

A GEOCHEMICAL AND STRUCTURAL STUDY OF THE
GNEISSES AND ECLOGITES ON THE
MOLDE PENINSULA, WEST NORWAY

Martin A. Harvey

Submitted in fulfilment of the
requirements for the
Degree of Ph.D.

Department of Geology,
University of Sheffield.

September, 1983

IMAGING SERVICES NORTH

Boston Spa, Wetherby

West Yorkshire, LS23 7BQ

www.bl.uk

CONTAINS
PULLOUTS

SUMMARY

The Molde Peninsula lies at approximately 64°N , in the Basal Gneiss Complex of W Norway, which represents a large area of basement rocks, mostly of Precambrian age and contains a large number of eclogites (i.e. gnt + omph. cpx rocks). To the NE of the Molde Peninsula lie several allochthonous units: the 'cover'. Previous mapping of the area had been of a reconnaissance nature and no systematic geochemical work had been done. Two major problems prevail in this area of Norway: the identification of and discrimination between true basement and true 'cover' rocks and the mode of formation of the eclogites. This study has been based on field mapping, petrography, geochemistry, mineral chemistry and some Rb-Sr isotope dating. Four major lithological units have been discerned. Basement rocks occur as two distinct types. The oldest is a calc-alkaline suite formed at ~ 2000 m.y. ago in an Andean type collision margin. These were subsequently intruded by the second type of basement rock at 1477 ± 21 m.y. ago (confirmed by Rb-Sr isotope dating) as a granitic pluton, related to the emplacement of the anorthosite-rapakivi suite, in a tensional crustal regime. A swarm of tholeiite dykes with a layered basic intrusion, was intruded into both types of basement rock at $\sim 1200-850$ m.y. ago in the waning stages of this crustal extension. The subsequent Caledonian orogeny between the Baltic and Greenland 'plates' involved considerable crustal thickening and nappe translation. One thrust unit of postulated Palaeozoic-aged marginal basin rocks occurs on the Peninsula. All four of these lithological units suffered eclogite facies metamorphism at $\sim 750^{\circ}\text{C}$ and 18-20 kbar during orogenesis and the dykes were disrupted into the pods of eclogite now seen. Subsequent rapid uplift instigated partial melting in the pelitic rocks, shearing and a variety of retrograde textures; eclogite facies assemblages are only sporadically preserved. Tight folding in the S of the area assisted in the extensive hydration of the rocks there.

ACKNOWLEDGEMENTS

Thanks go to Dr. D.A. Carswell for devising this project and for providing supervision throughout the period of study. Also to Professors C. Downie and J.B. Dawson for providing facilities in the Department of Geology during my rather extended stay.

Dr. R. Kanaris-Sotiriou for much help and useful advice with the X.R.F. analysis.

Dr. F.G.F. Gibb and Mr. H. Palmer for assistance with the temperamental E.M.P.

Professor W.L. Griffin for providing the Mass Spectrometer and other analytical facilities at Mineralogisk-Geologisk Museum, Oslo. Also to T. Enger and B. Sundvoll for technical assistance, and to H. Austrheim and S. Solheim for discussions on Rb-Sr methods at the same institution.

V. Somogyi, S. Burley, A. Saxby and A. Dawson for assistance and advice on wet-chemical methods.

Professor B. Leake for making X.R.F. facilities available at the University of Glasgow, and to Dr. C. Farrow for assistance with the same. Also to Dr. H. Williams for providing accommodation in Glasgow.

G. Mulhearn, D. Gregory and C. Otley for providing innumerable rock thin-sections.

M. Cooper for providing advice on draughting of the figures.

Steiner and Arne Sandvik for providing hospitality and accommodation at Molde Ungdomsheberge.

Various associates with whom discussion has prevented the polarised attitudes which result from solitary research and have assisted in the completion of this thesis: S.J. Cuthbert, J.R. Broadhurst, A. Al-Samman and P.C. Home.

S. Forster for performing several minor miracles with her typewriter.

Finally to Miss H. Steward for keeping me sane and assisting with the final preparation of this thesis.

CONTENTS

	<u>Page</u>
LIST OF TABLES	i
LIST OF FIGURES	iii
LIST OF PLATES	vii
<u>CHAPTER 1</u>	
INTRODUCTION	1
1.1 Geological Setting of Southern Norway	1
1.1.1 The Oslo Graben	1
1.1.2 The Southern Gneiss Region	2
1.1.3 The Jotun and Related Nappes	3
1.1.4 The Allochthonous Units and Sparagmites	6
1.1.5 The North-Western Gneiss Region	7
1.2 The Eclogite Controversy - Previous Studies and Interpretations	12
1.3 Previous Work on the Moldefjord Area	20
1.4 Aims of this Study	22
<u>CHAPTER 2:</u>	
GENERAL GEOLOGY AND STRUCTURES	24
2.1 Introduction	24
2.2 Structure	25
2.2.1 Foliation	26
2.2.2 Folds	28
2.2.3 Lineations	32
2.2.4 Faults and Joints	35
2.2.5 The Augen Gneiss as a Strain Marker	37
2.2.6 Conclusions	39

<u>CHAPTER 3</u>	THE TVERRFJELLA UNIT	42
	3.1 General Geology and Petrography	42
	3.1.1 The Garnet-Granulite	42
	3.1.2 The Marble	49
	3.1.3 The Heterogeneous Rocks	58
	3.1.4 The Nature of the Basal Contact of the Tverrfjella Unit	63
	3.1.5 Discussion of Petrography	65
	3.2 Geochemistry	81
	3.2.1 The Garnet Granulite	81
	3.2.2 The Mixed Rocks	89
	3.2.3 The Heterogeneous Rocks	91
	3.3 Discussion	95
	3.4 Mineral Chemistry and P-T Calculations	101
	3.4.1 The Garnet-Granulite	101
	3.4.2 The Kyanite Pelite	104
	3.4.3 Pressure and Temperature Calculations	105
	INTRODUCTORY STATEMENT TO CHAPTERS 4 and 5	109
<u>CHAPTER 4</u>	THE AUGEN GNEISS UNIT	113
	4.1 General Geology and Petrography	113
	4.1.1 Description	113
	4.1.2 Discussion of the Petrography	117
	4.2 Geochemistry	119
	4.3 Rb-Sr Whole Rock Dating	125
	4.4 Discussion	125

<u>CHAPTER 5</u>	THE HETEROGENEOUS QUARTZO-FELDSPATHIC GNEISS UNIT	141
	5.1 General Geology and Petrography	141
	5.1.1 Description	141
	5.1.2 Discussion of the Petrography	149
	5.2 Geochemistry	151
	5.3 Discussion	156
	5.4 Mineral Chemistry and P-T Conditions	161
 <u>CHAPTER 6</u>	 THE HETEROGENEOUS ROCKS OF MOLDEFJORD	 165
	6.1 General Geology and Petrography	165
	6.1.1 Rocks of the Moldefjord Coast	165
	6.1.2 Rocks of Bolsøy	172
	6.1.3 Discussion of the Petrography	179
	6.2 Geochemistry	181
	6.3 Discussion	187
 <u>CHAPTER 7</u>	 THE METABASIC AND META-ULTRABASIC ROCKS	 191
	7.1 Eclogites	191
	7.1.1 Field Relationships and Petrography	191
	7.1.2 The Metadolerites	191
	7.1.3 The Garnet-Peridotite	202
	7.2 Geochemistry	205
	7.2.1 Eclogites	205
	7.2.2 The Metadolerites	217
	7.2.3 The Garnet Peridotite	220
	7.2.4 Discussion of the Geochemistry	223
	7.3 MINERAL CHEMISTRY AND P-T CALCULATIONS	227
	7.3.1 The Eclogites	227
	7.3.2 The Metadolerites	231
	7.3.3 The Garnet-Peridotite	232
	7.3.4 Pressure and Temperature Calculations	233

<u>CHAPTER 8</u>	SUMMARY OF CONCLUSIONS	242
REFERENCES		242
		Following Page
<u>APPENDIX A</u>	ANALYTICAL METHODS	274
<u>APPENDIX B</u>	TEMPERATURE, PRESSURE AND MINERAL CALCULATIONS	All

LIST OF TABLES

Table number		Following page
1.1	Allochthonous units in the Trondheim region	6
1.2	Lithostratigraphic units in the Moldefjord-Kristiansund area	9
1.3	Radiometric ages relevant to the Basal Gneiss Region	11
2.1	Strain analysis of augen in the augen gneiss	38
2.2	Sequence of tectonic events in the Moldefjord area	41
3.1	Whole rock analyses and normative minerals of the Garnet-Granulite, Tverrfjella	83
3.2	Selected elements for oceanic and island arc basalts	88
3.3	Whole rock analyses of the mixed rocks - Tverrfjella	90
3.4	Whole rock analyses of the heterogeneous rocks - Tverrfjella	91
3.5	Selected elements in some major units of the Earth's crust	92
3.6	Analyses of garnets from the Garnet-Granulite	101
3.7	Analyses of clinopyroxenes from the Garnet-Granulite	101
3.8	Analyses of amphiboles from the Garnet-Granulite	101
3.9	Analyses of secondary feldspars from the Garnet-Granulite	101
3.10	Phases in the kyanite pelite in the heterogeneous rocks - Tverrfjella	104
3.11	Pressure and temperature data for the Garnet-Granulite	105
4.1	Whole rock analyses and normative minerals - Augen Gneiss Unit	119
4.2	Rb-Sr data	120
4.3	Averaged Rb-Sr data	128
5.1	Whole rock analyses - metasedimentary rocks in the Heterogeneous Quartzo-Feldspathic Gneiss Unit	151
5.2	Whole rock analyses - metaigneous rocks in the Heterogeneous Quartzo-Feldspathic Gneiss Unit	151
5.3	Analyses of clinopyroxene, garnets, feldspars and scapolites - Heterogeneous Quartzo-Feldspathic Gneiss Unit	161
5.4	P-T data for sample F4	162

Table number		Following page
6.1	Whole-rock analyses and normative minerals - Heterogeneous rocks of Moldefjord	182
6.2	Whole rock analyses and normative minerals - rocks of Bolsøy in the Heterogeneous rocks of Moldefjord	182
7.1	Whole rock analyses and normative minerals of the 'bimineralic' eclogites	205
7.2	Whole rock analyses and normative minerals of some eclogites	205
7.3	Whole rock analyses and normative minerals of the metadolerites	217
7.4	Whole rock analyses and normative minerals of the Kolmannskog garnet-peridotite body	220
7.5	Analyses of garnets from the eclogites	227
7.6	Analyses of clinopyroxenes from the eclogites	227
7.7	Analyses of amphiboles from eclogites	227
7.8	Analyses of feldspars associated with symplectite clinopyroxenes in eclogites	227
7.9	Analyses of garnets from metadolerite	231
7.10	Analyses of clinopyroxenes from metadolerite	231
7.11	Analyses of minerals occurring in the peridotite and associated eclogite at Kolmannskog	232
7.12	Pressure and temperature data for the metabasic and meta-ultrabasic bodies	233

LIST OF FIGURES

Figure number		Following page
1.1	Tectonostratigraphic units of Southern Norway	1
1.2	General geology of the Basal Gneiss complex	7
1.3	Isotherms of equilibration temperatures for eclogites and granulites	16
2.1(a)	Poles to foliation planes - Molde peninsula	26
2.1(b)	Poles to foliation planes - Moldefjord coast and Bolsøy	26
2.2(a)	Poles to foliation planes - Tverrfjella	26
2.2(b)	Poles to foliation planes - central sub area	26
2.3(a-f)	Various fold styles from throughout Molde peninsula	28
2.4(a-d)	Fold classification plots and fold styles	29
2.5	Geological map of fold structures between Moldefjord and Tingvoll	32
2.6(a)	Relationship between lineation directions and tectonic axes of a fold	32
2.6(b)	Poles to lineations on foliation planes from Moldefjord and Bolsøy	32
2.7(a)	Method of unfolding folds and reorientation of contained lineations	33
2.7(b)	Development of folds and resultant reorientation of contained lineation	33
2.8	Large-scale faulting at Tverrfjella	36
2.9(a)	Strikes to joints and faults throughout the Molde peninsula	36
2.9(b)	Changes in strain ratios with progressive deformation	36
3.1(a)	ACF diagram for the granulite facies	52
3.1(b)	T-X _{CO₂} diagram at 5 kbar with the univariant curve for reaction 3.H	52
3.2	Section of the Tverrfjella Unit	64
3.3	Phase diagram for the various melting curves	68
3.4	Phase diagram for high pressure minerals	72
3.5(a)	Isobaric T-X diagram - buffered fluid conditions	74
3.5(b)	Isobaric T-X diagram - externally controlled fluid conditions	74
3.6	T-X _{CO₂} diagram at 12 kbar	76

Figure number		Following page
3.7	Partial T-X _{CO₂} diagram at 5 kbar	79
3.8(a)	(Al + Fe + Ti) vs. (Ca + Mg) after Moine & de la Roche (1968)	82
3.8(b)	TiO ₂ vs. D.I. of Thornton & Tuttle (1960)	82
3.9	Selected elements plotted against Zr	85
3.10	Cr vs. Zr and Ni vs. Zr - sample trends	85
3.11	Cr vs. FeO ^t /(FeO ^t + MgO) and Ni vs. FeO ^t / (FeO ^t + MgO)	85
3.12(a)	Zr/TiO ₂ x 10,000 vs. Ga	85
3.12(b)	Zr/TiO ₂ x 10,000 vs. Nb/Y	85
3.13(a)	Zr/Y vs. Zr, log/log after Pearce & Norry (1970)	88
3.13(b)	V vs. Ti/1000 after Shervais (1982)	88
3.14(a)	Ti vs. Cr plot	88
3.14(b)	Zr-(Ti/100)-(Y x 3) after Pearce & Cann (1973)	88
3.15(a)	TiO ₂ vs. Zr with fields from Pearce & Cann (1973)	88
3.15(b)	TiO ₂ -(Mn x 10)-(P ₂ O ₅ x 10) with fields from Mullen (1983)	88
3.16(a)	TiO ₂ vs. Zr, log/log with fields of Gale & Pearce (1982)	88
3.16(b)	Cr vs. Y, log/log with fields of Gale & Pearce (1982)	88
3.17	Ti/100-(CaO x 3)-Zr - influence on Garnet- Granulite	88
3.18(a-c)	Zr/TiO ₂ x 10,000 vs. Ga, Ce, Nb/Y for quartzo- feldspathic rocks of the Tverrfjella Unit	94
3.19(a)	(Grossular + andradite)-(almandine + spessartine)- pyrope - after Coleman et al. (1965)	101
3.19(b)	Acmite-jadeite-augite after Essene & Fyfe (1967)	101
3.20	(Diopside & hedenbergite)-tschermakite-jadeite diagram	103
3.21	Pressure and temperature grid for Garnet- Granulite and kyanite pelite	105
A, B, C	Discrimination diagrams for the Augen Gneiss Unit and Heterogeneous Quartzo-Feldspathic Gneiss	111
4.1	Selected element oxides vs. Thornton & Tuttle's Differentiation Index	120
4.2(a)	K vs. Rb plot	120
4.2(b)	Ba vs. Sr plot	120
4.3(a)	Ca vs. Sr plot	120
4.3(b)	Rb-/Sr vs. Sr -differentiation trend for a mantle- derived granite magma	120

Figure number		Following pages
4.4(a)	Ba-Rb-Sr plot after Bouseily & Sokkary (1975)	121
4.4(b)	AFM plot with tholeiite/alkaline division	121
4.5(a)	Total alkalis ($\text{Na}_2\text{O} + \text{K}_2\text{O}$) vs. SiO_2 and CaO vs. SiO_2	123
4.5(b)	Al_2O_3 vs. An/(An + Ab) with tholeiitic/calc-alkaline division	124
4.6(a)	Ab-Or-An plot with fields from Streckeisan (1976)	124
4.6(b)	Ab-Or-An- H_2O diagram after Yoda et al. (1957)	124
4.7	Map of part of Moldefjord	125
4.8(a)	Rb-Sr whole-rock isochron diagram for the Augen Gneiss Unit	126
4.8(b)	Rb-Sr isochron diagram for Sr isotopic rehomogenisation	126
4.9(a)	Rb-Sr isochron diagram for Sr isotopic rehomogenisation on a small scale	126
4.9(b)	Sr evolution diagram	126
4.10(a)	Rb-Sr whole rock isochron diagram - averaged values of the Augen Gneiss Unit	128
4.10(b)	AFM plot with tholeiite/alkaline division for anorthositic suite	131
4.11(a)	Al_2O_3 vs. An/(An + Ab) with tholeiite/calc-alkaline division for anorthositic suite	131
4.11(b)	Ab-Or-Q- H_2O diagram after Tuttle & Bowen (1958)	131
4.12(a)	Relationship between the anorthosite-charnockite and leuconite-granite series as a function of $P_{\text{H}_2\text{O}}$	137
4.12(b)	Continental reconstruction for the mid-Proterozoic after Bullard et al. (1965)	137
5.1(a)	TiO_2 vs. SiO_2 - metasediment and metaigneous rocks	155
5.1(b)	Zr/($\text{TiO}_2 \times 1,000$) vs. Ni-metasediment and metaigneous rocks	155
5.2(a)	(Al + Fe + Ti) vs. (Ca + Mg) after Moine & de la Roche (1968)	155
5.2(b)	(Al + Fe + Ti)-K vs. (Al + Fe + Ti)-Na after Moine & de la Roche (1968)	155
5.3(a)	al-alk vs. c in Niggli normative minerals	155
5.3(b)	AFM diagram showing tholeiite/calc alkaline division	155
5.4(a)	$\text{Na}_2\text{O} + \text{K}_2\text{O} + \text{CaO}$ after Barker et al. (1981)	156
5.4(b)	Or-Ab-An of Streckeisen (1976)	156
5.5(a)	Tectonic features of Scandinavia, 2500-2000 m.y.	161
5.5(b)	P-T grid showing relationship between Garnet-Granulite and granulite F4 equilibration values	161

Figure number		Following pages
6.1(a)	K vs. Rb with $K/Rb = 230$ of Taylor (1964)	182
6.1(b)	Ca vs. Sr with possible differentiation trend	182
6.2(a)	TiO_2 vs. SiO_2 after Tarney (1976)	183
6.2(b)	$Zr/TiO_2 \times 1000$ vs. Ni of Winchester et al. (1980)	183
6.3(a)	AFM diagram with calc-alkaline/tholeiite division	185
6.3(b)	Ab-Or-An plot of Streckeisen (1976)	185
6.4(a)	(Al-Fe-Ti) vs. (Ca + Mg) of Moine & de la Roche (1968)	185
6.4(b)	Zr-(Ti/100)-(Y x 3) of Pearce & Cann (1973)	185
6.5(a)	Zr/Y vs. Zr after Pearce & Norry (1979)	186
6.5(b)	Cross-section of tectonostratigraphic relationship between Tverrfjella Unit and rocks on Bolsøy	186
7.1(a)	Garnet-peridotite outcrop at Kolmannskog	202
7.1(b)	(Al + Fe + Ti) vs. (Ca + Mg) after Moine & de la Roche (1968)	202
7.2	Covariance of various elements vs. Zr	208
7.3(a)	AFM diagram for eclogites and metadolerites	210
7.3(b)	$(Na_2O + K_2O)$ vs. SiO_2 for eclogites	210
7.4(a)	Zr-(Ti/100)-(Y x 3) after Pearce & Cann (1973)	211
7.4(b)	Zr/Y vs. Zr after Pearce & Norry (1979)	211
7.5(a)	Ti vs. Cr for eclogites and metadolerites after Pearce (1976)	212
7.5(b)	Ni vs. Cr (after Griffin & Råheim (1973)	212
7.6(a)	(Grossular & andradite)-(almandine + spessartine)- pyrope after Coleman et al. (1965)	227
7.6(b)	Acmite-jadeite-augite after Essene & Fyfe (1967)	227
7.7(a)	(Diopside & hedenbergite)-tschermakite-jadeite diagram	228
7.7(b)	Compositional zoning profiles across a clino- pyroxene and garnet	228
7.8(a)	Textural relationships between the clinopyroxenes and garnets of metadolerite	228
7.8(b)	Comparative pressure-temperature grid	228

In the following pictures scales are as follows:

Hammer = 40 cm long

Lens cap = ~ 5 cm diameter

Scale bar on photomicrographs = 500 μ

LIST OF PLATES

Plate number	Following Page
GENERAL GEOLOGY AND STRUCTURES	
2.1(a) Deformation of the Augen Gneiss, Mordal	41
(b) Deformation of the Augen Gneiss, Eidskrem	
(c) Flaggy foliationplanes in the heterogeneous rocks of Moldefjord, Mek	
(d) Isoclinal folds in the heterogeneous rocks of Moldefjord, Mordal	
(e) Isoclinal folds in the Augen Gneiss, Julaksla	
(f) Sheared Augen Gneiss, Eidskrem	
2.2(a) Flat-lying fold in the Garnet-Granulite, Tverrfjella	41
(b) Upright folds in the Augen Gneiss, Moldeheia	
(c) Large-open fold in the heterogeneous rocks of Moldefjord, Mordal	
(d) Flat-lying fold in the migmatitic rocks of the Tverrfjella Unit, Tverrfjella	
(e) Jointing in the heterogeneous rocks of Moldefjord, Mordal	
(f) Boudinage of the heterogeneous rocks of Moldefjord	
THE TVERRFJELLA UNIT	
3.1(a) The Garnet-Granulite in outcrop, Talstadhesten	108
(b) The Garnet-Granulite in thin-section	
(c) Mineralogical banding in the Garnet-Granulite, Talstadhesten	
(d) Quartz rich portion of the Garnet-Granulite with pyroxene 'strings'	
(e) Retrogressed Garnet-Granulite with kelyphites	
(f) Retrogressed Garnet-Granulite with symplectic clinopyroxene	
3.2(a) Partly retrogressed Garnet-Granulite with development of secondary plagioclase	108
(b) Heavily retrogressed Garnet-Granulite	
(c) Breakdown of kyanite in the Garnet-Granulite	

Plate number		Following page
(d)	Heavily retrogressed kyanite, to clays in the Garnet-Granulite	
(e)	General appearance of the small garnet peridotite within the Garnet-Granulite	
(f)	Contact of the marble and Garnet-Granulite, Langvatnet Quarry	
3.3(a)	'Plastic' contact of the Garnet-Granulite and marble, Langvatnet Quarry	108
(b)	Gradational contact of the Garnet-Granulite and marble, Talstadhesten	
(c)	Sharp contact between the Garnet-Granulite and marble, Talstadhesten	
(d)	Breakdown of clinopyroxene to tremolite + calcite	
(e)	Quartz + calcite in the impure marble	
(f)	Zoisite being replaced by scapolite in the marble	
3.4(a)	Scapolite breaking down to a symplectite of zoisite + Ca-plagioclase in the impure marble	108
(b)	Sphene + opaque producing rutile in the impure marble	
(c)	Melt + scapolite producing clinopyroxene, Garnet/ Granulite/marble mixed rock	
(d)	Layered nature of the heterogeneous rocks of the Tverrfjella Unit, Trolltindane	
(e)	Clinzoisite breaking down to plagioclase, quartzite band in the Garnet-Granulite	
(f)	Sillimanite appearing between K-feldspar and biotite, pelite in the heterogeneous rocks of Tverrfjella Unit.	
 THE AUGEN GNEISS UNIT		
4.1(a)	Undeformed Augen Gneiss, Fanghol	140
(b)	Calc-silicate pods in the Augen Gneiss, Eidskrem	
(c)	The Augen Gneiss in thin section	
(d)	Hornblende poikiloblastically enclosing plagioclase	
(e)	Mylonitised Augen Gneiss	
(f)	The granite sheets in thin section	
 THE HETEROGENEOUS QUARTZO-FELDSPATHIC GNEISS UNIT		
5.1(a)	The massive migmatite gneiss, Bjørnsnos Farm	164
(b)	Fine-scale migmatite gneiss, Helvatnet	
(c)	Palaeosome of the migmatites	
(d)	The banded gneiss, Elnesvågen	
(e)	The augen bearing gneiss, Hollingsholm	
(f)	The grey gneiss, Vagøy	

Plate number		Following page
5.2(a)	Protomylonitic fabric of the granitic gneisses	164
(b)	Garnet rim on a clot of mafic phases, quartzo- feldspathic gneiss	
(c)	Polygonal texture of feldspars with small clinopyroxenes	
 THE HETEROGENEOUS ROCKS OF MOLDEFJORD		
6.1(a)	Deformed quartzo-feldspathic rocks	190
(b)	Mylonitised quartzo-feldspathic rocks	
(c)	Orthite grain with a clinozoisite rim in the quartzo-feldspathic rocks	
(d)	A relict symplectic clinopyroxene in a garnet- amphibolite	
(e)	Banded nature of the pelitic rocks	
6.2(a)	Porphyroblastic hornblende enclosing quartz and plagioclase felsic schist, Bolsøy	190
(b)	Garnet with quartz inclusions in a snowball texture pelite, Bolsøy	
(c)	Plagioclase displaying two sets of twins, pelite, Bolsøy	
(d)	Relict and fragmented kyanite, pelite Bolsøy	
 THE META-BASIC AND META-ULTRABASIC ROCKS		
7.1(a)	A pod of eclogite in outcrop, Julneset	237
(b)	A 'zone' of eclogites, Vågøy	
(c)	A Class I eclogite	
(d)	Eclogite with small, rounded garnets	
(e)	A Class II eclogite	
(f)	A symplectite front in the clinopyroxene of an eclogite	
7.2(a)	A Class III eclogite	237
(b)	A Class IV eclogite	
(c)	A Class V eclogite	
(d)	Primary amphibole in the eclogites	
(e)	Eclogite containing a vein of omphacitic clinopyroxene Svartnakken	
7.3(a)	Corona texture in a metadolerite	237
(b)	'Fish-net' texture in a metadolerite	
(c)	Orthopyroxene in the garnet-peridotite at Kolmannskog containing needles of magnetite	
(d)	Symplectite development in the garnet-peridotite at Kolmannskog	

CHAPTER 1

INTRODUCTION

In this chapter a brief synopsis of the geology of southern Norway will be given, including a relatively extended section on the North-West Gneiss Region in which the area of study lies; followed by a history of the previous work in the Moldefjord area.

1.1 GEOLOGICAL SETTING OF SOUTHERN NORWAY

South of latitude 64°N , Norway may be divided into five geological units: the Oslo Graben; the Southern Gneiss Region; the Jotun and related nappes; the Allochthonous Units of the Trondheim area and Sparagmites; and the North-West Gneiss Region (see Fig. 1.1).

1.1.1. The Oslo Graben

This structure is a palaeo-rift, runs N-S, is approximately 200 km x 40 km and is a structural extension of the Rhine Graben. Much of the following is taken from Høltedahl (1960) and Oftedahl (1980).

The lowest rocks are Cambro-Silurian sediments, a sequence of sandstones, limestones and shales (often alum-bearing or bituminous) passing into continental sandstones (Ringerike Series) once thought to be comparable to the Old Red Sandstone of Great Britain. Only the northernmost part of the graben was affected by subsequent Caledonian tectonism. The succeeding Permian rocks are sediments (sandstones and shales) overlain by lavas (trachy-andesites and minor ignimbrites), intruded in three phases.

Igneous plutons were subsequently intruded, as both volcanic rocks and batholiths (Barth, 1945). The former are up to 1 km across, lie on tectonic lines and consist of gabbros and diorites; the latter make up a large part of the region, contain monzodioritic to granitic rocks, and

FIG. 1.1

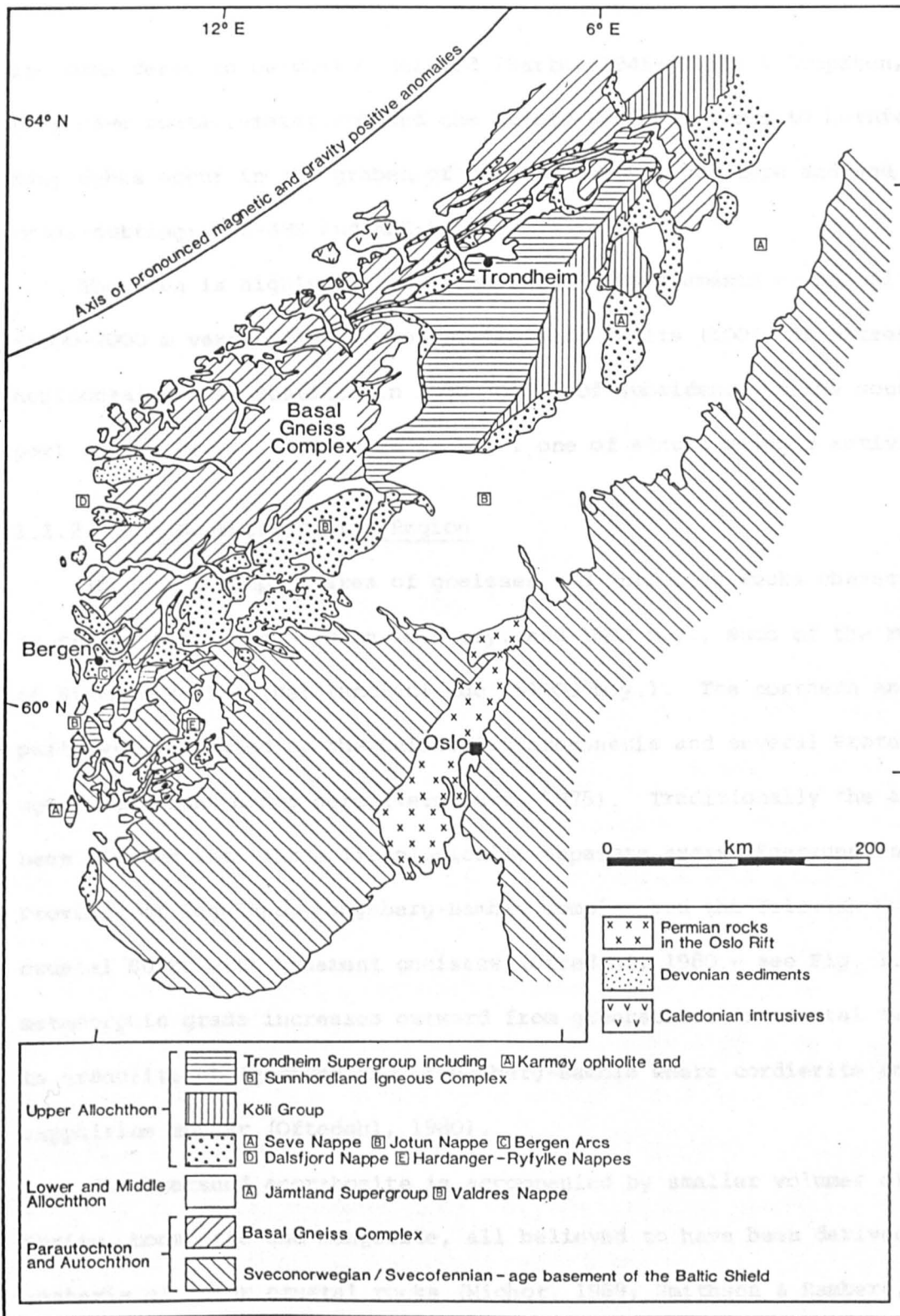


FIG. 1.1 The main tectonostratigraphic units of southern Norway (after Roberts et al., 1981).

are considered to be mantle derived (Barth, 1945; Heier & Compston, 1969), they have contact-metamorphosed the Cambro-Silurian rocks to hornfels. Many dykes occur in the graben, of various geochemical type and age, generally cross-cutting: NNW-SSE and NNE-SSW.

The area is highly faulted, the large displacements on normal faults (1000-2000 m vertically) and on strike slip faults (100's of metres horizontally) has resulted in 2000-3000 m of subsidence of the south-central part of the graben. The area is still one of strong seismic activity.

1.1.2. The Southern Gneiss Region

This is a complex area of gneisses and intrusive rocks characterised by radiometric ages between ~850 m.y. and 1600 m.y., much of the region is of Sveconorwegian (Dalslandian) age (~1000 m.y.). The northern and western parts were affected by the Caledonian orogenesis and several Proterozoic-aged intrusions occur here (Versteve, 1975). Traditionally the area has been divided into three lithologically separate areas: Egersund Anorthosite Province of Rogaland, Kongsberg-Bamble Complex and the Telemark Supracrustal Suite with basement gneisses (Oftedahl, 1980 - see Fig. 1.1). The metamorphic grade increases outward from greenschist in central Telemark to granulite at Egersund and Kongsberg-Bamble where cordierite and sapphirine appear (Oftedahl, 1980).

The Egersund anorthosite is accompanied by smaller volumes of leuconorite, norite, monzonite and mangerite, all believed to have been derived by anatexis of lower crustal rocks (Michot, 1969; Smithson & Ramberg, 1979) and intruded at ~1000 m.y. (Pasteels & Michot, 1975).

Kongsberg contains a variety of metamorphic rocks and intrusives. Both meta-dacite and meta-andesite, with geochemical affinities to island areas, have been identified here, also a possible eugeosynclinal sequence, all cut by post-tectonic granites. Two metamorphic events have been

revealed: 1600-1500 m.y. ('Kongsbergian') related to the failed opening of a supercontinent (Milne & Starmer, 1982) and ~1060 m.y. (Jacobsen & Heier, 1978; Field & Råheim, 1979): a reworking of older rocks. Bamble contains mixed gneisses with a complex history, the rocks have been intruded by many Proterozoic - aged intrusions which have been related to the anorthosite-charnockite suite of rocks (Starmer, 1972; Ploquin, 1975) as orogenic intrusions emplaced during the rifting of a supercontinent (Milne & Starmer, 1982).

The Telemark Supracrustals contain continental volcanics plus quartzitic sandstones, subsequent metamorphism and tectonism makes the distinction between these and the basement very difficult. The basement is dated ~1500 m.y. and the supracrustals ~1300-1200 m.y., both overprinted by a weak Sveconorwegian event. Porphyritic granites intruded both units ~960-850 m.y. On the very southern tip of Norway, the supracrustals are missing and the intrusive rocks are in direct contact with the basement, dated as ~900 m.y., these maybe related to the Egersund Anorthosite Complex (Wilson et al., 1977).

Torske (1977) noted a regional pattern in the rock types with a central continental area, surrounded by an andesitic belt, in turn surrounded by continental crust. This he related to a Cordilleran-type margin, originally situated off the present southern coastline, with subduction occurring ~1600-1500 m.y. ago, a rather different hypothesis to the failed tensional tectonics deduced from the intrusive rocks here.

1.1.3. The Jotun and related nappes

It has long been considered that the Jotun nappe represents a far-travelled body (>200 km), with a root off the present west coast of Norway, whose trailing edges formed the smaller nappe-like sheets on that coast (e.g. Dalsfjord-Skjerlie, 1969; Hossack, 1982). This thrust motion to the

SE was deduced from structures on the NW (Roberts, 1977) and SE sides (Valdres area - Hossack, 1978; Hossack et al., 1981) of the body. However, an alternative interpretation of the structures on the NW side suggests motion in that direction (Battey & McRitchie, 1973; Banham et al., 1979). From the presence of metasediments, metavolcanics, locally with pillow lavas and serpentinites (Banham et al., 1979; Elliot & Cowan, 1966) and a possible exotic olistostrome mélange there (Gibbs, 1982). The NW margin of the nappe has been suggested as the site of a Caledonian suture zone subsequent to the closure of a proto-Atlantic Ocean (Banham et al., 1979; cf. Dewey, 1969). The nappe possesses a gravity anomaly of +58 mgals, indicating a deep, dense root: ~16 km (Smithson et al., 1974) and it has been suggested that the body is an Ivea-type 'flake', of local origin, detached from the lower crust and rapidly raised to the surface (Battey & McRitchie, 1973; Smithson et al., 1974; Banham et al., 1979). Indeed, from the mineral chemistries, Griffin (1971) suggested initial crystallisation of the rocks at 25-30 km depth followed by rapid uplift.

To the SW lie the Hardanger-Ryfylke nappes lying above Proterozoic basement and its cover. Andresen & Faereth (1982) have correlated the lower part of these nappes to rocks in the Valdres area and the upper parts to the Jotun Nappe. Overlying these is the Sunnhordland Nappe Complex of ophiolites and island-arc volcanics, continental-rift volcanics/intrusives, allochthonous basement and sediments. The ophiolites were obducted onto an Andean-type Baltic margin in the Upper Ordovician prior to thrusting over the basement (Andresen & Faereth, 1982).

Similar rocks to those the Jotun-Hardanger nappes occur in the Bergen Arcs, a series of arcuate belts containing lower Palaeozoic metasediments, metavolcanics and gneisses with migmatites and anorthosites (Sturt et al., 1975; Sturt & Thon, 1978). These are divided into:

Major Arc

Anorthositic and charnockitic rocks

Minor Arc

Precambrian Basement

This was previously considered to be a continuous stratigraphic sequence from Precambrian gneisses to lower Palaeozoic rocks (Hernes, 1967), with the Arcs developed during the Caledonian orogeny (cf. Kolderup & Kolderup, 1940). Now all the units are interpreted as nappes, thrust from the west, onto a Precambrian gneiss complex (Sturt et al., 1975; Sturt & Thon, 1978; Austrheim, 1981). The Major and Minor Arcs contain ophiolite fragments and equate with the Sunnhordland Nappe Complex. Structurally above these is the Ulrikkens Gneiss Complex (Sturt & Thon, 1978) and the Anorthosite Complex. The latter contains preserved granulite facies rocks evolved from low pressure assemblages (Griffin & Heier, 1973). Austrheim (1981) has deduced a more complex sequence of deformational and intrusive events under granulite or pre-granulite facies conditions, followed by amphibolite facies reworking and the formation of eclogites along shear zones in rocks of suitable composition either during the Caledonian or Sveconorwegian orogens (Austrheim & Råheim, 1981; Austrheim & Griffin, 1982). This complex may correlate with the Jotun Nappe or may represent a higher structural level (Andresen & Faereth, 1982).

The small nappe units at Dalsfjord in Sunnfjord are of mangerites thrust over metagreywackes, in turn overthrust by an island-arc/ophiolite sequence prior to emplacement on the Precambrian gneisses (Skjerlie, 1969, 1974; Furnes et al., 1976).

The suggested correlations between the Hardanger, Bergen and Dalsfjord nappes with the Jotun nappe favour an allochthonous origin for the latter. The alternative explanation, of a local origin, would require some large-scale mechanism to uplift a large, dense mass and place it over less dense crustal material.

1.1.4. The Allochthonous Units and Sparagmites

The Allochthonous Units occur in the Trondheim area, are fossil-bearing Palaeozoic rocks and overly the North-West Gneiss Region (see Fig. 1.1). The rocks are folded together with the underlying gneisses in open, upright folds in the east which tighten towards the west. The nappes thin westwards and polyphase deformation is evident in each unit, related to a gradual build-up of a rock pile under progressive simple shear (Roberts & Gee, 1981; Krill, 1983).

The rocks are divided into the Särvi, Seve-Köli and Upper Nappes which pass eastwards into Sweden where a further unit, the Offerdal Nappe appears. The lithological units and suggested correlations of Gee (1978, 1980) and Krill (1980, 1983) are given in Table 1.1.

These allochthonous units are separated from the basement by a thin veneer of sediments, locally conglomeratic, which is considered to have acted as a décollement surface on which the nappes rode during their emplacement (Gee, 1980). The sequence includes rocks from a variety of environments: Precambrian basement, island-arc, back-arc and possibly oceanic derivation (Gale & Roberts, 1974). The nappes are considered to have originated up to 1000 km W of the present coast, with half this distance achieved through translation and the remainder by stretching (Gee, 1978).

These nappes structurally overlie the Jotun Nappe whereas the Sparagmites (Eocambrian/Cambro-Silurian sediments) underlie it. In the Valdres area the autochthonous Proterozoic basement is overlain by a veneer of mid-Cambrian shale, in turn overlain by two sheets of sediments roofed by the Valdres nappe, upon which the Jotun Nappe has been shown to have moved in a southward direction (Hossack, 1978; Hossack et al., 1981). Beneath the Valdres thrust sheet lie three other sheets: Strondafjord,

TABLE 1.1 Allochthonous units in the Trondheim Region

Gee (1980)	Krill (1980, 1983)	Lithological Notes
Upper Allochthon		
Trondheim Supergroup	Tronget-Støren Nappe	Rocks similar to Blåhø Nappe but only to greenschist facies. Mafic volcanics and volcanoclastics but lacking pelites. Silurian(?), Ordovician(?) from fossils.
Køli Nappe	'Abscherungszone'	Not present everywhere. Sediments and volcanics at greenschist facies. Silurian, Ordovician and older?
Seve Nappe	Surna Nappe?	Rocks similar to Blåhø Nappe but has abundant dykes and bodies of trondhjemite. Possessed a metamorphic foliation before emplacement. The Surna (Røros) schist dated by Råheim (1977) gave 'errorchrons' ~460 m.y. Upper amphibolite/granulite facies, equivalent to Gula Nappe? on trondhjemite intrusions. Silurian, Ordovician and older(?).
Särvi Nappe	Blåhø Nappe	Garnet-hornblende schist (+ kyanite), amphibolite plus serpentine bodies and ultramafite, marbles, psammite and gneiss. Difficult to date, but a maximum model age of ~800 m.y. given for sediments (Solheim, 1980).
Särvi Nappe	Saetra Nappe	Feldspathic psammite and amphibolite-originated as tholeiitic dykes in sedimentary layered fluvial sandstone. Rb-Sr whole rock dating gives 745 ± 37 m.y. as an igneous age for the dykes (Krill, 1981). Low amphibolite facies. Late Precambrian sediments.
Middle Allochthon		
Offerdal Nappe	Risberget Nappe	Coarse augen gneiss plus rapakivi granite, gabbro, anorthosite, felsic granite and heterogeneous gneiss with calc-silicates. Rb-Sr whole rock gives Precambrian ages (~1600 m.y. - Solheim, 1980) which Krill (1983) interpreted as the intrusive age of the Augen gneiss. This is probably equivalent to the Tännäs Augen Gneiss Nappe in Sweden.

Below these lie the Lower Allochthon (the Lønset and Åmotsdal Nappes of Krill (1980, 1983) and the Parautochthon including basement portions and relict eclogitic gabbros. The metamorphic grades of these rocks increases towards the west and down the tectonostratigraphy, from chlorite to garnet grade. Eclogites and granite intrusions then appear with calculated temperatures of formation ~660°C (Krill, 1983) apparently before the final emplacement of the Tronget-Støren and Surna Nappes. Much of the Caledonian metamorphism post-dated the nappe emplacement but in the west of the region it was prior to the thrusting (Gorbatshev et al., 1981).

Synnfjell and Aurdal. All these contain sparagmitic rocks, i.e. feldspathic sandstones, often coarsely conglomeratic with thin shales and limestones, and rare tillites. These are considered to represent fluvial and marine deposits and exhibit increasing grades of metamorphism to the NW, up to greenschist facies. Restoring the sheets to their pre-thrust positions to the NW, showed them to have covered >200 km of marine shelf. This area was progressively shortened during their emplacement in the Caledonian orogeny (Nickelson et al., 1981).

1.1.5 The North-West Gneiss Region

The area of this study lies in this region, also known as the Basal Gneiss Region (Holtedahl, 1944) and referred to as such throughout this work. The Region forms the deepest exposed level of the Scandinavian Caledonides and is the largest of a number of basement windows in the Caledonian nappes of Norway and Sweden (Holtedahl & Dons, 1960; Roberts et al., 1981). Fig. 1.2 shows the major geological units in the Region with the division into the Jostedal and Fjordane Complexes from Bryhni (1966).

Two major problems are encountered here: the recognition of, and the relationship between the 'basement' gneisses and the 'cover' rocks of the greenstone nappes. Early geologists (Irgens & Hiortdahl, 1864; Reusch, 1881; Kolderup, 1923, 1928) regarded the gneisses as an Archaean (Pre-cambrian) basement to the overlying lower Palaeozoic sediments. By contrast, Holtedahl (1936, 1938, 1944) considered that some of the gneisses were likely to be derived by feldspathisation of 'Caledonian' meta-sediments. Gjelsvik (1951) and Kolderup (1952, 1960) were of a similar opinion with the gneisses derived from 'Eocambrian' (i.e. late Pre-cambrian) or Cambro-Silurian sediments. In a series of papers, Hernes (1955, 1956a, 1965, 1967) suggested that all the gneisses represented an

FIG. 1.2

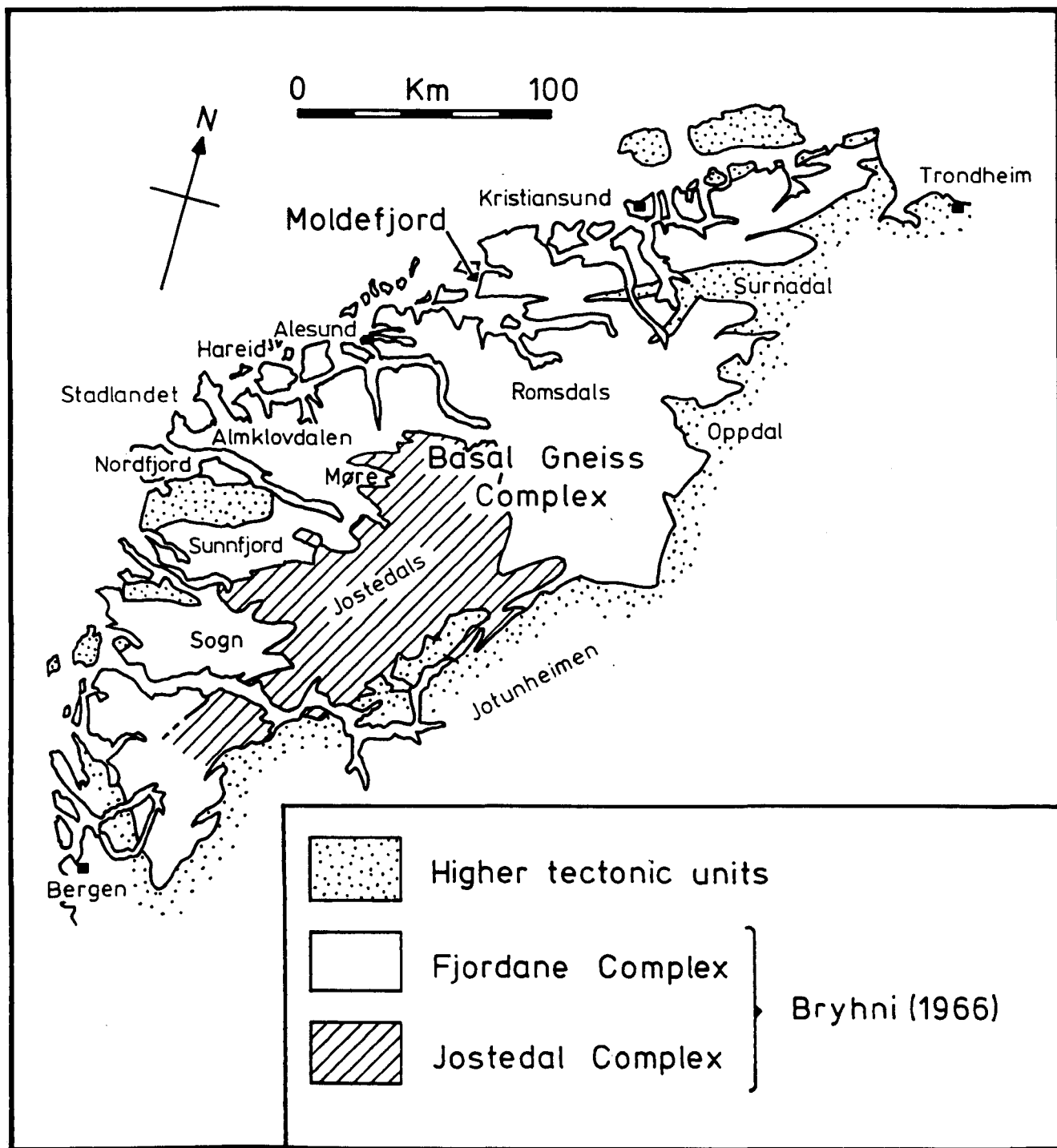


FIG. 1.2 The general geology of the Basal Gneiss Complex, with important localities.

altered late Precambrian succession. A more complex history was envisaged by both Strand (1960) and Muret (1960) with the Precambrian basement and the Cambro-Silurian deposits being intimately folded together during the Caledonian orogeny.

This situation was further complicated with the suggestion that perhaps the 'basement' gneisses themselves were composed of two distinct elements. In the SW part of the Region, Bryhni (1966) mapped a contact between a reworked Pre-Eocambrian (i.e. late Proterozoic) basement complex of homogeneous, migmatitic gneisses (the Jostedal complex) and an overlying heterogeneous series (the Fjordane complex) containing: quartzites, anorthosites, peridotites, mangerites and various supracrustal rocks. In the Grotli area, Strand (1969) mapped a similar contact between 'Caledonised' Precambrian basement (subsequently correlated with the Jostedal Complex: Skjerlie & Pringle, 1978) and overlying metasupracrustal rocks. Brueckner (1977a) also found two contrasting sequences in the Tafjord area, to the south of Grotli, naming them the Vikvatn sequence (heterogeneous) and the Fetvatn sequence (homogeneous), broadly correlating them with portions of the Fjordane and Jostedal Complexes respectively. To the SW of Grotli in the Gaular area, Skjerlie (1969) differentiated between a Precambrian gneissic basement and an overlying metasupracrustal sequence and considered them to be closely interfolded.

In the NW part of the Trondheim Basin there exists an area of undisputed Eocambrian-Silurian rocks in contact with the Basal Gneisses, even so the nature of the contact is unclear. Once again, a metasomatic and migmatitic alteration of the sediments was originally invoked to create the gneisses (Barth, 1938; Strand, 1949). Conversely, Rosenqvist (1941) and Oftedahl (1964) considered the contact to be primary, with the Eocambrian and Cambrian rocks deposited directly onto the older gneisses and the two folded together.

Roberts et al. (1970), Bryhni & Grimstad (1970) and Carswell (1973a) agreed that the Cambro-Silurian rocks are in contact with Precambrian gneisses, but considered the contact to be tectonic and any apparent conformity due to subsequent Caledonian deformation. From work at Oppdal, Krill (1980) has suggested that both autochthonous and allochthonous cover and basement are present, but so interfolded as to obscure the original relationships.

On the map of Holtedahl & Dons (1960) a lobe of schistose rocks from the Trondheim Basin extends into Surnadalen as the Surnadal synform (see Fig. 1.2). The nature of the 'basement'-'cover' relationships in Surnadalen are of particular significance since it has been considered that the rocks there are a discontinuous extension, along strike, of the rocks on the islands in Moldefjord (Strand, 1953). Originally, these schists were believed to be of lower Palaeozoic sediments with the gneisses below formed by migmatization of the former during the Caledonian event (Gjelsvik, 1953). The Surnadal synform was also formed at this time, one of several NE-SW trending tight, recumbent fold structures in the area (Hernes, 1956a, b; Løset, 1977, Krill, 1983). A similar migmatization origin was also postulated by Strand (1953) who was unable to find a structural break between the schists and gneisses.

Hernes (1955) has published a map of the geology between Molde and Kristiansund, including Surnadalen; along with a tectono-stratigraphy of the rocks based on a eugeosynclinal sequence of assumed late-Precambrian age (Hernes, 1967), subsequently expanded upon by Råheim (1972, 1979) from work at Kristiansund (see Table 1.2). However, Råheim queried the Caledonian age for the metamorphic event, and demonstrated that at least some of the rocks (Frei and Kristiansund Groups) possess a Svecofennian age (i.e. 1800-1600 m.y.) of 1708 ± 68 m.y. (Pidgeon & Råheim, 1972). The

TABLE 1.2 Lithostratigraphic units in the Moldefjord-Kristiansund area

Hernes (1967)	Råheim (1972, 1979)	Lithologies and possible origins and metamorphic grades from Råheim
<p>Upper Tingvoll Group } Lower Tingvoll Group }</p> <p>Raudsand Group</p> <p>- - TECTONIC BREAK - -</p> <p>Frei Group</p>	<p>Støren Group } - - TECTONIC BREAK - - } Trondheim Suite Røros Group (+ Gula ≡ Surna Group) }</p> <p>Sandvik Group</p> <p>Kristiansund Group</p> <p>Border Group</p> <p>Frei Group</p> <p style="text-align: center;">Lower ↑ Almandine-amphibolite/ granulite facies ↓ Upper</p>	<p>Low grade (greenschist) basic metavolcanics</p> <p>Garnet-micaschist, amphibolites, garnet-amphibolites, marbles, calc-silicates. At amphibolite facies.</p> <p>Heterogeneous gneisses with amphibolites, schists and marbles. Derived from basaltic volcanics plus terrigenous sediments.</p> <p>Homogeneous gneisses plus amphibolite. Derived from rhyodacitic volcanism or possibly arkoses.</p> <p>Heterogeneous gneisses. Derived from basaltic/rhyodacitic volcanics plus sediments to give calc-pelites.</p> <p>Heterogeneous gneisses: migmatitic pelites, augen gneiss, granitic gneiss with garnet-amphibolite-eclogite series and calc-silicate gneisses. Derived from rhyodacitic volcanics, basaltic tuffs/lavas and limestone/pelites respectively.</p>

N.B. Støren Group ≡ Tronget-Støren Nappe and the Surna Group is ≡ Surna Nappe in Table 1.1 Rickard (1981) considers that rock units in the Tingvoll Group are comparable to portions of the Tännäs, Särsv and Seve Nappes and represent thrust or fold-repeated slices of the trailing edges of these nappes. These rocks are equated with the Risberget nappe on the map of Krill (1983).

apparent lack of any structural or metamorphic break between these dated rocks and those in the Surnadal synform (Trondheim Suite) led him to suggest that these latter rocks were also of a similar age (Råheim, 1977), although this was then in conflict with the Caledonian age assigned to them by Hernes (1956a). To resolve this problem he postulated that perhaps two suites of rocks, both of almandine-amphibolite facies, had been juxtaposed with the contact between either the Røros and Støren Groups, or within the Støren Group itself. He subsequently demonstrated that the rocks in the Tingvoll Group do appear to have a Svecofennian age (1707 ± 63 m.y.). The Rb-Sr data for the Røros Group is more difficult to interpret: the isochron is not well constrained and gives a Caledonian 'age', although Råheim interprets this as a result of partial Sr re-equilibration during Sveconorwegian or Caledonian events on originally older (1700 m.y.) rocks by rather tenuous reasoning (Råheim, 1977) which will be discussed more fully in the conclusions to Chapter 3. Furthermore, he demonstrated the existence of a structural and metamorphic break between these Svecofennian aged rocks of the synform and the younger Støren Group (which he equated with the 'Caledonian' Støren Nappe of Gale & Roberts (1974) - Råheim, 1979). This would suggest that the Surnadal synform is not an integral part of the Palaeozoic rocks of the Trondheim Basin, and that the rocks on the Moldefjord islands, supposedly on strike with the synform are also of Svecofennian age.

By contrast, Krill (1981) regarded this tectonic break as an 'Abscherungszone' separating an infrastructure of high-grade metamorphism from a superstructure of low-grade metamorphism as found at Oppdal (Krill, 1980). From the suggested correlations in Table 1.2 it would appear that the rocks of the Surnadal syncline are (i) allochthonous, now interfolded with the basement and (ii) Caledonian in age; as a consequence the rocks in Moldefjord would be the same.

From his studies in the Moldefjord area, Carswell (1973a) noted that eclogites were apparently found only in the 'basement' gneisses and were lacking in the adjacent metasediments. From this he concluded that the former were significantly older than the latter and were thus part of the 'Caledonised' Precambrian basement with the Palaeozoic rocks deposited on them. Consequently he placed a lithological break within the Frei Group, in much the same place as a line on Hernes' map although the latter drew no importance to the feature. Carswell also discussed the inherent difficulties involved in discerning between units in a metamorphosed terrain, especially in the case of the Basal Gneisses where a basement complex has been severely deformed together with a cover of younger rocks. He pointed out that metamorphic overprinting of the basement will eradicate any previous metamorphic distinctions between the rocks, whilst migmatization will promote lithological convergence. Furthermore, he suggested that a full understanding of the situation was most likely to be obtained from radiometric dating. Table 1.3 lists some of the dates derived by various methods from the Basal Gneisses, with the interpretations of the various workers. The ages fall approximately into four groups implying a polymetamorphic history for the region (cf. Kratz et al., 1968):

- Caledonian orogenic events
- Sveconorwegian orogenic events
- Mid-Proterozoic igneous events
- Svecofennian orogenic events.

The Caledonian event affected all the Basal Gneiss Region with the deformation becoming progressively more plastic and intense towards the NW resulting in the difficulties with lithological distinction outlined above. The deposition of Devonian fluvial/alluvial sediments (correlated with the O.R.S. in Britain) in several basins along the west coast of Norway (see Fig. 1.1) marked the end of this orogenic event, although some of the rocks display late movements (Steel, 1981).

TABLE 1.3 Radiometric ages relevant to the Basal Gneiss Region

AGE (m.y.)	METHOD/LITHOLOGY	INTERPRETATION	SOURCE
~1800 1800-1600	K-Ar (amphibole)/eclogite Rb-Sr (WR)/gneisses	Svecofennian orogenic event Svecofennian	McDougall & Green (1964) Priem (1967)
~1880 1682 ± 70 (1646 ± 70) 1708 ± 60 (1672 ± 60)	Rb-Sr (WR)/Dombås supracrustals Rb-Sr (WR)/gneisses Rb-Sr (WR)/gneisses (Kristiansund Group)	crystallisation of rocks or isotopic homogenisation of sediments metamorphism of gneisses and contained eclogites age of amphibolite-grade metamorphism	Brueckner (1972) Mysen & Heier (1972) Pidgeon & Råheim (1972)
~1700	Rb-Sr (WR)/gneisses (Frei Group)	closure of Rb-Sr system	"
~1600 1682 ± 20 1707 ± 63 (1671 ± 63)	U-Pb (zircon)/gneisses (Kristiansund Group) Rb-Sr (WR)/gneisses Rb-Sr (WR)/gneisses (Tingvoll Group)	minimum of zircon crystallisation Svecofennian event Svecofennian high-grade metamorphism	" Hansen et al. (1973) Råheim (1977)
~1660 1625 ± 75 (1591 ± 75) 1775 ± 57 (1738 ± 57) 1760 ± 70 1688 ± 162 1653 ± 84 1700-1750	Rb-Sr (WR)/schists (Røros Group) Rb-Sr (WR)/gneisses Rb-Sr (WR)/supracrustals Rb-Sr (WR)/basement gneisses Rb-Sr (WR)/mylonite gneiss Rb-Sr (WR)/basement gneiss Rb-Sr (WR)/gneisses	age of high-grade metamorphism Svecofennian orogeny age of formation of gneisses age of pre-metamorphic rocks or age of amphibolite facies Svecofennian deformation Svecofennian age equivalent to similar ages in the Basal Gneisses	" Skjerlie & Pringle (1978) Brueckner (1979) Lappin et al. (1979) Råheim et al. (1979) " Solheim (1980)
~1550-1760	U-Pb (zircon)/eclogites	primary magmatic age	Gebauer et al. (1982)
~1550 1511 ± 64 (1479 ± 64) 1520 ± 10 1450-1500 1477 ± 21	⁴⁰ Ar/ ³⁹ Ar (pyroxene)/augen gneiss Rb-Sr (WR)/anorthositic suite U-Pb (zircon)/mangerite syenite Rb-Sr (WR)/augen gneiss + granites Rb-Sr (WR)/augen gneiss + granites	ancient element = Laxfordian in Lewisian related to ~1600 m.y. anorthosites and rapakivi granites most likely a magmatic crystallisation age minimum age of formation by deformation magmatic crystallisation of igneous precursor	Bryhni et al. (1971) Abdel-Monem & Bryhni (1978) Lappin et al. (1979) Solheim (1980) Harvey (this work)
1150-950 1000 ± 150 (1035 ± 150) 1113 ± 106 1022 ± 18 1253 ± 100 (1226 ± 100)	K-Ar (phlogopite + hornblende)/eclogite Rb-Sr (WR)/basement gneisses Rb-Sr (WR)/augen gneiss ⁴⁰ Ar/ ³⁹ Ar (pyroxene)/augen gneiss Rb-Sr (WR)/basement gneiss	metamorphism & secondary alteration Precambrian rocks Grenvillian event metamorphic overprinting Precambrian rocks	McDougall & Green (1964) Brueckner et al. (1968) Michot & Pasteels (1969) Bryhni et al. (1971) Brueckner (1972)
~1150 1033 ± 37 (1069 ± 37)	Rb-Sr (WR)/Dombås supracrustals Rb-Sr (WR)/Hestbrepiggen granite	crystallisation of rocks or isotopic homogenisation of sediments intrusion during Grenvillian orogeny	" Priem et al. (1973)
~1000 960 ± 10 (940 ± 10)	Rb-Sr (WR)/schists (Røros Group) Rb-Sr (WR)/gneisses	a possible 'age' age of formation, Svecofennian or Caledonian	Råheim (1977) Brueckner (1979)
~1200-1100 1200-1000	Rb-Sr (WR)/quartzites Rb-Sr (WR)/Seve nappe	possible Sveconorwegian effect Sveconorwegian age	Lappin et al. (1979) Reymer et al. (1980)
~1050 ~950	Rb-Sr (WR)/gneisses & flagstones U-Pb (zircon)/amphibolite	Sveconorwegian effect emplacement into basement during Sveconorwegian	Solheim (1980) Gebauer et al. (1982)
~400 383 ± 12 (396 ± 12) 463 ± 6	K-Ar (mica) & Rb-Sr (mica)/eclogite & gneiss K-Ar (mica)/gneiss ⁴⁰ Ar/ ³⁹ Ar (amphibole)/gneisses	Caledonian effect Caledonian effect upon Precambrian rocks minimum age of amphibolite metamorphism	McDougall & Green (1964) Brueckner et al. (1968) Strand (1969)
~380 524 ± 6 488 ± 2 405 ± 2	K-Ar (mica)/gneisses ⁴⁰ Ar/ ³⁹ Ar (amphibole)/amphibolite ⁴⁰ Ar/ ³⁹ Ar (mica)/augen gneiss ⁴⁰ Ar/ ³⁹ Ar (mica)/gneisses	phase of folding? Caledonian metamorphism " "	" Bryhni et al. (1971) " "
590 550 408	Rb-Sr (WR)/quartzite Rb-Sr (WR)/schists Rb-Sr (WR & mica)/gneisses	(calculated age with I.R. = 0.705) Caledonian sediment? " Caledonian recrystallisation	Brueckner (1972) " "
391 ± 12 (383 ± 12)	Rb-Sr (WR & minerals)/schists	complete mineral homogenisation during Caledonian	"
~400 393 ± 7 (385 ± 7)	U-Pb (zircon)/Kristiansund gneisses Rb-Sr (minerals)/pegmatites	disturbance of isotopic system Caledonian aged intrusives	Pidgeon & Råheim (1972) "
~385	Rb-Sr (WR)/granite dykes	"	"
~400-600 ~460 398-384	U-Pb (zircon)/eclogite Rb-Sr (WR)/Røros Group Rb-Sr & K-Ar (mica)/Røros Group	Caledonian event secondary 'isochron' gives Caledonian age late Caledonian effect	Krogh et al. (1973) Råheim (1977) "
396 ± 15 (388 ± 15) 392 ± 15 (384 ± 15)	Rb-Sr (WR)/gneisses "	Caledonian effect "	Skjerlie & Pringle (1978) "
~400 ~425 460	U-Pb (zircon)/migmatitic gneisses Sm-Nd (garnet & clinopyroxene)/eclogites Rb-Sr (WR)/Seve nappe	Caledonian influence age of high-pressure metamorphism Caledonian effect	Lappin et al. (1979) Griffin & Brueckner (1980) Reymer et al. (1980)
~400 ~400	Rb-Sr (WR & minerals)/gneisses U-Pb (zircon)/eclogites	Caledonian & weak effect on minerals Caledonian metamorphism	Solheim (1980) Gebauer et al. (1982)
598 ± 1 408 ± 8 414 ± 31	Sm-Nd (minerals)/eclogites Sm-Nd (WR & minerals)/eclogites Sm-Nd (WR & minerals)/gneisses	Caledonian metamorphism of Palaeozoic rock Caledonian metamorphism or post-orogenic crystallisation "	Griffin & Brueckner (1982) Mearns & Lappin (1982a) "

WR = whole rock

Ages in brackets are recalculated, when possible, using the current ⁸⁷Rb decay constant of 1.42×10^{-11} m.y. (Steiger & Jäger, 1977).

1.2 THE ECLOGITE CONTROVERSY - PREVIOUS STUDIES AND INTERPRETATIONS

The gneisses of the Basal Gneiss Region are dominated by amphibolite-facies mineralogy but enclose relics of higher grade rocks. One particular rock found within the gneisses has been the object of scrutiny and controversy for many years, and seemingly out of all proportion to its limited abundance namely: the eclogites. These are found as pods, layers or larger bodies, within the gneisses ('external' type) and as layers and lenses within ultramafic rocks ('internal' type). They are also found in association with the anorthosites N of Nordfjord (Bryhni, 1966; Brastad, 1983).

The 'external' eclogites are predominantly bimineralic (omphacitic clinopyroxene + almandine - pyrope garnet \pm quartz \pm rutile) with a tholeiitic, or more rarely, an alkali-olivine basalt chemistry. Mineralogical variations include: chloromelanitic omphacite (i.e. substantial actinolite component in the clinopyroxene) at Sunnfjord (Krogh, 1980a); impure jadeites from Selje (Lappin & Smith, 1978); kyanite, often with clinozoisite; orthopyroxene in Mg-rich, Ca, Na-poor compositions; glaucophanes, at Sunnfjord (Krogh, 1980a); tremolite and baroisite amphiboles; phengite in Al-rich; or phlogopite in Mg-rich compositions (Griffin et al., 1983). Often these hydrous phases appear to be in equilibrium with the clinopyroxene and garnet.

The 'internal' eclogites are of two types: the first is the 'Rødhaugen' type of Eskola (1921): bimineralic with Mg-Na-augite + pyrope garnet \pm orthopyroxene. There is no olivine, as seen in the enclosing peridotite. The chemistry is only broadly basaltic since the normative minerals comprise an An-rich plagioclase and less than 30% olivine. These occur as bands several metres long within the peridotite. The second is the 'Raudkleiva' type (Griffin et al., 1983), which appear

as lenses 1-30 m across, probably disrupted from tabular bodies. At Almklovdalen these have been interpreted as cogenetic with the garnet-peridotite (Lappin, 1974), whereas Griffin & Qvale (1981) consider them to be basaltic dykes intruded into the ultramafic body. The rocks are superferric (i.e. high $\text{Fe}/(\text{Fe} + \text{Mg})$), have much higher Na_2O and Al_2O_3 contents than the 'Rødhaugen' type (Griffin et al., 1983) and have been equated with the superferrian eclogites of the Alpine peridotites (Griffin & Qvale, 1981).

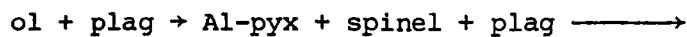
The eclogites associated with the anorthosites are up to 0.5 m thick and possess gradational contacts with the anorthosite (Brastad, 1983). They are similar in chemistry to the superferrian types but have higher Na_2O and K_2O contents and are essentially biminerally (cpx + gnt ± zo ± ky). REE patterns, coupled with high Al contents, genetically relate them to the enclosing anorthosites (Griffin et al., 1983).

The pioneering work on these rocks was done by Eskola (1921) who distinguished between those occurring within the gneisses and those with dunitic rocks. They were interpreted as fragments detached from larger eclogite rocks ('eclogite-magma') at depth and emplaced into the gneisses where they then suffered the same metamorphic and tectonic processes, which were considered to have formed the gneissic foliation. O'Hara & Mercy (1963) showed the 'internal' eclogites to be chemically different from those found in kimberlite pipes, but concluded that they were also fragments of the upper mantle. This interpretation has been supported by a number of workers: O'Hara et al. (1971), Carswell (1968a, 1968b), Lappin (1966, 1974), Lappin & Smith (1978) and extended to include the 'external' eclogites. The introduction of these bodies into the crust has been explained by the model of a 'tectonic mélange' involving the interdigitation of crust and mantle during the continent-continent collision of the Caledonian orogen (Smith, 1980).

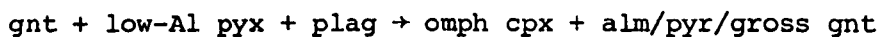
From a regional study of the gneisses and eclogites, Gjelsvik (1952, 1953) concluded that the eclogites were derived from crustal protoliths during a high-grade metamorphic event since some examples of dolerite displayed corona reactions developing from low-P assemblages towards eclogite assemblages:



This interpretation has subsequently been supported by a number of workers: Hernes (1954b), Kolderup (1960), Schmitt (1964), Bryhni (1966), Bryhni et al. (1969), Bryhni et al. (1970). Corona forming reactions have more recently been studied by Griffin & Heier (1973) and Griffin & Råheim (1973) for dolerites and other basaltic rocks and a simplified form of the reactions are given here:



IGNEOUS LOW-P GRANULITE



HIGH-P GRANULITE

ECLOGITE

These were considered to be a continuous sequence of reactions occurring during cooling and compression of an igneous mass (Griffin & Råheim, 1973). Field evidence from Sunnfjord has revealed the transformation of meta-gabbros into eclogites, through corona reactions such as these, with preserved intrusive contact relationships, igneous textures, structures and mineralogies (Cuthbert & Carswell, 1982). Also, an eclogite in gneisses near the Surnadal syncline exhibits preserved primary igneous mineralogy and structures of gabbro (Tørudbakken & Råheim, 1981).

Experimental work demonstrated that eclogites could be stable at crustal pressures in an anhydrous environment (Yoder & Tilley, 1962; Green & Ringwood, 1967a). The major argument used against the idea of

crustal (in situ) metamorphism of the eclogites is that they occur within almandine-amphibolite gneisses, rather than eclogite facies gneisses as would be expected if the whole terrain had been subjected to eclogite grade metamorphism (Lappin & Smith, 1978). However, it has been shown that there is a definite difference in water fugacity (f_{H_2O}) between the eclogites and the enclosing gneisses (Bryhni et al., 1970; Green & Mysen, 1972) supported by experimental work (Fry & Fyfe, 1969). Carswell (1973b) then suggested a dual origin for these rocks: a crustal metamorphism at high pressures to give 'external' eclogites and tectonic intrusion of ultramafic mantle fragments containing the 'internal' eclogites. The $^{87}Sr/^{86}Sr$ initial ratios from the clinopyroxenes in these rocks supported this hypothesis, with low ratios from the 'internal' and higher ratios from the 'external' eclogites suggesting crustal contamination of the latter (Brueckner, 1977b). It is now considered that the ultramafic rocks and 'internal' eclogites equilibrated to the prevailing crustal high P and T conditions, subsequent to their emplacement (Carswell & Gibb, 1980). More recently it has been shown that the gneisses also contain relics of high-grade assemblages (Krogh, 1980b) suggesting that they too have experienced an eclogite grade metamorphism. However, Rb-Sr whole-rock isotopic studies by Mearns & Lappin (1982b) have shown that this system is undisturbed in the gneisses suggesting that the rocks have not experienced a grade of metamorphism any higher than amphibolite facies.

Further evidence for a crustal origin for eclogites is present in the chemical zoning of the constituent minerals, and particularly so in the garnets; the routine use of the electron microprobe has facilitated the study of these features. The zoning in garnet is usually seen as a decrease in the Fe/Mg ratio from the core to the rim of a grain, often with concomitant decrease in Mn content (e.g. Bryhni & Griffin, 1971). After comparison with the experimental work of Raheim & Green (1974), this has been interpreted as

mineral growth with an increase in temperature, i.e. prograde (Råheim & Green, 1975). It has been noted that garnets often contain inclusions of other phases not present in the matrix of the eclogite, e.g. amphibole (Al-rich, Si-poor, Na-Ca-type), plagioclase, diopside, microcline, biotite and epidote (Bryhni & Griffin, 1971; Krogh, 1980a, 1982; Carswell et al., 1983; Griffin & Qvale, 1981). Towards the rim of the garnet the amphibole inclusions become progressively Al-poorer, Si-richer and more Na-types, whilst omphacitic clinopyroxenes, of compositions equivalent to those of the matrix clinopyroxene, and rutile begin to appear. This zoning of inclusions coincides with the chemical zoning and has been interpreted as the transition from a pre-eclogite amphibolite assemblage to an eclogite assemblage (Krogh, 1982). By contrast, Lappin & Smith (1978) relate these amphibole inclusions to incipient amphibolitisations of the rock. Retrograde zoning can also be found in the garnets, generally restricted to a narrow rim on the grain. These garnets generally contain only eclogite phases as inclusions and it has been suggested that these eclogites have been raised to temperatures $>700^{\circ}\text{C}$ which eradicated any zoning, mineral or chemical through ionic diffusion (Krogh, 1982).

$$\text{The distribution coefficient: } K_D = \frac{(\text{Fe}^{2+}/\text{Mg}^{2+})_{\text{gnt}}}{(\text{Fe}^{2+}/\text{Mg}^{2+})_{\text{cpx}}},$$

calibrated by Råheim & Green (1974) and Ellis & Green (1979) has been used on the coexisting garnet and clinopyroxene from numerous eclogites in the region in an attempt to elucidate their conditions of formation. The K_D values from these eclogites have been found to follow a consistent pattern across the region, and consequently so do the calculated temperatures of equilibration (Krogh, 1977) (see Fig. 1.3). The calculated temperature and pressure values define a gradient of about 200°C across the region with the lowest values around Sunnfjord ($\sim 500^{\circ}\text{C}$ and $\sim 10\text{-}12$ kbar) and the highest

FIG. 1.3

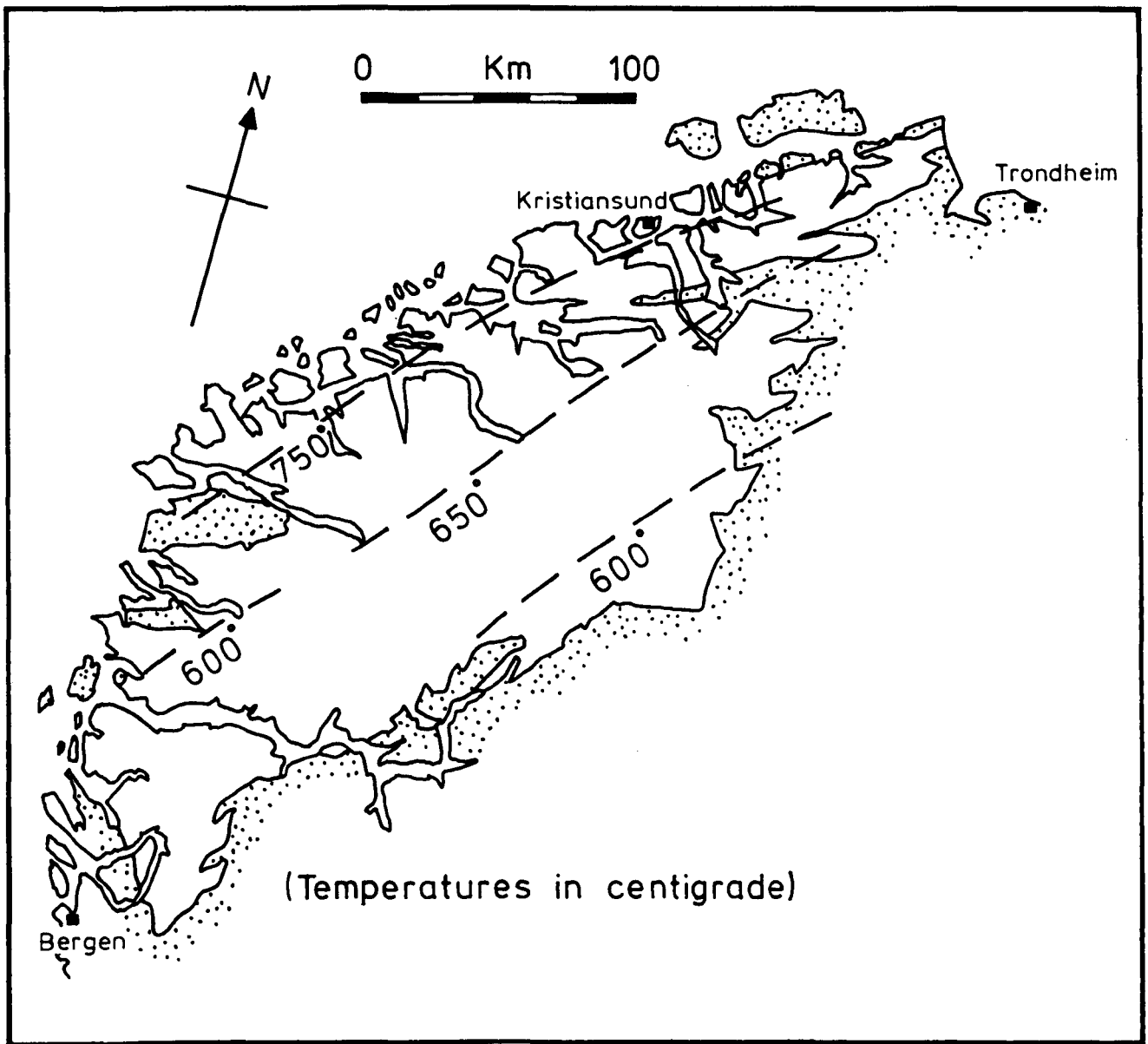


FIG. 1.3 Isotherms of equilibration temperatures for eclogites and granulites in the Basal Gneiss Complex (after Griffin et al., 1983).

along the coast of Møre og Romsdal ($\sim 800^{\circ}\text{C}$ and $\sim 18\text{--}20$ kbar) (Griffin et al., 1983). Krogh (1977) interpreted this gradient as the result of the underthrusting of the Baltic crustal plate, beneath that of Greenland, during a continent-continent collision in the Precambrian. The maximum P-T conditions lie at the deepest part of the underthrust unit. Such a scenario of continent-continent collision has also been suggested by other workers (Griffin et al., 1983; Cuthbert et al., 1983) with the event occurring during the Caledonian orogeny.

Many eclogites show varying degrees of retrogression. Initially the clinopyroxene develops a diopside + plagioclase symplectite texture in response to a decrease in the prevailing pressure (discussed by Mysen & Griffin, 1973). This diopside is subsequently hydrated to an amphibole whilst the garnet produces an amphibole or biotite as the eclogite is progressively down-graded, firstly to a granulite-facies assemblage, then to an amphibolite-facies assemblage. P-T conditions for the former have been calculated as $\sim 700\text{--}750^{\circ}\text{C}$ and 8-13 kbar (Krogh, 1977) suggesting rapid, isothermal, uplift of the subducted terrain. Those for the latter are put at $\sim 600\text{--}700^{\circ}\text{C}$ and 10-13 kbar (Lappin & Smith, 1978). The degree of retrogression between eclogites is very variable and is generally dependent upon the degree of deformation associated with the rock, which develops paths for hydrating fluids. Thus retrogression tends to be found at the contacts between eclogites and the enclosing gneisses, where the difference in rock competence aids deformation; or adjacent to cross-cutting pegmatite dykes, which are themselves fluid-rich. The often incomplete amphibolitisation of eclogites has been attributed to sluggish fluid transport (Heinrich, 1982). The alteration tends to affect the whole-rock chemistry of the rocks, mainly by introducing K^+ , H^+ (Al^{3+}) ions and removing Si^{4+} ions (Lappin, 1962, Bryhni et al., 1969).

A fluid phase may also have a part in the development of the anhydrous assemblage of the eclogite, although this appears to be a contradiction in terms. Both Bryhni et al. (1970) and Green & Mysen (1972) have suggested that partial melting, at the time of metamorphic maximum in the gneisses surrounding an eclogite would tend to draw water away from the eclogite thereby assisting its dehydration. This water would not necessarily be expelled from the gneisses, but would still be available for the subsequent hydration reactions described above. Furthermore, Glassley (1982) has demonstrated that as the SiO_2 content of this fluid decreases, the eclogite assemblage becomes stable at progressively lower pressures.

The absolute dating of eclogites is difficult due to common disequilibrium of the isotope systems in high-grade rocks and the lack of geologic controls. The low Rb contents of the rocks, giving low Rb/Sr ratios, does not allow the use of that system on whole rocks although it is possible on the constituent minerals. Both the K-Ar and ^{40}Ar - ^{39}Ar methods suffer from the problem of excess Argon, whilst the U-Pb method on zircon often gives inconclusive results (Hunziker, 1982). McDougall & Green (1964) dated the micas from bodies in Nordfjord and obtained an age of ~ 400 m.y. They also used K-Ar on amphiboles and micas and obtained ages of ~ 1800 m.y., 1150-950 m.y. and ~ 400 m.y., i.e. Svecofennian, Sveco-norwegian and Caledonian respectively. However, they concluded that many of the ages might be unreliable due to excess Ar in the minerals. Mysen & Heier (1972) dated gneisses at Hareid at 1646 ± 70 m.y. and related this to a metamorphic event which was assumed to have also affected the enclosed eclogites. Krogh et al. (1974) used U-Pb on zircons from the Ulsteinvik eclogite at Hareidland and obtained ages between 400 and 600 m.y. From these early studies no clear picture of the history of these rocks emerged, presumably due to the sensitivity of their isotopic systems to disturbances.

Griffin & Brueckner (1980) attempted to resolve these problems by utilising the Sm-Nd isotopic system which they considered to be resistant to metamorphic effects short of total recrystallisation. The ages obtained are internally consistent, between samples, with fairly low errors. This new isotopic evidence indicates that:

- (i) the rocks crystallised at ~ 425 m.y. ago (i.e. during the Caledonian orogeny);
- (ii) the protoliths separated from the mantle long before the Caledonian orogeny;
- (iii) the protoliths were of a wide range of compositions;
- (iv) the protoliths were probably exposed to the effects of the Svecofennian and Sveconorwegian orogenies.

From further work Griffin & Brueckner (1982) have found difficulty in obtaining meaningful Sm-Nd ages from eclogites which equilibrated at temperatures $> 700^{\circ}\text{C}$ due to disequilibrium between garnet and clinopyroxene. They obtained a Rb-Sr mineral age of 398 ± 1 m.y. with an I.R. of 0.7034 from the Verpeneset eclogite which they interpreted as Caledonian metamorphic age upon a Palaeozoic protoliths. They considered that the Sm-Nd ages previously obtained reflected the time of closure of that isotopic system upon uplift of the crustal unit containing the eclogites, whilst the Rb-Sr ages reflect a later cooling event.

Both Mearns & Lappin (1982) and Gebauer et al. (1982) have presented Caledonian ages for eclogites: 408 ± 8 m.y. (Sm-Nd) for the former, interpreted as a thermal resetting or recrystallisation of Proterozoic material; and ~ 400 m.y. (U-Pb) for the latter, interpreted as an eclogite facies event on Svecofennian or Sveconorwegian protoliths. Krill (1981) dated a gneiss interbanded with eclogite-bearing micaschists of the Blåhø group at Oppdal as 583 ± 60 m.y.

This prevalence of Caledonian ages from eclogites suggested that the metamorphism of that time was of a high grade (Griffin & Brueckner, 1980). As radiometric ages from the Basal Gneisses had tended to reveal Caledonian ages only from the mineral isochrons (see Table 1.3). This was interpreted as indicating that the Caledonian metamorphic event was one of only minor re-heating, otherwise the whole-rock isotopic systems would have been more severely disturbed (Pidgeon & Råheim, 1972; Solheim, 1980). Krill & Griffin (1981) have discussed this point and have compared the situation with that in the Alps where older Rb-Sr whole-rock systems have been shown to survive subsequent intense metamorphism and deformation. Furthermore, the severity of the Caledonian metamorphism is reflected in the mineral ages from pegmatites which cut eclogites, indicating temperatures sufficient for anatexis (Griffin et al., 1983).

One difficulty encountered with assigning an eclogite forming event to the Caledonian orogeny was that it required the surrounding gneisses to suffer both prograde and retrograde reactions during a relatively short space of time: ~75 m.y. However, Cuthbert et al. (1983) have demonstrated that this was perfectly feasible by effectively doubling the thickness of the crust during a continent-continent collision. This thickness of material gave both the pressure to realise eclogite grade conditions and the buoyancy for the subsequent, and necessary rapid uplift, of the rocks.

1.3. PREVIOUS WORK IN THE MOLDEFJORD AREA

At first, only one aspect of the geology here was of note, presumably for economic reasons: the marble deposits at Trerrfjella (see Map B). Vogt (1896), Bugge (1905) and Holtedahl (1953) described these rocks at Talstad, Nås and Visnes noting their purity and their relationship to the adjacent hornblende gneisses.

The islands in Moldefjord (Bolsøy, Saeterøy and Hjertøy) were also of particular interest. First mapped by Bugge (1934) as greenschists they were correlated with the Ordovician rocks in the Surnadal synform to the NE. Gjelsvik (1951) also referred to the rocks as greenschists and considered them to be derived from basalts, subsequent granitisation of which gave rise to the gneisses to the south. Hernes (1954a) also studied the rocks there, and in the S side of Fannefjord; he reiterated much of what Gjelsvik had said and again presumed the rocks to be derived from lavas/volcanics with sediments appearing as limestones and quartzites. Although Hernes calls the rocks greenschists, the mineral assemblages he gives (plag (An 35) + qtz + epidote + bi + gnt (66% almandine) ± musc ± pyrite ± apatite ± kspar) for the mica-schist and (hb + plag (An 40) ± qtz ± epidote ± pyrite ± kspar) for the greenschist seem to be more indicative of amphibolite facies (Turner, 1968, p. 308).

Hernes (1954b) also made a particular study of the meta-basic rock on Tverrfjella, concluding it was a large, retrograded, eclogite skarn containing marble, resulting from reactions between the marble and the surrounding gneisses. Vogt (1896) recorded the presence of this body as: "eclogite near marble". Eskola (1921) analysed the garnets from this body and considered it to be true eclogite but without any genetic connection with the marble.

As mentioned previously, Hernes (1955, 1967) made a preliminary geological survey of the area; the lithologies examined in the present study lie in his Frei Group (see Table 1.2). Råheim (1972) expanded upon Hernes' work and recognised two phases of folding: f_1 giving strong planar and linear structures, erasing all earlier events, and f_2 , folding f_1 . Included in f_1 were large ENE-WSW trending structures such as the Molde-Tingvoll Syncline (the SW extension of the Surnadal Synform) and the Halså anticlinorium (Hernes, 1965).

Carswell (1968b, 1973b) has studied the peridotites at Ugelvik on Otrøy and the enclosed garnet-websterite lens (Carswell et al., 1982), concluding that it represents a body from the upper mantle which has re-equilibrated to the prevailing P-T conditions when it was emplaced into the lower crust. Carswell (1973a) also looked at the country-rock gneisses and considered that it was possible to divide the Frei Group into eclogite-bearing and eclogite-free portions, the former being true basement and the latter the Caledonian aged cover which had been deposited on the basement and folded with it. Griffin & Carswell (1983) have also investigated an eclogite at Litledigerneset, on Midøy, which has been veined by the enclosing gneisses. These veins contain the assemblage: omphacitic cpx + gnt + kspar + plag + qtz + bi ± ky. The vein/gneiss/eclogite relations suggest that the veins originated before, or during the eclogite grade metamorphism and that all three were metamorphosed in situ.

1.4. AIMS OF THIS STUDY

From the foregoing introduction it can be seen that the elucidation of the geology in W Norway is still at an early stage. Several complications arise here: the growth of the terrain has been over an extended period of time, from at least 1800 m.y. to about 400 m.y. ago, with often very similar lithologies appearing at different times. The intimate mixing of these lithologies by three orogenic periods, coupled with migmatization, has confused the situation further. This lithological convergence makes the application of stratigraphical sequencing, as done by Hernes and Råheim, rather questionable. Unfortunately, the application of radiometric dating has only partially clarified the situation by setting time limits for major events: the successive overprinting of such events can obscure the original age of a lithology. Although it is

undoubtedly a powerful tool in geology, its often rather arbitrary use appears to give rise to 'errorchrons', i.e. a good-fitting isochron which, in fact, gives a spurious age. Such lines can arise for several reasons: 'open-system' behaviour of the rock during metamorphism with the loss or gain of isotopes; excess Ar; improper sampling techniques, i.e. over a too large an area, or from disparate rock-types which superficially appear to be the same lithology.

The purpose of this research project was to provide information from a relatively unexplored area of the Basal Gneisses to further the understanding of the Region as a whole. Two specific problems were tackled: firstly to try and clarify the tectono-stratigraphy of the southern part of the area, especially the nature of the 'basement'-'cover' contact, if it existed at all. To this end, geochemistry, allied with a Rb-Sr dating program was applied. Secondly, a study of the eclogite bodies, especially that at Trerrfjella, this was of special interest because of its apparent intimate relationship with the extensive marble deposits. Mineral chemical work would allow the calculation of pressure and temperature estimates of their formation, which would perhaps resolve a major controversy over their mode of origin.

CHAPTER 2

GENERAL GEOLOGY AND STRUCTURES

Following the introduction, the lithological units, dealt with in the succeeding chapters, will be briefly described followed by a discussion of the rock structures. Petrologic terms relating to migmatites are from Mehnert (1969) whilst those for cataclastic rocks are from Higgins (1971).

2.1 INTRODUCTION

The area of this study covers approximately 270 km² of the Molde Peninsula situated in the county of Møre og Romsdal (62° 52' N, 7° W), between Moldefjord to the south and the lakes of Langvatnet and Nåsvatnet to the north including the island of Bolsøy to the south (see Map A). The area is covered by sheets 1220/I, II and III, and 1320/III and IV of the M711 series 1:50,000. Mapping was done on the 1:20,000 'Okonomisk' series maps with some of the larger structures derived from aerial photographs, supplied by Fjellanger Widerøe A/S.

The terrain is fairly mountainous and can be divided into two topographic parts. Rising to about 600 m the well rounded hills of the southern part give the impression of a plateau-like surface, whilst those of the northern part are more peaked and lofty, rising to about 900 m. These differences appear to reflect the differing rock-types present in the two parts. The two are separated by the valley of Fraeneidet, one of a series of NE-SW trending glacial valleys which transect the region and include Moldefjord; the development of these features seems to be partly controlled by the strike direction of the rocks. Within Moldefjord are the low-lying, elongate islands of Bolsøy, Saeterøy and Hjertøy, beyond, to the south, lie the Romsdal mountains visible as the famous 'Molde Panorama'. A narrow strandflat forms the northern boundary to the area.

The majority of the exposure is at the coast and on the hills above the tree-line, at about 400 m; thanks to the policy of road straightening in Norway these are supplemented by numerous road cuts, which usually supply the better outcrops.

The area has been divided into four geological units on the basis of lithological type and structural pattern. The most northerly unit appears on the Tverrfjella mountains and includes an extensive garnet-granulite/eclogite body with enclosed marbles, capped by a series of heterogeneous amphibolitic and pelitic gneisses. Surrounding this unit on the lower ground is an expanse of heterogeneous, quartzo-feldspathic, migmatitic gneisses, including augen-bearing, banded and unbanded types, as far south as Jendem. Both of these units have fairly flat-lying, NE-dipping, foliations. To the south lies an augen gneiss unit containing massive augen-bearing and augen-free gneisses with more heterogeneous rocks as far south as Mordalsvågen. Here lies a series of well-foliated, steeply dipping, heterogeneous rocks of almandine-amphibolite facies including: amphibolites, pelites, semi-pelites, quartzo-feldspathic rocks and marbles; this unit incorporates the rocks of Bolsøy. Pods of eclogite, and more rarely meta-dolerites, appear in all these units, with the possible exception of Tverrfjella (see Maps A and D).

2.2 STRUCTURE

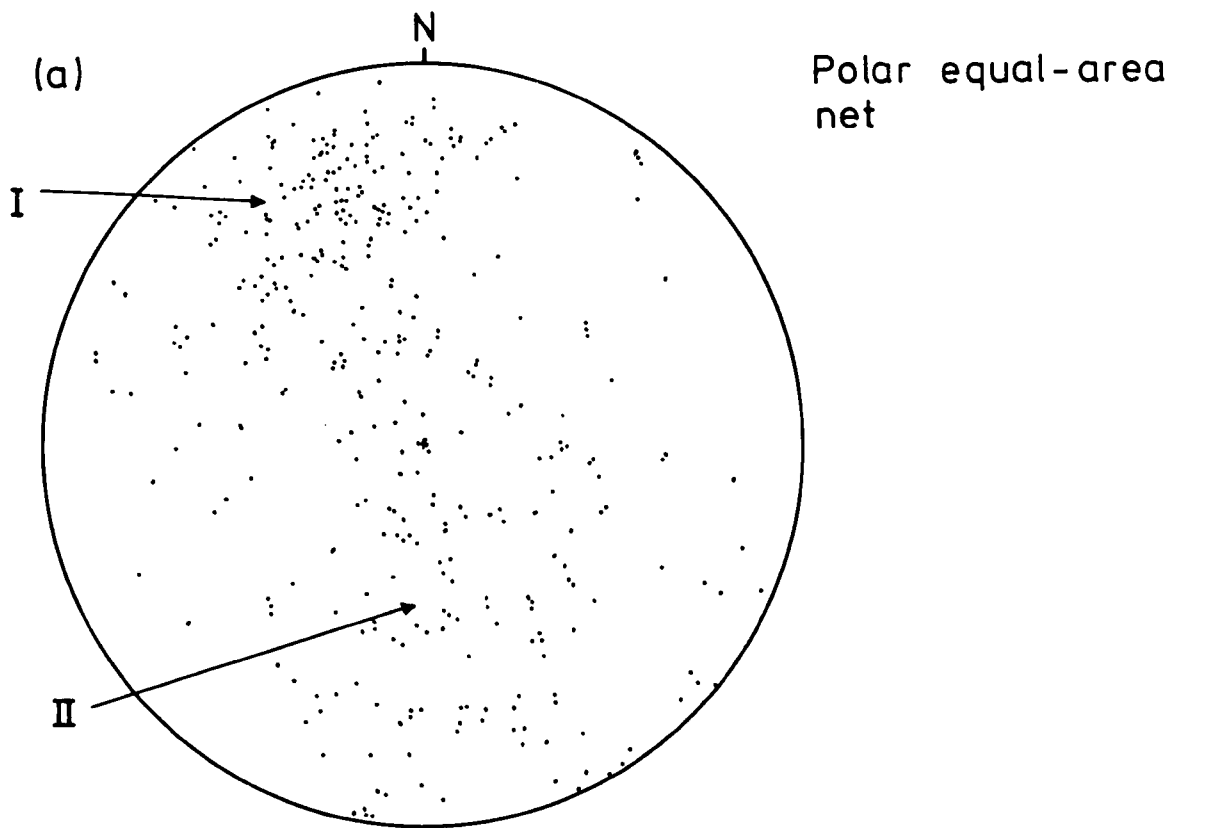
Apart from the dominant foliations throughout the area, sometimes displaying lineations, there are few other rock structures of note. Five structural elements are considered: foliations, lineations, folds (generally as isolated examples), faults (generally inferred from the orientation of pegmatite veins, displacement of rock units or from aerial photographs) and joints.

2.2.1 Foliation

Fig. 2.1(a) shows a stereographic plot of the orientation of poles to foliation planes throughout the mapped area and two maxima are clear: one corresponds to foliations dipping approximately $60^{\circ}/250^{\circ}$ (maximum I), the other to foliations dipping approximately $25^{\circ}/000^{\circ}$ (maximum II). Examined in conjunction with the structural data shown on Map A it can be seen that maximum I represents the dominant steeply dipping foliation along the Moldefjord coast and on Bolsøy whilst maximum II represents the more gently dipping foliations on and around the Tverrfjella mountains. Removing these two groups of readings from Fig. 2.1(a) and plotting them separately shows the concentrations more clearly (Figs. 2.1(b) and 2.2(a)). This also leaves two residual groups of points (maxima III(i) and (ii) - Fig. 2.2(b)) which can be assigned to the area of high ground between Elnesvågen and a line about 1 km north of Moldefjord where belts of both gently and steeply dipping foliation exist.

The rocks which comprise maximum II are mixed, but in general it is difficult to discern good foliation surfaces except in the most pelitic rocks, on Trolltindane, or in the migmatitic rocks on Tverrfjella peak and the lower ground north of Langvatnet. The former are flaggy whilst the latter exhibit a planar fabric in which the neosome lies (see Chapter 5, Plate 5.1(b)). Many of the rocks are massive and have blocky outcrops whilst others have a chaotic structure, especially if amphibolite bands and pods are present (see Chapter 5, Plate 5.1(a)). In the sequence of rocks on the Tverrfjella mountains the foliation is apparently sub-parallel to the banding in the rocks. The lowest unit, the garnet-granulite, generally lacks any fabric and is massive except in steep narrow shear zones striking NE-SW where the rock is converted to green-schist; these appear to be localised manifestations of the dominant

FIG. 2.1



I Moldefjord/Bolsoy sub-area
II Tverrfjella sub-area

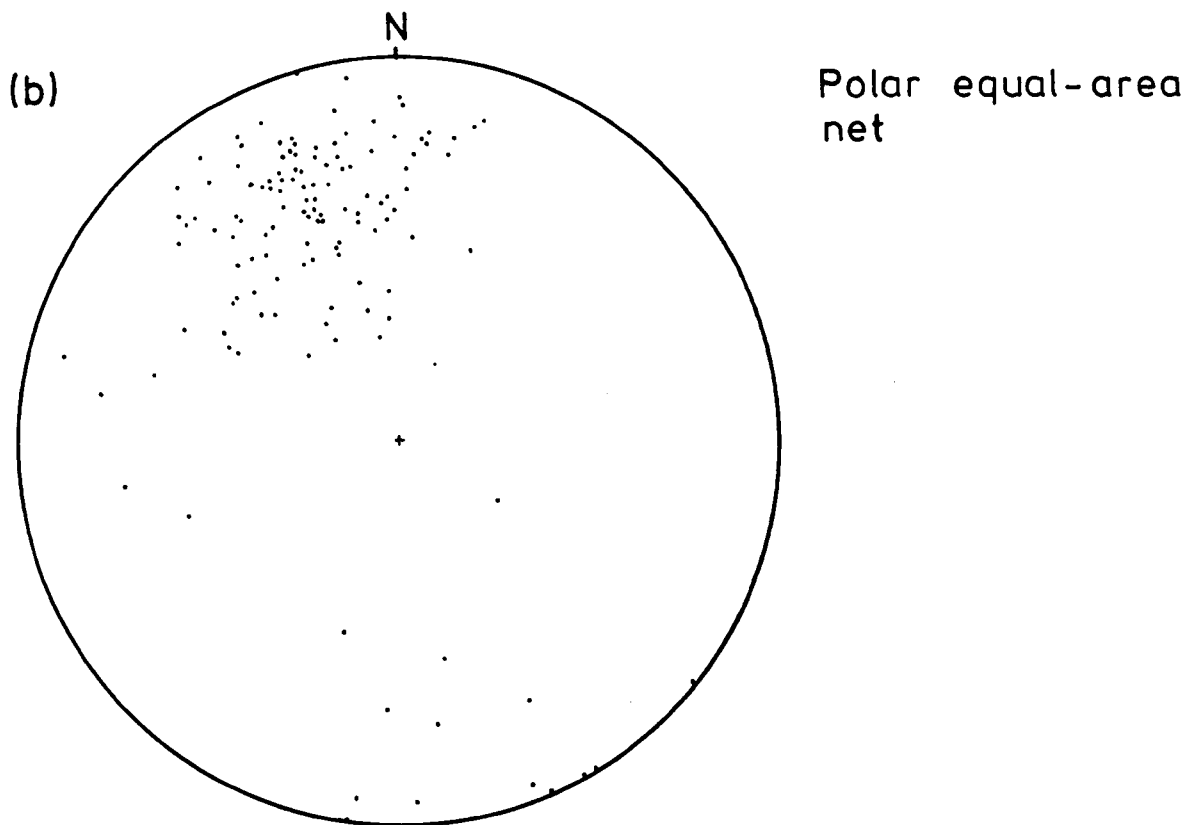


FIG. 2.1 (a) Poles to foliation planes, from throughout the Molde peninsula
(b) Poles to foliation planes, Moldefjord coast and Bolsøy

FIG. 2.2

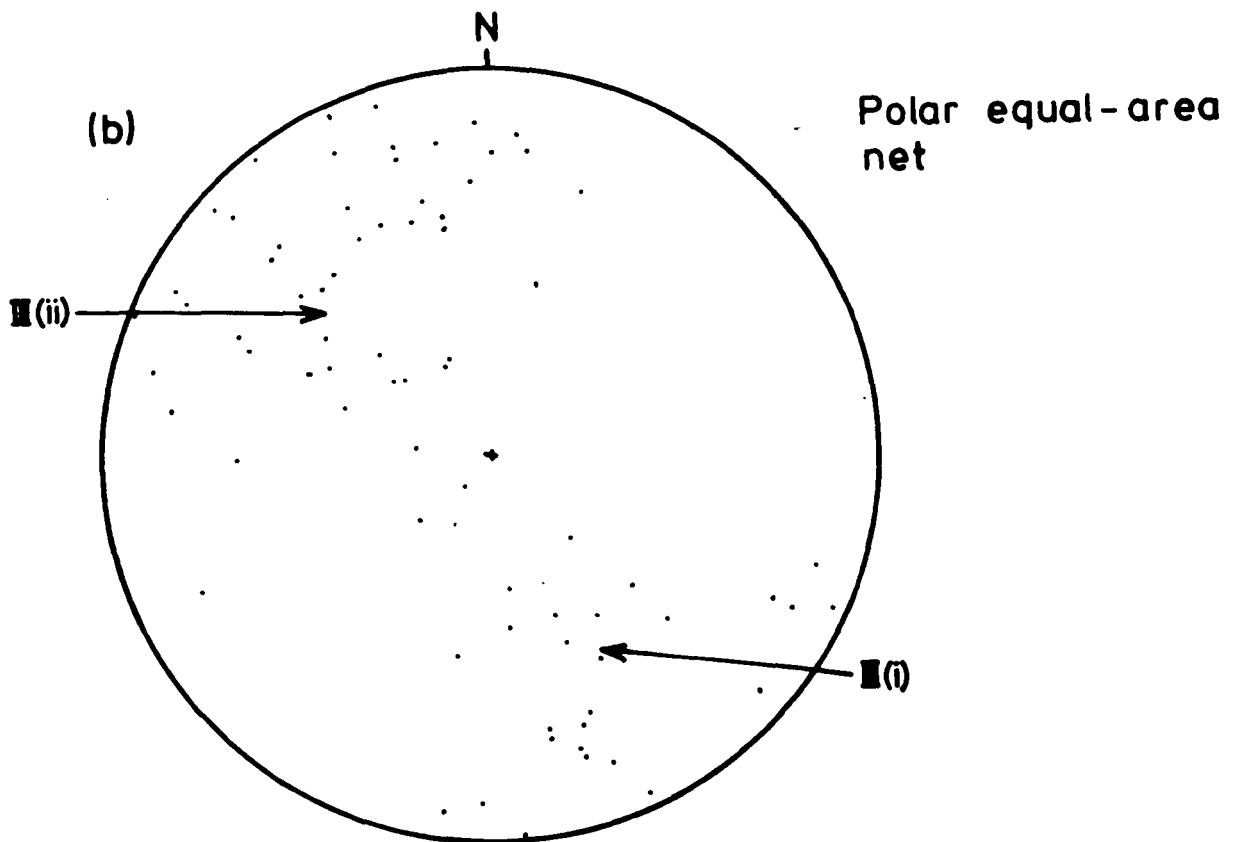
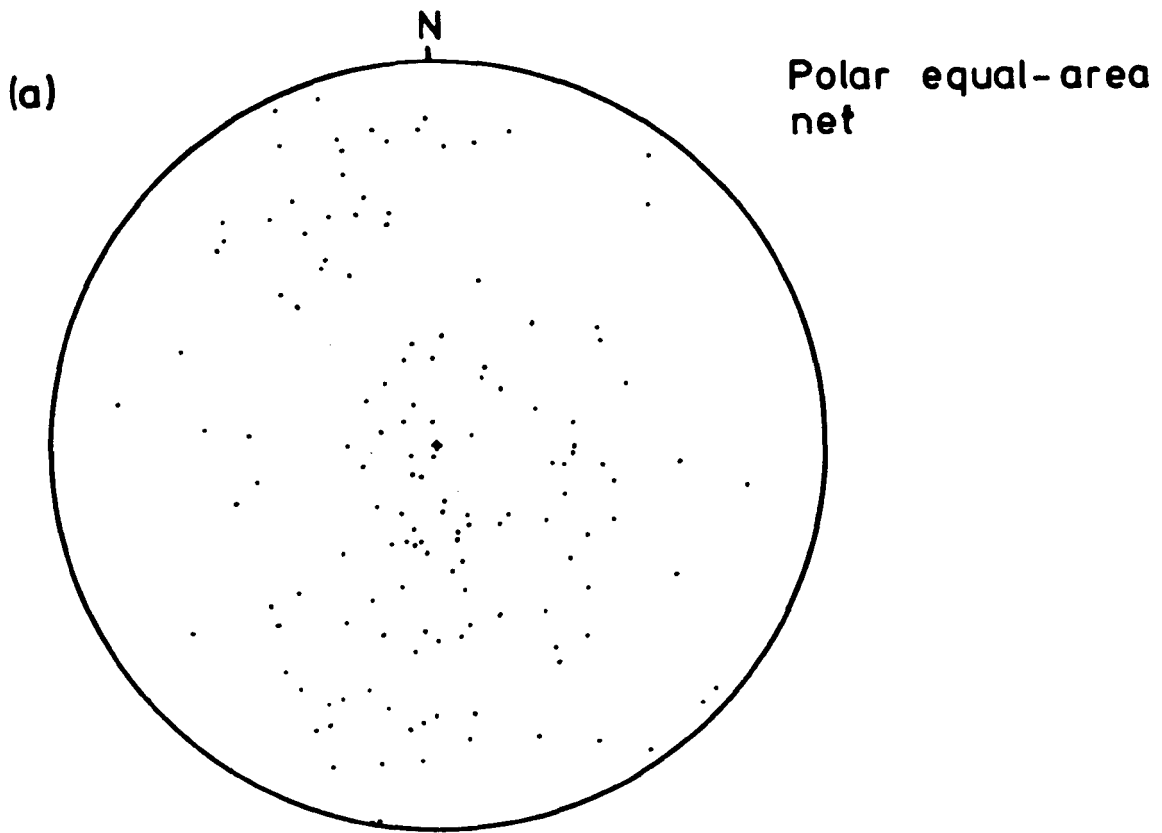


FIG. 2.2 (a) Poles to foliation planes, Tverrfjella
(b) Poles to foliation planes, central sub-area

foliation at Moldefjord. The formation of the secondary fabric can also be seen in many thin sections of the granulite as cracking of the garnet plus related retrogression (see Chapter 3, Plate 3.2(a)). It can also appear in the quartzo-feldspathic rocks as orientations of biotite perpendicular to the lines of garnet denoting the first foliation.

When the granulite is in proximity to the marble any foliation becomes inconsistent in strike suggesting interference from the latter. The distribution of the outcrops of marble as discontinuous lines of large pods (Map B) and the often complex, pygmatic nature of the contacts between the marble and granulite suggests that disruption of originally continuous limestone bands has occurred with concomitant distortion of the surrounding granulite.

The slight spread of points in maximum II (Fig. 2.2(a)) can be attributed to a shallow synclinal structure on Tverrfjella as discerned from the direction of dips on Map B (cf. Gjelsvik, 1953). The axial plane appears to run along the line of peaks although the extension of the structure onto Talstadhesten is doubtful.

The distribution of points in maxima III (i) and (ii) (Fig. 2.2(b)) can be attributed to the appearance of both the flat-lying and steep foliations in the rocks between Malmefjord and Moldefjord, although the steeper structures predominate. The influence of the steeper foliation upon the flatter is best seen in the exposures of the augen gneiss as the augen act as strain indicators. In most cases the foliation is steep, but not particularly pervasive; some intense deformation of the rock has converted it into a monotonous grey gneiss without augen, or ultimately into a mylonite which may be accompanied by faulting (Plate 2.1(a)). Some outcrops exist where the rock is being progressively deformed from flat-lying to steeply foliated (Plate 2.1(b)). The flatter foliation is

difficult to find any further south than Hollingsholm as the steeper structures predominate after this point. The foliations are generally visible on suitable surfaces (i.e. perpendicular to strike), but none of the rocks are sufficiently micaceous to permit any sort of fissility.

The foliation represented by maximum I (Fig. 2.1(b)) is well exposed in the road section of the E62 between Mordal and Molde with steeply dipping, flaggy surfaces (Plate 2.1(c)). The change from the variable foliation in the augen gneiss to this persistent form is remarkably abrupt, over a few tens of metres, and is best seen at Mordal and NE of Varden at Molde. The change appears to be due to a major difference in competence between the massive gneisses and the more mixed rocks to the south. The foliation is continued on the island of Bolsøy and is consistent regardless of the rock-type whether massive quartzo-feldspathic gneiss, amphibolite or pelite. Some of the surfaces exhibit large-scale undulations (√6 m amplitude) particularly around Mek, W of Molde, plunging down-dip and it is considered that these cause the spread of points on Fig. 2.1(b).

2.2.2 Folds

These structures rarely occur in the mapped area, but tend to be more common towards Moldefjord. In general three styles are present: tight intrafolials, similar folds and open folds. The paucity of data did not allow the construction of any meaningful stereographic plots.

The intrafolial folds are relatively common in the heterogeneous rocks at Moldefjord and are interpreted as having been coeval with the formation of the steep foliation there. They are often rootless and can have a monoclinial appearance with one short and one long limb (Plate 2.1(d) and Fig. 2.3(a & b)). These folds can also be found in those portions of the augen gneiss which display belts of steep foliation (Plate 2.1(e) and Fig. 2.3(c, d & e)). The deformation in the augen gneiss appears to have

FIG. 2.3

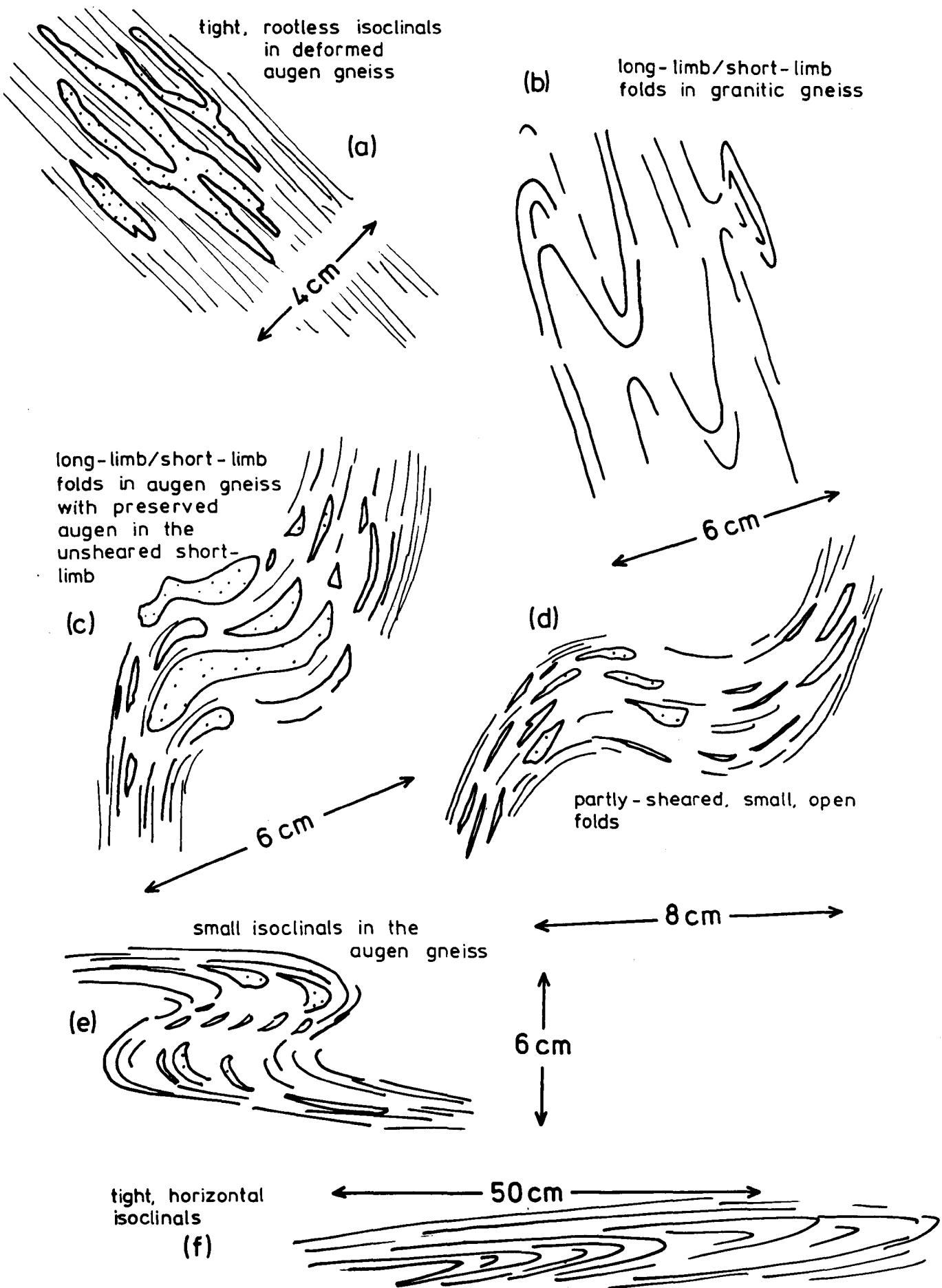


FIG. 2.3 Various fold styles from throughout the Molde peninsula

been rather inhomogeneous since some augen have survived intact, others are severely attenuated and some folds are only partially developed. In some instances this lithology takes on a pseudo-migmatitic appearance (Plate 2.1(e)) and it is thought that the augen became partially mobilised during deformation and congregated in the apices of the folds, the zone of least stress. As deformation proceeded some of these portions became very elongate with the rock taking on the appearance of a migmatitic grey gneiss (Plate 2.1(f)).

These intrafolial folds are very rarely seen N of Malmefjord and then only in steep shear zones but have much the same appearance as those further south (Fig. 2.3(f)).

The folds of similar style appear throughout the area, although those on Tverrfjella appear to be rather more attenuated and elongated than those in the south (compare Plates 2.2(a) and 2.2(b)). Furthermore, those in the north are flat-lying with almost horizontal axial planes whilst those in the south have axial planes sub-parallel to the regional foliation although this is not axial planar to the folds and is in fact folded by them. The folds shown in Plates 2.2(a) and 2.2(b) have been classified using the method of Ramsay (1967, p. 359): that from Tverrfjella is a Class 1C type (between types 2 and 3) whilst that from Moldefjord is a Class 3 but is very close to a type 2 (Fig. 2.4(a & b)). The thickness of the limbs parallel to the axial surface (T_{α}) is not constant in the Tverrfjella fold suggesting elongation of the limbs.

Ramsay (1967, p. 422) has suggested that there are only two possible mechanisms which can account for the formation of such folds: (i) progressive inhomogeneous simple shear, i.e. shear folding (Hobbs, Means & Williams, 1975, p. 185); (ii) a uniform homogeneous strain throughout the region plus a progressive inhomogeneous simple shear.

FIG. 2.4

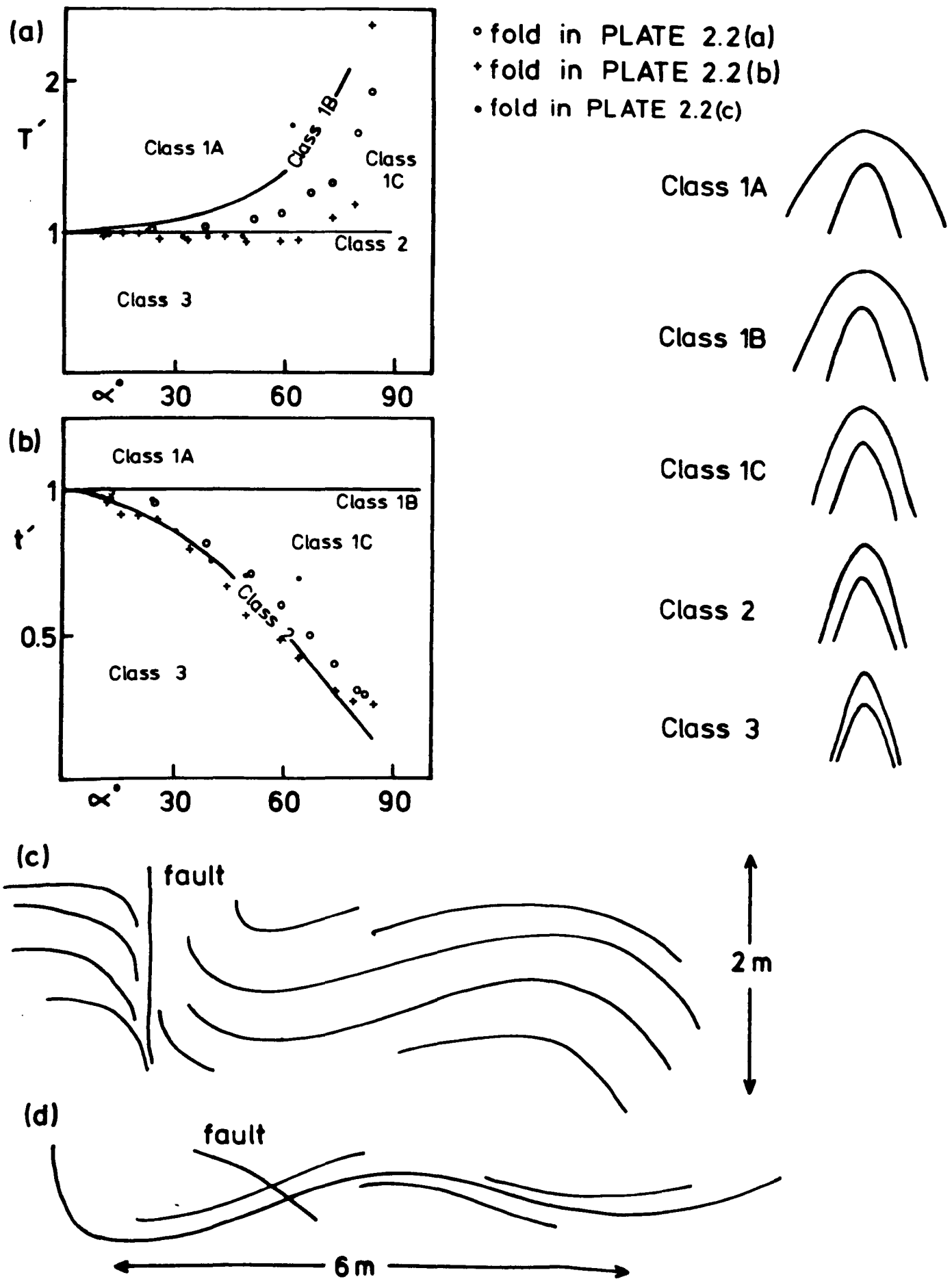


FIG. 2.4 (a) & (b) Fold classification plots (after Ramsay, 1967, p. 366) with the representative forms of each fold class. (c) & (d) Large, open, fold styles from Tverrfjella

Reservations are held over the first of these since it has been criticised as being mechanically unrealistic: Flinn (1962), Ramsay (1967, p. 436), Hudleston (1973).

The second mechanism produces folds of types 1 or 1B ('parallel' - Ramsay, 1967, p. 433 - see Fig. 2.4(a)) by buckling; subsequent 'flattening' (or uniform shortening perpendicular to the axial plane - Ramsay, 1967, p. 412; Hudleston, 1973) produces the similar fold, the greater the amount of 'flattening' the closer the fold style approaches that of type 2. However, it has been noted that the most common fold styles produced by this mechanism are of type 3 or Class 1C, both very close to type 2 (Hudleston, 1973) the very types found in the mapped area. Therefore it is suggested that these folds have been formed by this mechanism and that those at Moldefjord have perhaps undergone greater amounts of flattening than those elsewhere (thereby attaining a form closer to type 2) being proximal to the intensely flattened fabric. Even so the limbs of these folds still reflect vestigial parallelism with variable thickness T_{α} as reflected on Fig. 2.4(a) by the upward curving of the T_{α} trace, as given by parallel folds.

The folds at Tverrfjella also appear to have undergone a certain amount of 'flattening' (the curve in Fig. 2.4(a) approaches the type 2 form but is still upward curving) but are flat-lying which suggests that both the buckling and 'flattening' processes have had different orientations to those at Moldefjord. It seems unlikely that the structures seen at Tverrfjella have been reoriented to a more upright position at Moldefjord by the imposition of the steeper structure since it is this steep foliation which is involved in the more upright folds. Furthermore, the prevalence of intrafolial folds in the steeper foliation and their relative lack at Tverrfjella suggests that this steeper foliation is not

simply a reorientation of the Tverrfjella foliation, but the product of a new stress field. The appearance of folds similar in style in the two places would appear to be fortuitous, although of course both are very close to being Class 1C, the most common type.

Folds which approximate to type 2 are generally found in the central parts of orogenic belts with regional folding and metamorphism, the zones of crust affected being very ductile during deformation and residing at considerable depth (Ramsay, 1967, p. 421). This is in keeping with the grades of metamorphism seen in the deformed rocks (see Table 2.2).

Rather more open folds are also present at Moldefjord with a more parallel form (i.e. type 1 or 1B) and generally larger than the others (Plate 2.2(c)). These are rare and appear to be in two mutually perpendicular directions as seen at Hjellvika, they generally have vertical axial planes which strike approximately E-W and N-S. This type of fold is not seen at Tverrfjella, although a fold style occurs there which is not seen further south. These are open in style and large with vertical axial planes striking approximately N-S, they are characterised by one steep limb often sheared or faulted (Fig. 2.4 (c & d)). The presence of this faulted limb and the general open nature of the folds suggests folding at higher crustal levels and a resultant transition from ductile to brittle behaviour in the rocks (cf. Råheim, 1972 - at Kristiansund).

The folds described here are very similar to those documented by Løset (1977) at Surnadal on strike to the NE, he noted three phases with axial planes trending approximately E-W:

- (i) f_1 isoclinal;
- (ii) f_2 flattened flexural-slip folds;
- (iii) f_3 very open with vertical axial planes;

he included the Surnadal syncline with the f_1 phase. The similarity and

geographical proximity between these structures and those seen at Moldefjord suggests that they were formed by the same stress field. Hernes (1956(a & b)) showed the Surnadal syncline extending into Fannefjord where he termed it the Molde-Tingvoll syncline, and it would seem reasonable to extend it further SW onto the islands in Moldefjord although there is no repetition of rocks there to confirm this. This possibility arises from: the similarity between the rocks on Bolsøy/Fannefjord and Surnadal (see Fig. 2.5 - cf. Strand, 1953) and the existence of apparently complimentary large-scale structures to the NW on the Molde peninsula. One of these is considered to be the shallow synclinal structure on Tverrfjella (referred to in section 2.2.1), the other the Halså anticlinorium (Hernes, 1965 - shown on Fig. 1 of Råheim, 1972), the axes of these folds are shown on Map A. In addition, Hernes (1965) locates a further synclinal structure running parallel to the coast and through the Devonian-aged deposits there. The existence of a large synclinal structure in Moldefjord suggests that the steep foliation there forms the limbs of such a fold and may be axial planar to it signifying a coeval formation (cf. Løset, 1977).

Plate 2.2(d) shows one of the almost recumbent similar folds on Tverrfjella which exhibits gentle undulatory folds on the upper limb, these have axial planes parallel to the Tverrfjella syncline and are interpreted as being part of the same deformation event confirming that the folds at Tverrfjella preceded those at Moldefjord.

2.2.3 Lineations

The origin of lineations on rock surfaces has been the subject of much debate (Phillips, 1937; Anderson, 1948; Kvale, 1953; Hooper, 1968) since it was considered that 'a' and 'b' lineations were formed by different processes; Fig. 2.6(a) shows the supposed relationships of the

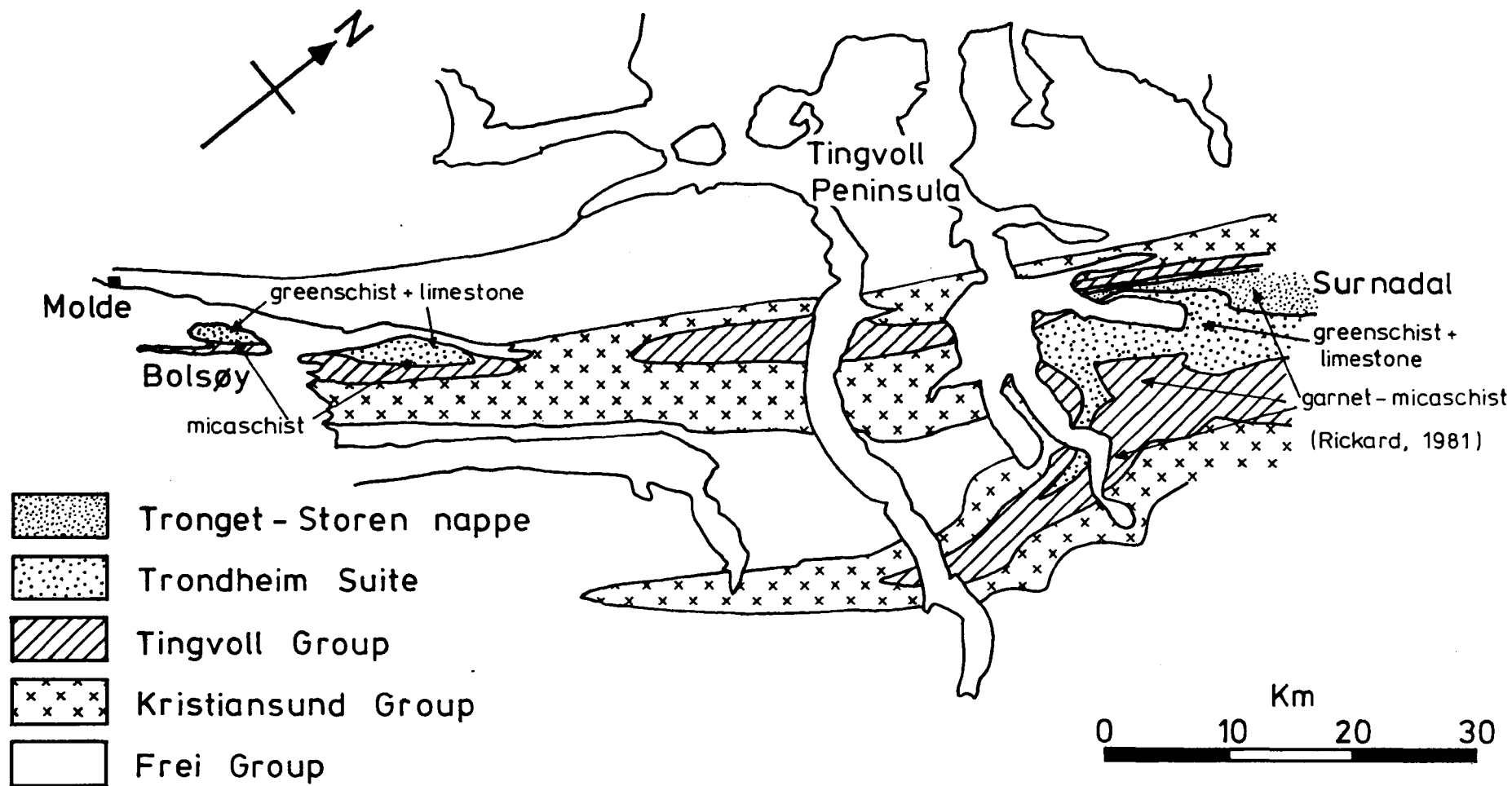


FIG. 2.5

FIG. 2.5 Simplified geological map of the fold structures between Moldefjord and Tingvoll (after Hernes, 1955 and Råheim, 1972), showing the lithological similarities between the two areas.

FIG. 2.6

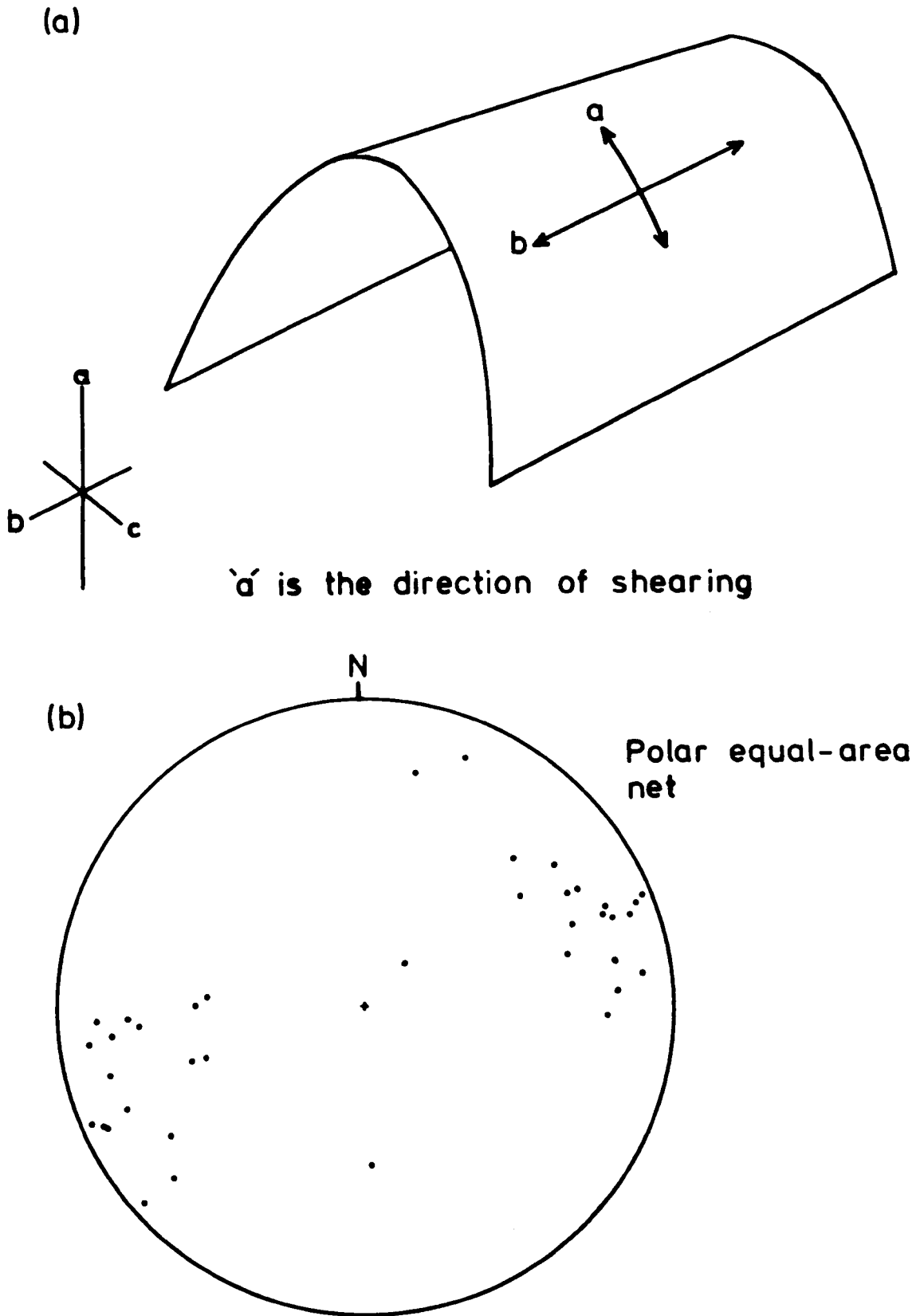


FIG. 2.6(a) Schematic representation of the supposed relationship between lineation directions and the tectonic axes of a fold.
(b) Poles to lineations on foliation planes, from Moldefjord and Bolsøy.

two to folding. However, Ramsay (1960) demonstrated that a lineation could form at any angle to the direction of stress and therefore the terms 'a' and 'b' were not universally applicable.

Fig. 2.6(b) shows a stereographic plot of the lineations throughout the mapped area, the two maxima represent lineations plunging between 10° and 20° in opposite directions. The lineations are non-penetrative being due to mica and hornblende growth, quartz rods, feldspar augen or micro-crenulations. The majority of these are developed in those rocks which have been affected by the imposition of the steeper foliation, i.e. the heterogeneous rocks along Moldefjord and in parts of the augen gneiss (see Plate 2.1(a & b)). It is considered that the spread of points on Fig. 2.6(b) can be attributed to the same large-scale undulations in the foliation which causes the spread of poles to the foliations as seen on Fig. 2.1(b). In an attempt to correct for this spread, each foliation containing a lineation was rotated on a Wulff (equal angle) stereonet to a datum, here 270° , thereby rotating the lineation to a new direction (cf. Phillips, 1971, p. 28). The plot of these reconstructed lineations is given in Fig. 2.7(a) and two compact groups now appear but no longer diametrically opposed, this pattern confirms the field observation of two mutually exclusive lineations (see Map A along Moldefjord coast). There could be two explanations for this division: the direction of stretching may not have been consistent during deformation or there has been folding subsequent to the lineation-formation. It is considered that the first possibility would produce a more random plot of the resulting lineations than is seen. The second possibility seems to be the more likely from the appearance of near-upright similar folds affecting the foliation at Moldefjord (see section 2.2.2). The hinges of these folds are rarely exposed which would explain the lack of data points between the two maxima,

FIG. 2.7

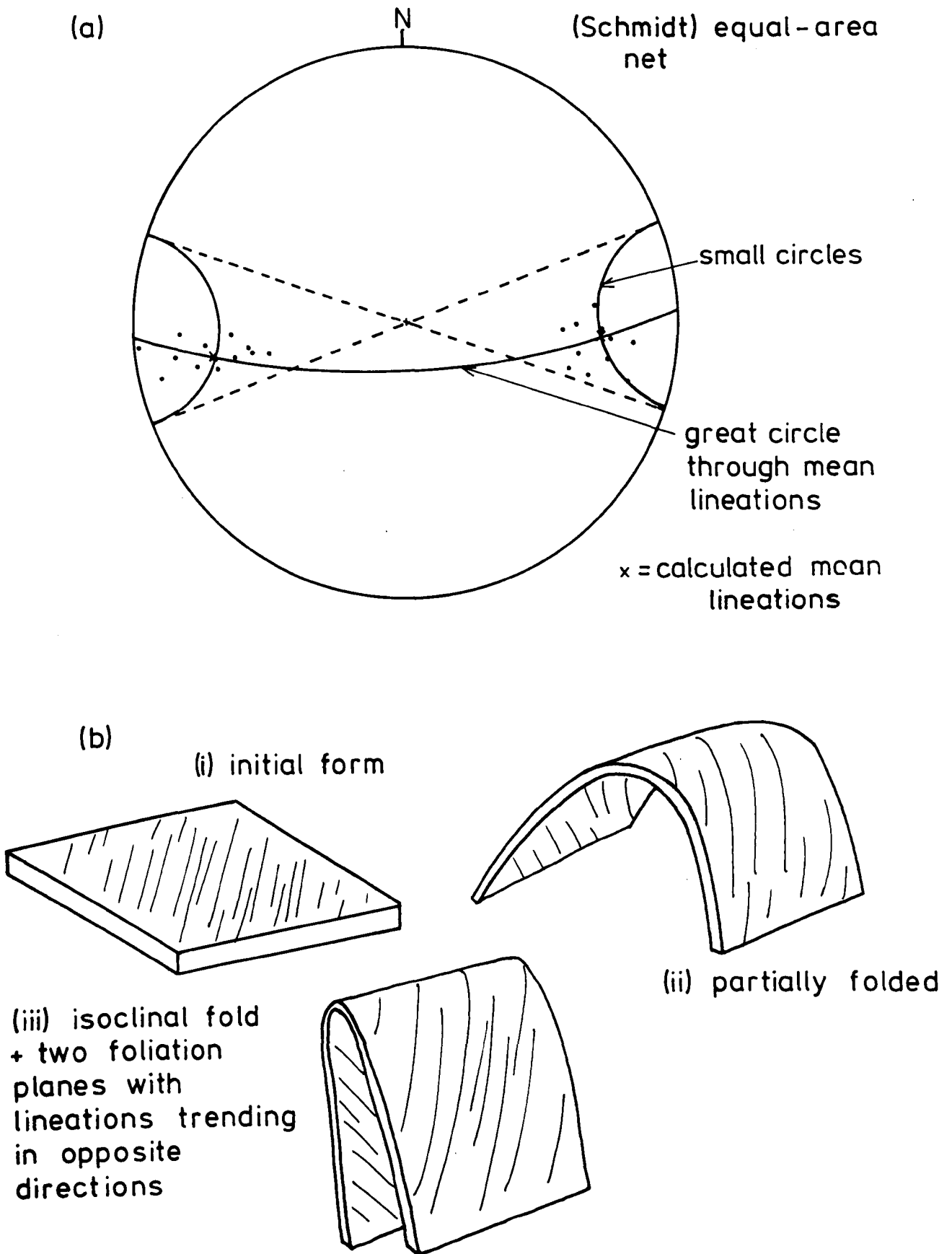


FIG. 2.7 (a) Method of unfolding the near-upright similar folds and resultant re-orientation of the contained lineations
(b) Diagrammatic representation of the development of the near-upright similar folds and resultant re-orientation of the contained lineation.

which then represent the lineations observed on the fold limbs. In addition, it was considered that the appearance of these two sets of lineations could be due to the effects of erosion upon these folds, such that it was purely arbitrary as to which limb and hence which lineation would be exposed (see Fig. 2.7(b)). To test this possibility, a stereographic construction was employed which allowed the unfolding of these similar folds. Theoretically, as the limbs of the folds are rotated to the horizontal (i.e. zero dip) the poles to the lineations should move to the primitive, 180° opposite, i.e. the same pole (Phillips, 1970, p. 61; Ramsay, 1967, p. 487). Initially, the mean pole for the lineations was calculated using the methods outlined in Ramsay (1967, p. 15) by computing the vectors for each pole and obtaining the mean vector from the sum of these. This was done on an equal-area stereonet (Schmidt net) to remove any angular discrepancies. The mean pole to the foliations bearing these lineations was also calculated, using the same method, and is shown in Fig. 2.7(a) with its corresponding great circle trace which passes very close to the two mean lineation poles confirming that the calculation method is correct. Since the limbs of the folds are ostensibly parallel, the representation of these folds by one plane on the stereonet seems permissible. When these planes are rotated to the horizontal the poles to the mean lineations do indeed move along the small circles to the primitive and lie opposite each other as expected (Fig. 2.7(a)). As the lineations had formerly been reoriented to a datum the direction of this unfolded structure is now meaningless, however it does show that the lineation preceded the imposition of the similar folds at Moldefjord and its formation was probably coeval with the development of the steep foliation there. The reorientation of a lineation in this manner by folding has also been noted by Løset (1977) in rocks to the NE at Surnadal where the rock structures are very similar (see section 2.2.2).

A lineation of a very different type can also be found in the rocks along Moldefjord as the orientation and alignment of pods of eclogite, lines of which can be traced for some distance along strike at favourable exposures, notably Julaksla Hill. From about Jendem northwards these pods become increasingly less well aligned and 'zones' of apparently randomly distributed pods are more typical, e.g. N coast of Vagøy (see Chapter 7; Plate 7.1(b)). Thus it would appear that the lineations of pods towards the S of the area is the result of the imposition of the steep foliation there.

2.2.4 Faults and Joints

The positions of most of these structures have been inferred from the aerial photographs, are shown on Map D, and fall into three groups: foliation surfaces exposed on the ground, large joints and faults. Some photo-cover was lacking over Bolsøy and Vagøy and most structures are only visible on the vegetation-free hill tops.

The profusion of approximately E-W trending structures in the southern part of the area is interpreted as the outcropping of the dominant steep foliation there which also gives rise to a number of similarly trending valleys particularly around Varden.

Cutting across these are a number of NE-SW trending lines which are interpreted as faults and which are often occupied by streams and/or lakes. The rocks at the outlet of Haukebølva are very disrupted and jointed, with much epidote mineral fill, indicative of rock brecciation and faulting. This fault in particular appears to be a fairly major structure, extending for ~10 km between Moldefjord and Malmefjord, furthermore it displaces lithological boundaries in a sinistral manner (see Map A).

The more infrequent NW-SE trending lineaments also appear to be faults from the examples seen on Julneset point which displace rock units and exposes rock surfaces exhibiting slickensides and epidote mineral fill.

The number of lineaments decreases dramatically in the rocks N of Malmefjord but these two dominant directions are still present. The E-W trending lines present here occur mainly in the areas of migmatitic gneiss and are almost totally absent on the Tverrfjella mountains suggesting that the latter rocks behaved in a more competent manner, a possibility partly supported by the field evidence which shows the garnet granulite to be profusely jointed.

The lineament running through Børresdalen is a major fault line with several displacements visible on the col at the head of the valley resulting in severe disturbance of the garnet-granulite with much pegmatite veining and concomitant rock hydration. Several faults also exist in the vicinity of Helvatnet. From the absence of the metasedimentary group on Talstadhesten, its restricted occurrence towards the E end of the mountains, and the displacement of the line of large marble bodies running through the garnet-granulite the relative movements of these major faults is postulated as shown in Fig. 2.8. The greater thickness of garnet granulite on Talstadhesten, compared to the remainder of the mountains suggests a wedge-shape for this rock unit, thickening southwards.

Jointing is abundant throughout the area and some of the larger, master joints may be visible on the aerial photographs; once again these are more profuse in the rocks towards Moldefjord (Plate 2.2(e)). The structures are often filled with clinozoisite, or more rarely hornblende, and are likely to be dilation joints. Some are probably related to the major fold structures, particularly the Halså anticlinorium, formed by extension on the fold crests (Hobbs, Means & Williams, 1976, p. 294); others may be pinnate joints directly related to the faulting (Hobbs, Means & Williams, 1976, p. 294).

The dominant strike directions of several faults and joints have been plotted in a rose-diagram (Fig. 2.9(a)) and display two dominant

FIG. 2.8

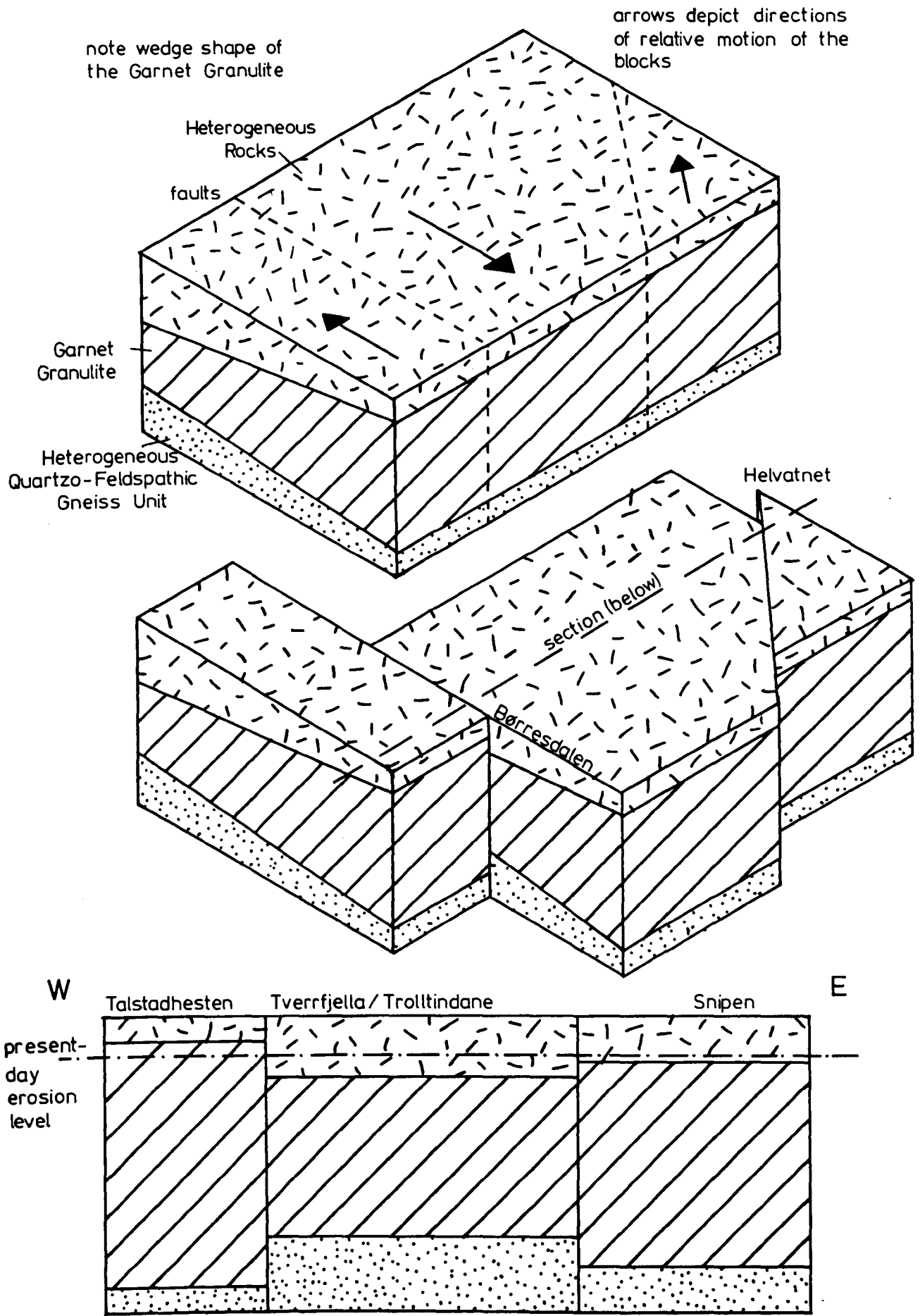
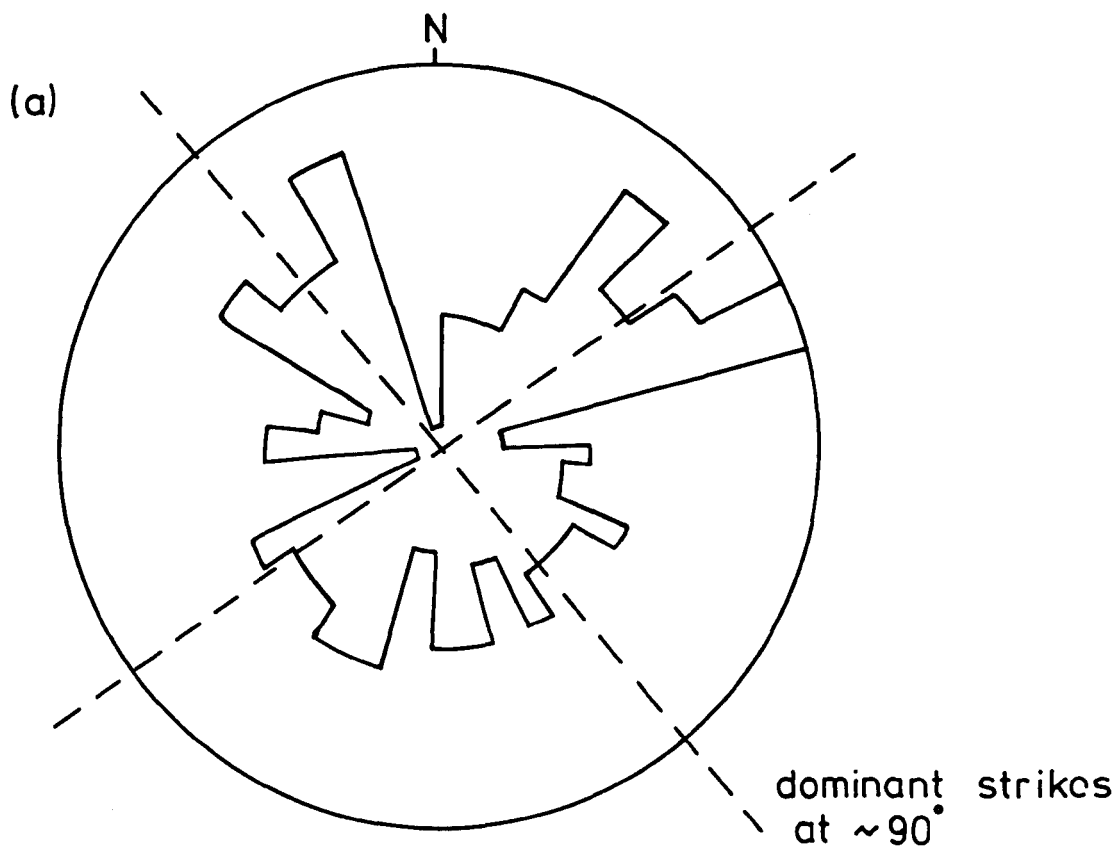


FIG. 2.8 Diagrammatic representation of the large-scale faulting at Tverrfjella.

FIG. 2.9



(b)

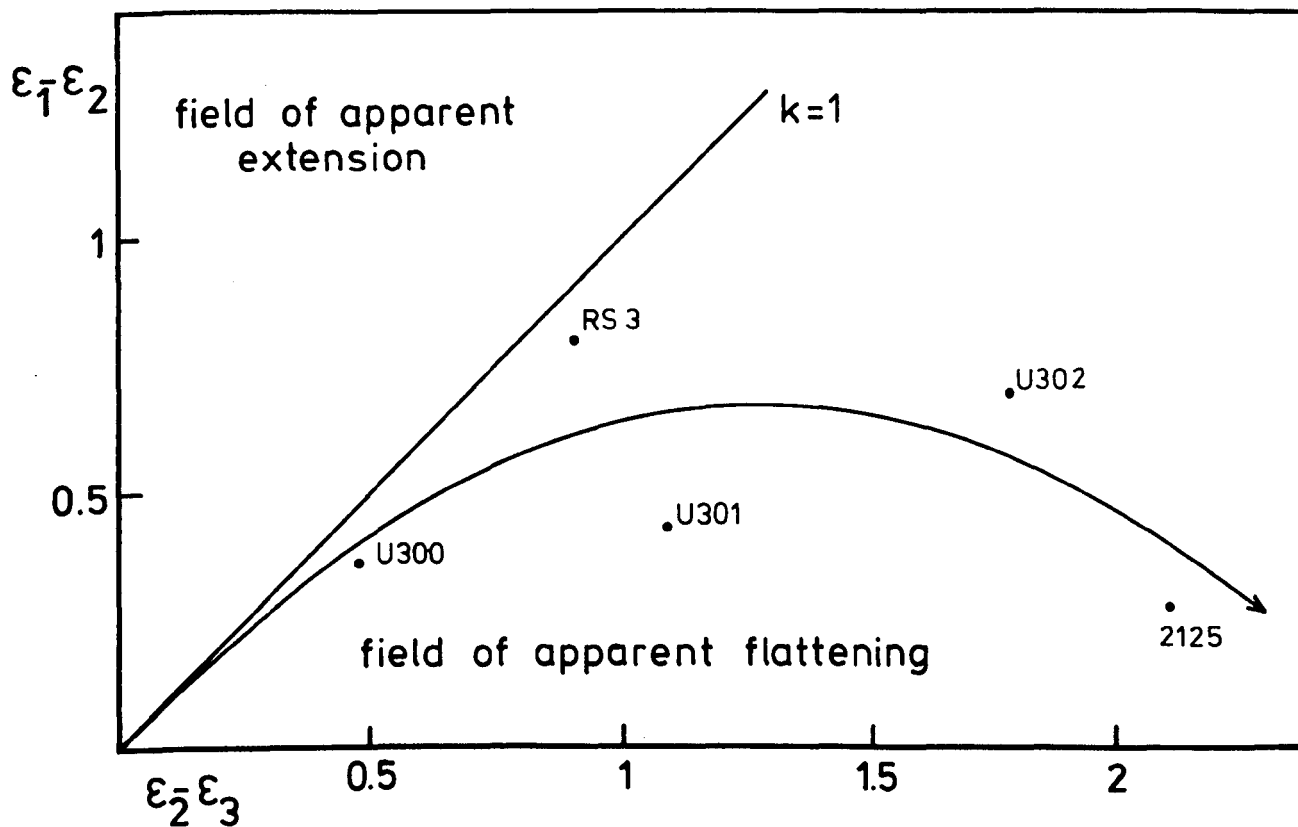


FIG. 2.9 (a) Rose diagram of strikes to joints and faults throughout the Molde peninsula
 (b) Plot using parameters from Table 2.1 illustrating changes in the ratios of the three principal strains ($\epsilon_1, \epsilon_2, \epsilon_3$) with progressive deformation (after Ramsay, 1967, p. 329). A postulated deformation path is shown.

directions almost exactly 90° apart and therefore at 45° to the principal compressive stress (Ramsay, 1967, p. 289). This is in accord with the stress direction in the strain ellipse deduced from the other structures, and the strike-slip nature of the faults.

Faults and joints are produced in rocks under conditions of brittle deformation (Ramsay, 1967, p. 289). It is suggested that the deformation at Molde was continuous during uplift of the rocks from deep crustal levels, with ductile deformation and folding, to higher levels with brittle deformation. Hydrous fluids must have been available throughout this deformation to produce the retrogressive metamorphism in the steep shear zones, particularly at Moldefjord, and the hydrous minerals in joints and the pegmatites along the fault lines.

2.2.5 The Augen Gneiss as a Strain Marker

In the field, the augen in the augen gneiss appear as ellipsoids which exhibit varying degrees of deformation (see Plate 2.1(b)) and a small exercise was undertaken to see if these variations could be used as strain markers (cf. Ramsay, 1967, Chapter 5; Hossack, 1968). Ramsay (1967, p. 122) has defined nine components necessary to define homogeneous strain in deformed objects in rocks: three changes in length of originally orthogonal lines and six changes in angles between these lines. Unfortunately it is rarely possible to measure these in geological material especially if the original form of the object is unknown, consequently only the changes in length of the axes of the ellipsoid are used: X, Y and Z (where $X > Y > Z$). Although this is limiting, the graphical representation can focus attention on some important aspects of the deformation.

Flinn (1962) defined the value 'k' as representing the ellipsoid where:

$$k = \frac{a - 1}{b - 1} \quad \text{with } a = \frac{X}{Y} \quad \text{and } b = \frac{Y}{Z}$$

when $k = \infty$ extension is implied, when $k = 1$: plane strain and when $k = 0$: shortening. The principal strains: e_1 , e_2 and e_3 can also be calculated by making an assumption as to the original form of the deformed object, for the augen the easiest assumption is a sphere, although it was more likely to be an ellipsoid (see Chapter 4). An important constraint on this assumption is that it is only valid if there is no volume change with deformation.

$$\text{Now the volume of an ellipse} = \frac{4}{3} \pi XYZ$$

$$\text{and the volume of a sphere} = \frac{4}{3} \pi r^3$$

Therefore $r^3 = XYZ$ where r is the radius of the original sphere.

$$\text{The principal strain } e = \frac{L - L_0}{L_0}$$

where L_0 = present lengths of the half axes and L = the original lengths of the half axes ($\equiv r$). When e is negative this implies shortening, when positive: extension, and when zero: plane strain.

Ramsay (1967, p. 330) prefers the parameter of natural strain:

$$\epsilon = \log_e (1 + e)$$

which can be readily used in the examination of the history of the deforming body. The volume change (Δ) of the ellipsoid can also be calculated:

$$\log_e (1 + \Delta) = \epsilon_1 + \epsilon_2 + \epsilon_3 \quad (\text{Jäeger, 1969})$$

Few of the samples of augen gneiss lent themselves to easy measurement as this required large pieces with a roughly cubic appearance to expose the three faces of the ellipsoids. Between 10 and 20 measurements of each axis were made in each sample and the calculated parameters are

TABLE 2.1 Data for strain analysis of the augen in the
augen gneiss

Parameters	RS3	U300	U301	U302	2125
e_1	1.32	0.49	0.92	1.85	1.39
e_2	0.04	0.04	0.25	0.44	0.83
e_3	-0.58	-0.35	-0.58	-0.76	-0.77
ϵ_1	0.85	0.40	0.65	1.05	0.87
ϵ_2	0.04	0.04	0.23	0.37	0.60
ϵ_3	-0.87	-0.43	-0.87	-1.42	-1.47
$(\epsilon_1 - \epsilon_2)$	0.798	0.363	0.425	0.683	0.26
$(\epsilon_2 - \epsilon_3)$	0.916	0.47	1.099	1.782	2.08
Δ	0.01	0.007	0.003	-0.009	0.0
$\bar{\Delta}$	0.01	0.007	0.003	-0.009	0.0
$\bar{\Delta}/\epsilon_3$	-0.012	-0.016	-0.003	0.001	0.0
k	0.816	0.73	0.265	0.198	0.16
r	0.6	0.77	0.6	0.66	0.7
X/Z	5.55:1	2.3:1	4.59:1	11.76:1	10.38:1

X/Z ratio indicates degree of extension in the strain ellipse

given in Table 2.1. Both RS3 and U300 have small values for e_2 signifying plane strain. In general e_3 is negative indicating shortening in that axis whilst Δ is always small implying little volume change and thereby justifying the assumption of original sphericity for the augen. The values for r are also fairly constant, perhaps signifying a constancy of original grain size between these samples. The value of k for each falls in the range $1 > k > 0$ indicating flattening ellipsoids, also shown by the positive values of ϵ_2 . ϵ_2 also approaches the values of ϵ_3 in successively deformed samples implying progressive flattening (Ramsay & Wood, 1973) as seen in the field.

The data is also presented graphically in Fig. 2.9(b) (after Ramsay, 1967, p. 330 and Ramsay & Wood, 1973). Since Δ is virtually zero the fields of 'apparent flattening' and 'true flattening' of Ramsay & Wood, (1973) coincide. The pattern of points seems to show a path of deformation (Flinn, 1962) progressing into the field of flattening and towards $k = 0$; the curve in this path implies that the shearing and/or the viscosity of the rocks was variable during deformation, also shown by the varying $\bar{\Delta} / \epsilon_3$ ratios.

Although this study does contain many uncertainties and assumptions partly due to a limited amount of data, it does show semi-quantitatively the deformation observed in the field.

2.2.6 Conclusions

From the foregoing study, two sets of deformation structures are apparent in the mapped area, one at Tverrfjella and surrounding ground, the other at Moldefjord. The latter is the younger and impinges to a certain degree upon the former.

The principal shortening strain direction for the deformation at Tverrfjella is considered to have been almost vertical, resulting in the

folds with horizontal axial planes and the sub-horizontal foliation. A certain amount of extensional strain accompanied this to produce the lines of disrupted marble boudins (see Map B) although this disruption was undoubtedly assisted by the plastic flow of the marble at elevated temperatures as discussed in Chapter 3. The occurrence of pods of eclogite in the quartzo-feldspathic gneisses surrounding the mountains, especially at Vagøy and Bollen, also suggests disruption by extension. The appearance of these eclogites in 'zones' of randomly distributed pods (see Chapter 7, Plate 7.1(b)) suggests that the disruption was of a 'chocolate-block' type, i.e. two perpendicular axes of extension (Ramsay, 1967, p. 113). This disruption was probably assisted by the ductile flow of the less competent migmatitic gneiss host rocks. It seems reasonable to extend the effects of these strains southwards to the rocks at Moldefjord, although the structures so formed have been obliterated by a subsequent deformation event except for small areas of relict flat foliation in the augen gneisses.

The principal strain directions for the deformation at Moldefjord are considered to be oriented as shown on Map D, from the nature of the folding and faulting the deformation appears to have been simple (irrotational) shear. The foliation planes at Moldefjord are parallel to the XY plane of the finite strain ellipsoid, cf. that for shear zones and the slaty cleavage in lower grade metamorphic rocks (Ramsay & Graham, 1970). Indeed the X/Z ratio from the most deformed augen gneiss sample (2125 - see Table 2.1) is very similar to that given for the slate belt in N. Wales, 6.5-10:1 (Wood, 1973). The dominant extension direction has not only reoriented the eclogite pods into zones and lines (see Map A) parallel to the regional strike, but has instigated boudinage within the heterogeneous rocks at Moldefjord (Plate 2.2(f)). The strong compressional

strain has formed the pervasive foliation here, the folding and the conjugate fault and joint sets at different stages in the progressive deformation as the rocks adopted different plastic and viscosity characteristics depending upon the prevailing temperature conditions (Hobbs, Means & Williams, 1976, p. 61).

The major folds were also formed by this event which affected the older structures on Tverrfjella by folding and localised shearing. The faulting can be shown to be the youngest of these structures as it truncates the Tverrfjella syncline at Børresdalen. The event is assigned to an uplift phase of the Caledonian orogeny, with high-level brittle failure coeval with metamorphic retrogression (cf. Hernes, 1956a; Løset, 1977; Krill, 1983 - see section 1.1.5), since the structures have a similar orientation and style to those to the NE whilst the regional orientation is similar to Caledonian structures in Scotland. The timing of the earlier deformation is more difficult to pinpoint, but appears to have been coeval with high temperatures; evidence from the rocks at Tverrfjella, including a Nd-Sm data of 418 ± 11 (Chapter 3) suggests that this also took place during the Caledonian but at an earlier stage. The presentation of the rocks at Tverrfjella as a definite sequence, including bands of marble, suggests that this unit has not suffered any deformation prior to the Caledonian orogenesis. However, the complexity of the surrounding migmatites and quartzo-feldspathic rocks suggests that those rocks may have been affected by a previous deformation, perhaps during the Svecofennian as suggested by Råheim (1972 - section 1.1.5).

Table 2.2 summarises the deformation events in the mapped rocks and their relationship to the metamorphic assemblages seen.

TABLE 2.2 Sequence of tectonic events in the Moldefjord area

Nature of metamorphism	Deformation
	PHASE 1
<p>Associated with eclogite-forming, high P-T metamorphism at deep crustal levels giving ductile deformation.</p>	<p>Near horizontal foliation, generally seen only in the northern part of the area around Tverrfjella, with 'chocolate-block' boudinage of eclogites.</p> <p>Similar style folds with near-horizontal axial planes preserved at Tverrfjella.</p> <p>?Open style folds with single steep/faulted limb preserved at Tverrfjella?</p>
	PHASE 2
<p>Uplift of rocks to increasingly higher crustal levels with high water activity resulted in amphibolite/green-schist retrogressive metamorphism in rocks affected by this phase.</p> <p>Deformation initially ductile, but progressively more brittle.</p>	<p>Intense compression perpendicular to line of Moldefjord coast forming: steep foliation, large fold structures (Molde-Tingvoll and Tverrfjella synclines plus Halså anticlinorium), intrafolial folds, lineations and reorientation of eclogite pods at Moldefjord.</p> <p>Steep shear zones at Tverrfjella.</p> <p>Near upright similar folds at Moldefjord, folding the lineation.</p> <p>Open folds at Moldefjord.</p> <p>Faults and joints throughout the area.</p>

PLATE 2.1

- (a) Transposition of the augen gneiss into a zone of flattening with production of a mylonite and brittle failure against fairly undeformed augen gneiss, Mordal (971575).
- (b) Transposition of the augen gneiss from a flat-lying foliation into a steeply dipping and flattened augen gneiss, Eidskrem (980602).
- (c) Flaggy foliation planes in the heterogeneous sequence, Mek (030577). Note the lineation on the foliation surface. The pinch-and-swell structure of the pegmatite implies syntectonic intrusion of the vein, also, the partial orientation of the biotites within the vein.
- (d) Isoclinal folds in the heterogeneous sequence, Mordal (975575).
- (e) Isoclinal folds in the augen gneiss, Julaksla (991586) with thickening of the augen in the crests of the folds. Note some shearing of the folds near to lens cap.
- (f) Flattened augen gneiss transversely by narrow shears, Eidskrem (980606). Note extreme extension of the augen of the left-hand side of the picture.

PLATE 2.1

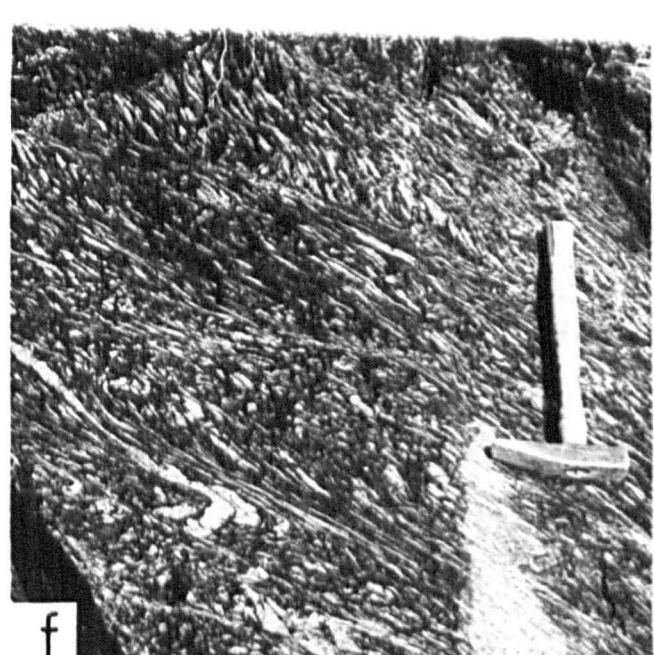
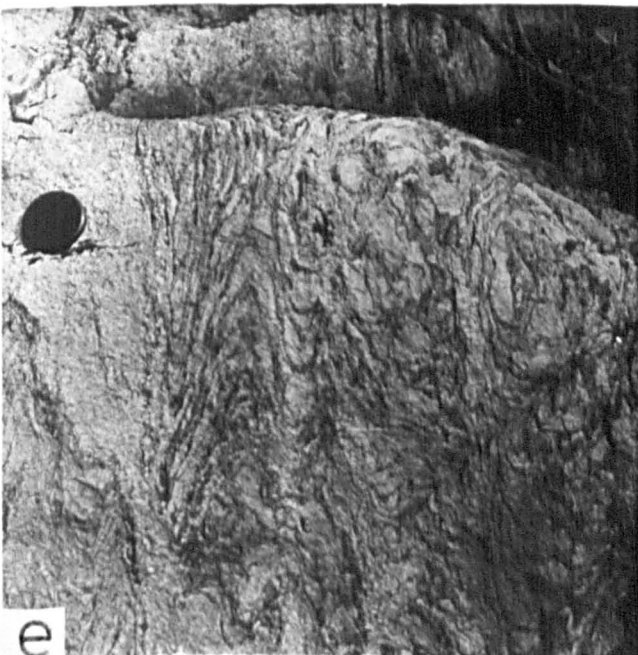
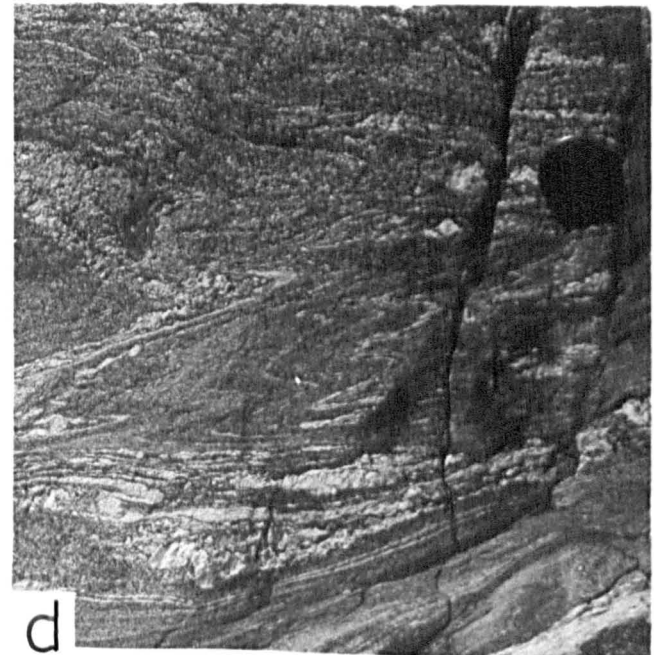
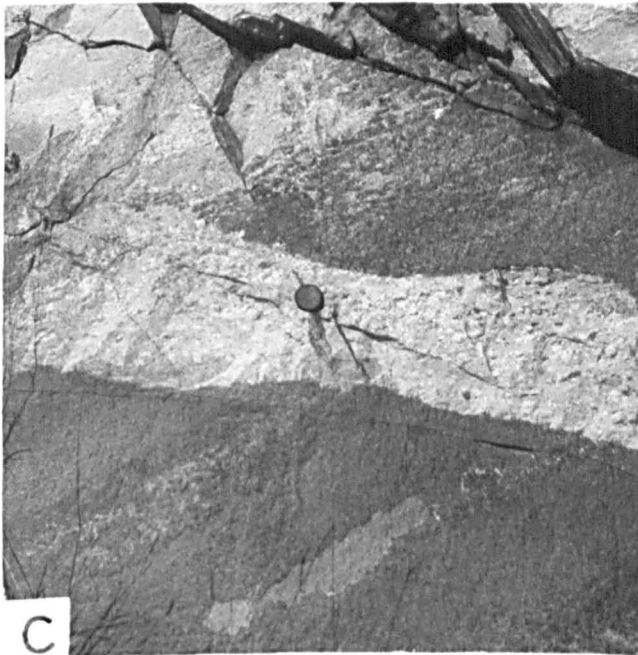
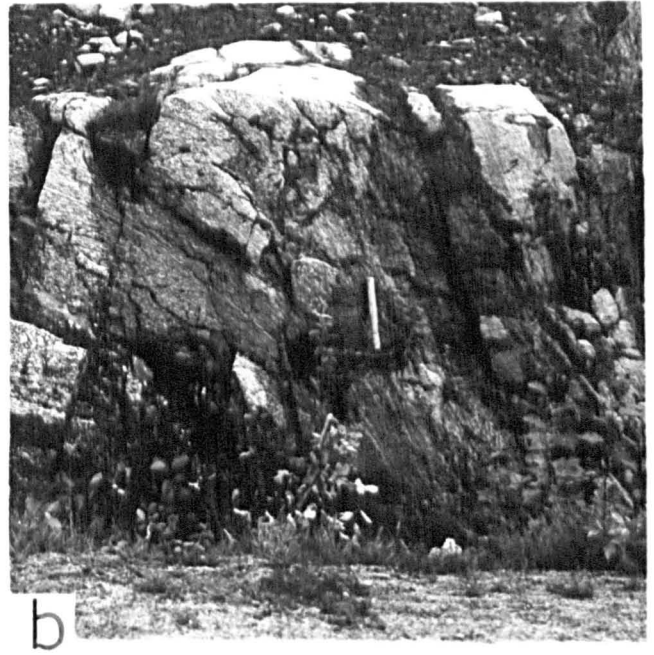
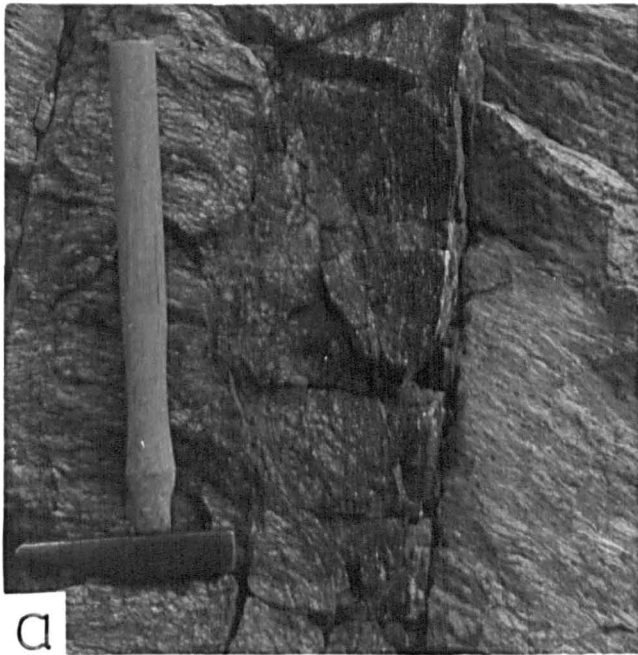
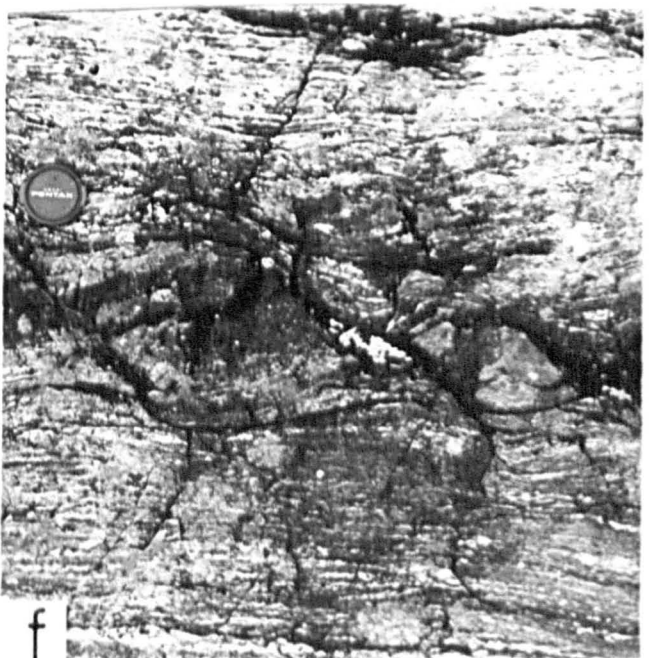
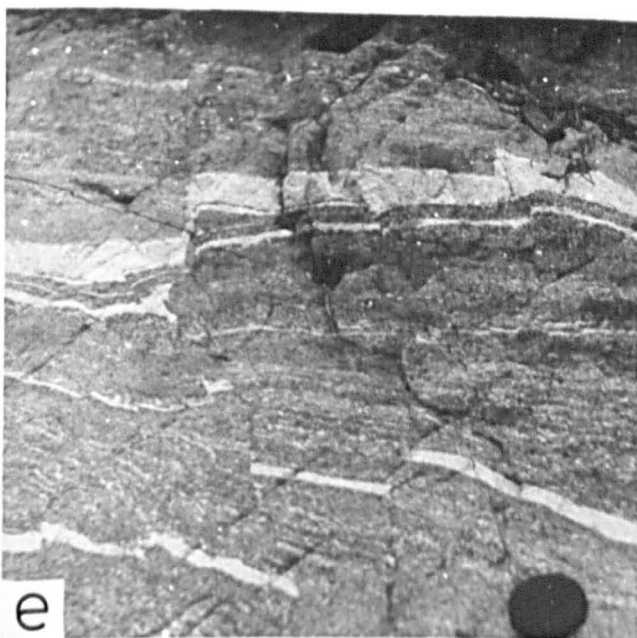
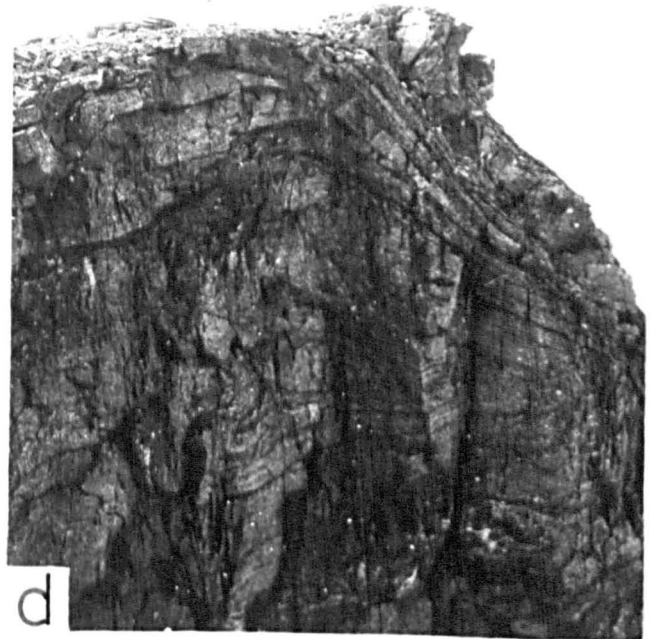
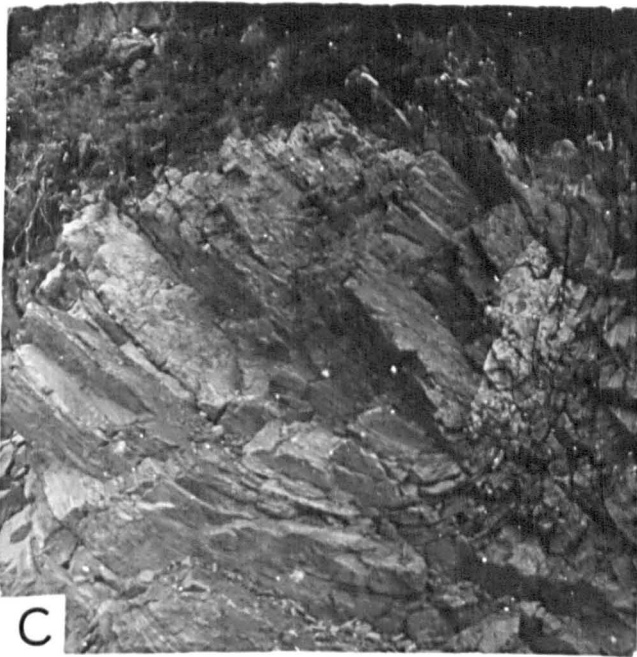
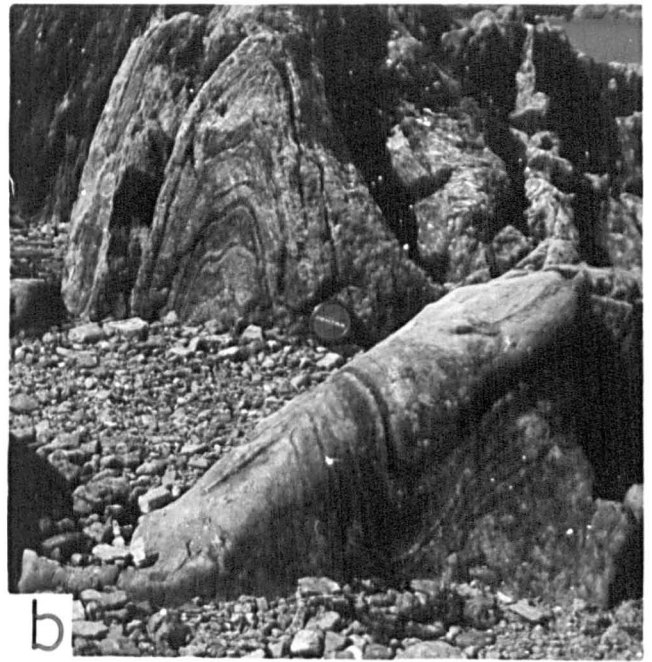
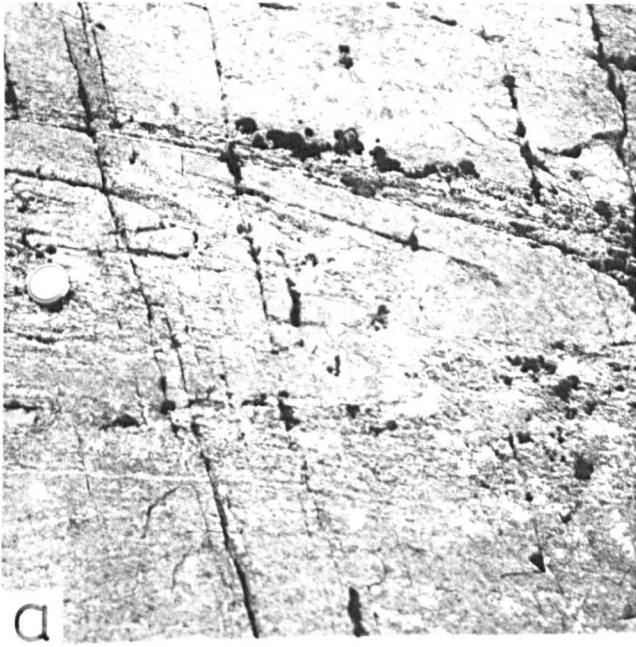


PLATE 2.2

- (a) A flat-lying similar fold in the garnet-granulite, Tverrfjella (101749). Note the prominent jointing.
- (b) Upright, similar folds in very attenuated augen gneiss, Moldeheia (060612). Relict augen appear above and to the right of the lens cap.
- (c) A very large, open, parallel fold in the heterogeneous rocks, Mordal (985572). Hammer at bottom of picture.
- (d) A large, flat-lying, similar fold in migmatitic rocks on Tverrfjella peak (112753). Note the undulations in the upper limb of the fold.
- (e) Joints cutting an epidote-amphibolite in the heterogeneous rocks, Mordal (978572).
- (f) Boudinage of a thin amphibole band in quartzo-feldspathic gneisses at Julneset point (970568). Note the rotation of the boudins and the jointing of the host rock.

PLATE 2.2



CHAPTER 3

THE TVERRFJELLA UNIT

3.1 GENERAL GEOLOGY AND PETROGRAPHY

The great lithological contrasts within this unit have allowed subdivision into: an extensive garnet-granulite enclosing large marble bodies and an overlying heterogeneous sequence; each will be described in turn. This area of ground has previously been studied by Hernes (1954b) although his map does not include the heterogeneous sequence. (All grid references refer to the 1:50,000 maps).

3.1.1 The garnet-granulite

This rock is best observed on the mountains of Talstadhesten and Heiane Allia (0873) at the western end of the Tverrfjella range. The rock is a monotonous, fairly homogeneous, medium-grained garnet-granulite forming large, blocky, well-jointed outcrops. The assemblage is remarkably consistent over such a large area: pink fractured garnet, pale green clinopyroxene, plagioclase (\sim An 20), quartz, hornblende (α pale yellow, β brown, γ brown-green, $\gamma^Z \approx 15^\circ$) + rutile (generally attached to opaque grains) + apatite \pm calcite with a generally subidioblastic, granoblastic (1 mm) texture. Concentrations of garnet, clinopyroxene or felsic minerals into bands 1-3 mm thick give the rock a layered appearance (Plates 3.1(a), (b) and (c)). Some portions are more quartz-rich (sample 1410) whilst others have either lighter or darker green clinopyroxenes, probably reflecting variations in their Fe-contents (Mysen, 1972). There is often a thin 'string' of clinopyroxene between the quartz and plagioclase (cf. Mysen, 1972 - his type 4 clinopyroxene - Plate 3.1(d)) or very thin rims of quartz between the mafic phases in the felsic portions of the rock. The lack of oriented minerals or foliation suggests that these variations

reflect an original compositional layering. The only manifestation of fabric development is lines of parallel fractures through the garnets, and to a lesser extent through the clinopyroxenes, which are associated with the retrogressive reaction leading to the production of blue-green hornblende from the garnet. Further evidence of retrogression appears as thin kelyphite rims on the garnets, of either a blue-green hornblende or of sub-microscopic intergrowths of hornblende and plagioclase (Plate 3.1(e)); some garnets develop small grains of opaque minerals at their rims. In general the garnets are little altered and are very consistent in both size and appearance. They generally contain tiny inclusions at their cores (plagioclase and quartz) although rutile and rare clinopyroxene also occur.

By contrast, the clinopyroxene always exhibits a symplectic texture with plagioclase (as seen by Hernes (1954b) in these rocks), generally developed at the centre of the original grain and approximately to the same degree throughout the garnet-granulite. The laths and 'blebs' of plagioclase are in the order of a few hundred microns across but can be large enough to display twin planes. These symplectites have the appearance of finger-prints and are identical to the textures described by Mysen (1972 - his type C2 - Plate 3.1(f)). In very coarse versions of the texture the plagioclase portions are visibly zoned (cf. Griffin & Råheim, 1973). Other clinopyroxenes display a brown, turbid colouration, again usually in the centres of the grains, which appears to be the incipient hydration of the mineral to an amphibole. Yet others develop small grains of opaque minerals within the plagioclase symplectite suggesting simultaneous expulsion of Fe during the alteration (Plate 3.1(f)).

Besides appearing in the symplectite, plagioclase also appears in the matrix, yet the compositions of the two are fairly consistent (\sim An 20). In both cases twins are sporadically developed and weakly defined. Matrix grains are in close association with both quartz, as rounded, slightly strained grains, and with small unaltered grains of clinopyroxene, the latter appearing to be a very advanced symplectitic texture (Plate 3.2(a)).

The hornblende appears to be secondary for several reasons:

(i) the larger grains form a poikiloblastic texture with respect to the plagioclase suggesting development from a symplectitic clinopyroxene by hydration;

(ii) some grains are oriented parallel to the fractures in the garnets and therefore are likely to have formed at the same time and under the same stress field as the secondary hornblende seen in these fractures;

(iii) any opaque minerals in contact with the hornblende cause a colour change in the hornblende from brown-green to orange-brown, implying disequilibrium between the two phases and a change in the Fe-oxidation state of the amphibole.

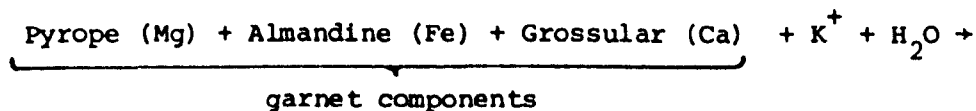
Amphibolitisation of the garnet-granulite is very variable. The rock appearing on the peaks of Heaine-Allia and Talstadhesten (0873), at the W end of the Tverrfjella range, is affected relatively little reflecting limited fluid mobility apparently prevented by a lack of foliation through the rock. The only amphibolitisation here is restricted to the localised fracture zones in the garnets. The nature of the retrogression textures in the rock are very similar to those described by Mysen & Heier (1972) and Mysen (1972) from the large (6 x 1 km) Ulsteinvik eclogite body at Hareid, and also to the eclogites elsewhere on the Molde peninsula (see Chapter 7), e.g. unamphibolitised symplectitic

clinopyroxenes and opaques on the rims of garnets. Mysen & Heier attributed the lack of hydrous phases (amphibole and biotite) to the sheer size of the body at Hareid which prevented access of fluids. Such an explanation seems applicable here, coupled with the lack of fabric development.

The garnet-granulite on the peaks at the E end of the range is more generally affected by amphibolitisation, particularly SW of Helvatnet (143756), with only a few areas of relict high-grade assemblages. This appears to be a result of the greater degree of disturbance suffered by the rocks there through faulting, shearing and jointing (Plate 3.2(b)). Where very severely deformed, the garnet-granulite is transformed into an amphibolite: hornblende (α yellow/brown, β dark green, γ dark green-blue, $\gamma^Z = 23^\circ$, -ve), plagioclase (An 45), sericite, white mica, chlorite (after biotite), zoisite, quartz + calcite + sphene. The fabric in these rocks is excellent with orientation of all the phases and mortar textures on the rims of the hornblende, zoisite and biotite. Relict garnet and clinopyroxene occur rarely (Sample 1427).

A major fault-line passes through Børresdalen and is manifest on the col at the head of the valley (097747) as severely disrupted garnet-granulite with pegmatite intrusion and concomitant amphibolitisation although the presence of relict rutile and clinopyroxene indicate the originally higher-grade assemblage present in these rocks. These rocks invariably display protocataclastic textures with mortared grain boundaries and ribboned quartz.

Biotite appears in the retrogressed garnet-granulite adjacent to these pegmatites, a product of the reaction:



can be seen to be composed of a low birefringence, high R.I. phase intergrown with quartz or plagioclase. In addition, this intergrowth can be seen to be developing from blades of kyanite and is itself surrounded by clusters of sub-idioblastic, granoblastic, polygonal plagioclase (An 60) (Plate 3.2(c)). This texture is virtually identical to those seen by Lappin (1960) and Bryhni (1966) in eclogites, and interpreted as symplectic intergrowths of corundum and oligoclase. Wikström (1970a) found a similar texture on kyanites in eclogites from Nordfjord which appeared to be a spinel intergrown with plagioclase (An 40). The reaction:



may have donated silica to the basic plagioclase in the surrounding rock producing a more acid oligoclase in the symplectite. Tilley (1937) found a similar texture in eclogites, described as an intergrowth of clinozoisite and quartz, with the plagioclase donating Ca^{2+} to the clinozoisite ($\text{Ca}_2\text{Al}_3\text{Si}_3\text{O}_{12}(\text{OH})$). In the garnet-granulite the phase with the high relief is difficult to identify but is thought to be corundum from its low birefringence. In other thin sections, hydration of the reaction products has produced the dark, turbid areas composed of sericite and clays with rare biotite with kyanite appearing within these patches (Plate 3.2(d)).

In the col between Heiane Allia and Talstadhesten (O91734), a thin (1 m) coarse-grained (5-10 mm) meta-ultrabasic band occurs, passing into heavily retrograded garnet-granulite on both contacts (sample 1413). It has the assemblage: hypersthene orthopyroxene, pale-green amphibole (α very pale yellow, $\beta = \gamma$ pale green, $\gamma^Z = 24^\circ$) probably pargasitic-hornblende, pale brown mica (phlogopite?), green spinel \pm calcite +

serpentinised (brown) olivine. The phases are well oriented and hydrated, with a blue-green hornblende and opaque minerals on the rims of the orthopyroxene, garnet producing green spinel + amphibole(?) intergrowth coronas, and olivine producing serpentine (Plate 3.2(e)). It is likely that a competence difference between this band and the surrounding garnet-granulite facilitated deformation and entry of fluids to produce these hydrous minerals. However, the mica and larger laths of amphibole appear to be primary and co-existing in equilibrium with the orthopyroxene, garnet and olivine suggesting that this may be a portion of a hydrous zone to a peridotite body not fully exposed here.

In a small abandoned marble quarry on the N face of Talstadhesten (O92746) the banding of the garnet-granulite is well displayed. Here a pale brown, sub-idioblastic amphibole (α colourless, $\beta = \gamma$ very pale brown/green, $\gamma^{\wedge}Z = 24^{\circ}$, +ve) occurs in an otherwise normal garnet-granulite assemblage (sample 143). From the optical data this phase is more likely to be pargasite than cummingtonite, as it has a $\alpha^{\wedge}a \approx 10^{\circ}$ and lacks twinning (Deer, Howie & Zussman, 1963, vol. II, p. 243 and 264). Moreover, it appears to be a primary phase, for three reasons:

(i) it is not associated with symplectic clinopyroxene or kelyphitic garnets; the latter display the typical secondary blue-green hornblendes with plagioclase;

(ii) the garnets contain inclusions of the mineral;

(iii) it is in apparent textural equilibrium with the garnet and clinopyroxene whilst contacts between it and grains of opaque minerals do not display the colour change, as seen in the secondary hornblendes. Mg-Ca-rich amphiboles such as these have been previously noted in rocks formed under eclogite-facies conditions (Lappin & Smith, 1978; Smith, 1982).

3.1.2 The Marble

Throughout the garnet-granulite, except in the very western part, several bodies of marble occur. These vary in size, from 1 x 0.5 km at Trollvatnet, down to a few metres, and take the form of elongate ovoids with long axes oriented E-W. From field mapping, distinct zones of these masses have been discerned (see Map B, cf. Hernes, 1954b) which are interpreted as mega-boudins disrupted from originally continuous bands. The rock weathers to blue-grey coloured, rounded outcrops with an abrasive surface of coarse (0.5-1 cm) crystalline calcite. The purity of the rock (see Table 3.3, analysis TL1) has resulted in quarrying at several localities for the production of carbide, although the rock is also used locally for agricultural lime and roadstone. The quarry roads provide relatively easy access to the mountains and excellent exposures of marble-granulite relationships at Langvatnet (085782), Talstadhesten (097751), Snipen (1675) and Langnes (174758).

The marble is generally blue-white in colour, massive, unfoliated and coarse-grained, typically 5 cm but up to 10 cm. In thin section it is almost mono-mineralic with a granoblastic texture of calcite plus tiny scattered grains of quartz and sulphides. There is no dolomite. At some contacts with the garnet-granulite the marble can take on a pale red, pink or orange colouring (cf. Vogt, 1896; Bugge, 1905) e.g. Langvatnet quarry (085752), although there is no visible reason for this in thin section, e.g. Fe-staining or the appearance of siderite.

Three types of contact between the garnet-granulite and the marble have been noted:

- (i) plastically interfolded, thin (5-10 cm) bands;
- (ii) gradational, with mixed rocks, i.e. clinopyroxene, hornblende, biotite in calcite;

(iii) sharp (Plates 3.2(f), 3.3(a), (b) and (c)).

Even when occurring as thin bands within the garnet-granulite the marble is still very pure, although pyrrhotite is a common accessory phase. This interbanding can be seen in the quarry at Langvatnet and displays intense, almost ptigmatic, deformation (Plate 3.2(f)). This plasticity is also visible on a larger scale at the NE end of Langvatnet quarry (O85752) where a large lobe of garnet-granulite extends into the marble (Plate 3.3(a)). Both of these examples suggest great differences in competence between the two lithologies, perhaps with the deformation of the marble assisted by gliding along the calcite twin/cleavage planes. It has been shown that at temperatures above about 400°C marble undergoes steady-stage flow causing recrystallisation and reorientation of the grains (Heard & Raleigh, 1972). The lack of oriented grains in this rock suggests that post-tectonic annealing has occurred (Heard, 1963).

It is considered that the disruption of the marble into these megaboudins played a major role in the disruption and associated retrogression of the adjacent garnet-granulite. In the vicinity of these bodies the dip and strike of the layering in the garnet-granulite is disturbed and assumes a random pattern. Furthermore, the garnet-granulite outcropping at the E end of the Tverrfjella range is even more disturbed, where there is a prevalence of marble bodies, than at the W end where the marble is absent (see Map B).

Running parallel to and a few centimetres on either side of the bands of garnet-granulite within the marble are thin (5 mm) discontinuous bands of green minerals, these are well exposed in the quarry at Langvatnet (O85752). They have variable assemblages, but overall are Ca-rich with some Fe phases:

Clinopyroxene, colourless and ragged with patchy alteration to a green Fe-actinolite (α pale-green, β green, γ blue-green, $\gamma^Z = 10^\circ$, -ve - Plate 3.3(d));

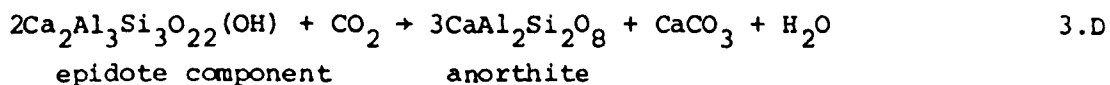
Scapolite as rounded grains with turbid cores and cleavages, the high birefringence of this phase suggests a melionitic (Ca) composition (Deer, Howie & Zussman, 1963, vol. IV, p. 328);

Bright-green clinopyroxene, typical of calc-silicate assemblages (Knorring & Kennedy, 1958);

+ zoisite + quartz + biotite (producing clays and/or chlorite) + opaques + brown hornblende (α brown-yellow, $\beta = \gamma$ dark green, $\gamma^Z = 16^\circ$, -ve) \pm plagioclase.

Many of these phases are in disequilibrium with each other. Quartz adjacent to calcite produces a thin rim of colourless-pale-green mineral, often pleochroic and associated with tiny grains of an opaque mineral. This is considered to be actinolite ($\text{Ca}_2(\text{MgFe})_5\text{Si}_8\text{O}_{22}(\text{OH})_2$ - Plate 3.3(e)).

Two distinct relationships are seen between scapolite and zoisite. Scapolite surrounds and replaces zoisite (cf. White, 1959) and a symplectic intergrowth of calcic plagioclase and zoisite replaces scapolite (cf. Parras, 1958; Aitken, 1983 - see Plates 3.3(f) and 3.4(a)). Both of these can be represented by two-stage reactions:



i.e. a dehydration/carbonation reaction.

The anorthite then reacts with the calcite to give scapolite.

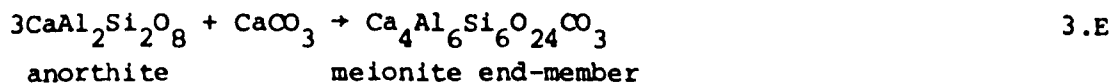


FIG. 3.1

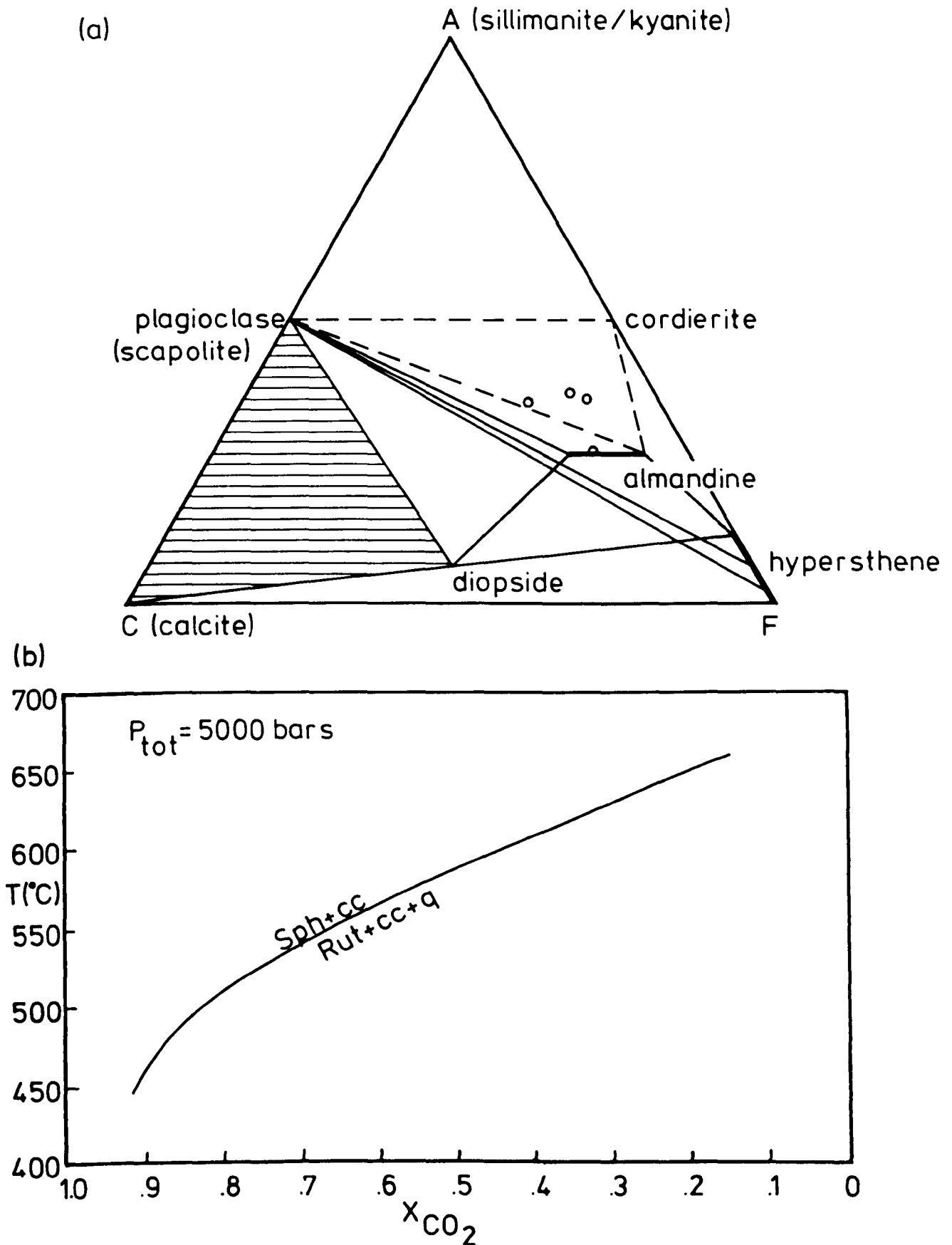
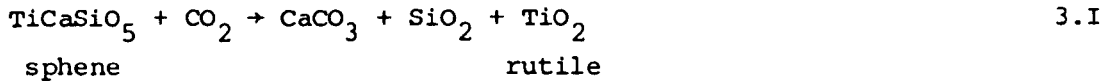


FIG. 3.1(a) ACF diagram for the granulite facies (Turner, 1968, p. 329) with excess SiO_2 and K_2O . The shaded field represents the assemblages recognised in the impure marbles. The points represent analyses of the pelitic rocks from the heterogeneous sequence (1018, T12, T13, T14).

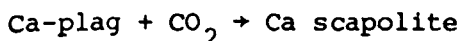
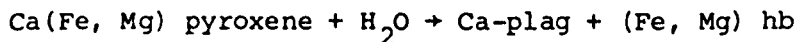
(b) T- X_{CO_2} diagram at 5 kbar with the univariant curve for reaction 3.H (Schilling & Vink, 1967; Hunt & Kerrick, 1977).

Similar bands are also exposed in the quarries on the north side of Talstadhesten (O97751). Here sphene produces rutile together with quartz, i.e.



a reversal of reaction 3.H. However the presence of a sulphide phase may be contributing Fe to the reaction or acting as a catalyst or nucleation point (Plate 3.4(b)).

Calcite and plagioclase also appears here; in clasts with white mica, the latter is both fibrous and coarse and the texture appears to be similar to the calcite + plagioclase + sericite products from scapolite observed by Parras (1958). Scapolite also appears in apparent symplectite intergrowth with green hornblende. If the scapolite is occurring instead of a plagioclase, a possible series of reactions could be:



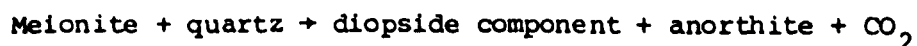
Besides these thin calc-silicate bands, coarser garnet-clinopyroxene rocks appear as thick (0.5 m) bands and pods, the latter apparently disrupted from the former, in several localities but particularly in the quarries at Snipen (1675) (Plate 3.3(c)). These generally display sharp contacts with the marble and can contain coarse garnets (~5 mm). They are unfoliated, porphyroblastic (clinopyroxene and garnet) and sub-idioblastic, with the general assemblage of: colourless clinopyroxene, meionitic scapolite, biotite, plagioclase (An 35-40), quartz + sphene + calcite ± Kspar ± garnet (sample 102). The plagioclase often displays a polygonal texture. The clinopyroxene has the typical ragged appearance,

poikiloblastic with respect to calcite and is also symplectic with plagioclase. The garnet is sieved with quartz and has ragged margins. The lack of any fabric suggests that the marble acted as a protective 'jacket' around these rocks and absorbed any stress by undergoing ductile flow.

The major differences between these bands and the calc-silicate type described earlier are:

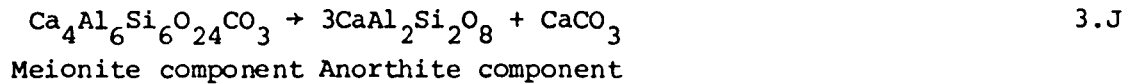
- (i) abundant garnet, implying higher Fe and Al concentrations;
- (ii) appearance of K-feldspar and biotite implying higher K concentrations;
- (iii) presence of anatectic material.

Even with these increased contents of Al and K, scapolite still appears suggesting either a high $\text{Ca}:(\text{Ca} + \text{Al} + \text{Na} + \text{K})$ value in these bands or perhaps a locally higher CO_2 . This scapolite exhibits extensive development of a brown turbid alteration generally confined to the centres of grains with thin, clear rims, which are only turbid along cleavages. This alteration appears to be sericite and calcite with trails of tiny opaques with the sericite often recrystallising into blades of white mica. The appearance of this K phase within the scapolite is most likely to have been assisted by the influx of the anatectic material. This appears as thin veins cutting across the calc-silicate phases, and can make up to 30% of the rock. The assemblage is: quartz + plagioclase (albite-oligoclase) + microcline, with antiperthites and perthites respectively. The quartz reacts with the scapolite to produce a clinopyroxene rim (cf. Plate 3.3(e)) which can be traced into, and is in optical continuity with, the primary clinopyroxene (Plate 3.4(c)). A proposed reaction is:



The anorthite product is not seen at the contact and may have contributed to the melt, although it may equally well have entered the scapolite.

Elsewhere, the scapolite is separated from the veining by a band of plagioclase, and there is no clinopyroxene present. It is possible that in these cases a localised high P_{H_2O} from the melt, caused the breakdown of scapolite (i.e. a reversal of reaction 3.E):



One isolated pod contains the unusual assemblage of: coarse, colourless, ragged clinopyroxene (+ve sign - diopsidic), meionitic scapolite, biotite, irregular calcite + quartz + plagioclase (An 33) in a sub-idioblastic unfoliated texture (sample 1416). However, the biotite is idioblastic and random, appears to overgrow the other phases and often forms a poikiloblastic texture with scapolite or is surrounded by a thin rim of the same. A major difference between this pod and the others described so far is the lack of garnet. It is possible that the biotite is a breakdown product of this phase via hydration, but it is difficult to see how the clinopyroxene could have escaped such hydration and how the scapolite was able to form in such an environment. However the rock is Al-poor (see Table 3.3) despite the appearance of a mica, which may have precluded the formation of garnet.

Rocks with abundant hydrous phases also appear as bands in the marble as clots of chlorite and hornblende, particularly at Langnes quarry (174758), often with grains up to 10 cm across. These suggest that large quantities of H_2O were present in localised areas of the marble presumably during the waning stages of metamorphism since the two minerals are seen to replace clinopyroxene and biotite.

At the northern end of these workings late pegmatites cut the marble and the clinopyroxene-bearing rocks within it. Very large hornblendes

appear at the contact between the mafic bands and the marble whilst scapolite appears as a pegmatite phase (cf. Deer, Howie & Zussman, 1963, vol. IV, p. 333). Compared to the scapolite previously described these grains are very coarse (~ 10 mm), possess low birefringence colours suggesting more sodic compositions and contain trails of tiny opaques. As pegmatitic scapolite forms in environments rich in volatiles such as CO_2 , Cl^- etc. (Deer, Howie & Zussman, 1963, vol. IV, p. 331) it suggests that this pegmatite was locally derived from the marble. The pods and bands in the vicinity tend to contain large amounts of hornblende and amphibolitised clinopyroxene, whilst sphene is ubiquitous.

The occurrence of the thin bands and layers of calc-silicate minerals within the marble, which are considered not to be the products of metasomatism, seem best related to impurities in an original sedimentary limestone:

<u>Detrital mineral</u>	<u>Donated element</u>	<u>Resultant phase</u>
sulphide	Fe	hornblende
	SO_4^{2-}	scapolite
	Ti	sphene
clays	K	{ biotite zoisite
	Al	
quartz	Si	quartz, silicates
calcite	Ca	calc-silicates
	CO_3^{2-}	scapolite
salt?	Na/Cl^-	scapolite
+ pore water?	H_2O	hydrous phases

The presence of Mg-phases (e.g. diopside) in a dolomite-free limestone, suggests that the limestone and the garnet-granulite were interbanded and mixed prior to the metamorphism.

3.1.3 The Heterogeneous Rocks

Above the garnet-granulite, with the enclosed marble bodies, at about 550 m, other more varied rocks begin to appear: quartzo-feldspathics, amphibolites and pelites. The layered nature of these rocks is well exposed on the N face of Trolltindane (117750 - Plate 3.4(d)).

On the N side of Børresdalen col (097741) there appears a thin (25 cm), white band interlayered with the garnet-granulite. This contains conspicuous, large (2 cm) pink garnets, sieved by quartz and clinozoisite in 'S-trails', set in a groundmass of anti-perthitic plagioclase (An 35) + quartz + bent kyanite + strings of colourless clinopyroxene. The kyanite is breaking down to biotite and plagioclase (+ corundum?) - see reaction 3.C). The clinozoisite inclusions show a symplectitic-like alteration to a plagioclase, which superficially appears to be similar to the texture seen in the marble (reaction 3.D) although no calcite is visible here (compare Plates 3.3(f) and 3.4(e)). The reason for including this particular rock here is that its assemblage shows a greater similarity to the heterogeneous quartz-feldspathic rocks described below, rather than to the variations previously described in the garnet-granulite. Furthermore, the band has sharp contacts with the garnet-granulite rather than gradational boundaries suggesting a distinct lithological type rather than a gradational compositional variant of the garnet-granulite.

On the E side of Børresdalen col (100750) well foliated, fine-grained, quartzo-feldspathic rocks appear, often with coarser migmatitic portions. The palaeosomes have the general assemblage of: sodic plagioclase, microcline, quartz, biotite, hornblende ± garnet. The neosomes have more equant, sub-idioblastic feldspars and unstrained quartz + biotite + apatite. One example possesses two fabrics, the primary alignment of garnet and biotite has been cut by later fractures resulting in retrogres-

sion of the garnets and sericitisation of the feldspars. These later fractures are related to the faults running through Børresdalen. These rocks become mylonitic or protomylonitic further up the ridge to Tverrfjella peak with relict feldspars and hornblende in a well comminuted matrix; such rocks are also found on the S-facing slope of Tverrfjella (108750). The neosome portions of these rocks are only slightly deformed, as granulation of the feldspar contacts, placing their time of formation towards the end of the deformation episode.

Further up this ridge a well defined gully appears in the hillside which can be traced for some distance downhill on the aerial photographs and is interpreted as part of the Børresdalen fault system. However, this dislocation does not seem to be the cause of the cataclastic textures in the rocks here since it cuts these rocks perpendicular to the mylonite fabric.

On the Tverrfjella peak (111753) these quartzo-feldspathic rocks become flaggy with a foliation well defined by both biotite and the neosome. Biotite is often sufficiently profuse to make the rock semi-pelitic. The palaeosome has a similar assemblage to the rocks already described, but in addition contains small garnets and rare kyanite which again reflect the pelitic and hence more aluminous nature of the rock. Deformation in the neosome is restricted to suturing of the quartz boundaries.

These flaggy rocks also appear on Blåfjellet peak (137750) with similar assemblages, although a certain amount of intermediate birefringence scapolite (i.e. intermediate Na-Ca composition) appears in the more mafic portions of the rocks. This phase exhibits the same turbid alteration products as the scapolite in the impure marble; here it co-exists with calcic plagioclase (\sim An 80). Again the neosome portions are only slightly deformed with granulated biotite and feldspar and strained quartz.

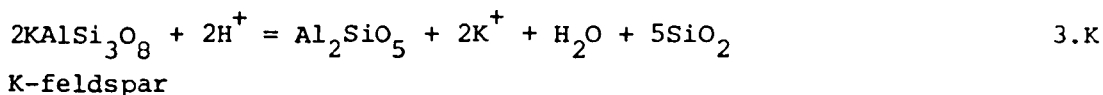
Approximately 10 m up the ridge from the gully at (102751), massive, dark, medium-grained garnetiferous amphibolites appear. A distinctive feature of these rocks in thin-section is the presence of poikiloblastic hornblendes (α yellow-brown, β green-brown, γ green-blue, $\gamma^{\wedge}Z = 16^{\circ}$) enclosing biotite, plagioclase (An 68), quartz and rarely, garnet. Also present, but not enclosed are green symplectic clinopyroxenes similar to those seen in the garnet-granulite. These are partially amphibolitised and it is considered that the poikiloblastic hornblendes are extreme versions of this hydration of the clinopyroxenes, resulting from the alteration and coalescence of several adjacent clinopyroxenes and their inclusions. The garnets are ragged, sieved with quartz and have kelyphite rims especially when they are adjacent to the poikiloblastic hornblendes which have apparently assisted in the hydration of the garnet. The plagioclase exsolved from the garnet during this alteration is evident as a thin rim between the garnet and poikiloblastic hornblende; the garnet can also appear as strings of rounded grains. Rutile is ubiquitous and associated with opaque phases whilst the biotite is transformed into chlorite + opaques. These rocks appear to have been original eclogite-facies rocks which have been even more heavily retrogressed than the garnet-granulite.

A further 50 m up the ridge from this locality, this rock is seen grading into a quartzo-feldspathic-rock over a distance of a few millimetres: In thin-section this junction is seen to be non-tectonic and is marked, in the mafic rock, by an increase in the proportion of oligoclase (heavily altered), a decrease in the proportions of clinopyroxene and amphibole and a diminution in the size of the garnets. The felsic rock is strongly altered, through shearing, with chlorite and white mica replacing biotite and feldspar respectively.

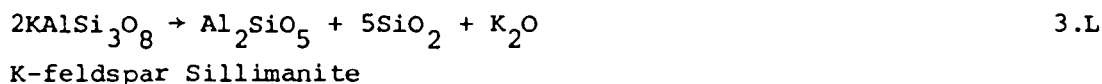
These eclogite-facies rocks with relict garnet and clinopyroxene also appear on Haldalstind peak (149750). Here the clinopyroxene is pale green and symplectic with coarse plagioclase (An 20) and some amphibolitisation (cf. Mysen's 1972 type Clb).

These rocks also appear on the W peak of Blåfjellet (140750), but differ from those described above by possessing narrow quartzo-feldspathic veins parallel to a crude sub-horizontal foliation. These differ from the migmatitic portions in the quartzo-feldspathic rocks by being heavily tectonised with much ribboned and strained quartz and are interpreted as original features rather than melt portions.

On Trolltindane (116751) pelites appear, both massive and well foliated, with foliation surfaces possessing a purple sheen but weathering to a rusty colour. They are highly aluminous with biotite, kyanite and garnet. Feldspars are porphyroblastic, antiperthitic oligoclase/albite, strained and cracked with granulated margins, and K-feldspar; both contain rounded 'blebs' of quartz. Quartz occurs in ribbons. Apatite and opaques are accessories. The biotite is very granulated but very well oriented with some later idioblastic blades overgrowing the fabric. The kyanite forms broad blades which are bent, strained and fractured (i.e. pre-tectonic) often altered to mica or sericite at the margins. The garnets are also syn-tectonic with 'S-trails' of quartz and zoisite. The K-feldspar is untwinned and typically displays a growth of fibrolite-sillimanite and quartz when adjacent to biotite (Plate 3.4(f)). A similar texture has been described by Tozer (1955) and Francis (1956), who both considered that the sillimanite was developing from the biotite, and Gavelin (1975) who suggested an addition of SiO_2 to and a loss of K^+ from the feldspar. Vernon (1979) suggested a base iron exchange reaction:



The free H^+ radical being derived from a cordierite + green biotite → brown biotite breakdown. However, no relict cordierite or green biotite is present here. An alternative reaction could be:



perhaps with the K_2O entering the biotite or the melt component. This melt is present in small migmatitic blebs and streaks of quartz and albitic anti-perthitic plagioclase with rare K-feldspar.

Semi-pelitic rocks occur on the ridge N of Trolltindane. Compared to the pelites these have greater amounts of plagioclase, less garnet (and smaller) and lack an aluminosilicate; the proportion of neosome is greater and coarser (5 mm) with equigranular albitic plagioclase and K-feldspar + rounded quartz all with slightly granulated boundaries.

An important feature of both the pelites and semi-pelites is that they lack any sort of white mica: phengite, paragonite or muscovite. Heinrich (1982) has studied pelites in the Alps containing: garnet + paragonite (Na-mica) + phengite (Mg-mica) ± kyanite ± quartz which he interpreted as an assemblage co-facial with the enclosed eclogites. Subsequent retrogression caused the breakdown of the phengite and garnet to a symplectic intergrowth of biotite and K-feldspar with the release of significant quantities of water, which hydrated the eclogites. The absence of this biotite-K-feldspar symplectite from the Tverrfjella pelites suggests that phengite was never present in those rocks, although the texture may have been obliterated during subsequent deformation and the formation of the biotite fabric.

Scattered calc-silicate rocks occur within this sequence of mixed rocks. The outcrop on the E ridge of Blåfjellet (144750) passes into the garnet-granulite and coarse marble, and contains the assemblage: pale green pleochroic clinopyroxene, hornblende (α straw, β dark-green, γ green, $\gamma^{\wedge}Z = 18^{\circ}$), meionitic scapolite, calcite, clinozoisite, sphene, opaques + K-feldspar + sodic plagioclase + biotite (to chlorite). This is a mixed calc-silicate/garnet-granulite rock of the type at Langvatnet quarry except that it has a greater areal extent and outcrops some distance from the marble. An interesting feature of the rock is that the clinopyroxene contains inclusions of scapolite. This may be a symplectic-like reaction, as seen in the garnet-granulite, with high P_{CO_2} producing scapolite rather than plagioclase (see reaction 3.E). Thin marbles also appear inter-layered with all these rocks. An example occurs in the flaggy migmatitic semi-pelite on Tverrfjella (111753); this is 1 m thick and fairly impure compared to the marbles occurring within the garnet-granulite, with the assemblage: meionitic scapolite, colourless diopsidic clinopyroxene, quartz, pale-green hornblende, biotite and calcic plagioclase (after zoisite?), profuse opaque minerals form a crude layering. The band displays a pinch and swell structure suggesting plastic deformation.

3.1.4 The nature of the basal contact of the Tverrfjella Unit

The rocks which appear below the garnet-granulite are heterogeneous, migmatitic quartzo-feldspathic gneisses, described in Chapter 4. The division between these rocks and those of the Tverrfjella Unit is based upon the apparently abrupt change in lithological type between the gneisses and the garnet-granulite. The words 'apparently abrupt' are used here because of uncertainty over the true nature of the basal contact.

Due to dense forestation and steep slopes the access to and examination of good localities is restricted. Only at one locality has a

physical contact been observed although a junction can be inferred at three other localities.

In Haukåselva (077730), on the W slopes of Talstadhesten, a sharp contact between the garnet-granulite and an underlying quartzo-feldspathic gneiss is visible. Unfortunately, the relationships are complicated by the intrusion of a pegmatite here, although the vein does not actually pass along the contact. The garnet-granulite contains an assemblage very similar to that of a moderately retrogressed example, as described earlier. However, in addition the rock contains blades of biotite, oriented into a crude foliation, for about 10 cm away from the contact. This biotite is the product of the alteration of the garnet in the garnet-granulite (see reaction 3A) and itself has been further altered to chlorite + opaques. Symplectic clinopyroxene is also present although the secondary pyroxene has been fairly well amphibolitised.

In the quartzo-feldspathic rock tiny garnets appear for about 10 cm away from the contact. Apart from this mineral the assemblage is similar to that seen in the quartzo-feldspathic rocks farther down the hillside (described in Chapter 5): sodic, antiperthitic plagioclase, quartz, biotite, K-feldspar ± hornblende. The nature of the contact is similar to those seen between eclogite pods and surrounding quartzo-feldspathic gneisses elsewhere on the Molde Peninsula. Although the appearance of biotite adjacent to the contact is common in the eclogite pods, the presence of garnet in the surrounding quartzo-feldspathic rock is quite rare. This type of contact, in the case of the eclogite pods, is interpreted as the result of local metasomatism and ionic exchange between the eclogite and quartzo-feldspathic gneiss (cf. Bryhni et al., 1969). Such an interpretation also seems applicable to the contact between the garnet-granulite and quartzo-feldspathic gneiss since the garnet-granulite is mineralogically similar to the eclogites.

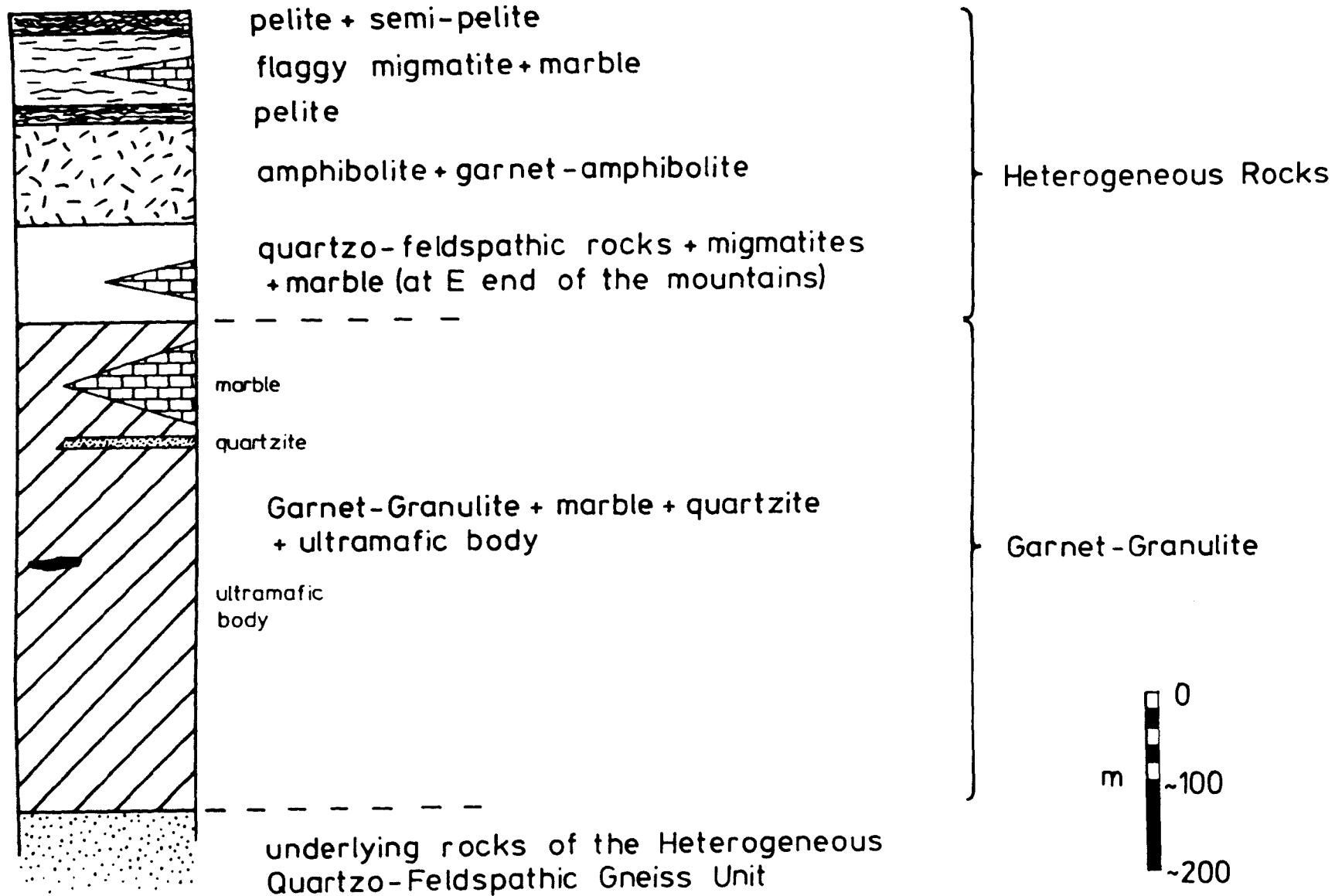


FIG. 3.2

FIG. 3.2 Schematic section of the Tverrfjella Unit with approximate thicknesses of the rock units.

The three localities where the basal contact can only be inferred are: Trolladalselva (122738); an approach road to Steinbrudd quarry (162745) and SW of Helvatnet (143755). At each of these localities quartzo-feldspathic gneisses appear; these rocks are all fairly massive and fine-grained with the general assemblage of: anti-perthitic plagioclase (An 10-30), quartz, K-feldspar (generally as microcline or as small 'augen' porphyroblasts) + biotite (often to chlorite) ± garnet ± hornblende. The gneiss at Helvatnet contains migmatite portions of: microcline, quartz and anti-perthitic, sodic plagioclase + biotite. These assemblages relate these rocks to the massive, heterogeneous, migmatitic, quartzo-feldspathic gneisses outcropping on the lower ground around the Tverrfjella mountains (Map B), rather than to the quartzo-feldspathic gneisses in the heterogeneous group of rocks within the Tverrfjella Unit itself which are more micaceous and flaggy, often with substantial contents of scapolite and garnet. Furthermore, the geochemistry of these rocks (samples 1114 and 1115 at Helvatnet and Steinbrudd respectively) relates them to the heterogeneous migmatitic gneisses as discussed in Chapter 5 (see Table 5.2).

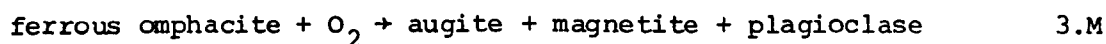
Although the evidence is restricted to one locality, the Tverrfjella Unit appears to lie directly on the heterogeneous migmatitic gneisses. However, it cannot be stated unequivocally that the junction is sharp everywhere on the basis of this one exposure.

Fig. 3.2 shows the vertical relationships of all the rock types described in this section with their estimated thicknesses.

3.1.5 Discussion of petrography

The general assemblage of the garnet-granulite observed at present (garnet + clinopyroxene + plagioclase + quartz) indicates that the rock formed under high-pressure granulite facies (as defined by Green &

Ringwood, 1967a). However, the rock displays certain textural features which suggest that it has suffered metamorphism at higher conditions. In this respect the most important of these textures is the intergrowth of sodic plagioclase with pyroxene, which is caused by the loss of jadeite component ($\text{NaAlSi}_2\text{O}_6$) from an original omphacitic clinopyroxene, a reaction driven by a decrease in P or an increase in T (Wikstrøm, 1970b). Several mechanisms for the breakdown reaction have been proposed and are reviewed by Mysen & Griffin (1973). The important feature of the breakdown reaction is that it cannot be isochemical if all the phases involved are to remain stoichiometric. Mysen & Griffin have suggested that stoichiometry of the clinopyroxene can be maintained during breakdown by the oxidation of Fe^{2+} in omphacite to Fe^{3+} in diopside (cf. Forster, 1947 and Wikstrøm, 1970c):



Such a reaction is visible in those clinopyroxenes in the garnet-granulite which exhibit grains of opaque mineral within the symplectic texture (Plate 3.1(f)). Mysen & Griffin suggested that the breakdown reaction is not only controlled by P and T, as proposed by Wikstrøm, but also by the oxygen fugacity. They also suggested that the breakdown could occur through the addition of SiO_2 (cf. Mysen, 1972):



although they considered that the supply of SiO_2 would not be fast enough for the breakdown to proceed to the degrees observed in eclogites unless the pyroxene involved was immediately adjacent to a quartz grain.

Wikstrøm (1970c) also demonstrated that the subsequent loss of Ca-Tschermaks component from the clinopyroxenes would cause the secondary

plagioclase to become progressively more calcic. This reaction can also be expressed as the addition of SiO_2 (cf. Mysen, 1972):



Both the composition of the plagioclase inclusions in the clinopyroxene symplectites observed in the garnet-granulite ($\sim\text{An } 20$), and the occurrence of zoning in some of these inclusions indicates that both the Ca-Tschermaks and jadeite components have been lost from the original clinopyroxene.

A feature of these symplectite textures in the garnet-granulite is their degree of development, compared to eclogites elsewhere on the Molde Peninsula, with the secondary plagioclase grains generally displaying triple-point contacts within scattered irregular grains of secondary clinopyroxene (see Plate 3.2(b)). This texture is interpreted as the result of the rocks being held at fairly high temperatures during the depressurisation and oxidation events necessary for the breakdown of the original clinopyroxene. This would then permit the annealing of the secondary plagioclase so formed.

The origin of the thin rims of clinopyroxene, between plagioclase and quartz in this rock (Plate 3.1(d)) are problematical. A similar texture described by Mysen (1972) from the Ulsteinvik eclogite, was attributed by him to clinopyroxene growth subsequent to the metamorphic culmination but prior to the formation of the symplectic clinopyroxenes. An alternative explanation is that since the rims of clinopyroxene in the garnet-granulite are in optical continuity with the secondary, symplectic clinopyroxene, they too are secondary clinopyroxenes with the expulsion of the plagioclase having been assisted by the proximity of the quartz as suggested by Mysen & Griffin (1973).

It is considered that the appearance of the symplectic texture implies that the clinopyroxenes were once omphacitic. This proposition, together with the observation of relict unsymplectic clinopyroxene in plagioclase-free assemblages, suggests that all this rock once possessed a typical eclogite assemblage: garnet + omphacitic clinopyroxene \pm rutile \pm quartz (Eskola, 1921). By way of confirmation, such clinopyroxene symplectic textures are also present in the eclogites present elsewhere on the Molde Peninsula (see Chapter 7). Furthermore, the garnet-granulite exhibits: kelyphitic garnets, paragonitic hornblendes and kyanite breakdown symplectites all of which have been described from other occurrences of eclogites in the Basal Gneiss Complex.

In his study of the eclogites of Norway, Eskola (1921, p. 19) analysed a garnet from this garnet-granulite and considered the rock to be a true eclogite but without any genetic connection with the enclosed marble bodies. Hernes (1954b) also considered the rock to be of eclogite facies and to have suffered retrogression to different degrees in different parts of the body. However, Hernes also described two textural features which were not noticed in this study: the occurrence of small garnets between the plagioclase and pyroxene, and the recrystallisation of plagioclase, through granulation, from larger laths of plagioclase. He compared both of these textures to similar ones found in meta-dolerites (Gjelsvik, 1952) and interpreted them as evidence of prograde reactions from an original gabbroic assemblage to eclogite. No texture remotely similar to the strings of garnet between plagioclase and clinopyroxene has been observed in this study; as stated in section 3.1.1 the garnets are very regular in both size and form. However, it is suspected that the recrystallised plagioclase from originally larger laths may be Hernes' interpretation of the texture of polygonal secondary

FIG. 3.3

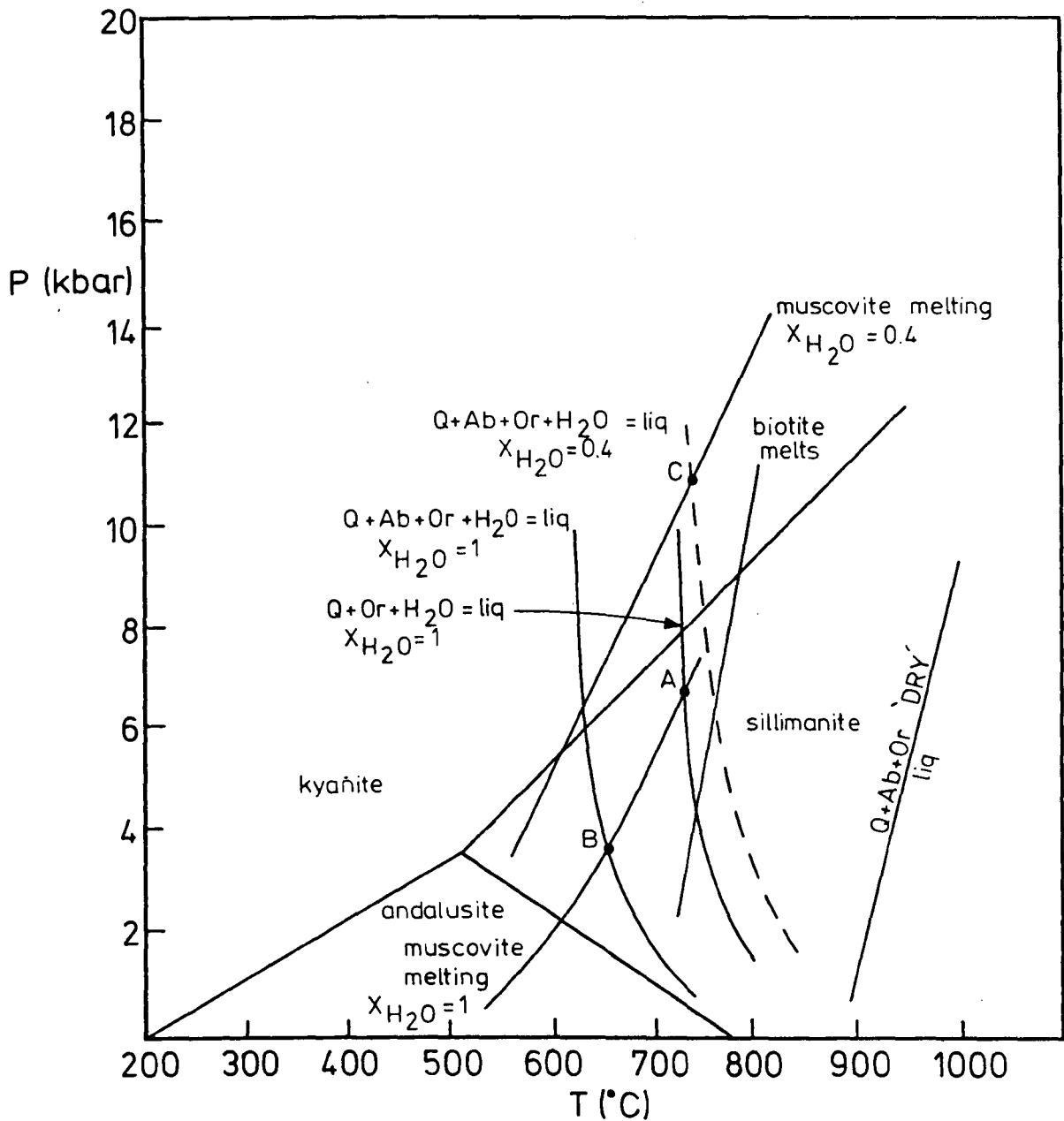


FIG. 3.3 Phase diagram for the various melting curves.

Al-silicate polymorph triple point from Holdaway (1971)

Muscovite melting curve at $X_{H_2O} = 1$ from Evans (1965)

Muscovite melting curve at $X_{H_2O} = 0.4$ from Holdaway & Lee (1977)

$Q + Or + H_2O \rightarrow Liq$ from Tuttle & Bowen (1958)

$Q + Ab + Or \rightarrow Liq$ 'DRY' from Winkler (1976, p. 306)

$Q + Ab + Or + H_2O \rightarrow Liq$ at $X_{H_2O} = 1$, and

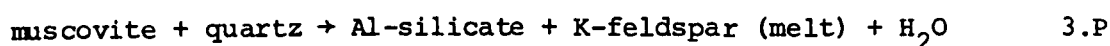
$Q + Ab + Or + H_2O \rightarrow Liq$ at $X_{H_2O} = 0.4$ from Kerrick (1972)

Biotite melting from Fyfe (1972)

Points A, B and C are explained in the text

plagioclase which can occur in fairly large clusters. Even so, these discrepancies in observation and interpretation of the textures present do not detract from the common interpretation of the garnet-granulite being a variably retrogressed eclogite.

The pelitic rocks in the heterogeneous sequence in the Tverrfjella Unit are mineralogically similar to the khondalites of Ceylon, which contain the assemblage: quartz + perthite + garnet (+ plagioclase + kyanite/sillimanite) and are interpreted as Al-rich sediments metamorphosed at granulite facies (Turner, 1968, p. 328). Two particular features of the pelites also suggest a high P-T origin: the appearance of biotite as a stable phase, and the present of quartz + K-feldspar ± plagioclase portions as veinlets and blebs. The latter are interpreted as melt portions for three reasons: they cut other phases, they are coarse-grained and they are relatively undeformed suggesting that they were not coherent until some time after the metamorphic/tectonic culmination. Furthermore, the absence of muscovite mica, except as secondary replacement of kyanite, suggests that the reaction:

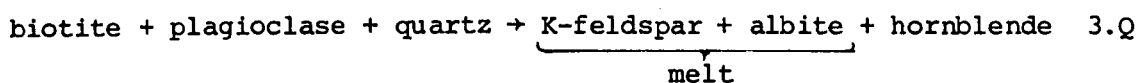


has occurred (Winkler, 1976, p. 308). This reaction is very dependent upon both the $X_{\text{H}_2\text{O}}$ in the rock (Kerrick, 1972) and the An content of the associated plagioclase (Winkler, 1976, p. 315). Fig. 3.3 shows the experimentally determined melting curves of several 'granite' systems. Point A shows that with only Or present muscovite will begin to melt at ~ 6.8 kbar and $\sim 730^\circ\text{C}$, with the addition of Ab component, the muscovite begins to melt at ~ 3.8 kbar and $\sim 650^\circ\text{C}$: point B. Both of these points fall within the stability field of sillimanite although kyanite is the stable Al-silicate in the pelites. However, at lower values of $X_{\text{H}_2\text{O}}$ the

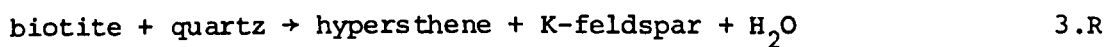
muscovite-melting reaction moves to lower temperatures (Chatterjee & Johannes, 1974), a curve at $X_{\text{H}_2\text{O}} = 0.4$ is shown on Fig. 3.3 (after Holdaway & Lee, 1977), and the granite melting curve moves to higher temperatures (Q + Ab + Or - 'dry' from Winkler, 1976, p. 306). These displacements cause the intersections of the two curves to occur at increasingly higher pressures as $X_{\text{H}_2\text{O}}$ falls (point C - cf. Kerrick, 1972 and Carmichael, 1978) into the kyanite stability field. Furthermore, once the rock begins to melt the $X_{\text{H}_2\text{O}}$ will continue to fall, unless there is an external source, as the melt will act as a 'sink' for H_2O (Turner, 1968, p. 468).

As described in section 3.1.3, the related white micas phengite (Mg-mica) and paragonite (Na-mica) are absent from these rocks, as is any evidence of the prior existence of phengite as the biotite-K-feldspar symplectite observed by Heinrich (1982). Phengite mica, although a high P phase, tends to lose the celadonite component $(\text{K}(\text{R}^{2+}\text{Al})\text{Si}_4\text{O}_{10}(\text{OH})_2)$ at high temperatures so that the mica composition approaches muscovite. Furthermore, Na substitutes for K at high T so that the mica composition approaches paragonite (Velde, 1965). Now, Heinrich (1982) deduced P-T conditions of 650°C and >15 kbar for his phengite-bearing pelites and it appears that the Tverrfjella pelites have suffered rather higher temperatures than this from the evidence of the melt portions in the rocks. Therefore, it is likely that phengite never existed in these rocks and was replaced by free paragonite or a paragonite-rich muscovite. However, paragonite melts to give albite + corundum, and this breakdown has not been observed in natural rocks (Turner, 1968, p. 123). Consequently it seems more likely that the paragonite existed as a muscovite component, this complicates the melting of that phase by displacing the curve to lower T (Thompson, 1982).

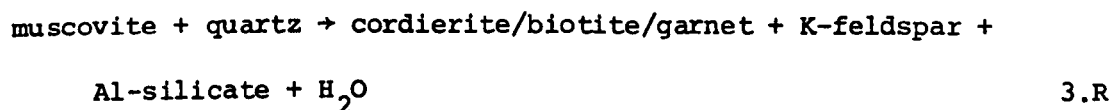
The relative scarcity of plagioclase in the melt portions suggests that this plagioclase has been derived from the paragonite component of the original white mica, rather than from the melting of biotite:



(Winkler, 1976, p. 213) which appears as a stable and fairly abundant phase in these pelites. This preservation of biotite in the rocks then places a maximum value on the temperature suffered by the rocks since the biotite melting curve lies at approximately 100°C above that for the beginning of anatexis (Winkler, 1976, p. 213 - see Fig. 3.3). The retention of biotite also implies that the following dehydration reaction has not occurred:

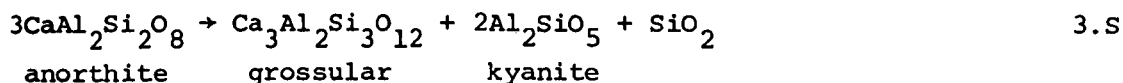


which is important for the recognition of high-grade rocks (Eugster & Wones, 1962). Although hypersthene is regarded as a diagnostic phase of the granulite facies (de Waard, 1965; Turner, 1968, p. 329 - see Fig. 3.1(a)), suggesting that biotite should therefore be absent from these rocks, it is perfectly feasible for biotite to exist in pelitic assemblages up to this metamorphic grade (Turner, 1968, p. 334; Bohlen et al., 1980). In addition, the bulk chemistry of the Tverrfjella pelites is too Fe-poor to have allowed the development of hypersthene (Fig. 3.1(a)). It has been suggested that biotite, or some other Fe-Mg phase, could be produced by the muscovite melting reaction and form part of the restite, if phengite was an important component of the white mica:



(Tracy, 1978).

The garnets in the pelites contain a certain amount of grossular component (see analysis 1018, Table 3.10) which indicates that the reaction:



has occurred (Hariya & Kennedy, 1968, Ghent et al., 1979 - see Fig. 3.4). In addition the garnets contain S-trails of inclusions, whilst the anatectic portions are relatively undeformed, suggesting:

- (i) the peak of metamorphism was accompanied by tectonism, and
- (ii) the anatexis was post-tectonic.

The appearance of sillimanite as a secondary phase after K-feldspar (Plate 3.5(a)) implies that the stability field of sillimanite was entered subsequent to the metamorphic culmination.

A postulated P-T path for the pelites which incorporates all these petrographic features is shown on Fig. 3.4. The curve phases below the stability curve for pure jadeite, which is absent from these rocks, into the kyanite stability field and finally into the sillimanite stability field where it crosses the melting curves discussed earlier.

It is likely that the fluid associated with the rocks during this metamorphic evolution was predominantly H_2O (Ghent et al., 1979), derived from dehydration reactions of sedimentary clays (Fyfe et al., 1958).

As melting proceeded, $X_{\text{H}_2\text{O}}$ would fall as it would be taken up by the melt (Kerrick, 1972); if $X_{\text{H}_2\text{O}}$ fell to a sufficiently low value, the Al-silicate and K-feldspar would co-exist without a melt (Carmichael, 1978). The existence of perthite textures in the feldspars in the anatectic portions suggests that the conditions were: $P_{\text{H}_2\text{O}} < 5000$ bars to permit the formation of a feldspar which subsequently unmixed on cooling (Morse,

FIG. 3.4

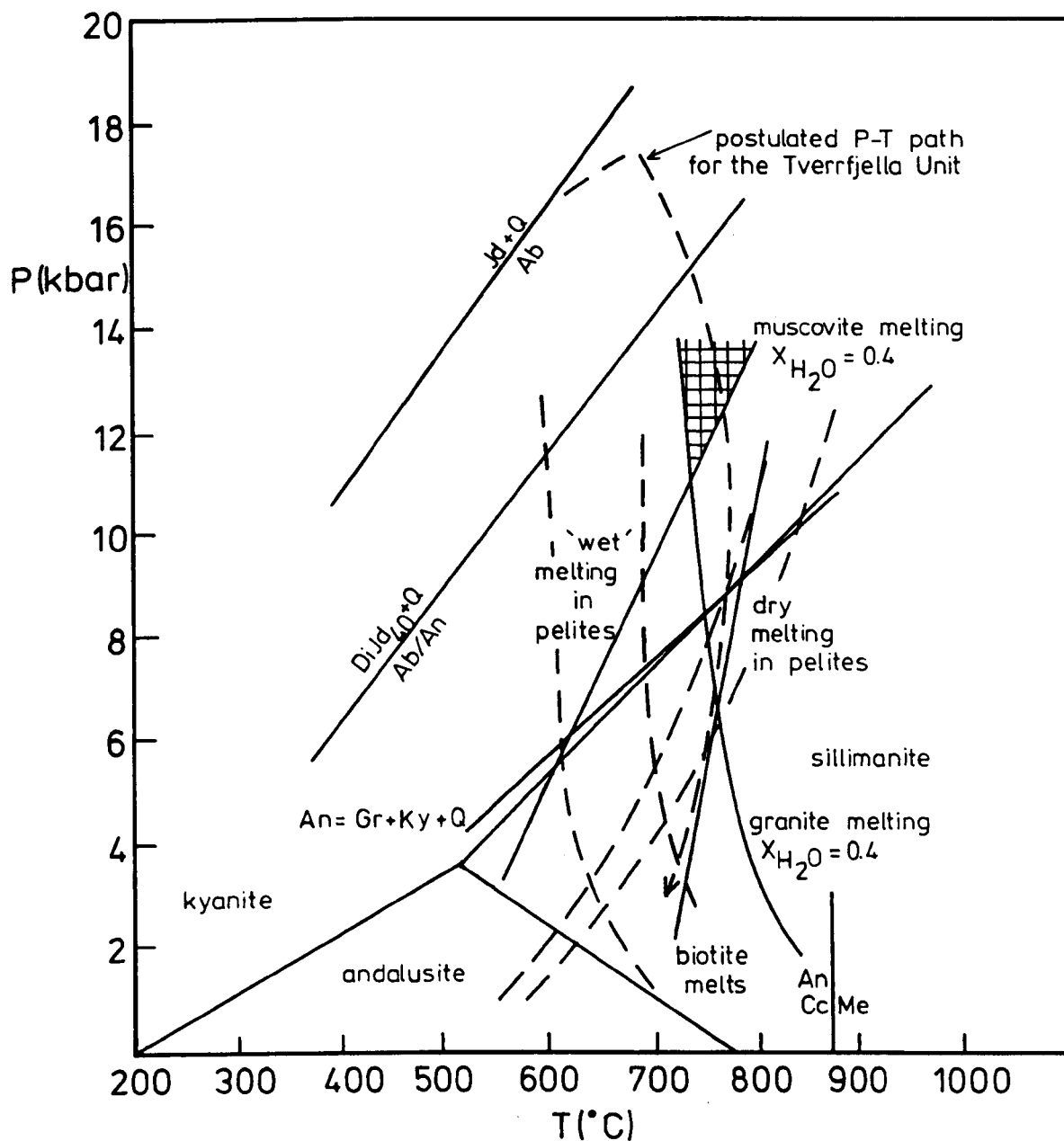


FIG. 3.4 Phase diagram for high-pressure minerals, the melting curves are from Fig. 3.3.
 $Ab \rightarrow Jd + Q$ from Holland (1979)
 $An + Ab \rightarrow Diop + Jd_{40} + Q$ from Holland (1979)
 $An + Gross + Ky + Q$ from Ghent et al. (1979) including effects of Alm and Pyr solid solution which depress the curve to this low P
 $An + Cc \rightarrow Me$ from Goldsmith & Newton (1977)
 Dry-melting and wet-melting curves in pelites from Thompson (1982)
 Shaded area represents the conditions where partial melting would be expected to occur in the pelitic rocks.

1970 and see section 5.4 for discussion in relation to the feldspars in the Augen Gneiss). The fact that the melt portions still reside in the pelites and have not been expelled also suggests that the $X_{\text{H}_2\text{O}}$ at the time of their formation was fairly low. Thompson (1982) has shown that melts formed at low $X_{\text{H}_2\text{O}}$ conditions are H_2O -undersaturated and, as a consequence, are more viscous and therefore are more difficult to remove from their source. This scenario of rapid uplift in initiate melting in pelites during exhumation of tectonically thickened crust has been elsewhere postulated by Thompson & Tracy (1979) and Thompson (1982).

Such a P-T path is also applicable to the garnet-granulite as it retains the high temperatures during depressurisation required to produce the textural pattern of recrystallised plagioclase and symplectitic clinopyroxene. The appearance of the symplectite implies that this curve passed through the lower stability limit of the $\text{JdDi}_{40} + \text{Qtz}$ assemblage (Holland, 1979) whilst the grossular component of the garnets (see Table requires the rocks to have lain on the high P side of the curve for the grossular forming reaction 3.S (see Fig. 3.4). These features suggest that both the garnet-granulite and the heterogeneous rocks acted as a single unit during metamorphism, and progressed along the same P-T trajectory.

The form of this trajectory is very similar to those postulated for the Moines in Scotland by Wells (1979). These 'hooked' paths have been discussed by England & Richardson (1977) in relation to the erosion of orogenic belts. They consider them to be a good reflection of the path taken by the rocks for two reasons:

(i) erosion is a fairly rapid process in relation to geological time so that the removal of overburden from a section of crust will have the effect of an instantaneous pressure change;

(ii) rocks at the highest grades of metamorphism and hence deep in the crust, will continue to heat up during their uplift due to energy sources in the mantle and from radioactive decay.

The combination of these two factors results in the type of P-T path shown in Fig. 3.4.

The mineral assemblages observed in the portions of impure marble for which reactions are given in section 3.1.2., are interesting in that there are both prograde (dehydration/carbonation) and retrograde (decarbonation/hydration) types, generally within a few centimetres of each other in one thin section. These observations have a bearing on the role of fluids in the metamorphism of these rocks.

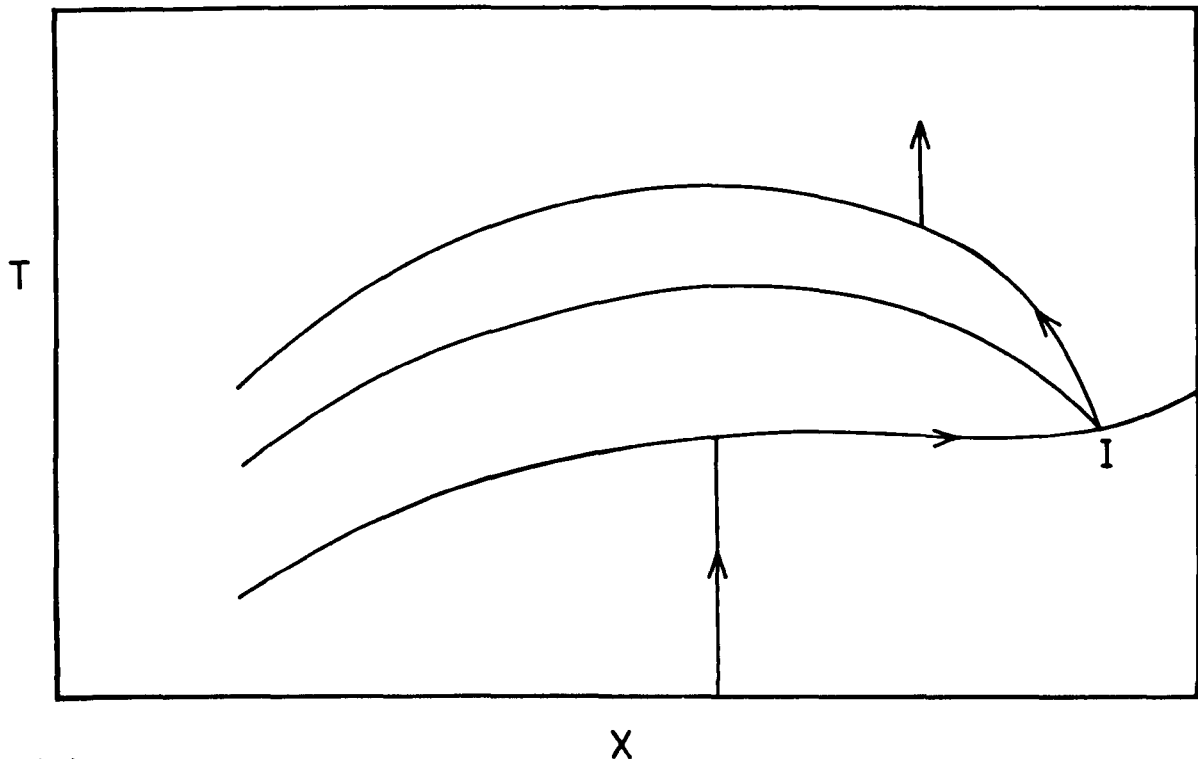
Most fluids in metamorphic rocks are composed of CH_4 , H_2O , CO_2 and H_2S , in decreasing order of abundance (Holloway, 1981). The lack of graphite and the scarcity of sulphides suggests that CH_4 and H_2S were negligible in these rocks, whilst the observed mineral assemblages suggest that H_2O and CO_2 were of importance. Indeed, most metacarbonate rocks can be assumed to have been metamorphosed in equilibrium with a simple H_2O - CO_2 binary fluid system, although this mixture can vary between pure CO_2 and pure H_2O (Ferry & Burt, 1982).

The devolatilisation reactions in metacarbonates will release CO_2 -rich fluids giving $X_{\text{CO}_2} > 0.5$ (Ferry & Burt, 1982) whilst dehydration reactions in granulites release H_2O -rich fluids (Valley & Essene, 1980). In the example of the rocks at Tverrfjella, both of these fluids would have been evolved in close proximity from the marble and garnet-granulite respectively.

Vidale & Hewitt (1973) considered that pore-water would be involved in the metamorphism of sedimentary rocks. However, such water is most likely to have been lost on compaction and diagenesis, although some

FIG. 3.5

(a)



(b)

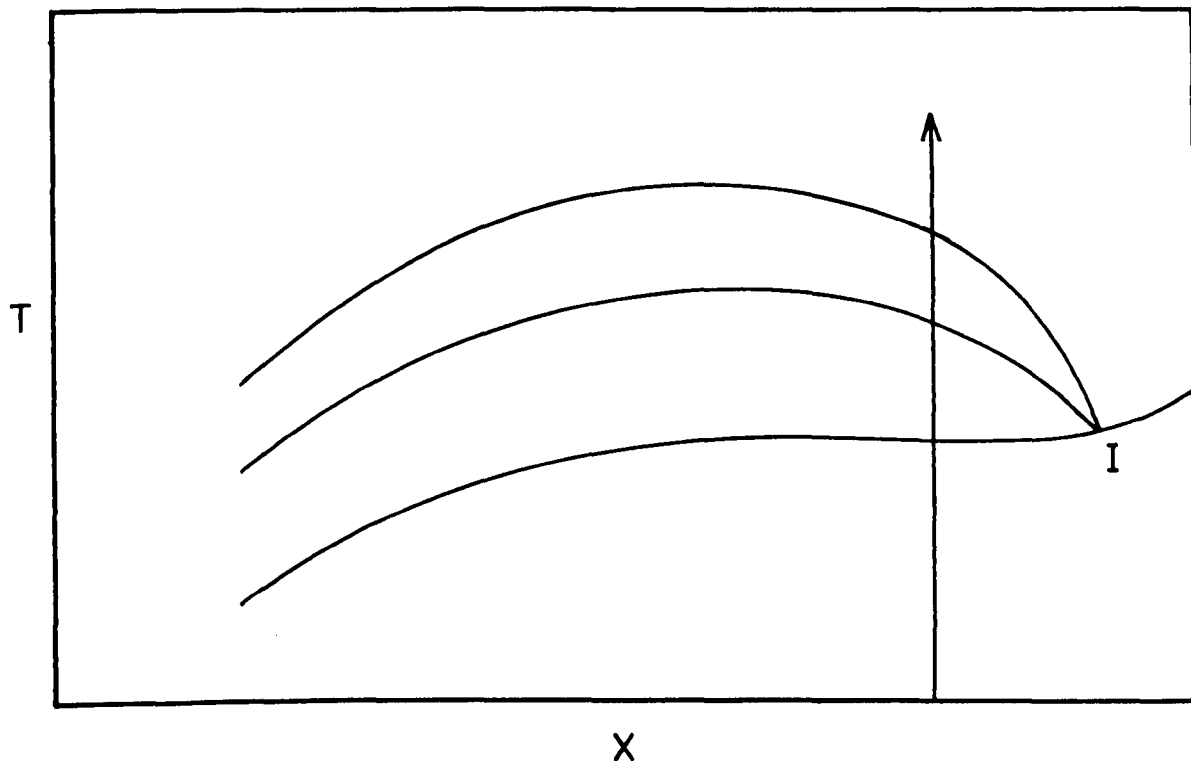


FIG. 3.5(a) Schematic, isobaric T-X diagram with the expected path of a rock system during metamorphism under buffered fluid conditions. I is the invariant point. (Several possible paths are possible depending upon the proportions of the phases formed and those originally present, and the compositions of the original and buffering fluid.)
 (b) Schematic, isobaric T-X diagram with the expected path of the same rock during metamorphism under externally controlled

combined water would still be available from the breakdown of hydrous minerals: e.g. clay, sericite and chlorite (cf. Fyfe et al., 1958). Furthermore, most metasediments have a porosity of <0.1%, which would prohibit the coexistence of large volumes of pore-fluid (Rice & Ferry, 1982). Therefore it is unlikely that there would be a great deal of H₂O generated by the marble.

In general, there are two types of system governing the composition of coexisting fluids in metamorphic rocks: internally buffered (closed), or infiltration, from an external source (open), although in most cases there is some degree of each (Rice & Ferry, 1982). In the case of meta-carbonate rocks the infiltrating fluid is mostly water generally derived from adjacent igneous plutons or dehydrating granulites. However, meta-carbonate rocks have the capacity to buffer this incoming fluid to a large degree, thereby necessitating the entry of large volumes of fluid before externally controlled equilibrium conditions are attained (Rice & Ferry, 1982). The concept of buffering in petrology is very similar to Le Chatelier's principle in chemistry which states that an equilibrium reaction will only stay in equilibrium if there is no change in the conditions affecting the reaction. If one component is added or removed the reaction will move in such a way so as to minimise the effect of that change on the reaction. In petrology, the mineral reactions are generally too sluggish to maintain a fixed value for the variable component (e.g. the H₂O content of the fluid) but can retard the changes caused by this variable (Rice & Ferry, 1982).

In metamorphic terrains with buffered fluid reactions, the metamorphism will follow the isobaric, univariant reaction curves on a T-X diagram resulting in the coexistence of reactants and products of these reactions in thin-section (see Fig. 3.5(a)). By contrast, in metamorphic

terrains controlled by externally derived fluids the metamorphism will follow near vertical paths, at the designated fluid composition, causing isobaric divariant assemblages to be very common whereas the coexistence of reactants and products from the univariant reactions will be rare (see 3.5(b), Rice & Ferry, 1982).

Some of the assemblages described in section 3.1.2. are of particular interest as they can be related to the system $\text{CaO-Al}_2\text{O}_3\text{-SiO}_2\text{-H}_2\text{O-CO}_2$, with SiO_2 and CaO in excess, which is a reasonable approximation to the bulk composition of impure limestones (Kerrick, 1974). Ellis (1978) provides schematic $T\text{-}X_{\text{CO}_2}$ diagrams for the system at 4 kbar and 12 kbar (see Fig. 3.6). With regard to this system, the absence of the phases margarite ($\text{Ca}_2\text{Al}_8\text{Si}_4\text{O}_{20}(\text{OH})_4$) and grossular garnet ($\text{Ca}_3\text{Al}_2\text{Si}_3\text{O}_{12}$) from the calc-silicate rocks is of importance. Frey & Orville (1974) demonstrated that margarite is only stable in the presence of an H_2O -rich fluid (i.e. $X_{\text{CO}_2} < 0.1$). Furthermore, the $T\text{-}X_{\text{CO}_2}$ diagram of Ellis (1978) shows that grossular garnet only appears at high H_2O fluid contents (see Fig. 3.6), confirmed by the experimental work of Aitken (1983), although its stability field enlarges with increasing T and CO_2 . Thus, the absence of these two minerals suggests the presence of a CO_2 -rich fluid in these calc-silicate rocks during metamorphism.

The observed assemblages which relate to this system are:

symplectite of Ca-plagioclase and zoisite replacing scapolite

(reactions 3.D and 3.E)

scapolite replacing zoisite (reaction 3.F)

Both of these assemblages appear as univariant equilibria on Fig. 3.6 suggesting that the fluid in equilibrium with the rocks was internally buffered at these high X_{CO_2} contents.

In relation to the symplectic assemblage, reaction 3.E (anorthite + calcite \rightarrow meionite) has been studied experimentally by Goldsmith & Newton (1977) and is shown on Fig. 3.4. The reaction is unusual in that it occurs at 875°C irrespective of the associated fluid composition, hence the horizontal topology of this reaction of the T-X_{CO₂} diagram (Fig. 3.6). However, there is a substitution of Na between meionite and any associated plagioclase which moves the reaction to lower temperatures with decreasing Na-content in the plagioclase and increasing Na-content in the scapolite (Goldsmith & Newton, 1977). Therefore, the observed coexistence of an An-rich plagioclase with scapolite in these rocks suggests temperatures somewhat lower than 875°C.

With regard to the two reactions involved in the development of this symplectite (meionite \rightarrow anorthite and anorthite \rightarrow zoisite), the anorthite \rightarrow meionite reaction was found to be difficult to reverse due to the large ΔS involved (~ 9.0 - Goldsmith & Newton, 1977), but appears to have done so in these rocks. This reversal has also been recognised by Aitken (1983) in calc-silicate rocks at Santa Lucia who, quite rightly, attributed it to a drop in temperature. A further drop in temperature would result in the anorthite reacting to produce zoisite (see path A on Fig. 3.6). However, Storre & Nitsch (1972) considered that the topology of the anorthite \rightarrow zoisite reaction on the T-X_{CO₂} diagram is a vertical straight line which would necessitate a decrease in X_{CO₂} of the co-existing fluid to drive the reaction. However, as all three phases: scapolite, zoisite and anorthite are seen to coexist in these rocks it suggests that the two reactions have not gone to completion which can be explained by a decrease in X_{CO₂} occurring simultaneously with a drop in temperature (path B on Fig. 3.6). Furthermore, the coexistence of zoisite and scapolite in the rocks requires that these reactions have occurred at fairly high pressures: the isobaric T-X_{CO₂} diagram of Ellis

(1978) at 4 kbar shows that zoisite and scapolite are unable to coexist whereas they are able to do so at 12 kbar (see Fig. 3.6).

From Fig. 3.6 the assemblage exhibiting the reaction: zoisite \rightarrow scapolite appears to be prograde and occurring without the intermediate anorthite phase. This reaction appears to occur at fairly low X_{CO_2} values and would introduce H_2O into the coexisting fluid as the reaction progressed along the $\text{zo} + \text{CO}_2 \rightarrow \text{me} + \text{H}_2\text{O}$ curve to the invariant point (I) where grossular would be produced (path C). However, as grossular is absent in these rocks it can be assumed that this reaction was driven by an increase in the CO_2 content of the coexisting fluid. In fact, if the vertical topology of this reaction (Storm & Nitsch, 1972) is correct, this reaction can only be driven by an increase in CO_2 content of the co-existing fluid.

All the above reactions occur within the same rock types, often within the same thin-section and often to varying stages of completion, whilst Fig. 3.6 shows that they require different temperatures and fluid compositions to occur. Therefore, it is likely that these reactions occurred at different times in the metamorphic evolution of the rocks, during both prograde and retrograde events, and with different coexisting fluids. This suggests that the fluid compositions were different in different parts of the marble, i.e. internally buffered. A similar situation has been deduced in other metasedimentary sequences (Hewitt, 1973; Vidale & Hewitt, 1973) especially if the interlayered rocks are of contrasting compositions, as at Tverrfjella, with different layers having fluids of different compositions, and little difference along the layers (Ferry, 1976a & b). Furthermore, very localised high $X_{\text{H}_2\text{O}}$ and X_{CO_2} conditions can occur, as is probably the case with the melt portion in the calc-silicate rock, in different parts of a metasedimentary rock (Valley & Essene, 1980).

To fully evaluate the nature of the fluids in the impure marbles would require further study involving systematic sampling over the marble-garnet-granulite contact and modal analyses of the assemblages. It is possible to calculate the expected fluid composition for the reactions above which could then be compared to the fluid composition estimated from the modal proportions of reactants and products. Any discrepancy could then be attributed to an external fluid source and its proportion calculated (cf. Rumble et al., 1982 in Rice & Ferry, 1982).

Other, more varied, assemblages also appear in these impure marbles, generally in the discrete pods within the marble, containing: garnet, tremolite, sphene, oxides, biotite and chlorite. With the addition of the components: FeO, MgO and K₂O to the system CaO-Al₂O₃-SiO₂-H₂O-CO₂, these assemblages are difficult to interpret on an idealised T-X_{CO₂} diagram. However, it is suspected that these assemblages equilibrated with rather more H₂O-rich fluids to allow the appearance of garnet and biotite. The appearance of tremolite, as a secondary phase after clinopyroxene, implies an increase in H₂O at some time as the stability-field of tremolite increases in size with increasing P_{H₂O} (Turner, 1968, p. 149). In relation to the isobaric univariant curve in the T-X_{CO₂} diagram for the system: MgO-CaO-SiO₂-H₂O-CO₂ (Fig. 3.7) it can be seen that a decrease in X_{CO₂} of the coexisting fluid from a high value (~1.0) will drive the reaction clinopyroxene → tremolite as will a drop in temperature at any fluid composition. The second of these possibilities is preferred in this case, as the change in composition of the coexisting fluid is then in accord with that postulated for the meionite → zoisite reaction discussed earlier.

Of interest is the assemblage clinopyroxene, plagioclase, secondary hornblende, sphene, oxides, biotite ± chlorite in one of these pods.

FIG. 3.7

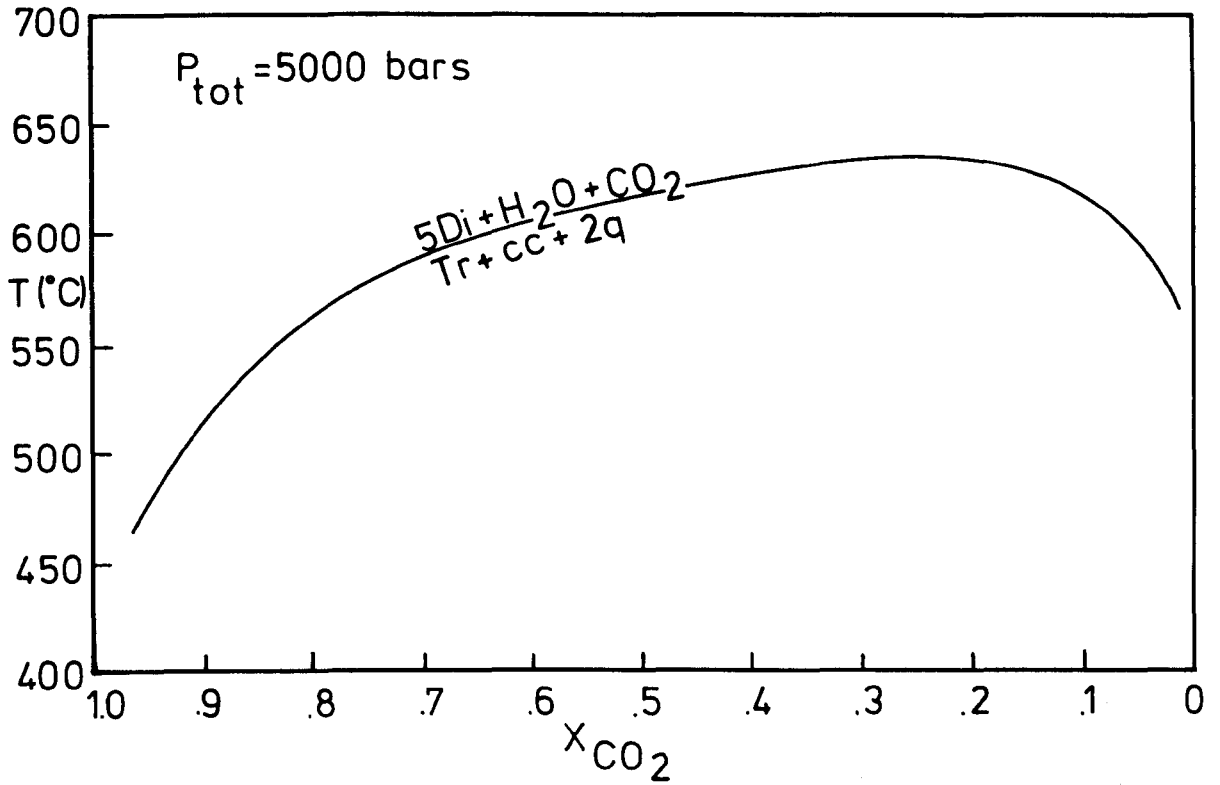
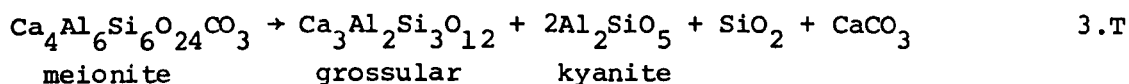


FIG. 3.7 Partial T-X_{CO₂} diagram at 5 kbar for the system: MgO-CaO-SiO₂-H₂O-CO₂ showing the topology of the univariant reaction 3.G (after Hunt & Kerrick, 1977, incorporating non-ideal mixing).

This pod lacks calcite suggesting lack of CO_2 in any coexisting fluid, or in very low concentrations. An unusual feature of the plagioclase is that it exhibits triple point boundaries and does not appear to have been derived from pre-existing omphacitic clinopyroxenes as does the polygonal textured plagioclase in the garnet-granulite. It is difficult to see why this particular assemblage should fail to produce any evidence of high-grade phases, e.g. symplectite, unless the coexisting fluid composition precluded such, perhaps by being H_2O -rich. Holland (1979) has described small knots of diopsidic pyroxene + tremolite + dolomite + calcite \pm quartz assemblages in marbles in the Tauern Window, Austria which he interpreted as relict high temperature, eclogite facies assemblages. He has also shown that the fluid in equilibrium with the marbles was $X_{\text{H}_2\text{O}} \approx 1.0$. Although the majority of the assemblages described above indicate an equilibrium fluid of high X_{CO_2} content ($>0.7?$), the limited degree of fluid mobility suggested does not preclude the possibility of some rocks equilibrating with very H_2O -rich fluids, as suggested by Holland, and this particular rock would appear to be one. It is possible that omphacitic pyroxenes once existed in this rock, but unmixing and re-crystallisation has been so complete (as postulated for the garnet-granulite) that no relics now exist.

From the intimate association between the marble and garnet-granulite seen as interlayering and mixing of the two rock types which has produced these unusual calc-silicate assemblages it seems certain that the marbles have followed the same P-T path as the garnet-granulite as shown in Fig. 3.4. This path crosses the grossular-in reaction and it has been suggested by Goldsmith & Newton (1977) that melonitic scapolite could transform to grossular, through the reaction:



(cf. reaction 3.5 and with a similar dP/dT slope). However, there appear to be two reasons why this phase has failed to appear in these calc-silicate rocks:

(i) Fig. 3.6 shows that grossular only appears at low X_{CO_2} values, and it has been shown that high X_{CO_2} values prevailed in the rocks.

(ii) Goldsmith & Newton (1977) were unable to reverse their experiments for reaction 3.E (i.e. meionite \rightarrow anorthite) because of the large ΔS of the reaction (~ 9.0), and it seems reasonable to suppose that an equivalent difficult of reaction would be experienced in any conversion of meionite to grossular and anorthite.

3.2 GEOCHEMISTRY

3.2.1 The garnet-granulite

From his study of the garnet-granulite, Hernes (1954b) considered a possible volcanic origin for this rock, considering its close association with the marble bodies, even though his observations suggested that the garnet-granulite had an original gabbroic (i.e. plutonic) assemblage. His preferred explanation was that the garnet-granulite represented a skarn formation between the granitised gneisses, surrounding the Tverrfjella Unit, and the marble bodies. The granitisation of the gneisses, which Hernes considered to have been originally sediments, was thought to have occurred through a granitisation 'front' which donated K and Si to the rocks, and removed Na, Mg and Fe from them. Furthermore, he considered the gneisses to be compositionally zoned, on a large scale, from quartz-diorite through granodiorite to granite at increasing distances from the garnet-granulite.

Such a granitisation process is not considered to be a feasible process in the case of these rocks, for several reasons:

(i) To produce the large volumes of gneiss present in the vicinity of the Tverrfjella Unit would require an enormous source of K and Si ions. Although meta-igneous granitic rocks are considered to exist elsewhere on the Molde Peninsula (see Chapter 4) which could have acted as a source for these ions, the rocks do not exhibit large depletions of K and Si.

(ii) A driving force is required to diffuse these elements in the rock being granitised. Although chemical or thermodynamic potentials are possible, these have been shown to take place over only very small distances (intercrystalline) and not over the large distances necessary for the production of these extensive tracts of gneisses (e.g. Krogh & Davis, 1973).

(iii) Although the gneisses around the Tverrfjella Unit are heterogeneous in both appearance and composition (see Chapter 5), they have not been found to be compositionally zoned as suggested by Hernes. Furthermore, Hernes' use of the word 'skarn' to describe the garnet-granulite implies that it is a rock composed of predominantly calc-silicate minerals produced by the thermal metamorphism (through granitisation) of the impure marbles. However, such calc-silicate assemblages are only locally present and generally at the marble/garnet-granulite contacts and not throughout the latter as a whole.

Considering the close association between the garnet-granulite and the marble, the presence of the overlying pelites, the appearance of mineralogical variations (e.g. carbonate-rich or kyanite-rich zones) and the compositional layering of the rock, another possibility which has to be examined is that the garnet-granulite represents a metamorphosed sediment. Examining the analyses of the garnet-granulite (presented in

FIG. 3.8

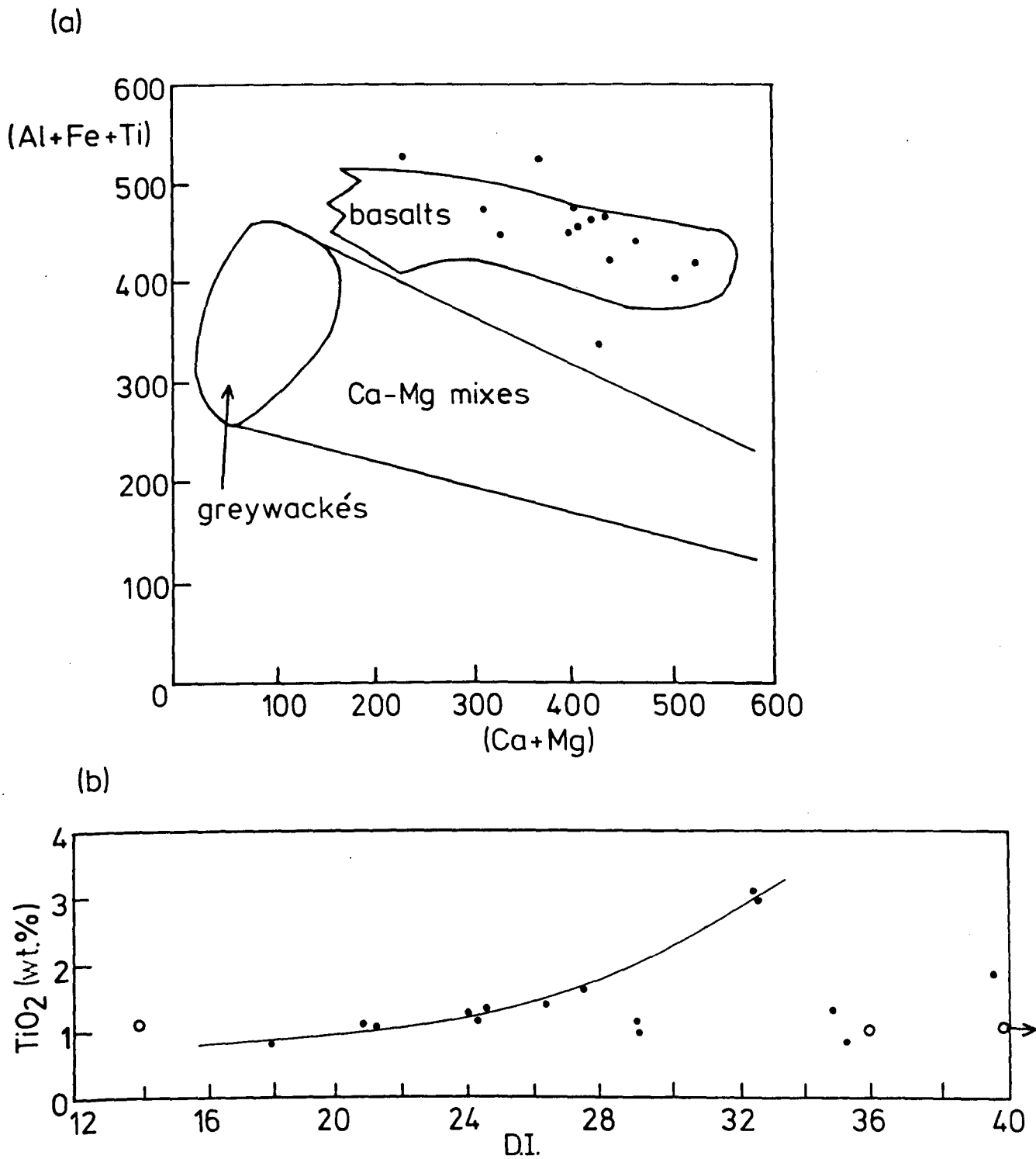


FIG. 3.8(a) (Al + Fe + Ti) vs. (Ca + Mg) in milliatoms after Moine & de la Roche (1968).

(b) TiO_2 vs. D.I. of Thornton & Tuttle (1960) (i.e. normative $q + or + ab + ne + lc + ks$). Dots = Garnet-Granulite, circles = amphibolites from the heterogeneous rocks.

Table 3.1 - plus an average composition) with this possibility in mind, three points can be made:

(i) The intimate mixing between the marble and the garnet-granulite suggests that the latter could be a very impure calcareous sediment. Although the analyses are fairly calcic and aluminous, perhaps suggesting the prior existence of calcite and clays respectively, the K contents are rather too low to support the contention of a clay-rich sediment. Also, the rocks are fairly Fe and Mg-rich.

(ii) The trace metal contents of Ni and Cr are rather high for a sedimentary rock (Turekian & Wedepohl, 1961).

(iii) The overall composition of the rocks is fairly consistent which may reflect a sedimentary parentage since great thicknesses of homogeneous sediments are present in the geological record.

Moine & de la Roche (1968) have produced diagrams specifically for the discrimination between sedimentary and igneous rocks. One of these has been used as an initial test of the chemical nature of the garnet-granulite and is shown in Fig. 3.8(a); this shows a basaltic chemistry for the rocks. The compositional consistency of the rocks is reflected by the fairly good grouping of the points in this diagram.

Leake has also attempted to graphically discriminate between meta-igneous and meta-sedimentary rocks, generally through the use of Niggli numbers (Leake, 1969; van de Kamp et al., 1979). He has also examined ortho- and para-amphibolites in relation to their concentrations of Cr, Ni and Ti (Leake, 1964) and considers that ortho-amphibolites contain higher contents of these elements, typically >100 ppm for Cr, >80 ppm for Ni and >1.0% for TiO_2 . Furthermore, he found negative correlations between Ni and Ti, and Cr and Ti. From the average analysis in Table 3.1 it can be seen that the contents of Cr and Ni (361 ppm and 138 ppm

TABLE 3.1 Whole-rock analyses and normative minerals for the garnet-granulite of the Tverrfjella Unit

	E10	OM1	D14	D17	D19	141	143	144	1410	1417	1423	1426	1428	1429	Average \bar{x}	σ
MAJOR ELEMENTS (wt. %)																
SiO ₂	49.16	49.64	46.71	45.81	48.16	49.15	48.54	49.53	53.04	51.36	48.82	48.27	47.10	50.75	48.98	1.79
TiO ₂	1.10	1.26	1.30	0.99	1.27	1.08	0.80	1.02	2.93	0.78	1.59	1.35	1.12	1.78	1.31	0.52
Al ₂ O ₃	15.41	14.27	14.48	14.53	15.13	15.07	14.57	16.12	13.57	15.16	13.81	14.28	17.99	14.21	14.90	1.07
Fe ₂ O ₃	2.41	3.84	3.84	3.01	2.43	4.40	3.45	4.49	4.89	0.36	2.58	4.30	7.26	4.07	3.67	1.51
FeO	9.13	7.53	6.66	6.32	7.47	7.13	5.53	5.86	11.28	7.84	9.39	7.55	4.87	8.63	7.51	1.64
MgO	8.09	7.85	9.77	9.13	5.13	9.78	13.33	9.03	4.07	6.31	8.22	7.47	5.90	6.81	7.92	2.23
MnO	0.16	0.20	0.17	0.15	0.11	0.13	0.12	0.18	0.27	0.12	0.17	0.19	0.16	0.26	0.17	0.05
CaO	11.26	11.40	12.33	11.73	11.43	10.71	10.67	11.25	7.30	9.93	10.98	12.22	12.48	8.03	10.84	1.46
Na ₂ O	3.24	2.33	3.06	4.17	4.24	2.37	2.01	2.40	1.69	2.40	2.71	3.04	2.55	4.64	2.92	0.85
K ₂ O	0.39	0.65	0.40	0.69	0.75	0.10	0.14	0.08	0.04	3.50	0.76	0.08	0.30	0.05	0.57	0.86
P ₂ O ₅	0.12	0.10	0.07	0.04	0.13	0.16	0.04	0.08	0.31	0.09	0.11	0.12	0.12	0.12	0.12	0.06
S	0.00	0.02	0.00	0.01	0.08	0.01	0.00	0.01	0.01	0.02	0.00	0.01	0.00	0.02	0.01	0.02
H ₂ O ^T	0.53	1.13	0.73	0.83	1.00	0.53	0.77	0.42	0.25	1.07	0.71	0.71	0.98	0.76	0.74	0.25
CO ₂	0.65	0.00	0.76	2.22	3.21	0.04	0.04	0.00	0.02	1.38	0.02	0.18	0.03	0.00	0.61	0.96
TOTAL	101.65	100.22	100.28	99.63	100.54	100.66	100.01	100.47	99.67	100.32	99.87	99.77	100.86	100.13	100.27	
TRACE ELEMENTS (ppm)																
Ni	70	102	262	222	255	178	362	112	0	123	61	92	20	76	138	100
V	360	343	274	242	294	-	-	-	-	171	-	-	-	-	281	63
Cr	351	344	567	606	592	456	717	320	80	244	178	203	193	203	361	189
Zn	92	82	76	77	93	54	57	57	95	85	87	100	13	61	74	22
Cu	84	138	76	114	29	4	53	151	4	6	0	89	14	0	54	52
Rb	10	9	6	9	13	1	2	4	2	100	8	4	0	3	12	25
Sr	81	103	99	72	126	89	71	179	65	128	80	189	32	71	99	42
Y	32	32	28	27	33	25	16	23	75	21	28	30	4	42	30	15
Zr	50	59	66	55	69	75	46	57	180	88	82	82	93	125	81	34
Pb	5	2	9	0	5	3	0	4	0	8	6	0	0	1	3	3
Ba	103	77	98	98	152	56	50	66	82	480	107	55	72	58	111	106
Ce	-	-	-	-	-	28	13	2	30	-	0	15	4	23	14	11
Ga	-	-	-	-	-	17	14	17	22	-	21	27	0	27	18	8
Nb	-	-	-	-	-	7	7	7	8	12	10	11	6	7	8	2
Th	-	-	-	-	-	4	0	3	1	-	4	4	0	0	2	2
NORMATIVE MINERALS (%)																
q	-	0.20	-	-	-	-	-	0.30	17.88	-	-	-	0.69	-	-	
or	2.31	3.84	2.36	4.08	4.43	0.59	0.83	0.47	0.24	20.68	4.49	0.47	1.77	0.30	3.37	
ab	25.56	19.72	17.60	12.59	23.64	20.06	17.01	20.31	14.30	16.89	22.93	25.73	21.58	39.26	24.71	
an	26.35	26.56	24.59	18.89	20.04	30.19	30.32	32.98	29.32	20.26	23.27	25.08	36.73	17.80	25.87	
ne	1.01	-	4.49	12.30	6.63	-	-	-	-	1.85	-	-	-	-	-	
di	23.43	23.67	28.84	31.27	29.34	17.53	17.70	17.76	4.05	23.35	24.84	28.03	19.14	17.27	21.88	
hy	-	16.67	-	-	-	20.60	16.21	19.40	19.94	-	4.59	2.81	6.84	6.41	7.19	
ol	15.79	-	12.53	10.94	5.73	2.17	10.39	-	-	12.46	11.85	7.47	-	8.48	7.63	
mt	3.49	5.57	5.57	4.36	3.52	6.38	5.00	6.51	7.09	0.52	3.74	6.24	10.53	5.90	5.32	
il	2.09	2.39	2.47	1.88	2.41	2.05	1.52	1.94	5.51	1.48	3.02	2.56	2.13	3.38	2.49	
py	-	0.04	-	0.02	0.15	0.02	-	0.02	0.02	0.04	-	0.02	-	0.04	0.02	
ap	0.28	0.23	0.16	0.09	0.30	0.37	0.09	0.19	0.72	0.21	0.26	0.28	0.28	0.28	0.28	
TOTAL	100.31	98.89	98.61	96.42	96.19	99.96	99.07	99.88	99.07	97.74	98.99	98.69	99.69	99.12	98.76	
D. I.	28.87	23.76	24.46	28.96	34.70	20.65	17.84	21.09	32.42	39.42	27.42	26.20	24.04	39.56		

D. I. is the Differentiation Index of Thornton & Tuttle (1960) i.e. normative q + or + ab + ne + lc + ks

respectively) in the garnet-granulite indicate a meta-igneous parentage on this basis. From the analyses as a whole, the two negative correlations seen by Leake also exist in the garnet-granulite, i.e. sample 1410 has the highest TiO_2 content (2.93%) and the lowest Ni and Cr contents (0 ppm and 80 ppm respectively), whilst sample 143 has the lowest TiO_2 content (0.80%) and the highest contents of Ni and Cr (362 ppm and 717 ppm respectively). From this evidence, a meta-igneous, basaltic parentage for the garnet-granulite is preferred here, rather than a sedimentary parentage.

Even so, the possibility exists that the rocks have been derived as sediments from an original basaltic rock and that the present basaltic classification is a remnant of that original chemistry. However, the actual process of weathering has a profound effect upon the chemistry of rocks particularly the ferro-magnesian minerals, as would be found in a basalt, with the loss of Na, Ca and Mg fairly quickly from the rock being weathered followed by K and Si (Krauskopf, 1979, p. 83-84). If such alterations had affected the precursor to the garnet-granulite, it is considered that any sort of original, igneous differentiation trend would have been significantly disturbed.

Fig. 3.8(b) shows the analyses plotted on a TiO_2 vs. the Differentiation Index (D.I.) of Thornton & Tuttle (1960), and a differentiation trend is fairly well defined thereby confirming an igneous precursor for the garnet-granulite. The points falling towards high D.I. values tend to be those samples displaying amphibolitisation (D17, D19), with increased K_2O contents, or those containing relatively greater amounts of plagioclase (E10, 1417, 1429), with increased Na_2O contents. It is interesting to note that there does not appear to be any deviation of points from the line in Fig. 3.8(b) as a result of large fluctuations in the TiO_2

contents of the samples. This element has been considered to be immobile in rocks metamorphosed up to amphibolite/granulite facies (Pearce & Cann, 1973; Floyd & Winchester, 1977). As the garnet-granulite has been shown to have suffered eclogite facies metamorphism it would appear that Ti is also immobile at this higher grade.

Certain other elements are also considered to be immobile during the high-grade metamorphism of basaltic rocks, e.g. Zr, Y, Nb, Ce and Ga (Pearce & Cann, 1973; Field & Elliot, 1974; Floyd & Winchester, 1978). To investigate the degree of alteration and disturbance suffered by the garnet-granulite during its metamorphic history, plots of various element oxides and trace elements were constructed against Zr (cf. Liégeois & Duchesne, 1981 - see Fig. 3.9). The majority of the major element oxides display fairly scattered patterns. From studies on eclogite rocks occurring elsewhere in the Basal Gneiss Complex Bryhni et al. (1969) found that during metamorphism the most mobile elements in these rocks were: K, Al and H (added) and Ca, Si and Na (removed - see Chapter 7, section 7.2.1). Fig. 3.9 shows that the very same element oxides in the garnet-granulite display the most random patterns and deviations from any sort of differentiation trend. However, FeO^t , MnO , P_2O_5 and Y show some degree of correlation with Zr, and Ti especially so. Binns (1967) considered that Cr would be mobile in eclogite rocks, but the good correlation of this element with Zr in Fig. 3.9 does not support this finding. Unlike the other elements in Fig. 3.9, both Cr and Ni show two correlation lines with Zr. The group of rocks with steeper metal/Zr slopes also have higher absolute metal contents (D14, D17, D19, 141 and 143). To give a greater separation of the points on these two plots, a log metals vs. Zr plot is shown in Fig. 3.10; plots of log metals vs. $\text{FeO}^t/(\text{FeO}^t + \text{MgO})$ are shown in Fig. 3.11. In all these diagrams two

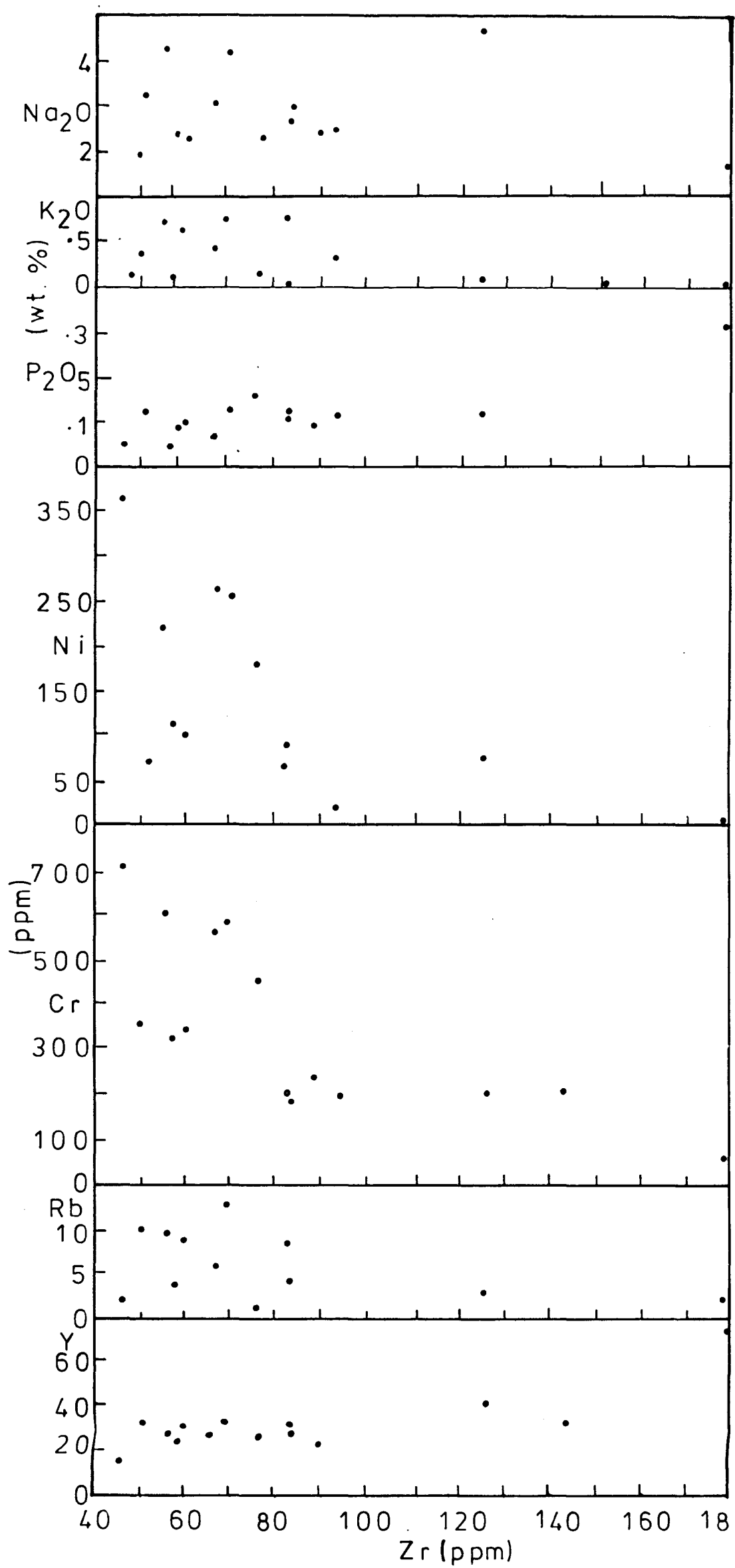
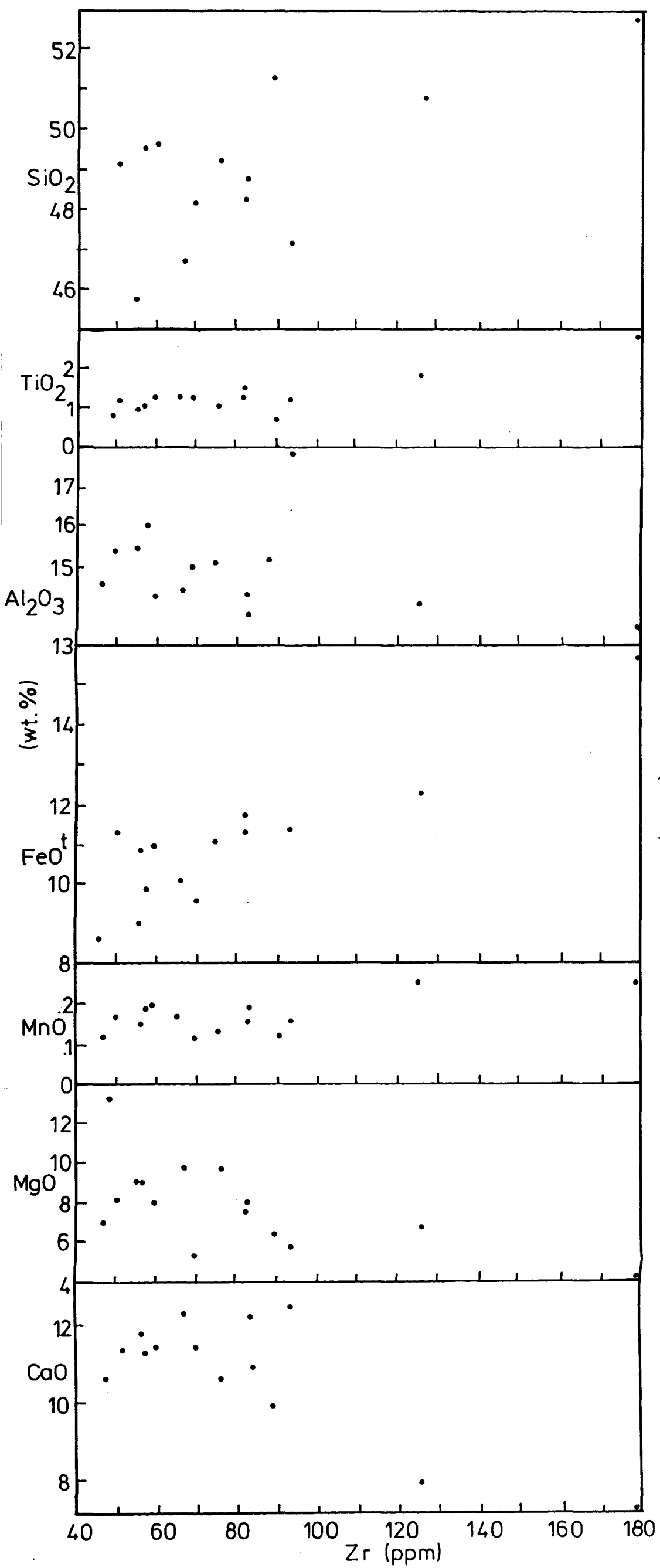
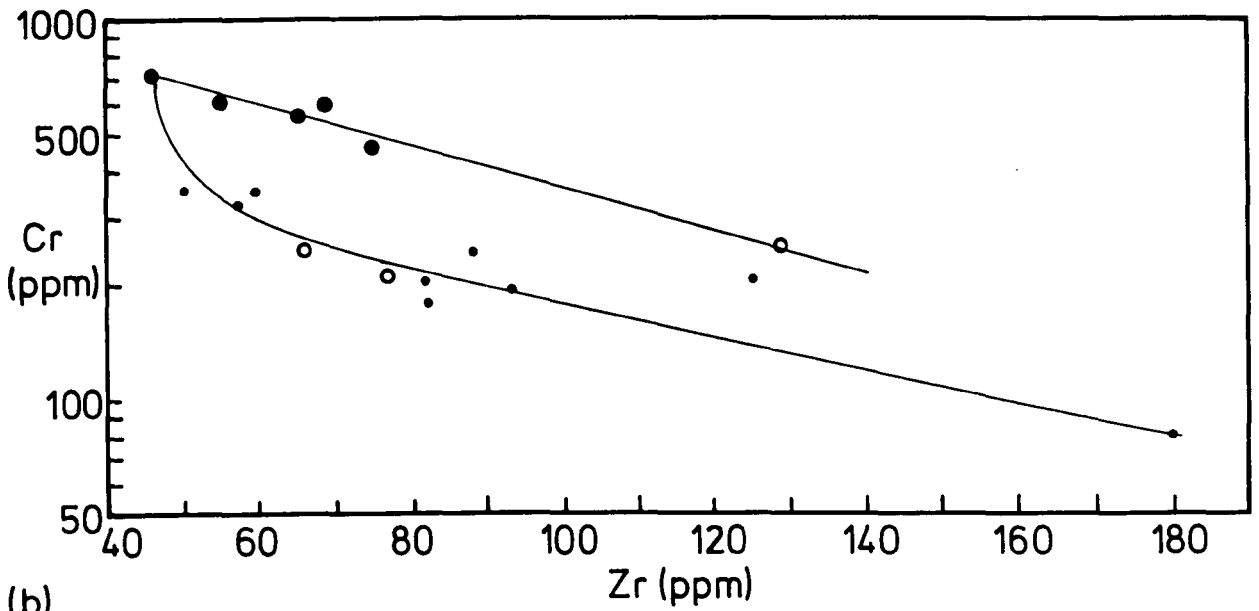


FIG. 3.9

FIG. 3.9 Selected elements plotted against Zr (cf. Liégeois & Duchesne, 1981).

FIG. 3.10

(a)



(b)

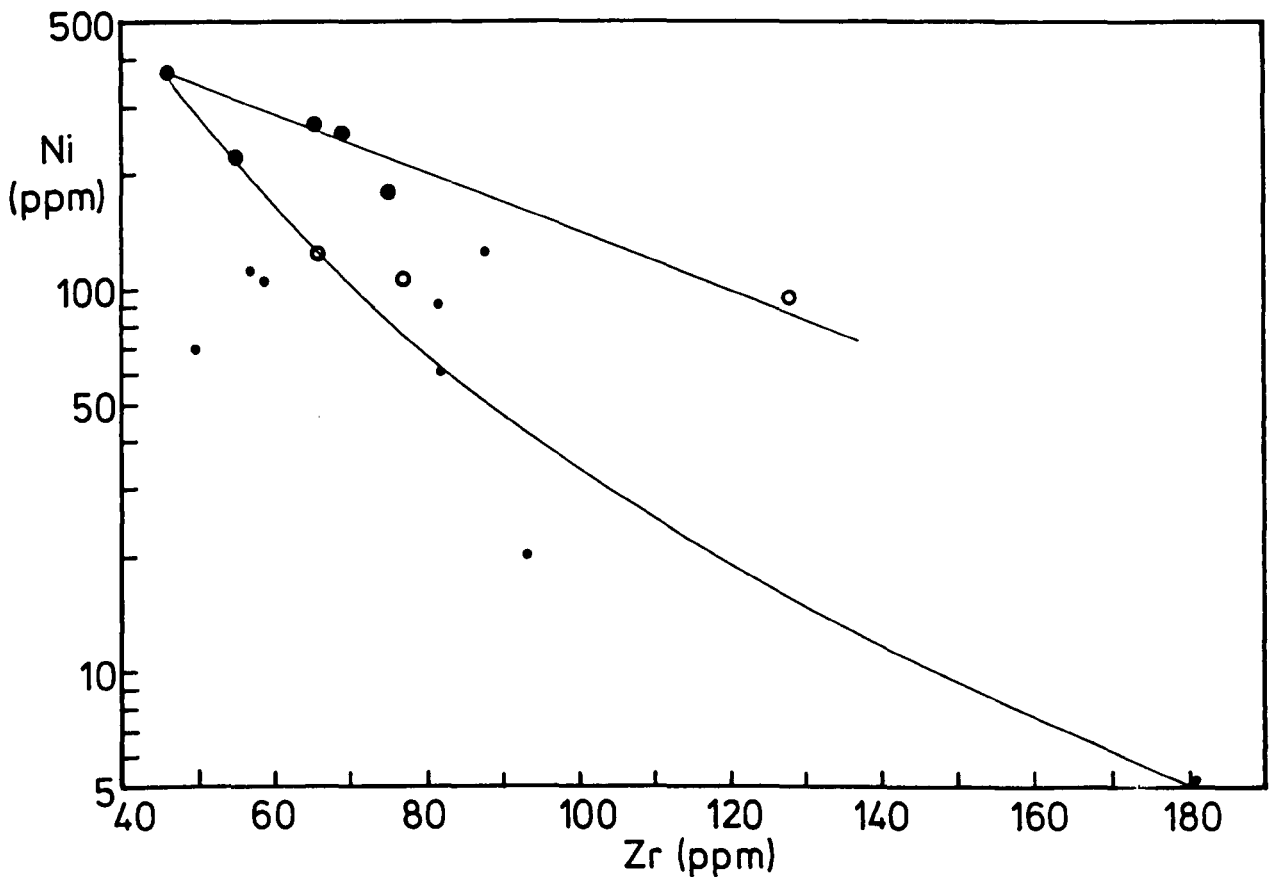


FIG. 3.10 Cr vs. Zr, and Ni vs. Zr, log/linear showing the division of the samples into two covariant trends. Large dots = samples with high metal contents; small dots = samples with low metal contents; circles = amphibolites from the Heterogeneous rocks higher in the Tverrfjella Unit (section 3.2.3).

FIG. 3.11

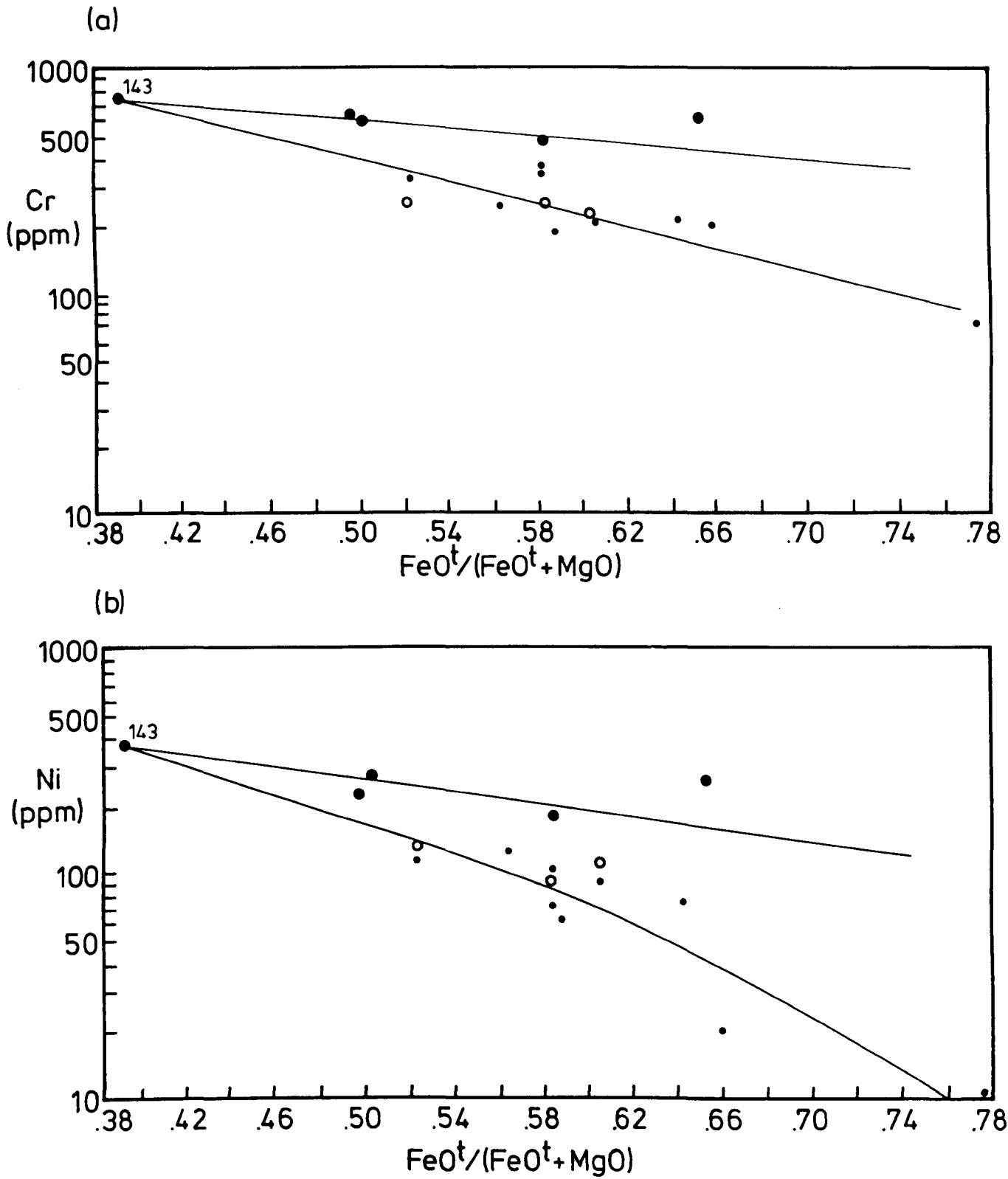
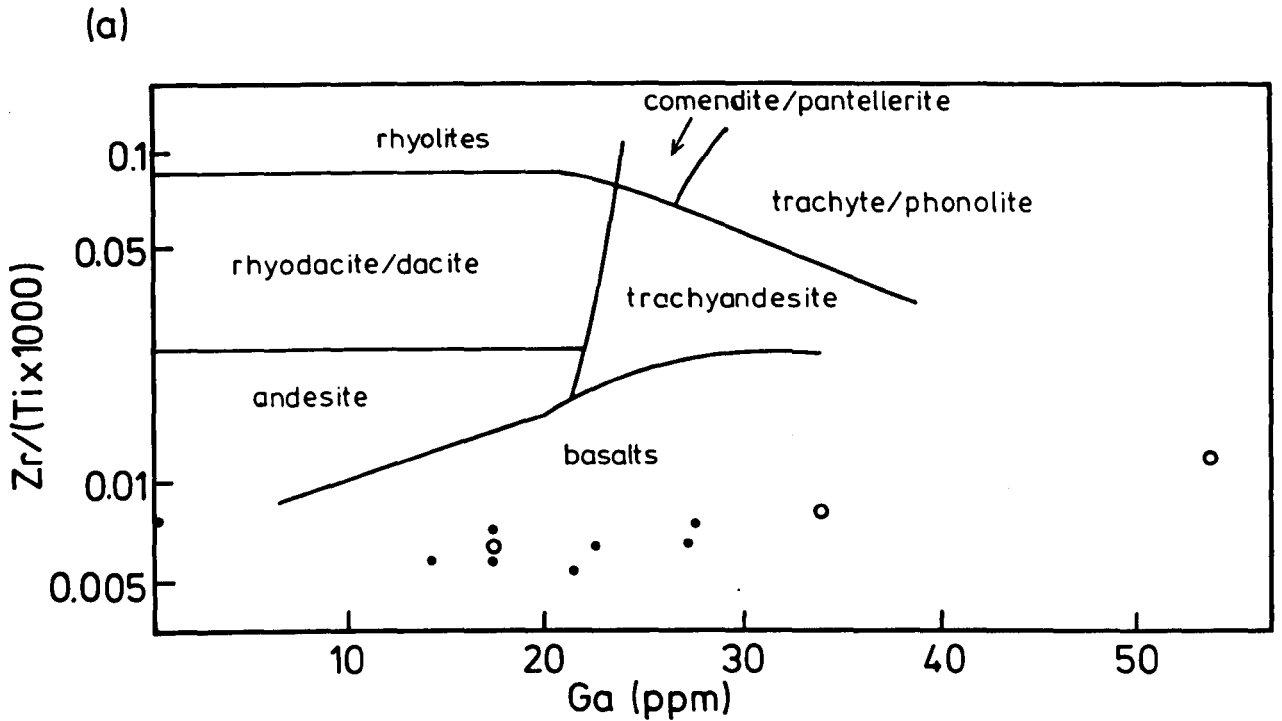


FIG. 3.11 Cr vs. $\text{FeO}^t/(\text{FeO}^t + \text{MgO})$, and Ni vs. $\text{FeO}^t/(\text{FeO}^t + \text{MgO})$, log/linear showing two covariant trends. Symbols as in FIG. 3.10.

FIG. 3.12



(b)

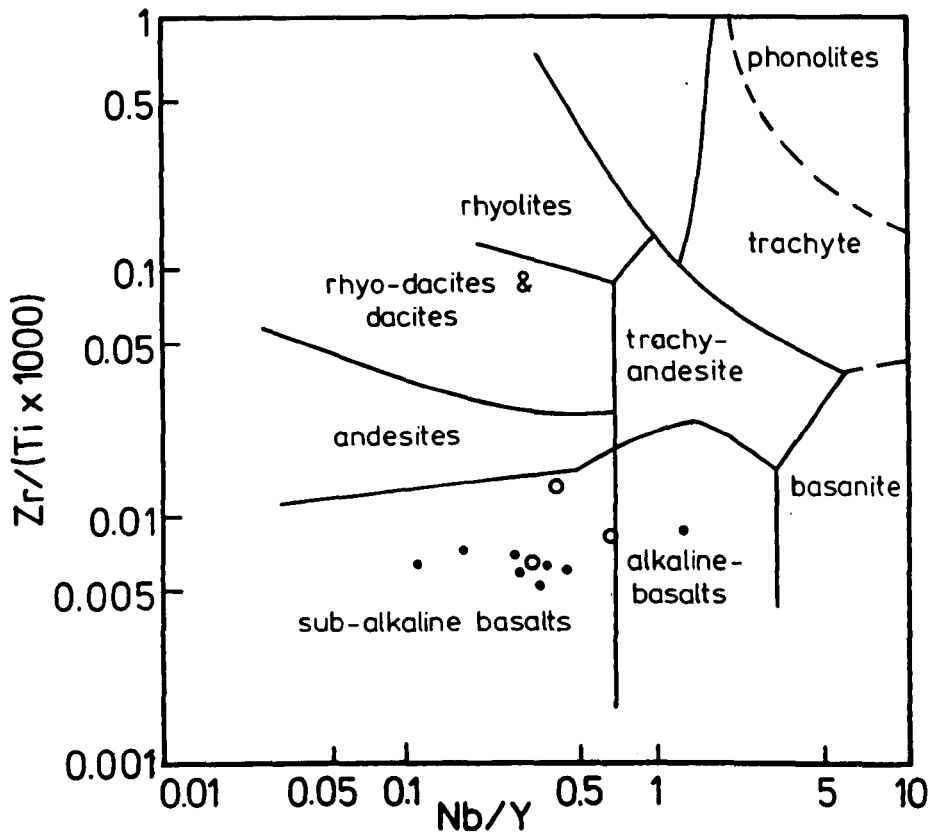


FIG. 3.12(a) $Zr/TiO_2 \times 10,000$ vs. Ga, log/linear after Floyd & Winchester (1978) for those samples of the Garnet-Granulite analysed for Ga. Dots = Garnet Granulite; circles = amphibolites from the Heterogeneous Rocks higher in the Tverrfjella Unit (section 3.2.3).

(b) $Zr/TiO_2 \times 10,000$ vs. Nb/Y, log/linear after Floyd & Winchester (1978) for those samples of the Garnet Granulite analysed for Nb. Symbols as in FIG. 3.12(a).

trends are clearly visible, although sample 1428 appears to have an anomalously low Ni value. The appearance of these correlation lines confirms the igneous nature of the precursor to the garnet-granulite and also suggests that there are two groups of rocks here with different differentiation trends. The good separation of the two trends against $\text{FeO}^{\text{t}}/(\text{FeO}^{\text{t}} + \text{MgO})$ (Fig. 3.11) suggests that the differentiation in this precursor was controlled by the fractionation of ferromagnesian minerals, in particular olivine and pyroxene which accept Ni and Cr into their respective structures. However, the appearance of an apparently continuous line of differentiation on other binary plots (e.g. Ti vs. Zr - Fig. 3.9) implies that these two groups were erupted at different times from different sources, whilst undergoing the same fractionation process (see Cox, Bell & Pankhurst, 1979, p. 37).

An important feature of these two trends is that both can be extrapolated back to a common point near to sample 143. Not only does this particular sample contain the largest amounts of Ni and Cr, it also has the largest amount of MgO (13.33%) and the lowest D.I. (17.84). These values suggest that this particular sample had a precursor which was particularly rich in ferromagnesian phases and therefore not a greatly fractionated assemblage.

A differentiation trend has also been discerned in eclogite rocks in the Alps (Liégeois & Duchesne, 1981) which was interpreted as the result of fractional crystallisation of a noritic gabbro (i.e. orthopyroxene ± olivine), thus indicating the occurrence of eclogite facies metamorphism of basaltic rocks within the crust (see discussion in section 1.2).

The scattered plots of the majority of the elements (Fig. 3.9) suggests a certain degree of mobility of those elements during metamorphism which makes it difficult to classify the original basalt type

of the garnet-granulite. However, a first approximation may be made by ignoring those samples which fall away from the differentiation trend on the Ti vs. D.I. plot (Fig. 3.8(b)) and assuming that the remaining samples do not possess greatly disturbed chemistries. With regard to the normative minerals, tholeiitic basalts are characterised by high hy, appreciable q and rare ol, whilst alkali-olivine basalts have conspicuous ol and often ne. Consequently, the samples falling on the curve in Fig. 3.8(b) appear to be tholeiites or olivine-tholeiites, i.e. they exhibit hy-normative \pm ol \pm q chemistries (see Table 3.1).

A few of the samples were analysed for Ga and Nb, both of which are considered to be immobile elements during metamorphism (Floyd & Winchester, 1978). Using their discrimination diagrams, the rocks again show a sub-alkaline (tholeiitic) character, with low Ga and Zr/TiO₂ values (Figs. 3.12(a) and (b)).

Various schemes, using both immobile major and immobile trace elements have been devised to classify basalts by geotectonic origin: Pearce & Cann (1973); Pearce & Norry (1973); Pearce (1975, 1976); Floyd & Winchester (1975, 1978); Winchester & Floyd (1977); Dixon et al. (1981); Gale & Pearce (1982); Shervais (1982); Mullen (1983). In particular, the Zr-(Ti/100)-(Y x 3) diagram of Pearce & Cann (1973) has been widely used in classification studies (see review by Zeck & Morthorst, 1982). The studies cited above have suggested that the elements: P, Mn and Cr are undisturbed by metamorphism up to greenschist facies, and Ti, Y and Zr are undisturbed up to granulite facies. However, the trends shown in Fig. 3.9 suggest that the elements Ti, Y, Zr and Cr appear to be unaffected by metamorphism up to eclogite facies, although P and Mn show some degree of scatter. Using the data in Table 3.1 the eigenvalue method of Pearce (1976) gave very scattered plots, whilst the Niggli-

number plots of Leake (1969) and van de Kamp et al. (1979) gave ambiguous results due to the restricted number of analyses available which could not define a satisfactory trend, necessary for these types of discrimination diagram.

The discrimination plots for the garnet-granulite are shown in Figs. 3.14-3.17 and in all of them the rocks fall into the fields of ocean-floor basalts and/or island-arc basalts. Samples 1428 and 1410 show erratic behaviour on these plots; 1428 has an extremely low Y content whilst 1410 has both high Y and high TiO_2 contents. Care has to be taken when interpreting these diagrams since some of them have overlapping fields (3.13(a), 3.15(a), 3.16(a) and (b)) which makes it difficult to be conclusive about the geotectonic paragenesis they indicate. Also, Fig. 3.13(b), cf. Shervais (1982), lacks the full complement of data due to the restricted number of V analyses, whilst Fig. 3.15 (b) of Mullen (1983) uses elements which have been shown not to be completely immobile (see Fig. 3.9 with respect to Mn and P). The most important plot of this group is Fig. 3.14(a) of Pearce (1975) since this makes a clear distinction between ocean-floor basalts and low-K-tholeiites (typical of island-arc volcanics, Windley, 1977, p. 246). By way of a cross-check on these diagrams it is constructive to examine the absolute values of elements in typical analyses of ocean-floor and island-arc basalts, in comparison with the garnet-granulite. Rivalenti (1976) gives ranges of values for both oceanic and island-arc basalts (see Table 3.2). According to Tarney et al. (1976) and Gale & Pearce (1982) the most valuable elements in such a comparison are: Ni, Cr, Ti, Y and the alkalies and LIL:K, Ba and Rb. Unfortunately, in the garnet-granulite the latter groups appear to be too greatly disturbed to be of any use. A comparison of Tables 3.1 and 3.2 shows that the majority of the Cr and Ni

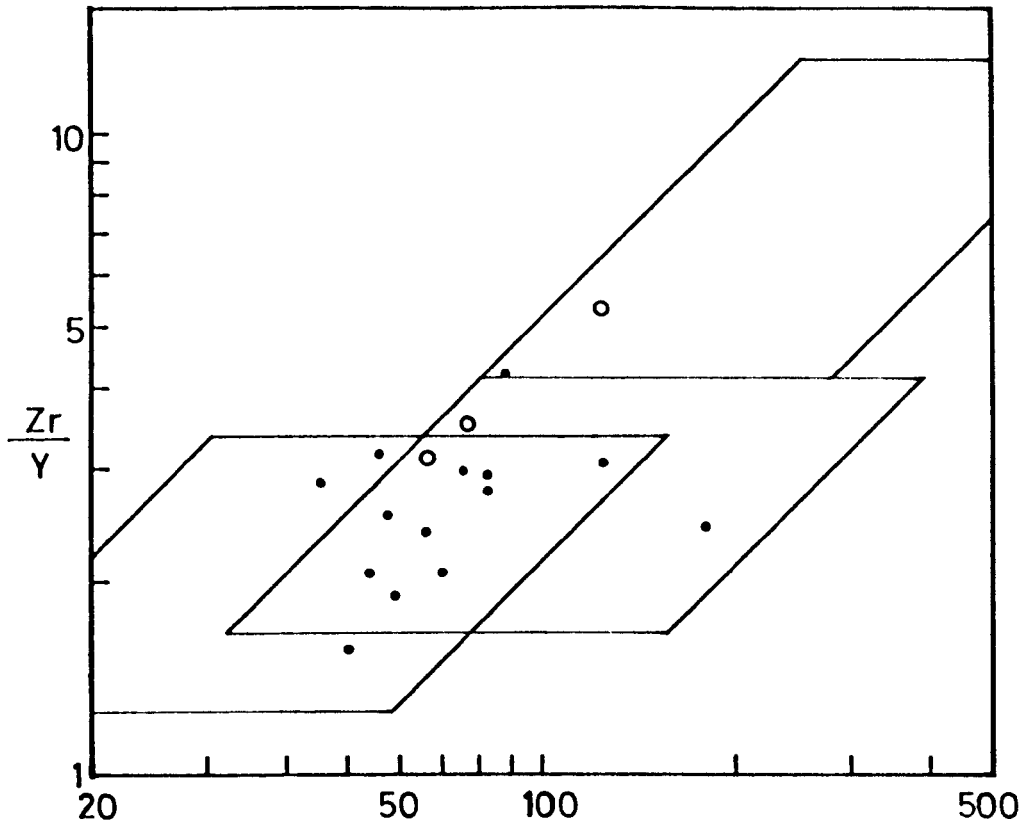
TABLE 3.2 Average contents of selected elements for oceanic and island-arc basalts, from Rivalenti (1976) with Y-values from Tarney et al. (1976) compared to the values from the garnet-granulite

	Oceanic	Island-arc	Garnet-granulite
TiO ₂ (wt. %)	1.4 - 2.4	0.5 - 1.5	0.78 - 2.93 (1.31)
Cr (ppm)	296 - 400	2 - 50	80 - 717 (361)
Ni (ppm)	97 - 170	6 - 30	0 - 362 (138)
Y (ppm)	43	~19	16 - 42 (28)

Average contents for the garnet-granulite are in brackets. The Y value for the garnet-granulite omits samples 1410 and 1428.

FIG. 3.13

(a)



(b)

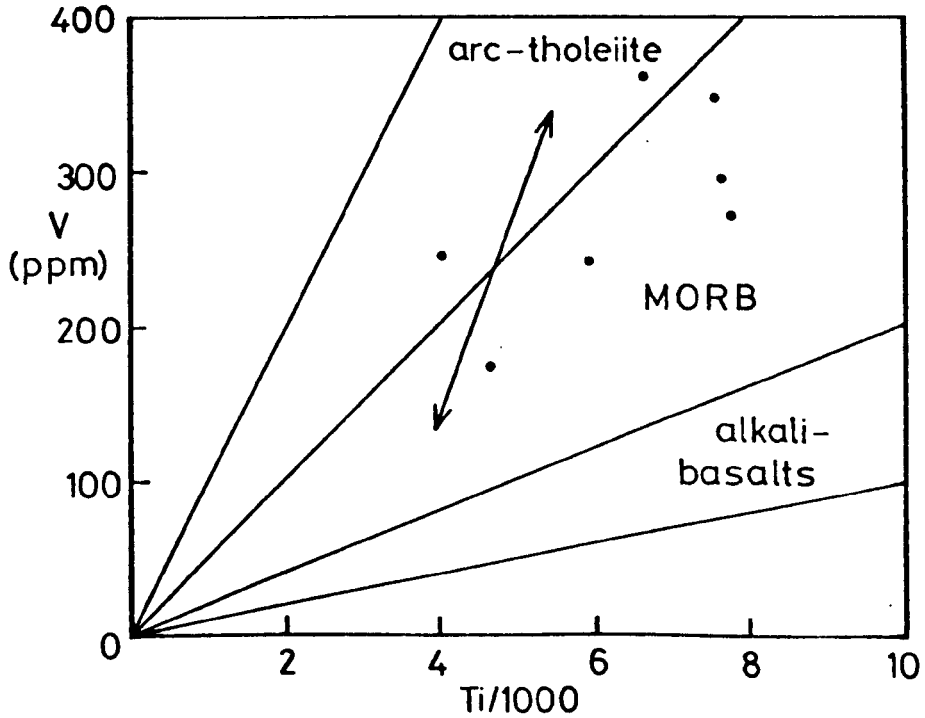
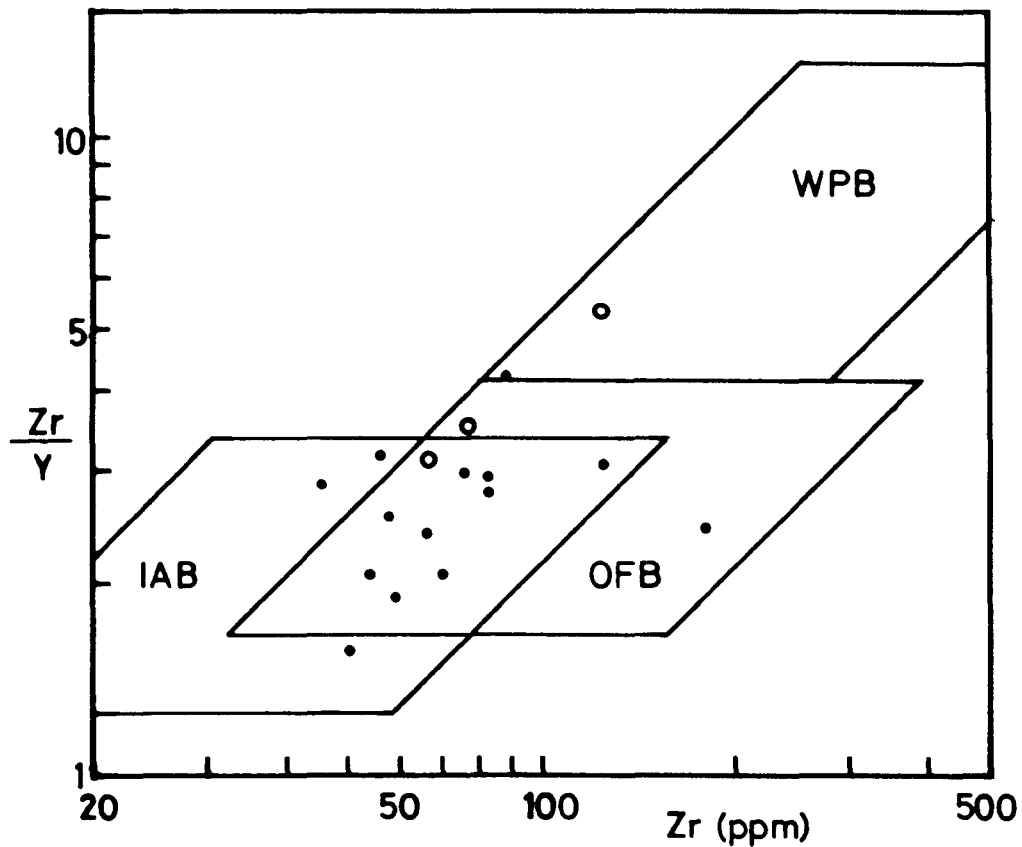


FIG. 3.13(a) Zr/Y vs. Zr , log/log after Pearce & Norry (1979).
 (b) V vs. $Ti/1,000$ after Shervais (1982) for samples of the Garnet-Granulite analysed for V . Symbols as in FIG. 3.12(a).

FIG. 3.13

(a)



(b)

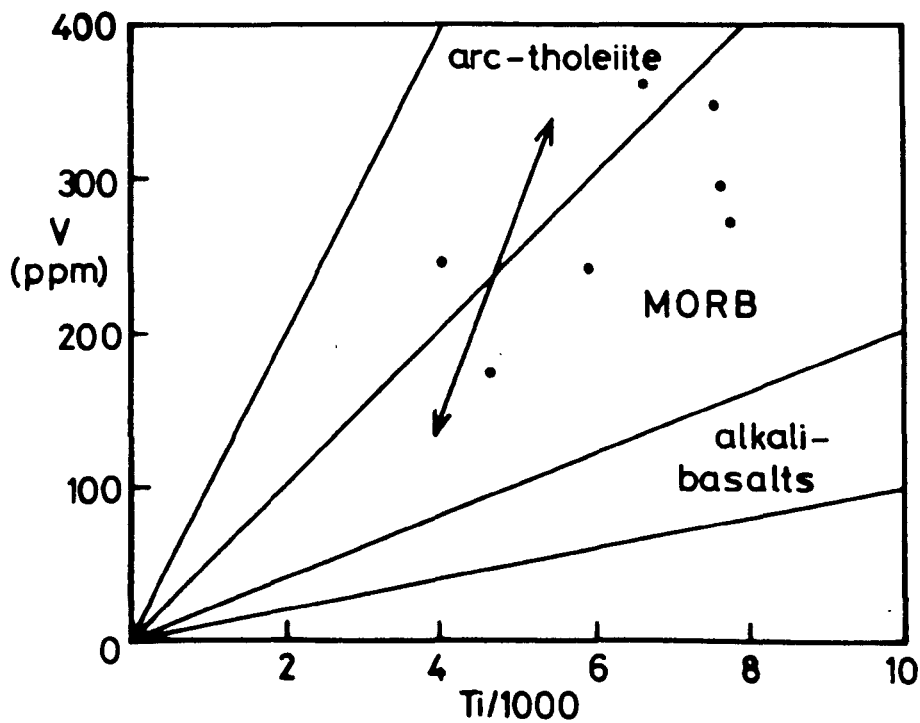


FIG. 3.13(a) Zr/Y vs. Zr, log/log after Pearce & Norry (1979).
 (b) V vs. Ti/1,000 after Shervais (1982) for samples of the Garnet-Granulite analysed for V. Symbols as in FIG. 3.12(a).

FIG. 3.14

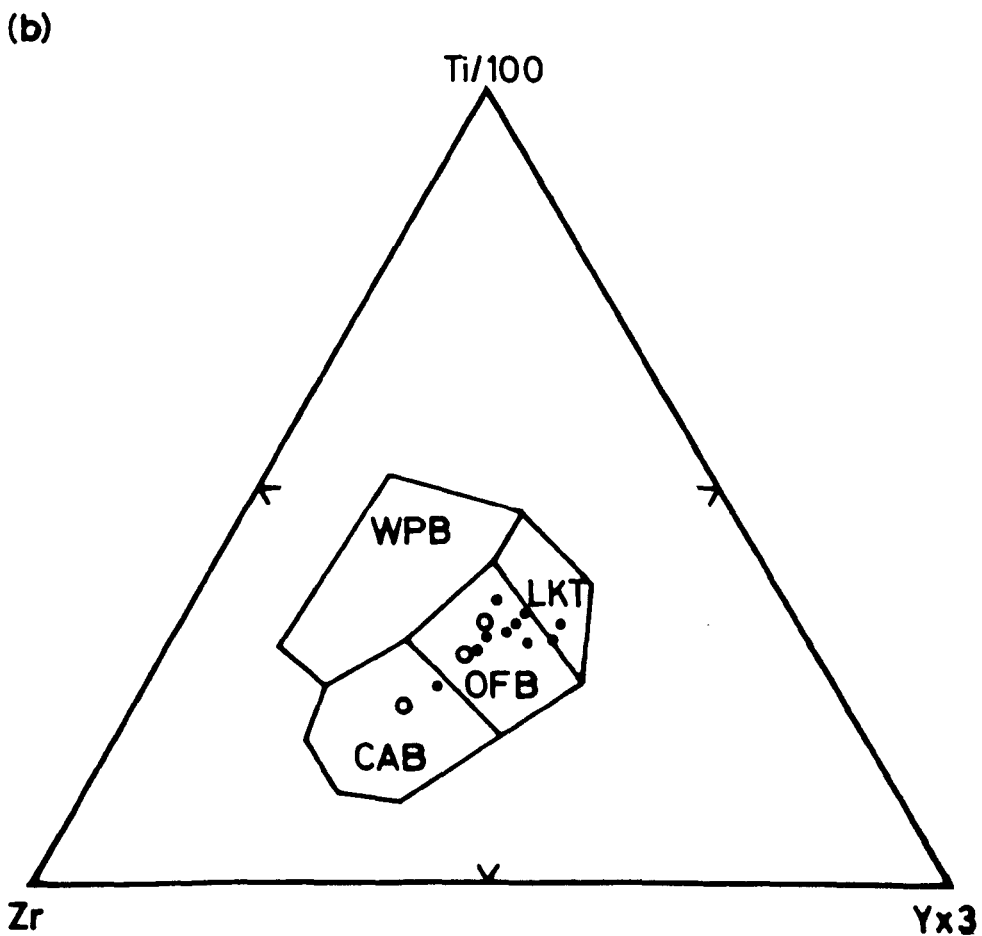
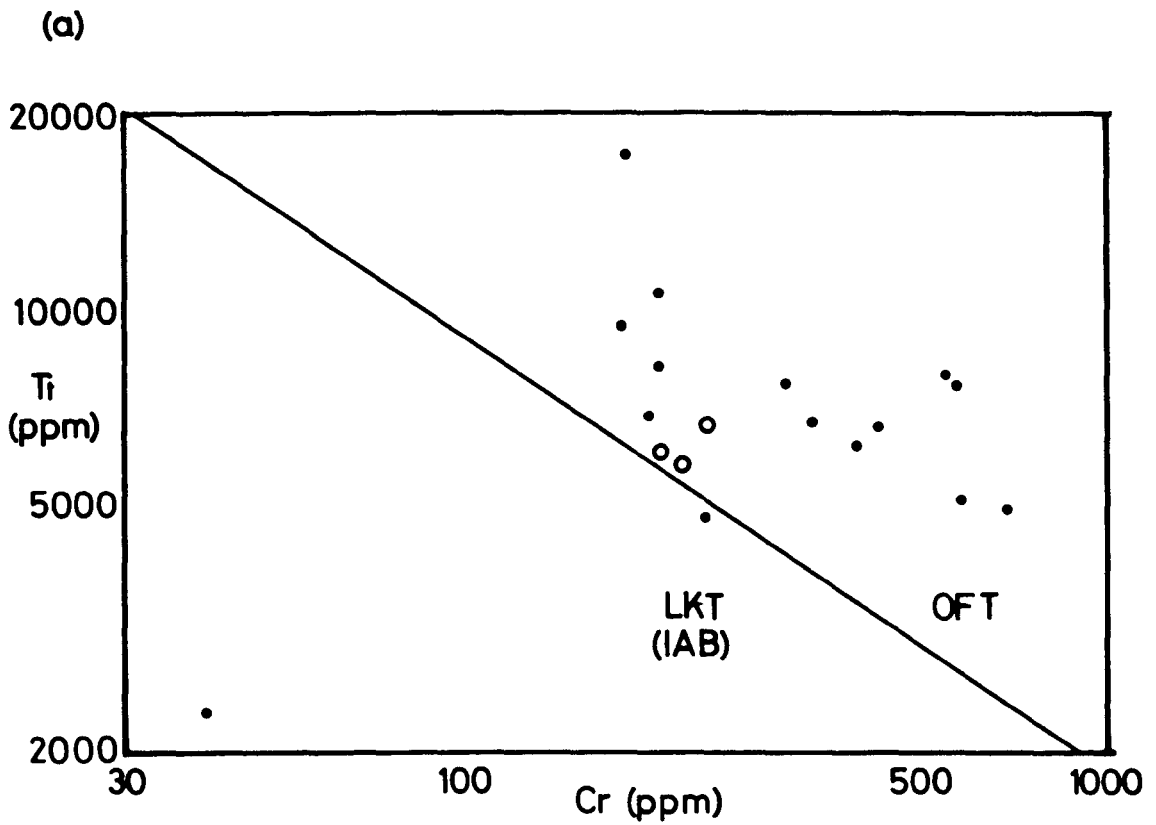


FIG. 3.14(a) Ti vs. Cr, log/log with division of low-k tholeiites and ocean-floor tholeiites from Pearce (1975).

(b) Zr-(Ti/100)-(Y x 3) after Pearce & Cann (1973). Symbols as in FIG. 3.12(a).

FIG. 3.15

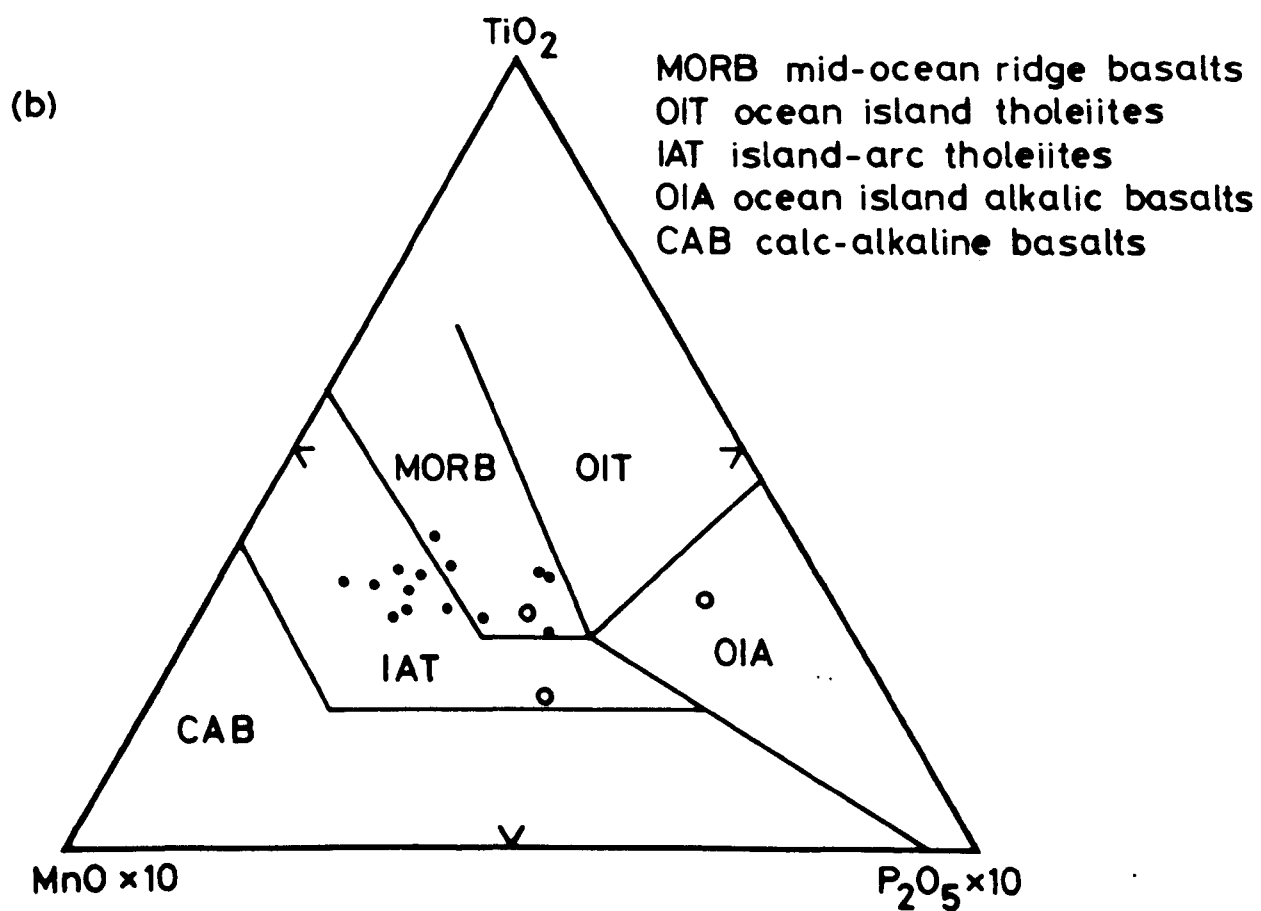
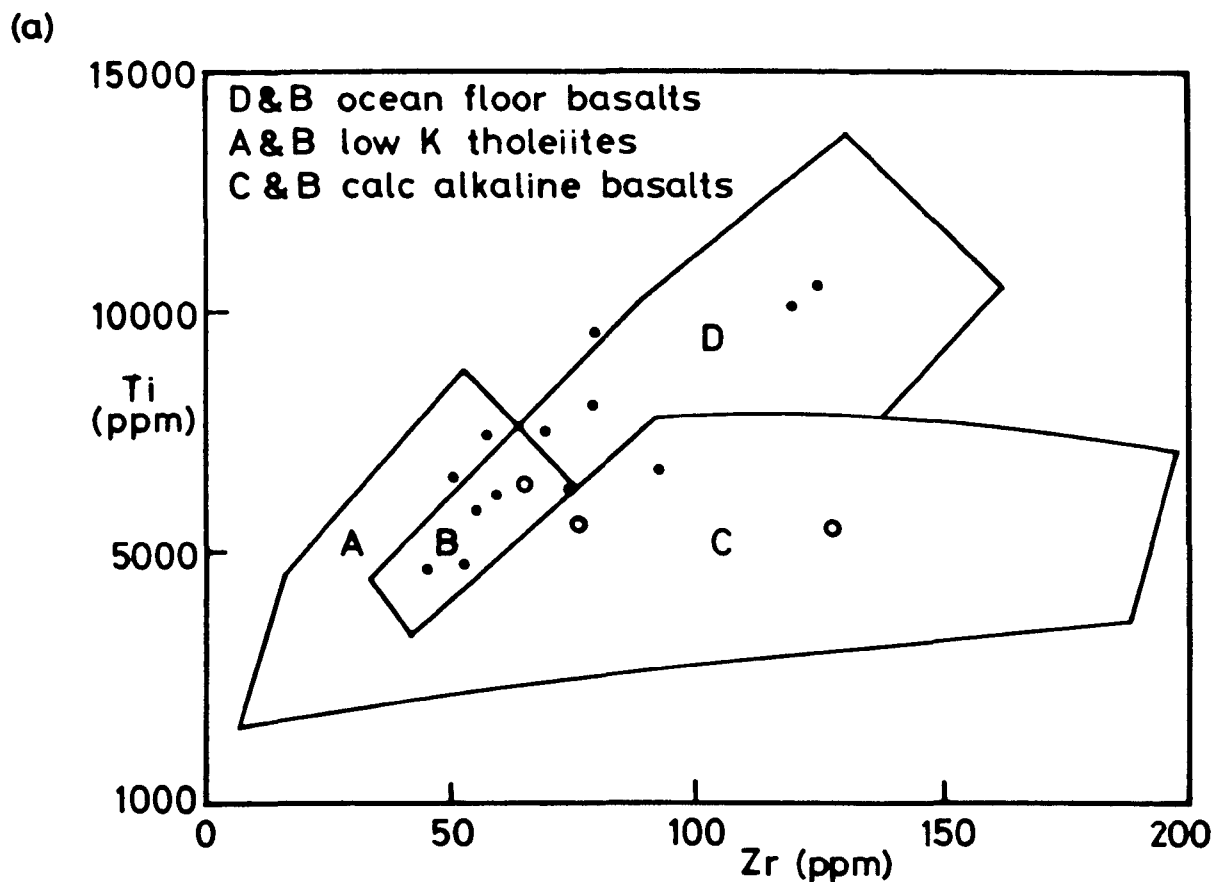
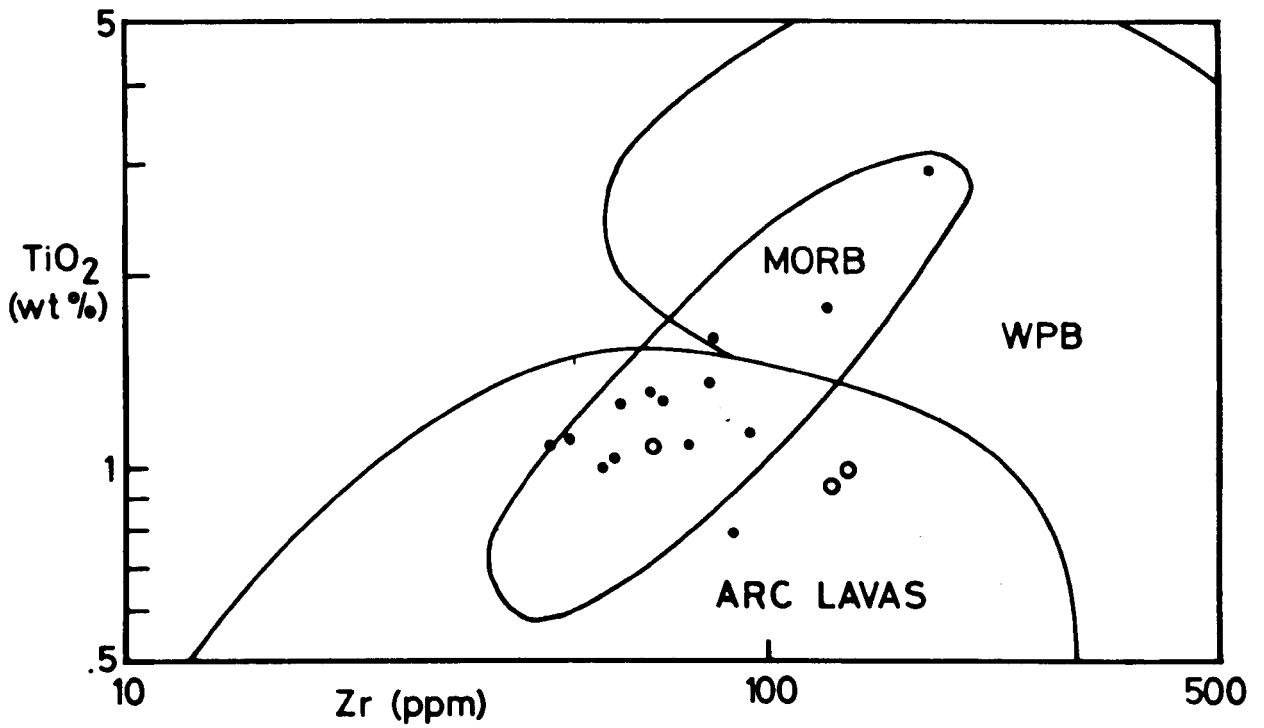


FIG. 3.15(a) Ti vs. Zr with fields from Pearce & Cann (1973).
(b) TiO₂-(Mn x 10)-(P₂O₅ x 10) with fields from Mullen (1983).
Symbols as in FIG. 3.12(a).

FIG. 3.16

(a)



(b)

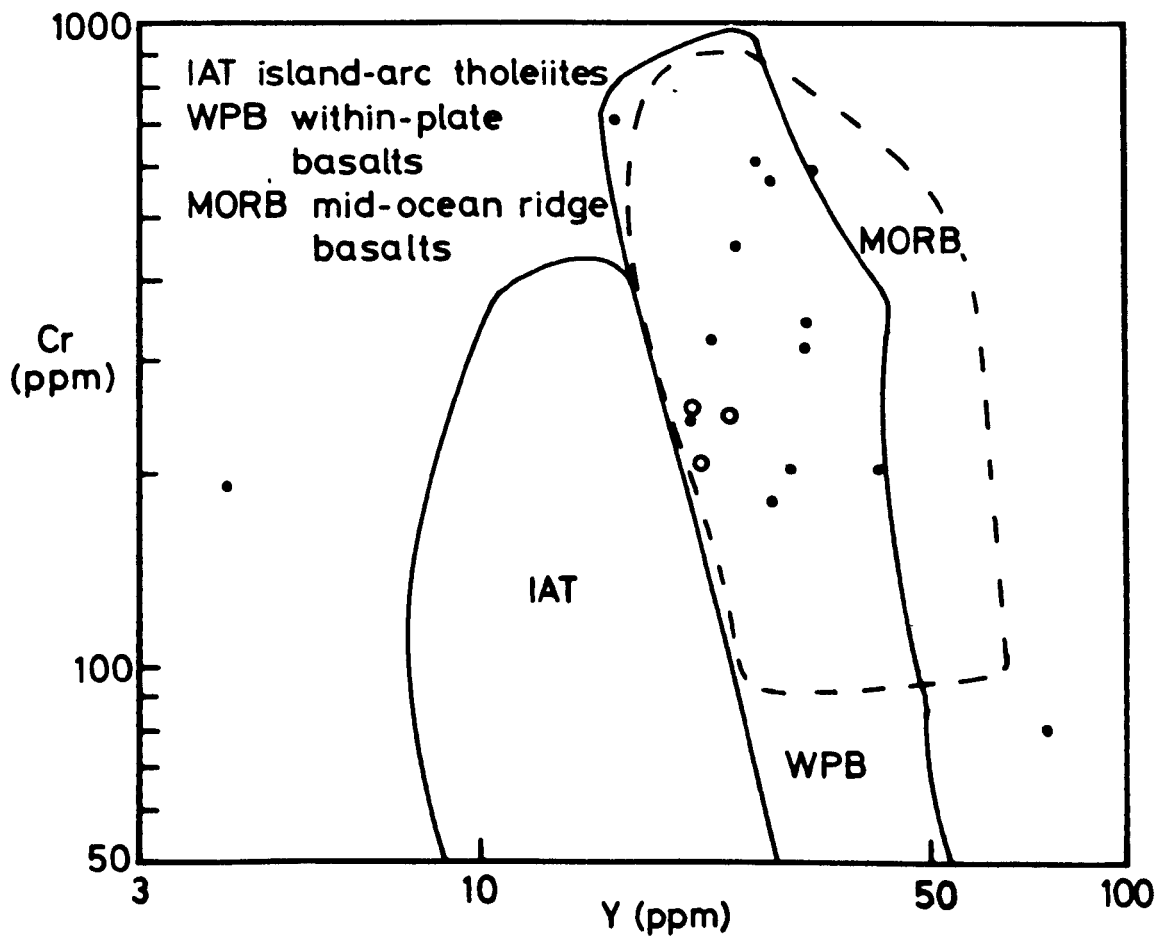


FIG. 3.16(a) TiO_2 vs. Zr, log/log with fields of Gale & Pearce (1982).
 (b) Cr vs. Y, log/log with fields of Gale & Pearce (1982).
 Symbols as in FIG. 3.12(a).

values for the garnet-granulite fall within the range for oceanic basalts. However, the ranges of values for both Y and TiO_2 in the garnet-granulite cover both oceanic and island-arc groups, whilst the averages for these elements in the garnet-granulite do not fall into either of the basalt groups. These data suggest that the majority of the rocks which formed the precursor to the garnet-granulite were of ocean-floor basalt type although it is tentatively suggested that some of the rocks may have island-arc affinities. Such an interpretation fits in well with the close association of the garnet-granulite with meta-limestones, whilst the layered nature of the rock suggests that it represents a meta-volcanic tuff/lava succession deposited in shallow-water conditions. The two fractionation trends shown in Figs. 3.10 and 3.11 were earlier interpreted as reflecting the presence of two sources of material for the precursors to the garnet-granulite. It now seems possible to extend this interpretation to two volcanic sources. It is interesting to note that Hernes (1954b) also postulated a volcanic origin for the precursor to the garnet-granulite, but discounted it in preference for the interpretation of a skarn formation for the rocks.

The interpretation of the garnet-granulite as a partly-retrogressed eclogite and a meta-volcanic unit, derived by fractional crystallisation from an olivine + pyroxene + plagioclase parent and interbedded with meta-sedimentary limestone is presented as further evidence for the occurrence of eclogite-facies metamorphism in the crust (cf. Liégeois & Duchesne, 1981).

3.2.2 The mixed rocks

As can be seen from Table 3.1 some of the samples of garnet-granulite contain more than the average amount of CO_2 (D17, D19, 1417). These samples also have rather more H_2O than average, a reflection of the

rather hydrated nature of their mineral assemblages. These three samples came from outcrops of garnet-granulite fairly close to, but not necessarily adjacent to, the marble. However, sample E10 came from immediately adjacent to the marble, but contains little CO_2 although it is a fairly hydrated rock. This suggests that CO_2 was introduced into the garnet-granulite at the retrogression phase of the metamorphism, apparently along cracks and joints formed during that phase, giving the veins of calcite seen in samples D17 and D19.

In addition, there has been direct pre-metamorphic mixing between the two precursors of the garnet-granulite and marble (i.e. volcanic tuff and limestone) resulting in the calc-silicate assemblages described in section 3.12. Analyses of these mixed rocks and the marble are given in Table 3.3 and plotted on Fig. 3.17 with the garnet-granulite; the marble itself is very pure as found by Vogt (1896) and Bugge (1905). To minimise the effect of the fractionation trend in the garnet-granulite Ti and Zr were used in the plot in Fig. 3.17 since the Ti/Zr ratio is fairly constant in all the samples of the rock, as seen in Fig. 3.9. The approximate fractionation trend of the garnet-granulite is shown; samples 143 and 1410 mark the extreme ends of this line.

Only sample E2 appears to show direct contamination by calcite on the garnet-granulite by lying a 'mixing-line', the increased calcite content is reflected in the relatively high content of CO_2 (4.7%) in this sample. The other mixed rocks also show the influence of Zr. This element has difficulty entering other phases due to its high charge and large ionic radius (0.79\AA) and tends to appear only in zircon (Taylor, 1965; Mason, 1966, p. 136) which is a common detrital mineral. However, it can also be concentrated in late magmatic differentiates such as the anatectic portions (K-feldspar + quartz \pm plagioclase) seen in some of these rocks.

TABLE 3.3 Whole-rock analyses of the mixed rocks from the Tverrfjella Unit

	E2	102	1416	TL1
MAJOR ELEMENTS (%)				
SiO ₂	45.11	54.75	42.57	0.43
TiO ₂	0.67	0.70	0.41	0.00
Al ₂ O ₃	13.69	16.00	7.21	0.14
Fe ₂ O ₃	0.00	1.05	0.41	0.05
FeO	8.10	6.70	5.78	0.02
MgO	6.60	4.25	12.34	1.09
MnO	0.12	0.12	0.02	0.00
CaO	17.29	9.72	20.36	54.84
Na ₂ O	2.79	1.72	2.42	0.16
K ₂ O	0.40	3.23	2.20	0.01
P ₂ O ₅	0.01	0.04	0.03	0.03
S	0.08	0.20	0.01	0.02
H ₂ O ^T	0.87	0.47	0.58	-
CO ₂	4.70	1.08	5.68	44.13
TOTAL	100.42	99.43	99.75	100.92
TRACE ELEMENTS (ppm)				
Ni	96	235	330	-
V	244	-	-	-
Cr	310	159	624	-
Zn	69	149	103	-
Cu	40	100	0	-
Rb	13	267	106	0
Sr	106	274	84	242
Y	20	49	0	-
Zr	39	270	51	-
Pb	5	33	2	-
Ba	50	467	152	-
Ga	-	60	17	-
Ce	-	62	11	-
Nb	0	52	8	-
Th	-	5	2	-

FIG. 3.17

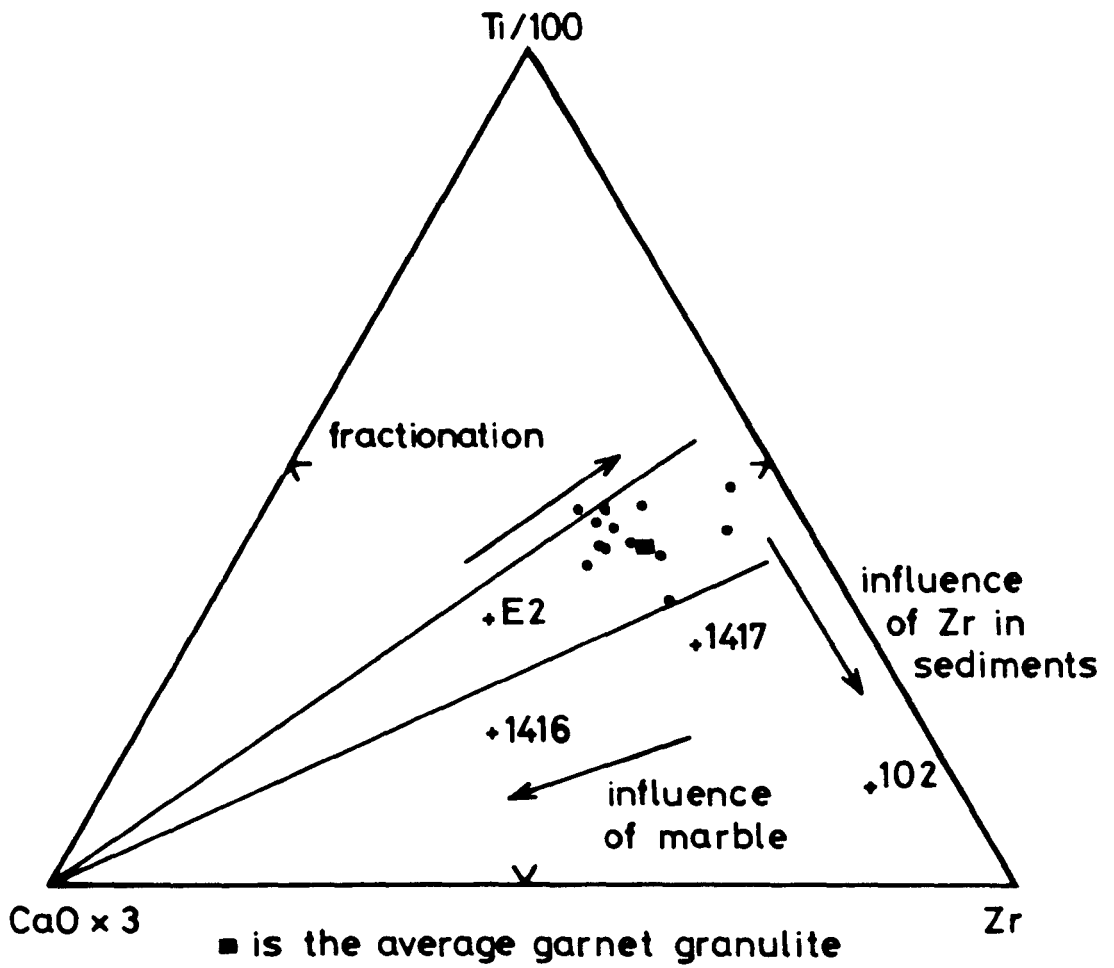


FIG. 3.17 $Ti/100-(CaO \times 3)-Zr$ to show the influences of those elements upon the Garnet-Granulite and the mixed rocks adjacent to the marble.

1417 is a sample of the garnet-granulite with a relatively high Zr value which appears to be due to the presence of anatectic material, probably originating in adjacent calc-silicate rocks. The relatively high Rb and Ba contents of this rock also reflect the presence of these anatectic portions (see Table 3.1).

Sample 102 also contains a relatively large amount of Zr and also contains anatectic portions. However, this particular rock also displays a relatively high Ga content (60 ppm); this element readily replaces Al, which is also fairly abundant in this sample (16.0%), and therefore tends to be concentrated in clay minerals (Mason, 1966, p. 164; Laporte, 1968, p. 66). Also, the relatively high Cu (100 ppm) and S (0.20%) contents of this sample perhaps indicate sedimentary sulphides, minerals commonly found in muds. Thus, there appears to be a certain amount of sedimentary influence in this particular sample.

Sample 1416 also displays the influence of calcite contamination, reflected in the CO₂ content of 5.68%, although the anatectic portions in this sample cause the plotted point to fall away from the direct 'mixing-line'.

3.2.3 The heterogeneous rocks

These rocks lie stratigraphically above the garnet-granulite and as far as possible, representative samples of each type were collected; the analyses are given in Table 3.4. Essentially, there are three rock types: amphibolites, quartzo-feldspathic rocks and pelites. From the interpretation of the garnet-granulite precursor as a meta-volcanic body, it would seem likely that these overlying rocks are also of igneous/sedimentary parentage. Leake (1969) has recommended the use of Niggli numbers to discriminate between meta-sedimentary and meta-igneous rocks. Unfortunately, the high-grade metamorphism suffered by these rocks,

TABLE 3.4 Whole-rock analyses of the heterogeneous rocks from the Tverrfjella Unit

	Pelites					Amphibolites			Quartzo-feldspathic rocks			
	1018	T12	T13	T14	HGP	1016	1017	T9	105	108	1015	T11
MAJOR ELEMENTS (wt. %)												
SiO ₂	55.88	60.40	56.37	68.63	63.51	45.97	61.25	49.94	74.11	66.76	81.27	64.39
TiO ₂	1.00	0.74	0.97	0.58	0.79	1.08	0.93	0.98	0.54	0.41	0.70	1.01
Al ₂ O ₃	20.98	15.52	19.59	14.64	17.35	16.22	14.79	15.77	9.85	16.68	9.63	15.04
Fe ₂ O ₃	0.45	0.99	2.01	0.84	2.00	3.53	1.53	2.99	2.27	0.52	0.00	2.53
FeO	7.85	8.04	6.00	3.36	4.71	5.76	6.22	8.08	3.10	2.98	1.52	4.47
MgO	2.99	4.44	2.98	1.70	2.31	8.21	5.40	7.05	2.68	1.01	0.74	2.22
MnO	0.15	0.21	0.16	0.08	-	0.13	0.05	0.20	0.13	0.05	0.00	0.13
CaO	2.44	3.79	2.62	2.42	1.24	16.12	4.78	8.61	3.34	4.14	1.42	3.44
Na ₂ O	2.41	2.32	2.65	3.13	1.96	1.50	0.70	3.08	1.82	4.07	3.00	2.39
K ₂ O	3.74	1.76	3.72	2.68	3.35	0.44	1.74	1.64	0.36	1.82	1.26	3.39
P ₂ O ₅	0.36	0.29	0.33	0.17	-	0.14	0.16	0.23	0.13	0.16	0.05	0.35
S	0.01	0.00	0.00	0.00	-	0.05	0.00	0.00	0.02	0.02	0.01	0.00
H ₂ O ^T	1.22	0.85	1.38	0.76	2.42	0.91	1.00	0.77	1.12	1.20	0.51	0.76
CO ₂	0.17	-	-	-	0.22	0.04	0.15	-	0.35	0.00	0.03	-
TOTAL	99.65	99.24	98.69	98.92	99.86	100.10	98.70	99.34	99.82	99.82	100.14	100.12
TRACE ELEMENTS (ppm)												
Ni	28	47	30	12		124	93	107	26	1	3	19
Cr	77	164	81	42		243	242	205	109	17	19	58
Zn	104	69	106	60		41	78	85	36	26	9	93
Cu	34	43	17	30		109	0	0	18	17	11	0
Rb	168	61	167	110		15	64	35	13	28	34	119
Sr	294	199	317	273		197	199	271	208	894	291	216
Y	47	21	41	28		21	24	22	20	10	1	45
Zr	134	85	133	241		66	128	77	123	202	91	312
Pb	10	15	20	16		7	10	12	6	14	11	19
Ba	877	420	897	611		73	257	397	160	1254	427	1201
Ga	103	20	18	65		17	54	34	57	63	29	98
Ce	27	19	27	18		19	18	19	13	18	8	21
Nb	18	9	19	15		7	16	9	11	10	10	17
Th	26	6	16	11		8	9	2	12	6	7	9
O.R.	4.9	10.0	23.2	18.3	27.6							

O.R. ≡ oxidation ratio: mol $\left(\frac{2\text{Fe}_2\text{O}_3 \times 100}{2\text{Fe}_2\text{O}_3 + \text{FeO}} \right)$ after Chinner (1960), for pelites

HGP is high-grade pelite from Shaw (1956)

reflected by the melt portions in the pelites and the symplectite omphacites in the amphibolites (see section 3.1.3) has had a profound effect upon the mineral chemistries causing the major Leake discriminant: (al-alk) vs. c to prove inconclusive for these rocks.

Nevertheless some of these rocks can be assumed to be sedimentary in origin from examination of their major element chemistries and mineral assemblages. Samples 1018, T12, T13 and T14 are all biotite-rich pelites and can contain kyanite and/or sillimanite, reflected in their high SiO_2 and Al_2O_3 contents. These rocks are interpreted as clay-rich sediments, which is partly supported in the cases of 1018 and T14 by relatively high Ga contents. Furthermore 1018 and T13 have slightly higher Th contents suggesting a concentration of radiogenic material, as found in shales (Krauskopf, 1969, p. 482). Table 3.4 also contains the average, high-grade, pelite of Shaw (1956). The pelites bear an overall similarity to this average analysis, except in the alkali contents and in the $\text{Fe}_2\text{O}_3/\text{FeO}$ ratio. The former discrepancy is likely to be the result of the production of melt components in the rocks which would have re-distributed these elements to some extent. The rocks taken by Shaw for his average appear to be only of amphibolite facies since they lack any melt portion and contain sillimanite as the stable Al-silicate. The $\text{Fe}_2\text{O}_3/\text{FeO}$ ratio has been expressed as the oxidation ratio (Chinner, 1960). Chinner has shown that the oxidation ratios in pelitic rocks decreases with metamorphic grade, being low in rocks with biotite, garnet and magnetite and higher in rocks with muscovite and hematite. Thus, the discrepancy between the oxidation ratio of Shaw's average pelite (27.6) and those of the Tverrfjella pelites (4.9-23.2) appears to be the result of the increased P-T conditions suffered by the latter rocks.

Sample 1015 has an extremely high SiO_2 content, coupled with the generally low metal concentrations, as found in sandstones (see Table 3.5),

TABLE 3.5 Abundances of selected elements in some major units of the Earth's crust in p.p.m. (after Turekian & Wedepohl, 1961).

	Sandstone	Granite	Granodiorite
Ni	2	4.5	15
Cr	35	4.1	22
Zn	16	39	60
Ca	X	10	30
Y	40	40	35
Zr	220	175	140
Pb	7	19	15
Ga	12	17	17
Ce	92	92	81
Nb	0.0X	21	20
Th	1.7	17	8.5
Ba	XO	840	420
Sr	20	100	440

X indicates an estimate of the order of magnitude

this rock is interpreted as an impure quartzite. The presence of relict kyanite in the rock and the appearance of Al_2O_3 as the major oxide second in concentration to SiO_2 suggests some clay contamination. The interbedding of this rock with the garnet-granulite, on the N side of the Børresdalen col, reinforces the volcano-sedimentary origin for the latter.

The remainder of the heterogeneous rocks are rather harder to interpret because of the limitations imposed by the alteration of the major element contents. However, the amphibolitic rocks display generally basaltic chemistries and can be treated in much the same way as the garnet-granulite; the analyses are shown on Figs. 3.13-3.16 with the garnet-granulite. In general, 1016 and T9 seem to be genuinely basaltic whereas 1017 gives contradictory information (see $\text{Zr}/(\text{TiO}_2 \times 10,000)$ vs. Ga, $\text{Zr}/(\text{TiO}_2 \times 10,000)$ vs. Nb/Y and Ti vs. Cr). The alkalis seem to be very disturbed in all three of the samples (reflected on the Ti vs. D.I. plot). Interestingly 1016 and T9 fall on the fractionation trend of the garnet-granulite (see Ni vs. Zr, Ni vs. $\text{FeO}^t/(\text{FeO}^t + \text{MgO})$, Cr vs. Zr and Cr vs. $\text{FeO}^t/(\text{FeO}^t + \text{MgO})$), but sample 1017 is not consistent, apparently due to its anomalously high Zr content. On the discrimination diagrams in Figs. 3.13-3.16 both 1016 and T9 fall in the ocean-floor basalt or island-arc tholeiite fields with the garnet-granulite; as expected, 1017 tends towards high Zr, although on Fig. 3.15(b) it lies towards low MnO values.

From these diagrams samples 1016 and T9 are interpreted as meta-volcanic rocks, possibly of the same origin as the garnet-granulite. T9 is suspected of containing some sedimentary component: not only is Zr relatively high (from zircon) but so is Ga (from clays) and SiO_2 (quartz/clays). Furthermore the rock displays small relict kyanite grains in thin section, again suggesting clay contamination, even though

the analysis is not particularly Al-rich. The majority of the metal trace elements reflect the basaltic component of the rock, these would not have been greatly affected by the addition of any sedimentary material in which metal concentrations are generally low (Turekian & Wedepohl, 1961).

The quartzo-feldspathic rocks proved to be the most difficult to interpret. Once again major element plots and the use of Niggli numbers for Leake (1969) and van de Kamp et al. (1976) discrimination diagrams proved inconclusive generally due to the variance in the LIL elements (K, Rb, Ba) and the limited number of samples preventing the definition of a trend necessary for these discrimination plots.

Table 3.5 gives the trace element contents for sandstones and granitic rocks (after Turekian & Wedepohl, 1961) against which the analysed samples have been compared. The metal contents: Ni, Cr and Zn are particularly low in 108 suggesting an igneous, granitic lithology, partly supported by the higher Pb contents when compared to sandstones. The high Zr content is ambiguous, this could be derived from either detrital zircon or is a result of the differentiated nature of the granitic precursor (Mason, 1966, p. 136). Both samples 105 and T11 have higher metal contents, especially in Cr pointing to a sedimentary influence. In addition, T11 contains an extreme Zr value, higher than any other meta-sediment in this unit and higher than the sandstone in Table 3.5 which may indicate detrital zircon.

In all these rocks, the Ce values are anomalously low for either sandstones or igneous rocks, and the Ga values are anomalously high. These two elements have been used on the discrimination diagrams of Floyd & Winchester (Fig. 3.18(a) and (b)) but the results from these samples are inconclusive. It is possible that the high Ga values have resulted from clay contamination, although sample 105 is not particularly Al-rich.

FIG. 3.18

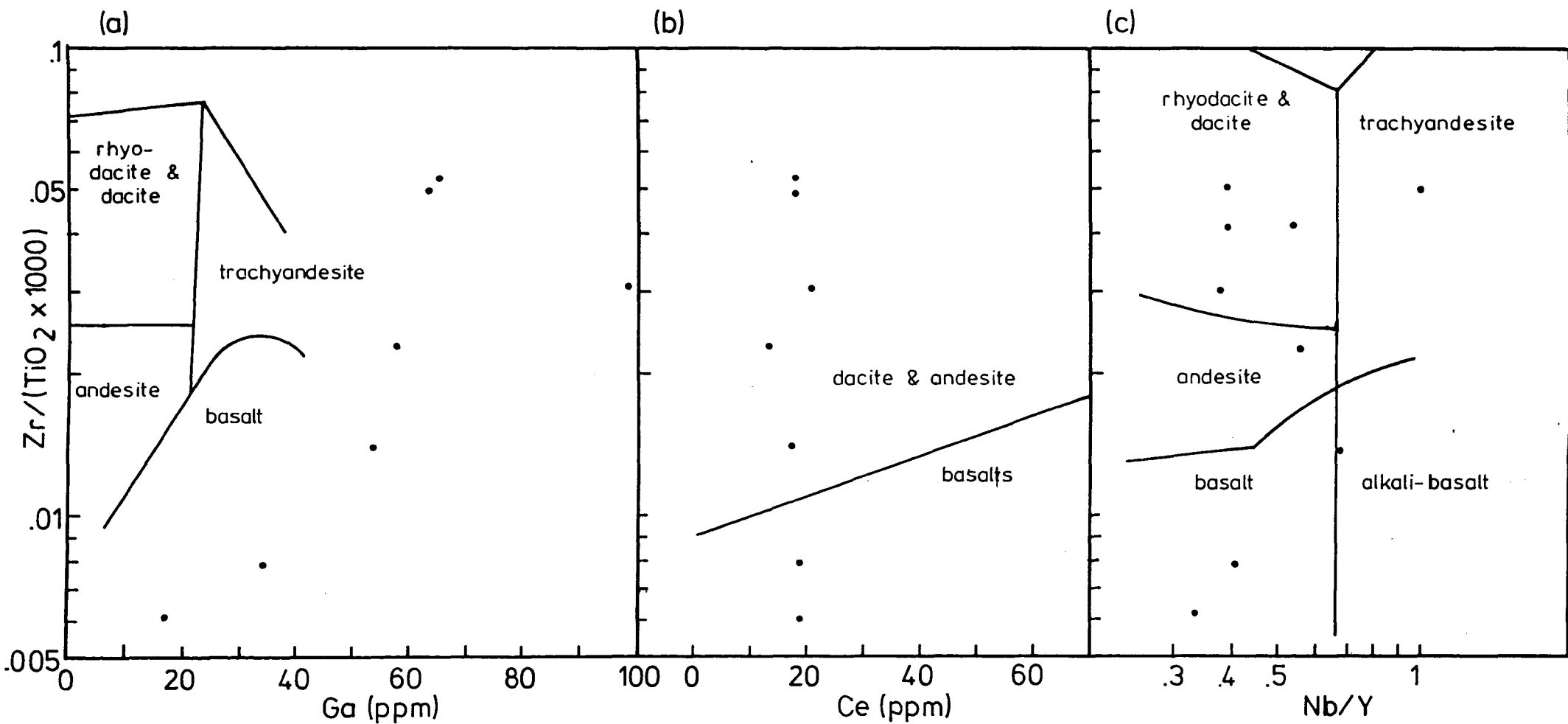


FIG. 3.18(a) $Zr/TiO_2 \times 10,000$ vs. Ga, log/linear after Floyd & Winchester (1978).
 (b) $Zr/TiO_2 \times 10,000$ vs. Ce, log/linear after Floyd & Winchester (1978).
 (c) $Zr/TiO_2 \times 10,000$ vs. Nb/Y, log/log after Floyd & Winchester (1978).
 All for the quartzo-feldspathic rocks of the Tverrfjella Unit.

The Th values are also relatively high, compared to sandstones, indicating radiogenic material from clay sediments. The Zr(Ti x 10,000) vs. Nb/Y plot (Fig. 3.17(c)) confirms the Zr/(Ti x 10,000) vs. Ce plot and suggests that the rocks are meta-igneous, subalkaline and probably rhyolites/dacites. Unfortunately, this interpretation places a further constraint on the trace element contents for the granite in Table 3.5 since Turekian & Wedepohl consider that extrusive granitic rocks often have variable and unusual contents of these elements.

The association of these rocks with others interpreted as meta-sediments/volcanics is in keeping with an interpretation of them being meta-acid tuffs, although the possibility of some sedimentary mixing with clay material cannot be discounted. Sample 108 approaches a chemistry most like that of a meta-igneous rock, whilst sample T11 appears to have suffered the most sedimentary influence.

3.3 DISCUSSION

On the maps of the Moldefjord Peninsula by Hernes (1955) and Råheim (1972) the Tverrfjella Unit is shown as part of the heterogeneous Frei Group, which has been dated as Svecofennian (i.e. 1800-1600 m.y.) by Pidgeon & Råheim (1973). However, from the geological relationships observed in the Tverrfjella Unit during this study, the Unit is considered not to be a part of the Frei Group, for three reasons:

(i) There is a distinct and apparently sharp lithological break between the Tverrfjella Unit and the underlying Heterogeneous Gneisses.

(ii) The underlying Heterogeneous Gneisses are very deformed often plastically, with extreme mobilisation of the migmatitic portions of the rocks (see Chapter 5 - Plate 5.1(a)). By contrast, the rocks in the Tverrfjella Unit display an original lithological layering, as seen on Trolltindane (Plate 3.4(d)). Although localised, small-scale

compositional layering is visible in the amphibolites of the underlying Heterogeneous Gneisses, this is not on the same large-scale seen in Trolltindane. This suggests that the rocks of the Tverrfjella Unit are younger than the underlying Heterogeneous Gneisses to have escaped this extreme deformation.

(iii) The Tverrfjella Unit lacks the pods of eclogite found elsewhere on the Molde Peninsula. Although the Unit does contain partly retrogressed and amphibolitised eclogite rocks, these have not been disrupted into pods and have been observed grading into the adjacent quartzo-feldspathic gneisses (see section 3.1.3). Furthermore, the retrogressed eclogites of the Tverrfjella Unit generally possess chemistries with oceanic affinities whereas the pods of eclogite have been interpreted as the metamorphosed equivalents of basaltic dykes and sills of a continental nature intruded during the late Proterozoic (~ 1200 m.y.) (see Chapter 7). This suggests that the Tverrfjella Unit was not present at the time of emplacement of the precursors to the eclogites.

These three features suggest two possibilities for the origin of the Tverrfjella Unit.

(i) The oceanic-derived volcanoclastics and sediments were deposited directly onto the underlying Heterogeneous Gneisses at some time after 1200 m.y. which therefore formed the basement.

(ii) The Tverrfjella Unit is allochthonous, thrust over the underlying Heterogeneous Gneisses.

A major difficulty with option (i) is that if the underlying gneisses formed the basement to these oceanic rocks, a section of oceanic crust would be expected here, i.e. an ophiolite. Where found, ophiolite complexes are often incomplete, but it is considered that some part of the units (ultra-mafic rocks, gabbros, dykes, pillow lavas,

pelagic (cherty) sediments (Windley 1977, p. 280)) should be present if the Tverrfjella Unit is to be autochthonous. The absence of these ophiolitic rocks suggests that the Tverrfjella Unit is allochthonous. The time of emplacement of this Unit is constrained by two events: the postulated time of intrusion of the eclogite-dyke precursors and the Caledonian metamorphism. (A sample from the Garnet-Granulite was dated by the Sm-Nd by Griffin & Brueckner (1980) and gave an age of 418 ± 11 m.y.) Although the contact between the Unit and the underlying Heterogeneous Gneiss is sharp, it is not imbricate, nor are mylonites apparent in the vicinity of the contact. Such structures would help to confirm the tectonic nature of the contact. However, it is likely that the subsequent high-grade Caledonian metamorphism would have masked such structures. Indeed, the identification of the contacts between the thrust sheets in the Allochthonous Units to the E, around Trondheim, has often proved to be impossible and their presence can only be inferred from other information (Andreasson & Gorbatschev, 1980).

Both Råheim (1972) and Hernes (1955) have mapped the rocks of the Tverrfjella Unit extending NE onto the adjacent island of Averøya. Råheim describes the rocks there as: eclogite-amphibolite, Ca-rich schist, calc-silicate gneisses, kyanite-garnet-biotite, schists; such descriptions can be applied to the rocks observed in the Tverrfjella Unit. The map of Hernes shows the rocks containing many marble and sulphide bodies. Råheim (1979) has attempted to correlate these sulphide deposits with those appearing in the Røros Group in the Surnadal Syncline (part of his Surna Group - see Table 1.2). Such a correlation is feasible on the basis of Råheim's tectonostratigraphy and the fact that he has dated the Røros Group as Svecofennian (~ 1700 m.y., Råheim, 1977). However, the validity of the Svecofennian age is questioned on two points:

(i) No actual isochron was produced for this age. Råheim initially plotted the data from the rocks of the Røros Group on the same Rb-Sr isochron diagram as that he used for the adjacent Tingvoll-Group rocks, which gave a Svecofennian age of 1707 ± 63 m.y. He then selected those samples from the Røros Group which fell close to the isochron for the Tingvoll Group rocks and claimed that this superimposition indicated a Svecofennian age for the Røros Group. Firstly, this selection procedure is false, taking only those data which fit in with a preconceived notion. Secondly, the samples from the Røros and Tingvoll Groups came from different localities and therefore are unlikely to have had the same rock precursor and hence the same $^{87}\text{Sr}/^{86}\text{Sr}$ initial ratio, a prerequisite for a true isochron.

(ii) Råheim considered that the Røros and Tingvoll Groups were structurally concordant and that the absence of a metamorphic or structural break between them implied that they were of the same (Svecofennian) age. However, as pointed out by Carswell (1973) such concordance may simply be due to the intense flattening suffered by these rocks during the folding of the Surnadal Syncline during the Caledonian. Such intensely flattened fabrics are also present on the Molde Peninsula (see Plate 2.1(c), section 2.2.1) which would have easily obliterated any pre-existing structures.

An alternative interpretation for the Røros Group, and that preferred here, is that the rocks are Silurian-Ordovician in age and form part of the Seve Nappe, one of the Allochthonous Units of the Trondheim area (Gee, 1980; Krill, 1980, 1981 - see Table 1.1). If the sulphide correlation of Råheim is correct this would result in the rocks of the Tverrfjella Unit also being Palaeozoic in age and would confirm an allochthonous origin for the Unit.

Unfortunately, the correlation of the sulphide deposits is viewed with some scepticism. Many such deposits occur in the area of the Allochthonous Units around Trondheim (Bugge, 1980) and the matching of any two deposits cannot be reliably taken as conclusive evidence of their stratigraphic equivalence.

Nevertheless, there are several features of the rocks in these Allochthonous Units which suggest that there is a stratigraphical equivalence between them and the Tverrfjella Unit:

(i) The lithological units in the Røros Group are broadly similar to those observed in the Tverrfjella Unit (Table 1.2).

(ii) The Seve Nappe contains rocks metamorphosed at granulite facies (Gee, 1980; Claesson, 1981) although this grade appears to be only a minimum since eclogite pods have been observed in parts of the Nappe (van Roermund, 1983).

(iii) Rocks of oceanic derivation have been recognised in several of the Nappes: Storen (Gale & Roberts, 1974; Gale & Pearce, 1982), Seve (Andreasson et al., 1981), Koli (Furnes et al., 1981).

Also, the Seve Nappe and other Nappe Units are recognised in tight infolds, with the basement gneisses, to the NE of the Molde Peninsula (Andreasson & Gorbatshev, 1980 and see Fig. 1.1) which may be further extensions, on strike of the rocks in the Tverrfjella Unit and on Averøya. The preservation of the high-grade metamorphic assemblages in the rocks on Tverrfjella appears to have been due to the rocks lying in relatively open synclinal structure, rather than being extensively flattened and sheared in the limbs of a tighter fold.

Not only are rocks of supposed oceanic derivation present in the Allochthonous Units, some of them display mixed basaltic chemistries between oceanic and island-arc basalts, as does the Garnet-Granulite.

Of particular interest are the greenstones at Løkken, near Trondheim, in the Støren Group (see Tables 1.1 and 1.2) (Gale & Roberts, 1974; Gale & Pearce, 1982). Gale & Roberts interpreted this mixed chemical association as the result of the rocks being generated in the transitional tectonic setting of a marginal (i.e. back-arc) basin. This interpretation was supported by the varied nature of the overlying sedimentary units at Løkken: shales, greenstones, greenschists, agglomerates, limestones plus rhyolite horizons higher in the sequence. Typical features of a marginal basin setting are: mixing of subaerial and submarine volcanics and sediments, conglomeratic horizons, deep-sea trace fossils, a bipolar provenance of clastic material and the local development of carbonates. The mixed basaltic parentage of the rocks in the Tverrfjella Unit may also indicate a margin at basin setting for their production. Table 3.2 showed that the Ti and Y values for the Garnet-Granulite were intermediate between oceanic and island-arc basalts (section 3.2.1), a feature cited by Tarney (1976) as evidence for petrogenesis in a marginal basin. Unfortunately, unlike the rocks at Løkken, the original sedimentary and stratigraphic nature of the associated rocks with the Garnet-Granulite is not nearly so well defined. The original presence of limestones is clear, and acid volcanics are considered to have occurred higher in the stratigraphic sequence; the pelitic rocks suggest original clay-rich sediments, perhaps shales. However, there is no evidence to suggest the prior existence of conglomerates or agglomerates in the Tverrfjella Unit.

The possibility of the Tverrfjella Unit being an allochthonous portion of a marginal basin related to one of the nappes in the Allochthonous Units of the Trondheim area should be taken purely as conjecture at present. However, there are several lines of enquiry which could be pursued to investigate this possibility further:

(i) A more rigorous comparison between the geochemistries of the Garnet-Granulite and the greenstones of the Allochthonous Units.

(ii) REE analysis of the Garnet-Granulite may clarify the nature and origin of the basalt precursor (cf. Gale & Pearce, 1982).

(iii) Further mapping of the basal contact of the Tverrfjella Unit may help to clarify the nature of the contact.

(iv) Further mapping, on strike, to the NE to Averøy and beyond to see if the rocks of the Tverrfjella Unit can be directly traced into the tight in-folds of the Allochthonous Units in that area.

3.4 MINERAL CHEMISTRY AND P-T CALCULATIONS

Mineral analyses were made on the Garnet-Granulite from several samples, including both relict eclogite facies assemblages and retrogressed assemblages with symplectic clinopyroxenes. Analyses were also made of the constituent phases of a pelite (1018) from the overlying heterogeneous rocks.

3.4.1 The Garnet-Granulite

The analyses of the phases in this rock are given in Tables 3.6 (garnets), 3.7 (clinopyroxenes), 3.8 (amphiboles) and 3.9 (feldspars).

Overall, the garnets are almandine-pyrope-grossular types with low calculated Fe^{3+} contents typical of eclogite facies garnets (e.g. Coleman et al., 1965; Mysen & Heier, 1972). The garnets show varying degrees of compositional zoning but always in a prograde fashion with increasing pyrope contents towards the rims of the garnets. On Fig. 3.19(a), after Coleman et al. (1965) the garnets fall into fields B and C, representing eclogites from migmatite, granulite and amphibolite rocks, and in glaucophane and low-amphibolite rocks respectively. The points are fairly scattered with a substantial range in grossular

TABLE 3.6 Analyses of garnets from the Garnet-Granulite

(wt. %)	E3	E3	E3	E9	E9	E9	E9	103	103	103	103	1410	1410	1410	1429	1429	1429	1429
	Core (1)	Rim (1)	(2)	Core (1)	(1)	(1)	Rim (1)	Core (1)	(1)	Rim (1)	(3)	Core (3)	(4)	Rim (3)	Core (1)	Rim (1)	(3)	(2)
SiO ₂	38.80	39.80	39.21	40.02	39.97	39.88	40.24	38.57	38.78	38.66	39.16	37.93	37.91	38.20	38.83	39.05	38.78	38.77
TiO ₂	0.05	0.04	0.06	0.02	0.02	0.02	0.00	0.04	0.04	0.04	0.03	0.02	0.02	0.02	0.02	0.02	0.03	0.02
Al ₂ O ₃	21.52	21.86	21.81	22.11	22.06	22.15	22.33	21.66	21.56	21.57	22.01	21.04	21.13	21.15	21.62	21.90	21.67	21.75
Cr ₂ O ₃	-	-	-	0.03	0.07	0.05	0.02	-	-	-	-	-	-	-	-	-	-	-
FeO	20.76	21.06	21.03	20.42	20.27	19.91	19.58	24.34	24.45	21.52	20.87	27.46	27.63	27.59	26.33	25.25	26.46	26.83
MnO	0.51	0.51	0.54	0.41	0.42	0.41	0.44	0.45	0.29	0.39	0.47	0.60	0.62	0.67	0.71	0.81	0.77	0.76
MgO	5.87	5.98	5.84	8.46	8.87	8.94	10.51	5.65	5.34	6.80	6.95	5.07	5.02	5.31	7.59	8.43	8.04	7.51
CaO	12.09	11.66	12.28	9.64	9.10	9.14	7.48	9.43	9.79	10.30	10.88	7.96	7.11	8.04	5.51	4.90	4.98	5.26
TOTAL	99.69	100.23	100.86	101.16	100.82	100.53	100.63	100.23	100.29	99.38	100.46	100.29	99.55	101.24	100.74	100.43	100.73	101.05
MINERAL FORMULA (12 OXYGENS)																		
Si	2.994	2.997	2.991	3.007	3.008	3.006	3.009	2.985	3.002	2.985	2.984	2.966	2.986	2.958	2.982	2.989	2.970	2.973
Ti	0.003	0.003	0.004	0.001	0.001	0.001	0.000	0.003	0.003	0.003	0.002	0.001	0.001	0.001	0.001	0.001	0.002	0.001
Al	1.957	1.976	1.961	1.958	1.957	1.968	1.968	1.976	1.967	1.963	1.977	1.939	1.962	1.930	1.957	1.976	1.957	1.966
Cr	-	-	-	0.002	0.004	0.003	0.001	-	-	-	-	-	-	-	-	-	-	-
Fe ³⁺	0.051	0.026	0.049	0.025	0.022	0.017	0.014	0.051	0.026	0.063	0.052	0.126	0.064	0.151	0.076	0.043	0.099	0.087
Fe ²⁺	1.289	1.325	1.292	1.259	1.254	1.238	1.210	1.524	1.557	1.327	1.278	1.669	1.757	1.635	1.615	1.575	1.596	1.634
Mg	0.675	0.684	0.664	0.948	0.995	1.004	1.171	0.651	0.616	0.783	0.789	0.591	0.589	0.613	0.868	0.962	0.918	0.858
Mn	0.034	0.033	0.035	0.026	0.027	0.026	0.028	0.029	0.019	0.026	0.031	0.039	0.042	0.044	0.046	0.053	0.050	0.049
Ca	0.999	0.958	1.004	0.776	0.734	0.738	0.599	0.782	0.812	0.852	0.889	0.667	0.600	0.667	0.454	0.402	0.409	0.432
TOTAL	8.002	8.002	8.000	8.002	8.002	8.001	8.000	8.002	8.002	8.002	8.002	7.998	8.001	7.999	7.999	8.001	8.001	8.000
END-MEMBERS (%)																		
ANDR	2.45	1.23	2.38	1.24	1.11	0.84	0.70	2.49	1.29	3.06	2.57	6.34	3.16	7.64	3.79	2.08	4.96	4.32
PYROPE	22.53	22.79	22.17	31.82	33.45	33.69	39.37	21.81	20.61	26.19	26.44	19.91	19.73	20.71	29.12	32.16	30.88	28.86
SPESS	1.11	1.11	1.17	0.88	0.90	0.88	0.94	0.99	0.64	0.85	1.02	1.34	1.39	1.49	1.55	1.76	1.68	1.66
GROSS	30.81	30.64	31.03	24.74	23.35	23.78	19.39	23.61	25.87	25.39	27.13	16.10	16.89	14.87	11.37	11.32	8.74	10.18
ALM	43.01	44.16	43.14	41.23	40.99	40.68	39.55	51.02	51.59	44.43	42.80	56.27	58.80	55.26	54.13	52.64	53.69	54.95
SCHORL	0.10	0.08	0.12	-	-	-	-	0.08	-	0.08	0.06	0.04	0.04	0.04	0.04	0.04	0.06	0.04
UVAR	-	-	-	0.09	0.21	0.15	0.06	-	-	-	-	-	-	-	-	-	-	-

Fe³⁺ calculated by charge-balance

Figures in brackets refer to the number of analysis points

TABLE 3.7 Analyses of the clinopyroxenes from the Garnet-Granulite

(wt. %)	E3	E3	E3	E3	E3	E9	E9	E9	E9	103	103	1410	1410	1410	1410	1410	1410	1410	1410	1429	1429			
	(2)	(2)	Symplectites			(1)	(1)	Core	(1)	Rim	(1)	(2)	(3)	(1)	Core	Rim	Core	Rim	(1)	(3)	(1)	(3)	(1)	(2)
SiO ₂	51.17	51.90	52.78	52.31	52.79	56.04	55.48	54.12	53.94	52.91	52.78	50.63	49.47	50.17	50.14	50.34	50.35	49.87	48.92	53.48	53.68			
TiO ₂	0.30	0.31	0.28	0.26	0.26	0.06	0.07	0.20	0.17	0.08	0.09	0.42	0.40	0.42	0.42	0.40	0.35	0.38	0.40	0.57	0.60			
Al ₂ O ₃	6.22	4.40	6.08	7.48	4.10	10.98	10.98	10.13	10.50	0.80	1.55	3.23	5.06	3.58	4.92	5.04	5.15	5.62	5.27	8.96	8.67			
FeO	7.62	8.20	5.74	5.60	6.22	3.59	3.92	4.89	4.89	7.89	9.95	10.50	11.34	11.24	11.12	11.08	11.68	11.20	11.74	9.86	9.70			
MnO	0.13	0.16	0.05	0.06	0.08	0.00	0.02	0.03	0.01	0.10	0.22	0.13	0.11	0.11	0.12	0.12	0.11	0.15	0.09	-	-			
MgO	11.13	11.55	11.69	11.15	12.74	9.06	9.08	9.64	9.56	13.58	12.34	12.05	11.17	12.04	10.84	10.65	10.06	10.52	10.22	7.81	8.48			
CaO	22.18	22.78	21.29	20.71	23.05	14.15	14.54	16.06	15.99	24.93	22.67	21.95	20.26	20.69	20.74	20.78	20.78	20.70	21.06	12.90	13.83			
Na ₂ O	1.04	0.94	2.03	2.25	0.57	6.37	6.06	4.91	5.02	0.12	0.38	0.70	1.03	0.79	1.21	1.32	1.87	1.24	1.12	6.14	5.53			
TOTAL	99.79	100.26	99.94	99.82	99.81	100.29	100.20	100.04	100.20	100.44	99.98	99.79	99.10	99.25	99.78	100.00	100.83	99.94	99.11	100.21	100.87			
MINERAL FORMULA (6 OXYGENS)																								
Si	1.899	1.927	1.934	1.914	1.946	1.943	1.970	1.983	1.932	1.969	1.979	1.907	1.874	1.900	1.885	1.888	1.875	1.872	1.862	1.943	1.941			
Ti	0.008	0.009	0.008	0.007	0.007	0.005	0.002	0.002	0.005	0.002	0.003	0.012	0.011	0.012	0.012	0.011	0.010	0.011	0.011	0.016	0.016			
Al	0.272	0.193	0.263	0.323	0.178	0.429	0.460	0.458	0.443	0.035	0.069	0.143	0.226	0.160	0.218	0.223	0.226	0.249	0.236	0.384	0.369			
Fe ³⁺	-	0.005	-	-	-	0.017	0.013	0.010	0.031	0.009	-	0.051	0.076	0.058	0.076	0.074	0.135	0.075	0.083	0.131	0.104			
Fe ²⁺	0.237	0.250	0.176	0.171	0.192	0.130	0.103	0.096	0.115	0.237	0.312	0.280	0.284	0.298	0.274	0.273	0.229	0.276	0.291	0.169	0.189			
Mn	0.004	0.005	0.002	0.002	0.002	0.001	0.001	-	-	0.003	0.007	0.004	0.004	0.004	0.004	0.004	0.003	0.005	0.003	-	-			
Mg	0.616	0.639	0.638	0.608	0.700	0.516	0.481	0.478	0.510	0.753	0.690	0.676	0.630	0.680	0.607	0.595	0.558	0.589	0.580	0.423	0.457			
Ca	0.882	0.906	0.836	0.812	0.911	0.618	0.553	0.536	0.614	0.994	0.911	0.885	0.822	0.840	0.836	0.835	0.829	0.833	0.859	0.502	0.536			
Na	0.075	0.068	0.144	0.160	0.041	0.342	0.417	0.437	0.349	0.009	0.028	0.051	0.076	0.058	0.088	0.096	0.135	0.090	0.083	0.433	0.388			
TOTAL	3.993	4.002	4.001	3.997	3.977	4.001	4.000	4.000	3.999	4.011	3.999	4.009	4.003	4.010	4.000	3.999	4.000	4.000	4.008	4.001	4.000			
END-MEMBERS (%)																								
Ca-Ti-Ts	0.85	0.87	0.77	0.72	0.75	0.54	0.19	0.16	0.46	0.23	0.26	1.20	1.14	1.21	1.19	1.13	0.98	1.07	1.16	1.56	1.63			
Ca-Ts	8.46	5.62	5.10	7.18	4.05	4.63	2.60	1.39	5.85	0.42	1.57	5.06	9.97	6.02	9.09	8.93	10.18	10.61	9.94	2.56	2.67			
Jd	7.56	6.29	14.43	16.04	4.23	32.52	40.40	42.70	31.72	-	2.77	-	-	-	1.24	2.16	-	1.50	-	30.14	28.34			
Ac	-	0.47	-	-	-	1.65	1.33	1.01	3.15	0.88	-	5.16	7.58	5.85	7.58	7.44	13.53	7.53	8.33	13.11	10.42			
Di	57.37	60.14	60.85	57.33	70.00	45.13	43.22	43.37	44.92	74.67	61.25	58.57	48.97	53.63	50.29	50.13	50.79	48.45	50.10	32.97	34.85			
Hd	22.04	23.51	16.77	16.16	19.18	11.40	9.27	8.73	10.13	23.49	27.72	24.21	22.02	23.52	22.68	23.00	20.81	22.75	25.15	13.14	14.42			
Jo	0.38	0.47	0.15	0.18	0.25	0.08	0.05	-	0.03	0.31	0.62	0.36	0.27	0.28	0.32	0.32	0.32	0.39	0.25	-	-			
En	2.41	1.88	1.51	1.88	1.22	3.22	2.42	2.20	3.06	-	3.98	3.83	6.90	6.58	5.23	4.70	2.40	5.21	3.36	4.66	5.42			
Fs	0.93	0.73	0.42	0.53	0.33	0.81	0.52	0.44	0.69	-	1.80	1.58	3.10	2.89	2.36	2.16	0.98	2.47	1.69	1.86	2.24			
Rh	0.02	0.02	-	0.01	-	0.01	-	-	-	-	0.04	0.02	0.04	0.03	0.03	0.03	0.02	0.04	0.02	-	-			

Fe³⁺ calculated on the basis of the structural formula, after Mysen & Griffin (1973)

Figures in brackets refer to the number of analysis points

TABLE 3.8 Analyses of amphiboles
from the Garnet-Granulite

(wt. %)	Calc-sil	
	E3 (2)	1410 (4)
SiO ₂	42.31	42.31
TiO ₂	1.44	2.07
Al ₂ O ₃	13.91	11.42
FeO	11.79	15.76
MnO	0.08	0.08
MgO	12.15	11.15
CaO	11.91	11.16
Na ₂ O	2.10	2.19
K ₂ O	1.95	0.31
TOTAL	97.64	96.45
MINERAL FORMULAE (23 OXYGENS)		
Si	6.263	6.308
Ti	0.160	0.232
Al	2.427	2.007
Fe ³⁺	0.000	0.656
Fe ²⁺	1.460	1.310
Mn	0.010	0.010
Mg	2.681	2.478
Ca	1.889	1.783
Na	0.603	0.633
K	0.368	0.059
TOTAL	15.861	15.476

Fe³⁺ calculated by the iterative
method of Leake (1978)

Figures in brackets refer to the
number of analysis points

TABLE 3.9 Analyses of secondary feldspars from the Garnet-Granulite

(wt. %)	E3 (1)	E3 (3)	103 (2)	1410 (2)	1410 (2)	1410 (2)	1429 (2)
SiO ₂	62.43	62.32	58.81	63.82	64.11	64.84	67.11
Al ₂ O ₃	23.78	24.04	26.06	22.75	22.17	22.13	20.57
FeO	0.16	0.12	0.07	0.20	0.15	0.14	0.16
CaO	5.27	5.59	8.31	4.19	3.54	3.43	1.69
Na ₂ O	8.60	8.24	6.79	9.21	9.49	9.53	10.80
K ₂ O	0.34	0.47	0.25	0.11	0.13	0.13	0.07
BaO	-	-	-	0.03	0.04	0.01	-
TOTAL	100.58	100.78	100.29	100.31	99.63	100.21	100.40
STRUCTURAL FORMULAE (8 OXYGENS)							
Si	2.756	2.746	2.622	2.813	2.839	2.851	2.933
Al	1.237	1.250	1.371	1.182	1.157	1.147	1.060
Fe ²⁺	0.006	0.005	0.003	0.007	0.006	0.005	0.006
Ca	0.249	0.262	0.396	0.198	0.168	0.162	0.079
Na	0.736	0.704	0.584	0.787	0.815	0.812	0.915
K	0.019	0.026	0.016	0.006	0.007	0.007	0.004
Ba	-	-	-	0.001	0.001	0.002	-
TOTAL	5.003	4.993	4.992	4.994	4.993	4.986	4.997
END-MEMBERS (%)							
Ab	73.3	71.0	58.6	79.4	82.2	82.6	91.7
An	24.8	26.4	39.8	19.9	16.9	16.4	7.9
Or	1.9	2.6	1.6	0.7	0.8	1.0	0.4

Figures in brackets refer to the number of analysis points

FIG. 3.19

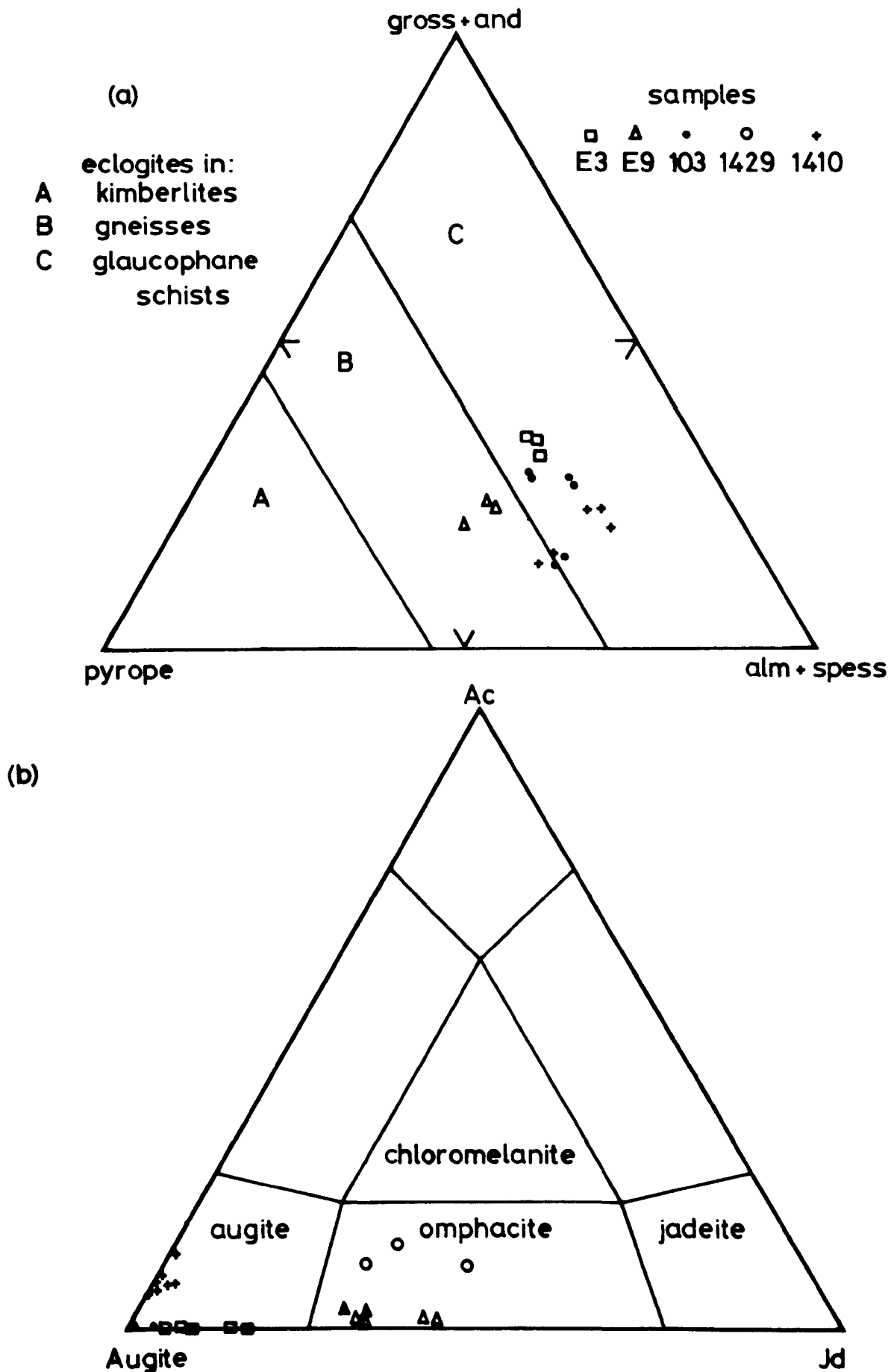


FIG. 3.19(a) (Grossular + andradite) - (almandine + spessartine) - pyrope diagram after Coleman et al. (1965) with their division of eclogite types.

(b) Acmite - jadeite - augite diagram and divisions after Essene & Fyfe (1967).

contents (9-31%). The compositions are broadly comparable to the garnets of the eclogites in the Seve nappe (van Roermund, 1983) but are more grossular than those of the Ulsteinvik eclogite at Hareid (Mysen & Heier, 1972).

The garnets richest in grossular come from sample E3 (\equiv E2 in Table 3.3) with > 30%, and sample 103 (\equiv 102 in Table 3.3) with \sim 26%. Both of these samples are of mixed Garnet-Granulite/marble rocks which have CaO contents higher than, and MgO contents lower than the average Garnet-Granulite in Table 3.1. By contrast, the sample with the lowest grossular content (1429) with \sim 10%, has a bulk chemistry lower in CaO than the average Garnet-Granulite. Sample 1410, with the most almandine garnets (\sim 57%) has the most Fe-rich bulk composition of the samples of Garnet-Granulite in Table 3.1 (15.68% total FeO). Consequently, it can be seen that the compositions of these phases fairly accurately reflect the bulk compositions of their respective rocks.

The analyses of the clinopyroxenes are given in Table 3.7, and are of both unaltered grains (E9, 1429) and symplectitic grains (E3, 103, 1410). All come from matrix clinopyroxenes. As shown on Fig. 3.19(b), after Essene & Fyfe (1967), there is a distinct compositional division between these two types of clinopyroxenes. The relict grains display jadeite contents up to 43%, equivalent to omphacites from eclogites elsewhere in Norway: 35-40% in the Ulsteinvik eclogite (Mysen, 1972); 44% in eclogites at Sunnfjord (Krogh, 1980a); 50% in the eclogites of the Seve Nappe (van Roermund, 1983). This compositional division is most likely to be a result of the sampling which included only well developed symplectites and unaltered grains. The development of the symplectite is reflected in the lower Na₂O, enrichment of FeO and lower calculated jadeite contents of the phases. Indeed the examples in

samples 1410 and 103 are almost entirely diopside-hedenbergite types as would be expected from the unmixing of plagioclase from an omphacitic clinopyroxene, through the reactions described in section 3.1.1.

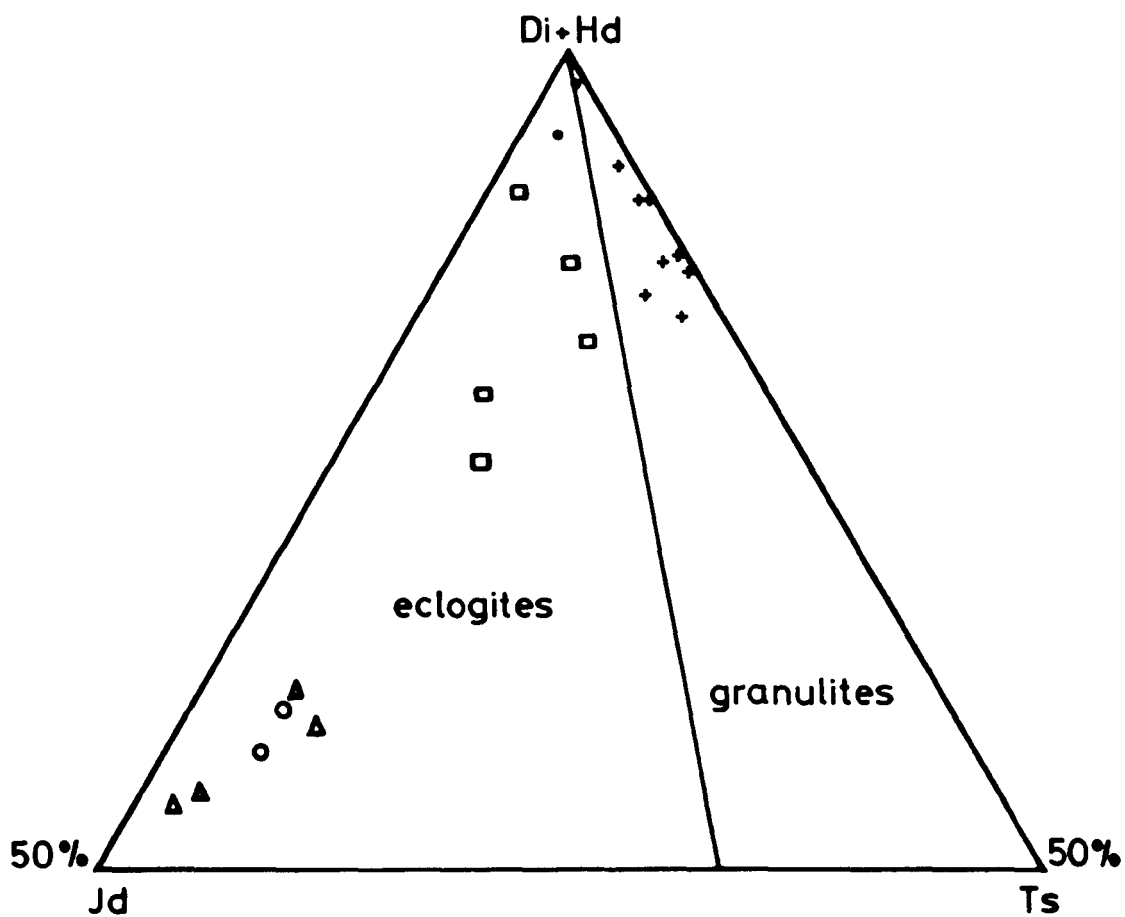
Plotting the data on Fig. 3.20 (after Lovering & White, 1969) shows that only the clinopyroxenes from sample 1410 are truly of granulite facies type, although sample 103 lies very close to the diopside-hedenbergite apex where the arbitrary division of $Jd:TS = 1.2$ may not be totally valid. Once again the chemical division between the symplectic and relict grains is well defined on this plot.

Of the relict grains only that from sample E9 shows any zoning, with an increase of jadeite from core to rim. The grains of clinopyroxene in E9 are fairly large ($\sim 4-5$ mm) compared to those in the other samples (~ 1 mm) which would have inhibited the process of volume diffusion (Tracy, 1982) and the eradication of compositional zoning.

Unfortunately, the presence of the symplectic clinopyroxenes makes it difficult to relate the mineral compositions to the bulk-rock compositions as with the garnets although it can be seen from Table 3.7 that the most calcic clinopyroxenes (E3 and 103) come from the mixed Garnet-Granulite/marble rocks which have CaO contents higher than the average Garnet-Granulite in Table 3.1.

The analysed amphiboles are given in Table 3.8, that from sample E3 is a primary phase whilst that from sample 1410 is secondary, after clinopyroxene. Both are Ca-rich amphiboles in the classification of Leake (1978) with $(Ca + Na) \geq 1.34$. The primary amphibole in E3 is more Mg, K and Al rich, but poorer in Fe than the secondary amphibole and classifies as a pargasite according to Leake of an equivalent type to the primary amphiboles observed in the Garnet-Granulite (section 3.1.1). The secondary amphibole classifies as a Tschermakite on Leake's

FIG. 3.20



see FIG. 3.19 for key to symbols

FIG. 3.20 (Diopside + hedenbergite)-tschermakite-jadeite diagram with eclogite-/granulite-pyroxene division of Lovering & White (1969).

method. As noted by Lappin & Smith (1978) secondary amphiboles in retrogressed eclogites are richer in Ti than the early (their 'primary') amphiboles which has been attributed to variations in oxidation conditions during eclogite facies and subsequent retrograde metamorphic events (Pinet & Smith, 1982).

The feldspars associated with the symplectic clinopyroxenes are given in Table 3.9 and bear the following relationships in these particular samples:

- E3: coarse symplectite
- 103: groundmass
- 1410: coarse symplectite and groundmass
- 1429: coarse groundmass adjacent to clinopyroxene

The phases display a wide range of compositions, from An 8 to An 40, but these are equivalent to those found by Krogh (1982) in eclogites with secondary symplectic feldspars elsewhere in the Basal Gneiss Complex. Although the degree of development of symplectite in samples E3 and 103 is no greater than that in sample 1410, the secondary feldspars are somewhat more calcic perhaps reflecting the more Ca-rich bulk-rock compositions of these mixed Garnet-Granulite/marble rocks.

3.4.2 The kyanite pelite

The analyses of the phases from sample 1018 are given in Table 3.10, and included garnet, biotite and plagioclase with the express purpose of calculating P-T conditions for this rock using the methods of Ferry & Spear (1978), Ghent et al. (1979) and Newton & Haselton (1981). The garnet is an almandine-pyrope variety with a little grossular and andradite, typical of garnets from metapelitic rocks (Miyashiro 1973, p. 214-221). The low MnO content of this phase, reflected in the low calculated spessartine value, is considered to reflect the high P paragenesis of the rock (cf. Miyashiro 1973, p. 221). The mica is a biotite with a Mg/Fe ratio < 2 and is fairly titaniferous.

TABLE 3.10 Analyses of phases in the kyanite pelite (1018) in the heterogeneous rocks of the Tverrfjella Unit

(wt. %)	GNT (3)	MICA (2)	FELD (4)
SiO ₂	37.85	34.46	60.56
TiO ₂	0.02	3.40	-
Al ₂ O ₃	21.28	18.68	24.53
FeO	31.41	19.65	0.13
MnO	1.21	0.11	-
MgO	4.94	9.01	-
CaO	4.00	0.01	6.53
Na ₂ O	-	0.10	7.82
K ₂ O	-	9.90	0.28
TOTAL	100.71	95.32	99.85
MINERAL FORMULAE			
	12 'O'	22 'O'	8 'O'
Si	2.972	5.285	2.701
Ti	0.001	0.392	-
Al	1.969	3.377	1.290
Fe ³⁺	0.085	-	-
Fe ²⁺	1.978	2.521	0.005
Mn	0.080	0.015	-
Mg	0.578	2.060	-
Ca	0.336	0.002	0.312
Na	-	0.029	0.676
K	-	1.937	0.016
TOTAL	7.999	15.618	5.000
END-MEMBERS (%)			
ANDR	4.23	Mg/Fe 0.817	Ab 67.3
PYROPE	19.44		An 31.1
SPESS	2.71		Or 1.6
GROSS	7.05		
ALM	66.53		
SCHORL	0.04		

(Fe³⁺ for garnet calculated by charge-balance)

Figures in brackets refer to the number of analysis points

3.4.3 Pressure and temperature calculations

The pressure and temperature data calculated for the Garnet-Granulite from the data in Tables 3.6, 3.7 and 3.9 are given in Fig. 3.21 and in Table 3.11; the P-T data for the pelite are given on Fig. 3.21. Only adjacent rim compositions have been used in these calculations to ensure, as far as is practicably possible, that the two phases are in equilibrium and will therefore reflect the P and T of final equilibration.

The P-T values for the non-feldspathic sample (E9) are shown as P-T lines on Fig. 3.21 using the calibration of Ellis & Green (1979) as there is no method of obtaining an estimate of the pressure of equilibration for these rocks from their assemblages. For the feldspathic samples the methods of Currie & Curtis (1976), Ellis & Green (1979), Krogh (1983) and Newton & Perkins (1982) were solved iteratively. The P-T values for the pelite were calculated using the methods of Ferry & Spear (1978), Ghent et al. (1979) and Newton & Haselton (1981). (See Appendix B for an explanation of these various methods.)

The P values from the method of Currie & Curtis (1976) are often negative or very low (1410, 103 and E3/4) which appears to be a result of these particular samples having little or no jadeite component in the clinopyroxene. Also, the T values for E3 and 103 are excessively high which seem to be a result of the calcic nature of the garnets in those samples. Both of these samples are of mixed Garnet-Granulite/marble rocks and the bulk rock composition is likely to be too calcic for the method of Ellis & Green (1979). The high T value for sample 103 is also partly a result of the low K_D for this sample which, in turn is a result of the high value for Fe^{2+} in this clinopyroxene (0.312). The P values from the method of Newton & Perkins (1982) are more realistic for

TABLE 3.11 Pressure and temperature data for the Garnet-Granulite

	PARAMETERS					METHODS				
	% Jd	K_D^*	K_D	X_{Ca}^{gnt}	X_{Ab}^{plag}	M & G T	E & G/C & C T	P	E & G/N & P T	P
FELDSPAR BEARING SAMPLES										
E3/1	7.56	5.23	5.06	0.335	0.733	711	904	8.5	929	15.3
E3/2	14.43	7.29	7.05	"	0.710	608	802	8.2	821	13.8
E3/3	16.04	7.15	6.92	"	"	613	817	11.7	1027	16.8
E3/4	4.23	7.34	7.72	"	"	606	732	-8.2	793	12.7
103	2.77	3.71	3.58	0.298	0.586	846	956	-3.0	1015	13.0
1410/1	-	5.06	5.81	0.225	0.794	722	754	5.7	778	11
1410/2	2.16	5.16	5.92	"	0.822	716	647	5.7	775	12
1410/3	-	4.58	5.32	"	0.826	759	681	-17.4	808	12.6
1429	30.14	2.94	4.77	0.145	0.917	961	789	19.4	785	17.3
NON-FELDSPAR BEARING SAMPLES										
E9	-	6.15	6.61	0.258	-	658				

K_D^* = gnt/cpx Fe-Mg partitioning with all Fe as Fe²⁺

K_D = gnt/cpx Fe-Mg partitioning with calculated Fe³⁺

M & G = Mori & Green (1970) E & G = Ellis & Green (1979)

C & C = Currie & Curtis (1976) N & P = Newton & Perkins (1982)

FIG. 3.21

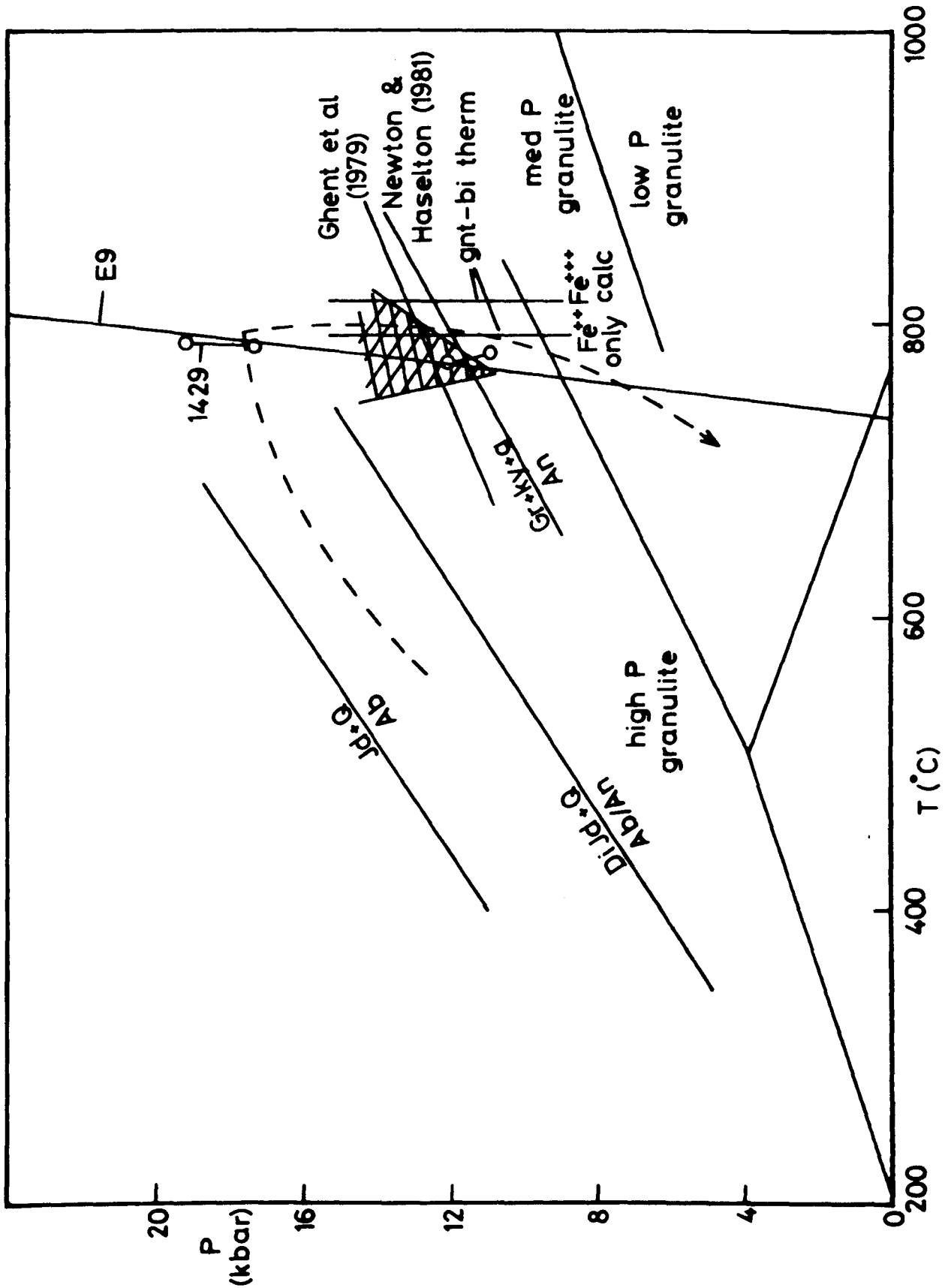


FIG. 3.2 Pressure and temperature grid for the data from the Garnet-Granulite and kyanite pelite (1018). Shaded area are the postulated conditions of melting for the pelites from Fig. 3.4.

Alb + Jd + Q from Holland (1979)

Alb + An + DiJd₄₀ + Q from Holland (1979)

Granulite fields from Green & Ringwood (1967a)

Dotted line is the postulated metamorphic path for the Tverrfjella Unit

a high-pressure granulite, although Newton & Perkins consider that their method may underestimate the pressure for a clinopyroxene-bearing assemblage. Again, the T values for samples E3 and 103 appear to be too high. Sample 1429, which contains the smallest amount of secondary plagioclase, and the most sodic, gives the highest P value for both of the methods: Currie & Curtis and Newton & Perkins. The values of ~ 18.5 kbar and 787°C are comparable to the P-T conditions calculated for eclogites elsewhere in the Basal Gneiss Complex (Griffin et al. 1983, and see Fig. 3.21).

On Fig. 3.21 the P-T data for samples 1429, 1410 and E9 are shown. If the method of Krogh (1983) had been used to calculate the P-T line for sample E9, temperatures of $\sim 50^{\circ}\text{C}$ would have resulted. Using the P estimate of 18.5 kbar from sample 1429 a temperature of $\sim 788^{\circ}\text{C}$ is obtained for sample E9, virtually identical to that for 1429. These P and T values reflect the relict eclogite facies mineralogies of these two samples and that of the original assemblage of the Garnet-Granulite as a whole. Furthermore these values fit in well with the regional distribution of temperatures derived from eclogites across the Basal Gneiss Complex from which temperatures $> 750^{\circ}\text{C}$ would be expected for eclogites in this area (Krogh, 1977; Griffin et al., 1983, and see Fig. 1.3).

The P-T data from sample 1410 (~ 12 kbar, $\sim 780^{\circ}\text{C}$) reflect the presently observed high-P granulite assemblage of the rocks. An important point here is that these P-T conditions for the retrogressed and symplectised rocks retain high temperature values reflecting the isothermal uplift of the rocks as deduced from the mineral textures (section 3.1.5).

The P-T data for pelite sample 1018 were calculated using the Al-silicate-quartz-plagioclase-garnet assemblage in the methods of Ghent

et al. (1979) and Newton & Haselton (1981). The P-T lines for these two methods are shown on Fig. 3.21 and agree very well. The method of Ferry & Spear (1978) was applied to the garnet-biotite pair in the same rock. Unfortunately, the biotite is rather titaniferous, which if excessive would result in unrealistic temperature estimates (Ferry & Spear, 1978). This phase gives a $(Al^{IV} + Ti)/(Al^{VI} + Ti + Fe + Mg)$ value of 0.187, only slightly higher than the limit of < 0.15 set by Ferry & Spear. The garnet is not particularly Ca or Mn rich and gives a $(Ca + Mn)/(Ca + Mn + Fe + Mg)$ value of 0.135 within the limit of < 0.2 set by Ferry & Spear.

Taking all Fe as Fe^{2+} gave a value for the partition coefficient (K) of 0.307 and a temperature of $792^{\circ}C$. The incorporation of Fe^{3+} into the calculation was found to have only a limited effect on the temperature value. Taking an arbitrary value of 2.25% Fe_2O_3 for the biotite (based on values of $\sim 0.5-4.0\%$ in Deer et al. 1963, vol. III, p. 62), and calculating Fe^{3+} in the garnet by charge balance altered the K only slightly to 0.321, which gave a temperature of $816^{\circ}C$. Consequently, the curve on Fig. 3.21 should be taken as a minimum temperature for this rock as should the P estimates where this curve cuts the anorthite \rightarrow grossular reaction curves. Interestingly the final equilibration conditions of this rock ($\geq 790^{\circ}C$, ≥ 12.5 kbar) are very similar to those of the high-P granulite assemblage in the Garnet-Granulite.

The derived P-T values for the Garnet-Granulite shown on Fig. 3.21 agree very well with the P-T path postulated for the Tverrfjella Unit in section 3.1.5 and shown on Fig. 3.4. Also, the calculated P-T conditions for the pelite lie very close to the 'dry-melting' conditions postulated for these rocks on a mineralogical basis (see Fig. 3.4).

It is considered that the high grade metamorphism of these meta-sedimentary/metavolcanic rocks, substantiated by the calculated P-T

conditions here is indicative of eclogite facies metamorphism in the crust as postulated by Bryhni (1966) for the 'external' eclogite pods in the Basal Gneiss Complex. However, Lappin & Smith (1978) consider that eclogite facies mineralogies cannot form within the crust and prefer P-T conditions of 30-45 kbar and 700-900°C for the equilibration conditions of these rocks, i.e. in the upper mantle. They consider that the eclogite pods were tectonically introduced into the lower crust, perhaps as part of the mega-mélange of Smith (1980), during continent-continent collision. However, it is difficult to envisage the tectonic processes required for such a large-scale lithological mixing which would allow the preservation of the stratigraphic sequencing observed in the Tverrfjella Unit.

PLATE 3.1

- (a) Appearance of the Garnet-Granulite in outcrop. Note the blocky, well-jointed nature of the rock. The banding is just visible, and is vertical. Talstadhesten top (O91743).
- (b) Appearance of the Garnet-Granulite in thin section. Garnet at bottom (note tiny inclusions of quartz and plagioclase); clinopyroxene above (note incipient symplectite at lower right of grain); plagioclase lower right (sample 1428, cross-polarised light).
- (c) Mineralogical banding of the Garnet-Granulite. Darkest bands are concentrations of opaque minerals, grey are garnet and clinopyroxene, lightest are plagioclase and quartz. N side of Talstadhesten (O92748).
- (d) Quartz-rich portion of the Garnet-Granulite exhibiting 'strings' of clinopyroxene between quartz and secondary plagioclase rims on garnet. Garnet is opaque at bottom. Note that the 'string' passes into the symplectitic clinopyroxene at the right of the picture. (Sample 1410, cross-polarised light).
- (e) Retrogressed example of the Garnet-Granulite with garnet displaying a well developed kelyphite rim of finely intergrown hornblende and plagioclase with exsolved opaque phases. (Sample 1421, plane-polarised light.)
- (f) Retrogressed example of the Garnet-Granulite with clinopyroxene displaying a symplectite texture with plagioclase. Note the exsolved magnetite grains within the symplectite portion of the grain. (Sample 1410, plane-polarised light.)

PLATE 3.1

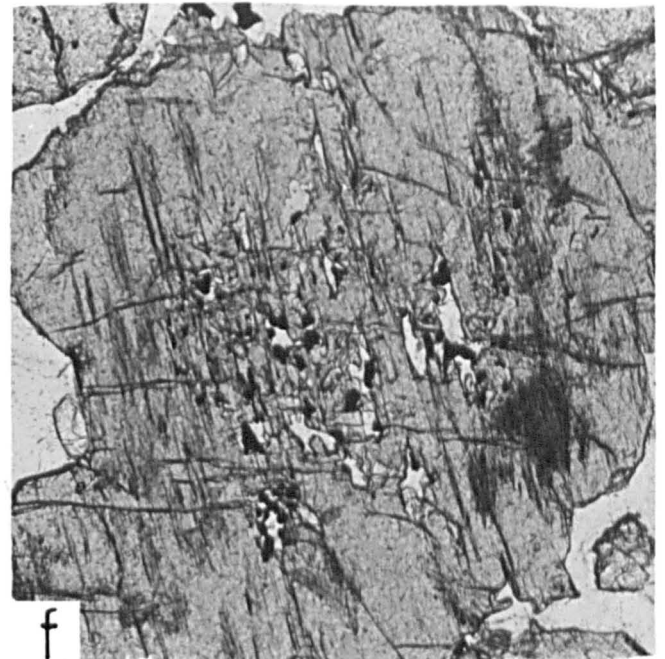
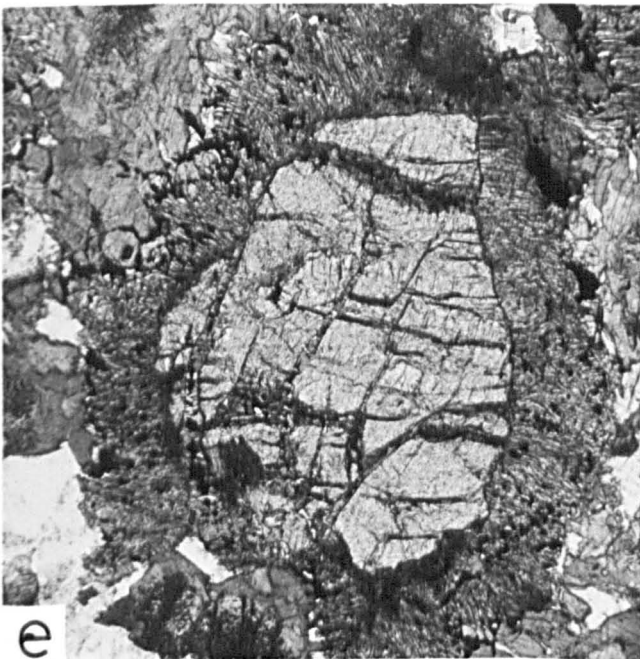
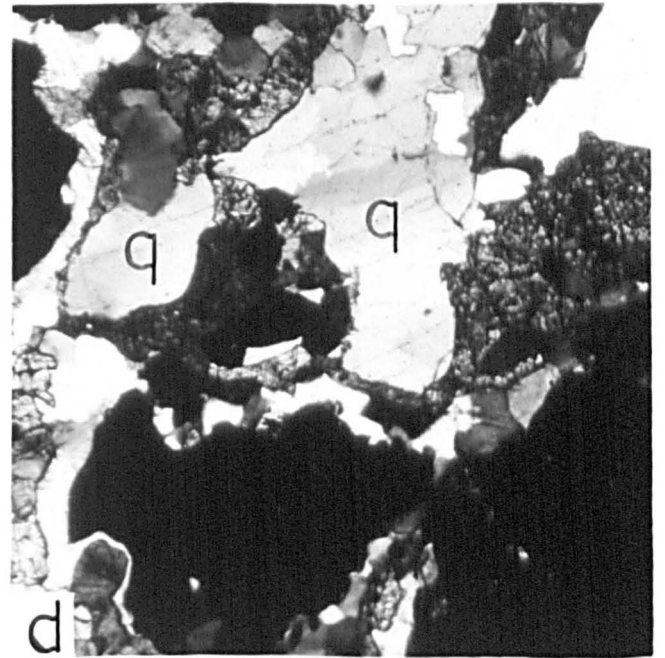
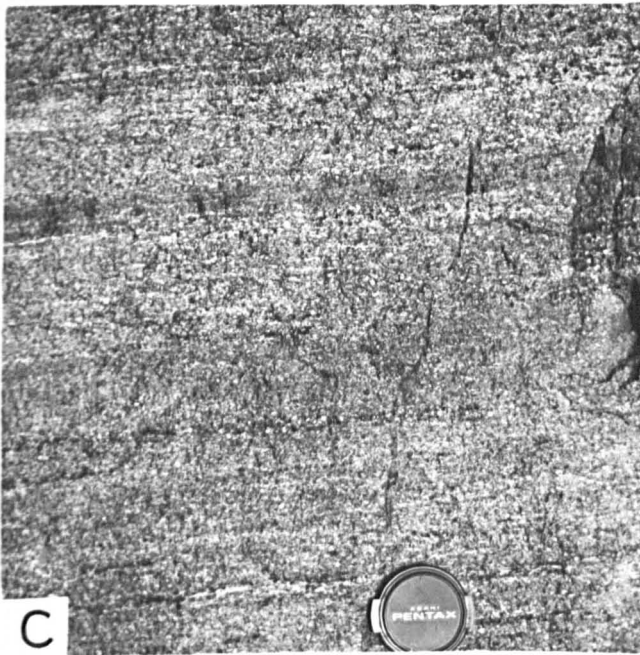
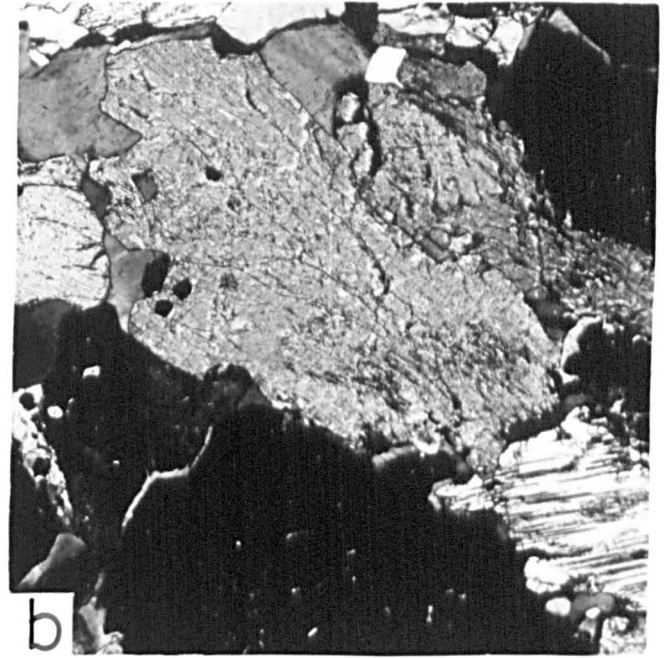
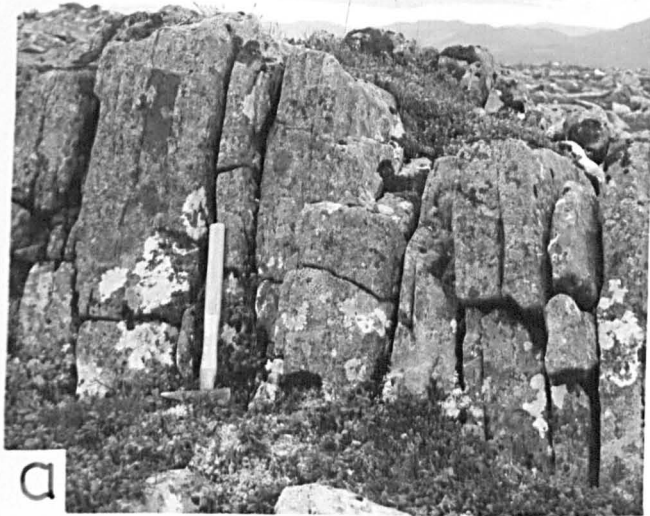


PLATE 3.2

- (a) General appearance of the partly retrogressed Garnet-Granulite. Plagioclase is fairly well developed in both fine symplectite with clinopyroxene to the right and more coarse replacement of both clinopyroxene and garnet, centre and left. Note cracking of the garnet and amphibolitisation with development of coarser amphibole grains at bottom left. (Sample 1422, plane-polarised light.)
- (b) Heavily retrogressed Garnet-Granulite displaying relict symplectic diopsidic clinopyroxene surrounded by irregular hornblende and plagioclase. Note ilmenite rimmed by sphene left of centre after rutile. (Sample 1423, plane-polarised light.)
- (c) Breakdown of kyanite, on right, to plagioclase and possibly corundum (the high-relief phase attached to the kyanite). (Sample 1434, plane-polarised light.)
- (d) Further breakdown of kyanite to plagioclase and clays in the murky area in centre of picture. Relict kyanite at top right of picture. (Sample 1425R, plane-polarised light.)
- (e) General appearance of the small garnet-peridotite S of Talstadhesten (O92734). Olivine is bottom right, mica top right. Note profuse opaque phases (magnetite) and spinel at centre top of picture. Also note orientation of orthopyroxene plus hydration on rim of garnet. (Sample 1413, plane-polarised light.)
- (f) Contacts of marble and the Garnet-Granulite, at top of quarry face and in a pygmatic band. Former contact is sharp; latter is gradational. Langvatnet quarry (O85752). Hammer at bottom right.

PLATE 3.2

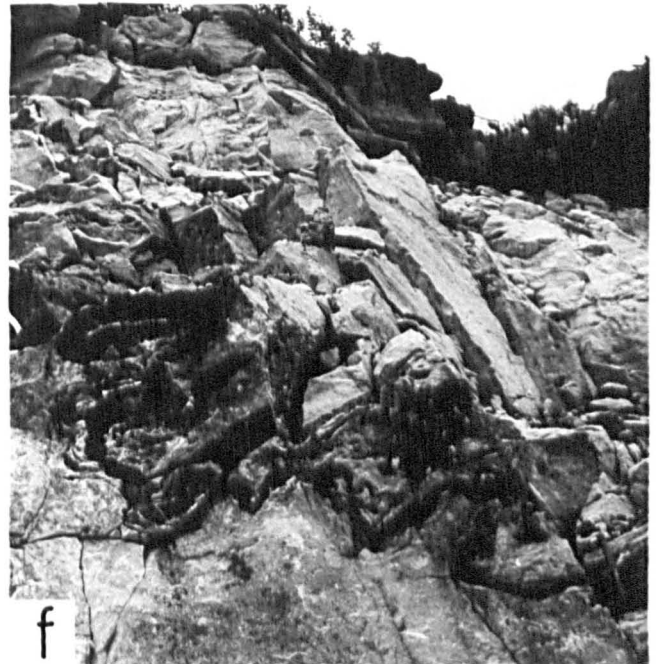
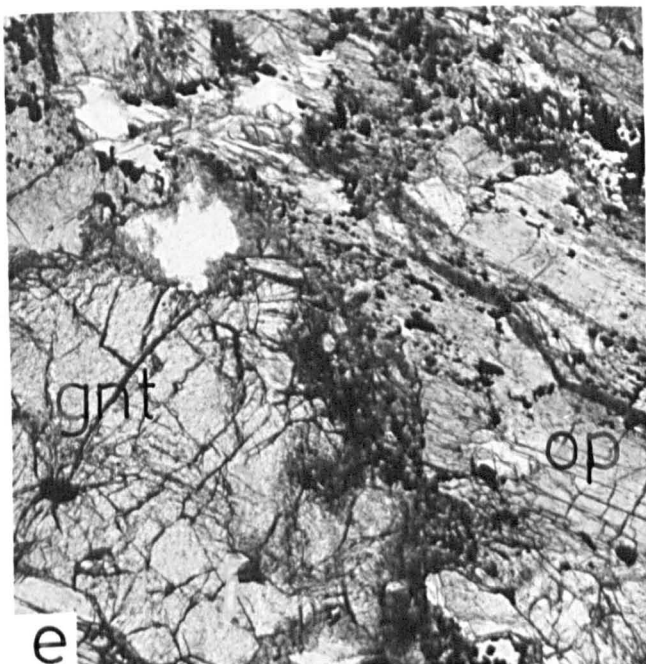
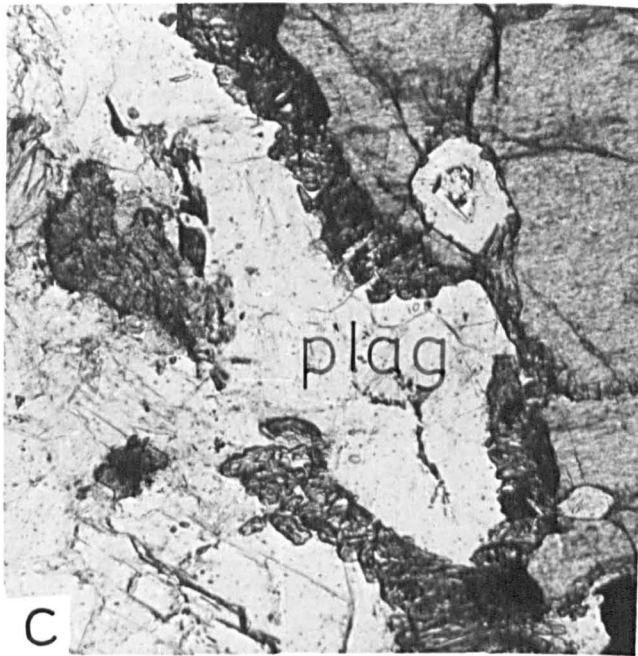
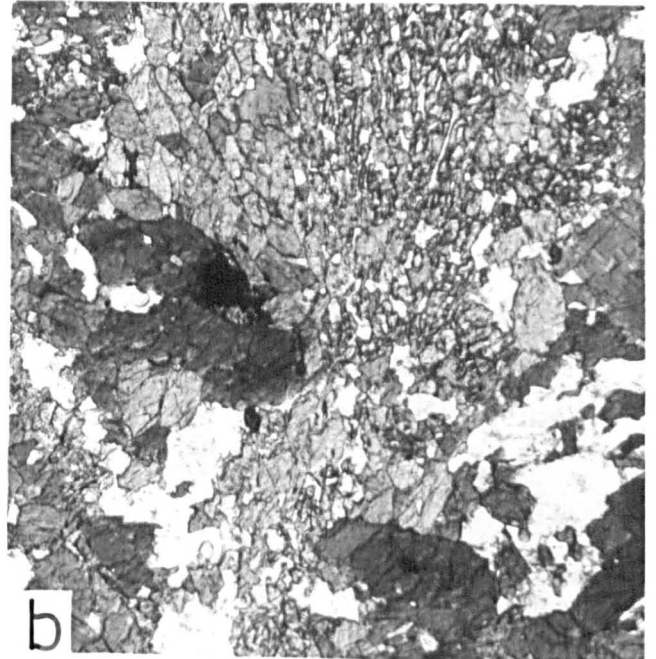
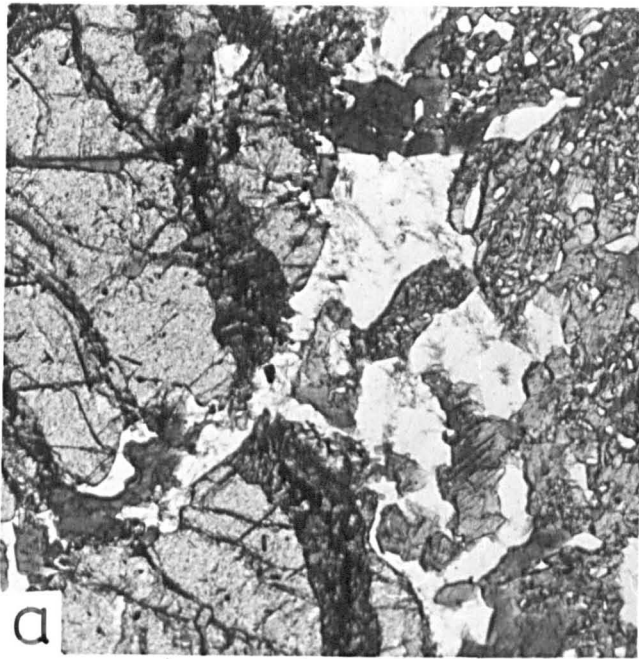


PLATE 3.3

- (a) Large lobe of the Garnet-Granulite extending into the marble at Langvatnet quarry (O85752), note banding in marble on left of picture. Snow barriers at top of face are \sim 2 m high.
- (b) Gradational contact of the Garnet-Granulite and marble, fallen block. N face of Talstadhesten (O92746).
- (c) Sharp contact between the Garnet-Granulite and marble, fallen block, N face of Talstadhesten (O92746). Note banding of Garnet-Granulite and disruption of the rock as boudins. Discolouration of marble (arrowed) is pink.
- (d) Breakdown of clinopyroxene (opaque) in the impure marble to tremolite (colourless) and calcite (speckled). (Sample 1418, cross-polarised light.)
- (e) Quartz against calcite in the impure marble producing a rim of colourless mineral possibly actinolite. (Sample 165, cross-polarised light.)
- (f) Zoisite being replaced by scapolite, impure marble. (Sample 165, cross-polarised light.)

PLATE 3.3

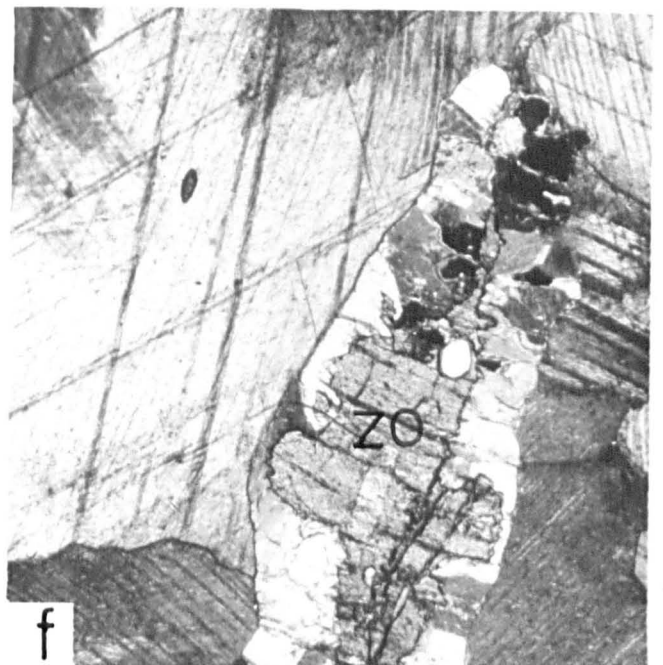
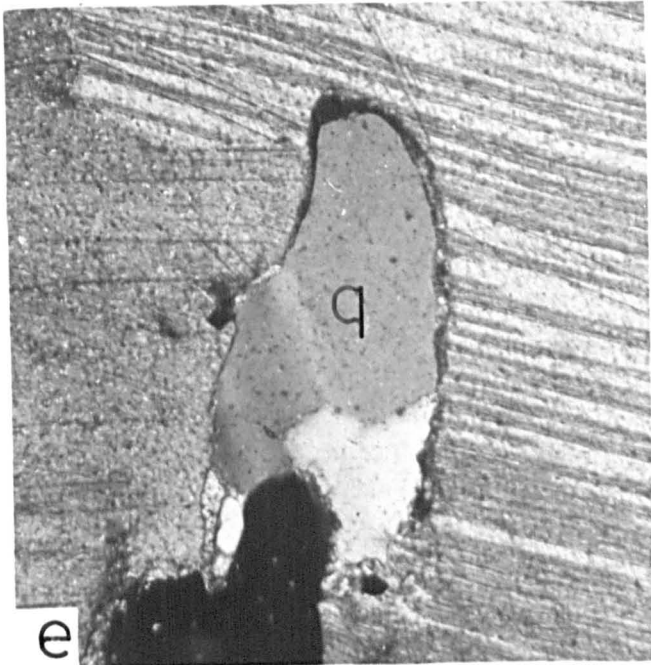
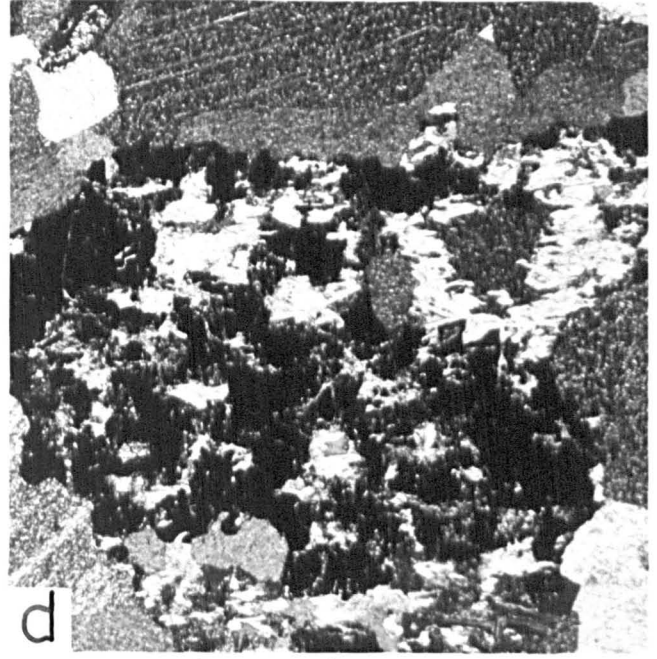
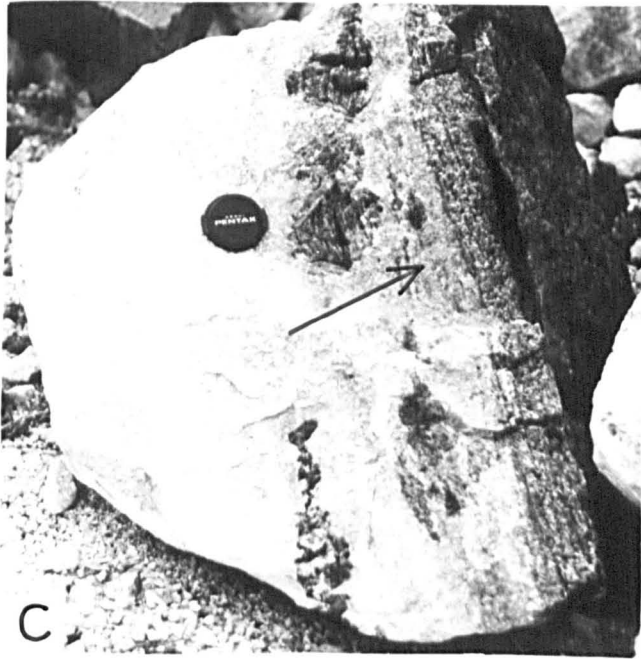
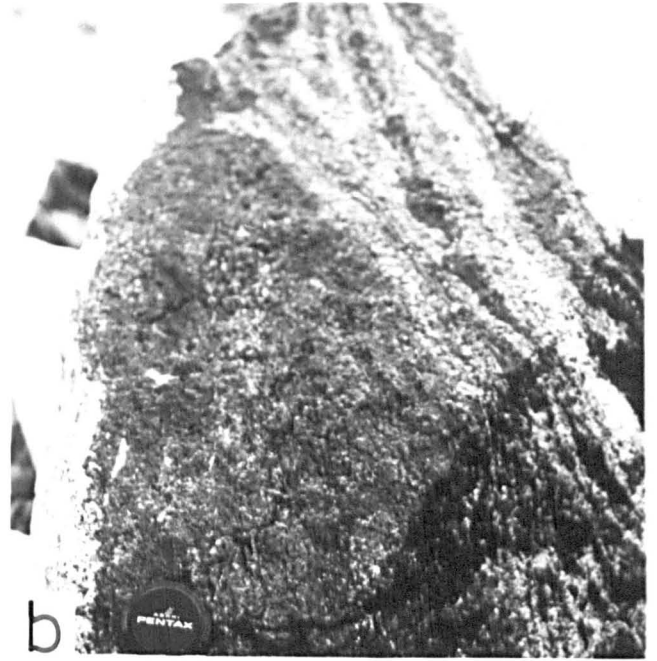
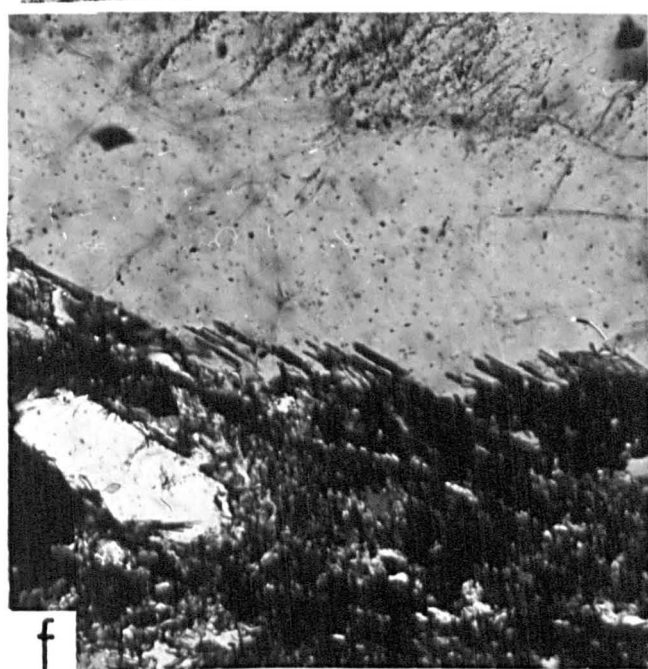
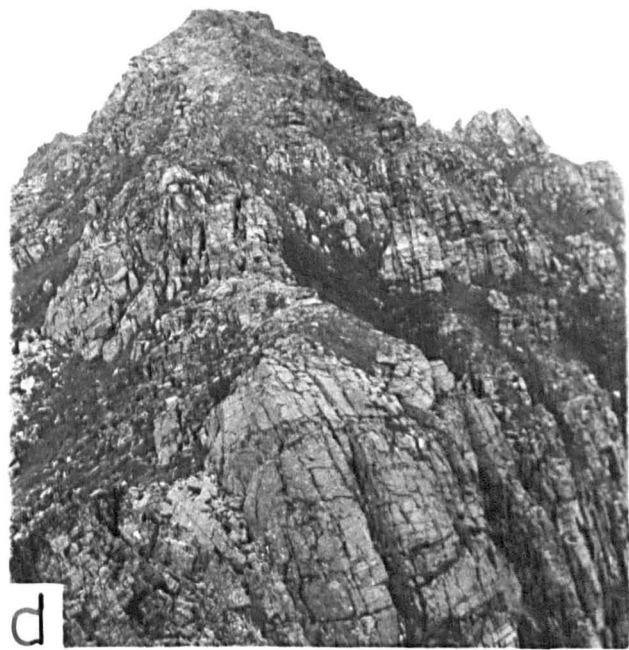
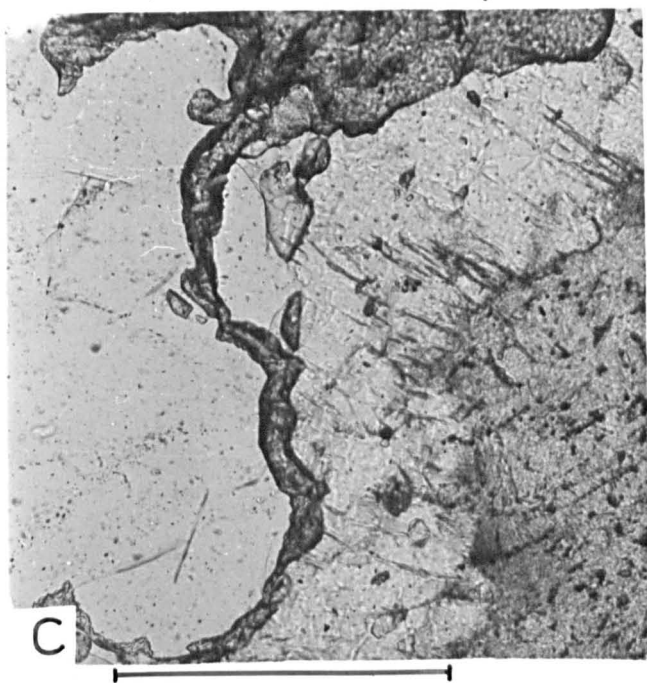
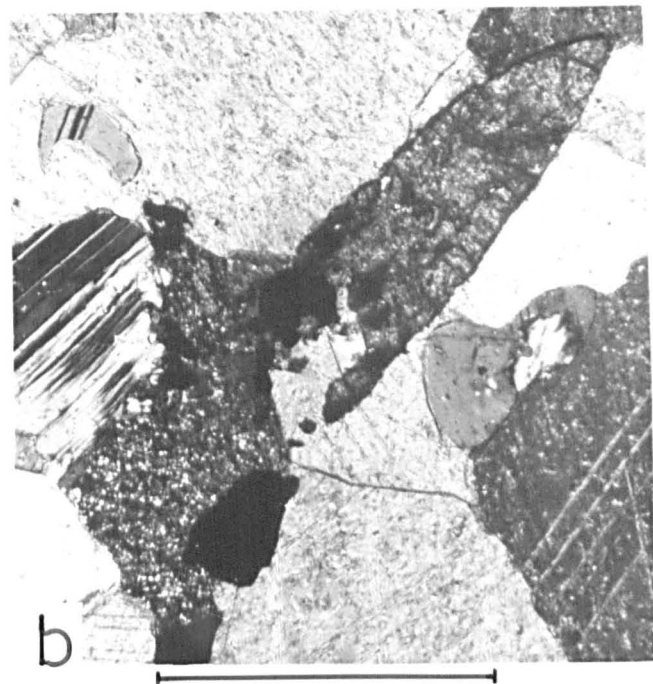
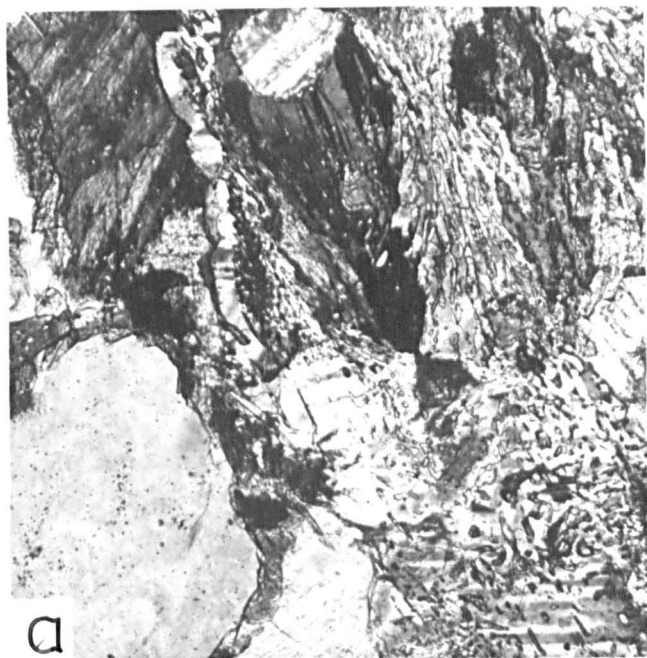


PLATE 3.4

- (a) Scapolite breaking down to a coarse symplectic intergrowth of zoisite (the high R.I. 'wormy' phase) and calcic-plagioclase. (Sample 165, cross-polarised light.)
- (b) Sphene + quartz producing rutile in the presence of an opaque phase. (Sample 167, cross-polarised light.)
- (c) Anatectic portion (on left of picture) against scapolite producing a rim of clinopyroxene which passes into a grain of primary clinopyroxene at top of picture. Note incipient alteration of scapolite to turbid mass of clays and opaques. (Sample 1417, plane-polarised light.)
- (d) Layered nature of the heterogeneous rocks of the Tverrfjella Unit seen on S face of Trolltindane (118751). Height of face ~ 150 m.
- (e) Clinozoisite breaking down to plagioclase adjacent to quartz in quartzite band within the Garnet-Granulite. (Sample 1012, cross-polarised light.)
- (f) K-feldspar (top of picture) adjacent to biotite, with fine, fibrous sillimanite growing at the contact. (Sample 1018, cross-polarised light.)

PLATE 3.4



INTRODUCTORY STATEMENT TO CHAPTERS 4 AND 5

In the following two chapters, the tract of quartzo-feldspathic gneisses, extending from Näs^ovatnet to Mordalsvå^ogen will be discussed; these rocks fall into the Frei Group of Rå^oheim (1972 - Table 1.2). From Map A it can be seen that this tract has been subdivided into an Augen Gneiss Unit and a Heterogeneous Quartzo-Feldspathic Gneiss Unit. Although the two groups of rocks are often intimately related in the field and appear conformable, it was found that they displayed fairly distinct geochemical patterns and hence deserved to be treated as separate rock units.

During the initial stages of mapping this tract of gneisses, some difficulty was experienced in being able to satisfactorily divide the rocks into mappable units. Although some fairly distinctive rock types were observed these generally did not occupy easily defined areas of ground but tended to be gradational over short distances with other rock types. Very generally, the gneisses show the following variations from N to S: at Näs^ovatnet (1576) the rocks are predominantly migmatitic with pink, coarse-grained neosomes set in a dark, fine-grained, biotitic palaeosome. Other massive, grey gneisses also appear along the W shore of Näs^ovatnet. The migmatitic gneisses appear along the N side of Langvatnet (0775); towards Elnesvå^ogen (0570) the migmatites become inter-mixed with massive, fine-grained, banded pink gneisses or augen-bearing gneisses. Further south, across Malmefjord onto Ytre Fraena (9967) the rocks become increasingly mixed with massive, grey gneisses, pink granitic gneisses and rare massive amphibolites. The proportion of the migmatitic gneisses is much less here. South of Ytre Fraena the coarse-grained Augen Gneiss appears and becomes increasingly dominant, with

most of the outcrop of this rock appearing between Hollingsholm (9762) and Mordalsvågen (9757). However, within this Augen Gneiss, other, non-augen-bearing rocks appear: generally homogeneous grey or pink gneisses, or striped pink and grey gneisses. From its striking appearance in the field, of pink-orange ovoidal augen set in a darker, mafic matrix, the Augen Gneiss was mapped as a separate unit within this tract of gneisses. However, in some places this proved to be fairly difficult for three reasons:

(i) N of Hollingsholm, the Augen Gneiss becomes increasingly limited in extent and intercalated with other granitic gneisses, some of which have augen-like structures.

(ii) When severely deformed the Augen Gneiss can be transformed into a banded gneiss, or an apparently augen-free grey gneiss which superficially appears very similar to other similarly textured gneisses (see Plate 2.2(d)). Only at certain localities where a banded or grey gneiss can be physically traced into a progressively deformed Augen Gneiss can a distinction be made.

(iii) In general, the migmatitic gneisses can be easily recognised in the field. However, when deformed the leucosome in these rocks breaks up into pale-coloured 'augen' and the rock can take on an appearance very similar to the deformed Augen Gneiss (see Plate 2.1(b)).

Some of these problems of rock recognition and subdivision were overcome when the geochemistries of the various rock types were examined. The major advantages in this respect were that the Augen Gneiss could be defined as a distinct geochemical group with a fairly well defined differentiation trend, and that the LIL element contents (Rb, K, Ba) of this rock were only slightly disturbed. Furthermore, this differentiation trend included the finer-grained, pink granitic sheets occurring

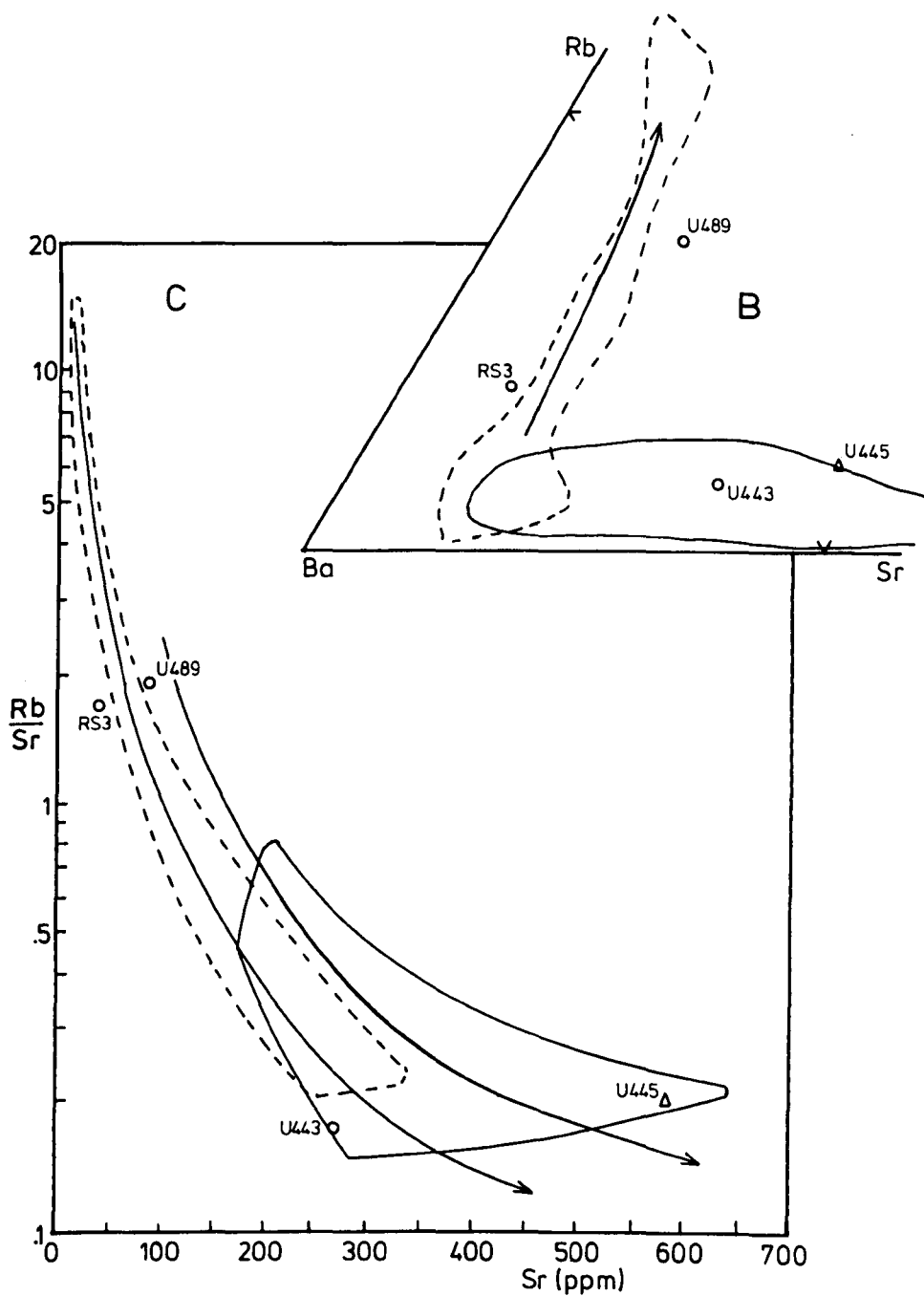
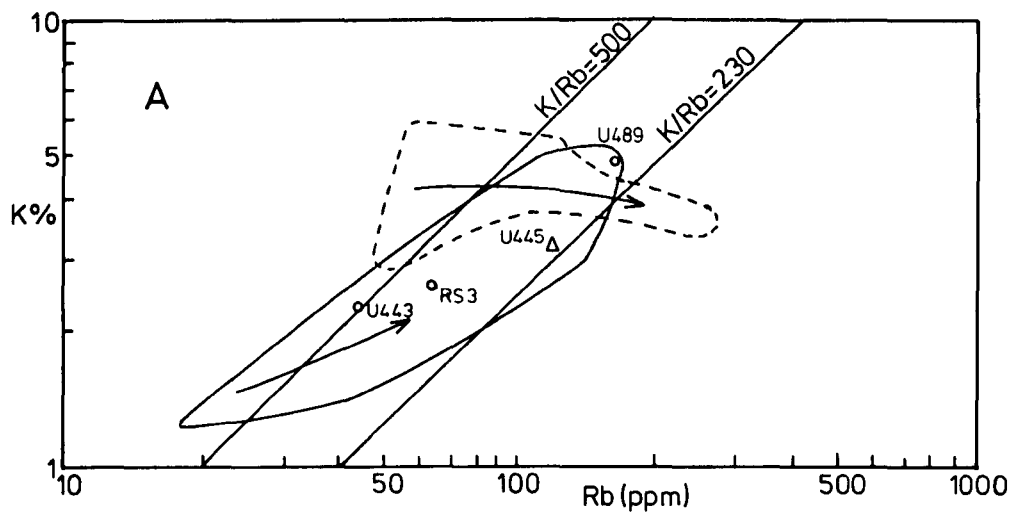
within the Augen Gneiss. The genetic connection between these two rock types was ultimately confirmed with the Rb-Sr isotopic data (see section 4.3). Initially, all rocks which, from field, petrographic or general geochemical similarity appeared to belong to the Augen Gneiss Unit, including the granite sheets, were treated as such. However, during investigation of the LIL contents of the Augen Gneiss Unit it became apparent that the differentiation trend of the Augen Gneiss was sufficiently well defined to be able to distinguish between the rocks in the Augen Gneiss Unit (s.s.) and other rocks which had been placed in this Unit on the basis of other evidence, notably: RS3, U443, U489 and U445. Three graphical plots show these distinctions well. (The data used in these plots is given in Table 4.1 for the Augen Gneiss Unit and in Tables 5.1 and 5.2 for the Heterogeneous Quartz-Feldspathic Gneiss Unit).

Fig. A (K vs. Rb) shows the fields of the Augen Gneiss Unit and that of the Heterogeneous Gneiss. The evolution trends of the two groups of rocks are different: in general the rocks of the Augen Gneiss Unit lie towards higher K/Rb ratios, whilst the Heterogeneous Gneisses lie at slightly lower K/Rb values and overall at lower K values.

Fig. B (Ba-Sr-Rb) shows the fields of the Units with the well defined trend of the Augen Gneiss Unit towards Rb enrichment in the granite sheets. The Heterogeneous Gneisses exhibit little Rb enrichment.

Fig. C (Rb/Sr vs. Sr) shows the fairly tight grouping of the Augen Gneiss Unit on the differentiation trend for these rocks. The Heterogeneous Gneisses fall mainly on a curve at higher Rb/Sr values, although a few fall on the curve for the Augen Gneiss Unit.

On all of these diagrams the 'problem rocks' always fall outside the field for the Augen Gneiss Unit, but not always inside the field for the Heterogeneous Gneiss Unit, particularly RS3 and U489. Sample RS3 appears



to be an undeformed Augen Gneiss with a granitic chemistry. However, it contains too little K, Rb and Sr to be equivalent to the Augen Gneiss (s.s.). Sample U489 was mapped as a pink granitic rock and considered to be part of the Augen Gneiss Unit. Now, Sr readily replaces Ca in plagioclase (Taylor, 1965) and this sample contains 91 ppm Sr and 0.85% CaO. For an equivalent CaO content, the granitic rocks in the Augen Gneiss Unit typically contain <50 ppm Sr (see Table 4.1). Even when deformed, the rocks of the Augen Gneiss Unit do not display such wide variations in their trace element contents and as a consequence these two samples have been placed with the Heterogeneous Gneiss Unit even though they contain rather more Rb than the majority of the rocks in that Unit.

CHAPTER 4

THE AUGEN GNEISS UNIT

4.1 GENERAL GEOLOGY AND PETROGRAPHY

From Map A it can be seen that this gneiss unit occurs as part of the tract of quartzo-feldspathic gneisses stretching from N^osvatnet to Mordalsv^ogen. For an explanation of how this tract was subdivided into the Augen Gneiss Unit and the Heterogeneous Quartzo-Feldspathic Gneiss Unit, see the Introductory Statement on p. 109. This Unit was termed the Augen Orthogneiss Complex in Carswell & Harvey (1983) and Harvey (1983).

4.1.1 Description

The main outcrop of this Unit occurs between Hollingsholm (9762) and Mordalsv^ogen (9756); as can be seen from Map A, portions of this Unit also occur within the Heterogeneous Quartzo-Feldspathic Gneiss Unit as far N as Jendem. Furthermore, a fairly extensive portion of the Heterogeneous Quartzo-Feldspathic Gneiss Unit has been mapped within the Augen Gneiss Unit. The actual northern boundary between these two Units is impossible to define accurately for two reasons: the often close similarity between the deformed rocks of the two Units and the lack of good exposure E of Jendem. However, the southern boundary of the Augen Gneiss Unit, against the Heterogeneous Group of rocks at Moldefjord is fairly well marked and can be observed running along the N side of the E662 road at Mordal farm (978576). This contact can also be found on the hills N of the town of Molde (around Varden - 044591). It is recognised that very attenuated portions of the Augen Gneiss Unit also occur within the Heterogeneous Group for approximately 0.5 km S of the main contact marked on Map A.

The dominant lithology of the Augen Gneiss Unit is a coarse-grained Augen Gneiss (capitals are used here to distinguish this rock from other augen gneisses described in subsequent chapters). When undeformed, the conspicuous pink/orange feldspar augen are ovoidal and typically ~1 cm across, although they may be up to 5 cm long (Plate 4.1(a)). The proportion of augen in relation to the darker matrix is fairly constant although some examples of the rock occur which have rather small, scattered augen, and others with larger, closer packed augen. The general appearance of the gneiss is quite variable depending upon the size and apparent proportion of the augen, and the degree of deformation affecting the rock, as shown in Plates 2.1 and 2.2. When deformed the augen appear as elongate 'pencils' (Plate 2.1(b)) although on breaking the rock these 'pencils' are simply the sections of 'plates'. These 'plates' are the product of the intense flattening and stretching imposed upon the originally ovoidal augen. The various forms of the augen were used as strain indicators in an attempt to quantify the progressive deformation path of the rocks (see section 2.2.5).

Locally, the Augen Gneiss contains massive, fine-grained, pink rocks which have sharp contacts with the Augen Gneiss and are deformed with it. They can be up to 3 m-4 m wide and take the form of dykes or sheets within the Augen Gneiss and consequently appear to be relatively younger than the gneisses. During the initial stages of mapping, these granite sheets were easily confused with the massive pink gneisses of the Heterogeneous Quartzo-Feldspathic Gneiss Unit; but were subsequently shown to be part of the Augen Gneiss Unit on geochemical grounds (see the Introductory Statement on p. 109).

At one locality, just N of Eidskrem (980608), where an expanse of the Heterogeneous Quartzo-Feldspathic Gneiss Unit appears within the

Augen Gneiss Unit small pods of calc-silicate rocks (epidote + garnet + sphene \pm plagioclase) are visible within the Augen Gneiss. These are generally involved in the deformation of the Augen Gneiss and display elongation in the strike direction; also, they are partly assimilated into the Augen Gneiss (Plate 4.1(b)). This assimilation has caused an increase in the proportion of garnet in the adjacent Augen Gneiss, with the feldspars taking on a greenish tinge due to epidote inclusions.

In thin section, the general assemblage of the Augen Gneiss is: perthitic K-feldspar (microcline), anti-perthitic plagioclase (An 20-30), quartz, hornblende (α straw, β dark-green, γ blue-green, $\gamma^{\wedge}Z \approx 20^{\circ}$), brown biotite, sphene, magnetite \pm garnet (Plate 4.1(c)). The equivalent rocks on Otrøy, mapped by D.A. Carswell have been found to contain relict symplectic clinopyroxenes similar in texture to those seen in the garnet-granulite on Tverrfjella (see Plate 3.1(f)).

In the undeformed examples of the gneiss the augen are composed of equant porphyroblastic, finely perthitic K-feldspar in a polygonal texture. A little plagioclase can appear in the augen. The plagioclase and quartz occur around the K-feldspar augen with smaller grains of K-feldspar. In some examples the plagioclase appears to form a discontinuous mantle around the augen. The quartz is generally deformed to some degree even in the most undeformed examples, and myrmekite often appears at the plagioclase-K-feldspar contacts. As the rocks become increasingly deformed the proportion of myrmekite increases appreciably and there appears to be a correlation between the degree of deformation and the appearance of this texture, suggesting that mechanical strain is the instigator of its formation (cf. Smith 1974, p. 577).

The mafic phases tend to appear as clots of hornblende and sphene surrounded by mats of well oriented biotite. In some examples of this

rock, small pink xenoblastic garnets appear as discontinuous 'strings' between the mafic clots and the feldspathic augen. These tend to appear in the more mafic examples. It has been noted that the proportion of mafic phases varies in these gneisses: some are mafic with garnet, others lack garnet and have smaller amounts of hornblende suggesting compositional variations in these rocks. In some examples, a texture of hornblende poikiloblastically enclosing plagioclase is seen (Plate 4.1(d)). Similar textures have been observed in the heavily retrogressed samples of the garnet-granulite (see Plate 3.2(b)), and it is possible that these hornblendes represent hydrated symplectic clinopyroxenes, and as such imply the prior existence of a high-pressure granulite assemblage of garnet-clinopyroxene (amphacitic)-quartz-plagioclase.

If isoclinally folded, the augen appear to have been partially mobilised into the crests of the folds, the zone of least of stress, giving the rocks a pseudo-migmatitic appearance (cf. Misch, 1969) (Plate 2.1(e)). As deformation proceeded, the augen became progressively smeared out and granulated to give a finely banded rock at amphibolite facies in which only relics of the augen now exist as aggregates of mosaic K-feldspar. The transition of rocks with large augen structures into banded rocks has also been observed in W. Greenland (McGregor, 1973). When very severely deformed the Augen Gneiss transforms into a mylonite with relic K-feldspars, and rarely hornblende (see Plate 2.1(a) and 4.1(e)).

The assemblages of the pink granitic rocks are dominated by micro-perthitic K-feldspar (microcline) and quartz + plagioclase (generally un-twinned albite) + biotite + opaques + apatite ± garnet in a fine-grained (~1 mm), equigranular, xenoblastic texture. Unlike the Augen Gneiss, these rocks have a consistent assemblage, without the variations in proportions of mafic phases. However, as with the Augen Gneiss, the rocks

display varying degrees of deformation and in general appear to have been more easily deformed than the Augen Gneiss. The quartz is always sutured and often 'ribboned' whilst the microcline has granulated margins and produces myrmekite when adjacent to plagioclase (cf. the Augen Gneiss). The biotite is fairly well aligned, as are the opaques (Plate 4.1(f)). These rocks can also be mylonitised with relict K-feldspars in a highly comminuted matrix of quartz and plagioclase; small neoblasts of zoisite appear in the fabrics of these mylonites.

4.1.2 Discussion of the petrography

The augen structures in augen gneisses are considered to be formed in two ways; either by metasomatism (Mehnert 1968, p. 35) or by deformation (Bryhni, 1966).

Metasomatically formed augen are generally K-feldspar, or more rarely sodic-plagioclase, either rounded or tending towards idiomorphic forms. In most cases the augen grew in a pre-existing fabric, i.e. 'feldspathisation'. However, the general form of an augen gneiss is one formed syntectonically with mono-mineralic augen in a schistose matrix. Augen can also be composed of aggregates of feldspar and quartz, and are related to the veins and schlieren of pegmatoid neosomes often occurring in nearby rocks (such 'augen' appear in the deformed rocks of the Heterogeneous Quartzo-Feldspathic Gneiss Unit - see section 5.1). The augen gneisses described by Bryhni (1966) occur at the junction of major lithological units and he considers that such rocks are typical of abrupt tectonic breaks. In general, the formation of an augen gneiss requires some degree of deformation during its evolution.

The augen in the Augen Gneiss do not appear to be the products of deformation from a migmatite for two reasons: the augen are not of a pegmatoid assemblage (K-feldspar + quartz + plagioclase), and they are

not accompanied by relict veins and schlieren of leucosome material. Furthermore, the augen do not appear to have formed by metasomatism since the augen are not mono-crystalline and idiomorphic. It is possible that the rocks have suffered recrystallisation under high grade metamorphic conditions which may have resulted in the polygonal texture seen in the augen, which then resided as competent bodies around which the quartz and mafic minerals were deformed. However, such recrystallisation is considered unlikely since the augen are very consistent in both size and distribution through the rock, features which are considered unlikely in an augen gneiss formed by metasomatism, as shown in the examples in Figs. 17 and 18 in Mehnert (1968, p. 34-35).

Indeed it is the very constancy of appearance of this Augen Gneiss, when undeformed, which suggests the other possible origin for the augen: as deformed porphyroclasts of an original igneous rock. In addition, three particular features of the augen suggest a possible relation of this pre-existing igneous rock to the rapakivi granites:

- (i) The appearance of discontinuous mantles of fairly sodic plagioclase on the augen (the rapakivi texture: Sahama, 1945; Dawes, 1966). Vidal et al. (1980) have discussed the behaviour of feldspar augen during deformation and found that the perthitic portions of the K-feldspar can recrystallise as albite or myrmekite onto the rims of the augen (cf. White, 1975). However, the plagioclase mantles in the Augen Gneiss do not appear to have formed in this way for three reasons:
- (a) the plagioclase is oligoclase rather than albite;
 - (b) the K-feldspar neoblasts observed by Vidal et al. are absent;
 - (c) the plagioclase mantles are best seen in the undeformed rocks rather than the deformed rocks.

(ii) The ovoidal form to the augen. Although it is possible that this form is a result of the deformation suffered by these rocks (compression/elongation and rotation in the matrix) these ovoids also exist in the most undeformed examples of the Augen Gneiss. Ovoidal phenocrysts are a feature of rapakivi granites (Sahama, 1945; Dawes, 1966).

(iii) Perthites and anti-perthites. Although these textures are indicative of grades of metamorphism at granulite facies (Sen, 1959) they may be original magmatic features, as found in rapakivi granites (de Waard, 1969).

The idea of an augen gneiss derived by deformation from an igneous rock is not new. Both McGregor (1973) and Myers (1978) demonstrated that augen gneisses in W. Greenland were the products of deformation of originally porphyritic igneous rocks.

The overall grade of metamorphism of the Augen Gneiss Unit is amphibolite facies, although the mylonites are transformed into greenschists with biotite altering to chlorite, and the appearance of epidote minerals. However, the appearance of rare symplectic clinopyroxene relics and fairly abundant garnet implies that these rocks were once subjected to high-pressure granulite facies conditions. Indeed, P and T equilibration conditions of 9.3 kbar and 806°C have been calculated for these rocks using the combined methods of Newton & Perkins (1981) and Ellis & Green (1979) (see Appendix B) on the assemblage: garnet-clinopyroxene-plagioclase-quartz (Carswell & Harvey, 1983; Harvey, 1983).

4.2 GEOCHEMISTRY

Whole-rock analyses and normative minerals for the Augen Gneiss and granite sheets are given in Table 4.1. Samples prefixed by 'U' are from Otrøy, all others are from the Molde Peninsula. The reason for grouping these two rock types in this chapter is explained in the Introductory Statement on p. 109.

The recognition of variations in the mineral assemblages of the Augen Gneiss suggested that a compositional trend existed in these rocks. The analyses are shown in a series of variation diagrams in Fig. 4.1 with various element oxides plotted against Thornton & Tuttle's Differentiation Index (i.e. normative $q + ab + or + ne + lc + kp$), in each case a fairly well defined trend is present. Furthermore, the Augen Gneisses appear to fall into two, or possibly three groups with divisions at about 68 and 80 on the D.I. axis. These divisions may be artificial, resulting from the sampling, but they may suggest that there is more than one chemical type of Augen Gneiss present, as suspected from the petrographic evidence. Consequently, the analyses in Table 4.1 have been tentatively divided into 'basic', 'intermediate' and 'acid' groups. These groups seem to have a spatial distribution with the most 'acid' variety occurring around Fanghol, with the 'intermediate' and 'basic' varieties to the N and S of that locality.

Essentially, the Augen Gneisses are intermediate to acid in composition with SiO_2 varying between 61% and 70%, total alkalies ~9%-10% with K_2O dominant in the 'acid' and 'intermediate' varieties, and CaO dominant in the 'basic' variety. The rocks are peraluminous ($Al_2O_3 > Na_2O + K_2O$, molecular) according to the terminology of Shand (1947). The normative minerals show the rocks to be oversaturated with a ubiquitous presence of hy, even in the most 'acid' varieties. The appearance of normative corundum ('c') reflects the peraluminous nature of the rocks.

Figs. 4.2(a) and (b) and 4.3(a) and (b) show plots of the LIL elements (Rb, K) and Ca and Sr; as with the major elements regular trends are visible. Rb selectively substitutes for K in minerals (K-feldspar) whilst Sr substitutes for Ca (in plagioclase) (Taylor, 1965). The trends shown are typical for a highly differentiated granitic series where there

FIG. 4.1

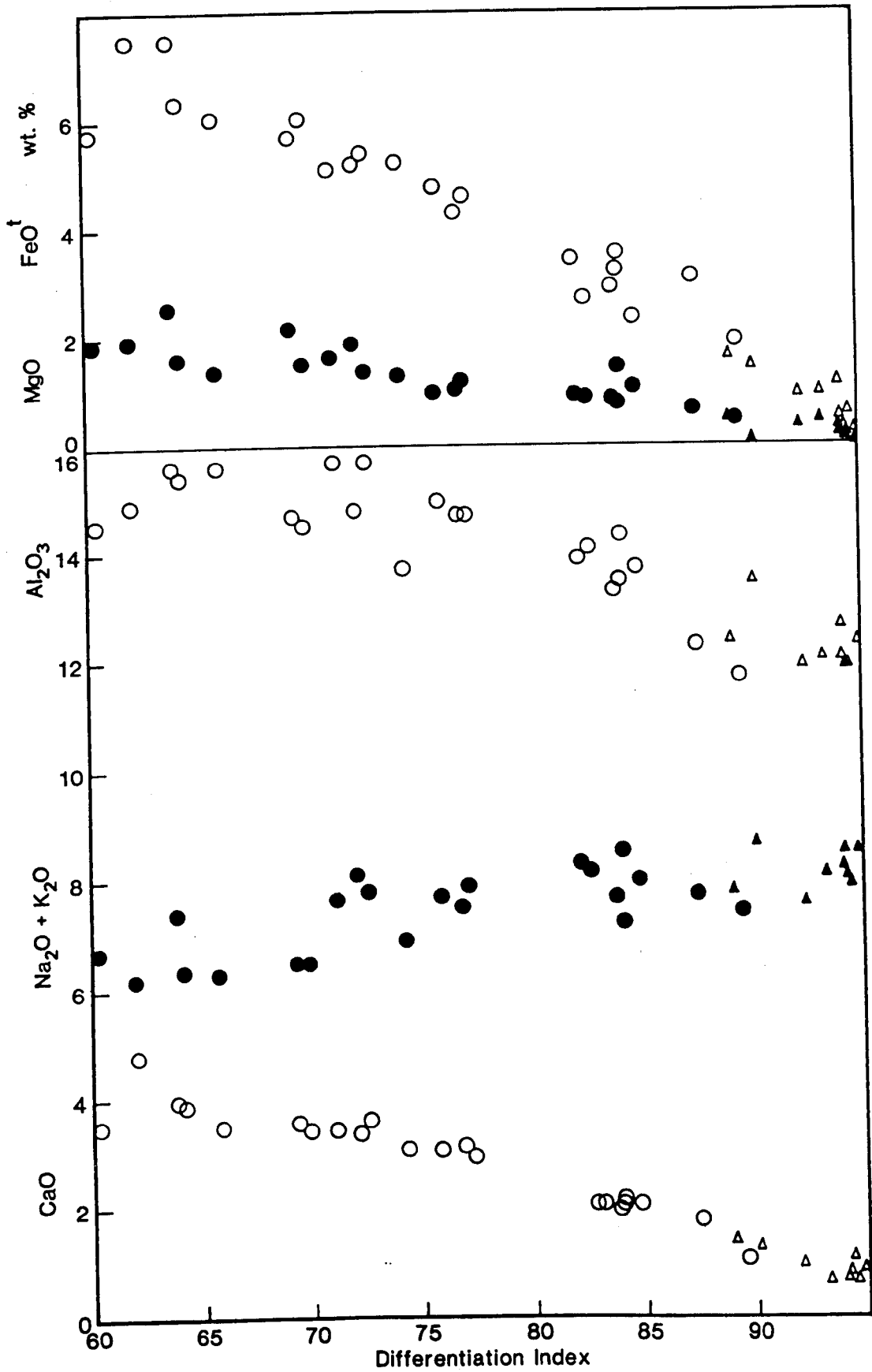
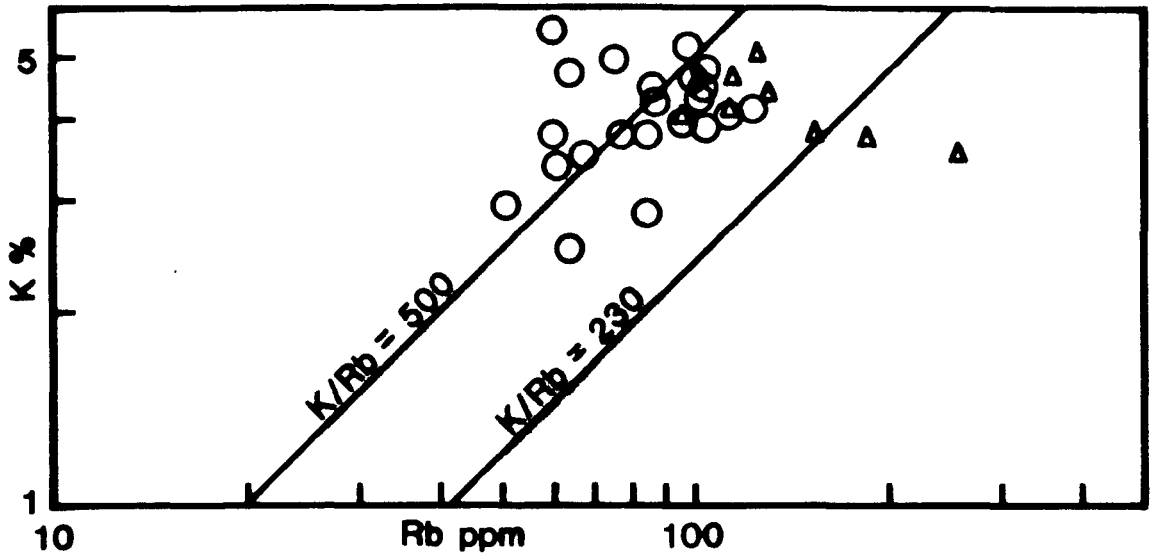


FIG. 4.1 Selected element oxides plotted against Thornton & Tuttle's Differentiation Index. Note divisions at 68 and 80 on the D.I. axis. Circles: Augen Gneiss, triangles: granite sheets.

FIG. 4.2

(a)



(b)

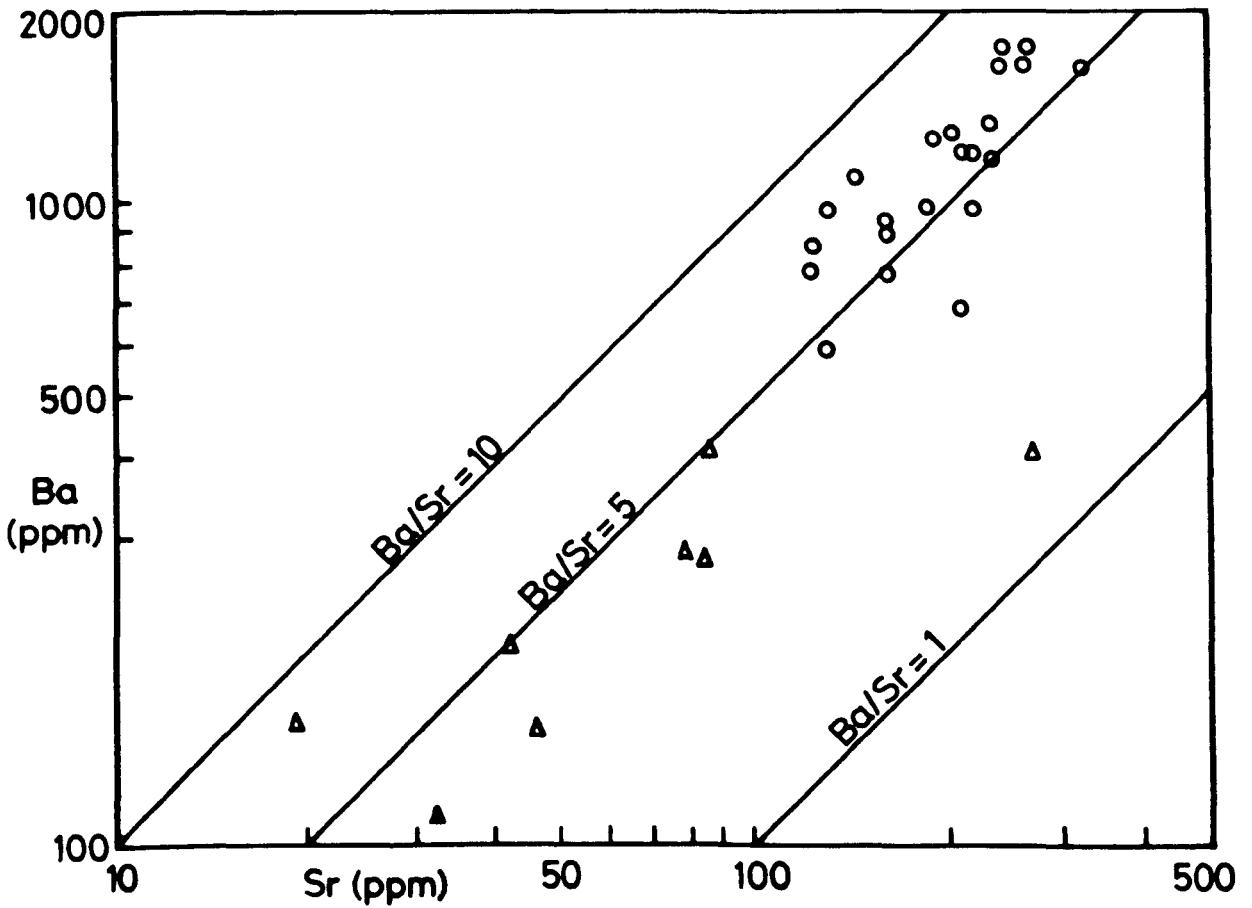
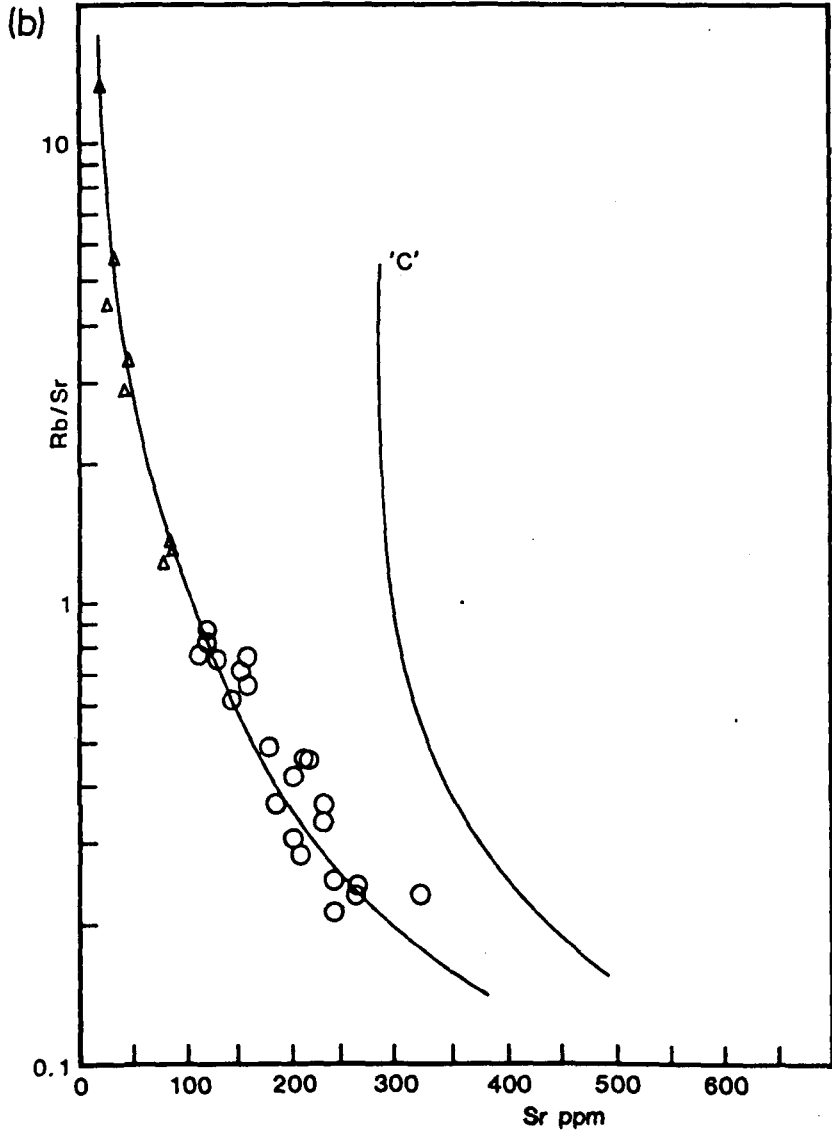
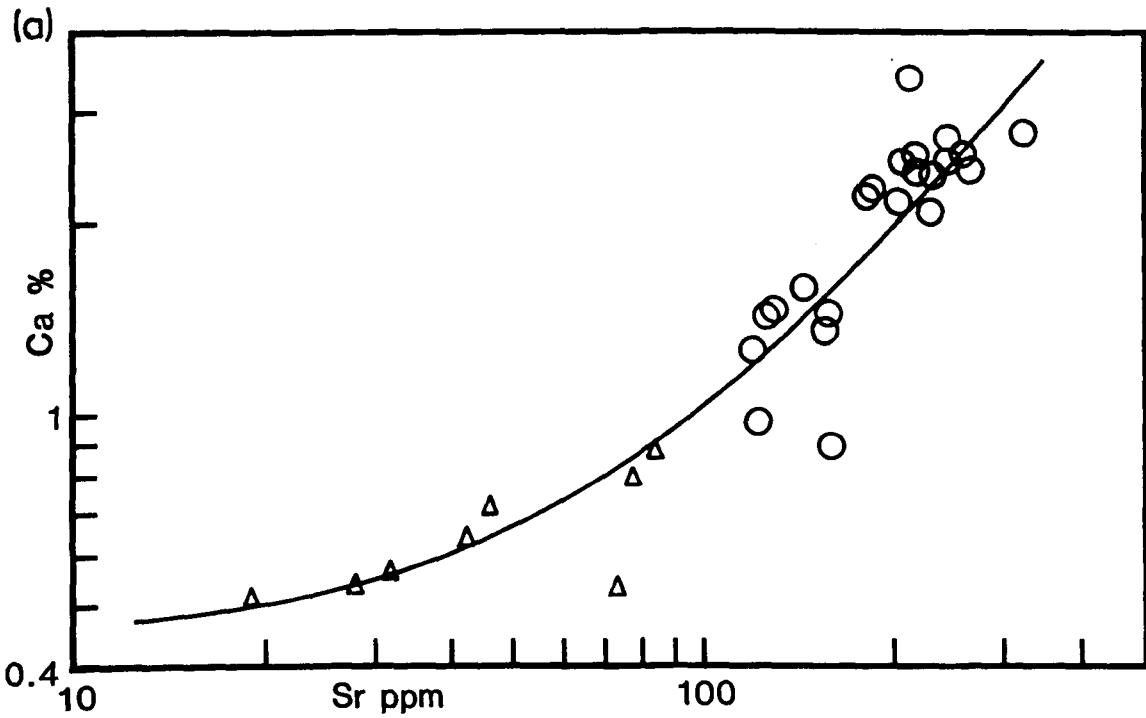


FIG. 4.2(a) K vs. Rb with the upper crustal K/Rb ratio of 230 after Taylor (1964). $K/Rb = 500$ also shown. Symbols as in FIG. 4.1.

(b) Ba vs. Sr, with $Ba/Sr = 5$ shown. Symbols as in FIG. 4.1.

FIG. 4.3



G. 4.3(a) Ca vs. Sr with trend reflecting lowering of the An content of the plagioclase with differentiation in the Augen Gneiss Unit. Symbols as in FIG. 4.1.

(b) Rb/Sr vs. Sr. Curve through points is a differentiation trend for a mantle-derived granite magma; curve 'C' is a trend for a granite magma derived by fusion of the crust (after Petersen, 1980a). Symbols as in FIG. 4.1.

is Rb and K enrichment simultaneous with Ba and Sr depletion (Nockolds & Allen, 1953; Kolbe & Taylor, 1966), i.e. biotite, plagioclase (and hornblende) fractionation. The enrichment of Rb is particularly noticeable on the K vs. Rb plot (Fig. 4.2(a)). The linear trend at about Ba/Sr = 5 (Fig. 4.2(b)) reflects the constant partitioning of these two elements throughout the formation of the Gneiss series. The Ca vs. Sr plot (Fig. 4.3(a)) mirrors the lowering of the An content of the plagioclase with differentiation, as seen in the normative minerals (Table 4.1). Ba tends to be concentrated, relative to K, in the early, most 'basic' rocks and not depleted until the very late stages of differentiation (cf. Bouseily & Sokkary, 1975). Similar trends to those shown in Figs. 4.2 and 4.3 have been observed in the charnockitic, Kleivan granite in S Norway (Petersen, 1980a) and in the metamorphosed rapakivi granite of Aggeneysberge in S Africa (Lipson, 1980).

The depletion of Ba in the later differentiates of this Gneiss series appears to be due to the mechanism postulated by Petersen (1980a). He considered that as differentiation proceeded the water content of the melt would increase to values ~2.5%-3.0% thereby inverting the biotite/K-feldspar crystallisation boundary (cf. Maaløe & Wyllie, 1975). Once biotite was crystallising before K-feldspar it would remove Ba from succeeding portions of the melt by acting as a fractionating phase.

The relationships between Ba, Sr and Rb are also shown on Fig. 4.4(a) (after Bouseily & Sokkary, 1975). Here the Augen Gneisses fall between the fields of 'normal granites' and 'anomalous granites' (i.e. metasomatic/migmatitic) and define a differentiation trend. The presence of this trend is important since Bouseily & Sokkary found that metasomatic/migmatitic rocks plotted as clusters rather than as trends; consequently such an origin does not seem to apply to these Augen Gneisses. The

FIG. 4.4

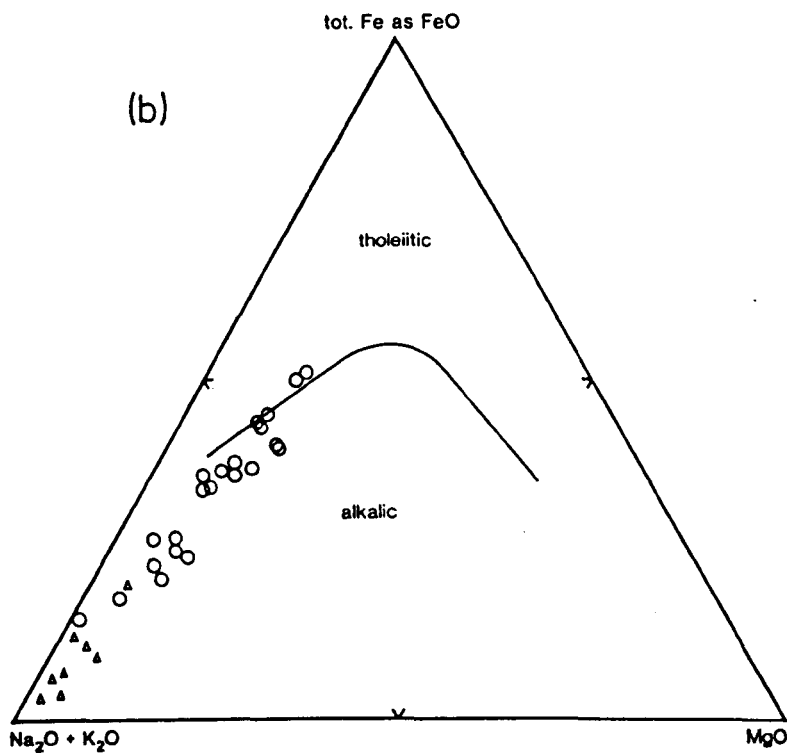
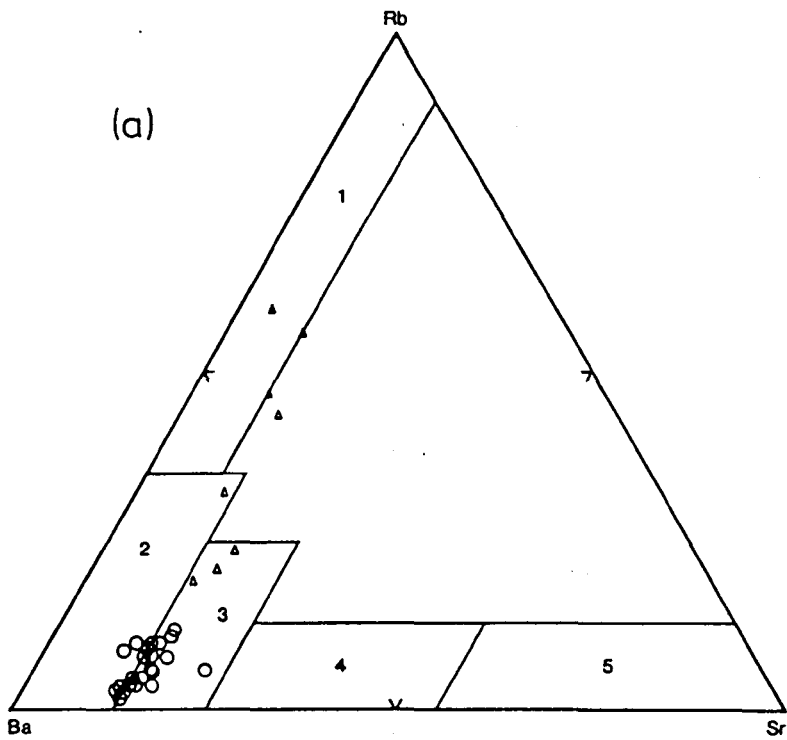


FIG. 4.4(a) Ba-Rb-Sr plot after Bouseily & Sokkary (1975) showing Rb-enrichment in the granite sheets. Symbols as in FIG. 4.1. (b) AFM plot with tholeiitic/alkaline division after Irvine & Barager (1971). Symbols as in FIG. 4.1.

differentiation trend is continued by the granite sheets into the field of 'strongly differentiated granites' with extreme Rb enrichment.

The curve shown in Fig. 4.3(b) is identical to the one derived by Petersen (1980a), by petrogenetic modelling, for the Kleivan granite which he considered to be the product of fractionation from a mantle-derived igneous body. Petersen found that a granitic magma derived by fusion of the crust would display a curve displaced to higher Rb/Sr values for comparable compositions (curve 'C'). The slight scattering of the points around the curve suggest that there has been some disturbance of the Rb-Sr system in the rocks.

It is important to note that the granite sheets, although of more differentiated compositions than the Augen Gneisses, follow all these elemental trends which implies that they are magmatically related to the Gneisses.

It is generally considered that there is a loss of certain elements, including the LIL elements (Rb, K, Th, U, Pb) from rocks during metamorphism above amphibolite facies (Lambert & Heier, 1968; Heier & Thoresen, 1971). Heier & Thoresen demonstrated that granulites have higher K/Rb ratios than the assumed upper crustal average K/Rb ratio of 230 (Taylor, 1964). Lambert & Heier considered that the loss of LIL elements from granulites was due to a partial melt, of granitic material, migrating upwards from the rocks taking these elements with it. An alternative possible process suggested by them was the increased efficiency of sub-solidus transport of these elements at medium- to high-pressure granulite facies. By way of confirmation they pointed to the lack of granitic fractions in granulite facies terrains. However, Tarney (1976) considered that the removal of LIL elements by partial melting was unlikely since the Lewisian granulites, although depleted in K and Rb

displayed pegmatites veins. He postulated that the loss of K, Rb and U, via hydrous fluids, will only occur at granulite facies if open-system conditions occur simultaneously with the metamorphism. He also considered that it was possible to attain granulite facies conditions under closed-system conditions when there would be a retention of the LIL elements. As an extreme example he indicated the granulite-eclogite rocks of the Bohemian Massif in central Europe which have relatively high K and Rb plus low K/Rb values but possess anhydrous assemblages.

Examining the plots of the trace elements in Figs. 4.2 and 4.3 in relation to these findings it would appear that the Augen Gneisses and granite sheets have not suffered a major loss of LIL elements even though they exhibit relics of high-grade assemblages. Although the K vs. Rb plot (Fig. 4.2(a)) shows the Gneisses clustering around the 500 ratio line, the absolute Rb values are still higher than in normal granulites (Lambert et al., 1976); also the rocks possess a granitic chemistry implying that there has been no loss of a partial melt. If the conjecture of Tarney (1976) is correct, it would appear that these rocks attained a high-grade assemblage under closed-system conditions allowing the retention of the LIL elements. Even during deformation and the related retrogression of the rocks, there apparently has not been any loss or addition of trace elements (cf. Heier & Thoresen, 1971). For example: samples 2120, 2123 and 2124 are very attenuated, exhibiting strained quartz and granulated feldspars, and yet have trace element compositions comparable to the less deformed samples, e.g. RS1.

Plotting the major element analyses on an AFM diagram (Fig. 4.4(b)) gives a trend which appears to be intermediate between calc-alkaline and tholeiitic. On the $\text{Na}_2\text{O} + \text{K}_2\text{O}$ vs. SiO_2 plot (Fig. 4.5(a)) of Irvine & Baragar (1971) the rocks fall into the subalkaline field; in

FIG. 4.5

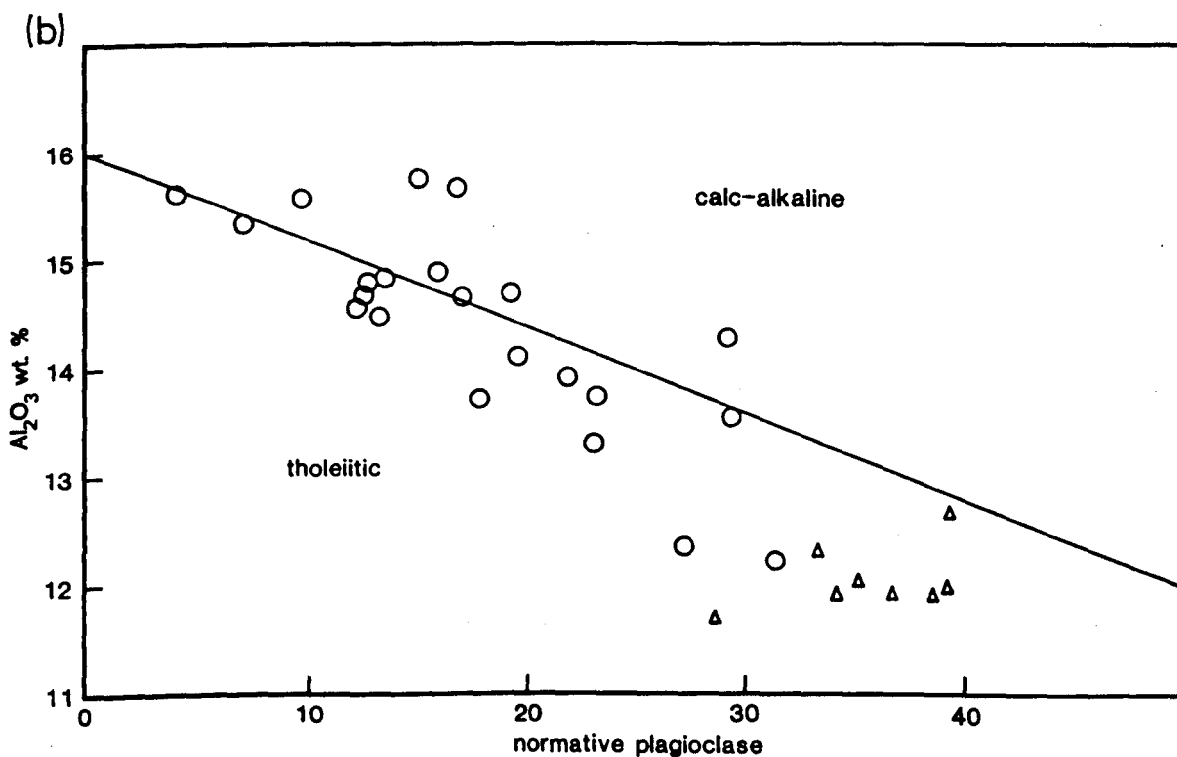
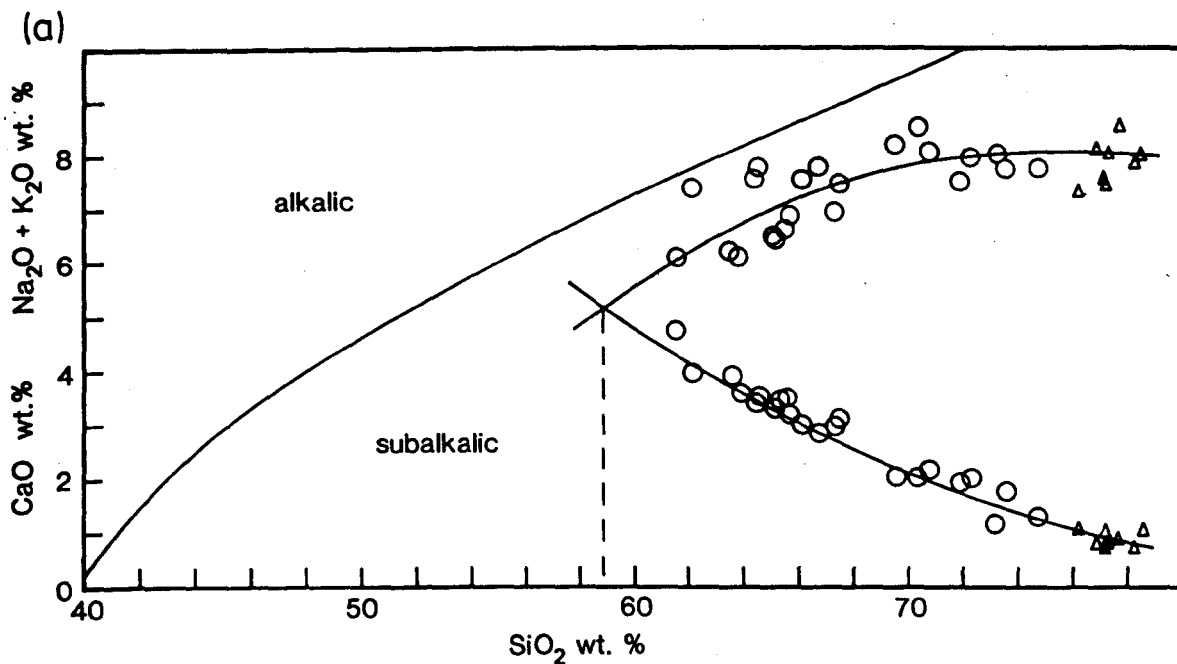


FIG. 4.5(a) Total alkalis (Na₂O + K₂O) vs. SiO₂, and CaO vs. SiO₂. The alkaline/subalkaline division is after Irvine & Baragar (1971). The intersection of the two trends marks the alkali-lime index of Peacock (1931). Symbols as in FIG. 4.1.

(b) Al₂O₃ vs. An/(An + Ab) with the tholeiitic/calc-alkaline division from Irvine & Baragar (1971). Symbols as in

conjunction with the CaO vs. SiO_2 plot, also shown on this diagram the alkali-lime index of 58% implies that they are calc-alkaline (Peacock, 1931). However, an important aspect of the chemistry of the Augen Gneiss is that they are K-rich, even in the 'basic' variety, with $\text{K}_2\text{O}/\text{Na}_2\text{O}$ ratios generally >1 . True calc-alkaline igneous rocks derived through the interaction of oceanic crust, mantle-derived mafic magmas and continental crust at an Andean-type convergent margin (Barker et al., 1981) typically have $\text{K}_2\text{O}/\text{Na}_2\text{O}$ ratios <1 (Mitchell, 1975) with $\text{K}_2\text{O}/\text{Na}_2\text{O}$ ratios >1 only occurring in the most differentiated, granitic, portions of the rock series. Therefore the relatively high $\text{K}_2\text{O}/\text{Na}_2\text{O}$ ratios in the Augen Gneiss and granite sheets appear to be more indicative of rocks of a continental origin (Mitchell, 1975).

Hence, a paradox arises: the Fe-poor nature of the Augen Gneiss and granite sheets points to a calc-alkaline affinity, but the alkali contents do not support this and yet still indicate a sub-alkaline character (see Fig. 4.5(a)), which cannot be tholeiitic because of the low Fe-contents. It is pertinent to note that on the Al_2O_3 vs. An' plot of Irvine & Baragar (1971) (Fig. 4.5(b)) the rocks straddle the dividing line, suggesting that they are transitional in chemistry between calc-alkaline and tholeiitic.

In an attempt to classify these rocks further, the normative feldspar diagrams of Streckeisen (1976) were employed (Fig. 4.6(a)); the majority of the rocks are oversaturated in this scheme (i.e. normative $q > 17\%$). Although the points do not fall exactly in the defined fields it is considered that they vary between: syenites/monzonites (depending upon q content), granodiorites, monzo-granites, syeno-granites and alkali-granites.

Consideration of the rocks in the Ab-Or-An system, studied by Yoder et al. (1957), shows the differentiation trend of the rocks

FIG. 4.6

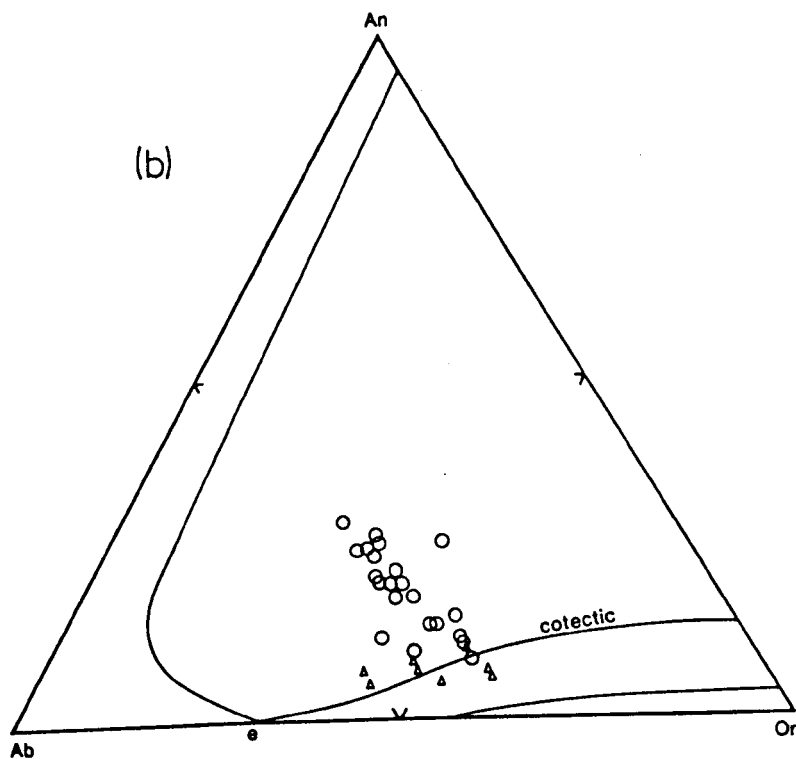
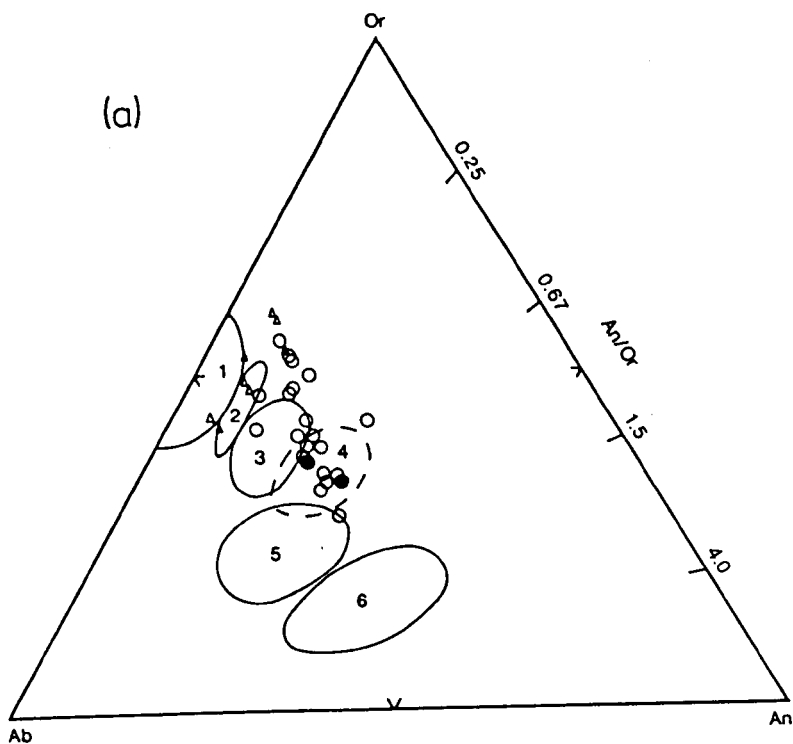


FIG. 4.6(a) Ab-Or-An plot with fields from Streckeisen (1976) for rocks with normative $q > 17\%$. Dashed fields are for rocks with normative $q < 17\%$ - solid ornament. Symbols as in FIG. 4.1. (b) Ab-Or-An-H₂O diagram after Yoder et al. (1957) at 5000 bars H₂O solid lines, apart from the cotectic represent the intersection of the solidus and solvus in the system. Symbols as in FIG. 4.1.

towards the cotectic, and then following the cotectic, with the granite sheets, towards the eutectic point (Fig. 4.6(b)). Since the crystallisation of a magmatic series would follow such a trend, it is considered that the chemistry of these rocks reflects a true igneous pattern.

As it was apparent that the Augen Gneiss Unit represented an orthogneiss series an Rb-Sr dating program was undertaken in order to place some sort of age constraint on either their time of intrusion or their time of metamorphism. The apparently well preserved LIL element patterns in the rocks suggested that a meaningful age could be obtained.

4.3 Rb-Sr WHOLE-ROCK DATING

The majority of the samples came from the outcrops at Fanghol where relatively homogeneous outcrops occur; other scattered samples were also taken including some from Otrøy. Fig. 4.7 shows their distribution. Samples with varying degrees of deformation were also taken to ascertain the effect this had on the Rb-Sr system. All were of litre size or larger and weighed 4-5 kg. Rb and Sr were determined by X.R.F. and the Sr isotopes by mass spectrometry (V6 Micromass 30) at the Mineralogisk-Geologisk Museum, Oslo, duplicate Rb and Sr analyses were also made at Sheffield University; the results are given in Table 4.2. The analytical procedures are given in Appendix A. Isochrons were fitted using the least squares method with correlated errors of York (1969) and an Rb decay constant (λ) of $1.42 \times 10^{-11} \text{ yr}^{-1}$ (Steiger & Jäger, 1977); all errors are quoted at the 2σ level. The value of $^{87}\text{Sr}/^{86}\text{Sr}$ obtained for standard SrCO_3 NBS 987 was 0.71030 ± 0.00010 over 20 runs.

From the evidence of co-magmatism for the Augen Gneisses and granite sheets, as shown by the continuous chemical trends on Figs. 4.1 to 4.6, the two rock types have been combined on a single isochron on the assumption that they would have the same initial $^{87}\text{Sr}/^{86}\text{Sr}$ ratio.

TABLE 4.2 Rb-Sr data used for the isochron in Fig. 4.8(a)

Sample Number	Rb	Sr	$^{87}\text{Rb}/^{86}\text{Sr}$	$^{87}\text{Sr}/^{86}\text{Sr}$	2σ	Description
Augen Gneisses						
2117	123	159	2.24748	0.75116	0.00010	Deformed
2120	113	156	2.08066	0.74773	0.00012	Sheared
2122	102	130	2.26695	0.75073	0.00014	Undeformed
2123	101	122	2.38314	0.75582	0.00012	Sheared
2124	78	231	0.97711	0.72361	0.00010	Sheared
2125	68	186	1.02893	0.72600	0.00008	Slightly Sheared
2134/1	78	231	0.68764	0.71913	0.00014	Deformed
2134/2	64	263	0.70476	0.71879	0.00014	Deformed
RS1	105	120	2.54395	0.75854	0.00010	Undeformed
U417/1	64	203	0.91360	0.72495	0.00026	Undeformed
U417/2	70	206	0.97500	0.72527	0.00016	Undeformed
U492	98	217	1.32334	0.73274	0.00016	Undeformed
U493	99	214	1.38279	0.73315	0.00016	Undeformed
Granite Sheets						
D121	97	77	3.80698	0.78699	0.00008	Undeformed
204	125	42	8.73983	0.88896	0.00010	Deformed
U418	115	84	4.05825	0.78956	0.00008	Undeformed

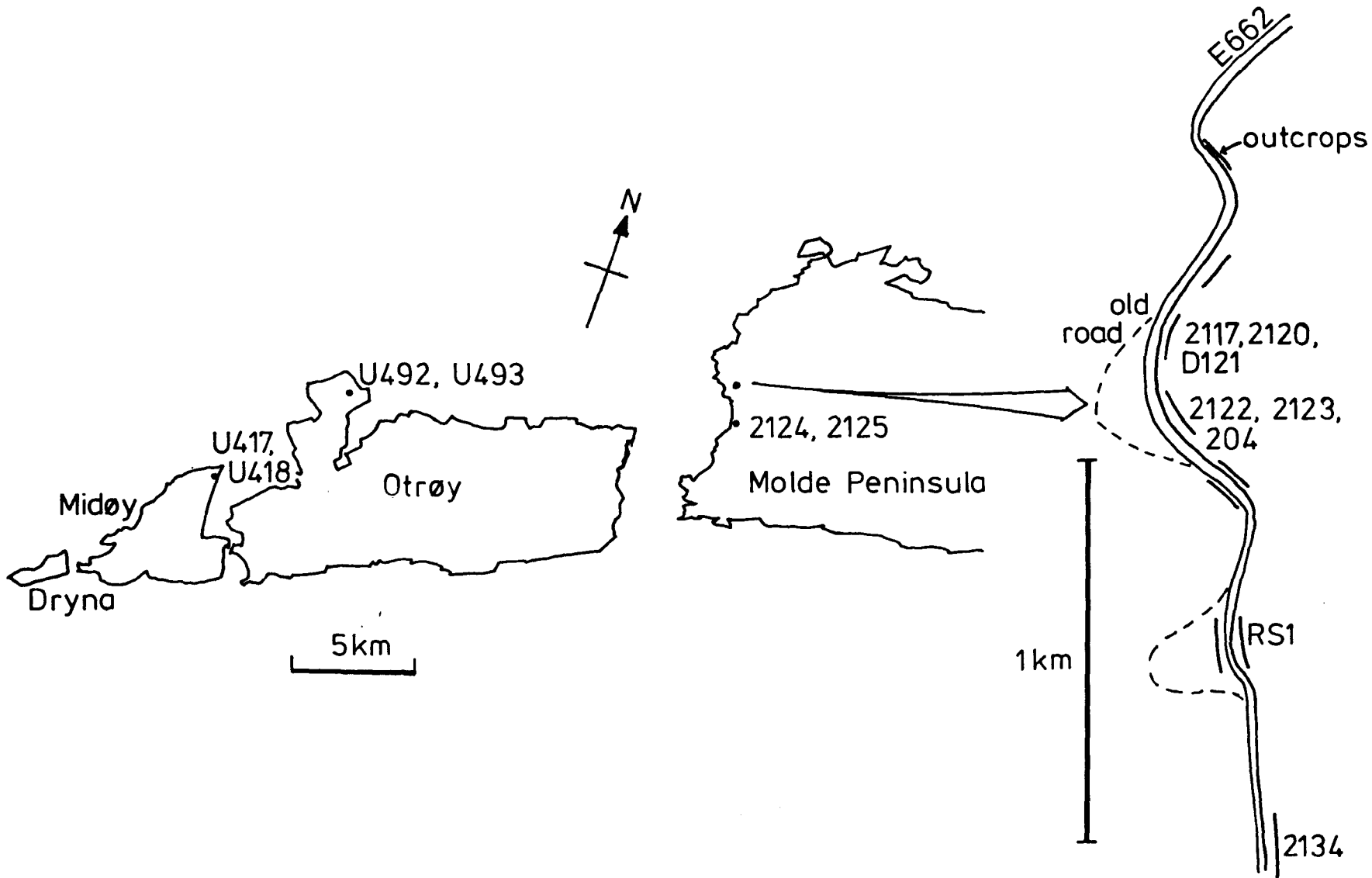


FIG. 4.7

FIG. 4.7 Map of part of Moldefjord, and a larger-scale map of the road-cuts at Fanghol, showing the localities of samples of the Augen Gneiss Unit used for the Rb-Sr whole-rock dating.

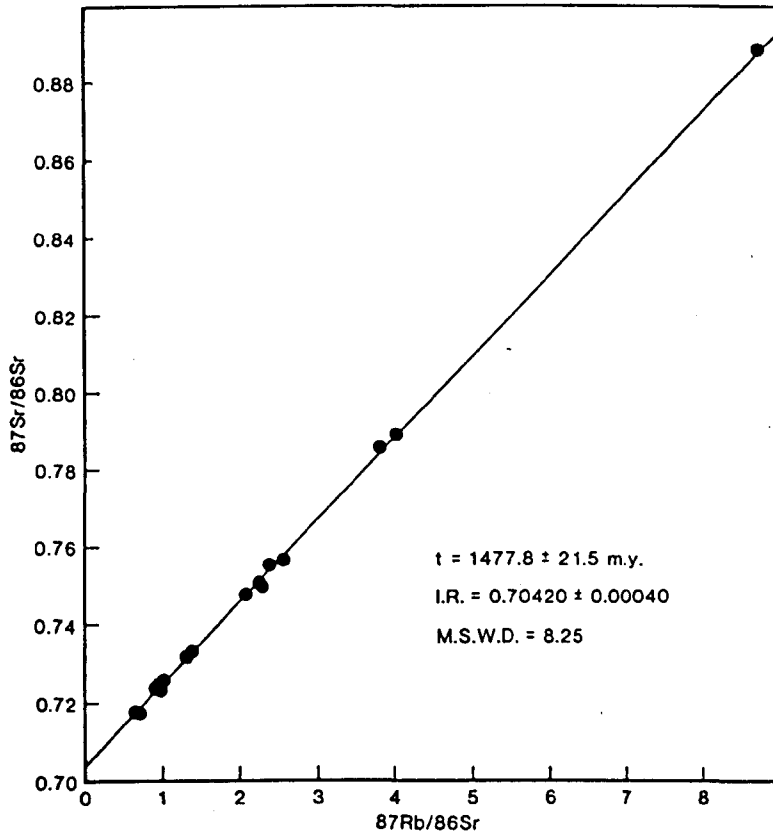
Fig. 4.8(a) shows this isochron with an age of: 1477.8 m.y. \pm 21.5 m.y.; an Initial Ratio ($^{87}\text{Sr}/^{86}\text{Sr}$) of 0.70420 ± 0.0004 and an M.S.W.D. of 8.25. The fairly high mean square of weighted deviates (M.S.W.D.) which reflects the goodness of fit of the isochron, suggests that there has been some disturbance of the isotopic system; Brooks et al. (1968) consider that only values <2.5 can be due to experimental error alone.

Radiometric ages obtained with the Rb-Sr whole-rock methods from rocks which have suffered grades of metamorphism of amphibolite facies or above are usually interpreted as representing a metamorphic event since it is assumed that there is a homogenisation and resetting of the isotopic system at these grades. At first sight this would appear to be the case with the Augen Gneisses and granite sheets as they fall on the same isochron and yet the field evidence suggests that the granite sheets are somewhat younger. This type of metamorphic homogenisation is depicted graphically in Fig. 4.8(b) and shows that a high initial ratio is a result of the rehomogenisation, which is not the case with the Augen Gneisses and granite sheets. Furthermore, this type of homogenisation requires large-scale movements of Sr to have occurred in the rocks, which have been shown to be unreal (Krogh & Davis, 1973). A slight redistribution of Sr (on a cm scale) is depicted in Fig. 4.9(a); in this case there is a scattering of the data points, which raises the M.S.W.D. but affects the initial ratio and age only slightly. It is considered that this was probably the situation with these rocks and that the age given represents that of the original igneous protolith, rather than a metamorphic event, intruded during the mid-Proterozoic.

The inhomogeneity of Rb is reflected in the distribution of points on the isochron, which fall into the same groups as seen on the major element plots (Fig. 4.1), with those points at higher Rb/Sr values

FIG. 4.8

(a)



(b)

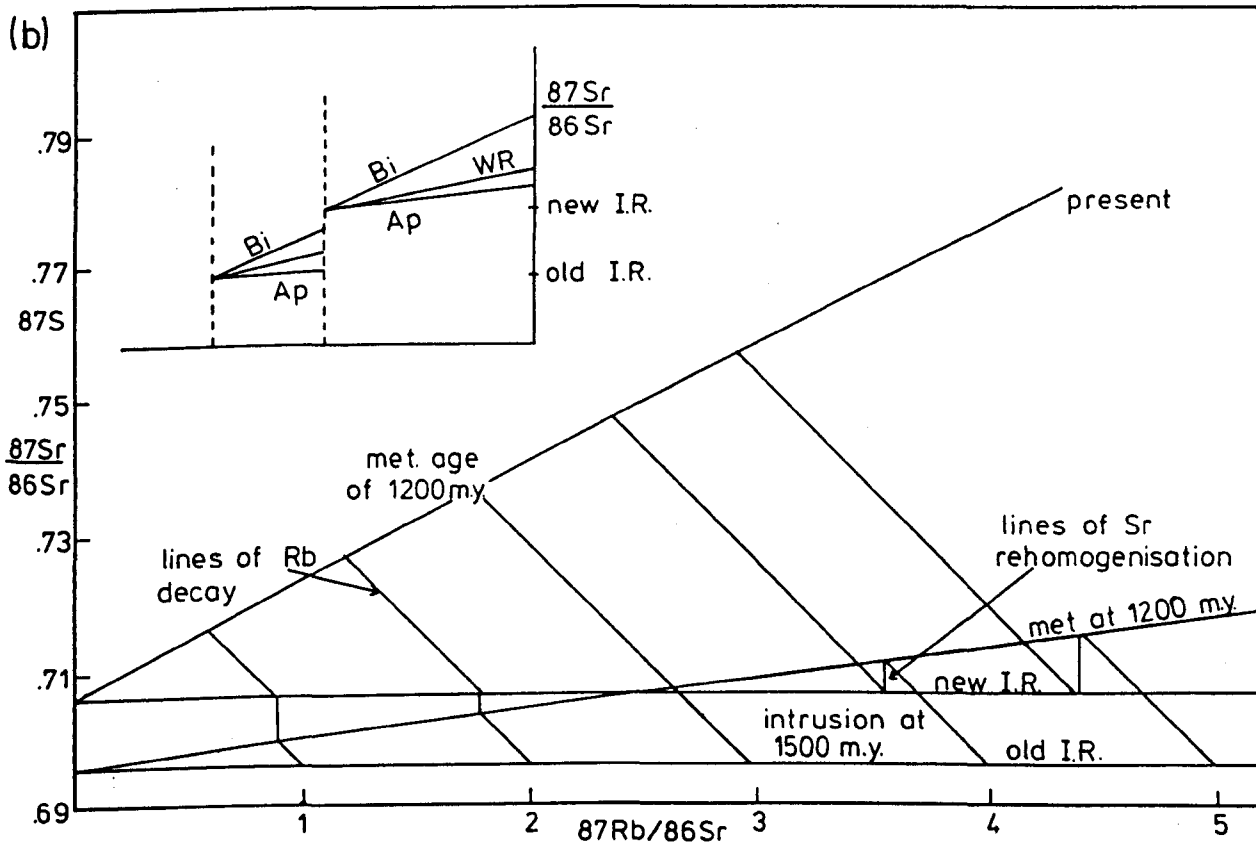


FIG. 4.8(a) Rb-Sr whole-rock isochron diagram for the Augen Gneiss Unit, from the data in TABLE 4.2.

(b) Schematic Rb-Sr isochron diagram for Sr isotopic rehomogenisation on a large scale; metres-kilometres. Inset shows the same represented as Rb-Sr growth curves for minerals and whole-rock where both are reset.

FIG. 4.9

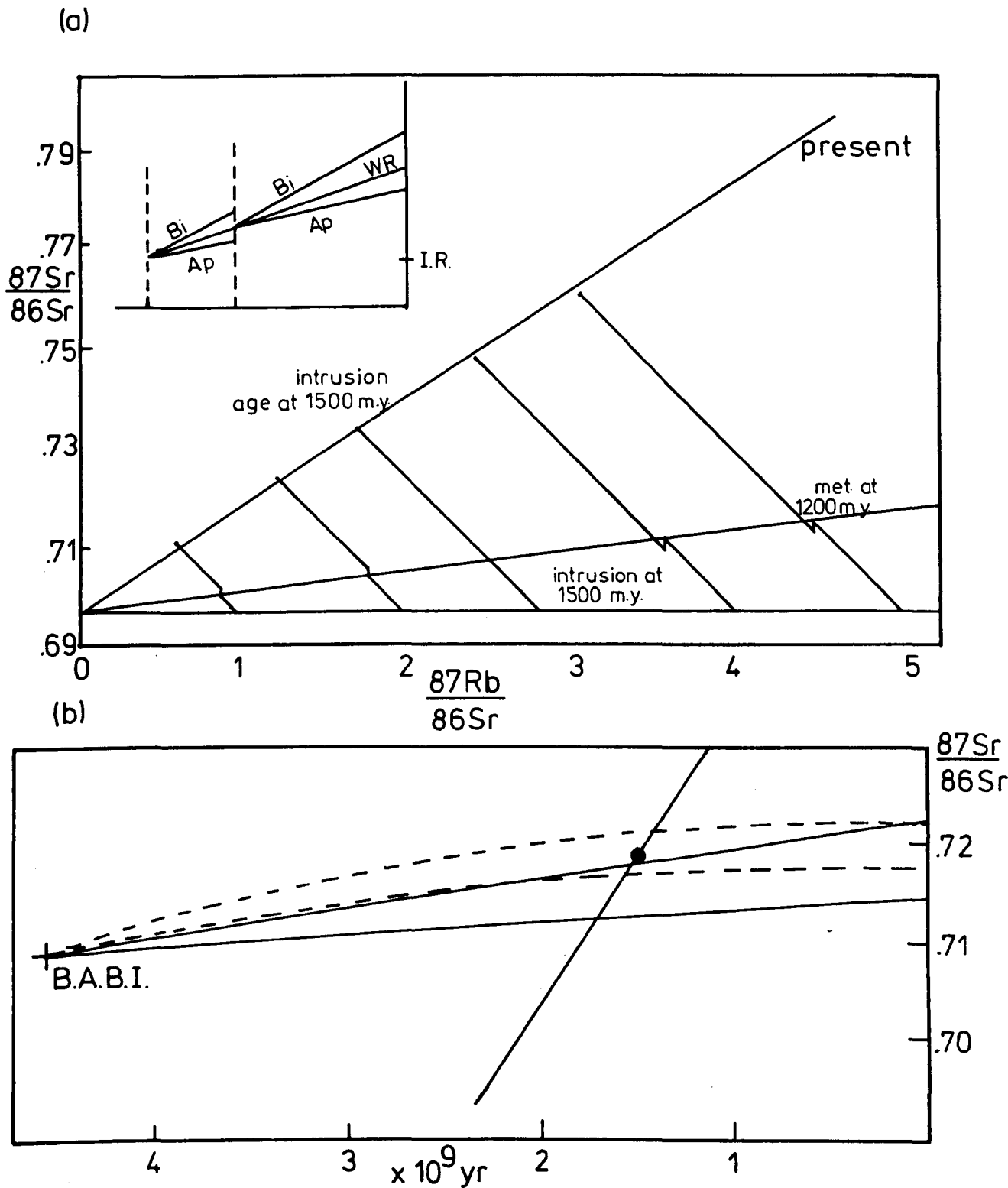


FIG. 4.9(a) Schematic Rb-Sr isochron diagram for Sr isotopic rehomogenisation on a small scale: millimetres-centimetres. Inset shows the same represented as Rb-Sr growth curves for minerals and whole-rock. Note resetting of minerals but not the whole-rock system.

(b) Sr evolution diagram with idealised mantle growth curves (solid) and those allowing for loss of Rb over time (dashed). B.A.B.I. (Basaltic Achondrite Best Initial ratio) from Papanastassiou & Wasserburg (1969). Solid circle represents the position of the Augen Gneiss Unit at ~ 1477 m.y. and I.R. of 0.07045.

coming from the area of more 'acid' Gneisses at Fanghol. There is a further division between the Gneisses and granite sheets, which have Rb/Sr ratios >3 . This inhomogeneity suggests two possibilities:

(i) The igneous protolith was of a mantle origin where the distribution of Rb and Sr is also considered to be inhomogeneous (Hofmann, 1975). This is in agreement with the Rb/Sr vs. Sr plot (Fig. 4.3(b)) which indicated a differentiation curve for a mantle-derived magma.

(ii) There was more than one pulse of magma, with the most differentiated portion at Fanghol. This would be similar to other zoned granitic plutons, e.g. in California (Bateman & Chappell, 1979).

The first possibility can be investigated further by examining the $^{87}\text{Sr}/^{86}\text{Sr}$ initial ratio in relation to the mantle growth curves given by Faure & Powell (1972, p. 45). In Fig. 4.9(b) the solid lines represent growth curves joining B.A.B.I. and the maximum and minimum values of $^{87}\text{Sr}/^{86}\text{Sr}$ initial ratios from modern ocean-floor basalts. The Augen Gneisses fall towards higher values of $^{87}\text{Sr}/^{86}\text{Sr}$ than would be expected for a mantle-derived igneous rock of this age (i.e. ~ 0.702), perhaps implying some crustal contamination increasing the $^{87}\text{Sr}/^{86}\text{Sr}$ ratio. However, the mantle growth curves are more likely to take the form shown by the dashed lines (cf. Faure & Powell, 1972, p. 132) since the supply of mantle Rb will have decreased over time through removal in magmatic events (Hart & Brooks, 1970). The initial ratio for the Augen Gneisses now falls well within the area bounded by these dashed lines, and together with the evidence from the Rb/Sr vs. Sr curve (Fig. 4.3(b)) a mantle origin for the igneous precursor to the Gneisses seems most likely.

The existence of the groups of points on the isochron can be used to make certain inferences as to the possible scale of Sr rehomogenisation

during metamorphism (cf. Roddick & Compston, 1977). When more than one sample of Augen Gneiss or granite sheet was taken from an outcrop (see Fig. 4.7), the Rb and Sr figures for these have been averaged to give mean $^{87}\text{Sr}/^{86}\text{Sr}$ and $^{87}\text{Rb}/^{86}\text{Sr}$ values for that 'outcrop'. These values approximate to those that would have been obtained if the whole outcrop had been sampled; they are given in Table 4.3 and are used to give a new isochron in Fig. 4.10(a). Neither this age, nor the initial ratio are very different from those of the isochron in Fig. 4.8(a) although the M.S.W.D. is improved. This implies that any Sr rehomogenisation was restricted to volumes no larger than 'outcrop' size. If the rehomogenisation had progressed between the 'outcrops' this isochron would display an M.S.W.D. similar to that in Fig. 4.8(a), therefore it is likely that any Sr homogenisation occurred on a scale smaller than 'outcrop', i.e. between hand-specimens (cf. Roddick & Compston, 1977). This agrees with the findings of Krogh & Davis (1973). Since the granite sheets lie within the Augen Gneisses it is likely that any rehomogenisation on this scale would have caused a convergence of the respective Sr isotopes in these rocks perhaps causing them to lie on the same isochron, as seen. However, the likelihood of a co-eval intrusion of the granite sheets and the igneous precursor to the Gneiss is favoured here from the evidence of the differentiation trends.

What is more difficult to ascertain is the time of metamorphic disturbance. Two major metamorphic events have occurred in Norway post 1500 m.y.: the Sveconorwegian (1200-900 m.y.) and the Caledonian (600-360 m.y.). The Molde Peninsula lies at about the accepted northern limit of the Sveconorwegian effect in south Norway (Zwart & Dornsiepen, 1978). Therefore it is more likely that the disturbance was Caledonian although it may have overprinted an earlier Sveconorwegian event. The

TABLE 4.3 Averaged Rb-Sr data used for the isochron in Fig. 4.10(a)

Sample Groups	Mean $^{87}\text{Rb}/^{86}\text{Sr}$	Mean $^{87}\text{Sr}/^{86}\text{Sr}$
2117	2.24453	0.75136
2120		
2122		
2123		
2124	1.00302	0.72482
2125		
2134/1	0.69620	0.71896
2124/2		
U417/1	0.94430	0.72511
U417/2		
U492	1.35307	0.73294
U493		
D121	6.27341	0.83798
204		

FIG. 4.10

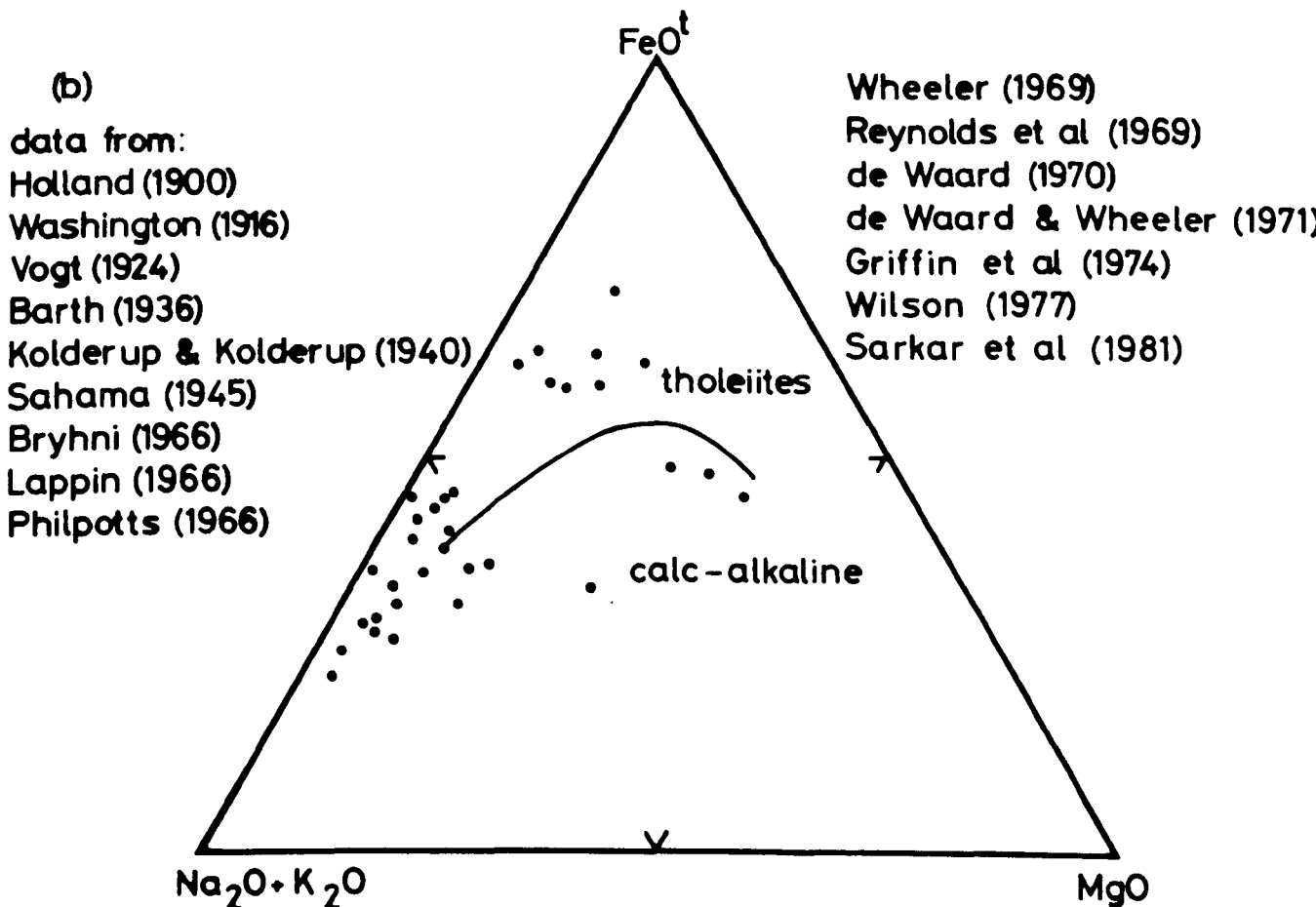
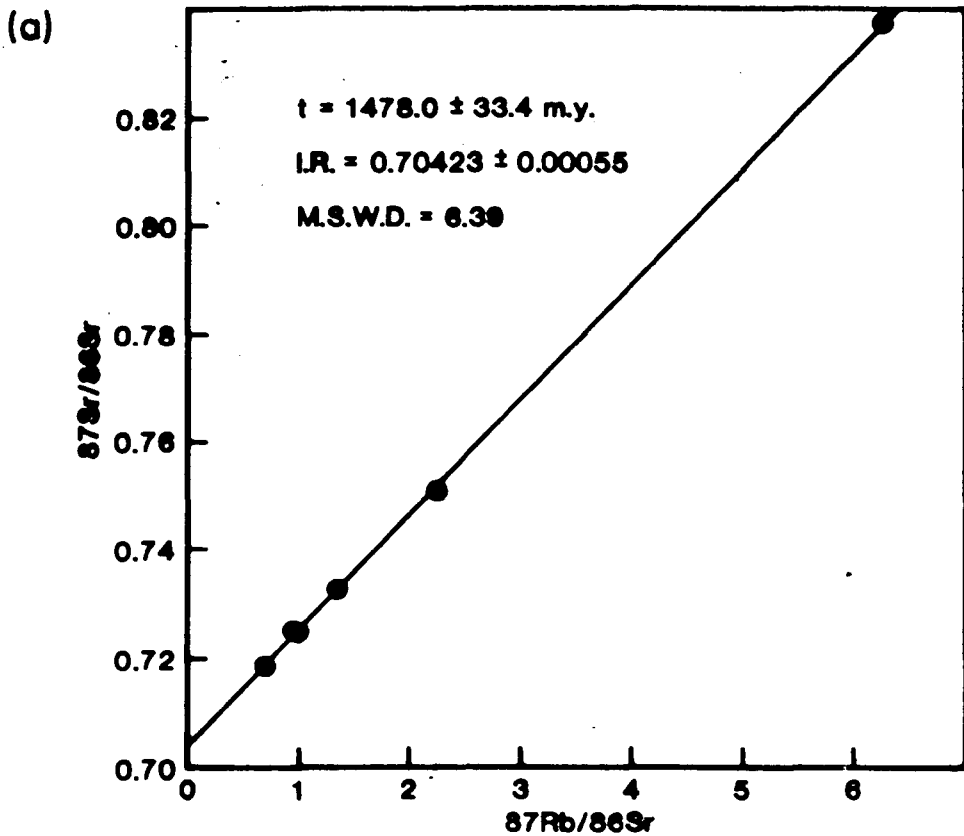


FIG. 4.10(a) Rb-Sr whole-rock isochron diagram for the averaged values of the Augen Gneiss Unit from the data in TABLE 4.3.

(b) AFM plot with the tholeiite/alkaline division after Irvine & Baragar (1971) for the anorthositic suite. Note the Fe enrichment.

suggestion that the Caledonian metamorphism was of a high enough grade to produce eclogite assemblages (Griffin & Brueckner, 1980) lends support to the idea of a disturbance at that time. However, dating of rocks in W Norway has tended to produce Precambrian ages, with only the minerals giving Caledonian ages (see Table 1.3). This feature has previously been interpreted as indicating that the Caledonian metamorphic effect represented only a minor reheating here (Pidgeon & Råheim, 1972; Skjerlie & Pringle, 1978; Råheim et al., 1979; Solheim, 1980). Krill & Griffin (1981) have discussed this point and have compared the situation with that in the Alps where older Rb-Sr whole-rock systems have been shown to survive subsequent intense metamorphism and deformation. They consider that a similar situation has prevailed in W Norway. The evidence from the Molde Peninsula: severe deformation with extreme flattening, stretching and mylonitisation of the rocks with a preserved igneous age and Rb and Sr contents seems to support such a contention. Although there was undoubtedly an influx of water at that time, to assist retrogression, the LIL element contents of the rocks were not greatly disturbed even in the shear zones and appear to give a meaningful isochron.

4.4 DISCUSSION

Unfortunately, the consideration of the Augen Gneiss Unit as a meta-igneous series is based on the geochemical and Rb-Sr isotope work, and as yet no evidence of igneous contacts with the adjacent Heterogeneous Quartzo-Feldspathic Gneiss Unit have been observed, although the severity of the subsequent Caledonian deformation has undoubtedly played a part in the concealment of such features. However, the appearance of partially assimilated calc-silicate pods in the Augen Gneiss, rocks which are seen within the Heterogeneous Quartzo-Feldspathic Gneiss

Unit (see section 5.1) suggests that the Heterogeneous Gneisses acted as the host rocks into which the Augen Gneiss Unit was intruded, and that these calc-silicate pods represent meta-xenoliths of those gneisses.

The mid-Proterozoic (1500 ± 300 m.y.) is considered to represent a period of prolonged crustal formation and of fundamental change in the evolution of the continents (Bridgewater & Windley, 1973). The existence of a supercontinent is postulated for this period (Piper, 1976) containing two elongate, orogenic ('mobile' - Anhaeusser et al., 1969) belts, the most prominent extending from the Ukraine to California (see Fig. 4.12(b)). The rock types produced in this belt were many and various: anorthositic suites, acid volcanics, red continental sandstones, plateau basalts, dyke swarms and large layered igneous intrusions, and alkaline complexes associated with carbonatites. Tensional conditions, with incipient rifting of the crust, are considered to be the conditions of formation for both alkaline complexes (Bowden, 1974) and intra-continental dyke swarms (Clifford, 1968). The relation of anorthositic suites to these rock types suggested that tensional crustal conditions were also responsible for the formation of that suite, with the continental sandstones being deposited in the resulting graben structures (Bridgewater et al., 1974). These workers also suggested that the anorthositic and alkalic plutonic suites may have been intruded along the same fault lines, and that the overall pattern of magmatism was diachronous with events in the E ~ 200 m.y.-300 m.y. earlier than those in the W.

The anorthositic suite contains: anorthosites, jotunites, opdalites, farsundites, mangerites, charnockites and possibly rapakivi granites (Isachsen, 1969; Emslie, 1973, 1978). The suite is tholeiitic with high Fe and low Mg contents. An orthopyroxene (hypersthene) or fayalite + quartz are diagnostic phases in the more differentiated members; also

present are antiperthitic oligoclase and a mesoperthitic K-feldspar (de Waard, 1969; de Waard & Wheeler, 1971). The rapakivi granites often exhibit mantling of oligoclase on K-feldspar phenocrysts, i.e. the 'rapakivi texture' (Sahama, 1945; Dawes, 1966). The alkaline suite contains: alkaline gabbros and granites, syenites, nepheline syenites and peralkaline rocks including carbonatites (Sørensen, 1974). These two rock suites are mentioned here since these appear to be the two chemical types between which the Augen Gneisses and granite sheets fall. However, Sørensen (1974) considers alkaline rocks to be characterised by the presence of feldspathoids and/or alkali-pyroxenes and amphiboles; also, he prefers the classification of Shand (1922) in which either Si or Al, or both can be deficient in the rock. Since the Augen Gneisses and granite sheets are peraluminous and oversaturated (see Table 4.1) they do not conform to the above requirements for the alkaline rocks and therefore are unlikely to have ever contained feldspathoids. Consequently it is considered unlikely that they have any real magmatic connection with that suite. However, from the evidence of possible relict rapakivi textures and the appearance of perthites and antiperthites in the Augen Gneisses (section 4.1) it is tentatively suggested that these orthogneisses have some affinity with the higher differentiates of the anorthositic suite, although they are rather Fe-poor. To give some degree of comparison rocks from the anorthositic suite have been plotted on similar diagrams as used for the Augen Gneisses and granite sheets (Figs. 4.10(b) and 4.11(a)). On the AFM plot the rocks of the anorthositic suite give a good tholeiitic trend; although on the Al_2O_3 vs. An' plot, which removes the effect of Fe, the field defined by these rocks appears in much the same position as that for the Augen Gneisses and granite sheets even to the extent of straddling the dividing line (see Fig. 4.5(b)). A direct comparison of the two sets of analyses shows that the 'basic'

FIG. 4.11

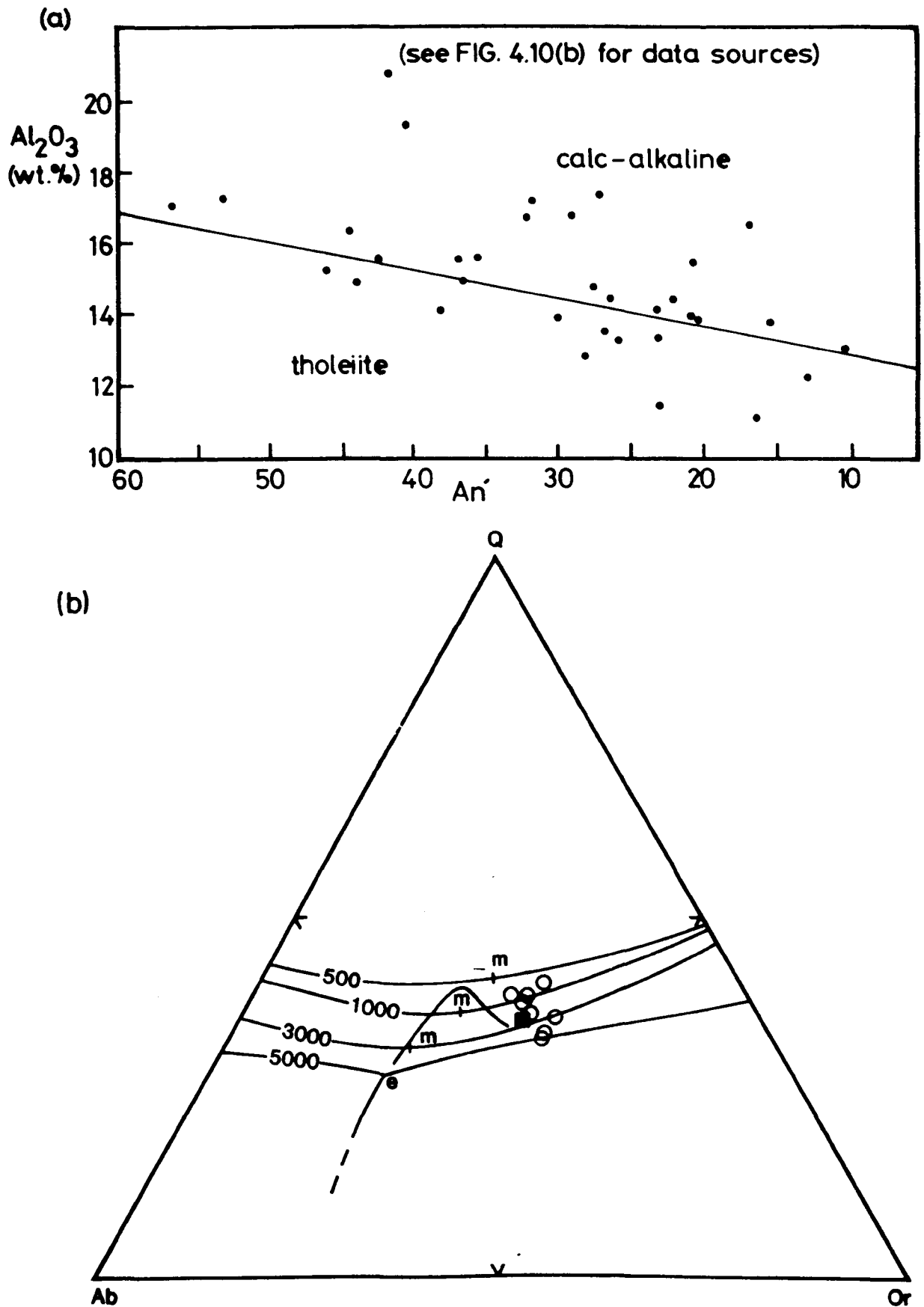


FIG. 4.11(a) Al_2O_3 vs. $\text{An}/(\text{An} + \text{Ab})$ with the tholeiitic/calc-alkaline division from Irvine & Baragar (1971) for the anorthositic suite. Symbols as in FIG. 4.10(b).

(b) Ab-Or-Q- H_2O diagram after Tuttle & Bowen (1958). Plotted points are samples with normative $\text{ab} + \text{or} + \text{q} + \text{ne} + \text{lc} \geq 80\%$. Curve is the hypothetical cooling path of a rapakivi granite as derived by Tuttle & Bowen. Solid square is the average rapakivi granite of Sahama (1945).

Augen Gneisses are most similar to the mangerites, but as the more 'acid' rocks are approached major differences in FeO and MgO contents become apparent with the Augen Gneisses possessing lower FeO and higher MgO contents for comparable compositions in the charnockites and rapakivi granites. A high FeO/MgO ratio is considered to be a major diagnostic character of the rapakivi granites (Anderson & Cullers, 1978; Emslie, 1978; Petersen, 1980b).

These differences in Fe and Mg contents could have arisen for several reasons: the anorthositic magma may have been more olivine-rich, fractionation of which would have resulted in residual melts having high Fe/Mg ratios. Conversely, the formation of olivine may have been inhibited in the parental magma to the igneous precursor of the Augen Gneisses, perhaps by silica saturation causing retention of Mg in the residual melts. The physical conditions of intrusion and fractionation of the two rock types may also have been different, e.g. in P_{load} , $P_{\text{H}_2\text{O}}$, P_{O_2} etc., to allow retention of Fe in one magma but not in the other.

Unfortunately it is impossible to derive a hypothetical parent magma for the Augen Gneisses, using mixing models as the original, igneous mineralogy no longer exists. A comparison with the parental magma of the anorthositic suite is also made difficult by the fact that uncertainty persists over the true nature of this parent. Emslie (1978) lists three possibilities, from various authors:

(i) gabbroic composition, derived from the mantle, and varying between gabbro, anorthositic-gabbro, 'plagioclase' basic magma and high-alumina gabbro;

(ii) calc-alkaline;

(iii) granodioritic-tonalitic, by anatexis of the continental crust.

Another possibility is a highly feldspathic magma derived by fractional crystallisation from a tholeiitic parent (Wiebe, 1980). Ryder (1974) considered that perhaps two types of parental magma were required: andesitic and high-alumina basalt producing andesine and labrodorite anorthosites respectively. Since it is considered that the tectonic regime in this mobile belt was tensional (Bridgewater & Windley, 1973; and see above), it is unlikely that calc-alkaline rocks would have been generated, being confined to Andean-type margins (Barker et al., 1981) which eliminates hypothesis (ii), and Ryder's suggestion of andesitic and high-Al-basalt parents. The low initial $^{87}\text{Sr}/^{86}\text{Sr}$ ratio of the Augen Gneisses and granite sheets (section 4.3) would seem to preclude hypothesis (iii) which is based upon evidence of some anorthositic suite granites having high initial ratios: ~ 0.7087 . The low Fe nature of the Augen Gneiss Unit precludes the suggestion of Wiebe for a tholeiitic parent. Therefore, it is considered that the magmatic precursor to the gneisses was probably derived by fractionation from a gabbroic mantle source.

It is generally thought that the anorthositic suite is developed under high-pressure, anhydrous conditions (Martignole, 1979). The lack of H_2O has two effects on the developing mineralogy: firstly, it will cause the crystallisation of pyroxene (hypersthene), rather than a hornblende (Robertson & Wyllie, 1971). Secondly, the low $P_{\text{H}_2\text{O}}$ will give a low and variable P_{O_2} thereby retaining the Fe in the melt and giving a tholeiitic character, rather than allowing it to enter the mafic phases and magnetite which would fractionate out (Osborn, 1959; Letteney, 1969). However, the most fractionated members of this suite are considered to be intruded at higher levels in the crust (Tuttle & Bowen, 1958; Dawes, 1966; Key & Wright, 1982), a fact which may have a bearing upon the textures seen in the Augen Gneisses.

From their studies of the Ab-Or-Q-H₂O system, Tuttle & Bowen (1958) explained the presence of rapakivi texture and the large phenocrysts in those granites by invoking a high-level intrusion with an increasing P_{H₂O} during cooling. The envisaged crystallisation path is shown in Fig. 4.11(b). A low initial P_{H₂O} is required to allow the crystallisation of K-feldspar first; the lower the H₂O content of the melt the further the feldspar-quartz boundary moves towards the Q apex, thereby giving a larger feldspar field and more opportunity for large crystals to grow. The increase in P_{H₂O} (assuming there is no loss of water) ultimately causes the intersection of the solvus by the solidus in the Ab-Or-H₂O system at ~5000 bars (Yoder et al., 1957; Morse, 1970) resulting in the simultaneous crystallisation of the two feldspars, often with the Ab nucleating on the Or to give the rapakivi texture. A sudden loss of H₂O results in new growth centres and a second generation of quartz and feldspar appearing, a feature often seen in rapakivi granites. To allow for such a loss of H₂O Tuttle & Bowen suggested fracture of the overburden on the magma, which is in accord with the tensional setting envisaged for the development of the anorthositic suite (Bridgewater et al., 1974).

Since the Augen Gneiss and granite sheets are depleted in Fe, compared to the anorthositic suite, it is suspected that a higher P_{H₂O} was present in the igneous precursor during its fractionation, maintaining a constant P_{O₂} and resulting in the removal of this element (Osborn, 1959). This Fe would enter the magnetite, hornblende or even biotite which would then fractionate out. The decrease in Ti and V (compatible with Ti) contents from the 'basic' to 'acid' varieties of the Augen Gneiss suggests that this fractionating magnetite was titaniferous. Rather fortuitously, the mafic phases generally presented by the Augen

Gneisses and granite sheets at present (hornblende, biotite and magnetite) are similar to those that would have been present at the time of the intrusion of the igneous precursor. Consequently, it seems permissible to compare the assemblages of the various types of Augen Gneiss to this fractionation pattern. Indeed, the proportions of hornblende and biotite decrease from 'basic' to 'acid' varieties of the Augen Gneiss, with the hornblende disappearing in the granite sheets. This pattern is consistent with that inferred from the trace-element plots (Figs. 4.2 and 4.3). Although there is no evidence for a basic, residual, fractionate in the Molde area, the presence of positive magnetic anomalies over the areas of the Augen Gneiss may indicate such a mass at depth.

Since the augen in these rocks are considered to represent relict K-feldspar phenocrysts, the P_{H_2O} in the igneous precursor must have been low enough to permit the growth of such large grains, as in the rapakivi granites. A low P_{H_2O} implies a hypersolvus magma which, in turn, implies that the perthites seen in the feldspars may have been, ultimately, of an igneous origin. It is possible that the igneous precursor followed a crystallisation path similar to that envisaged for the rapakivi granites, resulting in the formation of mantled phenocrysts. Although the evidence for mantles is equivocal (section 4.1), the possibility of their presence is reinforced by the Na-poor nature of the rocks. Tuttle & Bowen (1958) considered that melts rich in Na would begin crystallisation in the plagioclase field in the Ab-Or-Q-H₂O system, rather than the K-feldspar field, thereby preventing the formation of such mantles. Due to the subsequent high-grade metamorphism and deformation of the rocks it is not clear whether a second generation of quartz and feldspar ever existed in these rocks. However, it is not unreasonable to speculate that a loss of H₂O may have occurred from this

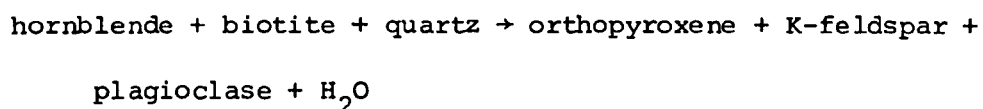
magma, in a manner similar to that suggested for the rapakivi granites: by overburden fracture, to explain the lack of early pegmatites in the Augen Gneisses (i.e. not Caledonian). It is possible that the granite sheets represent the equivalents of these missing veins, judging by their extremely differentiated chemistries (see Table 4.1), but lack the pegmatite texture which results from crystallisation from a volatile phase. Such a lack of pegmatites is also a feature of rapakivi granites (Key & Wright, 1982).

Although it is likely that the ovoidal feldspar augen now seen in the augen were formed during deformation (see section 4.1), it is interesting to note that the rapakivi granites also tend to have ovoidal feldspar phenocrysts (Sahama, 1945). Tuttle & Bowen (1958) suggested that these developed through a lack of surface tension between the growing crystal and a surrounding viscous melt (cf. Sederholm, 1928). In their experiments on the Ab-Or-An-H₂O system, they found that the most viscous mixes occurred around the Q-Or join. Fig. 4.11(b) shows that the majority of the Augen Gneiss analyses lie close to this join suggesting that such a mechanism may have also occurred in these rocks. The position of Sahama's (1945) average rapakivi granite is shown for comparison.

In conclusion it is considered that although the parental magma of the igneous precursor to the Augen Gneiss, and the tectonic setting of the intrusion may have been very similar to those of the anorthositic suite, it was a major difference in H₂O content which controlled the ultimate, and somewhat dissimilar, mineralogies and chemistries.

This interpretation is very similar to an idea suggested by de Waard (1969) who considered that the anorthosite-charnockite suite is closely related to the leucodiorite-granite suite in chemistry but not

in mineralogy. This difference was attributed to differences in P_{H_2O} at the time of formation with hypersthene or fayalite/quartz appearing in the anhydrous rocks (charnockites etc.), and hornblende and biotite in the hydrous rocks (granites etc.) (Fig. 4.12(a)). This he expressed as an equation:



From this study on the Augen Gneiss it would appear that the situation is rather more complex than envisaged by de Waard, with the higher P_{H_2O} not only giving hydrous mafic phases, but also causing a loss of Fe from the suite as a whole.

Rare earth element studies on the Augen Gneisses may help to clarify their origin. Hubbard & Whitley (1978) found that the Torpa granite, associated with the Varberg charnockite in SW Sweden, displayed a REE pattern similar to that of the Finnish rapakivi granites and that both were different from other granites of comparable major element composition, notably in LREE enrichment. Petersen (1980b) found a similar pattern in the Farsund charnockite but the pattern became gradually LREE depleted and HREE enriched towards the more fractionated portions.

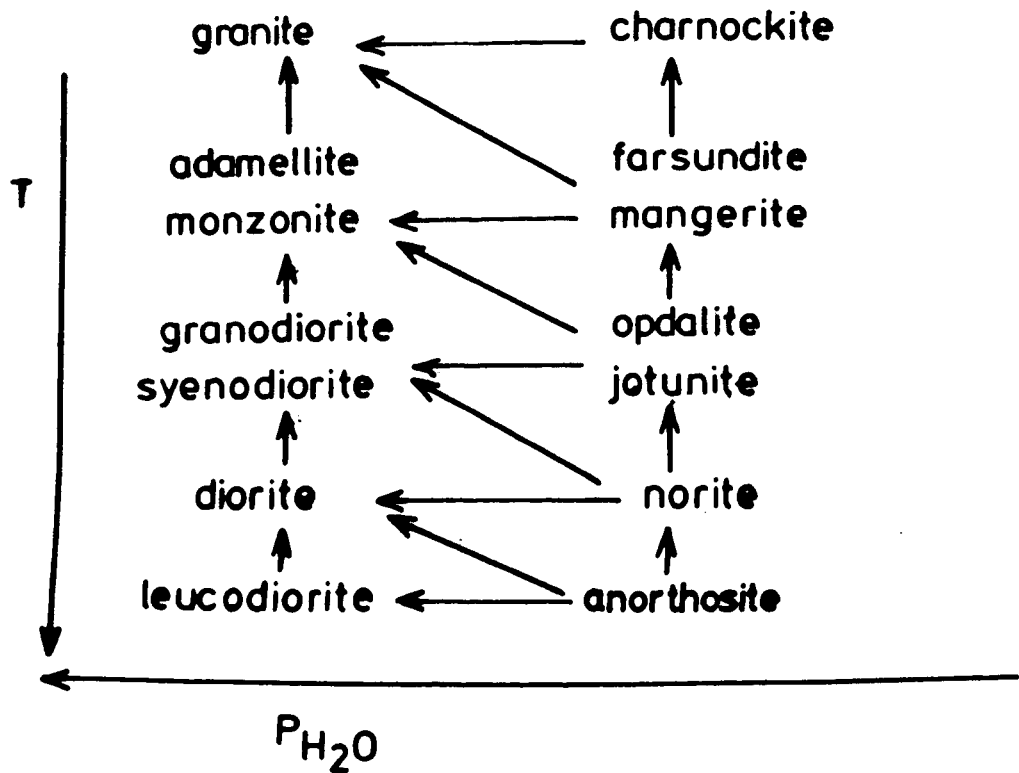
Elsewhere in W Norway and Central Sweden, other augen gneisses have been interpreted as derivatives from rapakivi-like igneous bodies, often with Proterozoic ages:

Abdel-Monem & Bryhni (1978) dated rocks from Eikefjord at 1479 ± 64 m.y. and related them to the anorthosite suite in N America;

Krill (1980) dated rocks, including augen gneisses, at Oppdal at 1450-1750 m.y.;

FIG. 4.12

(a)



(b)

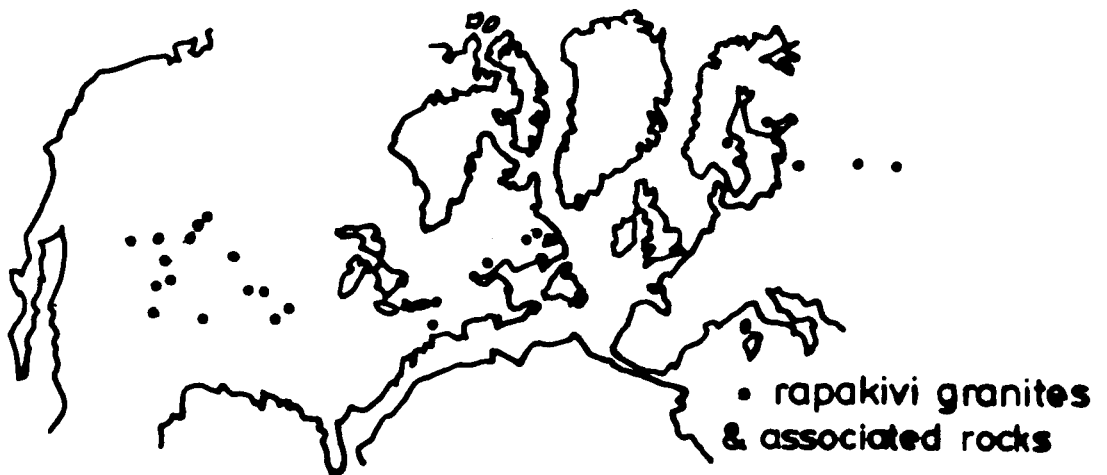


FIG. 4.12(a) Schematic relationship between the anorthosite-charnockite and leuconite-granite series as a function of P_{H_2O} . Arrows indicate possible transitions between members of the two series. After de Waard (1969).

(b) Continental reconstruction for the mid-Proterozoic after Bullard et al. (1965) with the positions of the major rock-types of Proterozoic age, Bridgewater & Windley (1973).

Andresen (1980) dated granites at Troms, N Norway at 1706 ± 15 m.y. and related them to the period of mangerite intrusion at Lofoten (see below);

Quernardel & Ploquin (1980) and Krill (1980) related the Tännäs augen gneisses in central Sweden, and the Andbergshøi Complex at Dombås to these rapakivi-like rocks. Point (1975) and Roshoff (1978) considered the Tännäs orthogneisses to be of Proterozoic origin.

It is interesting to speculate whether the augen gneisses at Oppdal, dated by Solheim (1980) at 1463 ± 68 m.y. are of a similar origin, although Solheim interprets the age as a metamorphic event.

Furthermore, mangerites have been described from various parts of Norway:

Kolderup & Kolderup (1940) considered those in the Bergen Arcs (see section 1.1.3) to be granulites, as did Bryhni (1966) with those on Måløy. Austrheim (1981) dated the former at 1328 ± 47 m.y. and interpreted them as igneous rocks with a granulite facies overprint;

Lappin (1966) and Lappin et al. (1979) dated those at Stadlandet at 1520 ± 10 m.y. and considered them to be igneous in origin;

Romey (1971) and Griffin et al. (1974) both considered the Lofoten mangerite to be igneous in origin, the latter workers dated the body at 1664 ± 20 m.y., whilst a date of 1737 ± 30 m.y. was obtained by Heier & Compston (1969).

The southern gneiss region of Norway has also produced Proterozoic ages, often from charnockitic rocks:

Hermans et al. (1975) suggested an igneous or metamorphic event at 1500 m.y., or 1200 m.y. for the charnockites of Rogaland;

Versteve (1975) found relic 1600-1700 m.y. ages in charnockites and gneisses;

Jacobsen & Heier (1978) considered that there were major additions to the crust in S Norway at around 1600 m.y. including andesitic rocks. (It has been speculated that Proterozoic rifting may have ultimately produced oceanic crust in N mid-Europe (Zwart & Dornsiepen, 1978) subduction of which would result in such rocks appearing here.);

Ploquin (1975, 1977) assigned an age of 1398 m.y. to the Kallingsheia massif in Telemark and considered it to be chemically and petrographically related to the anorthosite suite of N America;

Michot & Pasteels (1969) dated the Egersund anorthosite at 1050 m.y.;

Field & Råheim (1979) considered a charnockite 'event' to have occurred in the Bamble area around 1540 m.y. ago;

Pederson & Falkum (1975) dated the Farsund charnockite at ~900 m.y.

Unfortunately, a certain degree of confusion arises with the terms charnockite and mangerite. As it is difficult to find suitable criteria which allow for the unambiguous distinction between those rocks formed at granulite facies and those which were intruded into a similar deep-crustal environment, these terms are often applied to any rock containing hypersthene and mesoperthite. Consequently, some rocks thought to be metamorphic in origin could well be igneous (i.e. those of Kolderup & Kolderup or Bryhni). Conversely, those rocks thought to be igneous could be metamorphic; these would be better termed as granulites.

From this evidence it would appear that Proterozoic magmatism in Norway was more extensive than has usually been considered, especially so in the Basal Gneiss Complex. Also, from a study of the large, positive aeromagnetic anomalies in Sweden, Dyrelius (1980) proposed that these features were caused by the presence of large volumes of strongly magnetic Proterozoic-aged granites in the basement.

Fig. 4.12(b) is the continental reconstruction for the mid-Proterozoic after Bullard et al. (1965) with the positions of the major

igneous features formed at that time (after Bridgewater & Windley, 1973). Although Norway lies well within the mobile belt, igneous rocks are shown only in the southern gneiss region. There appear to be several reasons for the earlier notions of a lack of igneous rocks of this age in the Basal Gneiss Complex:

(i) There has been a general acceptance that Rb-Sr whole-rock ages reflect metamorphic, rather than igneous events because of the belief that the Rb-Sr isotopic system is easily upset by high-grade metamorphism. Such a disturbance does not seem to have occurred in the Auger Gneisses and may not have done so in other rocks.

(ii) Auger gneisses have usually been interpreted as being products of metasomatism (Mehnert, 1968) or deformation (Bryhni, 1966) rather than as igneous relics.

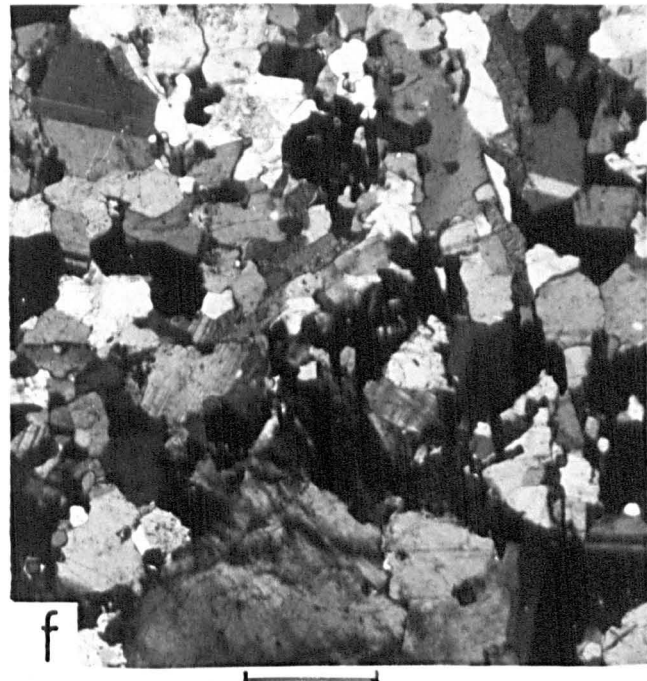
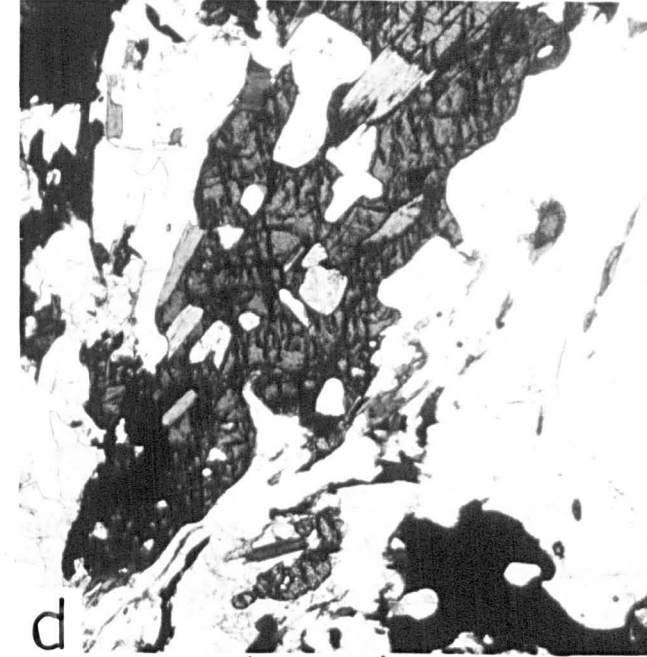
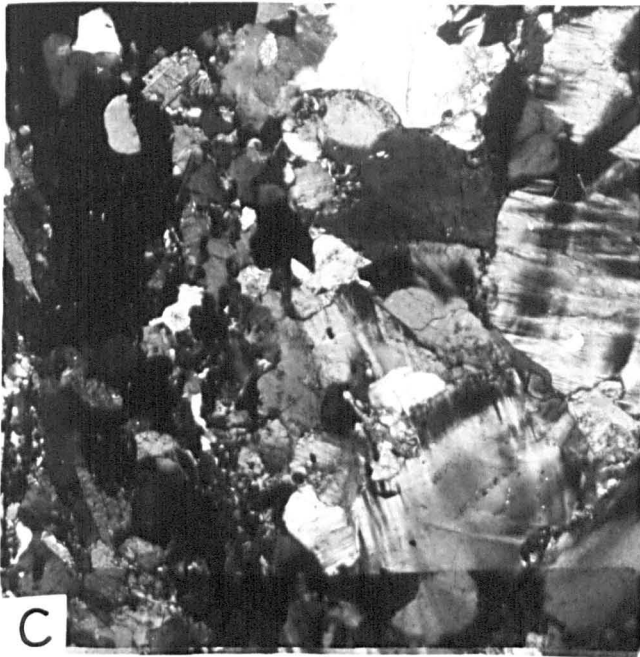
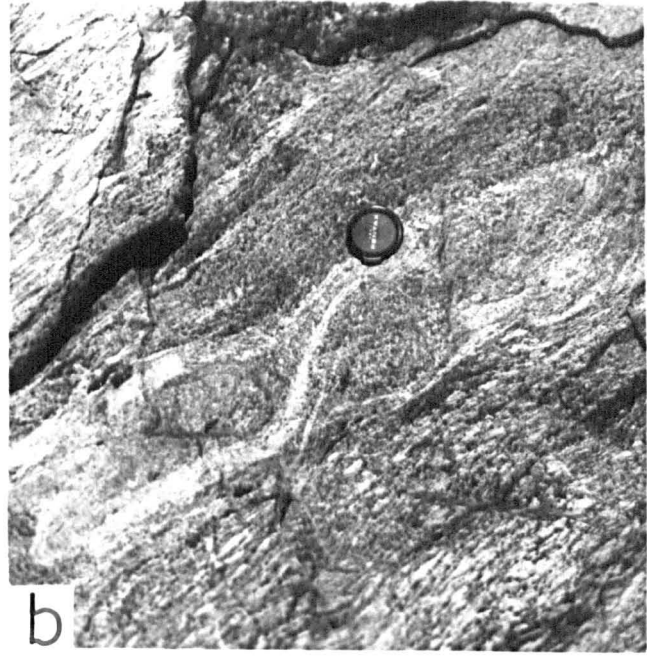
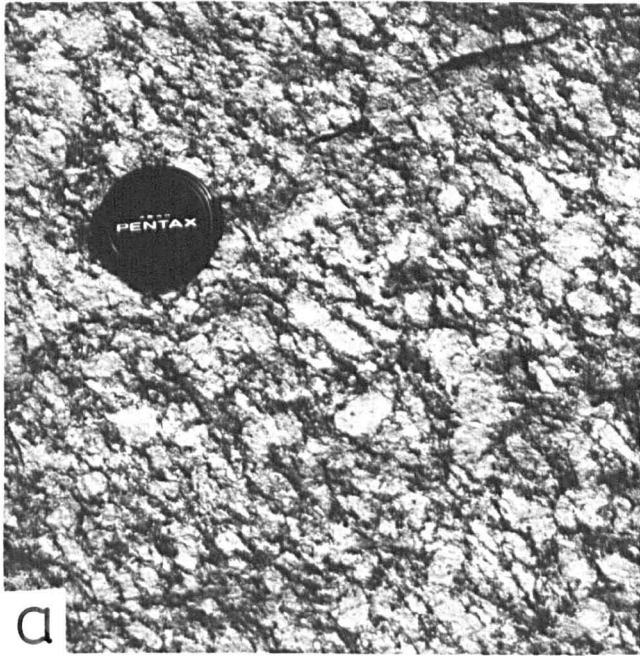
(iii) There has probably been some mis-identification of igneous mangerites as metamorphic rocks.

(iv) The Basal Gneiss Complex has been severely affected by later Caledonian deformation making interpretation of the rocks very difficult.

PLATE 4.1

- (a) Appearance of the Augen Gneiss in outcrop when undeformed. Fanghol (977614).
- (b) Small, partly-assimilated pods of calc-silicate rocks in the Augen Gneiss. Note orientation of the pods parallel to the extension of the augen. Eidskrem (980607).
- (c) The Augen Gneiss in thin-section. K-feldspar of the augen on right, biotite of the matrix on the left. Note the small grains of plagioclase on the edge of the augen and the development of myrmekite there. (Sample 2123, cross-polarised light.)
- (d) Hornblende poikiloblastically enclosing plagioclase, after clinopyroxene? (Sample 2125, crossed-polarised light.)
- (e) Mylonitised Augen Gneiss with relict hornblende and K-feldspar in a comminuted matrix. (Sample 2120, crossed-polarised light.)
- (f) General appearance of the granite sheets in thin section. (Sample D117, crossed-polarised light.)

PLATE 4.1



CHAPTER 5

THE HETEROGENEOUS QUARTZO-FELDSPATHIC GNEISS UNIT

5.1 GENERAL GEOLOGY AND PETROGRAPHY

The rocks included in this Chapter appear in a tract of gneisses extending from Näs^ovatnet to Mordalsvå^ogen, and occur in the southern part of the Frei Group of Rå^oheim (1972 - see Table 1.2).

See the Introductory Statement on p. 109 with respect to the relationship between these gneisses and the Augen Gneiss Unit, which also occurs in this tract of gneisses.

5.1.1 Description

The gneisses outcrop on the ground around Näs^ovatnet (~ 1576), along the N side of Langvatnet (~ 0775) and across Malmefjord to Hollingsholm (1962 - see Map A). Included in this group of rocks are those appearing within the Augen Gneiss Unit which can be distinguished from it on chemical grounds. The exposures in the northern part of this tract, in the valley of Oselva (1377), are poor but improve towards Elnesvå^ogen (~ 0672). On the S side of Malmefjord, the coastal exposures provide the better outcrops as the hills tend to be fairly heavily forested or have lichen covered rock surfaces on their tops.

(i) Migmatitic, with both massive neosomes and small, intrafolial neosomes.

(ii) Banded gneisses, on scales of centimetres or metres, generally pink and grey. These can be easily confused with the severely deformed Augen Gneiss.

(iii) Augen-bearing gneisses, these generally have smaller and more widely disseminated augen than the Augen Gneiss (s.s.).

(iv) Massive, grey gneisses, generally with an almost schistose foliation and small, pink porphyroblasts and veins.

Also, smaller amounts of the following rocks were found: pink, microcline-bearing gneisses, massive banded amphibolites, granulites and calc-silicate rocks.

The migmatitic rocks occur mainly on the N and NE sides of Langvatnet and N of Helvatnet (1476). They can be massive, pale (pink/white) coarse-grained rocks dominated by the neosome portions which can be up to 1 m wide (Plate 5.1(a)), or rather finer-grained, semi-pelitic rocks dominated by the palaeosome in which the neosome appears as thin streaks and veins ~2-5 cm wide, which weather out into small ridges (Plate 5.1(b)). In the massive variety, the rocks possess the characteristic chaotic, plastic deformation style typical of migmatites (Mehnert, 1968, p. 34) whereas the finer-grained variety are well foliated with the neosome lying within the foliation planes. In the terminology of Mehnert (1968, p. 39) these migmatites have the megascopic texture of 'Schlieren' i.e. elongate light and dark streaks, which is considered to be a feature of an advanced stage of a migmatite formed at high P-T conditions.

The rocks contain pods of eclogite in varying states of preservation but rarely are these totally amphibolitised. The rocks also contain massive amphibolites ~1 m wide which have been intruded by the neosome of the migmatite and deformed with it (Plate 5.1(a)). The eclogites do not display this intrusive feature and appear to reside in the migmatites as competent bodies.

The palaeosome in the migmatites consists of: brown biotite, anti-perthitic plagioclase (An 38), quartz + microcline + opaques. These are fine-grained (1-2 mm) and foliated with oriented biotite, sutured and strained quartz and granulated plagioclase (Plate 5.1(c)). The neosome

consists of: coarse (5 mm), perthitic microcline, slightly sausseritised plagioclase (An 10-25), quartz + biotite (to chlorite) + zircon + apatite + kyanite + rare colourless garnet. These phases show some evidence of deformation as granulated feldspar margins and slightly strained and sutured quartz; in general the neosome is less deformed than the palaeosome. White mica is uncommon but can appear as large blades in the neosome or in a more acicular habit attached to biotite in the palaeosome. The kyanite is generally replaced by fibrolite-sillimanite and/or muscovite. When deformed the rocks tend to be hydrated with heavily sausseritised plagioclase and sericitised K-feldspar. An unusual feature of the feldspar in these migmatites is the appearance of rounded 'blebs' of quartz scattered through the grains. According to Mehnert (1968, p. 58) these 'quartz-drops' are typical of migmatites and probably represent relics of the palaeosome.

Some of the migmatites contain very little neosome portion and appear to be semi-pelites. These rocks occur as fairly wide bands within the more neosome-dominated rocks and contain the assemblage: oriented biotite, porphyroblastic garnet, plagioclase (An 42), quartz + opaques + apatite + white mica + microcline. These rocks are fairly heavily deformed with sutured quartz smeared into zones of 'ribbons'.

The banded gneiss is shown in Plate 5.1(d), although this rock type can occur with much wider bands. This type of rock is fairly common, particularly N of Elnesvågen (0672), E of Helvatnet (1576), N of Hollingsholm (9963) and at Ytre Fraena (0167). The bands consist of coarse granitic material set in a finer-grained, foliated rock; there is a good segregation of the quartzo-feldspathic minerals and more micaceous portions. The quartzo-feldspathic portions contain: microcline, anti-perthitic plagioclase (An 12) + quartz + biotite and are moderately de-

formed with ribboned quartz and some granulation of the feldspars; the plagioclase develops myrmekite when adjacent to the K-feldspar. As in the Augen Gneiss this texture appears to be the result of deformation induced exsolution (Smith, 1974, p. 577). The finer grained portions contain: biotite, microcline, plagioclase (An 38) + hornblende (α straw, β dark-green, γ blue-green, $\gamma^Z \approx 18^\circ$) + quartz + sphene + opaques + orthite (with clinozoisite rims) + tiny garnets + apatite + white mica. The plagioclase is difficult to identify as it is often untwinned which may be the result of deformation (Smith, 1974, p. 348). These rocks appear to be deformed and flattened examples of the migmatitic rocks with the neosome now represented by the concentrations of quartzo-feldspathic minerals in a deformed palaeosome.

These gneisses also contain thin (~ 5 cm) veins and streaks of quartzo-feldspathic rocks containing idiomorphic porphyroblasts of hornblende, generally parallel to, and incorporated within, the foliation although they are also observed cutting across the rock fabric. These are termed sticholithic or 'fleck' structures by Mehnert (1968, p. 37). The quartzo-feldspathic portion is dominantly very coarse (5 mm) microcline, plagioclase (An 20), quartz + apatite. The porphyroblasts are green hornblende, altering to biotite, poikiloblastic to plagioclase + some sphene. This assemblage and texture is identical to that described by Mehnert (1968, p. 37). He considers that these veins do not form by partial melting (confirmed by Chenall et al., 1980), but rather by metamorphic differentiation from the palaeosome through the reaction:



Gavelin (1975) considers that the veins tend to form in meta-arenites (i.e. psammites) and generally in pre- or syn-tectonic metamorphic condi-

tions. As the veins observed in these gneisses are seen cutting the steeply-dipping foliation and incorporated within that foliation, it would appear that they have formed as syn- and post-tectonic features in this case.

The augen-bearing gneisses appear towards Hollingsholm, but are also seen at Steinbrudd (160745) and E of Helvatnet (151759). These can be easily confused with the Augen Gneiss, although the augen tend to be whiter and more pegmatitic in appearance than the pink-orange form seen in the Augen Gneiss. Furthermore, the augen are generally small (1 cm maximum) and scattered in a very deformed grey matrix (Plate 5.1(e)). The augen are composed of polygonal microcline, quartz + a little plagioclase (oligoclase) + myrmekite + 'quartz-drops' in a granulated texture. The matrix is almost schistose with: biotite; hornblende (α green-yellow, β dark brown-green, γ green-blue, $\gamma^Z \approx 19^\circ$) + K-feldspar + opaques + apatite + strings of tiny garnets (altering to biotite) + plagioclase. As in the banded gneisses this plagioclase is rarely twinned. The biotite in the matrix tends to sweep around the augen thereby delineating their outline.

These rocks are interpreted as extremely deformed migmatitic rocks. Plate 2.1(d) shows the streaks of quartzo-feldspathic material passing into larger, partially formed augen; it is considered that further flattening and stretching of this rock would result in the type seen in Plate 5.1(e).

The proportion of extended and disrupted neosome in these deformed migmatites is significantly less than the proportion of palaeosome. This observation suggests that the most pelitic migmatites, i.e. those with the greatest proportion of palaeosome have suffered the most deformation. This is not surprising as they contain easily disrupted and

foliated phases such as biotite and hornblende, whereas the neosome contains coarser more competent feldspars in a more structurally coherent, polygonal texture. However, highly deformed, massive migmatite portions have been observed in this tract of gneisses, albeit rarely. These rocks retain the large perthitic microclines (5-10 mm) + myrmekite + 'quartz-drops' + plagioclase (oligoclase) + quartz. The quartz is strained and sutured, whilst the feldspars have granulated margins. The small amount of palaeosome present in these rocks is dominated by hornblende, breaking down to biotite which itself is being altered to chlorite + large sphenes + biotite + plagioclase (An 40) + quartz. The presence of this small amount of palaeosome distinguishes these rocks from deformed Caledonian-aged pegmatites.

The grey gneisses are fairly common but do not appear to form particularly extensive outcrops; they are generally seen intercalated with the massive pink granite sheets within the Auger Gneiss Unit, around Hollingsholm and on Vågøy. They are well foliated with the assemblage: green hornblende, biotite, garnet, plagioclase (An 15-30), quartz, K-feldspar + opaques + apatite + sphene. The rocks are generally more mafic and intermediate in composition than the rocks previously described and less pelitic (Plate 5.1(f)). The mafic phases occur in clots with the hornblende poikiloblastically enclosing plagioclase and quartz; the biotite interpenetrates the hornblende and replaces it. The highest proportion of garnet occurs in the most mafic rocks of this type. Small pink, K-feldspar porphyroblasts and streaks can occur giving the rocks an appearance somewhat like that in Plate 5.1(e), but much less schistose and without the banding.

The 'granitic' (s.l.) rocks are fairly massive and appear throughout this tract of gneisses, particularly at Helvatnet and within the Auger

Gneiss Unit where they were confused with the granite sheets occurring in that Unit. However, they are well foliated, whereas the granite sheets generally are not, with granulated feldspars, oriented biotite and sutured quartz plus relict polygonal microcline and plagioclase (An 20-30) (Plate 5.2(a)). Also present is a blue-green hornblende, generally associated with biotite in mafic clots, or appearing in clusters with quartz and plagioclase, which may be a very advanced symplectic texture after a clinopyroxene, cf. that in the Augen Gneiss, see Plate 4.1(d). Some of these rocks have been retrogressed to greenschist facies assemblages with heavily chloritised mafics + exsolved opaques, sausseritised plagioclase, zoisites and orthites. The feldspars in these 'granitic' rocks do not contain 'quartz-drops' and therefore do not appear to be the products of migmatization.

Generally speaking, the gneisses in this tract contain assemblages indicative of the amphibolite facies, although some contain garnet and possible amphibolitised symplectic textures after clinopyroxene which may indicate an original high-pressure granulite assemblage. At some localities, where the younger, steeply-dipping foliation has been instigated, the rocks produce assemblages intermediate between amphibolite and greenschist facies, with the appearance of chlorite and epidote.

At two localities relict, high pressure granulites were found: S of Skoften Hill (080665) and on the W side of Surendalen (182722); the latter locality lies outside the main mapping area (see Map A). Both examples of granulite have a distinctive mottled appearance in outcrop, caused by 'strings' of small garnets growing as coronas around clots of hornblende (α yellow, β dark-green, γ green-blue, $\gamma^Z \approx 15^\circ$), pale-green clinopyroxene, biotite, sphene and rutile (Plate 5.2(b)). Scapolite appears rarely, of an intermediate composition from the birefringence colour.

Around these mafic clots the matrix is dominantly plagioclase (An 15-30), rarely twinned and rarely anti-perthitic + quartz + rare microcline in an excellent polygonal texture (Plate 5.2(c)). The rocks show very little evidence of deformation, generally as a slight orientation of the biotite. The hornblende does not appear to be secondary, from clinopyroxene or garnet, nor does the clinopyroxene display any form of symplectite with plagioclase, as seen in the garnet-granulite on Tverrfjella (see Plate 3.1(f)). However, at the Skoften Hill locality (sample M22) the clinopyroxene occurs as both porphyroblasts and as small discontinuous strings lying between large quartz grains and smaller polygonal plagioclase grains. In contact with the clinopyroxene, and between it and the matrix plagioclase (\sim An 20) lies another, untwinned, plagioclase. This can only be detected through it having a lower R.I. than the matrix plagioclase and as a consequence appears to be highly sodic (see Plate 5.2(c)). This texture is interpreted as the clinopyroxene producing albite in the presence of quartz, similar to that seen in the garnet-granulite (see Plate 3.1(d) and the discussion in section 3.1.5). This suggests that these clinopyroxenes once contained jadeite and therefore were once omphacitic.

Other, more mafic rocks appear within this tract of quartzofeldspathic gneisses, particularly on Vaggø where massive amphibolites occur (996675) with the assemblage: hornblende (α straw, β dark-green-brown, γ blue-green, $\gamma^Z \approx 19^\circ$), biotite, garnet + plagioclase (An 12) + quartz + sphene \pm K-feldspar + clinozoisite + apatite + scapolite. All these phases are well aligned. The rocks appear to be compositionally layered with thin 1-5 mm hornblende-rich, quartz-rich and plagioclase-rich layers. The scapolite tends to occur only in the biotite-rich portions whilst garnet appears with hornblende.

The mapping of D.A. Carswell on the island of Otrøy, on strike to the W of the Molde peninsula, has found more extensive exposures of units of amphibolitic rocks intercalated with the Augen Gneiss Unit; these are well exposed on the E end of the island (9456). Besides the amphibolites, the rocks include psammitic biotite-rich rocks, and calc-silicate rocks with well foliated epidote, sphene ± garnet + plagioclase + quartz assemblages. The assemblages of the calc-silicate rocks are virtually identical to those found in the partially assimilated pods in the Augen Gneiss at Eidskem, which were interpreted as meta-xenoliths (see section 4.4).

5.1.2 Discussion of the petrography

Råheim (1972) described all the rocks seen in the Heterogeneous Quartzo-Feldspathic Gneiss Unit in his Frei Group, although he included several other metasedimentary rocks such as quartzites and marbles not seen here. From his mapping he considered that the conformable banding of the various rock types was the result of metamorphism of an original sedimentary layering and consequently interpreted the rocks as clay-rich sediments ± arkosic portions ± calcic portions. The more granitic rocks he interpreted as dacitic and rhyodacitic volcanics mixed with sedimentary material (see Table 1.2). His favoured interpretation for the rocks was deposition in a eugeosynclinal basin with subsequent metamorphism at ~1700 m.y. ago (from a Rb-Sr whole rock date by Pidgeon & Råheim, 1972) at granulite facies (~700°/~10 kb) to give partial melting of the pelitic rocks in association with kyanite.

Comparing the migmatitic rocks appearing around Langvatnet to those on Tverrfjella (section 3.1.3) certain similarities are apparent, although the latter generally have less neosome portion. Both sets of rocks are aluminous with much biotite, and the appearance of kyanite

and/or sillimanite plus garnet. Also, the neosomes in both sets of rocks are comparatively undeformed compared to the palaeosome. The anatectic portions in the pelites on Tverrfjella were interpreted as having been produced during rapid, post-tectonic uplift of the rocks from eclogite facies conditions of metamorphism (see section 3.1.5). The same interpretation seems applicable to the migmatites in this gneiss unit. However, the excellent segregation of the neosome and palaeosome in the Heterogeneous Gneiss Unit and the plastic style of deformation, neither of which are seen at Tverrfjella, suggests that these rocks have been through more than one phase of metamorphism and mobilisation of the neosome. Although many of the rocks interpreted as deformed equivalents of the migmatitic rocks, with 'schlieren' and 'augen' of neosome within a well defined foliation, appear within the belts of younger, steeply dipping foliation these rocks have also been observed in areas dominated by the older, flat-lying foliation. This suggests these rocks have also suffered more than one period of deformation and segregation of the neosome portions. It is the polyphase metamorphic nature of these migmatitic rocks which differentiates them from those on Tverrfjella; the latter were interpreted as pelites metamorphosed once during the eclogite facies event in the Caledonian (see section 3.1.5).

The meta-sedimentary interpretation of Råheim (1972) seems applicable to many of the rocks in this tract of gneisses. The banding in the amphibolites, with the appearance of Al-phases and scapolite, the occurrence of calc-silicate rocks and mica-rich psammities in addition to the migmatitic pelites would seem to confirm such an interpretation. However, the more massive 'granitic' rocks and grey gneisses were more difficult to interpret from their mineral assemblages and a study of their whole-rock chemistries was necessary to clarify their origin.

5.2 GEOCHEMISTRY

The analyses of the rocks from this tract of gneisses are given in Tables 5.1 and 5.2. Table 5.1 contains the migmatitic rocks, with pelitic palaeosomes, and the assumed meta-sedimentary rocks; Table 5.2 contains the massive pink 'granitic' rocks and grey gneisses. The latter also includes some banded and augen-bearing rocks, probably derived from original migmatites but lacking in any pelitic portion. Samples prefixed by 'U' are from Otrøy, all others are from the Molde Peninsula.

Table 5.1 shows the migmatitic gneisses to be variable in composition, reflecting the varying proportions of palaeosome and neosome in the samples. The more siliceous samples with $K_2O > Na_2O$ are those dominated by the 'granitic' neosomes (e.g. D28A and D28F). The samples dominated by the pelitic palaeosome tend to be Si-poor often with $K_2O < Na_2O$ and richer in Fe, Mg and trace metals (Ni and Cr). Overall, the rocks are only moderately aluminous for pelites (compared to those in Table 3.3 for the pelites on Tverrfjella). There does not appear to be any correlation between the proportion of neosome and the Rb and Zr contents of these rocks. Both of these elements should be preferentially concentrated in the 'granitic' melt portions of these rocks, with Rb entering K-feldspar, and Zr in zircon (Taylor, 1965). Samples D28A and D28F are the most K-rich samples and yet they do not possess equivalent high concentrations of Rb. This suggests that these rocks have suffered a depletion of Rb at some time. However, there is a very rough correlation between the Sr contents and the proportion of neosome in these rocks. This element usually tends to be concentrated in the palaeosome portion of migmatites (Iden, 1981).

The group of metasedimentary rocks have variable compositions but overall are fairly aluminous and titaniferous, and not particularly

TABLE 5.2 Whole-rock analyses and normative minerals for the meta-igneous rocks in the Heterogeneous Quartzo-Feldspathic Gneiss Unit

	Massive 'granitic' rocks						Grey, banded and 'augen'-bearing rocks								
	RS3	1115	U340	U443	U446	U489	D93	D94	D95	D117	F5	1114	M22	U362	U445
MAJOR	ELEMENTS (wt. %)														
SiO ₂	72.54	70.73	76.26	78.85	70.08	77.22	62.53	66.56	63.23	66.57	54.67	67.42	63.47	68.07	63.80
TiO ₂	0.36	0.45	0.24	0.10	0.24	0.03	1.11	0.71	0.65	0.88	0.99	0.84	0.58	0.39	0.67
Al ₂ O ₃	13.43	14.35	12.05	12.19	14.77	12.42	15.46	14.88	16.82	14.63	16.77	14.93	16.64	15.52	16.15
Fe ₂ O ₃	1.97	1.42	0.81	0.12	1.33	0.02	2.75	2.01	2.05	2.40	3.91	1.42	2.03	0.89	2.70
FeO	1.82	2.12	0.77	0.76	0.78	0.51	4.14	2.86	3.13	3.33	4.76	3.85	2.83	2.57	2.43
MnO	0.11	0.05	0.02	0.02	0.05	0.03	0.16	0.07	0.11	0.15	0.17	0.09	0.10	0.07	0.11
MgO	0.78	0.89	0.44	0.28	0.75	0.19	2.45	1.51	2.32	1.70	4.89	1.33	2.38	1.44	2.50
CaO	2.19	2.05	1.28	1.60	1.84	0.85	4.18	3.16	4.97	3.38	7.36	3.05	4.35	3.38	3.72
Na ₂ O	4.12	2.58	2.85	2.09	2.93	2.75	3.45	3.05	4.32	2.32	3.44	3.02	3.52	3.77	3.85
K ₂ O	3.09	4.97	4.76	2.79	5.99	5.81	3.08	4.05	1.53	3.40	2.19	3.81	2.79	2.89	3.76
P ₂ O ₅	0.16	0.18	0.07	0.01	0.10	0.01	0.35	0.23	0.21	0.32	0.57	0.25	0.16	0.17	0.29
S	0.01	0.00	0.01	0.00	0.00	0.00	0.02	0.02	0.01	0.01	0.01	0.00	0.00	0.02	0.01
H ₂ O ^T	0.50	0.46	0.30	0.21	0.20	0.03	0.48	0.37	0.65	0.49	0.65	0.24	0.53	0.50	0.40
TOTAL	100.08	100.25	99.86	99.02	99.06	99.87	100.16	99.48	100.00	99.58	100.38	100.25	99.38	99.68	100.39
TRACE ELEMENTS (ppm)															
Ni	2	27	1	0	1	0	9	5	6	9	36	15	15	2	2
V	12	36	10	9	25	6	84	62	60	59	198	66	-	30	70
Cr	11	5	11	15	13	25	23	21	16	20	122	10	28	9	12
Zn	-	58	15	16	-	9	-	-	-	-	-	77	62	54	-
Cu	-	48	9	5	-	6	-	-	-	-	-	19	10	11	-
Rb	69	111	82	47	118	173	69	106	19	114	59	117	66	54	123
Sr	42	205	184	269	870	91	326	254	330	214	727	214	283	254	585
Y	35	18	14	12	17	39	40	35	16	51	34	34	6	19	45
Zr	226	237	158	83	290	78	305	246	212	295	178	343	133	167	280
Pb	21	25	6	10	22	40	5	17	14	20	12	17	10	20	1
Ba	276	1121	499	404	2451	231	885	1106	552	847	1021	962	1504	813	553
NORMATIVE MINERALS (%)															
q	31.00	30.57	38.09	51.66	25.32	36.50	17.65	23.85	17.65	29.96	5.00	25.39	18.72	24.65	15.81
or	18.26	29.37	28.13	16.49	35.40	34.34	18.20	23.94	9.04	20.09	12.94	22.52	16.49	17.08	22.22
ab	34.86	21.83	24.12	17.69	24.79	23.27	29.19	25.81	36.56	19.63	29.11	25.56	29.79	31.90	32.58
an	9.03	8.99	5.89	7.87	8.48	4.15	17.60	14.17	21.99	14.68	23.85	13.50	20.54	15.66	15.68
c	-	1.43	0.05	2.85	0.36	0.09	-	0.28	-	1.75	-	0.89	0.30	0.45	-
di	0.64	-	-	-	-	-	0.69	-	1.05	-	7.16	-	-	-	0.70
hy	2.73	4.19	1.42	1.83	1.87	1.34	9.22	6.14	8.23	6.89	12.61	7.82	8.49	6.89	7.00
mt	2.86	2.06	1.17	0.17	1.82	0.03	3.99	2.91	2.97	3.48	5.67	2.06	2.94	1.29	3.92
il	0.68	0.86	0.46	0.19	0.46	0.06	2.11	1.35	1.24	1.67	1.88	1.60	1.10	0.74	1.27
py	0.02	-	0.02	-	-	-	0.04	0.04	0.02	0.02	0.02	-	-	0.04	0.02
ap	0.37	0.42	0.16	0.02	0.23	0.02	0.81	0.54	0.49	0.74	1.33	0.58	0.37	0.40	0.67
TOTAL	100.45	99.72	99.51	98.77	98.73	99.80	99.50	99.03	99.24	98.91	99.57	99.62	98.74	99.10	99.87
$\frac{K_2O}{Na_2O}$	0.75	1.93	1.67	1.33	2.04	2.11	0.89	1.33	0.35	1.47	0.64	1.26	0.79	0.77	0.98

siliceous. Samples 235, U343 and U365 are all calc-silicate rocks with epidote, garnet, plagioclase, quartz, sphene assemblages, as reflected by the high Ca and often high Al contents of the rocks. Epidote typically has a chemical composition with a high $\text{Fe}_2\text{O}_3/\text{FeO}$ ratio (Deer, Howie & Zussman, 1964, Vol. 1, p. 179-199); samples U343 and U365 reflect the high proportion of epidote in their assemblages with $\text{Fe}_2\text{O}_3 > \text{FeO}$ in their chemical compositions. The trace element contents in these calc-silicates reflect the major element contents with very high Sr contents (which enters Ca-phases, such as epidote, Taylor, 1965) and Zr contents (in detrital zircon?). Pb is unusually high in these rocks, which is generally an indication of igneous rocks (Turekian & Wedepohl, 1961 - see Table 3.5). However, Pb has a similar ionic radius to Sr and is a divalent ion, and therefore can also enter the Ca sites in minerals (Taylor, 1965). Therefore it is considered that these high Pb values are another reflection of the calcic nature of the rocks. An important point here is that sample 235 is one of the partly assimilated calc-silicate pods with the Augen Gneiss at Eiksrem (see Plate 4.1(b)). Samples U343 and U365 appear as discrete bands within the amphibolitic rocks, on strike, on the E coast of Otrøy, and yet the compositions of the three rocks are broadly similar. This observation suggests that these meta-sedimentary rocks formed part of the rock sequence into which the igneous precursor of the Augen Gneiss was intruded.

Sample M36 is also fairly calcic, and has a high Sr content, but is a fairly pelitic rock, reflected in the higher trace metal (Ni and Cr) contents and Al content. Samples U435 and U444 are psammites (i.e. a higher feldspar:mica ratio than the pelites) with high contents of total alkalis and Ba (in K-feldspar) but lower Al contents. Zr is moderately high in these two samples perhaps reflecting the presence of detrital zircon.

Samples M19 and U371 are hornblende, garnet, mica, plagioclase \pm scapolite bearing rocks. Comparing the chemical compositions of these two rocks with the amphibolites in the Tverrfjella Unit, several differences are apparent (see Table 3.4). Samples M19 and U371 have higher contents of K, and less Ca and Mg. However, the major differences occur in the trace element contents with the greater proportion of feldspar in these two rocks reflected in the higher contents of Ba, Sr and Rb. The trace metal contents are lower than those in the amphibolites from the Tverrfjella Unit which typically have Ni > 100 ppm and Cr > 200 ppm; low metal contents are typical of sediments (Turekian & Wedepohl, 1961). A sedimentary parentage of these two rocks is also suggested by their high values of Zr. The amphibolites at Tverrfjella were interpreted as meta-igneous rocks, although some mixing with detrital material was postulated for one sample (1017) which has a higher content of Zr than the others. A meta-sedimentary parentage for these two amphibolites is preferred here. It is considered that little mixing with basaltic igneous material has occurred in these rocks, prior to metamorphism, as this would have substantially increased their contents of trace metals.

Overall, the chemistries of these rocks are rather unusual and appear to reflect original sedimentary parents, as inferred from the petrographic evidence, dominated by clays or clay/limestone mixtures (marls). A puzzling feature of the calc-silicate rocks (235, U343 and U365) is the lack of carbonate in the observed metamorphic assemblages as would be expected in such calcic rocks (compare with the calcite-bearing calc-silicate rocks in the Tverrfjella Unit which also have high CaO contents - Table 3.3). It is possible that these rocks have suffered the loss of large volumes of CO₂ at some time in their evolution, although such a loss would have been very selective since marbles have been

observed in equivalent Frei Group rocks at Kristiansund (Råheim, 1972) and in the amphibolites on the Otrøy. Epidote-quartz bearing nodules have been observed in shales and sandstones at New Brunswick, Canada by Percival & Helmstaedt (1978), which they interpreted as thermally metamorphosed ironstone concretions. However, these nodules were rich in both Ca and Fe, whilst the calc-silicate rocks here are not particularly Fe-rich (see Table 5.1) which would seem to preclude such a parent for them. Consequently, the exact sedimentary parent to these unusual rocks is still obscure although some sort of impure calcareous rock is favoured here.

The two groups of gneisses in Table 5.2 are other rocks of interest here since little could be gleaned from the petrography of these rocks to indicate their parentage.

The 'granitic' rocks have a generally similar composition to the migmatites, with a similar alkali balance, but contain less Al and slightly more Si, a reflection of the lack of pelitic portions in these rocks. The group of mixed rocks is more intermediate in composition, with $\text{SiO}_2 < 70\%$, $\text{Na}_2\text{O} > \text{K}_2\text{O}$ and higher normative hy than the 'granitic' rocks. Sample D94 is unusually low in K, reflected in its low Rb content (19 ppm) and moderately low Ba content (552 ppm) compared to the other rocks in this group. The two granulites are included in this group: F5 and M22. The former is moderately calcic with a high Sr value (727 ppm) and has the lowest Si content of this group of rocks reflected in the low q content.

Two types of parental rocks appear feasible for these gneisses either metasedimentary, perhaps of the same original stratigraphic unit as the metasediments described above; or meta-igneous, as suggested by Råheim (1972).

Tarney (1976) has recommended the use of a TiO_2 vs. SiO_2 discriminant plot for quartzo-feldspathic gneisses of unknown parentage, Fig. 5.1(a) shows this plot with the meta-igneous/meta-sedimentary dividing line of Tarney and most of the gneisses in Table 5.2 are divided between the two fields. However, the discriminant plot of Winchester et al. (1980), which uses Ti and Zr to avoid the possible effects of element mobility during metamorphism, shows that most of these gneisses have a meta-igneous parentage, although sample 1115 falls well within the meta-sedimentary field (Fig. 5.1(b)). The discrimination plots of Moine & de la Roche (1968) give inconsistent information for these gneisses. Fig. 5.2(a) shows the rocks clustering in the greywacke field, whereas in Fig. 5.2(b) the rocks plot outside the equivalent field. However, it was noted that the gneisses fell on a fairly well defined compositional trend in both of the diagrams of Moine & de la Roche, particularly Fig. 5.2(a). The discrimination plot: al-alk vs. c (Niggli normative minerals) of Leake (1969) also produced a compositional trend for these rocks, and one indicative of an igneous parent (Fig. 5.3(a)).

In general these discrimination diagrams indicate an igneous parentage for these gneisses although the influence of sedimentary material, perhaps through pre-metamorphic mixing, cannot be discounted for some of the samples as suggested by the position of some of the points on Fig. 5.1(a). The discrimination between meta-igneous and meta-sedimentary parents for quartzo-feldspathic rocks is notoriously difficult since most quartzo-feldspathic rocks have the general composition of greywackes or arkoses (van de Kamp et al., 1975). However, the most important piece of evidence for an igneous origin for these gneisses is the presence of a compositional trend on several of these diagrams. Such trends are also visible on Figs. A and B which were used in the discrimination between

FIG. 5.1

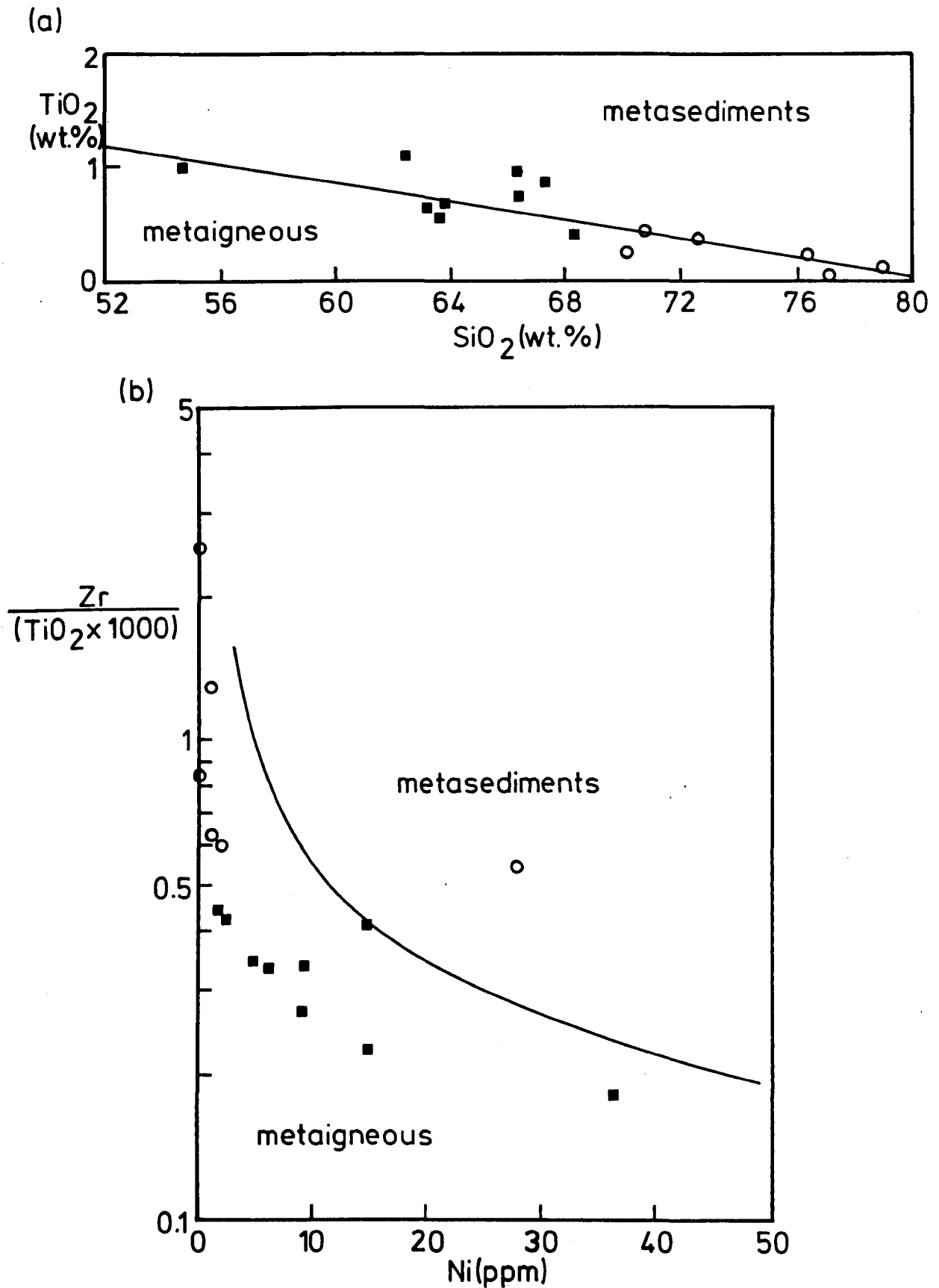


FIG. 5.1(a) TiO₂ vs. SiO₂ discriminant diagram for metasediment and metaigneous rocks, after Tarney (1976).

(b) Zr/(TiO₂ × 1,000) vs. Ni discriminant for meta-igneous and meta-sedimentary rocks, after Winchester et al. (1980). Squares = grey, banded and 'augen'-bearing rocks; circles = 'granitic' rocks.

FIG. 5.2

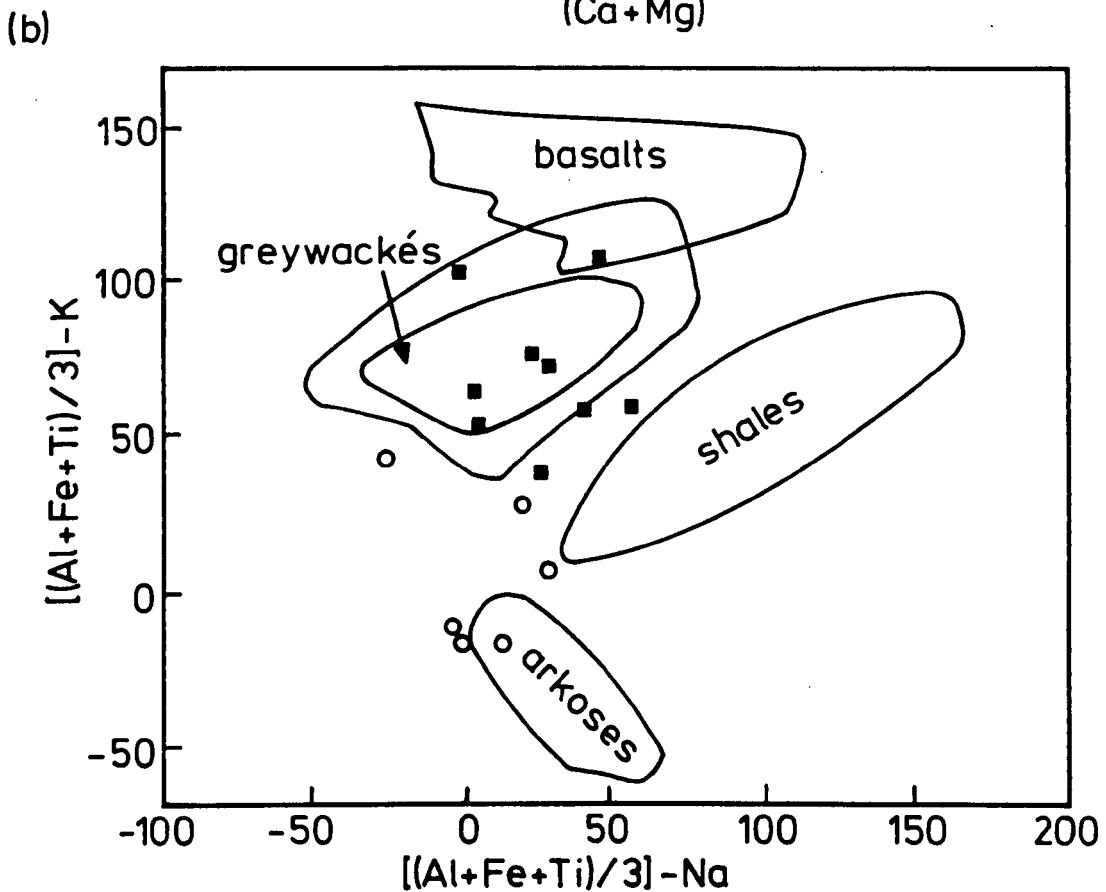
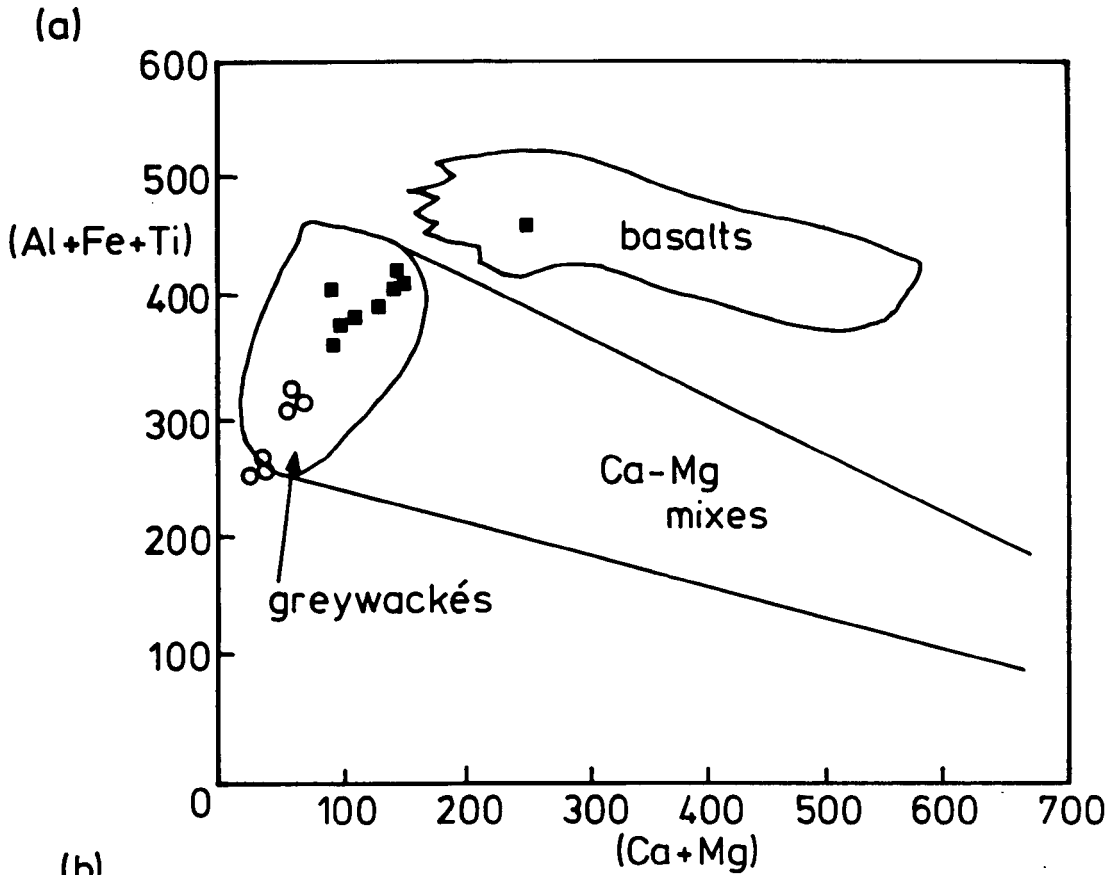


FIG. 5.2(a) (Al + Fe + Ti) vs. (Ca + Mg) in milliatoms, after Moine & de la Roche (1968) with discriminant fields. Note the compositional trend of the samples.

(b) (Al + Fe + Ti)-k vs. (Al + Fe + Ti)-Na in milliatoms, after Moine & de la Roche (1968) with discriminant fields. Note the scatter of points on this plot compared to FIG. 5.2(a). Symbols as in FIG. 5.1.

FIG. 5.3

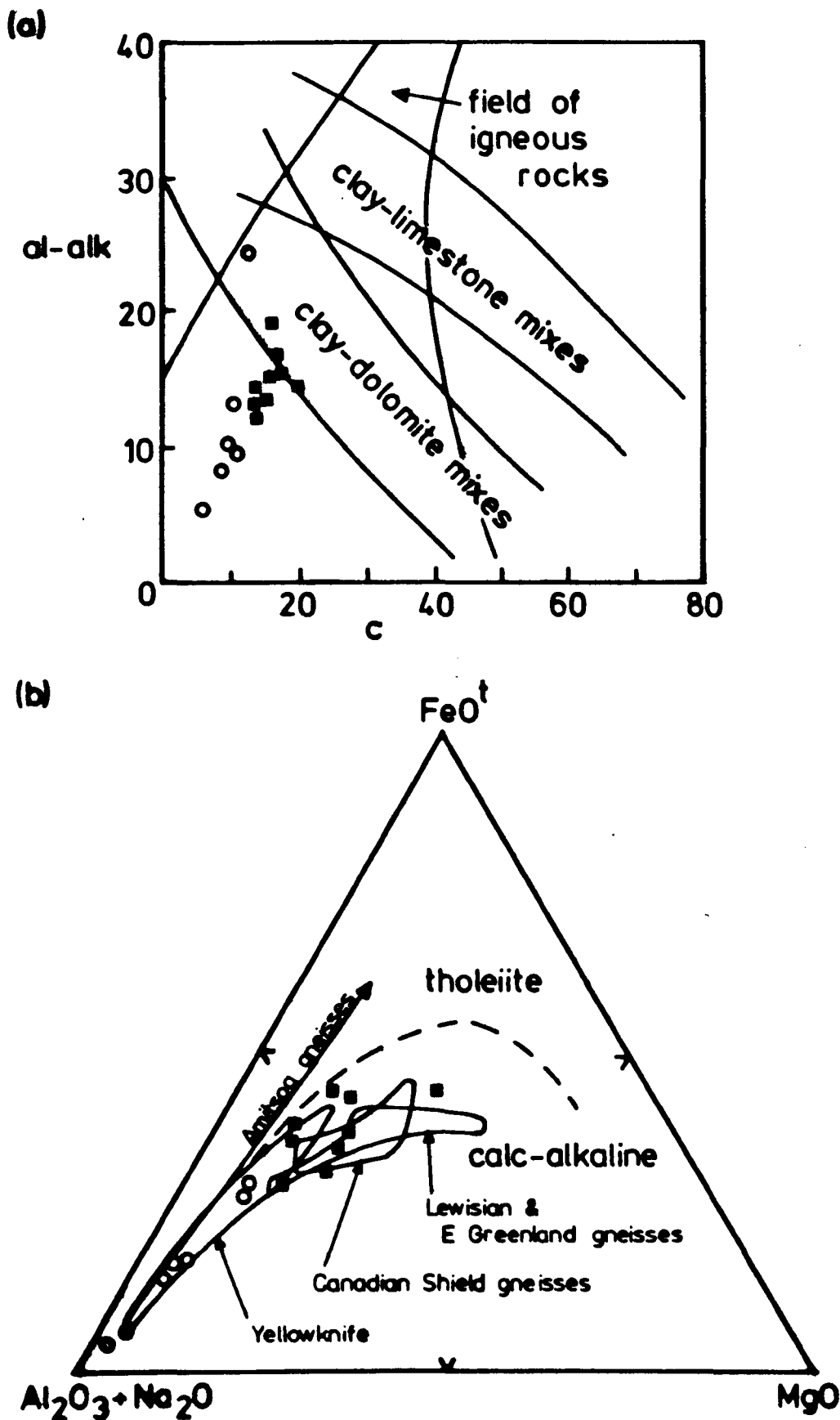


FIG. 5.3(a) al-alk vs. c in Niggli normative minerals after van de Kamp et al. (1976). The rocks define a compositional trend indicative of an igneous parentage.

(b) $(\text{Al}_2\text{O}_3 + \text{Na}_2\text{O})$ - FeO^t -MgO plot with fields of Archaean calc-alkaline complexes from Lambert et al. (1976). Symbols as in FIG. 5.1.

the Heterogeneous Quartzo-Feldspathic Gneiss Unit and the Augen Gneiss Unit (see the Introductory Statement on p. 109).

Plotting the data from Table 5.2 on an AFM diagram confirms the presence of an igneous trend and shows it to be calc-alkaline (Fig. 5.3(b)), a similar trend is shown on a K_2O-Na_2O-CaO plot (cf. Barker et al., 1981 - Fig. 5.4(a)) and an Ab-Or-An plot (cf. Streckeisen, 1976 - Fig. 5.4(b)). It has been shown by Robinson & Leake (1975) that many meta-sedimentary sequences plot as calc-alkaline trends on AFM diagrams, which can result in misleading information about the rock parents. However, Fig. 5.1(b) provides two pieces of information which supports the interpretation of an igneous origin for the gneisses in question:

(i) The rocks define a fairly good curve on this diagram implying consistent behaviour of Zr in the rocks. Zr has been shown to have variable concentrations in meta-sediments (van de Kamp et al., 1976).

(ii) The Ni contents in the rocks are fairly low, nearly all <20 ppm, typical of meta-igneous rocks; greywackes typically have contents \sim 50 ppm (van de Kamp et al., 1976).

As a consequence the calc-alkaline trend shown on these diagrams is taken as an igneous feature, and is presented as further evidence of the chemical diversity between these gneisses and the Augen Gneiss, which was shown to have a chemistry transitional between calc-alkaline and tholeiitic igneous rocks (see section 4.2). The classification of Streckeisen 1976, in Fig. 5.4(b) show the rocks to vary between tonalite, granodiorite, and granite; or the respective volcanic equivalents: dacite and rhyolite.

5.3 DISCUSSION

Three features of this tract of gneisses are of note:

(i) The rocks are heterogeneous with intercalations of meta-sediments, meta-igneous and migmatitic rocks.

FIG. 5.4

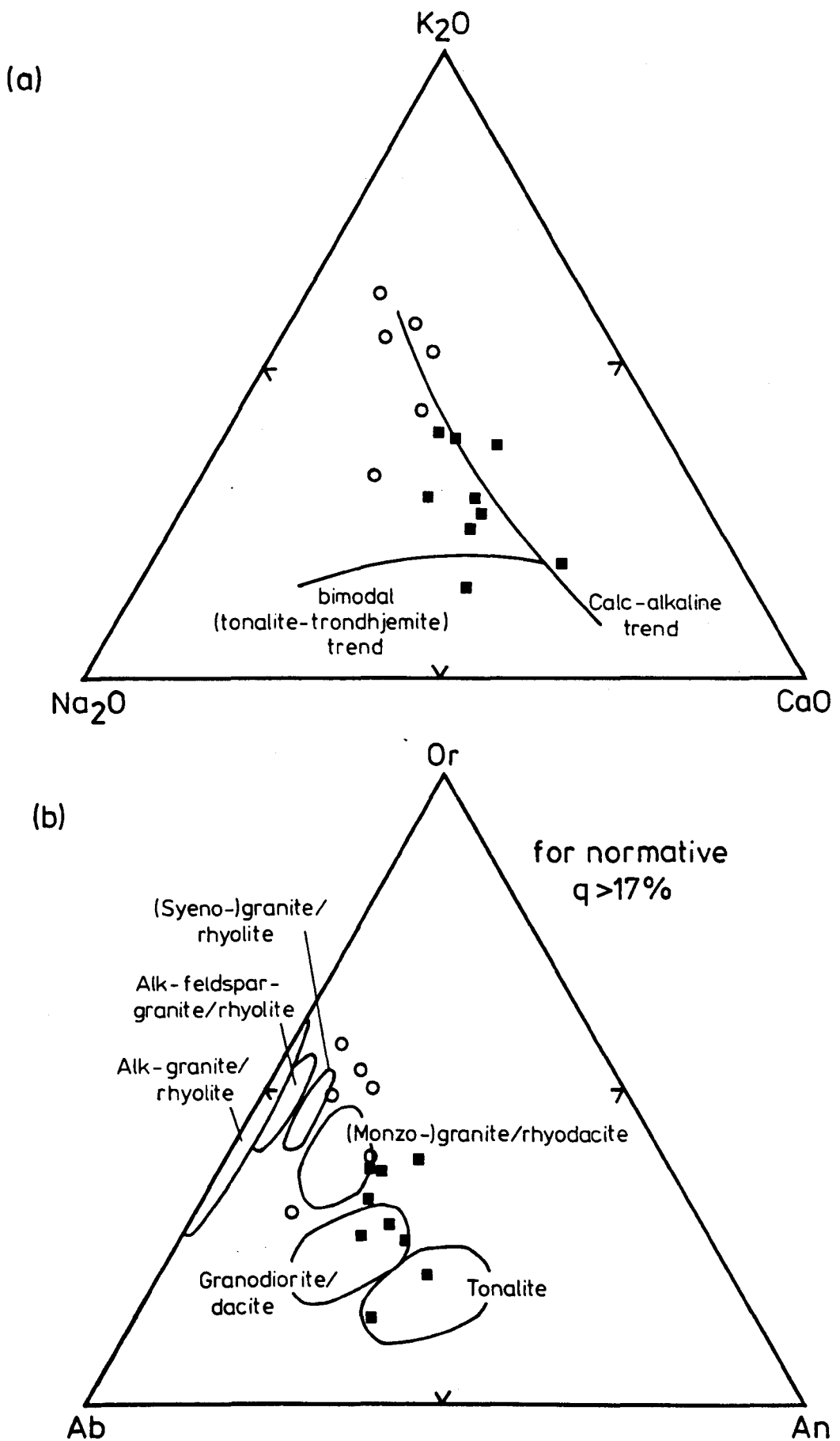


FIG. 5.4(a) $Na_2O + K_2O + CaO$ diagram after Barker et al. (1981).
 (b) $Or-Ab-An$ diagram of Streckeisen (1976) with fields as shown. Symbols as in FIG. 5.1.

(ii) The meta-igneous rocks are of calc-alkaline composition.

(iii) The Rb-Sr whole-rock age of 1708 ± 60 m.y. from Pidgeon & Råheim (1972) on equivalent rocks at Kristiansund places an age constraint on the rocks.

The first two points are features typical of Archaean (~ 3900 -2500 m.y. ago) basement complexes as found in Greenland (McGregor, 1973); Scourie in Scotland (Holland & Lambert, 1973) or Assynt in Scotland (Sheraton et al., 1973). A chemical comparison between several Archaean terrains and these gneisses is provided in Fig. 5.3(b), with trends from Lambert et al. (1976).

Windley (1977, p. 3) gives a synopsis of the rock units in Archaean regions and notes that up to 80-90% of these regions may be composed of quartzo-feldspathic rocks with or without biotite, hornblende and diopside (cf. Wynne-Edwards & Hasen, 1972). These are well foliated rocks, intercalated with other rock types or containing evidence of partial melting. Windley (1977, p. 5) also shows that the elucidation of the precursors of these quartzo-feldspathic gneisses is difficult for three reasons:

(i) Archaean terrains are generally depleted in LIL elements (Rb, K, Y, Th), e.g. Tarney et al. (1972).

(ii) Chemical analyses cannot readily distinguish between volcanic and plutonic igneous rocks unless field evidence such as layering, veining or igneous contacts are visible.

(iii) Some volcanic rocks may have been intermixed with sedimentary material.

A feature of these gneisses which distinguishes them from Archaean terrains is the undepleted nature of their LIL elements as shown on Fig. A on p. 109. As shown in the previous section, the chemical compos-

ition of the gneisses can indicate volcanic or plutonic parental rocks. Admittedly, it is tempting to assign a volcanic origin to the gneisses, considering their close association with metasedimentary rocks (cf. Råheim, 1972). The close association of metasedimentary rocks with ortho-gneisses in gneiss terrains has tended to favour the interpretation of intermixing of volcanoclastics with sediments in such terrains (Windley, 1977, p. 6). However, work by McGregor (1973) and Myers (1978) in W Greenland has shown that many gneiss terrains are probably composed of severely deformed plutonic rocks tectonically intercalated with supra-crustal rocks, although this does not preclude the possibility of the presence of meta-volcanic rocks. Indeed, the work on the Augen Gneiss on the Molde Peninsula has shown that deformation of an originally plutonic rock can result in an apparently homogeneous grey gneiss. As a consequence, it is possible that some of these gneisses represent severely deformed plutonic rocks.

Now, Archaean calc-alkaline suites appear to be bimodal tonalite-trondhjemite associations at the proto-continental (i.e. pre-plate-tectonic) stage of the Earth's history (3800-2900 m.y. ago); and to show a continuous fractionation trend, from gabbro to granite at the plate-tectonic stage of the Earth's history (2200 m.y. age - present). The more recent tectonic scenario results in the production of andesite-rhyolite volcanism with the plutonic rocks: granite and tonalite (Barker et al., 1981). Fig. 5.4(a) shows the gneisses following the gabbro-granite trend, rather than the bimodal trend thereby indicating formation under a plate-tectonic regime.

Igneous rocks of the calc-alkaline suite are usually formed at convergent oceanic-continental plate margins and are produced through the interaction of the subducted oceanic crustal rocks, mantle derived

mafic magmas and continental crustal rocks (Barker et al., 1981). The generally small amount of continental crust involved in the generation of these rocks results in low K_2O/Na_2O ratios, typically <1 (cf. Mitchell, 1975). (Note that the Augen Gneiss has K_2O/Na_2O ratios >1 and was interpreted as forming in an extensional crustal regime).

The gneisses in Table 5.2 have K_2O/Na_2O ratios of around 1; the 'granitic' rocks have the highest ratios whilst the more 'intermediate' rocks have ratios generally <1 . The K_2O/Na_2O ratios >1 in the 'granitic' rocks appear to contradict the expected values of <1 for a calc-alkaline suite. However, it has been shown that rocks erupted at increasing distances from the subduction zone have suffered a greater influence of crustal material in their production resulting in the production of granitic rocks with K_2O contents $\sim 4-5\%$ and K_2O/Na_2O ratios >1 (Bateman & Dodge, 1970). Consequently, these meta-igneous gneisses are interpreted as the differentiated portion of a calc-alkaline suite formed at some time between $\sim 2200-1700$ m.y. ago. As previously stated both plutonic and volcanic rocks may form parts of this tract of gneisses. It seems reasonable to include the meta-sedimentary gneisses, discussed in section 5.2, in this crust-forming event as it has been shown that they must have been placed ~ 1500 m.y. ago to be intruded by the precursor to the Augen Gneiss. The close association between these meta-igneous and meta-sedimentary rocks presently observed in outcrop may be primary, but could equally well be the result of intense tectonic intercalation. Rocks formed at $\sim 2200 \pm \sim 300$ m.y. ago would have suffered three subsequent metamorphic/deformation events in this part of Scandinavia: Svecofennian ($\sim 1850-1600$ m.y.), Sveconorwegian (1200-900 m.y.) and Caledonian (600-360 m.y.) (see Table 1.3).

Similar, calc-alkaline/migmatitic/metasedimentary gneiss terrains have been described elsewhere in Scandinavia: in Lofoten, N. Norway

(Griffin et al., 1974; Iden, 1981) and in much of Finland (Eskola, 1963; Simonen, 1980) and Sweden (Lundqvist, 1980).

All of these gneiss sequences have been interpreted as mixed sequences of volcanic calc-alkaline rocks and metasediments, generally greywackes and arkoses. The time of formation of the precursors to these gneisses in Finland (the Karelides and Svecofennides) has been placed at ~2800 m.y. ago (Kuovo & Tilton, 1966; Hietanen, 1975) whilst those in Lofoten have been dated at ~2500-2000 (Griffin et al., 1974). Bowes (1976) correlates these two events, in the two areas, and also with the Scourian event (~2800 m.y.) in Scotland considering it to be a time of major addition of material to the continental crust. The deposition of the rocks in Finland has been modelled as an Andean-type orogeny (i.e. an oceanic-continental plate convergent margin) with the volcanics and sediments deposited on an older basement, 3000-3500 m.y. old - Hietanen, 1975) and subsequently metamorphosed in the Svecokarelide orogeny (~1900-1800 m.y. - Bowes, 1976). Similarly, the calc-alkaline rocks in Lofoten are considered to have been deposited on older basement (~3400 m.y. old - Taylor, 1975) and metamorphosed at ~1800 m.y. ago (Heier & Compston, 1969; Griffin et al., 1974).

The S Gneiss Region of Norway is also considered to be the product of an Andean-type subduction event, resulting in a mixed sequence of calc-alkaline volcanics and sediments (see section 1.1.2). However, older basement, comparable in age to that described above, has not been found in S. Norway probably due to the substantial isotopic reworking suffered by the rocks during widespread plutonic intrusion ~1500 m.y. ago and during the Sveconorwegian metamorphism (Oftedahl, 1980).

The calc-alkaline nature of some of the Heterogeneous Gneisses on the Molde Peninsula and their association with meta-sediments, with a

postulated time of formation $\sim 2200 \pm 300$ m.y., is presented as further evidence of crustal addition in the early Proterozoic in Scandinavia. Furthermore, the formation of the precursors to these rocks may have occurred in the same Andean-type subduction event postulated for the other areas of calc-alkaline gneiss in Scandinavia. It is considered that the plate geometry at the early stages of plate tectonics consisted of many small micro-plates which, when subducted, were quickly assimilated into the newly formed continental crust giving a rapid crustal growth (Windley, 1977, p. 62-64). The hypothetical Andean-type orogeny of Hietanen, for Finland, would be easily extended to include the calc-alkaline gneiss terrains described elsewhere in Scandinavia, with an elongate subduction zone assimilating many micro-plates and gradually migrating southwards over a fairly short period of time (Fig. 5.5(a)). To confirm such a hypothesis a radiometric dating program on the calc-alkaline rocks on the Molde Peninsula is required, which would also place a more exact age constraint on the time of their formation. Since Moldefjord lies at the supposed N limit of the Sveconorwegian metamorphic event (Zwart & Dornsiepen, 1978) the rocks would not have been extensively reworked (as evinced by the mid-Proterozoic age obtained from the Auger Gneiss Unit) and may reveal an older igneous precursor event. Careful sampling and preliminary geochemical work would be required to ensure that the calc-alkaline rocks alone were included in such a dating program.

5.4 MINERAL CHEMISTRY AND P-T CONDITIONS

Analyses of minerals from selected rocks in the Heterogeneous Quartzo-Feldspathic Gneiss Unit are given in Table 5.3. It was hoped that these data would supply an independent estimate of the P-T conditions for these gneisses using the clinopyroxene-garnet-plagioclase-quartz assemblage in the granulite, F5. (Although the mineral analyses

TABLE 5.3 Analyses of clinopyroxene, garnets, feldspars and scapolites from rocks in the Heterogeneous Quartzo-Feldspathic Gneiss Unit

(wt. %)	Cpx		Garnet		Feldspar			Scapolite			
	F4 (3)		F4 (2)	M36 (1)	F4 (2)	M19 (1)	M36 (3)	M19 (3)	M36 (2)		
SiO ₂	50.42		38.85	38.67	61.62	60.20	63.57	46.68	47.51		
TiO ₂	0.37		0.02	0.02	-	-	-	-	-		
Al ₂ O ₃	5.08		21.47	21.26	23.81	24.71	22.36	25.53	24.87		
Cr ₂ O ₃	-		0.00	0.00	-	-	-	-	-		
FeO ^T	10.65		24.72	23.44	0.22	0.14	0.18	0.13	0.11		
MnO	0.16		1.24	1.12	-	-	-	-	-		
MgO	10.57		5.07	4.69	-	-	-	-	-		
CaO	20.54		9.68	11.06	5.99	7.11	4.40	16.56	15.92		
BaO	-		-	-	-	-	-	0.04	0.06		
Na ₂ O	1.47		-	-	7.90	7.46	8.65	4.12	4.29		
K ₂ O	-		-	-	0.53	0.23	0.72	0.18	0.15		
S	-		-	-	-	-	-	2.51	3.48		
Cl	-		-	-	-	-	-	0.18	0.10		
TOTAL	99.26		101.05	100.26	100.07	99.85	99.88	95.93	96.49		
MINERAL FORMULAE											
	6' O'		12' O'	12' O'	8' O'	8' O'	8' O'	(Si + Al) = 12	(Si + Al) = 12		
Si	1.897		2.994	2.999	2.740	2.688	2.819	7.296	7.421		
Ti	0.010		0.001	0.001	-	-	-	-	-		
Al	0.225		1.950	1.944	1.248	1.300	1.169	4.704	4.579		
Cr	-		-	-	-	-	-	-	-		
Fe ³⁺	0.068		0.061	0.055	-	-	-	-	-		
Fe ²⁺	0.267		1.533	1.466	0.008	0.005	0.007	0.017	0.014		
Mn	0.005		0.081	0.074	-	-	-	-	-		
Mg	0.593		0.582	0.542	-	-	-	-	-		
Ca	0.828		0.799	0.919	0.285	0.340	0.209	2.773	2.665		
Ba	-		-	-	-	-	-	0.003	0.004		
Na	0.107		-	-	0.681	0.646	0.744	1.248	1.299		
K	-		-	-	0.030	0.013	0.041	0.018	0.015		
S	-		-	-	-	-	-	0.074	0.102		
Cl	-		-	-	-	-	-	0.048	0.026		
CO ₂	-		-	-	-	-	-	0.878	0.872		
TOTAL	4.000		8.001	8.001	4.992	4.992	4.989	17.059	16.997		
END-MEMBERS (%)											
Ca-Ti-Ts	1.05	Andr	3.00	2.75	Ab	68.4	64.7	74.9	Me	68.8	67.1
Ca-Ts	8.25	Pyr	19.44	18.08	An	28.6	34.0	21.1	'W'	4.059	3.997
Jd	3.93	Spess	2.70	2.46	Or	3.0	1.3	4.1			
Ac	6.97	Gross	23.65	27.92							
Di	50.36	Alm	51.17	48.80							
Hd	22.70	Schorl	0.04	-							
Jo	0.43	Uvar	-	-							
En	4.45										
Fs	2.01										
Rh	0.04										

$$Me = (Ca + Ba + Fe) / (Ca + Ba + Fe + Na + K)$$

CO₂ in scapolite calculated on the assumption of the anion site total = 1 (cf. Rollinson, 1980)

Figures in brackets give the number of spot analyses on each grain

Fe³⁺ for garnet calculated by charge-balance, for clinopyroxene on the basis of the structural formula (cf. Mysen & Griffin 1973)

FIG. 5.5

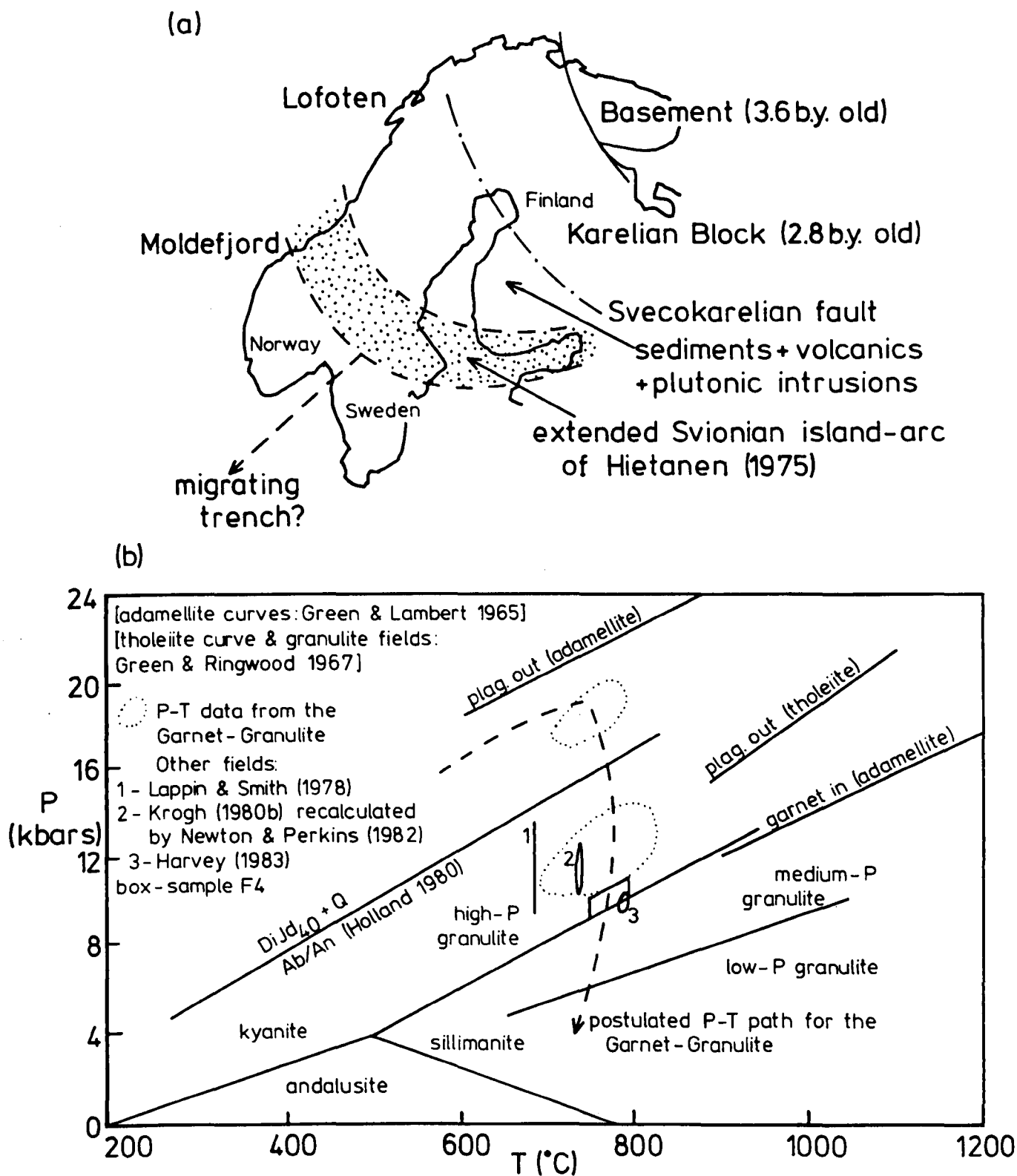


FIG. 5.5(a) Tectonic features of Scandinavia in the period 2500-2000 m.y. ago, after Nietanen (1975). Her postulated subduction zone has been extended across to W Norway to allow the development of calc-alkaline rocks in that area.
 (b) P-T grid showing the relationship between the calculated equilibration values from the Garnet-Granulite and the granulite F4.

were done on sample F4, this is part of the same original sample). Furthermore, the scapolite bearing rocks M19 and M36 could perhaps supply an estimate of the temperature conditions of the metamorphism from the plagioclase-scapolite assemblages, if the compositions were favourable. (See Appendix B for the P-T calculation methods.)

The clinopyroxene in the granulite is fairly comparable to the symplectic clinopyroxenes in the Garnet-Granulite on Tverrfjella (see sample E3 in Table 3.7), although it is slightly Fe-richer. The Jd/Ts ratio of 0.42 for this phase places the rock in the granulite facies according to the division of White (1964 - $Jd/Ts < \frac{1}{2}$ for granulite facies, and $> \frac{4}{5}$ for eclogite facies clinopyroxenes). The garnet is broadly comparable to those in the Garnet-Granulite (see Table 3.6). Neither of these phases are compositionally zoned. The feldspar is slightly more An and Or than those in the Garnet-Granulite (see Table 3.9).

The P-T data for this sample is given in Table 5.4 and are plotted on a P-T grid in Fig. 5.5(b). The figures agree well with the data from the retrogressed samples of the Garnet-Granulite, although the pressure is slightly lower, and the data of Krogh (1980b) from clinopyroxene-bearing quartzo-feldspathic gneisses in the Frei Group at Kristiansund, recalculated by Newton & Perkins (1982). However, the figures are $\sim 100^\circ\text{C}$ more than the metamorphic conditions calculated by Lappin & Smith (1978) for the amphibolite-facies quartzo-feldspathic gneiss at Stadlandet/Selje area.

Although the analysed clinopyroxenes in this rock are not symplectic they give similar P-T conditions to the symplectic clinopyroxenes from the Garnet-Granulite. Green & Ringwood (1967) found that for basaltic compositions the conversion of plagioclase to a garnet-clinopyroxene assemblage occurred at increasingly higher pressures for increasingly

TABLE 5.4 P-T data for sample F4 from the Heterogeneous Quartzo-Feldspathic Gneiss Unit

Jd (%)	K_D	x_{Ca}^{gnt}	x_{Ab}^{plag}	P(kbar)	T(°C)	Method
3.93	5.85	0.2668	0.684	9.9	808	Ellis & Green (1979) and Currie & Curtis (1976)
				8.8	756	Krogh (1983 - rectilinear equation) and Currie & Curtis (1976)
				11.2	811	Ellis & Green (1979) and Newton & Perkins (1982)
				10.6	762	Krogh (1983 - rectilinear equation) and Newton & Perkins (1982)
				10.1	784	Average

N.B. The method of Krogh (1983) gives temperatures lower by $\sim 60^\circ\text{C}$ than Ellis & Green (1979) whilst Currie & Curtis (1976) give pressures lower by ~ 2 kbar than Newton & Perkins (1982).

less basaltic compositions (expressed as $100 \text{ Mg}/(\text{Mg} + \text{Fe})$). Also, the work of Green & Lambert (1965) on an adamellite at high P and T conditions showed that a rock of this composition will retain plagioclase in its assemblage to much higher pressures than a basaltic composition, at the same temperature (see the 'plag-out' curves on Fig. 5.5(b)). Therefore, the appearance of the large amounts of plagioclase in sample F4, compared to the Garnet-Granulite at the same P and T, is the result of the less basaltic composition of the rock.

Although the scapolite-bearing rocks are not of particularly similar bulk compositions, the compositions of the scapolites are very similar. M36 is a semi-pelite with a high Al content, whilst M19 is more amphibolitic and siliceous (see Table 5.1). The feldspar compositions are slightly different with a more Ab-rich plagioclase in sample M36, reflecting the more sodic bulk composition of that sample. As CO_2 cannot be measured on the EMP, it has been calculated in the scapolites by assuming that the anion site total = 1 (cf. Rollinson, 1980) even though a small amount of OH^- ion can enter this site in sodic scapolites (Goldsmith, 1976). The mineral formulae have been calculated on the basis of $(\text{Si} + \text{Al}) = 12$ (cf. Evans et al., 1969 and Rollinson, 1980). The remaining cations ($\text{Na} + \text{Ca} + \text{K} + \text{Fe} + \text{Ba}$) are added to give the parameter 'W'. From their studies of the stoichiometry of scapolite, Evans et al. obtained a range of values for this parameter of: 4.068-3.927, with a mean of 3.981. The 'W' values for the two samples here fall within this range indicating good stoichiometry of the analyses.

Using the data from the coexisting scapolite and plagioclase temperatures in excess of 1300°C were obtained with the method of Goldsmith & Newton (1977). This is not surprising since the plagioclase is fairly sodic and falls outside the compositional limit of $>\text{An} 70$ set

by Goldsmith & Newton for the calculation of meaningful temperatures by their method. Applying the method of Rollinson (1980) for CaCO_3 -scapolites to these mineral pairs gives equally unrealistically high temperatures of 1249°C for M19 and 2185°C for M36 which again appears to be due to the sodic nature of the plagioclase.

PLATE 5.1

- (a) Appearance of massive migmatite gneiss with extreme chaotic appearance. Note partial intrusion of the massive amphibolite by the migmatite, bottom right of picture. Bjørnsnos farm (078760).
- (b) Appearance of the finer-scale migmatite with the anatectic portion lying within the well-defined foliation planes. Helvatnet (1476).
- (c) General appearance of the palaeosome of the migmatites. Note the fibrous sillimanite in centre of picture. (Sample D9, cross-polarised light.)
- (d) The banded gneiss in outcrop, with relatively small-scale banding N of Elnesvågen (0672).
- (e) The augen bearing gneiss, note the small scattered feldspar augen and compare to Plate 2.1(d). Hollingsholm (965628).
- (f) The grey gneiss. N coast of Vågøy (994683).

PLATE 5.1

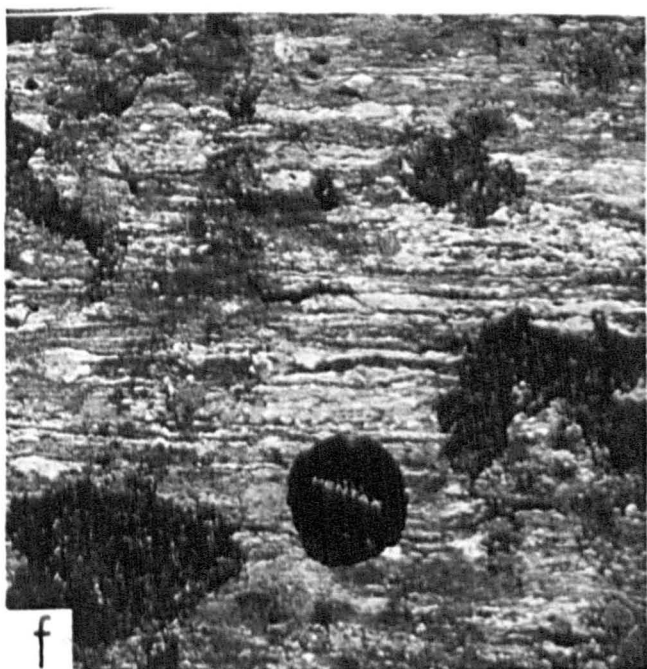
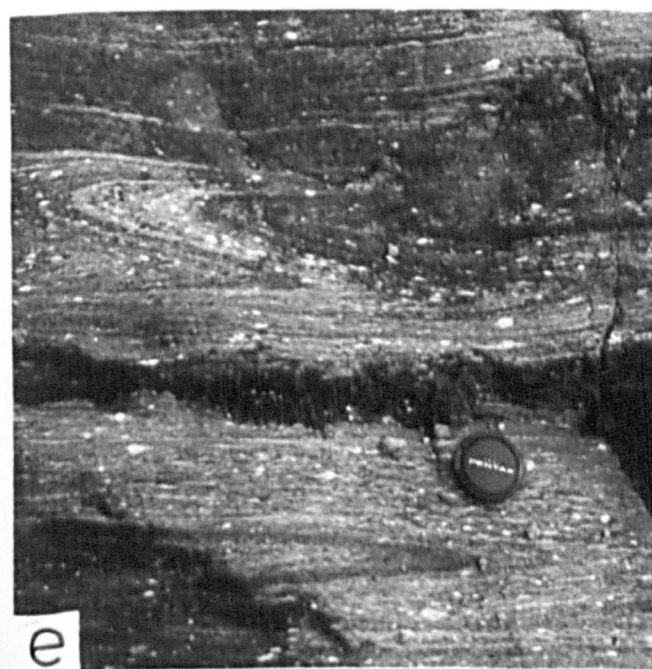
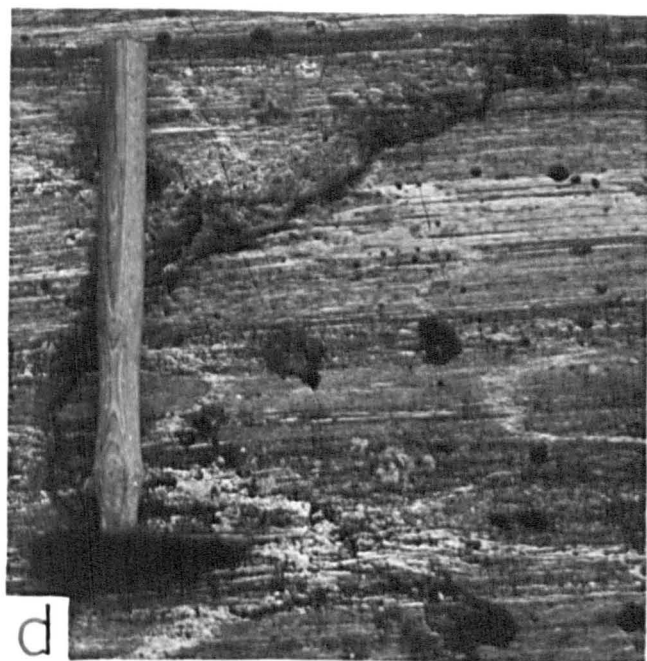
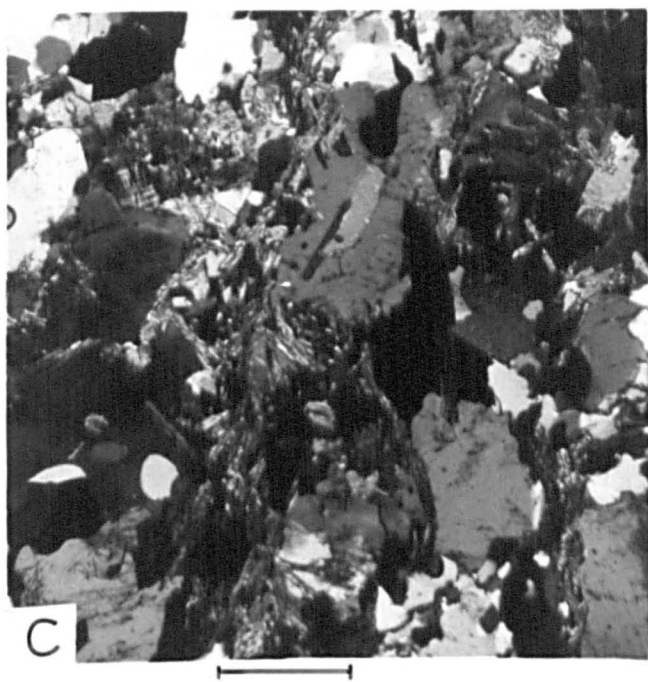
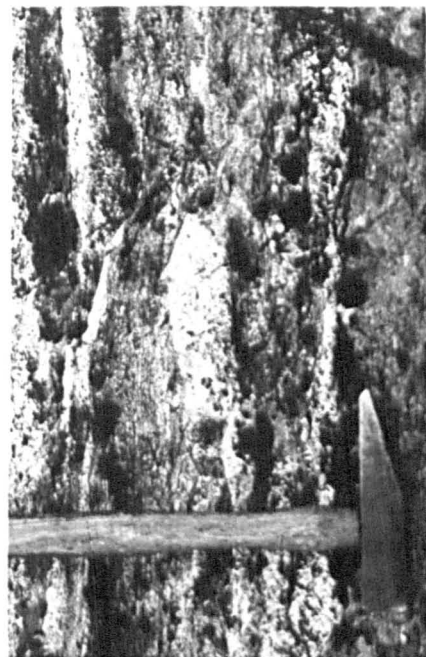


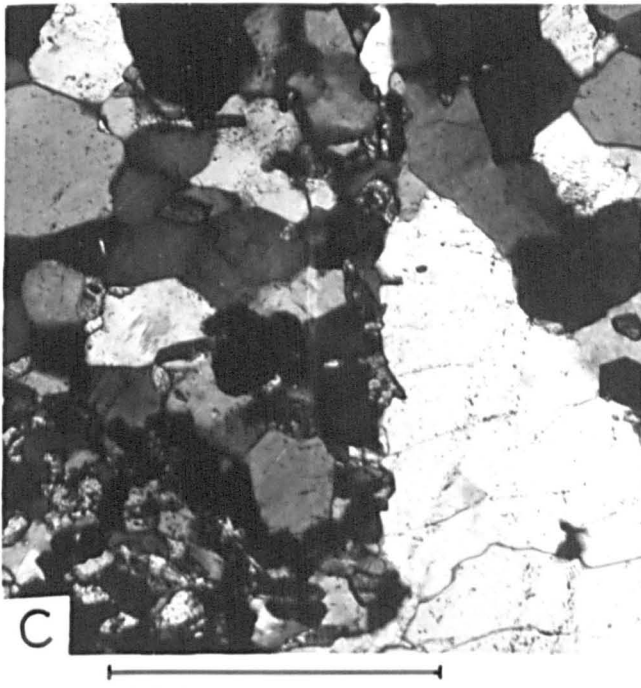
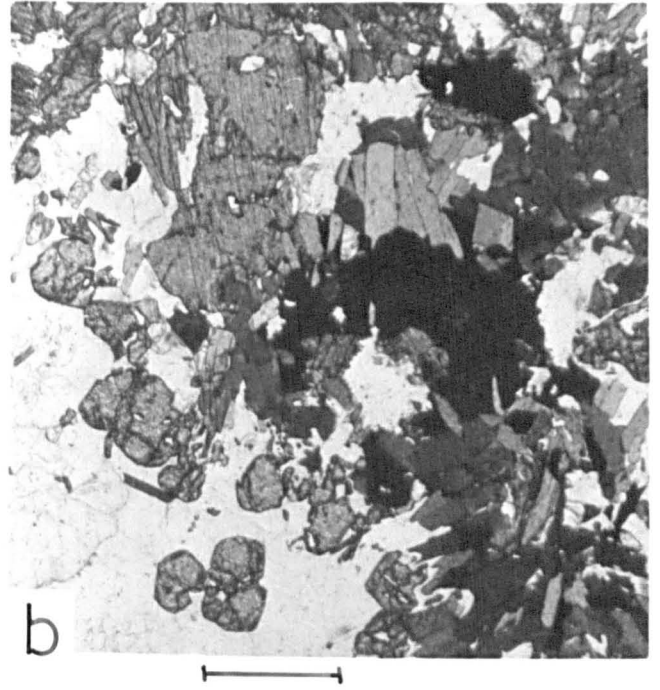
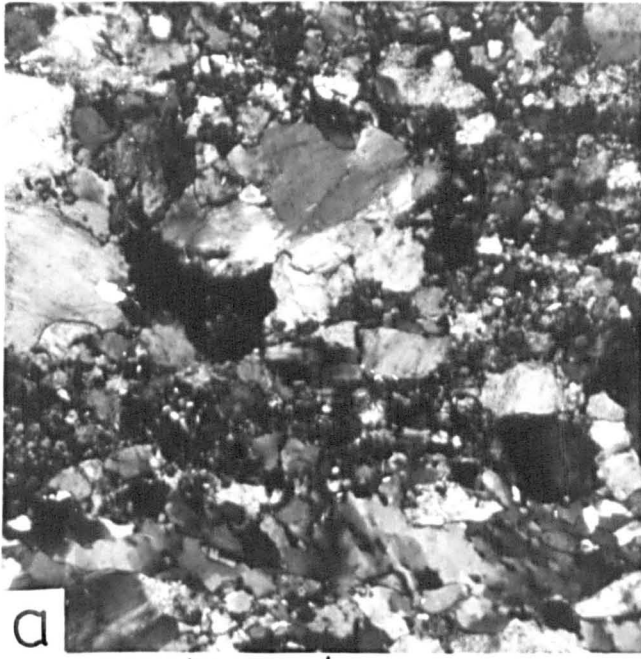
PLATE 5.2

- (a) General appearance of the granitic gneisses, note the protomylonitic fabric and compare to the granite sheets in Plate 4.1(f). (Sample 2136, cross-polarised light.)

- (b) Mafic clot of clinopyroxene, hornblende and biotite surrounded by a rim of small garnets. (Sample F4, plane-polarised light.)

- (c) Polygonal feldspar texture and a string of small clinopyroxene grains between the feldspars and quartz. These small clinopyroxenes have exsolved albite adjacent to the quartz. (Sample M22, cross-polarised light.)

PLATE 5.2



CHAPTER 6

THE HETEROGENEOUS ROCKS OF MOLDEFJORD

The rocks of this Unit lie on the S side of the Molde Peninsula and include the rocks mapped on the island of Bolsøy in Moldefjord (see Maps A and C). From the mapping of Hernes (1955), the rocks on the mainland, along the Moldefjord coast, are part of the Frei Group of Precambrian age (~ 1700 m.y. - Pidgeon & Råheim, 1972). The rocks on Bolsøy represent parts of the Tingvoll, Røros and Støren Groups (see Table 1.2) which have been mapped, on strike, from the Surnadal area (Strand, 1953 - see Fig. 2.5) where they are considered to be of Cambro-Silurian age. Radiometric dating by Råheim (1977) has shown that the Tingvoll Group is also Precambrian in origin with a date of 1707 ± 63 m.y. However, the Precambrian age given for the Røros Group by Råheim (1977) is considered invalid (see section 3.3) and the interpretation of Krill (1983) that this Group is Ordovician-Silurian in age is preferred here. Because of the apparent age differences between the rocks on the mainland and those on Bolsøy they are treated separately in this Chapter. (Grid references are for the 1:50,000 maps.)

6.1 GENERAL GEOLOGY AND PETROGRAPHY

6.1.1 Rocks of the Moldefjord coast

These rocks have been followed along strike from Julneset point, where their width of outcrop is about 1 km, to about 3 km E of the town of Molde where their width is about 2.5 km (Map A). The exposures are fairly good in road cuts along the E662 W of Molde, particularly so in the cuts along the road to the ferry point at Mordalsvågen (5797) where their heterogeneous nature is well displayed. These cuts also show the

very consistent steep, flat foliation surfaces, which often appear flaggy (Plate 2.1(c)). The rocks are also found on the high ground around Varden (O44592), N of Molde. Elsewhere the rocks are obscured by dense tree cover.

The contact between these rocks and those of the Augen Gneiss Unit has already been mentioned in section 4.1.1. At the best exposure of the contact, W of Mordal farm (978576) the contact was found to be very well defined. However, portions of the Augen Gneiss Unit have been recognised with the Heterogeneous Rocks of Moldefjord at several localities; around Varden (O44591), at Mekvatnet (O24538) and on the coast W of Mordal farm (O257) (see Map A).

Very simply the rocks consist of quartzo-feldspathic units and amphibolitic units; both have varying proportions of: garnet, feldspar, quartz and mica. Some rocks approach semi-pelitic compositions, others have calc-silicate assemblages dominated by epidote minerals; also, rare, thin sugary-textured marbles appear at Mordalsvågen and on Varden. The rocks are very variable over short distances and can appear compositionally banded in some localities, e.g. Julneset. This small scale variation made it impossible to map the rock types as distinct units along strike although it was noted that the quartzo-feldspathic rocks were relatively more abundant on the S shore of Julneset, the headland at Mek and E of Molde whilst the amphibolitic rocks tended to occur further inland. The rocks have been severely affected by flattening during the Caledonian orogeny (Chapter 2) and consistently display large flaggy foliation planes in outcrop often incorporating a lineation of amphibole or mica. They are also well jointed, generally filled with epidote or more rarely calcite. Thin granitic veins intrude the rocks, particularly at Mek, whilst larger coarse pegmatite veins tend to be more profuse here than

in the rocks further N. The profusion of veins reflects the fractured nature of these rocks (Plates 2.1(c) and 2.2(e)). The extreme stretching accompanying this deformation has caused partial or complete boudinage of some of the lithological bands (Plate 2.2(f)). Pods of eclogite can be found in these Heterogeneous Rocks notably on Julneset and N of Molde (see Map A) although they are invariably strongly retrogressed and amphibolitised which makes their recognition very difficult, especially when they occur in amphibolitic rocks.

In thin-section the Heterogeneous Rocks reflect the severe deformation suffered as cataclastic textures; the quartzo-feldspathic rocks tend to display these textures more often than the amphibolitic rocks. The typical appearance of a quartzo-feldspathic rock is shown in Plate 6.1(a) and consists of: porphyroblasts of strained, perthitic microcline set in a matrix of strongly ribboned and sutured quartz, granulated plagioclase (An 20) and K-feldspar. Plagioclase rarely survives as porphyroblasts. Biotite is well oriented and smeared out, often transformed to chlorite; opaque phases appear as thin strings. The severe deformation has tended to promote the formation of myrmekite between adjacent plagioclase and K-feldspar and the appearance of two sets of twin-planes in the plagioclase (cf. the Augen Gneiss (section 4.1.1) and see Smith 1974, p. 577). Both of the feldspars in these rocks are altered to sericite (K-feldspar) and sausserite (plagioclase) to varying degrees, often assisted by cracking perpendicular to the fabric of the rock. These quartzo-feldspathic rocks have variable assemblages with both granitic (dominated by K-feldspar) and more intermediate (dominated by plagioclase) compositions. The latter tend to be more biotite and/or garnet-rich. The former phase is well aligned and generally transformed to chlorite; the latter occurs in strings of

rounded grains and are extensively cracked and altered to amphibole or chlorite. Some examples of the quartzo-feldspathic rocks contain significant quantities of amphibole (α yellow-brown, β green, γ green-blue, $\gamma^Z = 19^\circ$) as thin bands; garnets associated with these amphibole bands tend to be more severely hydrated than otherwise, often with the development of kelyphite rims (cf. those in the Garnet-Granulite, Plate 3.2(a)). These deformed rocks can be termed protomylonites in the nomenclature of Higgins (1971). Some rocks show very severe cataclasis with little evidence of pre-existing phases (Plate 6.1(b)), generally limited to small, rounded amphiboles or feldspars in a very fine comminuted matrix. These are mylonites in the terminology of Higgins (1971). Other rocks are only slightly deformed but do exhibit severe hydration of all the constituent phases, making identification of the feldspars difficult. Both K-feldspar and plagioclase have been altered to sericite and sausserite respectively giving a turbid, cloudy appearance to the rock in thin-section. The high degree of sausseritisation in these rocks can give the rock an orange tinge in outcrop.

An interesting feature of a large number of these quartzo-feldspathic rocks is that the K-feldspars contain perthites and 'quartz-drops'. The latter have also been observed in K-feldspars in the rocks of the Heterogeneous Quartz-Feldspathic Gneiss Unit and were interpreted as representing relics of a deformed migmatite (section 5.1.1 and see Plate 5.1(c)); such an interpretation also seems applicable to these rocks.

A very common feature of these quartzo-feldspathic rocks is the appearance of orthite (a Rare-Earth bearing epidote mineral, rich in Fe^{2+}) as brown, metamict grains rimmed by clinozoisite in a post-tectonic growth (Plate 6.1(c)). This sharp zoning is interpreted as the

growth of the mineral under oxidising conditions. Initial growth of orthite with Fe as Fe^{2+} allows entry of Rare-Earth elements into the mineral structure (Ce^{2+} , Y^{2+} , Deer et al. 1963, vol. I, p. 212); subsequent oxidising conditions permit the growth of clinozoisite, with Fe as Fe^{3+} , which then precludes the entry of divalent ions into the mineral structure. Very little other post-tectonic mineral growth is present in these rocks, some small zircons can be discerned, and calcite appears in rocks adjacent to the marbles, which originally may have been derived from veins.

Some of the quartzo-feldspathic rocks contain significant quantities of biotite and garnet (sample D75) and appear semi-pelitic. Again the garnets are cracked and in strings whilst the biotite is well aligned and tends to sweep around the garnets. These rocks are fairly plagioclase rich (An 15) which tend to display two sets of twins at right angles, a feature considered to be stress-induced (Smith 1974, p. 577) (see Plate 6.2(c) for an example in the pelites on Bolsøy); accessory phases include quartz, apatite, opaques and K-feldspar. An important feature of these semi-pelites is the limited amount of quartzo-feldspathic material they contain, in contrast to similar rocks in the Heterogeneous Quartzo-Feldspathic Gneiss Unit (section 5.1.1) or in the Tverrfjella Unit (section 3.1.3), although muscovite is absent. This suggests that although the muscovite-melting reactions have occurred in these rocks, e.g. $\text{muscovite} + \text{quartz} \rightarrow \text{Al-silicate} + \text{K-feldspar (melt)} + \text{H}_2\text{O}$

(and see section 3.1.5), these melts have subsequently been expelled from the rocks, presumably during the severe flattening deformation during the Caledonian.

Some of the more mafic quartzo-feldspathic rocks display large, ragged grains of green, finely-twinned epidote. These lie in contact

with porphyroblastic hornblende (α brown-yellow, β green, γ green-blue, $\gamma^{\wedge}Z = 21^{\circ}$) in a matrix of plagioclase (An 20), and quartz + sphene + zircon + K-feldspar (sample 2413). Such Ca-rich rocks tend to occur in proximity to the thin marbles at Mordalsvågen (982573).

The more mafic rocks in these sequence along the Moldefjord coast tend to be less profoundly deformed than the quartzo-feldspathic rocks. They contain the general assemblage of: hornblende (of varying pleochroic schemes, generally blue-green although brown-green varieties also appear), plagioclase (An 28), quartz, biotite (to chlorite) sphene \pm garnet. These phases can appear in both well foliated rocks and in more granoblastic textures in which only the biotite is oriented. Even when undeformed the rocks display evidence of retrogression with both biotite and hornblende altering in chlorite and sausseritisation of the plagioclase. The garnets are generally sub-idioblastic and often cracked with concomitant amphibolisation or even to biotite or chlorites + opaques. Kelyphite rims are common. In some heavily retrogressed rocks, the previous existence of garnet can be inferred from rounded clots of acicular blue-green hornblende + quartz + white mica surrounded by generally well oriented tabular amphiboles (sample D65).

Some of the rocks contain hornblende which display relict symplectite textures with plagioclase (cf. those in the Augen Gneiss - Plate 4.1(d)). Yet others display small relics of clinopyroxene symplectites in the cores of these hornblendes (Plate 6.1(d)) suggesting that these secondary textures have been derived from original omphacitic clinopyroxenes, as observed in the Garnet-Granulite in the Tverrfjella Unit (section 3.1.5 and see Plate 3.2(b)). Careful inspection of any surviving garnets in these rocks reveals the presence of relict rutile grains within these minerals. Consequently, it is considered that some

of these garnet-amphibolites possessed the high-grade assemblage of garnet + omphacite + rutile equivalent to the eclogite facies Garnet-Granulite at Tverrfjella. Unfortunately, conclusive evidence for such, the preservation of grains of omphacite within the garnets has not yet been found in the rocks. Other possible evidence of these rocks once suffering high-grade metamorphism is the appearance of rare pale brown amphiboles poikiloblastically intergrown with garnet (α pale yellow, β pale yellow-green, γ pale green-brown, $\gamma^Z \approx 20^\circ$), suggestive of paragonitic hornblende. Such amphiboles are considered to be indicative of high-pressure metamorphism (Mysen & Boettcher, 1975); also, the associated garnets contain rutile grains (sample D64).

A few rocks contain the unusual calc-silicate assemblages: clinozoisite/epidote + sphene \pm hornblende (often difficult to identify) in a schistose fabric (sample D57) similar to those observed on Otrøy by D.A. Carswell and those at Eidskrem (section 4.1.1) although these examples do not contain garnet. Other calc-silicate rocks are very well inter-banded with semi-pelites (Plate 6.1(e)); this particular example contains: clinozoisite, quartz, sphene, calcite, plagioclase (An 50) \pm apatite (sample D72).

Other, thinly-banded rocks (on scale of thin-section) occur on Varden, generally amphibolitic semi-pelites with concentrations of hornblende, biotite and quartz. Furthermore, these rocks contain scattered grains of low birefringence scapolite (i.e. sodic end-member), generally within the biotite-rich portions. Overall, the rocks are very similar in appearance to those occurring in the Heterogeneous Quartzo-Feldspathic Gneiss Unit on Vågøy even to the extent of the scapolite only appearing within the biotite-rich portions (see section 5.1.1).

Besides the general low metamorphic grade exhibited by these assemblages (generally amphibolite- to greenschist-facies) the rocks are

also cut by micro-shears and veins which cause very local hydration of the rocks. However, these appear to be relatively late features and the majority of the low-grade assemblages appear to have formed during the severe deformation of the Caledonian orogeny.

6.1.2 Rocks of Bolsøy

This island is fairly heavily wooded with little inland exposure, except along the roads around Heimdal (129567). The northern coastline also offers fairly good exposures whilst the coasts to the E and S are flat and pebble strewn.

The map of Hernes (1955) shows a three-fold division of the rocks here: greenschists, mica-schists and 'granitic' gneisses + augen gneisses. The units mapped here are very similar to his (see Map C) although the nomenclature of Hernes is not always followed. Hernes also mapped a thin limestone unit at approximately the same position as the 'augen' gneiss on Map C. No limestones were found at this locality although scattered marbles occur in the schistose units to the NW. One extra rock division has been made here, in addition to those of Hernes, of an amphibole-rich quartzo-feldspathic schist on the most NW coast of the island. As can be seen from Map C, the rocks on Bolsøy maintain a very constant dip, as do the rocks along the Moldefjord coast, although the large, flaggy foliation surfaces of the latter are not so well developed on Bolsøy.

The felsic schist is well banded, on the scale of a few cm, and contains the assemblage: amphibole (α straw, β green, γ blue-green, $\gamma^Z \sim 16^\circ$) possibly tremolitic, plagioclase (An 75-90), quartz + biotite (to chlorite) + clinozoisite + opaques. The amphibole appears as subidioblastic, post-tectonic porphyroblasts which cut across the foliation. An interesting feature of these porphyroblasts is that they are

poikiloblastic with quartz and appear very similar to the amphibolitised symplectites in the Augen Gneiss (see Plate 6.2(a) and compare with Plate 4.1(d)). The amphiboles can also appear as porphyroblasts of multiple, oriented grains, almost in optical continuity, which also contain tiny oriented inclusions of quartz and plagioclase. The late-stage nature of this mineral suggests that these grains are simply overgrowing the quartz and plagioclase rather than representing relict symplectite textures. The amphibole can also appear as a matrix phase in the more equigranular examples of this rock unit and is then well aligned, together with the quartz and plagioclase, both of which are strained and sheared; the plagioclase is also partially sausseritised. The rocks are very brittle and reflect this nature in profuse jointing, often filled with epidote minerals or quartz. On the N coast of the island (\sim 133576) the contact between this unit and the amphibole schist is well marked and can be followed SW, across the island as a small feature.

The amphibole schist is a very monotonous, massive, fine-grained well-foliated rock with the assemblage: hornblende (α pale yellow, β green, γ green-blue, $\gamma^Z \sim 16^\circ$) + plagioclase (An 25) + quartz + biotite \pm K-feldspar in a foliated texture. Fairly profuse bodies of fine-grained, sugary marble occur within this rock. These tend to be rather impure, with hornblende being the major addition (α pale yellow, β green, γ green-blue, $\gamma^Z \sim 12^\circ$ - tremolitic) + biotites and opaques, in a foliation, + clinozoisite + sphene + chlorite + quartz. Also, a small calc-silicate body, adjacent to a marble, but disturbed by a pegmatite intrusion, occurs near the ferry stage (120572). This has the assemblage: ferroactinolite (α pale yellow, β pale green, γ very blue-green, $\gamma^Z \sim 9^\circ$), often porphyroblastic, calcite and calcic scapolite. The scapolite occurs in a symplectitic texture with plagioclase, which appears to be

replacing it, cf. that in the marble in the Tverrfjella Unit (see Plate 3.4(a)) although the secondary zoisite of that example is not visible here.

Micaceous rocks on Bolsøy are flaggy or phyllitic depending upon the proportion of mica present. The rocks are best exposed on the N shore of the island (~ 138575) and at Heimdalen (127567); the outcrops are generally heavily weathered and rust coloured although the rocks display a characteristic purple sheen on fresh surfaces. Quartzo-feldspathic streaks and 'blebs' can be seen in outcrop running parallel to the foliation which itself can be micro-folded and kinked. The general assemblage of the rocks is fine-grained: biotite, garnet, plagioclase (An 35-55), quartz + amphibole + K-feldspar + orthite ± kyanite ± calcite. The biotite is red-orange in colour with some chloritisation and zircon inclusions; three generations exist, usually in one rock sample:

Pre-tectonic: strained and bent, and butting against the garnet

Syn-tectonic: unstrained and following the limbs of microfolds and sweeping around the garnets; these are the most numerous

Post-tectonic: cutting across the limbs of the microfolds

The garnet is variably sized: some are tiny and in trails parallel to the foliation others are porphyroblastic and irregular with corroded rims. They are usually sieved with quartz and plagioclase although some have inclusions of biotite; others have inclusions only in the core of the grains, yet others have orange (grossular-rich) cores and colourless rims. The porphyroblastic forms appear to be in two generations.

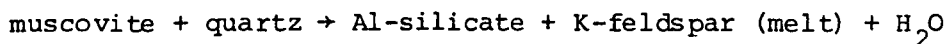
Pre-tectonic: very corroded rims and squarish outlines, the trails of inclusions are at high angles to the dominant foliation.

Syn-tectonic: inclusion trails form 'S'-shapes (Plate 6.2(b)).

The plagioclase in the groundmass is irregular and often untwinned.

Much of the twinning is in two sets at right angles, with one twin set pinching out as it approaches the other (Plate 6.2(c)). These twin sets appear to be albite and pericline twins, which invariably accompany each other in deformed plagioclases (Smith 1974, p. 348). Some difficulty was encountered in deciding which twin set was the albite twin in order to evaluate the An content of the plagioclases. The lack of twinning in some plagioclase grains in these rocks may also be a result of mechanical deformation (Smith 1974, p. 348).

Quartz appears in both the groundmass and in pre-tectonic segregations. In the latter it is heavily strained and sutured, cuts across other phases and occurs with a more acidic, porphyroblastic, anti-perthitic plagioclase (An 25) + rare untwinned K-feldspar. In conjunction with the lack of white mica except as a secondary phase, these segregations are interpreted as representing strongly deformed anatectic portions implying that these rocks have suffered a high-T metamorphism to instigate the reaction:



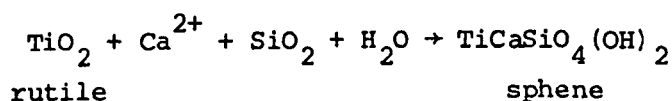
as interpreted for the pelites of the heterogeneous rocks in the Tverrfjella Unit (see section 3.1.5). The aluminosilicate phase is only rarely seen in the pelites on Bolsøy, but relict grains of kyanite can be found (Plate 6.2(d)). These are always severely disrupted and strained indicating a pre-tectonic formation.

The amphibole in these rocks is variable in composition; Fe-actinolite appears to be the most common (α pale yellow, β yellow-green, γ green-blue, $\gamma^Z \sim 18^\circ$) although more Ca-Mg types do appear, tending towards more pargasitic compositions (α pale yellow, $\beta = \gamma$ pale green, $\gamma^Z \sim 16^\circ$). These amphiboles are pre-tectonic in formation and are

disrupted; they are also often poikiloblastic with quartz and overgrown by biotite. This poikiloblastic texture with the quartz may simply be a result of the amphiboles overgrowing the groundmass phases, as inferred for the similar texture observed in the amphiboles of the felsic schists on the W coast of Bolsøy. However, some examples occur in which the quartz appears as oriented laths, parallel to the cleavage of the host amphibole, perhaps implying exsolution of silica during a change in composition of the amphibole with metamorphic conditions.

Of the accessory phases, orthite is fairly profuse and exhibits sharply zoned rims of clinozoisite, as seen in the rocks of the Moldefjord coast (see Plate 6.1(c)), reflecting a change from reducing to oxidising conditions during metamorphism.

Within the unit of mica-schists several amphibolite or amphibole-rich rocks occur (e.g. sample 37), and sugary, fine-grained marbles; both of these rock types are best seen along the N coast (1357) of the island. The amphibolitic rocks occur as small, very elongate pods (2-3 m long) and it was considered that perhaps these represented highly deformed and attenuated forms of the pods of eclogite seen on the mainland. The cores of these pods were carefully scrutinised in an attempt to find evidence of relict eclogite facies assemblages, but to no avail. The rocks are fine grained and cut by chlorite and calcite-filled joints. The mineralogy is well oriented and consists of hornblende (α pale yellow, β green-brown, γ blue-green, $\gamma^Z \sim 18^\circ$), plagioclase (An 46), again exhibiting two sets of twin planes, quartz \pm K-feldspar \pm sphene. Rare, ragged garnets can be found, oriented parallel to the fabric and sieved with quartz. The sphene is generally seen as a rim on an opaque phase, after rutile:



The Ca may have been donated by plagioclase but is more likely to have been derived from the hydrating fluids which can be seen to have carried CaCO_3 , now visible as calcite veins. Indeed, one outcrop of this amphibolite was observed grading into an adjacent marble (139574). Here the amphibole is rather more tremolitic (α colourless, β pale green, γ vs. pale blue-green, $\gamma^Z \sim 19^\circ$) and contains inclusions of quartz, clinozoisite and calcite; it has also suffered slight chloritisation. The marble is very fine grained and pure, with rare quartz, K-feldspar and plagioclase, generally in clots. Some of these clots contain idocrase and a pale brown mica, phlogopite; both are typically found in marbles metamorphosed at amphibolite facies (Deer et al. 1963, vol. III, p. 50). Some of these marbles display cataclastic textures (146574) with intense granulation of the calcite and bending of the porphyroclasts of mica. Accessories include: phlogopite, scapolite and relict clinozoisite apparently altering to plagioclase (cf. that in the marble, and that observed in the impure quartzite, sample 1012, both in the Tverrfjella Unit (see sections 3.1.2 and 3.1.3, and Plate 3.4(e)).

Cataclastic rocks such as these appear to be concentrated at the junction between the mica-schists and the more quartzo-feldspathic rocks on the E side of the island. Intensely deformed quartzo-feldspathic rocks can be observed at (145569) and consist of: feldspar, zoisite, chlorite and quartz. The feldspars are heavily sericitised and sauseritised, and granulated; the quartz occurs as ribbons around the other phases. The sphene and biotite are strongly disrupted with the latter altering to chlorite. Only the zoisite is undeformed and appears to be a post-tectonic phase. Some parts of the rock approach a mylonite fabric in which porphyroblasts of K-feldspar lie in a matrix of quartz, plagioclase chlorite, biotite \pm zoisite such that the rocks adopt an 'augen' texture.

To the E of these cataclastic rocks, the rocks are predominantly fine grained two-feldspar-quartz grey gneisses, extensively flattened with a pronounced banding. On scale of metres (e.g. 155569) the rocks are massive rather than flaggy. K-feldspar is the dominant feldspar and generally appears as porphyroblasts; both the K-feldspar and the plagioclase (An 10-15) are generally untwinned although both exhibit quartz 'drops' as seen in certain rocks of the Heterogeneous Quartzo-Feldspathic Gneiss Unit which were interpreted as the representatives of deformed migmatites (section 5.1.1 and see Plate 5.1(c)). Such textures have also been noted in the quartzo-feldspathic rocks of the Moldefjord coast. These feldspars can appear in both polygonal textures, with only slight suturing of the grain margins, and in more protocataclastic textures in which the grains are fairly heavily granulated. In both of these textures quartz appears as thin 'ribbons' or 'strings' and biotite is always well aligned. An interesting point here is that the biotite in these rocks is of a green-brown adsorption colour, whilst the biotite occurring in the rocks to the west is of an orange-brown colour. The latter are considered to be Ti-rich biotites, whilst the former are dominated by ferric iron (Deer et al. 1963, vol. III, p. 71). Accessory phases include: green hornblende, sphene, relict garnet and ubiquitous orthite, again zoned with clinozoisite rims. Although the rocks are brittle and profusely jointed, generally filled with chlorite, competence differences between these quartzo-feldspathic rocks and the amphibolites they contain have produced some pinch-and-swell structures. These amphibolites can appear as both discrete pods or as bands, both possess well defined foliations that have the general assemblage of: hornblende, plagioclase (An 35) + quartz ± K-feldspar.

6.1.3 Discussion of the petrography

On the map of Hernes (1955) the rocks are simply described as: schistose quartz dioritic-granodioritic gneisses and he appears to have missed the wide lithological diversity of this group of rocks. Also, Carswell (1973), in his regional synopsis of the Basal Gneiss Complex, did not note the occurrence of eclogite pods in this group of rocks; on his criterion of only the Precambrian basement having eclogites he considered that these rocks were of Palaeozoic age.

Several other points can be made about this group of rocks from the observations above:

(i) The rocks generally display assemblages indicative of almandine-amphibolite facies or amphibolite facies, but where assisted by shearing this grade can be as low as greenschist facies.

(ii) Evidence for a previous high-grade metamorphism exists in several of the rocks. Quartz 'drops' point to old, deformed migmatites whilst the relics of symplectic clinopyroxene indicate the prior existence of omphacitic clinopyroxene (cf. the Garnet-Granulite, section 3.1.1).

(iii) The presence of calc-silicate rocks with epidote and scapolite, semi-pelites, marbles and compositionally banded rocks all tend to suggest that sedimentary deposits formed the precursors to some of the rocks in this group even though such meta-sedimentary rocks are in the minority here.

As mentioned in section 1.3 the rocks on Bolsøy were originally mapped as greenschists (Bugge, 1934) and were correlated with the Ordovician rocks to the NE. Fig. 2.5 shows the lithological similarities between the two areas. Both Gjelsvik (1951) and Hernes (1954a) also referred to the rocks as greenschists and considered them to have been derived from lavas/volcanics and sediments.

Again, several points can be made about the rocks on Bolsøy

(i) Most of the rocks display assemblages indicative of the amphibolite facies although in strongly deformed rocks greenschist facies assemblages can occur.

(ii) Evidence for a previous high-grade metamorphic event is present in several of the rock types here: kyanite as the dominant aluminosilicate, anti-perthites in the plagioclases, deformed anatectic portions and quartz 'drops' in the more felsic rocks.

(iii) There is a predominance of lithologies which can be considered to have had sedimentary deposits as their precursors: pelites, marbles and calc-silicate rocks.

As can be seen from these lists for the rocks of the Moldefjord coast and those of Bolsøy, the two groups of rocks are fairly similar. However, there are two differences:

(i) Bolsøy is dominated by metasedimentary rocks whereas the Moldefjord coast is dominated by quartzo-feldspathic and amphibolitic rocks.

(ii) Eclogites have been found in the rocks of the Moldefjord coast and not on Bolsøy.

An important feature of the geology of Bolsøy is the presence of a distinct lithological and tectonic break, considered to occur between the mica schists to the W and the more felsic rocks to the E (see Map C) along which the 'zone' of mylonites lies. Not only are the rock types on either side of this 'zone' very different but it was also noted that the colour of the biotite changed across the 'zone', from orange brown in the rocks to the W to green-brown in the rocks to the E. This junction coincides with the contact between the Røros Group and Tingvoll Group of Hernes (1955) and consequently between rocks considered to be

of different ages. In the introductory statement to this chapter it was stated that an Ordovician-Silurian age is considered valid for the Røros Group (from Krill, 1983) whilst a Precambrian age is preferred for the Tingvoll Group: 1707 ± 63 m.y. (from Råheim, 1977). Although Råheim (1977) has also postulated a Precambrian age for the Røros Group, his derived age is not considered valid here on the basis of the sampling and data selection he used (see discussion in section 3.3). It is considered that this 'zone' of discordance marks a major temporal discontinuity between the rocks on Bolsøy and in consequence adds weight to the arguments of Krill (1980, 1983) and Gee (1980) concerning the tectonostratigraphy of this area. However, it must be remembered that the evidence for the younger age of the Røros and Støren Group rocks on Bolsøy, and indeed these very lithostratigraphic names, is based on earlier workers' mapping and cannot be substantiated in this study.

Although there is some degree of uncertainty, it appears that part of the rock sequence on Bolsøy is of Precambrian age (Tingvoll Group) as are the rocks of the Moldefjord coast: ~ 1700 m.y. In an attempt to clarify the problem of the distinction between the Groups of rocks on Bolsøy and those on the mainland, the geochemistries of the rocks were studied.

6.2 GEOCHEMISTRY

Many of the rocks in the Moldefjord area display cataclastic or well foliated textures, whilst the observed relict assemblages indicate that these rocks have suffered a reworking from grades of metamorphism of at least high-P granulite facies, if not eclogite facies, down to amphibolite facies. Such reworking in shear zones has been shown to have pronounced chemical effects upon certain elements in the affected rocks through hydrothermal alteration and metamorphism (Drury, 1974;

Beach & Tarney, 1978; Floyd & Winchester, 1983). In amphibolitic rocks, contents of K, Rb and Ba were found to increase during reworking whilst Ca, Mg, Mn, Na and Sr were depleted or redistributed (Floyd & Winchester, 1983). In a range of rock compositions, Beach & Tarney (1978) showed that K and Ca were depleted from and Na was enriched in the rocks. Also, oxidation prevailed and the Mg/Fe ratios were increased. With regard to the relative mobility of the LIL elements (K, Rb, Ba), the findings of these two groups of workers appear to be contradictory. As a further complication, Drury (1974) found that K, Rb and Th were added to rocks during the granulite-amphibolite transition whereas Ba, Sr and P were lost from the rocks. Although these findings are rather mixed there is some consensus of opinion as to which elements are mobile: K, Rb, Ba, Ca, Sr, and it is these which must be viewed with care in the rocks of Moldefjord.

Besides the problem of element mobility and redistribution, this group of rocks is very heterogeneous in both grade of metamorphism, general assemblage (i.e. mafic or felsic) and degree of deformation, all of which can affect the bulk rock composition.

The analyses for the rocks of the Moldefjord coast are given in Table 6.1; those for the rocks of Bolsøy are given in Table 6.2. Of the quartzo-feldspathic rocks in Table 6.1 it is immediately apparent that a wide range of compositions exists. The analyses are shown on a K vs. Rb plot in Fig. 6.1(a) where they cluster slightly above the upper crustal average K/Rb ratio of 230 (Taylor, 1964). Three particular samples fall away from this cluster: D51, D59 and D68. These three have exceptionally low K and Rb values, although neither D59 or D51 have particularly well developed cataclastic textures which would be expected to have assisted in the depletion of these elements (Beach & Tarney,

TABLE 6.1 Whole-rock analyses and normative minerals of the rocks along the Moldefjord coast in the Heterogeneous Rocks of Moldefjord

	Quartzo-feldspathic rocks										Semi-pelites			Amphibolites		
	D44	D51	D53	D59	D68	D74	D84	D97	211	M31	D73	D75	D54	D62	D64	D49
MAJOR ELEMENTS (wt. %)																
SiO ₂	76.34	65.72	72.14	76.20	63.05	75.11	65.74	69.32	68.93	70.62	59.85	60.67	45.97	48.69	45.66	46.99
TiO ₂	0.12	0.43	0.38	0.26	0.50	0.37	0.98	0.27	0.29	0.24	0.75	0.66	0.81	1.52	0.88	1.86
Al ₂ O ₃	12.28	14.81	13.39	11.93	15.96	12.70	14.16	15.96	16.03	15.49	17.51	17.28	15.26	14.58	15.78	16.26
Fe ₂ O ₃	0.60	2.76	1.06	1.00	1.75	1.56	3.06	1.04	1.47	0.25	2.69	1.94	3.10	5.02	4.22	4.18
FeO	0.23	4.01	1.49	2.10	5.01	1.14	3.21	0.89	1.04	1.66	3.31	3.56	7.79	7.13	9.18	9.38
MnO	0.06	0.17	0.08	0.08	0.07	0.04	0.15	0.05	0.05	0.06	0.11	0.09	0.18	0.20	0.18	0.21
MgO	1.00	2.32	1.24	1.76	3.53	0.88	2.10	0.85	0.93	0.55	2.82	3.35	8.69	8.03	11.25	7.64
CaO	0.88	6.11	2.08	1.48	2.80	1.54	3.38	1.96	2.91	1.86	5.27	5.90	12.92	11.12	8.88	9.19
Na ₂ O	3.33	3.26	2.58	3.74	3.30	2.22	3.08	4.14	4.26	4.22	4.39	3.60	2.17	2.63	1.97	2.77
K ₂ O	4.51	0.14	4.23	0.55	1.87	3.63	3.60	4.77	3.04	4.28	2.26	2.15	1.05	0.47	0.58	0.79
P ₂ O ₅	0.06	0.15	0.11	0.02	0.09	0.11	0.31	0.09	0.13	0.08	0.34	0.25	0.05	0.20	0.12	0.33
S	0.00	0.00	0.02	0.01	0.03	0.02	0.14	0.00	0.00	0.00	0.04	0.00	0.00	0.01	0.00	0.04
H ₂ O ^T	0.17	0.38	0.71	0.51	0.82	0.76	0.58	0.46	0.45	0.43	0.50	0.60	1.13	0.54	0.86	0.86
TOTAL	99.38	100.76	99.73	99.64	98.87	100.08	100.40	99.80	99.47	99.76	99.84	100.05	99.12	100.17	99.56	100.31
TRACE ELEMENTS (ppm)																
Ni	0	3	9	0	28	7	8	0	0	0	7	36	114	86	217	97
V	4	75	37	23	-	38	84	20	-	-	104	96	-	322	-	257
Cr	8	23	18	9	114	35	23	8	9	12	15	53	365	213	137	69
Zn	-	68	-	-	114	-	-	-	34	29	81	63	75	95	73	111
Cu	-	28	-	-	52	-	-	-	18	9	32	8	163	48	9	79
Rb	128	2	135	9	66	110	116	98	64	91	43	83	13	4	20	21
Sr	85	225	323	320	295	272	180	647	955	571	874	570	158	149	235	362
Y	19	17	39	96	14	41	55	28	0	13	28	25	24	49	10	35
Zr	79	90	221	258	93	206	341	233	117	183	311	192	56	104	71	133
Pb	23	5	25	10	23	20	17	20	17	22	9	10	6	0	0	2
Ba	238	91	883	119	332	749	787	1430	2358	1594	1714	625	76	94	166	362
NORMATIVE MINERALS (%)																
q	37.65	29.41	34.39	45.40	22.66	43.91	23.99	21.61	25.15	23.99	10.51	13.46	-	-	-	-
or	26.65	0.83	25.00	3.25	11.05	21.45	21.28	28.19	17.97	25.29	13.36	12.71	6.21	2.78	3.43	4.67
ab	26.49	27.59	21.83	31.65	27.93	18.79	26.06	35.03	36.05	35.71	37.15	30.46	11.06	22.26	16.67	23.44
an	3.97	25.36	9.60	7.21	13.30	6.92	14.18	9.14	13.59	8.71	21.40	24.64	28.80	26.59	32.50	29.60
c	0.79	-	1.05	2.54	3.63	2.58	-	0.64	0.75	0.73	-	-	-	-	-	-
ne	-	-	-	-	-	-	-	-	-	-	-	-	3.96	-	-	-
di	-	3.23	-	-	-	-	0.45	-	-	-	2.03	2.42	28.29	21.83	8.68	11.24
hy	2.49	7.55	4.28	6.96	15.41	2.34	6.48	2.45	2.53	3.82	8.59	11.02	-	13.57	12.07	7.94
ol	-	-	-	-	-	-	-	-	-	-	-	-	13.30	1.72	17.11	11.80
mt	0.39	4.00	1.54	1.45	2.54	2.26	4.44	1.51	2.13	0.36	3.90	2.81	4.50	7.28	6.12	6.06
il	0.23	0.82	0.72	0.49	0.95	0.70	1.86	0.51	0.55	0.46	1.42	1.25	1.54	2.89	1.67	3.53
py	-	0.94	0.04	0.02	0.28	0.04	0.26	-	-	-	0.08	-	-	0.02	-	0.08
hm	0.33	-	-	-	-	-	-	-	-	-	-	-	-	-	-	-
ap	0.14	0.35	0.26	0.05	0.21	0.26	0.72	0.21	0.30	0.19	0.79	0.58	0.12	0.47	0.28	0.77
TOTAL	99.13	100.08	98.71	99.02	97.96	99.25	99.72	99.29	99.02	99.26	99.23	99.35	97.38	99.41	98.53	99.13

TABLE 6.2 Whole-rock analyses and normative minerals of the rocks of Bolsøy in the Heterogeneous rocks of Moldefjord

	Quartzo-feldspathic rocks			Amphibolites		Pelites		
	BD 109	BD 110	313A	BD 103	37	BD 105	BD 108	315C
MAJOR ELEMENTS (wt. %)								
SiO ₂	74.85	70.16	71.74	50.32	48.24	59.08	55.69	58.77
TiO ₂	0.19	0.39	0.38	1.67	1.90	0.94	0.81	1.16
Al ₂ O ₃	13.14	15.00	13.86	15.16	14.95	15.85	17.78	18.18
Fe ₂ O ₃	0.55	1.28	1.42	3.39	2.76	4.65	3.30	1.44
FeO	0.53	1.00	0.96	7.32	8.54	6.61	4.17	6.65
MnO	0.11	0.06	0.08	0.09	0.19	0.42	0.18	0.07
MgO	0.45	1.39	0.62	6.51	8.61	3.69	3.40	3.98
CaO	1.00	1.69	1.51	9.63	9.86	2.69	6.24	1.13
Na ₂ O	2.76	3.71	3.65	4.51	2.84	2.43	3.64	1.12
K ₂ O	5.66	5.65	5.09	0.15	0.31	2.38	2.78	4.57
P ₂ O ₅	0.04	0.10	0.10	0.24	0.22	0.06	0.34	0.18
S	0.00	0.00	0.00	0.02	0.00	0.03	0.01	0.02
H ₂ O ^T	0.47	0.52	0.23	0.54	1.38	1.09	0.86	1.48
TOTAL	99.75	100.95	99.64	99.55	99.72	100.05	99.38	98.75
TRACE ELEMENTS (ppm)								
Ni	0	0	1	113	70	77	13	38
V	9	21	10	326	-	123	146	-
Cr	10	9	7	325	234	166	32	133
Zn	-	-	-	36	74	100	93	117
Cu	-	-	-	16	0	47	16	15
Rb	139	128	85	0	11	87	96	166
Sr	133	374	162	116	301	189	584	139
Y	40	42	22	38	31	64	59	23
Zr	141	303	288	108	145	315	297	238
Pb	20	30	17	1	2	9	13	19
Ba	635	1099	779	67	67	436	920	618
NORMATIVE MINERALS (%)								
q	34.32	21.50	27.23	-	-			
or	33.45	33.39	30.08	0.89	1.83			
ab	23.36	31.39	30.89	37.44	24.03			
an	4.70	7.59	6.40	20.68	27.13			
c	0.75	-	-	-	-			
ne	-	-	-	0.39	-			
di	-	0.11	0.34	20.65	16.46			
hy	1.33	3.55	1.39	-	12.56			
ol	-	-	-	10.16	8.10			
mt	0.80	1.86	1.99	4.92	4.00			
il	0.36	0.74	0.72	3.17	3.61			
py	-	-	-	0.04	-			
hm	-	-	0.05	-	-			
ap	0.09	0.23	0.23	0.56	0.51			
TOTAL	99.16	100.36	99.32	98.90	98.23			

FIG. 6.1

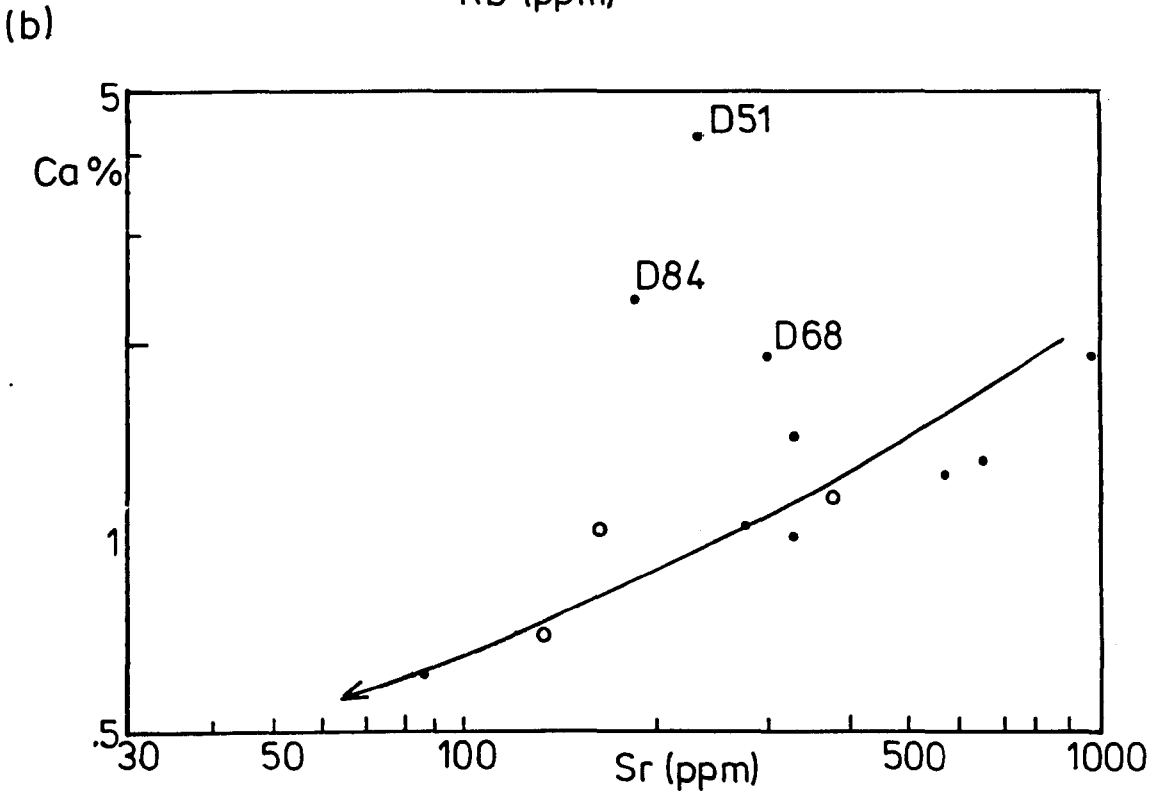
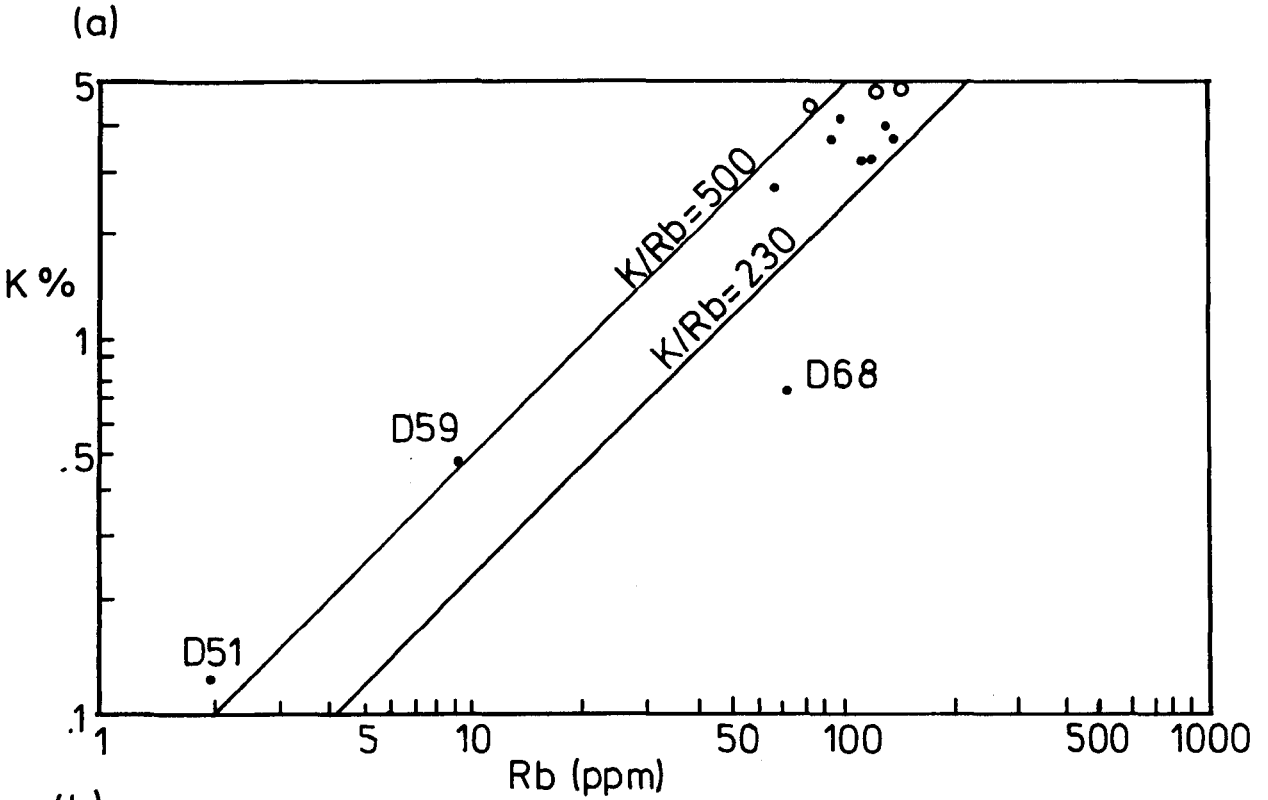


FIG. 6.1(a) K vs. Rb with $K/Rb = 230$ of Taylor (1964). Dots = rocks from the Moldefjord coast, circles = rocks from Bolsøy.
 (b) Ca vs. Sr, a possible differentiation trend is indicated. Symbols as in Fig. 6.1(a).

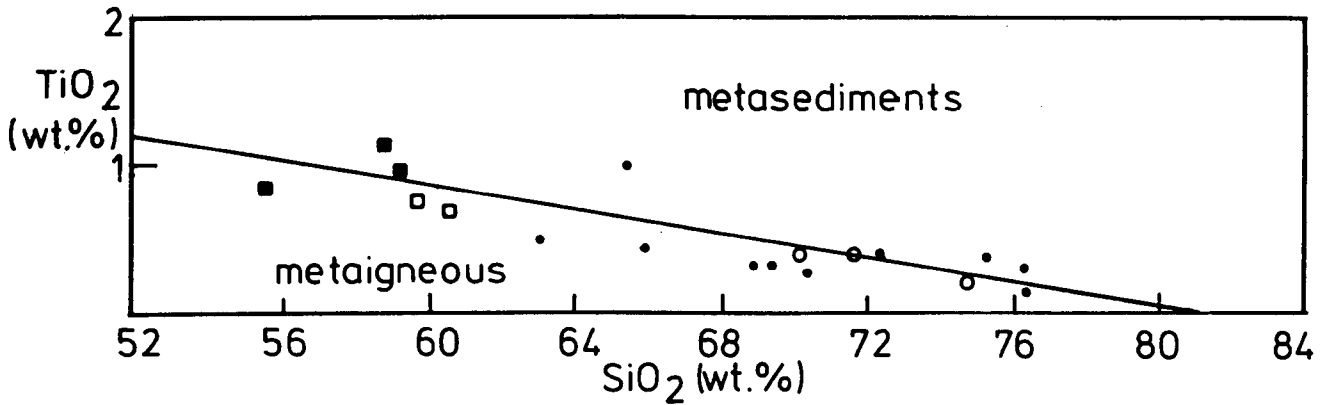
1978). Furthermore, sample D68 is a relatively biotite-rich rock and as such would be expected to have a fairly high content of K. Fig. 6.1(b) shows the rocks on a Ca vs. Sr plot and the majority lie on a covariance trend indicative of differentiation (see Fig. 4.3(a) for a similar trend in the Augen orthogneisses). Again three samples fall away from this trend: D51, D68 and D84; on this plot sample D59 lies on the trend. From Figs. 6.1(a) and (b) it is considered that both samples D51 and D68 have suffered a depletion of K and an enrichment of Ca relative to the other rocks, although it would appear that deformation of the rock is not necessary to invoke such chemical changes. Other rocks such as D84 (a cataclasite) and D59 appear to show variable behaviour. However, some of the most strongly deformed rocks, e.g. D44 (see Plate 6.1(a)) do not appear to show chemical variations on either of these two plots.

The quartzo-feldspathic rocks from E Bolsøy have been included on both Fig. 6.1(a) and (b), and it is interesting to note that they lie with the rocks from the Moldefjord coast on Fig. 6.1(a), although at higher K values, and on the same trend on Fig. 6.1(b). This chemical equivalence suggests that perhaps the rocks on the Moldefjord coast and those on Bolsøy are of the same parentage, or even of the same lithological unit, as suggested in section 6.1.3. However, such a suggestion is partly based upon the possibility of the trend seen on the Ca vs. Sr plot (Fig. 6.1(b)) reflecting an igneous sequence. The discrimination between sedimentary and igneous parents for metamorphosed quartzo-feldspathic rocks has already been attempted for the Heterogeneous Quartzo-Feldspathic Gneisses (section 5.2) and was found to be fairly successful.

The TiO_2 vs. SiO_2 discrimination plot of Tarney (1976) is given in Fig. 6.2(a) and shows that the rocks lie mainly in the meta-igneous field. However, this plot was found to be ambiguous for the data from

FIG. 6.2

(a)



(b)

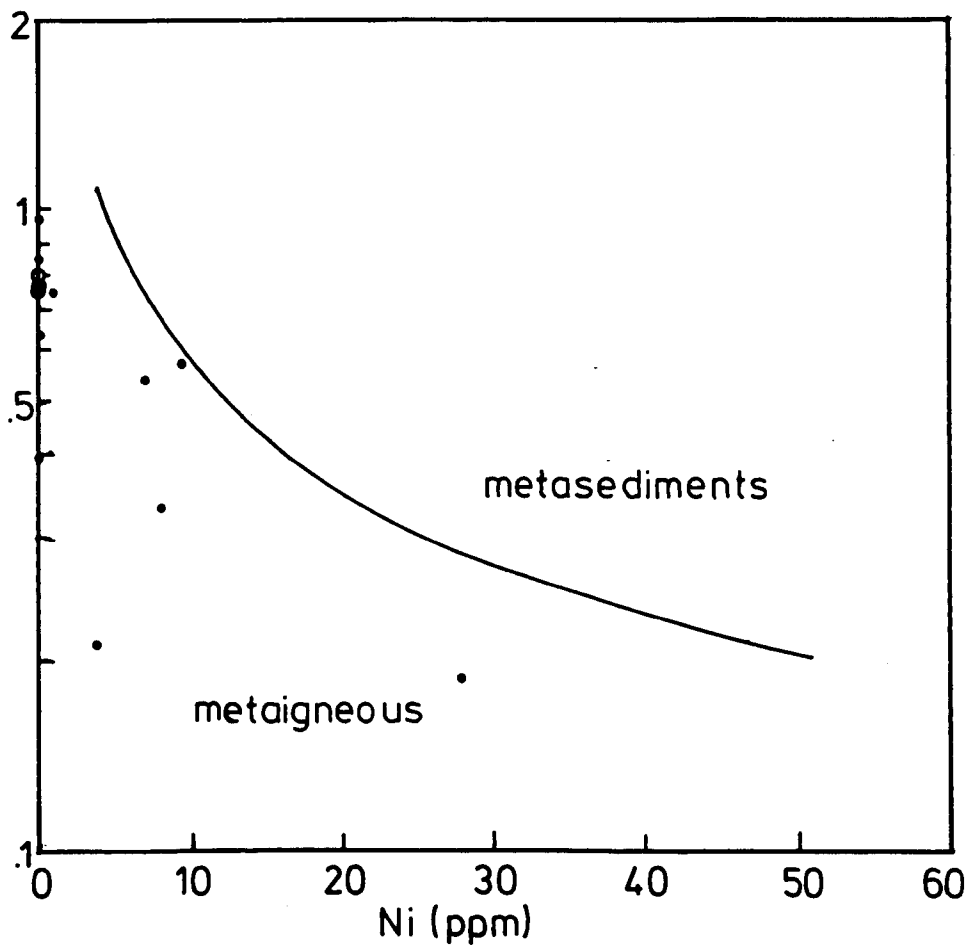


FIG. 6.2(a) TiO_2 vs. SiO_2 after Tarney (1976) with his division. Symbols as in Fig. 6.1(a), open squares = semi-pelites of the Moldefjord coasts, solid squares = pelites of Bolsøy.
 (b) $\text{Zr}/(\text{TiO}_2 \times 1000)$ vs. Ni of Winchester et al. (1980) with their fields. Symbols as in Fig. 6.1(a).

the Heterogeneous Quartzo-Feldspathic Gneiss Unit, and also appears to be so with the rocks of Moldefjord. The semi-pelites of the Moldefjord coast and the pelites of Bolsøy are also shown on this figure, rocks which are considered to represent metasediments and the plot also gives an ambiguous interpretation to these rocks.

The discriminant: $Zr/(TiO_2 \times 1000)$ vs. Ni of Winchester et al. (1980) has also been used for the quartzo-feldspathic rocks; although a meta-igneous parentage is indicated, the generally low Ni contents of the rocks must question the validity of such an interpretation from this diagram (Fig. 6.2(b)). Furthermore, unlike the quartz-feldspathic rocks of the Heterogeneous Quartzo-Feldspathic Gneiss Unit, the rocks of Moldefjord do not show a consistent trend on this plot, the presence of which was interpreted as an igneous feature for the former. Regarding the Ni contents absolutely, the data of Turekian & Wedepohl (1961 - see Table 3.5) shows that low Ni contents are typical of sandstones rather than igneous rocks. However, van de Kamp et al. (1976) have stated that greywackés have typical Ni contents of ~ 50 ppm. This contradiction can be resolved by examining some of the other trace elements in the quartzo-feldspathic rocks. Both Pb and Ba are of note here, these elements occur in substantially lower contents in sandstones (< 10 ppm Pb and < 100 ppm Ba) than in igneous rocks (> 15 ppm Pb and > 100 ppm Ba) (Turekian & Wedepohl, 1961 - see Table 3.5). In virtually all the quartzo-feldspathic rocks on the Moldefjord coast and on Bolsøy the Pb is > 15 ppm and the Ba is > 100 ppm indicating an igneous parentage for these rocks.

It is interesting to note that the two samples which deviate from these Pb and Ba values are D51 and D59. It is possible that the lower contents of Pb and Ba in these two particular samples are a reflection of the chemical modification which they appear to have suffered, or

they may represent true metasedimentary material. The latter interpretation is feasible for two reasons, and is preferred here:

(i) Other meta-sedimentary rocks are present elsewhere along the Moldefjord coast.

(ii) It is difficult to see why only these two samples should have suffered element mobility (as suggested by Figs. 6.1(a) and (b)) when none of the other adjacent rocks have, especially when the undeformed textures of samples D51 and D59 are taken into account.

Plotting these samples considered to be igneous in parentage on an AFM diagram (Fig. 6.3(a)) shows that they define a calc-alkaline trend similar to that in the Heterogeneous Quartzo-Feldspathic Gneiss Unit (section 5.2). Although such chemical trends can be obtained from meta-sedimentary sequences (Robinson & Leake, 1975) it is considered that the trace element data convincingly indicates an igneous parentage for these rocks. On the classification plot of Streckeisen (1976) (Fig. 6.3(b)) the rocks fall between granodiorites, monzogranites and syenogranites, or the volcanic equivalents (dacites to rhyodacites). On both of these diagrams, the quartzo-feldspathic rocks from Bolsøy still fall on the same calc-alkali trends, reinforcing the suspected lithological connection between the rocks on Bolsøy and those on the Moldefjord coast.

The amphibolites from the Moldefjord coast and Bolsøy have been plotted on Fig. 6.4(a), the $(Al + Fe + Ti)$ vs. $(Ca + Mg)$ plot of Moine & de la Roche (1968), and they fall in or near the basalt field. The rocks are also shown on the AFM plot (Fig. 6.3(a)) where they fall into the tholeiite field, as reflected in their normative mineralogies, with appreciable hy and q contents. Although two samples: D54 and BD103 have a little normative nepheline present, indicative of alkali-olivine basalts, these contents may simply be an artifact of either high alkali

FIG. 6.3

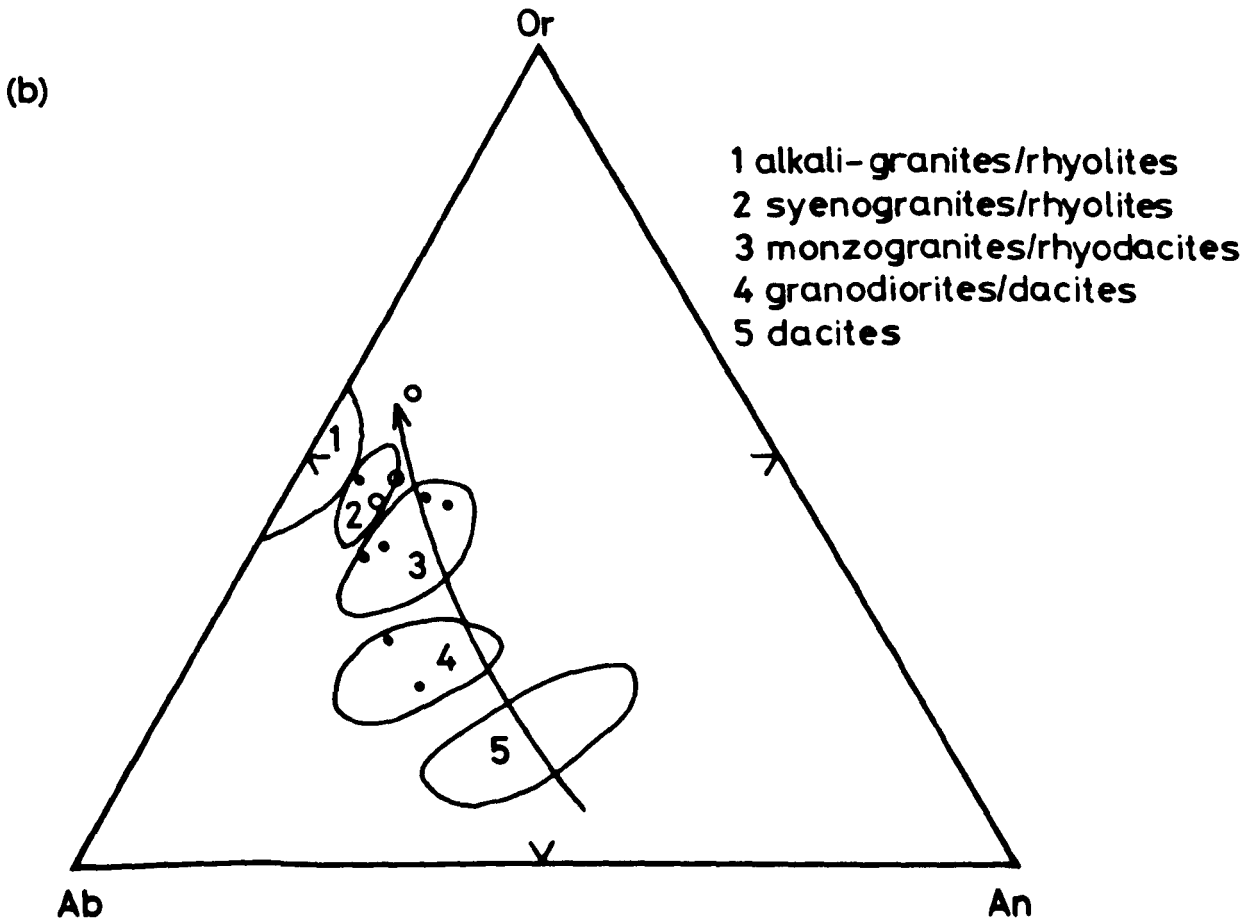
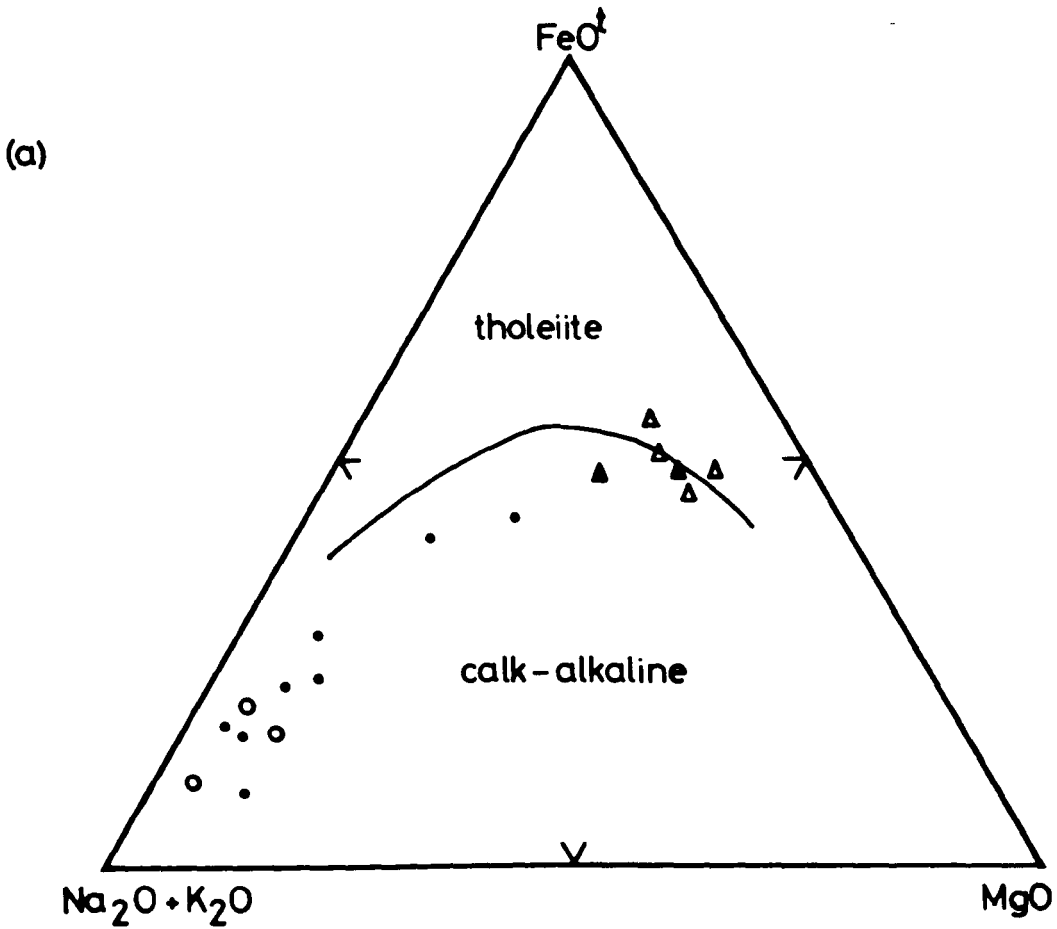


FIG. 6.3(a) AFM diagram with the calc-alkaline/tholeiite division of Irvine & Baragar (1971). Symbols as in Fig. 6.1(a), open triangles = amphibolite of the Moldefjord coast, solid triangles = amphibolites of Bolsøy.

(b) Ab-Or-An plot of Streckeisen (1976) with his fields and calc-alkaline trend. Symbols as in Fig. 6.1(a).

FIG. 6.4

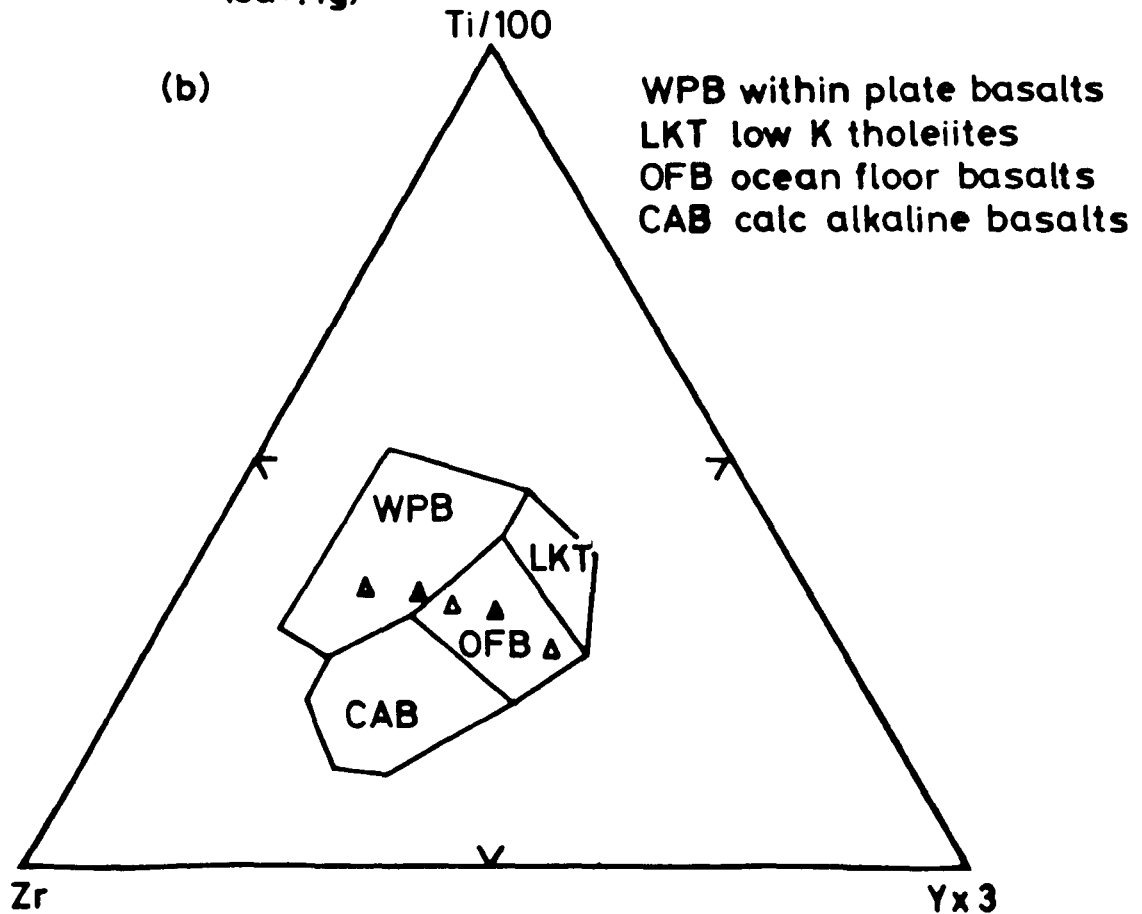
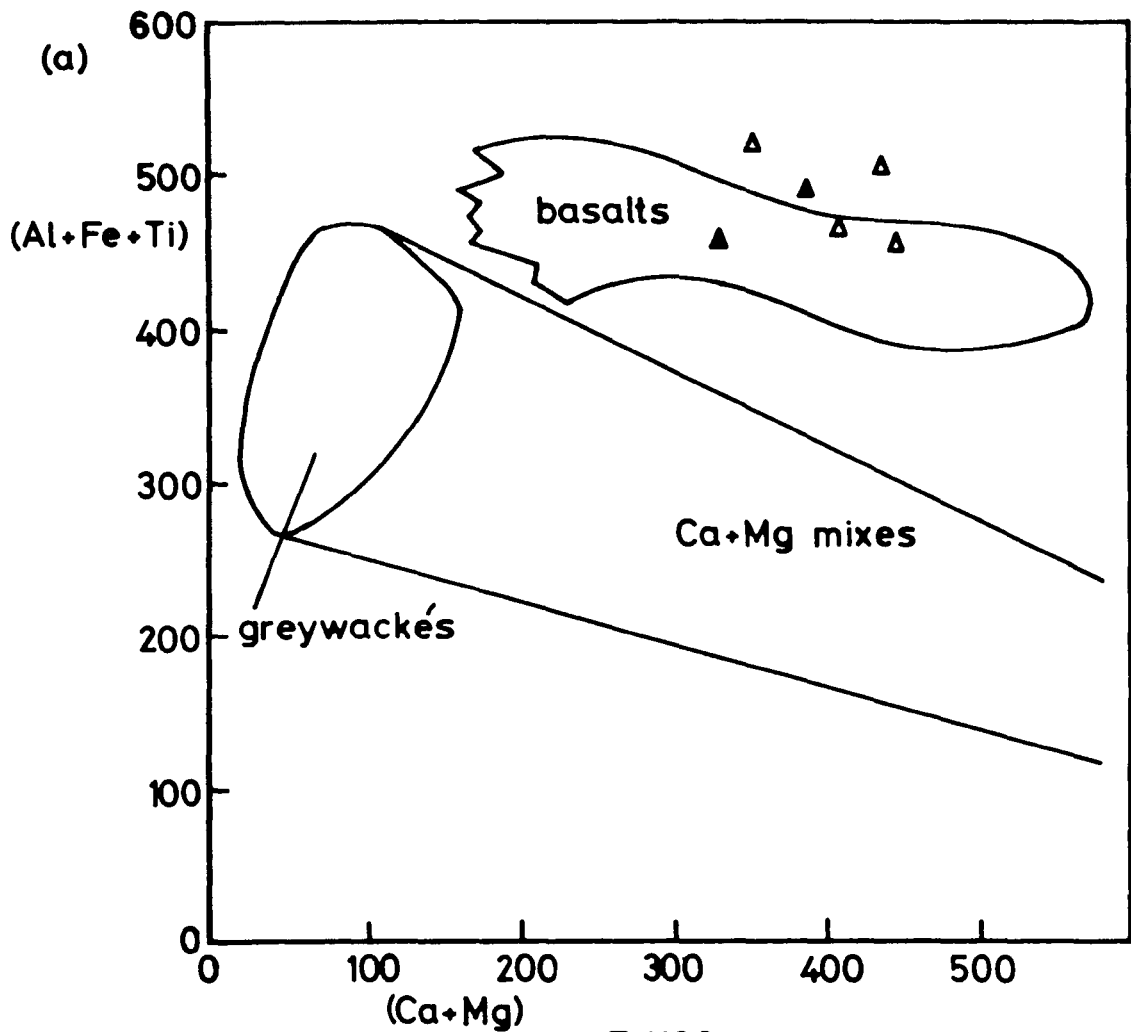


FIG. 6.4(a) (Al + Fe + Ti) vs. (Ca + Mg) in milliatoms of Moine & de la Roche (1968) with their fields. Symbols as in Fig. 6.3(a).

(b) Zr-(Ti/100)-(Y x 3) of Pearce & Cann (1973) with their fields. Symbols as in Fig. 6.3(a).

contents (e.g. BD103) or a low Fe_2O_3 value (see discussion on errors in normative mineral calculations in Appendix B.3). On both of these plots the rocks are fairly closely clustered, and although there is no well defined compositional trend visible, there are no samples which deviate markedly from these clusters a feature which would perhaps indicate some evidence for element mobility in these rocks. From their work on amphibolites in shear zones, Floyd & Winchester (1983) found that although the major elements may be disturbed, the immobile elements: TiO_2 , P_2O_5 , Zr, Y and Nb do not appear to be markedly altered. On the basis of this finding, several geotectonic discrimination diagrams were applied to the amphibolites of Moldefjord to see if any consistent groupings occurred (cf. the Garnet-Granulite: section 3.2.1, and the eclogites: section 7.2.1).

Two of these plots are shown in Figs. 6.4(b) and 6.5(a) and they show good divisions between within-plate basalts (WPB) and ocean-floor basalts (OFB). Samples 37 (from Bolsøy) and D64 (from the Moldefjord coast appear to be of a within-plate character, although sample D64 does not fall into any defined field on Fig. 6.5(a), whilst the others appear to be of an ocean type, although sample D54 is perhaps too far removed from the OFB field on Fig. 6.4(b) to be precise in that case. Unfortunately, the limited amount of data available here makes it impossible to state any definite judgements as to whether the amphibolites from these two localities are of the same parentage. The only conclusion that can be made at this point is that both the Moldefjord coast and Bolsøy contain amphibolites of both within-plate and oceanic affinities. The use of other discrimination diagrams, for basalts, e.g. Ti vs. Cr (Pearce, 1976) or Ti vs. Zr (Pearce & Cann, 1973) only hindered in the interpretation of these amphibolites as the rocks did not fall into any consistent field on those diagrams.

FIG. 6.5

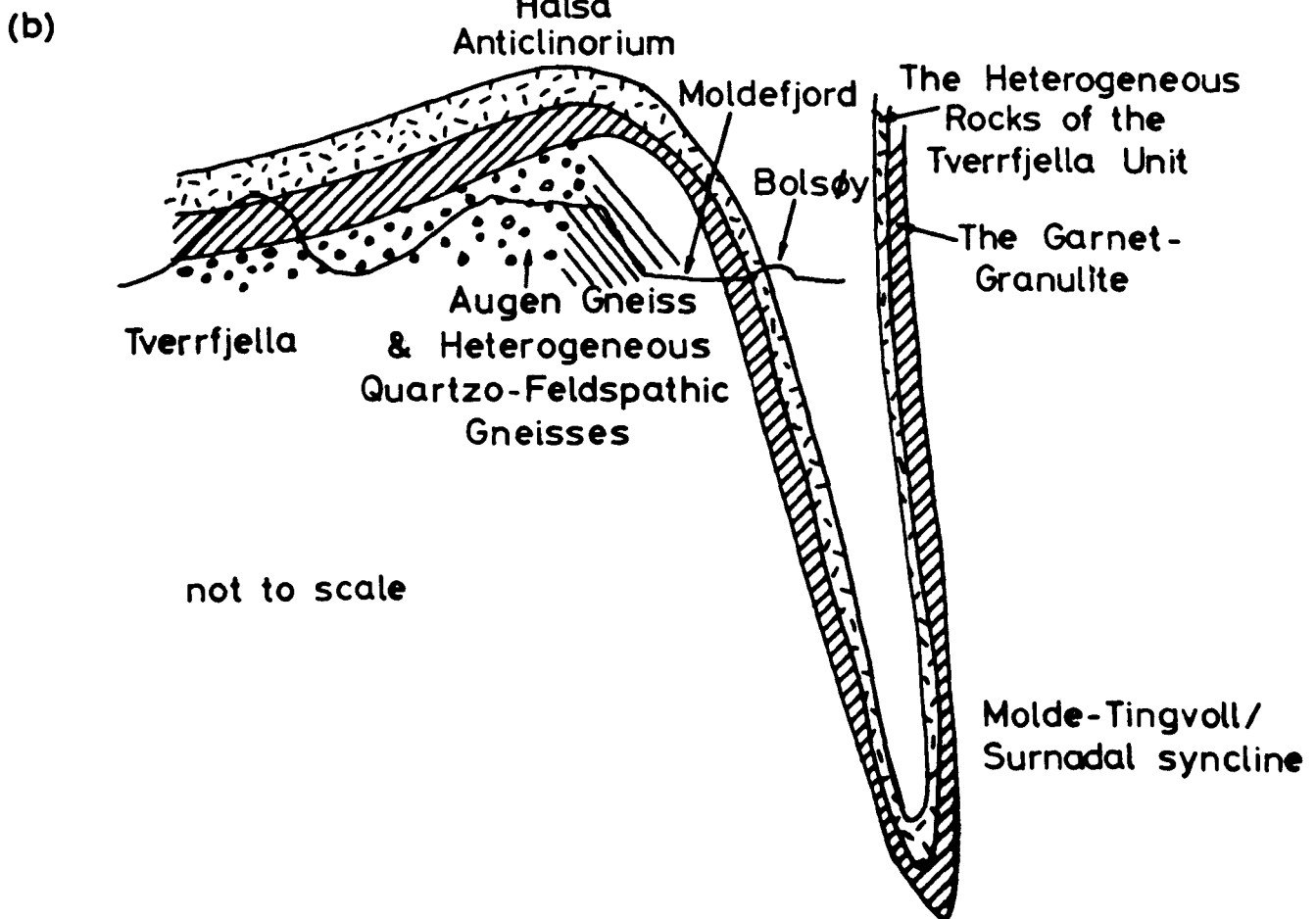
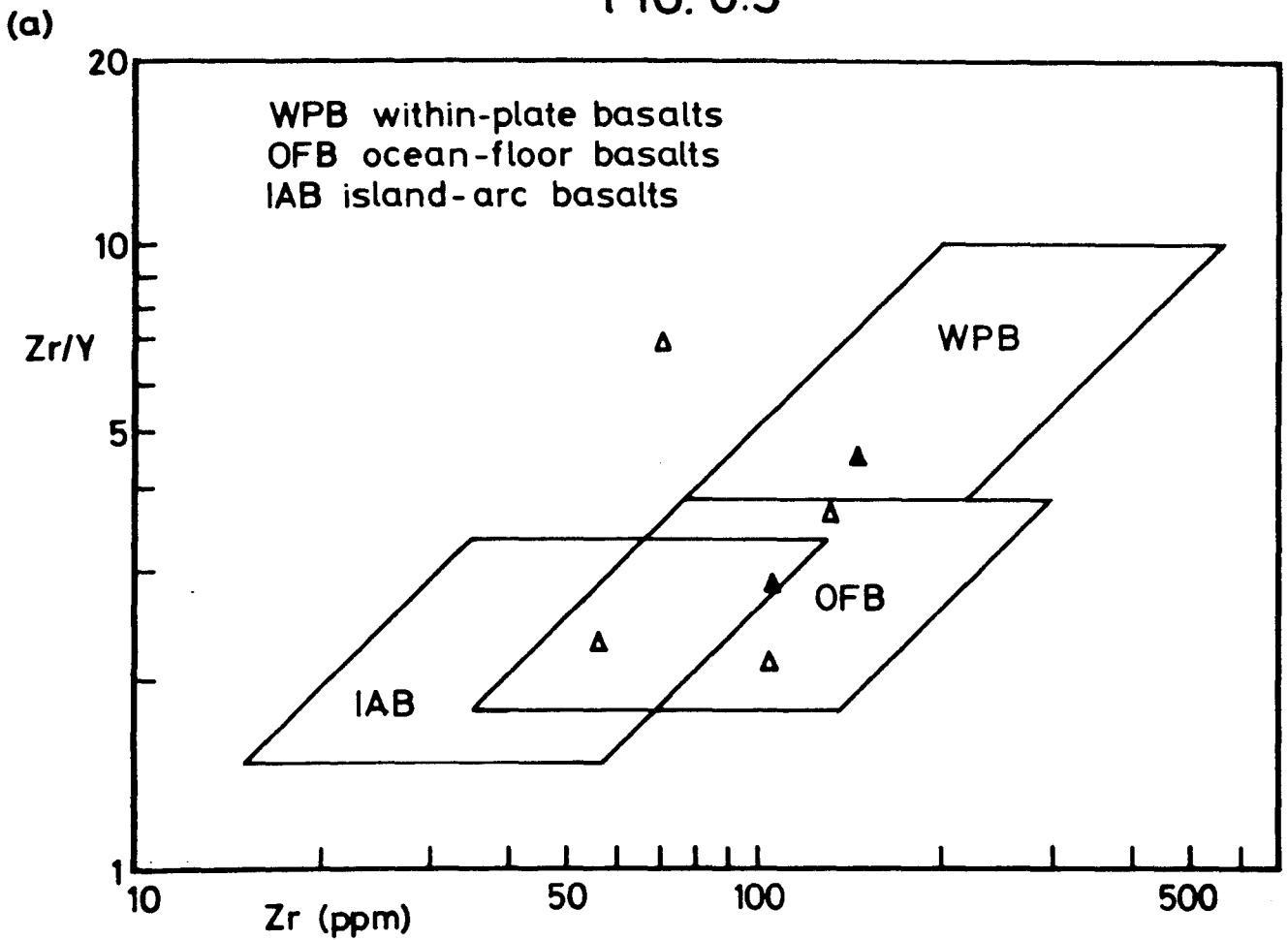


FIG. 6.5(a) Zr/Y vs. Zr after Pearce & Norry (1979) with their fields. Symbols as in Fig. 6.3(a).

(b) Schematic cross-section of the possible tectonostratigraphic relationship between the Tverrfjella Unit and the rocks on Bolsøy.

The mica/garnet rich semi-pelites and pelites on the Moldefjord coast and on Bolsøy respectively possess generally aluminous chemistries indicative of clay-rich sediments as precursors to these rocks. Overall, the chemistries of the pelites from the two areas are very similar, although those from Bolsøy are perhaps more Fe-rich with generally higher trace-metal contents. The oxidation ratio in pelites ($2\text{Fe}_2\text{O}_3 \times 100 / (\text{Fe}_2\text{O}_3 + \text{FeO})$) can be used as an indication of the grade of metamorphism suffered by the rocks (Chinner, 1960). In all of the pelitic rocks here this ratio is fairly high (> 60), although sample 315C has a ratio of 30.2, which indicates a low grade of metamorphism: amphibolite facies or lower. As these pelites display relics of a previous high-grade metamorphism, as anatectic material and kyanite, which would be expected to result in lower values for this ratio through reducing conditions at high grade (Chinner, 1960 - note that the high grade pelites of the Tverrfjella Unit have ratios of 5-23, section 3.2.3), it can be concluded that oxidising conditions prevailed in these rocks during retrogression.

6.3 DISCUSSION

Several general points can be made about the rocks of Moldefjord:

(i) The chemistries of the rocks are not particularly disturbed, in either the quartzo-feldspathic or amphibolitic types even though the rocks are often severely deformed. However, oxidation has prevailed during the retrogression of the rocks as shown by the zoning of clinozoisite on orthite and the oxidised chemistries of the pelitic rocks. It is interesting to note that oxidising conditions have been inferred for the retrogression of other rock types on the Molde Peninsula: for the formation of the symplectic clinopyroxenes in the Garnet-Granulite (section 3.1.5), and for the production of the exsolved magnetite

observed in several phases of the garnet-peridotite at Kolmannskog (see section 7.1.3).

(ii) The quartzo-feldspathic rocks of the Tingvoll Group on Bolsøy appear to be chemically equivalent to those of the Moldefjord coast, and both exhibit a calc-alkaline nature. Not only are calc-alkaline rocks considered to make up a major part of the Heterogeneous Quartzo-Feldspathic Gneiss Unit, but a mineralogical similarity between the meta-sedimentary rocks of Moldefjord and those of the Heterogeneous Quartzo-Feldspathic Gneiss Unit has been noted (section 6.1.1). Unfortunately, no satisfactory age has yet been obtained for the rocks on the Moldefjord coast. A preliminary Rb-Sr whole-rock project was based on a large amphibolite band on Julneset point but the data obtained was scattered meaninglessly on a Rb-Sr isochron diagram. However, as stated previously these rocks do lie in the Frei Group of Råheim (1972) which has been dated at Svecofennian (~ 1700 m.y.), whilst the equivalent Tingvoll Group rocks at Surnadal, to the NE, have also been dated as Svecofennian by Råheim (1977).

(iii) The metasedimentary rocks on NW Bolsøy are rather more dominated by pelites and marbles than those on the Moldefjord coast. Unfortunately, the chemical data from the amphibolites in both of these areas did not allow a rigorous comparison between the two sets of rocks. However, it was noted that these rocks of the Røros and Støren Groups on Bolsøy did not contain eclogites although amphibolites were found. This lack may be due to the strong deformation and retrogression the rocks have suffered, although the rocks on the Moldefjord coast have also suffered this same deformation and retrogression and yet relict eclogite pods have been found in them. This may suggest that the rocks on Bolsøy have escaped the emplacement of the precursors to the eclogites, which

are postulated as a suite of dykes intruded \sim 1200 m.y. ago (see Chapter 7), which then supports the Palaeozoic age for these rocks. However, the apparent lack of eclogites on Bolsøy may simply be due to the limited exposure on the island.

The lack of good radiometric dates on the rocks of Moldefjord is rather limiting. However some stratigraphic control is supplied by the presence of both eclogites and portions of the Augen Gneiss Unit in the rocks along the Moldefjord coast (see Map A). Initially, it was considered that the portions of the Augen Gneiss Unit were perhaps tectonic intercalations within the Moldefjord rocks and that the sharp junction observed between these two Units at Mordal was a tectonic feature, either a fault or a thrust. However, mapping by D.A. Carswell on Otrøy, to the W, has shown that these portions of the Augen Gneiss Unit reside in the rocks of Moldefjord for some distance away from this major contact, up to 1 km away. A second possibility to consider is that these portions represent igneous emplacements of the precursors to the Augen Gneiss at \sim 1500 m.y. ago; if so, then the rocks of Moldefjord must be older than 1500 m.y. The inclusion of the pods of eclogite in these rocks implies that they were in place at \sim 1200 m.y. ago to have received the emplacement of the precursors to the eclogites. An older age for the rocks at Moldefjord is preferred for two reasons:

(i) The rocks are part of the Frei Group, which elsewhere has been dated as Svecofennian.

(ii) If the rocks were formed after 1500 m.y. ago and before 1200 m.y. they would be part of the tensional tectonic conditions which prevailed in Scandinavia at that time (see Chapters 4 and 5, and Bridgewater et al., 1974) in which calc-alkaline rocks are not found, being confined to compressive, Andean-type orogenic margins (Mitchell, 1975).

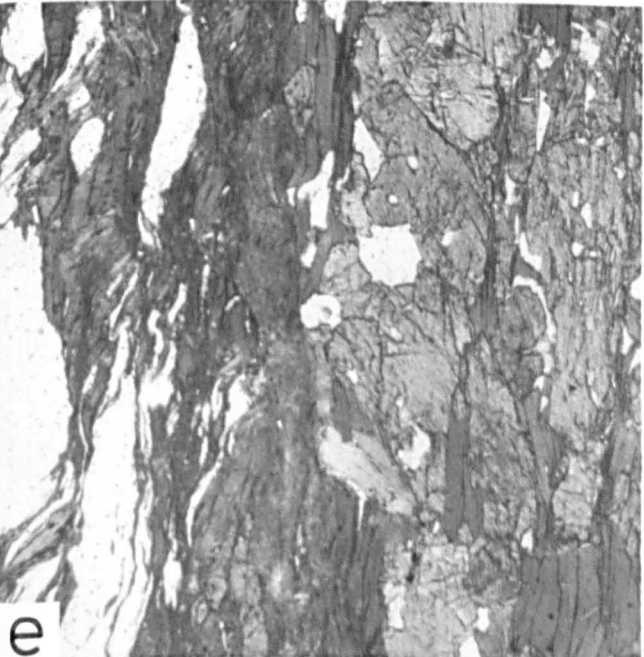
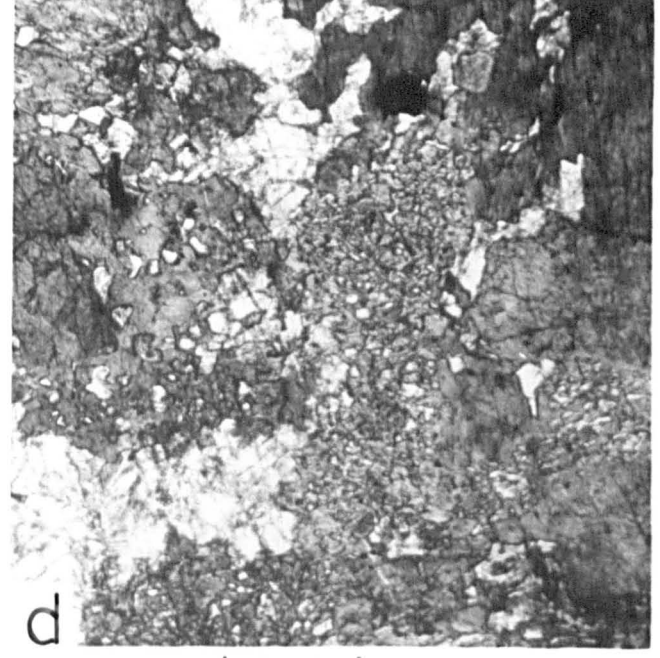
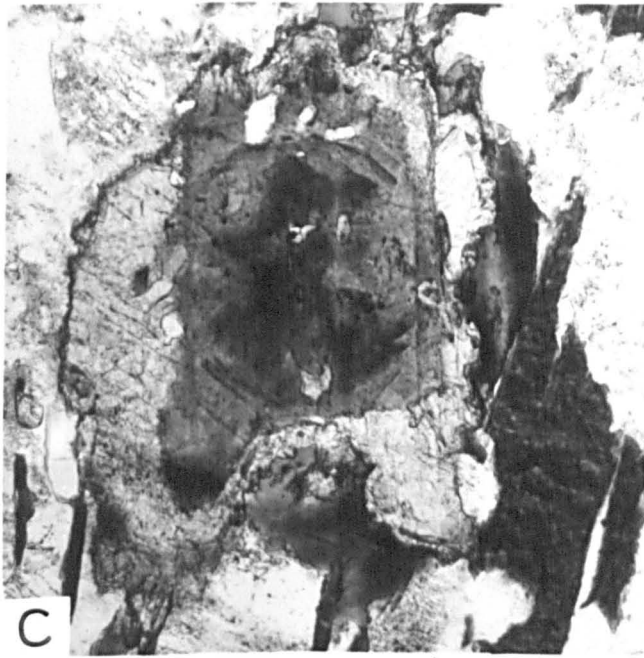
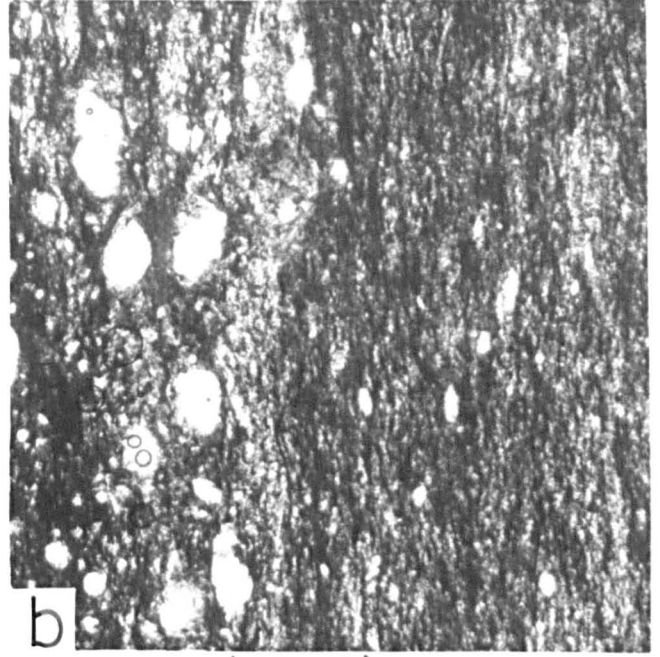
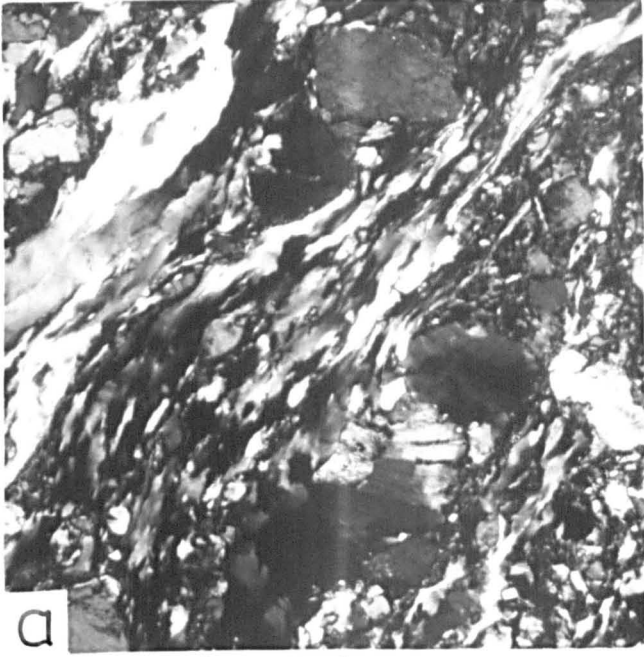
As a consequence, the rocks of the Moldefjord coast are tentatively placed with the Heterogeneous Quartzo-Feldspathic Gneiss Unit as part of the calc-alkaline suite and sediments which are considered to have been deposited in this part of Norway ~ 2500-2000 m.y. ago (see Chapter 5).

If the Palaeozoic age for the rocks of Bolsøy, from the correlations of Bugge (1934) and Shand (1953), is accepted, an interesting possibility arises. These rocks are considered to lie on strike with the equivalent rocks in Surnadal which have been interpreted as part of the Seve Nappe in the Allochthonous Units of the Trondheim Area (Gee, 1980; Krill, 1980, 1981 - see Table 1.1). Furthermore, the Garnet-Granulite in the Tverrfjella Unit has been postulated as being related to these same Allochthonous Units on rock type and chemistry (see section 3.3). Indeed, the lithological similarity between the rocks on Bolsøy and those of the heterogeneous rocks in the Tverrfjella Unit is striking with felsic schists, amphibolites, kyanite-bearing schists and marbles appearing in both areas. A major omission from the rocks of the Tverrfjella Unit seen on Bolsøy is the Garnet-Granulite which would be expected to appear as a massive amphibolite on Bolsøy. It is possible that this rock unit now lies along the line of Moldefjord between Bolsøy and the mainland. Although the evidence is scant, it is suggested that the Tverrfjella Unit and the rocks on Bolsøy, in the Røros and Støren Groups are equivalent lithostratigraphic units. Unfortunately the chemistry of the amphibolites on Bolsøy is too limited to go towards confirming this hypothesis by displaying an oceanic nature. It is interesting to note that the major fold structures in the Molde Peninsula do allow such a lithological equivalence as shown in Fig. 6.5(b).

PLATE 6.1

- (a) General appearance of the deformed quartzo-feldspathic rocks with sheared and strained quartz and feldspars with granulated margins. (Sample D44, cross-polarised light.)
- (b) General appearance of a thoroughly mylonitised quartzo-feldspathic rock where only small, rounded relict grains of feldspar lie in a comminuted and foliated matrix. (Sample 202, plane-polarised light.)
- (c) Orthite grain showing metamict alteration in centre and sharp zoning with a rim of clinozoisite. (Sample D76, plane-polarised light.)
- (d) Garnet-amphibolite displaying partially amphibolitised symplectic clinopyroxene (centre and right). (Sample D60, plane-polarised light.)
- (e) Banded appearance of the pelitic rocks. Biotite + quartz on the left and hornblende + clinozoisite + quartz on the right, note parallelism of banding and foliation. (Sample D72, plane-polarised light.)

PLATE 6.1



CHAPTER 7

THE META-BASIC AND META-ULTRABASIC ROCKS

Two types of meta-basic rock occur on the Molde Peninsula: eclogites (the most numerous) and metadolerite. Meta-ultrabasic rocks are represented by garnet-peridotites. All these rock types appear as discrete masses surrounded by more massive gneisses. The three types are treated together here for three reasons: they have a similar form in outcrop; they have broadly similar mineralogies and chemistries; and they provide several independent estimates of pressure and temperature of equilibration.

7.1 ECLOGITES

A synopsis of the previous work on these rocks in the Basal Gneiss Complex as a whole is given in section 1.2, in addition, many of the features of the Garnet-Granulite at Tverrfjella (see Chapter 3) are also seen in these rocks.

7.1.1 Field relationships and petrography

Eclogites are typically found as ellipsoidal pods, generally 1-3 m long and about 0.5-1 m wide, with the long axes oriented parallel to the local strike direction of the enclosing rock (Plate 7.1(a)). When the foliation direction of the host rock is unclear, and the general appearance of the rock is chaotic, the enclosed pods tend to be more rounded, as seen in the migmatitic rocks in the north of the area. The more ellipsoidal forms appear in the rocks towards Moldefjord where the pervasive, younger foliation is more developed. These pods have been referred to as boudins in the literature (e.g. Bryhni et al., 1969) although this nomenclature presupposes that the bodies have been

disrupted from originally continuous masses by the process of boudinage (Ramsay 1967, p. 103; Hobbs et al. 1976, p. 278). The term pod is being increasingly used in current literature on these rocks (e.g. Lappin & Smith, 1978; Griffin et al., 1983) and is preferred here.

These pods can be mapped out in zones (Plate 7.1(b)) and it is these which are marked on Map A, except for the very largest bodies (e.g. at Svartknakken). From the presence of these zones it is considered that the pods were disrupted from originally larger bodies as 'chocolate-block' structures. Subsequent plastic deformation and rotation has rounded these blocks into the pods seen at present whilst the flattening fabric in the south of the area has given these pods an ellipsoidal form (see section 2.2.6). At no time are the pods seen to be disrupted from original layers or bands as true boudins (see Plate 2.2(f) for an example of such structures in the Heterogeneous rocks of Moldefjord at Mordalsvågen^o). As a result of this disruption the pods nearly always display sharp contacts with the enclosing gneisses irrespective of the latter's composition, i.e. the eclogites are always the most competent even in the amphibolitic rocks. An exception to the general appearance of sharp contacts is an eclogite at Litledigerneset on Midøy which displays apparent igneous backveining from the enclosing gneisses and is mentioned in section 1.3. The occurrence has been discussed by Griffin & Carswell (1983) and is presented as evidence for eclogite facies metamorphic conditions in the crust.

In outcrop the eclogites have a mottled appearance, of red garnet and pale green clinopyroxene; the majority of the pods exhibit a darker green rim adjacent to the host rock as a result of amphibolitisation of the garnet and clinopyroxene. This amphibolite rim varies greatly in width with some rocks appearing to be totally amphibolitised such that

only careful inspection in thin section discloses relict garnet and clinopyroxene. The amphibolitised portions display an orientation of minerals, often emphasised by the appearance of biotite, which lie sub-parallel to the strike direction of the host rocks. It is considered that the development of the foliation in the host rocks, through deformation in the Caledonian, often extended into the eclogite pods and provided pathways for H_2O which then retrogressed the foliated margins of the rocks. The degree of foliation development in the pod and concomitant amphibolitisation appears to be related to two factors:

(i) The nature of the host rocks: eclogites in amphibolite gneisses tend to be more altered than those in quartzo-feldspathic rocks.

(ii) Degree of imposition of the younger foliation: eclogites in the Heterogeneous rocks of the Moldefjord coast are less well preserved than those further north.

Consequently, the best examples of eclogite are to be found in the migmatitic rocks around Elnesvågen. Exceptions to the general rule of foliated eclogite \equiv amphibolitised eclogite exist as almost totally amphibolitised rocks (i.e. garnet/clinopyroxene-free) with a recrystallised, unoriented crystalline fabric. The rocks are also locally hydrated when cut by pegmatites.

The eclogites often display a fine mineralogical banding on the scale of a few mm (Plate 7.1(a)) which has also been described by Mysen & Heier (1972) from the Ulsteinvik eclogite at Hareid. They attributed this feature to low P (< 9 kbar) igneous crystal sorting of olivine, clinopyroxene and plagioclase rather than the metamorphic segregation of garnet and clinopyroxene. This banding is often at an angle to the foliation of the host rock (Plate 7.1(a)) reflecting the rotation of the pod during deformation.

Most of the eclogite pods are jointed to some degree; these joints do not pass into the surrounding gneisses and tend to be quartz-filled; the contact between the eclogite and host rock may also be quartz-filled (Plate 7.1(a)). The jointing could be a product of disruption and rotation of the pod, or perhaps reflects a volume reduction of the rock during high-grade metamorphism as the mineralogy adopted the closely-packed crystal structures of pyrope-garnet and omphacitic-clinopyroxene.

The typical assemblage of an eclogite, as defined by Eskola (1921), is: omphacitic clinopyroxene + pyrope-almandine garnet \pm rutile + quartz although there are several additional phases which can be stable in the assemblage as given in section 1.2 (kyanite, clinozoisite, orthopyroxene, glaucophane, phlogopite). None of the eclogites examined in this study had totally anhydrous assemblages even though attempts were made to sample such from the cores of the pods. The rocks show varying degrees of retrogression with the development of diopsidic clinopyroxene-plagioclase symplectites and amphibolitisation identical to that described in the garnet-granulite at Tverrfjella (see section 3.1.1).

In the best preserved eclogites the clinopyroxene is the typical apple-green colour of omphacite (Deer et al. 1963, vol. II, p.) generally sub-idioblastic and tabular. The garnets are rounded, often appearing as clusters or 'strings', and can contain inclusions: generally quartz and rutile or more rarely clinopyroxene and amphibole in the centres of the grains. The rocks are fine-grained: 1 mm-2 mm, although garnet can be up to 10 mm. In some examples of eclogite in the Basal Gneiss Complex these inclusions are observed in zones in the garnet from amphibole in the core to clinopyroxene at the rim interpreted as mineral growth under prograde metamorphic conditions (Krogh, 1982). No such pattern is visible in these rocks. There appear to be three

textural forms which the garnet adopts: large amorphous, xenoblastic grains; clusters of discrete, rounded grains; and strings of small rounded grains (see Plates 7.1(c), (d) and (e)). The last of these forms occurs in those eclogites displaying some degree of fabric development, but without any related amphibolitisation, in which the garnet strings are parallel. Lasnier (1982) has described similar textural forms of garnet and considered that they represented successive stages in the crystallisation of the eclogite from its protolith. In his scheme, the discrete rounded grain form (Plate 7.1(d)) occurs earlier in the crystallisation sequence than the xenomorphic form (Plate 7.1(c)). He also noted the presence of preserved sheared textures in eclogites giving a 'flaser' structure (cf. that in Plate 7.1(e)).

The eclogites have been grouped into Classes, depending upon the degree of retrogression they display; naturally there is a continuum between the Classes, but they do serve to show the development of the textures.

Class I These are the best preserved eclogites, even so the clinopyroxenes invariably contain some incipient symplectite as brown turbid patches. The garnets exhibit thin, green kelyphite rims often with a little plagioclase development (Plate 7.1(c)).

Class II Further development of clinopyroxene gives 'hair'- or 'fingerprint'-type intergrowths lobate to the centres of the grains (cf. Eskola 1921 - Plate 7.1(f)). These 'fronts' only seem to occur when the altered clinopyroxene is adjacent to another clinopyroxene and not when adjacent to a garnet.

- Class III Here the symplectites are coarser and the low birefringence of the plagioclase can be readily seen. The kelyphite on the garnets tends to be more fibrous (cf. Alderman, 1936), although the garnet can also display replacement by biotite and plagioclase at the rim. Some amphibolitisation of the secondary clinopyroxene is generally visible (Plate 7.2(a)).
- Class IV The symplectite is coarse, often with the plagioclase twins visible. Amphibolitisation is extensive, that produced from clinopyroxene and garnet coalesce into optically continuous grains. Both symplectite development and amphibolitisation tend to follow the clinopyroxene cleavages. The degree of kelyphitisation of the garnets is often no greater than in Class I, although biotite extends some way into the grains (Plate 7.2(b)).
- Class V Ostensibly a garnet-amphibolite, although relict symplectitic clinopyroxene can be discerned within areas of coarse amphibole-plagioclase symplectite. The plagioclase is of oligoclase-andesine composition implying expulsion of both the jadeite and Ca-Tschermaks components from the clinopyroxene (see reactions 3E and 3F, section 3.1.1). The garnets are often cracked with extensive amphibolitisation and development of biotite (which can be chloritised). Rutile apparently remains stable and shows no alteration to sphene (Plate 7.2(c)).

Such textures have also been described from the Garnet-Granulite of the Tverrfjella Unit, although in that rock the degree of retrogression and development of the textures was fairly constant, equivalent to Class III or IV in the eclogites. Rare examples of relict garnet-

omphacitic clinopyroxene were also found (equivalent to a Class I eclogite) as were garnet-amphibolites (equivalent to a Class V eclogite), although the latter tended to be restricted to local shear zones (see section 3.1). In the Class I eclogites the clinopyroxene in thin-section is very pale green or almost colourless, whereas in Class III eclogites, where the clinopyroxene has exsolved plagioclase, the mineral is a distinctly deeper green colour due to the addition of Fe during the retrogression.

Accessory phases in these eclogites include: opaques (ilmenite, or more rarely, sulphides), rutile, amphibole, kyanite, orthopyroxene, apatite, mica and quartz.

The ilmenite and rutile tend to be attached to each other and can occur as both interstitial grains and as inclusions; the ilmenite tends to be associated with the garnet but rutile can appear within any phase. In addition, these two phases tend to be separated from the kelyphitised garnets by a thin rim of plagioclase. It was noted that some samples had particularly high contents of these two phases.

Amphibole occurs mainly as a secondary phase after clinopyroxene and garnet. However, a primary amphibole also appears in a few examples (e.g. M26) as an interstitial phase and in apparent equilibrium with the garnet and clinopyroxene. With a pleochroic scheme of (α very pale brown, β brown, γ brown-green, $\gamma^Z \approx 20^\circ$ Plate 7.2(d)) they appear to be very similar to the paragenetic hornblende seen in the garnet-granulite (section 3.1.1) and hence equivalent to similar amphiboles observed in eclogites elsewhere in the Basal Gneiss Complex (Smith, 1982). The secondary amphiboles can be both green-brown (derived from the clinopyroxene), and blue-green (derived from the garnet) in colour. However, these two seemingly different amphiboles are seen to coalesce

into optically continuous grains in Class III and IV eclogites which suggests compositional uniformity. It is suspected that these differences in colour may result from variations in $\text{Fe}^{3+}/\text{Fe}^{2+}$ ratios rather than bulk composition.

The orthopyroxene-bearing eclogites of northern Moldefjord have been mineralogically studied by Carswell et al. (1983a). The assemblage: garnet + clinopyroxene + orthopyroxene is technically a garnet-websterite, although Carswell et al. prefer to retain the traditional nomenclature of orthopyroxene eclogite. In these rocks the clinopyroxene and orthopyroxene generally display exsolved garnet, whilst the clinopyroxene shows typical secondary symplectite textures. The rocks are often heavily amphibolitised. Rutile is scarce in this type of eclogite, but quartz is more common than in the 'bimineralic' eclogites. A pale-brown mica (Ti-rich phlogopite) is a common accessory as inclusions in pyroxene and garnet, and in the matrix.

At one particular locality, on Svartnakken (9861), the large eclogite pod displays a small (~ 2 cm wide), localised clinopyroxene vein containing large (~ 1 cm) garnets (Plate 7.2(e)). In thin section, the host eclogite is a typical Class I/II type with the unusual feature of the garnets being crammed with small clinopyroxene and rutile inclusions in the central two-thirds of the grain. The vein is virtually pure clinopyroxene displaying Class III symplectites. The large garnets in the vein appear to be composed of several coalesced garnet grains each with the same large number of clinopyroxene inclusions as seen in the host rock. Similar veins have been noted in eclogites by: Lappin (1966), Krogh (1980a), Morgan (1970) and Cuthbert & Carswell (1982) and in each case high fluid activity during eclogite facies metamorphism has been the postulated cause for the vein formation, possibly assisted by the

formation of fractures in the eclogite as the mineralogy adopted the smaller volume space of pyrope-garnet and omphacitic-clinopyroxene.

7.1.2 The metadolerites

In the Basal Gneiss Complex, this rock type is considered to occur mainly N of a line running E from Ålesund (Gjelsvik, 1952) and to take the form of lensoidal bodies, of varying size, often several hundred metres in length.

The examples found on the Molde Peninsula typically occur as small pods similar in size and form to the lensoidal pods of eclogite found there, although they are relatively more scarce compared to the eclogites. Specific localities of metadolerite are marked on Map A. One body mapped by D.A. Carswell on Midøy, to the SW of the Molde Peninsula, is particularly large, at about 1 km long.

In outcrop the rocks exhibit a fine-grained mottled, or 'patterned' appearance, the result of pink garnets growing as coronas around the other, mafic phases of the rock. Griffin & Råheim (1973) have termed these rocks either: coronitic metadolerites, or eclogitic dolerites depending upon the degree of advancement of the reactions from a dolerite assemblage to an eclogite assemblage. According to Gjelsvik (1952) there are two types of metadolerites: olivine-bearing or olivine-free, the latter being more abundant.

As with the eclogites, these rocks have a sharp margin to the host gneisses and exhibit zones of amphibolitisation at these contacts. Unlike the eclogites, they are not mineralogically banded and do not display fabric development except when amphibolitised but rather, possess an igneous appearance.

The general assemblage of these rocks is: garnet + clinopyroxene + hornblende + plagioclase (An 35) + biotite + opaques + rutile + apatite ±

orthopyroxene ± quartz(?). Olivine-bearing metadolerites have been found by D.A. Carswell on Otrøy and Midøy. Photomicrographs are given in Plate 7.3(a) and (b). The clinopyroxenes are irregular in form and are typically pigmented, considered to be due to Ti-inclusions (Griffin & Råheim, 1973); collars of brown sub-idiomorphic hornblende surround these clinopyroxenes. Other clinopyroxenes appear to be breaking down at the rims to a very fine intergrowth of secondary clinopyroxene and biotite, with a colourless phase, possibly hornblende, and a very high relief phase, possibly spinel. Many of these dusty clinopyroxenes contain exsolution lamellae as observed by Griffin & Råheim, which they interpreted as reflecting the original 'primary' igneous nature of these pyroxenes.

The plagioclase forms an excellent polygonal texture in one example (Plate 7.3(a)) containing small xenoblastic grains of garnet and possibly spinel. Plagioclase is difficult to observe in the other example (Plate 7.3(b)) as it appears to be being overgrown by garnet. In this particular rock the garnet has almost totally replaced the plagioclase, but has preserved an ophitic texture as described by Battey et al. (1979) (the 'fish net' structure of Griffin & Råheim, 1973). In the other example the garnet forms coronas around the clinopyroxene/hornblende clots and has only partly replaced the feldspar.

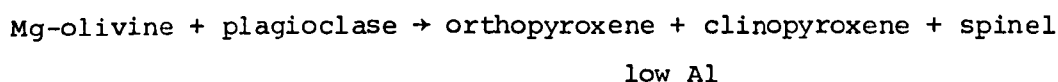
Orthopyroxene is difficult to identify, due to the masking of the pleochroism by the Ti-inclusions, but is mantled by clinopyroxene. As with the 'primary' clinopyroxenes it has exsolution lamellae.

No evidence of symplectite formation with plagioclase has been observed in the clinopyroxenes in these rocks (cf. the eclogites, and Griffin & Råheim, 1973).

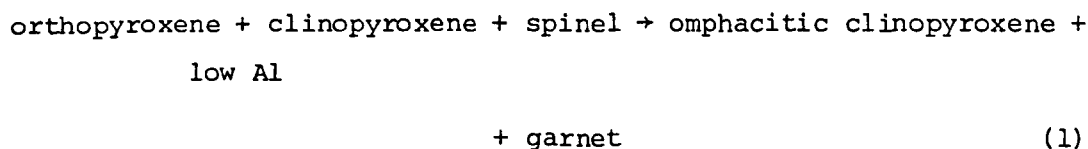
The textures observed in these rocks are very similar to those described by both Gjelsvik (1952) and Griffin & Råheim (1973). The

latter authors interpreted the textures as the conversion of doleritic, high T assemblages (clinopyroxene + plagioclase + ore ± olivine ± orthopyroxene) to the low T, high P assemblage of clinopyroxene + garnet + rutile + quartz through the reactions given on p. 14 of Chapter 1.

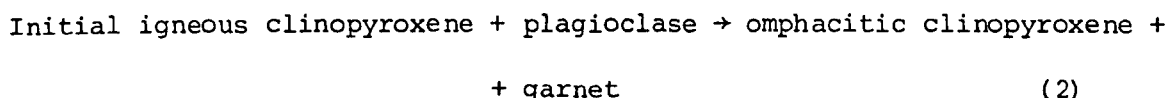
Griffin & Heier (1973) considered that the alteration of the doleritic phases was due to an isochemical alteration rather than any form of metasomatic process. They formulated two reactions to explain the coronitic textures and metamorphic mineralogy:



These products react further:



Simultaneous with, or shortly after this reaction was:



The lack of olivine in these rocks, and the lack of metamorphic orthopyroxene associated with spinel suggests that reaction (1) has gone to completion. However, the appearance of the relict primary clinopyroxenes suggests that reaction (2) has been only partially completed.

From her study of the metadolerite on Flemsøy, Mørk (1982) considered that a fluid phase played a major part in the 'eclogitisation' of the dolerite with a concomitant oxidation of the rock chemistry (cf. Emmett, 1982). High fluid activity has been considered to be important in the formation of the anhydrous eclogite assemblages by other workers (see section 1.3).

7.1.3 The garnet-peridotite

The body of interest occurs in a road cut ~ 800 m E of the junction between the E662 and the gravel road to Eide (113773), S of Kolmannskog farm. A smaller body occurs nearer the farm at about (106778) and is probably related to the larger outcrop. In addition, small hydrated bodies occur in a cut on the road between Elnesvågen and Bud (026702), and at Indre Hoem (016671).

The body S of Kolmannskog is limited in size, only 15 m long and ~ 6 m high; Fig. 7.1(a) shows a sketch of the outcrop with positions of the samples taken. The western contact with the migmatitic pelite (Chapter 5) is not seen, but a large mass of enstatite + clogs of garnet + 1 cm wide veins of tremolite occurs there. This appears to be part of a reaction selvage between the peridotite and the country rocks, typical of this type of peridotite (Curtis & Brown, 1969; Carswell et al., 1974; Evans, 1977). Brueckner (1975) used $^{87}\text{Sr}/^{86}\text{Sr}$ ratios to show that these selvages are the product of the interaction between the peridotite and hydrous fluids emanating from the enclosing gneisses. A further outcrop of enstatite + tremolite veins is found ~ 200 m W of this main body. The E contact with the host gneisses is tectonic and occupied by a quartz vein. This junction has permitted the ingress of fluids resulting in the hydration of the peridotite immediately adjacent to the contact. This type of contact is similar to that seen in the eclogites, although a zone of biotite has been formed here 4-5 cm wide in preference to the amphibole in the eclogites.

Several fairly distinct rock types occur in this one outcrop although it has not been possible to delineate them precisely (see Fig. 7.1(a)). They are dominated by olivine, orthopyroxene (hypersthene) and garnet with minor clinopyroxene, accessory phases include: rutile,

FIG. 7.1

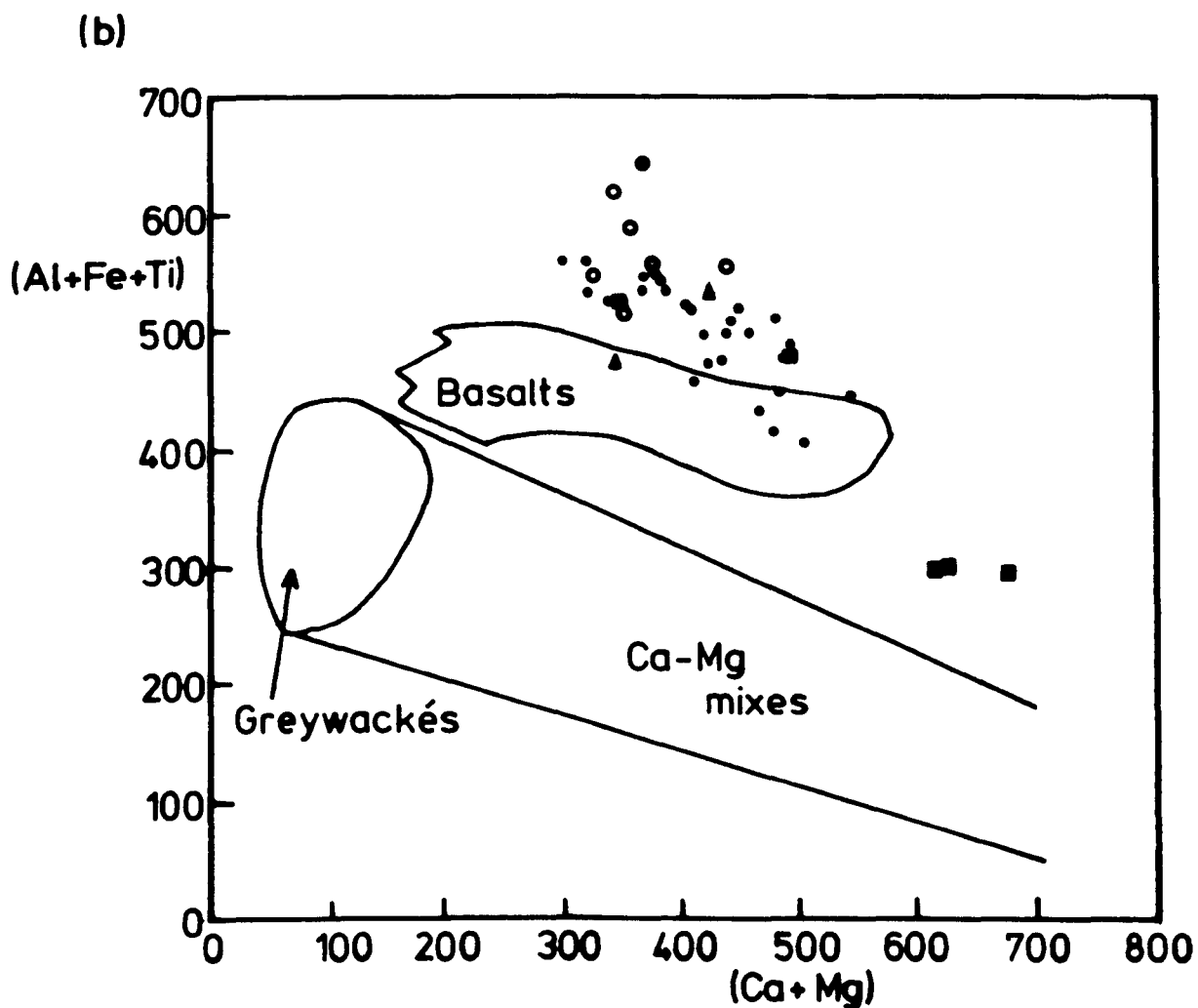
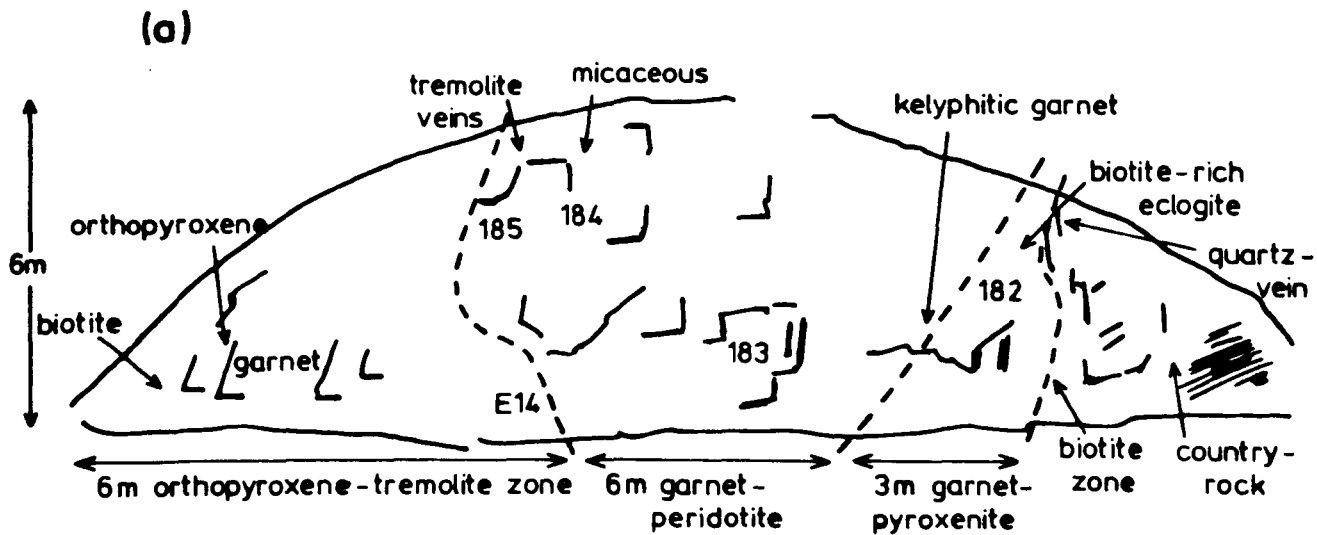


FIG. 7.1(a) Sketch of the garnet-peridotite outcrop at Kolmannskog with approximate lithological divisions. Numbers refer to rock samples.

(b) $(Al + Fe + Ti)$ vs. $(Ca + Mg)$ (milliatom) after Moine & de la Roche (1968). Dots = 'bimineralic' eclogites; circles = Fe-Ti type eclogites; squares = orthopyroxene-bearing eclogites; triangles = kyanite-bearing eclogites.

opaques, green pleonaste spinel, mica and secondary ferroctinolite. The mica is green-brown pleochroic, and can be quite profuse in some parts giving the rock a foliation. It is suspected that the green colour is due to a low Fe^{3+}/Fe^{2+} ratio in the mineral. The major assemblages of these phases are:

garnet + orthopyroxene + olivine + spinel (garnet-spinel harzburgite)

garnet + orthopyroxene + clinopyroxene + olivine + spinel (garnet-spinel lherzolite)

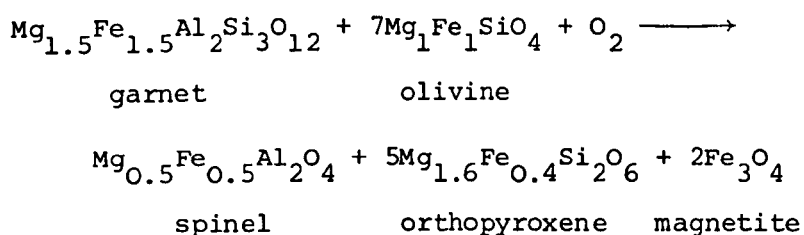
garnet + orthopyroxene ± olivine ± clinopyroxene (garnet-pyroxenite)

garnet + clinopyroxene (eclogite)

The rocks are fairly coarse grained (~ 5 mm) especially the orthopyroxene which typically occurs as large sub-idioblastic grains lobate with other phases, particularly olivine. Orthopyroxene also occurs as smaller polygonal grains. Olivine is irregular but is well preserved with only slight, brown, serpentinisation. The clinopyroxene is green and pleochroic and hence augitic, except in the eclogite where it adopts the paler green colour of omphacite. The garnet is fairly small, generally as rounded, sub-idioblastic grains in 'strings'. The eclogite displays variable degrees of retrogression and hydration with textures typical of Class I to Class IV types.

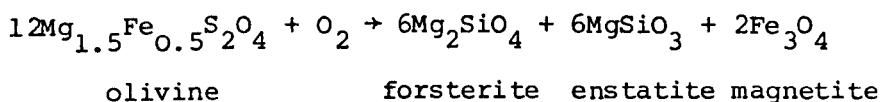
Spinel is a prominent accessory in all these rocks, except the eclogite, dark green and generally attached to the opaque grains (Plate 7.3(c)). Magnetite is also a predominant feature of these rocks, as both interstitial grains and as needle and 'bleb' inclusions in the olivine and orthopyroxene (Plate 7.3(c)). Furthermore, coarse symplectites of magnetite and orthopyroxene occur (Plate 7.3(d)). The garnets also display symplectite textures of spinel + opaques + amphibole when adjacent to olivine which appear to pass into the orthopyroxene-

opaque symplectites with increasing distance from the garnet (Plate 7.3(d)). Carswell et al. (1983b) interpreted these textures as reflecting the decompression of the rocks from eclogite facies garnet-peridotite to granulite facies pyroxene-spinel peridotite with concomitant oxidation. Excluding the grossular component of the garnet, their derived equation was:



In the Kolmannskog peridotite this secondary orthopyroxene appears to have been hydrated to a colourless amphibole, although the symplectites around the garnets are too fine-grained to make a positive identification of the phases involved.

Olivine also may have undergone oxidation, simultaneously with this reaction, to give the inclusions of magnetite observed in that phase:



The occurrence of abundant oxides as primary metamorphic phases, as well as in secondary replacement textures indicated that the oxidation of the rock also occurred during the formation of the primary peridotite assemblage.

7.2 GEOCHEMISTRY

7.2.1 Eclogites

Samples were taken from eclogite pods throughout the northern Moldefjord area, from both fresh and retrogressed examples. The whole-rock analyses and normative minerals for the typical 'bimineralic' eclogites are given in Table 7.1; whilst those for the Fe-Ti type, orthopyroxene- and kyanite-bearing eclogites are given in Table 7.2.

As shown in section 6.1, the development of retrograde textures in these rocks was found to be very variable although it was possible to group the rocks into five Classes based upon the varying degrees of retrogression seen. In addition, these degrees of retrogression are reflected in the chemical compositions of the rocks allowing them to be grouped into the same five Classes in Table 7.1.

In general, the compositions in Table 7.1 are fairly variable, a feature of eclogites noted by other workers (e.g. Bryhni et al., 1969). Those in Table 7.2 have been placed into their respective groups on the basis of their mineral assemblages: the Fe-Ti types tend to contain more rutile and opaque phases, whilst the orthopyroxene- and kyanite-bearing types are self explanatory.

Excluding the more unusual chemistries (in Table 7.2) the data in Table 7.1 have been plotted on the discrimination diagram of Moine & de la Roche (1968). The points do not fall exactly within the defined basalt field, but slightly above it towards higher Fe and Ti contents (Fig. 7.1(b)). However, the rocks do not fall into the sedimentary fields, and appear to define an igneous trend. Adding the data from Table 7.2 to this diagram shows that the Fe-Ti type eclogites also fall onto this trend. The orthopyroxene-bearing eclogites are fairly scattered, but the group of three points towards high Ca + Mg values

TABLE 7.1 Whole-rock analyses and normative minerals of the 'bimineralic' eclogites

CLASS	I					II									III				IV						V		
	U152	U484	H1	D102	186	U124	U128	U404	U476	U517	M1	M26	T3	285	U237	U321	U366	U367	U127	U339	U356	U409	U485	284	291	U276	U405
MAJOR ELEMENTS (wt. %)																											
SiO ₂	47.67	45.63	47.80	47.54	47.01	45.45	45.31	45.80	46.35	46.65	48.06	45.86	46.63	45.48	47.43	48.44	45.67	47.70	44.99	49.35	45.66	46.04	47.40	48.37	48.14	47.49	46.99
TiO ₂	0.38	0.91	1.64	1.40	2.02	1.60	0.99	1.79	1.49	2.75	1.21	1.22	1.02	1.11	1.51	1.19	1.24	1.74	2.01	0.78	2.34	1.66	1.88	1.82	0.81	2.55	1.81
Al ₂ O ₃	15.77	16.62	13.86	12.22	12.18	15.00	15.87	16.58	15.31	12.16	16.32	16.40	15.13	15.46	12.52	15.03	16.57	16.41	16.20	16.51	16.26	17.37	18.85	15.64	15.43	16.67	18.21
Fe ₂ O ₃	1.47	3.55	1.91	2.06	2.48	2.05	1.91	3.19	2.39	0.45	1.32	3.15	1.45	1.66	2.62	1.05	2.18	1.87	2.04	0.53	3.01	1.79	1.51	2.15	1.60	1.71	2.11
FeO	8.11	9.26	10.97	10.78	10.90	12.54	12.49	11.65	12.29	9.85	10.56	8.89	10.53	10.86	7.70	12.47	9.84	11.89	12.74	8.24	11.35	10.76	10.57	11.98	10.39	12.72	9.08
MnO	0.16	0.18	0.16	0.21	0.18	0.18	0.18	0.19	0.19	0.18	0.18	0.17	0.18	0.18	0.18	0.19	0.16	0.28	0.17	0.15	0.20	0.15	0.18	0.23	0.22	0.20	0.13
MgO	14.23	12.92	7.12	10.42	10.90	9.79	12.21	8.69	9.85	9.81	10.83	11.62	11.91	12.45	12.06	9.05	10.50	9.36	9.07	8.96	7.59	8.01	5.02	6.70	11.43	5.32	6.69
CaO	10.33	8.73	13.56	11.55	11.58	9.23	7.69	8.77	8.87	12.98	9.37	9.30	10.20	9.85	11.23	10.49	9.89	7.25	8.39	10.27	9.18	10.42	10.61	9.23	8.14	9.18	8.45
Na ₂ O	1.69	1.77	2.20	1.61	2.17	2.64	2.10	3.05	2.60	2.65	2.13	2.14	2.01	2.33	2.21	2.23	2.21	2.72	2.57	3.06	2.23	2.45	2.72	2.36	1.28	3.29	3.20
K ₂ O	0.04	0.02	0.02	0.08	0.02	0.16	0.49	0.03	0.01	0.08	0.27	0.31	0.27	0.02	1.23	0.12	0.55	0.16	0.90	0.98	1.06	0.36	0.72	0.56	0.54	0.76	2.10
P ₂ O ₅	0.09	0.13	0.16	0.18	0.21	0.42	0.14	0.04	0.31	0.80	0.20	0.10	0.15	0.16	0.13	0.09	0.19	0.19	0.38	0.25	0.32	0.07	0.30	0.20	0.31	0.32	0.51
S	0.02	0.01	0.00	0.00	0.00	0.02	0.00	0.00	0.01	0.44	0.01	0.00	0.00	0.00	0.11	0.12	0.02	0.01	0.00	0.12	0.02	0.00	0.03	0.00	0.00	0.00	0.01
H ₂ O ^T	0.48	0.16	0.46	0.70	0.29	0.33	0.34	0.24	0.22	0.45	0.29	0.91	0.21	0.20	0.94	0.42	0.34	0.33	0.91	0.79	0.56	0.40	0.39	0.46	0.98	0.39	0.68
TOTAL	100.43	99.89	99.86	98.75	100.00	99.40	99.72	100.02	99.89	99.03	98.74	100.08	99.69	99.76	99.82	100.83	99.35	99.91	100.48	99.93	99.77	99.48	100.18	99.64	99.27	100.60	99.97
TRACE ELEMENTS (ppm)																											
Ni	512	292	75	116	385	218	400	189	180	184	196	251	255	280	124	212	239	207	253	136	165	184	46	74	226	60	139
V	138	148	249	-	-	174	87	181	174	263	-	-	-	-	341	256	210	202	175	175	224	151	254	-	-	249	130
Cr	715	82	51	569	565	257	103	313	245	814	90	115	251	126	168	321	149	177	82	219	144	113	90	143	229	73	102
Zn	68	-	97	83	81	100	104	111	104	104	77	73	56	79	75	114	101	173	118	98	122	116	99	111	85	132	90
Cu	122	-	63	20	50	21	72	14	32	45	41	20	26	42	259	121	45	56	46	40	175	13	56	39	58	199	18
Rb	3	0	3	3	4	1	16	0	0	5	8	9	8	3	40	6	19	4	26	20	25	5	13	17	17	24	61
Sr	63	333	303	350	180	430	332	142	345	537	609	166	168	170	225	89	226	221	456	355	91	148	418	264	332	246	432
Y	13	16	26	18	20	25	19	28	22	40	13	12	12	13	29	24	24	35	32	16	34	26	28	29	11	35	24
Zr	36	76	103	77	122	120	70	114	121	376	77	87	81	79	80	39	70	118	136	115	140	109	131	132	68	165	121
Pb	0	3	9	12	11	24	5	0	243	9	4	1	6	7	12	3	5	9	9	10	2	241	6	13	0	4	18
Ba	44	61	153	45	67	78	132	66	60	254	207	140	122	94	238	90	253	85	512	519	222	129	347	247	173	217	839
NORMATIVE MINERALS (%)																											
or	0.24	0.12	0.12	0.47	0.12	0.95	1.88	0.18	0.06	0.47	1.60	1.83	1.60	0.12	7.27	0.71	3.25	0.95	5.32	5.79	6.26	2.13	4.26	3.31	3.19	4.49	12.41
ab	14.30	14.98	18.62	13.62	18.36	22.34	17.77	25.18	22.00	21.07	18.02	18.11	17.01	19.38	16.02	18.87	18.70	23.02	21.15	23.88	18.87	20.73	23.02	19.97	10.83	27.84	20.51
an	35.33	37.35	27.89	25.88	23.44	28.61	32.43	31.46	30.08	21.05	34.17	34.23	31.47	31.67	20.61	30.65	33.67	32.10	30.01	28.42	31.23	35.34	37.10	30.43	34.76	28.43	29.12
ne	-	-	-	-	-	-	-	-	-	0.73	-	-	-	0.18	1.45	-	-	-	0.32	1.09	-	-	-	-	-	-	3.56
di	12.32	4.11	31.61	24.63	26.49	11.84	3.92	9.65	9.75	30.87	8.96	9.06	14.75	13.11	27.40	17.14	11.49	2.16	7.50	17.00	10.03	13.05	11.30	11.64	2.92	12.52	7.75
hy	13.89	17.84	5.80	20.32	8.08	3.36	7.60	1.71	10.69	-	16.73	8.85	6.60	-	-	14.18	1.91	20.88	-	-	8.33	1.82	4.77	22.16	37.31	1.11	-
ol	20.63	17.96	8.96	6.86	15.13	24.78	29.61	22.67	19.87	15.76	16.20	19.79	23.50	30.04	18.80	14.48	23.84	13.72	27.33	19.78	14.71	19.96	12.65	4.40	4.48	17.51	18.11
mt	2.13	5.15	2.77	2.99	3.60	2.97	2.67	4.63	3.47	0.65	1.91	4.57	2.10	2.41	3.80	1.52	3.16	2.71	2.96	0.77	4.36	2.60	2.19	3.12	2.32	2.48	3.06
il	0.72	1.73	3.12	2.66	3.84	3.04	1.88	3.40	2.83	5.22	2.30	2.32	1.94	2.10	2.87	2.26	2.36	3.31	3.82	1.48	4.44	3.15	3.57	3.46	1.54	4.84	3.44
py	0.04	0.02	-	-	-	0.04	-	-	0.02	0.82	0.02	-	-	-	0.21	0.23	0.04	0.02	-	0.23	0.04	-	0.06	-	-	-	0.02
ap	0.21	0.30	0.37	0.42	0.49	0.98	0.33	0.09	0.72	1.86	0.47	0.23	0.35	0.37	0.30	0.21	0.44	0.44	0.88	0.58	0.74	0.16	0.70	0.47	0.72	0.74	1.19
TOTAL	99.81	99.56	99.26	97.85	99.55	98.91	98.09	98.97	99.49	98.50	100.38	98.99	99.32	99.38	98.73	100.25	98.86	99.31	99.29	99.02	99.01	98.94	99.62	98.87	98.07	100.01	99.17

TABLE 7.2 Whole-rock and normative minerals of the Fe-Ti, orthopyroxene- and kyanite-bearing eclogites

	Fe-Ti type							Orthopyroxene-bearing					Kyanite-bearing	
Class	I	I	II	IV	IV	IV	IV	II	II	III	III	IV	III	III
	D8	D37	D89	U69	U160	U277	D118	U19	U408	U206	U243	U26	U30	U358
MAJOR ELEMENTS (wt. %)														
SiO ₂	44.04	41.24	40.77	39.63	43.15	45.17	45.15	51.90	45.09	48.78	49.51	46.06	54.56	45.43
TiO ₂	1.25	5.40	6.79	3.61	3.04	4.44	2.52	0.24	1.11	0.31	0.32	4.50	1.04	0.24
Al ₂ O ₃	14.88	11.96	6.85	15.69	16.59	10.45	15.11	9.59	11.71	8.09	7.83	11.21	15.52	20.19
Fe ₂ O ₃	2.07	3.84	4.00	3.32	2.59	2.68	4.59	1.80	2.72	2.04	1.40	0.81	0.73	1.49
FeO	15.33	18.90	20.27	17.75	13.32	15.60	11.47	6.07	14.94	7.98	8.80	17.44	10.45	8.23
MnO	0.21	0.32	0.32	0.34	0.23	0.25	0.26	0.20	0.23	0.20	0.18	0.24	0.19	0.18
MgO	8.58	6.40	7.49	5.68	7.21	6.87	6.31	17.69	15.10	17.91	19.96	7.14	7.29	8.27
CaO	12.38	10.06	10.44	9.61	9.87	10.07	9.12	9.89	6.23	10.34	10.13	9.24	8.96	12.04
Na ₂ O	1.31	1.24	2.11	1.60	2.32	2.62	2.69	0.91	0.55	0.74	0.65	1.75	0.91	1.76
K ₂ O	0.02	0.04	0.44	0.08	0.15	0.52	0.71	0.40	1.08	0.14	0.67	0.13	0.01	1.14
P ₂ O ₅	0.02	0.28	0.06	1.43	0.67	0.35	0.32	0.06	0.20	0.87	0.09	0.38	0.12	0.03
S	0.00	0.01	0.00	0.04	0.03	0.39	0.01	0.03	0.03	0.02	0.00	0.57	0.01	0.00
H ₂ O	0.37	0.58	0.58	0.32	0.46	0.71	0.59	0.35	0.47	1.73	0.60	0.93	0.31	0.43
TOTAL	100.66	100.27	100.12	99.08	99.62	99.93	99.15	99.12	99.45	99.71	100.14	100.12	100.09	99.34
TRACE ELEMENTS (ppm)														
Ni	57	58	27	22	142	57	89	441	451	518	536	79	214	44
V	765	1127	-	356	232	763	272	137	119	138	143	894	225	218
Cr	307	40	108	13	66	37	124	1896	219	2031	1952	54	183	76
Zn	96	141	109	197	111	148	109	69	126	87	101	142	64	83
Cu	74	116	156	62	21	436	113	14	45	34	40	536	89	52
Rb	3	3	8	1	4	8	17	18	78	26	24	0	0	32
Sr	52	109	126	187	306	442	199	49	284	122	136	279	50	927
Y	9	37	28	87	58	38	42	16	21	6	1	47	28	20
Zr	19	118	132	124	173	141	177	18	69	37	34	174	43	96
Pb	6	7	6	4	12	4	0	6	8	8	7	8	6	45
Ba	64	82	295	100	60	208	265	37	201	173	237	63	18	348
NORMATIVE MINERALS (%)														
or	0.12	0.24	2.60	0.47	0.89	3.07	4.20	2.36	6.38	4.37	3.96	0.77	0.06	6.74
ab	11.09	10.49	14.69	13.54	19.63	22.17	22.76	7.70	4.65	6.01	5.50	14.81	7.70	9.60
an	34.66	26.95	7.92	35.40	34.41	15.22	27.06	20.90	26.30	16.70	16.47	22.35	38.24	43.83
ne	-	-	1.71	-	-	-	-	-	-	-	-	-	-	2.87
di	22.14	17.69	36.22	2.47	8.41	26.91	13.24	22.05	2.69	23.08	26.52	17.53	4.48	12.82
hy	2.74	21.26	-	16.20	6.13	5.96	9.37	41.02	32.25	31.94	25.15	31.78	32.79	-
ol	23.91	6.24	17.24	15.29	18.33	11.87	9.48	1.27	19.91	10.09	18.91	(q 0.19)	(q 12.99)	20.83
mt	3.00	5.57	5.80	4.81	3.76	3.89	6.66	2.61	3.94	2.96	2.03	1.17	1.06	2.16
il	2.37	10.26	12.90	6.86	5.77	8.43	4.79	0.46	2.11	0.59	0.61	8.55	1.98	0.46
py	-	0.02	-	0.08	0.06	0.73	0.02	0.06	0.06	0.04	-	1.07	0.02	-
ap	0.05	0.65	0.14	3.32	1.56	0.81	0.74	0.14	0.47	2.02	0.21	0.88	0.28	0.07
TOTAL	100.08	99.37	99.22	98.44	98.95	99.06	98.32	98.57	98.76	97.80	99.36	99.10	99.60	99.38

also appear to lie on an extrapolation of this trend. Although these three points fall towards the field of calcic sediments, their position here is largely controlled by the Mg-rich nature of their chemistries. The overall basaltic nature of these eclogites relates them to the other eclogite pods observed in the Basal Gneiss Complex (Griffin et al., 1983).

Although eclogites tend to be generally basaltic in chemistry, they are very difficult to relate to any specific basalt type (cf. Bryhni et al., 1969). Not only does the heterogeneity of the rocks prevent this, but so do the chemical effects of both the prograde and retrograde metamorphism, and their limited size (Liégeois & Duchesne, 1981). Bard & Moine (1979) noted that there was little metasomatic effect on thick (several metres) sequences of metabasalts up to amphibolite/granulite facies. Similarly, Mysen & Heier (1972) attributed the lack of hydration of the Ulsteinvik eclogite at Hareidland to the very large size of the body which prevented easy ingress of fluids. Similar reasoning was applied to the large, essentially anhydrous retrogressed eclogite at Tverrfjella, in this study (section 3.1.1).

Lappin (1962) examined the amphibolitisation of eclogites and considered that there was a loss of Si^{4+} and Fe^{2+} from, and addition of: K^+ and H^+ to the bodies during the process; the behaviour of other elements was variable, Bryhni et al. (1969) compared the analyses of unaltered eclogite to an altered epidote-biotite-plagioclase rock, on the rim of an eclogite pod, and derived two sets of mobile elements. The most affected were: K^+ , Al^{3+} , H^+ (added), and Ca^{2+} , Si^{4+} , (Na^+) (removed). Bryhni et al. also considered that K^+ could be lost during prograde metamorphism since neither garnet nor clinopyroxene accept this element, as observed by Griffin & Murthy (1968). Forbes (1965) found that K_2O

was generally lower in eclogites than in basalts. Krogh (1980a) also noted that chemical alteration could occur prior to the final equilibration of the eclogite assemblage as well as during subsequent retrogression. He considered that portions of the margin to the eclogite pod suffered an introduction of material from the adjacent quartzofeldspathic gneiss causing an increase in Th, U and Zr in the eclogite. Evidence for chemical interaction between eclogites and the host gneisses has also been given by Brueckner (1977), who found that although eclogites have low Rb/Sr ratios they have high $^{87}\text{Sr}/^{86}\text{Sr}$ ratios, which he interpreted as Sr transfer from the gneiss to the eclogite. Krogh (1980a) also noted that the retrogressed samples had increased K_2O , and decreased Cr contents. The latter effect he attributed to the breakdown of the omphacitic clinopyroxene, which readily accepts Cr^{3+} into its structure (cf. Binns, 1967), and the non-acceptance of this element by the secondary amphiboles. However, such a situation is difficult to envisage since amphibole contains both Al^{3+} and Fe^{3+} for which Cr^{3+} may substitute, as in omphacitic clinopyroxenes.

Examining the analyses in Table 7.1 in relation to the degree of retrogression suffered by the rocks certain similarities exist with these findings. In Classes I and II, the best preserved eclogites, both K_2O and Rb, which substitutes for K in minerals (Taylor, 1965), are lower than in the other Classes, representing retrogressed rocks. However, K_2O is not particularly enriched in the retrogressed rocks, as found by Krogh, although sample U405 in Class V is an exception with 2.1 wt.% K_2O . Cr appears to show higher values in Class I (eclogites containing omphacitic clinopyroxenes) than in Classes IV and V. However, none of the other elements considered to be mobile by the authors above (e.g. Si, Ca, Al) appear to behave as such in these particular eclogites.

In fact Na behaves in a manner converse to that found by Lappin (1962) by increasing in value in the most retrogressed samples (Class V). In addition, Ba appears to increase in value in the retrogressed samples, again an element which substitutes for K in minerals (Taylor, 1965). The fairly constant Zr contents through the five Classes suggests that there has been little contamination by the host gneisses, as considered by Krogh (1980a).

As with the Garnet-Granulite (section 3.2.1), various elements have been plotted against Zr to investigate which of these have been mobilised during the metamorphic history of the rocks, the plots are shown in Fig. 7.2 and include the Fe-Ti types, and the kyanite- and orthopyroxene-bearing eclogites. The majority of the plots show very broad trends, often with substantial scattering of the points, particularly with K, Rb, Ni and Cr as expected. The most linear trends occur with P_2O_5 , Na_2O , TiO_2 , MgO and Y, typical of an igneous fractionation series (cf. Liégeois and Duchesne, 1981). Of these elements, Y, Ti and P are considered to be immobile during secondary alteration processes (Floyd & Winchester, 1978). However, the apparent covariance of Y and P_2O_5 , particularly well shown in the Fe-Ti types (Table 7.2) implies that Y is entering the apatite, as suggested by Krogh (1980a), perhaps making it a potentially mobile element. However, the apatite in the eclogites is in textural equilibrium with the eclogite facies garnet and clinopyroxene and is considered to be a primary phase which has survived any subsequent retrogression of the rocks and as such prevents Y from behaving as a mobile element.

In section 1.2 it was stated that the current debate over the origin of the eclogites in W Norway revolves around the question of whether the rocks are mantle-derived fragments, tectonically emplaced

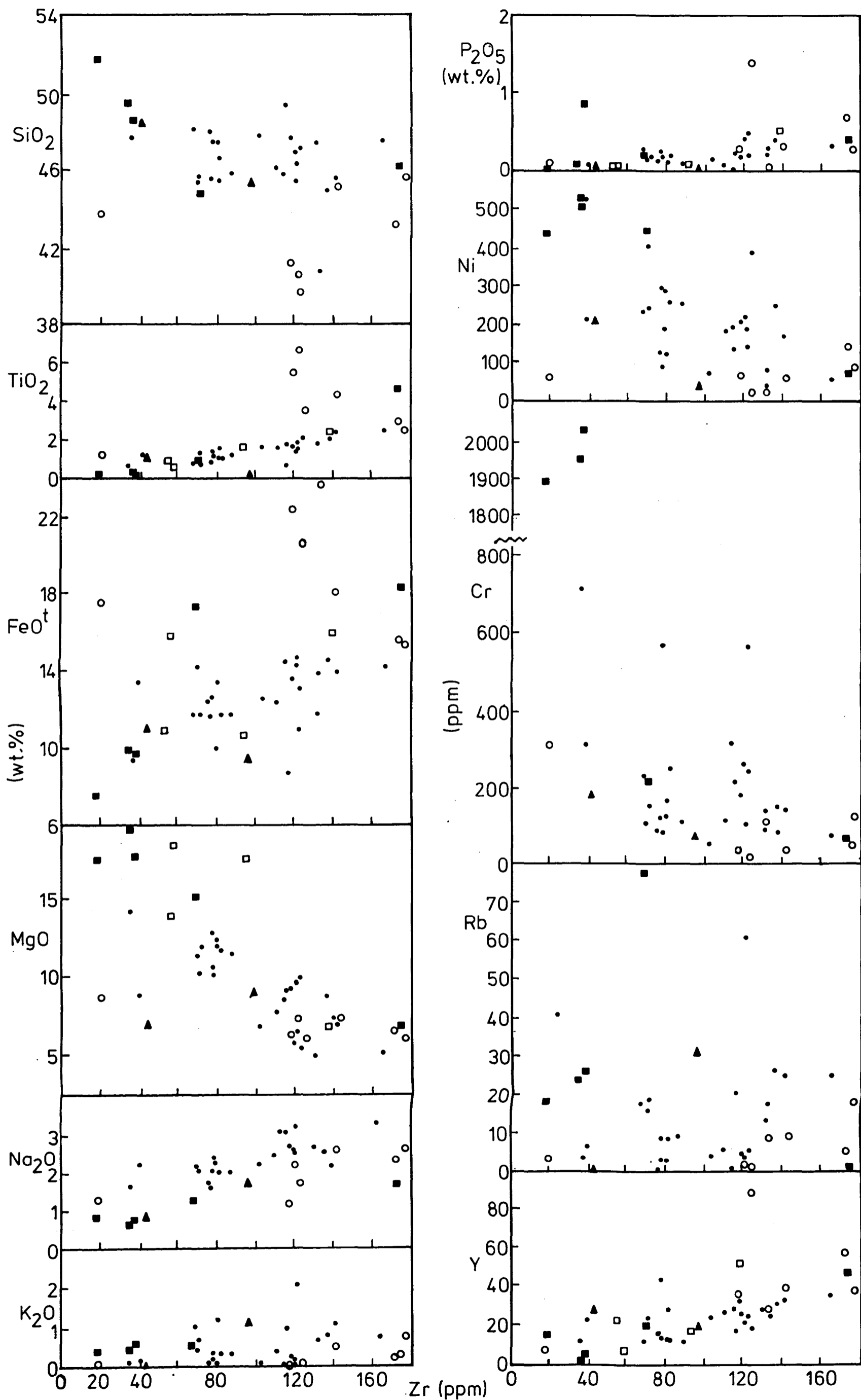


FIG. 7.2 Various elements vs. Zr, showing varying degrees of covariance. Symbols as in Fig. 7.1(b), open squares = garnet-peridotite.

into the crustal gneisses, or whether they are basaltic rocks metamorphosed within and together with the gneisses. The main proponents of the first hypothesis (M.A. Lappin and D.C. Smith) have never included a general geochemical investigation of the eclogites in their work (see section 1.2 for references), but rather rely on the mineral chemical data the rocks provide to infer high P (17-29 kbar) and T (700-900°C) conditions for the equilibration conditions of the rocks, indicative of the upper mantle. The apparent reluctance of these workers to utilise all the evidence provided by these rocks is regarded as a major omission. As seen here, the data from this fairly extensive suite of eclogites at Moldefjord defines a fairly good differentiated igneous trend, as seen by other workers who use the rock geochemical data of eclogites: e.g. Morgan (1970); Mysen & Heier (1972); Liégeois & Duchesne (1981); van Roermund (1983).

The distinction between different types of basalt is not always easy even for unmetamorphosed rocks; furthermore it has been shown that ". . . the composition of a given [eclogite] sample, particularly one from a small body [as here] may not be simply related to its original magmatic composition." (Griffin et al., 1983). Nevertheless, an attempt will be made here to classify the basaltic types involved from the analyses in Table 7.1 and 7.2.

In terms of normative minerals, tholeiitic basalts are characterised by high hy, appreciable q and rare ol, whilst alkaline-olivine basalts have conspicuous ol and often ne. From Tables 7.1 and 7.2 it appears that the majority of these eclogites are tholeiitic, often ol-tholeiitic with a few alkaline-olivine basalts, as found elsewhere in the Basal Gneiss Complex (Griffin et al., 1983). A few samples (e.g. U128, 285) have exceptionally high normative ol contents. If the

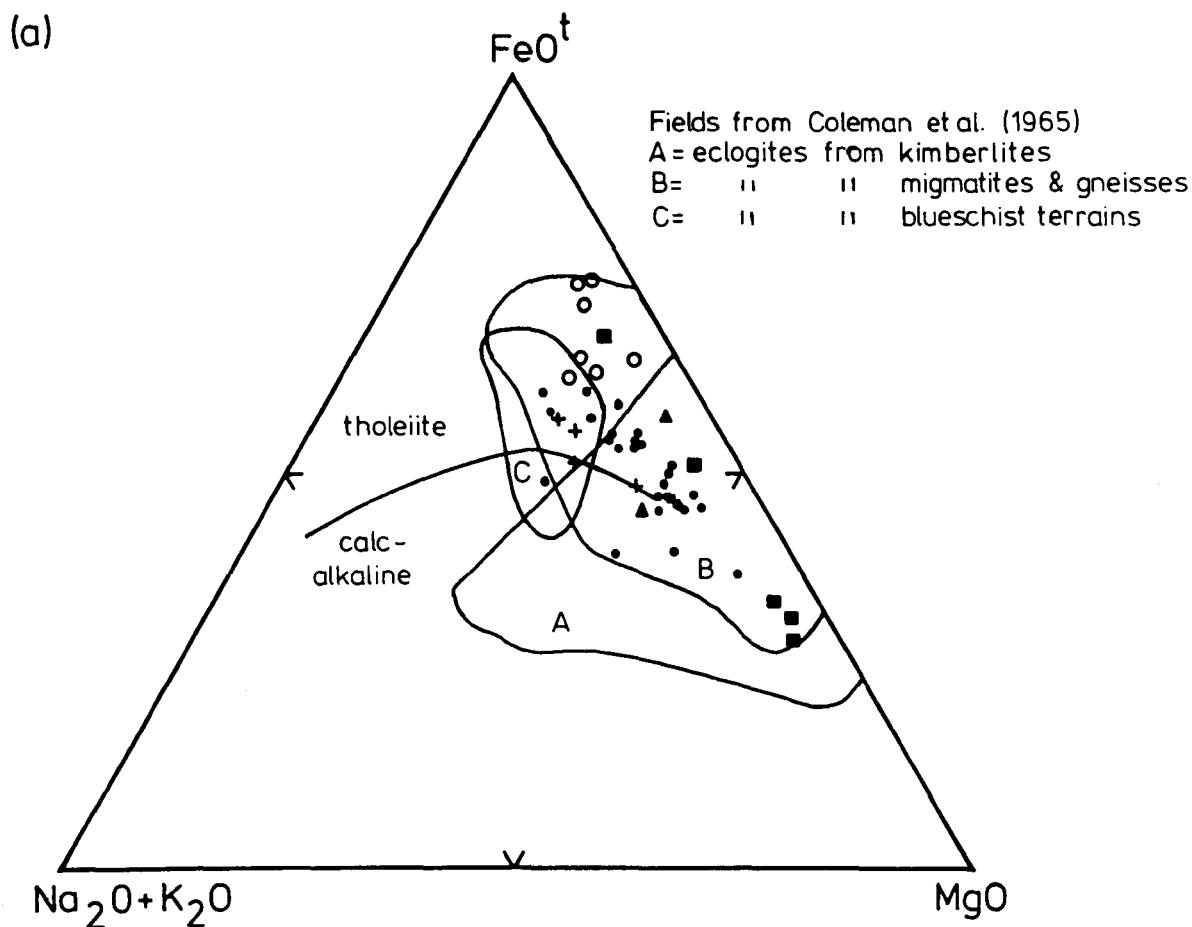
alkalies (Na_2O and K_2O) had been increased by metasomatism during retrogression and hydration of the eclogite, ne may appear in the norm., especially if the rock is particularly low in SiO_2 (e.g. U127 - see Appendix B for a discussion on the errors in normative mineral calculations). Consequently, the appearance of apparent normative alkali-olivine basalt type eclogites may simply be a reflection of the degree of metasomatism suffered by originally normative tholeiite type eclogites (cf. van Roermund, 1983).

As MgO , FeO^{t} and Na_2O give fairly good trends against Zr in Fig. 7.2, the AFM plot may be used with discretion with regard to the K_2O contents. Fig. 7.3(a) shows that the rocks describe a good tholeiitic trend with the Fe-Ti-type and orthopyroxene-bearing eclogites at the extremities of this trend. The spread of points towards the alkalies apex may be taken to reflect the metasomatic effects suffered by the rocks during retrogression. Otherwise, the points generally fall into field 'B' of Coleman et al. (1965), i.e. eclogites "with migmatite gneisses". Fig. 7.3(b) shows that the rocks plot across the alkaline/subalkaline division line of Irvine & Baragar (1971). However, the majority which plot in the alkaline field are interpreted to be the result of the metasomatic addition of K_2O to these samples during the retrogression of the rocks. However, the position of the majority of the points for the Fe-Ti type eclogites within the alkaline field may reflect a true alkali basalt composition for those rocks, for two reasons:

(i) Compared to the majority of the 'bimineralic' eclogites the Fe-Ti type eclogites do not contain large amounts of alkalies (Fig. 7.3(b)).

(ii) They also contain substantial quantities of TiO_2 , and lesser P_2O_5 as found in the eclogites of Sunnfjord which were classified as having alkali-olivine basalt chemistries by Krogh (1980a). Both plots

FIG. 7.3



(b)

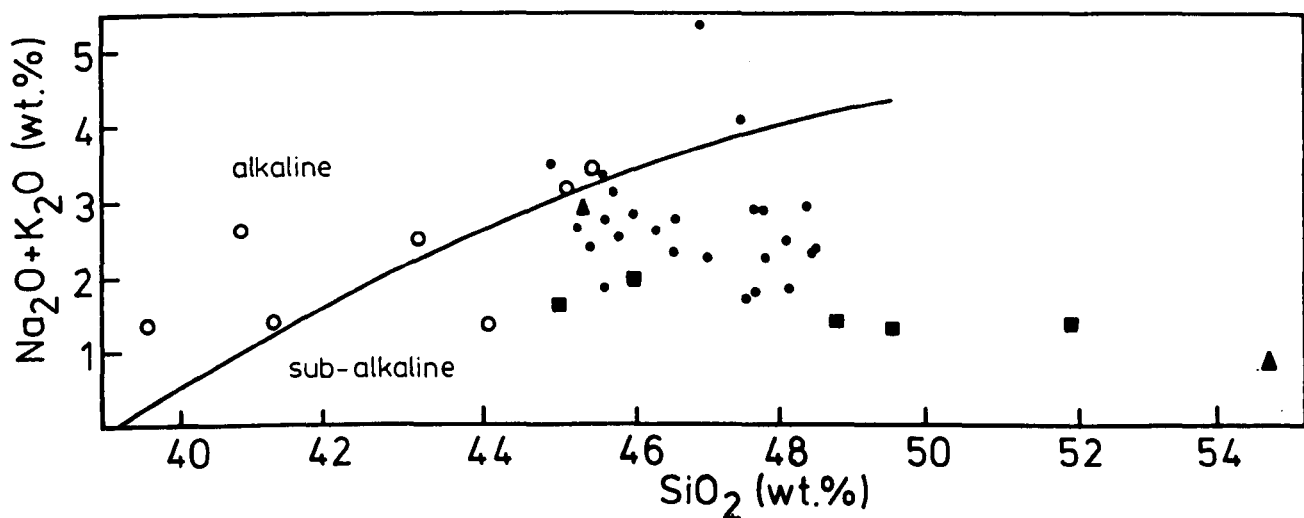


FIG. 7.3(a) AFM diagram for the eclogites and metadolerites, with tholeiite-alkaline division of Irvine & Baragar (1971). Note the large compositional range of the eclogites. Symbols as in FIG. 7.1(b), crosses = metadolerites.

(b) (Na₂O + K₂O) vs. SiO₂ for the eclogites. Alkaline-tholeiite division is after Irvine & Baragar (1971). Symbols as in FIG. 7.1(b).

7.3(a) and (b) show patterns very similar to those given by Griffin et al. (1983) for other eclogites in the Nordfjord area.

Various classification schemes based on the geotectonic origin of basalts have been devised using major and trace elements: Pearce & Cann (1973); Pearce (1975, 1976); Floyd & Winchester (1975, 1978); Winchester & Floyd (1976); Pearce & Norry (1979). In particular, the Zr-(Ti/100)-(Y x 3) diagram devised by Pearce & Cann (1973) has been widely used in classification studies (see a review by Zeck & Morthorst, 1982). The mobility of the major elements in these eclogites makes the use of the major elements for this classification unwise (e.g. the eigen values of Pearce, 1976).

The Zr-(Ti/100)-(Y x 3) diagram in Fig. 7.4(a) shows that the majority of the eclogite cluster in the centre of the plot; the Fe-Ti types tend towards the Ti apex, whilst the orthopyroxene- and kyanite-bearing eclogites are scattered and so not seem to follow any pattern. Using the diagram at the simplest level, the eclogites fall mainly into the within-plate-basalt (WPB) field, with a few in the ocean-floor-basalt (OFB) field. However, care has to be taken when interpreting this diagram in relation to rocks which plot within the WPB field since both Holm (1982) and Zeck & Morthorst (1982) consider that Pearce & Cann (1973) did not use sufficient data from continental tholeiites to define the WPB field sufficiently well. As a result, it is often the case that obviously continental tholeiites plot within the OFB field (e.g. the Palisades Sill - Zeck & Morthorst, 1982). Unfortunately, the alternative plot suggested by Holm ($TiO_2-K_2O-P_2O_5$) is unsuitable for the eclogites in question because of the mobility of K_2O . Even using the Zr/Y vs. Zr plot of Pearce & Norry (1979) gives an ambiguous pattern with the points falling between the WPB and OFB fields (Fig. 7.4(b)), whilst the Ti vs.

FIG. 7.4

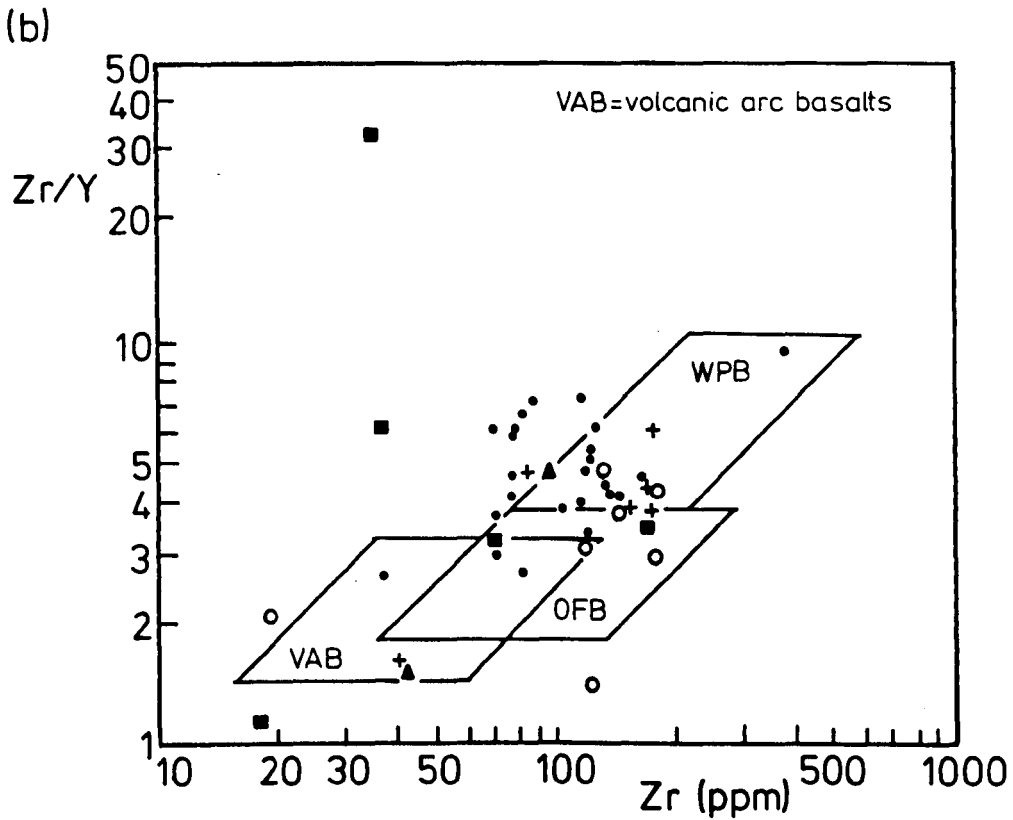
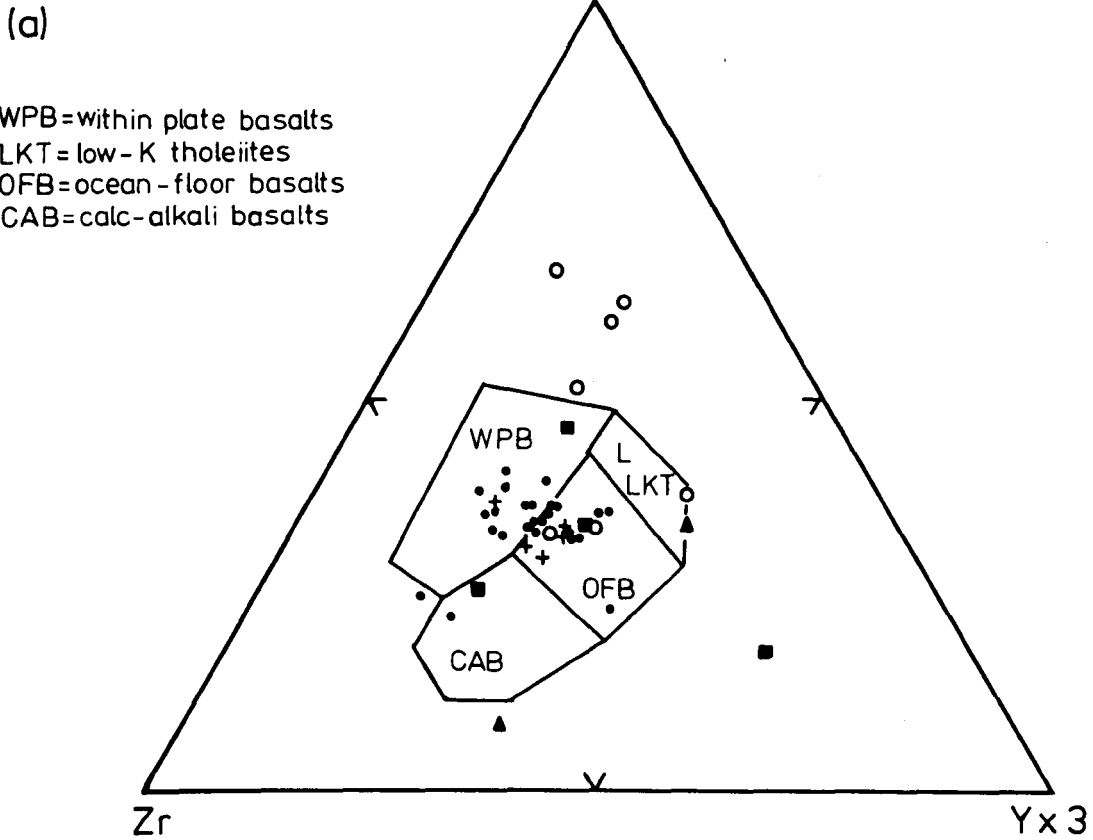


FIG. 7.4(a) Zr-(Ti/100)-(Y x 3) diagram after Pearce & Cann (1973) for the eclogites and metadolerites. Symbols as in FIG. 7.3(a).
(b) Zr/Y vs. Zr, log/log, diagram after Pearce & Norry (1979) for the eclogites and metadolerites. Symbols as in FIG. 7.3(a).

Cr plot of Pearce (1975) shows more points falling in the OFB field than in the tholeiite field (Fig. 7.5(a)).

The ambiguous geotectonic classification of the eclogites makes it difficult to make any definite conclusions as to their petrogenesis. If the rocks are accepted as representing metamorphosed oceanic basalts, which presently reside in gneisses interpreted as continental in origin, this would lead weight to the arguments of Lappin & Smith (1978) that the eclogites may represent fragments of ocean-floor basalt tectonically emplaced into the lower crust during continent-continent collision and subsequent subduction. If a continental WPB origin for the rocks is accepted, the present situation of the eclogites in continental gneisses need not be explained by invoking a tectonic introduction. The alternative explanation offered by Griffin et al. (1983) is that the eclogites represent in situ metamorphosed tholeiitic dykes and sills which have been subsequently disrupted into pods.

The Fe-Ti type eclogites, typified by increased amounts of rutile and ilmenite in their assemblages appear to be the most differentiated members of this basaltic suite of intrusions with lower Cr and Ni values, and higher Y and P_2O_5 values than the eclogites in Table 7.1. Apart from sample D8, these rocks have MgO values $< 8 \text{ wt.}\%$ and $FeO^t > 14 \text{ wt.}\%$ and as such can be classed as 'superferrian' (Griffin & Qvale, 1981). Eclogites of this type are present in the French Alps where they have been interpreted as representing meta-ferrogabbro dykes intruded into ophiolitic rocks (e.g. Mottana, 1977). The superferrian eclogites described by Griffin & Qvale (1981) at Raudkleivane Almklovdaalen were similarly interpreted. Since oceanic rocks are conspicuous by their absence in the vicinity of the eclogite pods at Moldefjord, such an origin can be discounted here. The high values of incompatible elements

FIG. 7.5

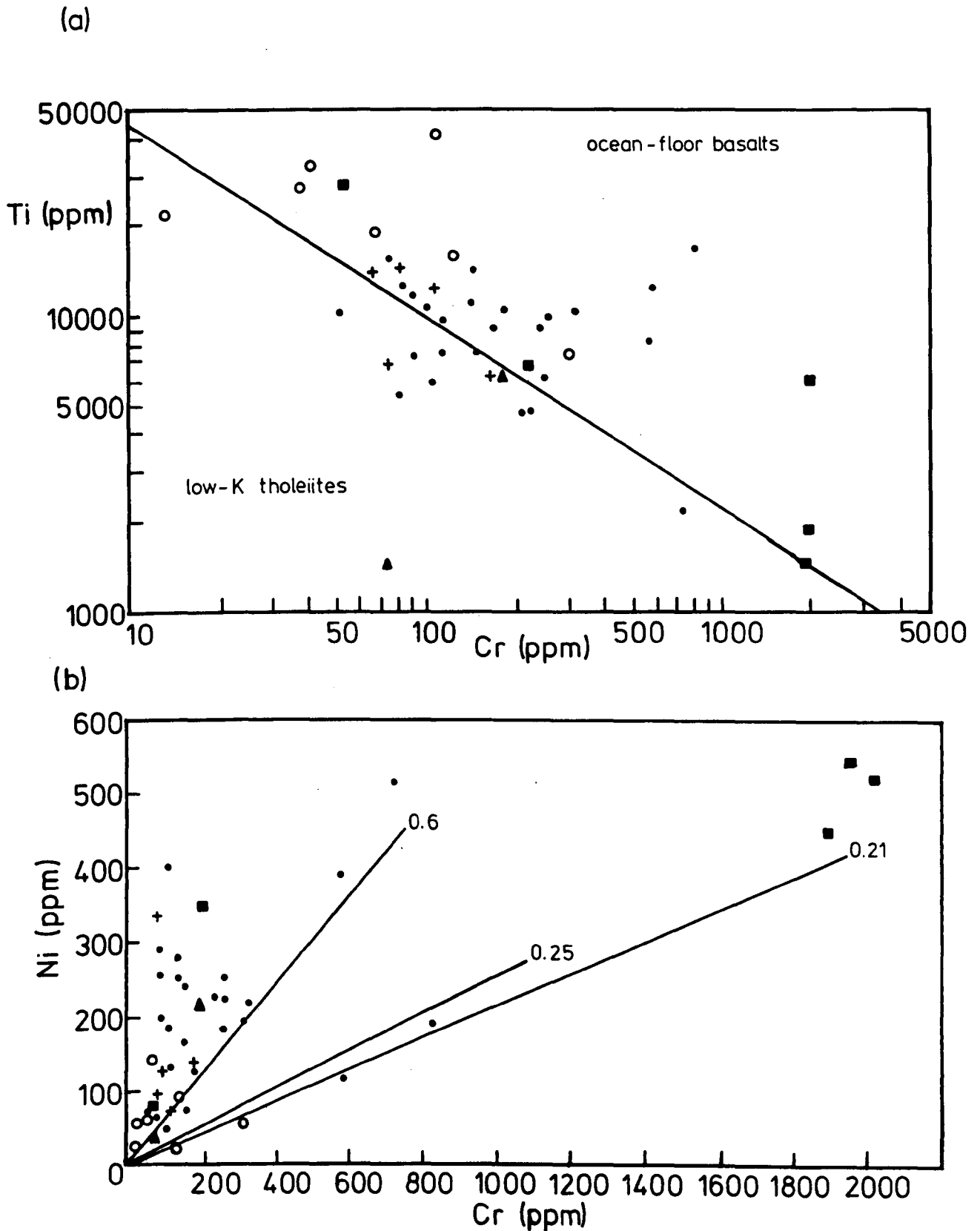


FIG. 7.5(a) Ti vs. Cr diagram after Pearce (1976) for the eclogites and metadolerites. Symbols as in FIG. 7.3(a).

(b) Ni vs. Cr after Griffin & Raheim (1973). Symbols as in FIG. 7.3(a).

(Ti, P and to a certain degree, Zr) suggest that these rocks represent late stage differentiates, perhaps with ilmenite and apatite appearing as cumulate phases. Indeed, the majority of the rocks plot away from the differentiation trends for FeO^t and TiO_2 in Fig. 7.2, typical of cumulate rocks which have extreme compositions and do not reflect liquid lines of descent (Cox et al., 1979, Chapter 12). Also, normative il is high in these rocks. Rocks similar in both chemistry and origin have been found in the Skaergaard layered intrusion in Greenland (Wager & Brown, 1947, p. 153, Analysis No. X) as ferrodiorites in the late-stage differentiates of the Upper Zone (UZ) of the intrusion. As at Skaergaard, the Fe-Ti type eclogites tend to have fairly high Mn and V contents (both enter ilmenite and magnetite, Taylor, 1965; Mason, 1966) and high Y (entering apatite). Some of the eclogites in Table 7.1 also display increased Fe, Ti and P contents (e.g. 186 and U217) suggesting that these are also rather more differentiated examples.

The orthopyroxene-bearing eclogites tend to have lower Al_2O_3 , TiO_2 , FeO and Na_2O , and higher SiO_2 , MgO, Ni and Cr contents than the non-orthopyroxene-bearing eclogites; they also have much higher normative hy contents. Sample U26, and to a certain extent sample U408, do not seem to fit in chemically with the other three samples of this type. In fact U26 has high Fe, Ti and V contents, with low MgO, Ni and Cr values more typical of Fe-Ti type eclogites, also, this sample is q-normative.

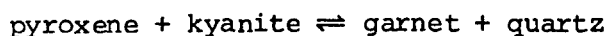
Excluding sample U26, the remaining samples have high hy and di with low ol and normative plagioclase compositions of $\sim \text{An } 75$, and as such can be termed eucrites. These fairly 'primitive' basalt compositions are also reflected in the position of the rocks on the AFM diagram (Fig. 7.3(a)), at the most magnesian end of the different-

iation trend. In their paper on orthopyroxene-eclogites, which included several of the samples analysed here (U19, U206, U243), Carswell et al. (1983) interpreted these rocks as representing the metamorphosed cumulates of igneous pyroxenes.

As the number of kyanite-bearing eclogites is limited to only two samples it is difficult to make any definite appraisal of this type. The situation is made more difficult by the fact that these two samples have rather different chemistries. Sample U358 has increased Al, Ca, Sr, Zr and Ba, and depleted Ni, Cr and Ti, when compared to the eclogites in Table 7.1, which may indicate some influence from the surrounding gneisses. Sample U30 does not show any significant increase in Al_2O_3 , as would be expected for a kyanite-bearing rock, but does possess a markedly increased SiO_2 value resulting in a fairly high q value in the norm. Unlike sample U358 this rock does not have increased alkali or Zr contents. Also, it possess a rather low MgO value.

From work in the Alps, Mottana (1977) found that eclogites contained in metasediments tended to have increased values of Si and Al. However, this sort of relationship does not appear to be the cause of the increased Sr and Al contents in these particular samples which are sited within the meta-igneous rocks of the Heterogeneous Quartzo-Feldspathic Gneiss Unit (U358) and the Augen Gneiss Unit (U30).

Godovikov & Kennedy (1968) have shown that the appearance of kyanite in eclogites is not actually due to the absolute Al_2O_3 content of the rock, but rather to the MgO:FeO:CaO ratio of the rock, and the prevailing pressure during metamorphism. The reaction:



goes to the right for FeO-rich eclogites and to the left in eclogites rich in MgO and low in FeO at high P. Their kyanite-bearing eclogites had MgO:FeO:CaO ratios of approximately 42:17:41, whilst the kyanite-free eclogites had ratios of 36:28:37. These ratios in samples U30 and U358 are 27:39:34 and 29:29:42 respectively which, from a comparison within the data of Godovikov & Kennedy, should prevent the formation of kyanite. This suggests that the high SiO_2 and Al_2O_3 contents of samples U30 and U358 do in fact play a part in the appearance of kyanite in those rocks, contrary to the opinion of Godovikov & Kennedy.

Although the two kyanite eclogite samples fall within the differentiation trend on the AFM plot (Fig. 7.3(g)), their trace element contents are variable and the rocks do not fall into any consistent field on the discrimination plots (Figs. 7.4 and 7.5). This variability in trace element composition, together with the increased Si and Al contents of these rocks makes it tempting to assign them to some sort of sedimentary protolith, perhaps quartz/clay mixes with basaltic volcanoclastics, to give the high Ni and Cr contents (see discussion in sections 3.2.3 and 5.2). However, kyanite-bearing eclogites are found elsewhere in the Basal Gneiss Complex (e.g. Bryhni, 1966; Lappin, 1966) although chemical analyses are mostly lacking for them. One of these examples is at Verpeneset, Nordfjord and an analysis is presented by Bryhni & Griffin (1971). Besides being low in FeO and rich in CaO, which should prevent the appearance of kyanite in eclogites according to Godovikov & Kennedy (1968), the rock is also rich in Al_2O_3 (19.97 wt. %), cf. sample U358. This particular rock appears as a layer within a bimineralic (clinopyroxene + garnet \pm quartz) eclogite, rather than as a discrete pod, and was interpreted as a metamorphosed gabbroic rock. Therefore, from this particular interpretation it appears perfectly feasible for the

two above samples (U30, U358), to have been derived from originally igneous rocks, although the relationship between these precursors and the tholeiites of the other eclogite types is unknown.

The consideration that perhaps some of these eclogites were originally igneous cumulates (e.g. the Fe-Ti and orthopyroxene-bearing types) suggested that the Ni-Cr plot would be diagnostic in that respect since Ni enters the olivine structure and Cr enters the clinopyroxene structure. A Ni vs. Cr plot is shown in Fig. 7.5(b) and shows that the majority of the eclogites have Ni/Cr ratios > 0.6 . Those samples falling towards high Ni/Cr ratios with high absolute Ni values (> 300 ppm) are considered to have had a predominance of olivine in their igneous precursors, perhaps with an almost picritic composition (cf. Krogh, 1980a). Unfortunately, this supposition is not supported by those particular samples having the highest normative ol contents (U152, 186, U128), although they are generally higher than the remainder of the eclogites. The interesting feature of this plot is that several samples fall away from this main group and form a trend with a Ni/Cr ratio ~ 0.21 which includes the three most Mg-rich orthopyroxene-bearing eclogites (U19, U206, U243) at very high Cr values. The position of these samples on this diagram is considered to support the interpretation of Carswell et al. (1983a) that these rocks had igneous precursors of clinopyroxene cumulates. The other four points on this separate trend represent both Fe-Ti type and bimineralic type eclogites. The former have been interpreted as late differentiate cumulates and their generally low Ni contents reflect the low olivine contents of such rocks, although it would appear that perhaps clinopyroxene was an important component of the cumulate assemblages in some of the rocks of this type. The two examples of bimineralic-type eclogite (D102 and U517) are, by virtue of

this low Ni/Cr ratio, distinct from the other eclogites of this type. However, the relatively high Cr contents of these two particular rocks are not supported by increased MgO contents, as found in the orthopyroxene-bearing types (see Tables 7.1 and 7.2) and their relationship to the other biminerally eclogites remains unknown at present. Indeed, the reason for the existence of this trend of seven samples at a fairly constant Ni/Cr ratio and one much lower than that observed in the remainder of the samples is also unknown. Griffin & Råheim (1973) used this diagram to illustrate the chemical difference between eclogites and metadolerites occurring at Kristiansund, where eclogites have Ni/Cr = 0.25 and metadolerites have Ni/Cr = 0.6. It is difficult to see why these seven particular rocks should be distinguished from the other eclogites on this basis as they all display a continuous sequence on the other elemental plots. However, it is interesting that these samples have Ni/Cr ratios more in line with the eclogites from the Kristiansund area.

7.2.2 The metadolerites

The chemical analyses of these rocks are given in Table 7.3. Overall they are broadly comparable in chemistry to the biminerally eclogites, although they contain slightly more K, Rb, Ba and Sr, and less Cr and Pb. Also, the chemistries are very similar to those published by Gjelsvik (1952) and Griffin & Råheim (1973) for metadolerites elsewhere in the Basal Gneiss Complex. Higher contents of Na₂O as well as K₂O were noted by Griffin & Råheim in their examples of metadolerite. As would be expected, the normative mineralogies of the eclogites and metadolerites are also similar, with the metadolerites displaying tholeiitic affinities and often substantial contents of normative olivine (e.g. U262 has 32.12% ol). As found in the eclogites,

TABLE 7.3 Whole-rock analyses and normative minerals of the metadolerites

	D41	286	U262	U266	U379	Average x σ	
MAJOR ELEMENTS (wt. %)							
SiO ₂	48.17	46.12	44.94	46.66	47.77	46.73	1.16
TiO ₂	1.03	2.38	1.12	2.09	2.30	1.78	0.59
Al ₂ O ₃	17.70	16.93	15.92	16.12	15.46	16.43	0.79
Fe ₂ O ₃	0.68	1.06	1.86	1.80	1.96	1.47	0.51
FeO	9.43	12.76	11.45	11.13	12.28	11.41	1.15
MnO	0.09	0.19	0.18	0.18	0.17	0.16	0.04
MgO	8.62	7.03	12.66	7.54	6.49	8.47	2.21
CaO	10.60	8.66	8.69	8.06	8.03	8.81	0.94
Na ₂ O	2.26	2.90	2.17	3.21	2.96	2.70	0.41
K ₂ O	0.45	0.98	0.38	1.14	1.11	0.81	0.33
P ₂ O ₅	0.11	0.44	0.17	0.39	0.53	0.33	0.03
S	0.00	0.00	0.05	0.00	0.12	0.03	0.05
H ₂ O	0.41	0.17	0.28	1.39	1.01	0.65	0.22
TOTAL	99.55	99.62	99.87	99.71	100.19	99.78	
TRACE ELEMENTS (ppm)							
Ni	138	130	336	80	93	155	92
V	-	-	154	266	241	220	48
Cr	168	84	74	110	67	101	37
Zn	65	109	97	113	132	103	22
Cu	67	80	55	92	55	70	14
Rb	17	23	11	28	26	21	6
Sr	377	390	321	443	309	368	49
Y	18	29	20	40	41	30	10
Zr	85	176	76	169	155	132	43
Pb	2	2	3	0	13	4	5
Ba	180	479	184	594	577	403	185
NORMATIVE MINERALS (%)							
or	2.66	5.79	2.25	6.74	6.56	4.79	
ab	19.12	24.02	18.36	26.11	25.05	22.85	
an	36.82	30.29	32.58	26.21	25.62	30.32	
ne	-	0.28	-	0.57	-	-	
di	12.30	8.13	7.65	9.23	8.91	9.22	
hy	9.81	-	1.13	-	12.45	3.97	
ol	15.05	23.68	32.12	21.80	11.93	21.48	
mt	0.99	1.54	2.70	2.61	2.84	2.13	
il	1.96	4.52	2.13	3.97	4.37	3.38	
py	-	-	0.09	-	0.23	0.06	
ap	0.26	1.02	0.40	0.91	1.23	0.77	
TOTAL	98.97	99.27	99.41	98.15	99.19	98.97	

high contents of K_2O in the metadolerites favours the appearance of ne in the norm (samples 286 and U266).

When plotted on the AFM diagram with the eclogites (Fig. 7.3(a)) the rocks lie on a similar tholeiitic trend to the eclogites although they are displaced towards the alkalis apex of the plot. On the other discrimination diagrams (Figs. 7.4 and 7.5(a)) these rocks generally fall within the group of points for the eclogites and display a comparable overlap between OFB and WPB fields.

As described in section 7.1.2, several other workers (e.g. Griffin & Råheim, 1973; Tjørudbakken, 1981; Mørk, 1982) have interpreted these metadolerites as representing the metastable relics of the transition between gabbroic igneous rocks and eclogites. From the preserved igneous textures in the samples studied here, and with their basaltic chemistries being akin to those of the eclogites, such an interpretation seems applicable to these rocks. As found with the eclogites the immobile elements appear to indicate an oceanic affinity for the igneous precursors to the metadolerite, but their occurrence within continental rocks is more favourable for an interpretation of these intrusions as dykes or sills.

Although Griffin & Råheim (1973) related the eclogites and metadolerites through their mineralogical relationships, they considered that the two rock types were chemically distinct, on the basis of their Ni and Cr contents (see section 7.2.1). However, when the data from Table 7.3 are plotted on Fig. 7.5(b), with the eclogites, the two rock types on the Molde Peninsula can be seen to have Ni/Cr ratios ≥ 0.6 and therefore are not chemically distinct on this basis.

From this chemical data it would appear that the eclogites and metadolerites are of the same geotectonic origin and therefore may be part

of the same intrusive event. If this is so, then a major question is: why have the metadolerites only developed partial eclogite facies assemblages and retained igneous textures? Griffin & Råheim (1973) attempted to answer this by saying that the eclogites and metadolerites were different rock suites, and that the metadolerites were intruded into a pre-existing eclogite-bearing terrain at high P and cooled from the basalt solidus to P-T conditions of $\sim 700^{\circ}\text{C}$ and 7-8 kbar where they achieved partial equilibration to eclogite assemblages. A slightly modified version of this interpretation, which allows the metadolerites and eclogites to be part of the same rock suite could be: the eclogite facies metamorphism followed soon after the intrusion of the majority of the basalts, but the precursors to the metadolerites were the very last stage of these intrusives and were emplaced at, or soon after the metamorphic culmination which allowed for only partial equilibration to eclogite facies assemblages. However, there are two points against such an idea:

(i) The chemistries of the metadolerites would be expected to show more differentiated chemistries, somewhat akin to the Fe-Ti type of eclogite, if they were the last intrusives of this basaltic suite.

(ii) Basaltic dyke intrusions are symptomatic of tensional crust-forming conditions (Clifford, 1968) rather than compressional orogenies and metamorphism. This second point would also seem to refute the idea of Griffin & Råheim (1973) that the metadolerites intruded into a regionally metamorphosed terrain.

An alternative answer to the question of the partly 'eclogitised' metadolerites could perhaps lie in the kinetic properties of the rocks and their constituent minerals. The preserved igneous textures of these rocks suggests that deformation could provide the necessary energy input

to allow the rocks to achieve eclogite-facies assemblages, i.e. the undeformed metadolerites have not gained full eclogite assemblages.

Indeed, Griffin & Råheim (1973) noted that those examples of metadolerite with sheared margins had been transformed to eclogite in those shears. Furthermore, such deformation may assist the influx of fluid phase, considered by many to be an integral part of the 'eclogitisation' process (e.g. Mørk, 1982, and see section 1.3).

7.2.3 The garnet peridotite

Qvale & Stigh (1983) have recently surveyed the occurrences of garnet-peridotites in Norway and have placed them into five groups:

- (i) layers and lenses within basic intrusions
- (ii) high temperature ultramafic intrusions
- (iii) ultramafic nodules/xenoliths
- (iv) so-called 'alpine-type' ultramafites
- (v) detrital serpentinites

Alpine-type peridotites are the most common in Norway and many attempts have been made to classify them on various bases: rock association, mineral assemblages or geotectonic origin (Jackson & Thayer, 1972; den Tex, 1969). From the lithological associations observed in the peridotite at Kolmannskog, it can be placed into the lherzolite sub-type of Jackson & Thayer (1972) whilst the association of the body with eclogite-bearing gneisses puts it in the 'root-zone' type of den Tex (1969). From the chemical analyses, given in Table 7.4, the rocks fall into the lherzolite sub-type of Qvale & Stigh (1983). However, from the minor occurrence of clinopyroxene in the Kolmannskog peridotite (section 7.1.3) the classification of the rocks as lherzolic does not seem really applicable. Also, it has been demonstrated by Carswell et al. (1983b) that two types of garnet peridotite occur in the Basal

TABLE 7.4 Whole-rock analyses and normative minerals of the Kolmannskog garnet-peridotite body

Rock Type	Gnt-Perid. EL7A	Gnt-Perid. 185	Eclogite 182	Gnt-Lherz E14
MAJOR ELEMENTS (wt. %)				
SiO ₂	47.12	44.18	48.24	44.73
TiO ₂	1.59	0.41	0.90	2.45
Al ₂ O ₃	9.31	6.34	8.99	16.37
Fe ₂ O ₃	4.60	5.75	5.95	2.91
FeO	6.60	10.77	5.30	13.44
MnO	0.20	0.28	0.23	0.21
MgO	17.92	26.67	13.92	7.02
CaO	8.67	3.51	14.73	10.01
Na ₂ O	1.21	0.06	1.04	2.76
K ₂ O	1.55	0.77	0.09	0.07
P ₂ O ₅	0.07	0.03	0.03	0.51
S	0.00	0.01	0.00	0.00
H ₂ O	1.05	0.75	0.39	0.28
CO ₂	0.20	0.12	0.11	0.30
TOTAL	100.09	99.65	99.92	101.06
TRACE ELEMENTS (ppm)				
Ni	812	469	152	64
V	236	106	-	350
Cr	1566	101	739	153
Zn	119	95	32	119
Cu	148	42	14	63
Rb	111	24	3	4
Sr	58	33	175	124
Y	17	8	23	52
Zr	93	56	53	138
Pb	20	6	35	6
Ba	57	130	57	104
NORMATIVE MINERALS (%)				
or	9.16	4.55	1.71	0.41
ab	10.24	0.51	8.80	23.36
an	15.40	14.76	19.60	32.07
di	21.42	1.96	41.89	11.81
hy	13.90	36.89	17.01	2.10
ol	18.68	30.64	0.95	20.47
mt	6.67	8.34	8.63	4.22
il	3.02	0.78	1.71	4.65
py	-	0.02	-	-
ap	0.16	0.07	0.07	1.19
TOTAL	98.65	98.52	100.37	100.28
$\frac{100 \text{ Fe}^{2+}}{(\text{Fe}^{2+} + \text{Fe}^{3+})}$	76.13	80.63	66.44	91.12
$\frac{100 \text{ Mg}}{(\text{Mg} + \text{Fe})}$	81.73	74.88	69.95	43.79
$\frac{100 \text{ Cr}}{(\text{Cr} + \text{Al})}$	1.62	0.16	0.80	0.09

Gneiss Complex of Norway designated Mg-Cr and Fe-Ti types and that only the Mg-Cr type can be labelled as 'alpine-type'. The Kolmannskog body was one of the peridotites used by Carswell et al. (1983b) to demonstrate the existence of the two chemical types of peridotite, and it falls into their Fe-Ti type. The analyses in Table 7.4 have low $100 \text{ Mg}/(\text{Mg} + \text{Fe})$ values (< 82) and low $100 \text{ Cr}/(\text{Cr} + \text{Al})$ values (generally < 1); peridotites in their Mg-Cr sub-type have values of 80-92 and > 1 for these respective ratios.

With regard to the normative minerals of these rocks, with the exception of sample 185, they can be related to basaltic, olivine-tholeiite compositions, although the contents of ol, hy and di are fairly variable. Sample 185 has high values of both ol and hy and normative plagioclase content of An 97. These rocks seem best related to compositional layers in an originally cumulate igneous body with varying proportions of olivine, orthopyroxene, clinopyroxene and plagioclase, whilst the extreme chemistry of sample 185 would appear to reflect an olivine-free orthopyroxene cumulate layer (+ plagioclase?) which cannot be realistically expressed in a normative composition (cf. Carswell et al., 1983b). One of the other Fe-Ti type garnet-peridotites cited in Carswell et al. (1983b) occurs at Eiksunddal on Hareidlandet. Originally studied by Schmidt (1963) he similarly interpreted the inter-layered eclogites, garnet-peridotites and garnet-pyroxenites as the metamorphosed equivalents of clinopyroxene-olivine norites with plagioclase-free olivine and orthopyroxene rich layers, an interpretation which has been supported by more recent whole-rock analyses (Carswell et al., 1983b).

Several interesting similarities exist between the Kolmannskog garnet-peridotite and certain types of the eclogites:

(i) the peridotite is generally Fe and Ti rich as are some of the eclogites, in addition these Fe-Ti type eclogites have generally low contents of Cr;

(ii) the orthopyroxene-bearing eclogites bear a broad mineralogical similarity to parts of the garnet peridotite body;

(iii) the Fe-Ti type eclogites, the orthopyroxene-bearing eclogites and the Fe-Ti garnet-peridotite have all been interpreted as having cumulate, igneous rock precursors.

From these similarities it is interesting to speculate whether there exists any genetic connection between the Fe-Ti garnet-peridotite and these eclogites.

Adding the data for the garnet-peridotite rocks to Fig. 7.2, which displays differentiation trends for the precursors of the eclogites shows that the garnet-peridotite rocks very broadly follow these trends, and particularly well on the Ti vs. Zr and Y vs. Zr plots. However, on the MgO vs. Zr and FeO^t vs. Zr plots, which show fairly well defined trends for the eclogites, the peridotite data is rather more scattered. This probably results from the fact that both MgO and FeO would be incorporated in the cumulate phases (olivine and pyroxene) of the igneous precursors to the peridotite. If a genetic association exists between the eclogites and the peridotite, these varying patterns could be related to the fractionation of a parental magma forming a layered igneous intrusion (the precursor to the peridotite). Successive fractionated liquids from this parent would be erupted as dykes or sills, as satellites to the layered intrusion (the precursors to the eclogites), which then display a constant liquid line of descent of the fractionating magma as shown on Fig. 7.2. The bulk rock compositions of the cumulate portions from the layered body do not generally reflect such a line of

descent because of their extreme chemistries (Wager & Brown, 1968; Cox et al., 1979, Chapter 12) (cf. the Fe-Ti type eclogites with cumulate Fe-Ti phases - see section 7.2.1) as seen with the MgO and FeO contents of the peridotite on Fig. 7.2. The fact that the TiO_2 and Y contents of the peridotite fall on the differentiation trend of the eclogites suggests that these elements were not incorporated into the cumulate phases of the original layered body.

7.2.4 Discussion of the geochemistry

As stated previously (section 7.2.1), the geotectonic classification of the eclogites and metadolerites based on their chemistries is ambiguous between ocean-floor and continental tholeiites, furthermore, much of the field evidence from these rocks is ambiguous. From the disposition of the pods in 'zones' with tectonic margins to the gneisses (Map A) it has been suggested that they have been disrupted from originally larger bodies (section 2.2.6). These larger bodies may have been fragments of oceanic crust tectonically emplaced into the crust, as suggested by Lappin & Smith (1978). Alternatively, they may have been in the form of dykes and sills of originally igneous rocks intruded into the crust. However, an eclogite on Midøy exhibits a back-veined relationship with the host gneisses. The vein contains an eclogite facies assemblage (omphacitic clinopyroxene + garnet + k-feldspar + plagioclase + quartz + biotite ± kyanite) and the vein/gneiss/eclogite relationships suggest that the vein originated before or during the eclogite facies metamorphism and that all three were metamorphosed in situ (Griffin & Carswell, 1983). This occurrence of a non-tectonic contact with the host gneisses suggests that not all of the eclogite pods have been tectonically emplaced into the crust and that an igneous dyke or sill origin for such examples is more likely. Evidence for a crustal,

igneous intrusive origin for the precursors to the eclogites is also supplied in the interpretation for the origin of the Kolmannskog garnet-peridotite. This is considered to represent a metamorphosed cumulate igneous body with a possible parental relationship to the precursors of the eclogites. Such igneous cumulates are not generally found in oceanic crust, although Mg-ultramafic cumulates are present (Windley, 1977, p. 280), and a continental, crustal igneous origin for such a body is preferred. If a genetic connection does exist between the precursor to the garnet-peridotite and the precursors to the eclogites it suggests that the latter were also originally intruded as igneous rocks.

The nature of the relationship between the pods of eclogite and the Garnet-Granulite of the Tverrfjella Unit (Chapter 3), which contains relict eclogite facies assemblages, is also important in this respect. Three points are important:

(i) The Tverrfjella Unit lacks pods of eclogite and is interpreted as a thrust unit of Palaeozoic rocks, emplaced prior to the metamorphic culmination (section 3.3).

(ii) The Garnet-Granulite reflects P-T estimates comparable to those of the eclogites elsewhere in the Basal Gneiss Complex ($\sim 770^{\circ}\text{C}$, 18 kbar) (section 3.4).

(iii) Radiometric dating of the Garnet-Granulite has shown that the eclogite facies mineralogy of the rocks equilibrated at the same time as that in the pods of eclogite, ~ 425 m.y. ago (Griffin & Brueckner, 1980). From these observations and interpretations it can be seen that if the pods of eclogite had been tectonically emplaced into the crust during Caledonian orogenesis, as suggested by Lappin & Smith (1978), they would be expected to occur in all the gneisses, including the Tverrfjella Unit since those rocks would also have been in a suitable position in

the crust to receive the bodies. However, as the pods of eclogite are absent from the Tverrfjella Unit it is considered that the precursors to the eclogites were not emplaced tectonically, but rather as igneous bodies, prior to the thrust emplacement of the Tverrfjella Unit.

This interpretation of the eclogites and metadolerites being disrupted from originally continuous sheets, perhaps as dykes and sills, in conjunction with their tholeiitic chemistries suggests that the Molde Peninsula has suffered a major period of igneous activity. This event may have been in several phases, giving the distinct chemical types of eclogites and perhaps involving a layered igneous intrusion now represented by the Kolmannskog garnet-peridotite. If such a hypothesis can be extended to cover the other occurrences of 'external' eclogites in the Basal Gneiss Complex it suggests that this part of Scandinavia has suffered the intrusion of a large number of igneous bodies, perhaps as a dyke swarm. 'External' eclogites elsewhere in Norway have been interpreted as representing metadolerite dykes, e.g. Krogh (1980a) with alkali-olivine basalts at Sunnfjord. The intrusion of large-scale dyke swarms has been noted in other parts of the world, often in association with layered basic/ultrabasic intrusions (Windley 1977, p. 69 and 107) and has been associated with tensional crustal conditions (Clifford, 1968).

The age of this igneous activity on the Molde Peninsula is constrained by two events:

(i) the age of the intrusion of the precursor to the Augen Gneiss Unit, at ~ 1500 m.y., within which the eclogites now lie;

(ii) the Caledonian ages derived from the eclogites, marking the minimum age of intrusion for their precursors (e.g. Griffin & Brueckner, 1980 at ~ 425 m.y.).

In the extensional tectonic regime for the N. Atlantic in the Proterozoic (2000-1000 m.y. ago) Bridgewater & Windley (1973) noted the extensive

development basic dykes in N America, Greenland, Sweden and Finland at $\sim 1200-1000$ m.y., generally with tholeiitic or olivine-tholeiitic chemistries in the same mobile-belt which instigated the formation of the anorthosite-rapakivi suite of intrusives (see Chapter 4 for discussion in relation to the Auger Gneiss Unit). Consequently, it seems reasonable to consider that the igneous precursors to the eclogites constituted part of this same period of dyke intrusion. By way of possible confirmation, recent Sm-Nd work has suggested that these meta-basic rocks are a manifestation of early Sveconorwegian (~ 1200 m.y.) basic magmatism (Mearns & Lappin, 1982). A U-Pb study by Gebauer et al. (1982) has suggested that some eclogites possess primary magmatic ages as old as 1500 m.y., Tørudbakken (1981) also produced a mid-Proterozoic age for the Vindøldalen dolerite at Surnadal (1517 ± 60 m.y.). These dates suggest that this phase of intrusion was a prolonged event perhaps not terminating until the opening of Iapetus ocean at ~ 850 m.y. (Windley 1977, p. 144).

If the timing of the intrusion of these basaltic rocks is correct it brings into question the Precambrian ages obtained for some eclogites (see Table 1.3). However, the date of ~ 1800 m.y. by McDougall & Green (1964) was obtained by the K-Ar method and it has been suggested that this age is inaccurate due to excess Ar in the amphibole used (Lappin & Smith, 1978). Mysen & Heier (1972) also suggested that the eclogite metamorphism was a Precambrian event (1682 ± 70 m.y.) from their dating of the gneisses enclosing the eclogites. The inference that the eclogite and gneisses were coeval is not considered sufficient reason for assigning the age derived from the gneisses to the eclogite.

Unfortunately the effects of the Sveconorwegian orogeny ($\sim 1200-900$ m.y.) on these intrusives are unknown. Although these effects are likely to have been minimal at the Molde Peninsula which lies at the

supposed N extent of the event (Zwart & Dornsiepen, 1978), the rocks further south must have been affected to a greater extent.

Although the suggestion of widespread basic dyke intrusion in the Basal Gneiss Complex during the late Proterozoic is only speculation, it does have two points in its favour:

(i) The extensional geotectonic regime of that period allows the formation of such a suite of rocks. As noted in Chapter 4, the map of Bridgewater & Windley (1973) for the Proterozoic shows Norway to be almost devoid of rocks of that age and this model helps to fill that gap.

(ii) The postulated time of intrusion fits in with the other events in the Basal Gneiss Complex constrained by radiometric work.

7.3 MINERAL CHEMISTRY AND P-T CALCULATIONS

7.3.1 The eclogites

The analyses of the phases in these rocks are given in Tables 7.5 (garnets), 7.6 (clinopyroxenes), 7.7 (amphiboles) and 7.8 (feldspars).

The garnets are very homogeneous and show little compositional zoning (see below). The compositions are plotted on Fig. 7.6(a) (after Coleman et al., 1965) which shows them to be essentially almandine-pyrope-grossular garnets with low calculated Fe^{3+} contents typical of eclogites (e.g. Coleman et al., 1965; Mysen & Heier, 1972). The minerals fall into fields B and C of Coleman et al., i.e. eclogites in migmatite, granulite and amphibolite rocks, and in glaucophane and low-amphibolite rocks respectively. In general they are very similar in composition to those of the Ulsteinvik eclogite on Hareidlandet (Mysen & Heier, 1972) but slightly less grossular rich than those from the eclogites in the Seve Nappe (van Roermund, 1983). Compared to the garnet in the high-pressure granulite in the Heterogeneous Quartzo-Feldspathic Gneiss Unit

TABLE 7.5 Analyses of garnets from the eclogites

(wt. %)	D8 Core (3)	D8 Rim (3)	D30 Core (1)	D30 Rim (1)	D38 Core (2)	D38 Rim (2)	D102 Core (1)	D102 Rim (1)	D102 Rim (1)	283 Core (4)	283 Rim (4)	284 Core (1)	284 Rim (1)	284 Rim (1)	M7 Core (1)	M7 Rim (1)	M26 (4)
SiO ₂	36.47	38.15	39.73	39.73	37.36	37.82	39.25	39.42	39.66	40.05	40.23	38.45	38.34	38.60	38.11	38.04	40.28
TiO ₂	0.06	0.05	0.02	0.04	0.03	0.05	0.02	0.02	0.02	0.03	0.03	0.02	0.02	0.02	0.04	0.02	0.02
Al ₂ O ₃	21.20	21.24	22.09	22.03	20.61	20.45	21.81	21.99	21.94	22.42	22.48	21.53	21.44	21.15	21.13	21.19	22.54
Cr ₂ O ₃	0.04	0.05	0.00	0.00	0.01	0.01	0.13	0.08	0.08	0.02	0.01	-	-	-	0.02	0.00	0.03
FeO	24.55	24.56	22.38	22.64	31.90	32.65	23.96	23.58	23.45	21.59	21.65	25.13	25.54	26.38	27.32	28.08	19.81
MnO	0.32	0.35	0.47	0.39	1.01	1.08	0.54	0.50	0.51	0.35	0.37	0.57	0.68	0.67	0.66	0.62	0.33
MgO	6.63	6.54	8.90	9.18	4.75	4.85	9.96	10.22	10.47	12.98	13.07	6.56	6.58	6.39	5.32	4.98	12.77
CaO	9.43	9.26	7.24	6.46	4.60	4.36	4.81	4.72	4.64	3.59	3.46	8.17	7.71	7.29	7.51	7.50	4.93
TOTAL	101.00	100.51	100.88	100.48	100.56	101.57	100.64	100.67	100.89	101.23	101.48	100.64	100.53	100.68	100.27	100.62	100.82
MINERAL FORMULAE (12 OXYGENS)																	
Si	2.950	2.941	3.001	3.010	2.953	2.964	2.975	2.979	2.987	2.965	2.970	2.962	2.960	2.984	2.976	2.969	2.983
Ti	0.004	0.003	0.001	0.003	0.002	0.003	0.001	0.001	0.001	0.002	0.002	0.001	0.001	0.001	0.003	0.001	0.001
Al	1.916	1.930	1.967	1.968	1.920	1.889	1.948	1.959	1.948	1.956	1.956	1.955	1.951	1.927	1.945	1.949	1.967
Cr	0.003	0.003	-	-	0.001	0.001	0.008	0.005	0.005	0.001	0.001	-	-	-	0.002	-	0.002
Fe ³⁺	0.175	0.179	0.029	0.008	0.170	0.178	0.093	0.076	0.071	0.109	0.100	0.120	0.127	0.105	0.097	0.110	0.064
Fe ²⁺	1.400	1.405	1.384	1.427	1.938	1.963	1.425	1.415	1.406	1.228	1.237	1.498	1.522	1.601	1.687	1.723	1.163
Mn	0.021	0.023	0.030	0.025	0.068	0.072	0.035	0.032	0.033	0.022	0.023	0.037	0.045	0.044	0.044	0.041	0.021
Mg	0.758	0.751	1.002	1.037	0.559	0.567	1.125	1.151	1.175	1.432	1.438	0.753	0.757	0.736	0.619	0.579	1.409
Ca	0.775	0.765	0.586	0.525	0.389	0.366	0.390	0.382	0.375	0.285	0.274	0.674	0.638	0.604	0.629	0.627	0.391
TOTAL	8.002	7.997	8.000	8.003	8.000	8.003	8.000	8.000	8.001	8.000	8.001	8.000	8.001	8.002	8.002	7.999	8.001
END-MEMBERS (%)																	
ANDR	8.73	9.01	1.48	0.41	8.61	8.87	4.65	3.76	3.53	5.45	4.99	6.07	6.41	5.20	4.81	5.53	3.19
PYROPE	25.66	25.62	33.46	34.98	18.94	19.09	37.80	38.62	39.33	48.27	48.39	25.42	25.57	24.66	20.79	19.50	47.23
SPESS	0.70	0.78	1.00	0.85	2.29	2.42	1.17	1.07	1.09	0.74	0.78	1.26	1.50	1.47	1.47	1.38	0.69
GROSS	17.26	16.72	18.09	17.28	4.49	3.34	8.04	8.79	8.72	4.03	4.14	16.66	15.09	14.99	16.15	15.55	9.80
ALM	47.41	47.72	45.97	46.48	65.69	66.15	47.91	47.48	47.05	41.39	41.62	50.57	51.39	53.64	56.65	58.00	38.97
SCHORL	0.12	0.10	-	-	0.06	0.10	0.04	0.04	0.04	0.06	0.06	0.04	0.04	0.04	0.08	0.04	0.04
UVAR	0.12	0.16	-	-	0.03	0.03	0.39	0.24	0.24	0.06	0.03	-	-	-	0.06	-	0.09

Fe³⁺ calculated by charge balance

Figures in brackets refer to the number of analysis points

TABLE 7.6 Analyses of clinopyroxenes from the eclogites

(wt. %)	D8 Core (1)	D8 Rim (4)	D30 Core (1)	D30 Rim (1)	D38 Core (2)	D38 Rim (2)	D102 Core (1)	D102 Rim (1)	283 Core (4)	283 Rim (3)	284 Symplectites (1)	284 Symplectites (1)	M7 Symp. (1)	M26 (3)
SiO ₂	52.80	53.13	51.88	52.78	52.77	52.72	54.63	54.69	55.56	55.58	50.38	50.55	50.63	55.36
TiO ₂	0.22	0.22	0.17	0.07	0.11	0.13	0.09	0.13	0.15	0.16	0.31	0.29	0.50	0.15
Al ₂ O ₃	6.41	6.06	6.34	8.08	2.46	2.84	5.43	5.86	7.11	7.12	4.81	4.21	3.98	8.73
Cr ₂ O ₃	0.07	0.06	-	-	0.04	0.01	-	-	0.02	0.01	-	-	-	0.02
FeO	8.57	8.52	7.09	6.48	15.43	15.52	6.60	6.92	5.48	5.49	9.80	9.21	11.66	4.41
MnO	0.03	0.03	0.13	0.10	0.12	0.14	0.06	0.10	0.03	0.03	0.14	0.13	0.15	-
MgO	10.49	10.54	11.88	10.74	9.17	9.30	11.58	11.35	11.31	11.36	11.52	12.05	10.85	10.35
CaO	19.11	19.09	20.81	18.39	17.31	17.50	17.47	16.99	16.44	16.40	20.64	21.55	20.44	15.71
Na ₂ O	3.05	3.10	1.67	3.04	3.30	3.01	4.06	4.15	4.85	4.76	1.19	0.94	1.15	5.28
TOTAL	100.75	100.75	99.97	99.68	100.71	101.17	99.92	100.19	100.95	100.91	98.79	98.93	99.36	100.01
MINERAL FORMULAE (6 OXYGENS)														
Si	1.924	1.935	1.908	1.929	1.965	1.958	1.977	1.976	1.975	1.977	1.898	1.900	1.913	1.978
Ti	0.006	0.006	0.005	0.002	0.003	0.004	0.002	0.004	0.004	0.004	0.009	0.008	0.014	0.004
Al	0.275	0.260	0.275	0.348	0.108	0.124	0.232	0.250	0.298	0.299	0.214	0.187	0.177	0.368
Cr	0.002	0.002	-	-	0.001	0.000	-	-	0.001	0.000	-	-	-	0.001
Fe ³⁺	0.079	0.074	0.019	0.006	0.192	0.169	0.094	0.083	0.079	0.067	0.060	0.065	0.053	0.034
Fe ²⁺	0.182	0.185	0.199	0.192	0.288	0.313	0.106	0.126	0.084	0.097	0.248	0.224	0.315	0.098
Mn	0.001	0.001	0.004	0.003	0.004	0.004	0.002	0.003	0.001	0.001	0.004	0.004	0.005	-
Mg	0.570	0.572	0.651	0.585	0.509	0.515	0.625	0.611	0.599	0.602	0.647	0.675	0.611	0.551
Ca	0.746	0.745	0.820	0.720	0.691	0.696	0.678	0.658	0.626	0.625	0.833	0.868	0.827	0.601
Na	0.215	0.219	0.119	0.215	0.238	0.217	0.285	0.291	0.334	0.328	0.087	0.069	0.084	0.366
TOTAL	4.000	3.999	4.000	4.000	3.999	4.000	4.001	4.002	4.001	4.000	4.000	4.000	3.999	4.001
END-MEMBERS (%)														
Ca-Ti-Ts	0.60	0.60	0.47	0.19	0.31	0.36	0.25	0.35	0.40	0.43	0.88	0.82	1.42	0.40
Ca-Ts	6.43	5.26	8.26	6.75	2.85	3.50	1.79	1.74	1.74	1.44	8.47	8.35	5.88	1.41
Ko	0.20	0.17	-	-	0.12	0.03	-	-	0.06	0.03	-	-	-	0.06
Jd	13.46	14.29	10.03	20.91	4.48	4.70	19.10	20.77	25.49	26.12	2.66	0.32	3.12	33.13
Ac	7.88	7.43	1.88	0.62	19.23	16.94	9.39	8.30	7.87	6.68	6.03	6.53	5.30	3.39
Di	51.12	51.79	55.84	48.80	41.88	40.70	56.05	52.56	52.94	52.20	53.17	58.01	49.50	49.53
Hd	16.36	16.77	17.09	16.00	23.73	24.72	9.50	10.85	7.44	8.37	20.43	19.27	25.56	8.80
Jo	0.08	0.08	0.35	0.26	0.31	0.35	0.17	0.26	0.08	0.08	0.37	0.36	0.39	-
En	2.92	2.71	4.64	4.84	4.51	5.38	3.21	4.27	3.48	4.01	5.75	4.75	5.80	2.79
Fs	0.93	0.88	1.42	1.59	2.55	3.27	0.54	0.88	0.49	0.64	2.21	1.58	2.99	0.50
Rh	0.01	0.01	0.03	0.03	0.03	0.05	0.01	0.02	0.01	0.01	0.04	0.03	0.05	-

Fe³⁺ calculated on the basis of the structural formula after Mysen & Griffin (1973)

Figures in brackets refer to the number of analysis points

TABLE 7.7 Analyses of amphiboles
from eclogites

(wt. %)	284 (5)	M7 (2)	M26 (3)
SiO ₂	41.27	41.17	44.12
TiO ₂	1.78	1.86	0.97
Al ₂ O ₃	12.30	11.42	13.57
FeO	15.32	18.84	8.22
MnO	0.07	0.09	-
MgO	10.89	9.31	15.72
CaO	11.29	10.65	10.80
Na ₂ O	1.84	2.07	2.95
K ₂ O	1.34	1.18	0.93
TOTAL	96.10	96.59	97.28
MINERAL FORMULAE (23 OXYGENS)			
Si	6.223	6.242	6.291
Ti	0.202	0.212	0.104
Al	2.186	2.041	2.281
Fe ³⁺	0.520	0.753	0.642
Fe ²⁺	1.412	1.636	0.339
Mn	0.009	0.012	-
Mg	2.448	2.104	3.342
Ca	1.824	1.730	1.650
Na	0.538	0.609	0.816
K	0.258	0.228	0.169
TOTAL	15.620	15.587	15.634

Fe³⁺ calculated by the iterative method
of Leake (1978)

Figures in brackets indicate the number
of analysis points

TABLE 7.8 Analyses of feldspars associated with symplectic clinopyroxenes in eclogites

(wt. %)	284	M7
SiO ₂	63.54	64.84
Al ₂ O ₃	22.67	21.86
FeO	0.15	0.19
CaO	4.00	3.35
BaO	0.06	-
Na ₂ O	9.05	9.88
K ₂ O	0.30	0.39
TOTAL	99.77	100.51
MINERAL FORMULAE (8 OXYGENS)		
Si	2.815	2.852
Al	1.184	1.133
Fe	0.006	0.007
Ca	0.190	0.158
Ba	0.001	-
Na	0.778	0.842
K	0.017	0.022
TOTAL	4.991	5.014
END-MEMBERS (%)		
Ab	78.9	82.4
An	19.3	15.5
Or	1.8	2.1

FIG. 7.6

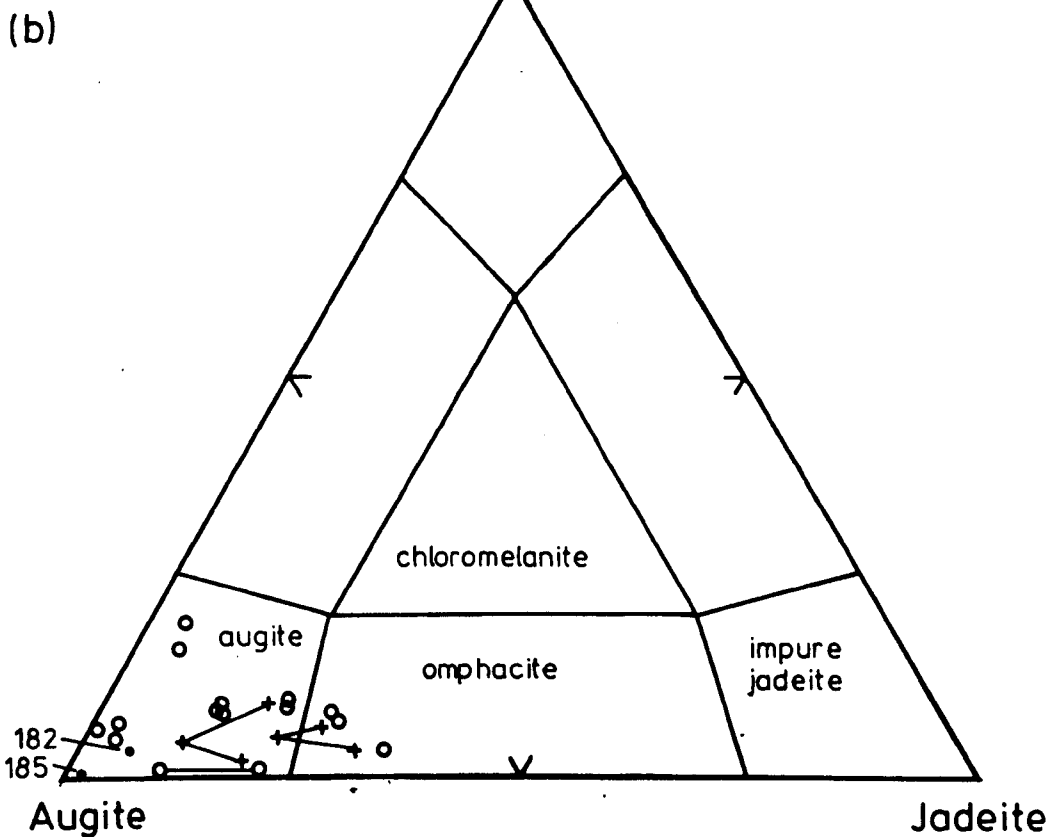
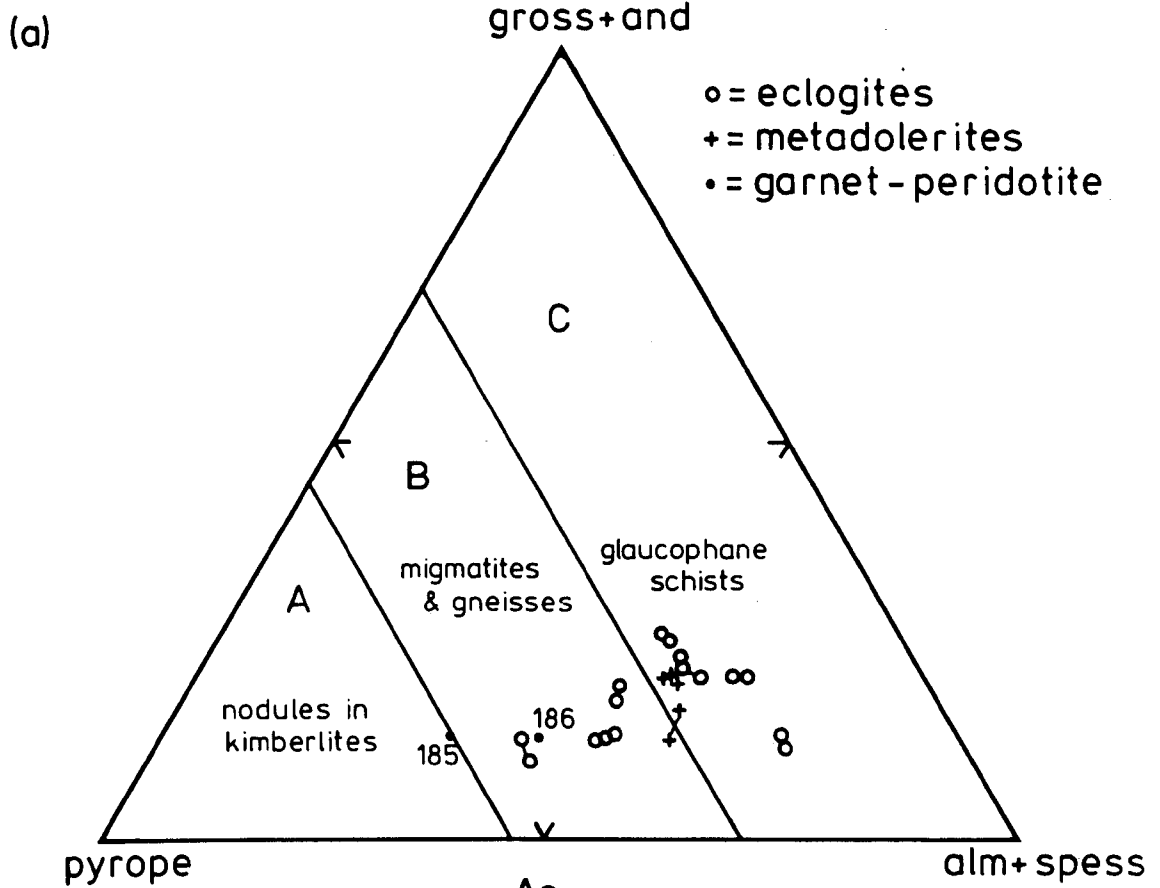
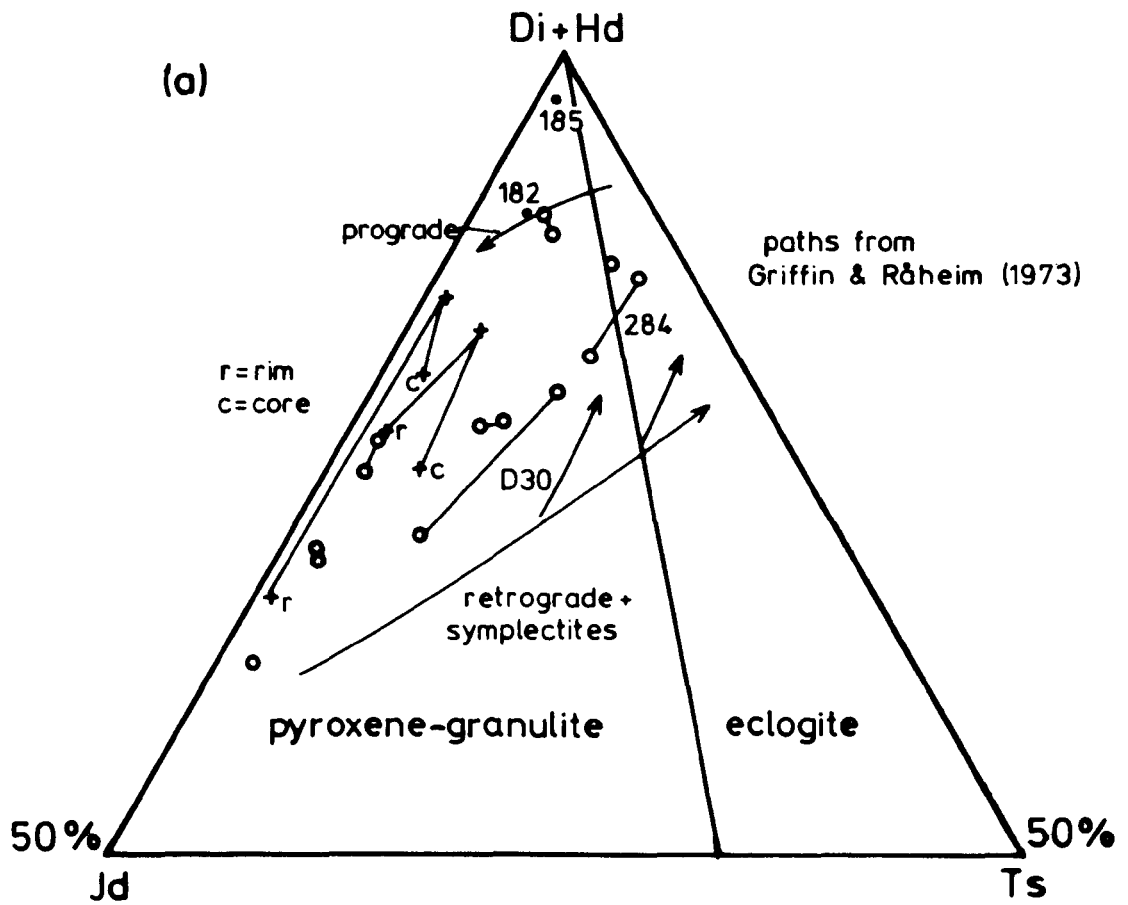


FIG. 7.6(a) (Grossular + andradite)-(almandine + spessartine)-pyrope diagram after Coleman et al. (1965) with their divisions of eclogite types. Note lack of any consistent zoning in the garnets.

(b) Acmite-jadeite-augite diagram and divisions after Essene & Fyfe (1967).

FIG. 7.7



(b)

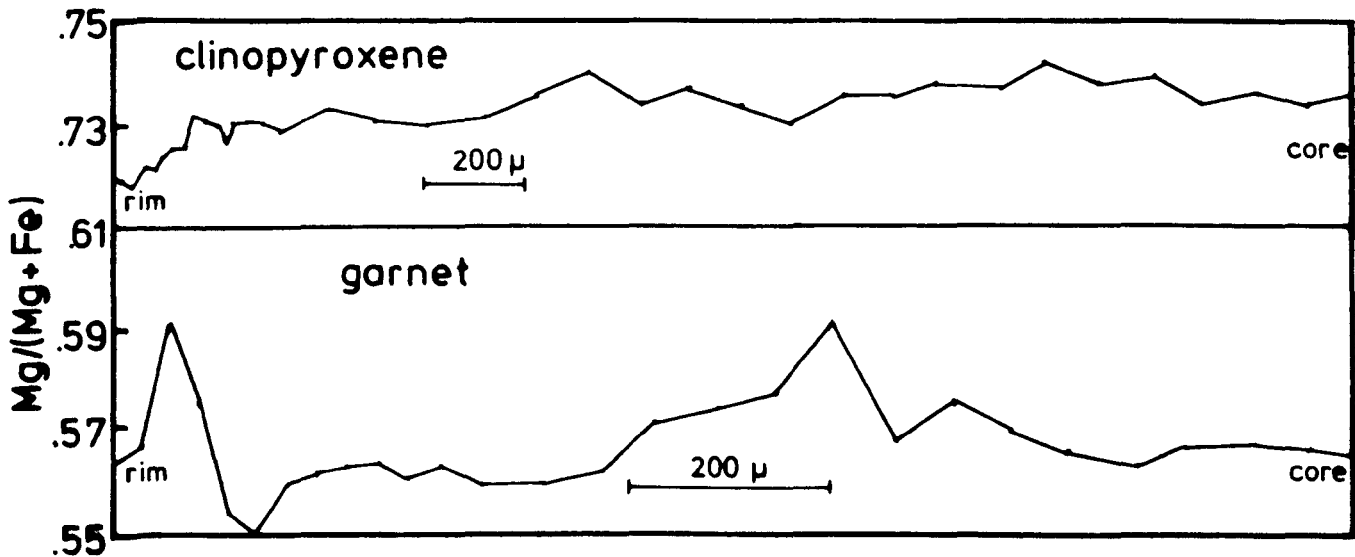


FIG. 7.7(a) (Diopside + hedenbergite)-tschermakite-jadeite diagram with eclogite/pyroxene-granulite division of Lovering & White (1969). Note the zoning profiles of the metadolerite clinopyroxenes.

(b) Compositional zoning profiles across a clinopyroxene and a garnet from sample D8.

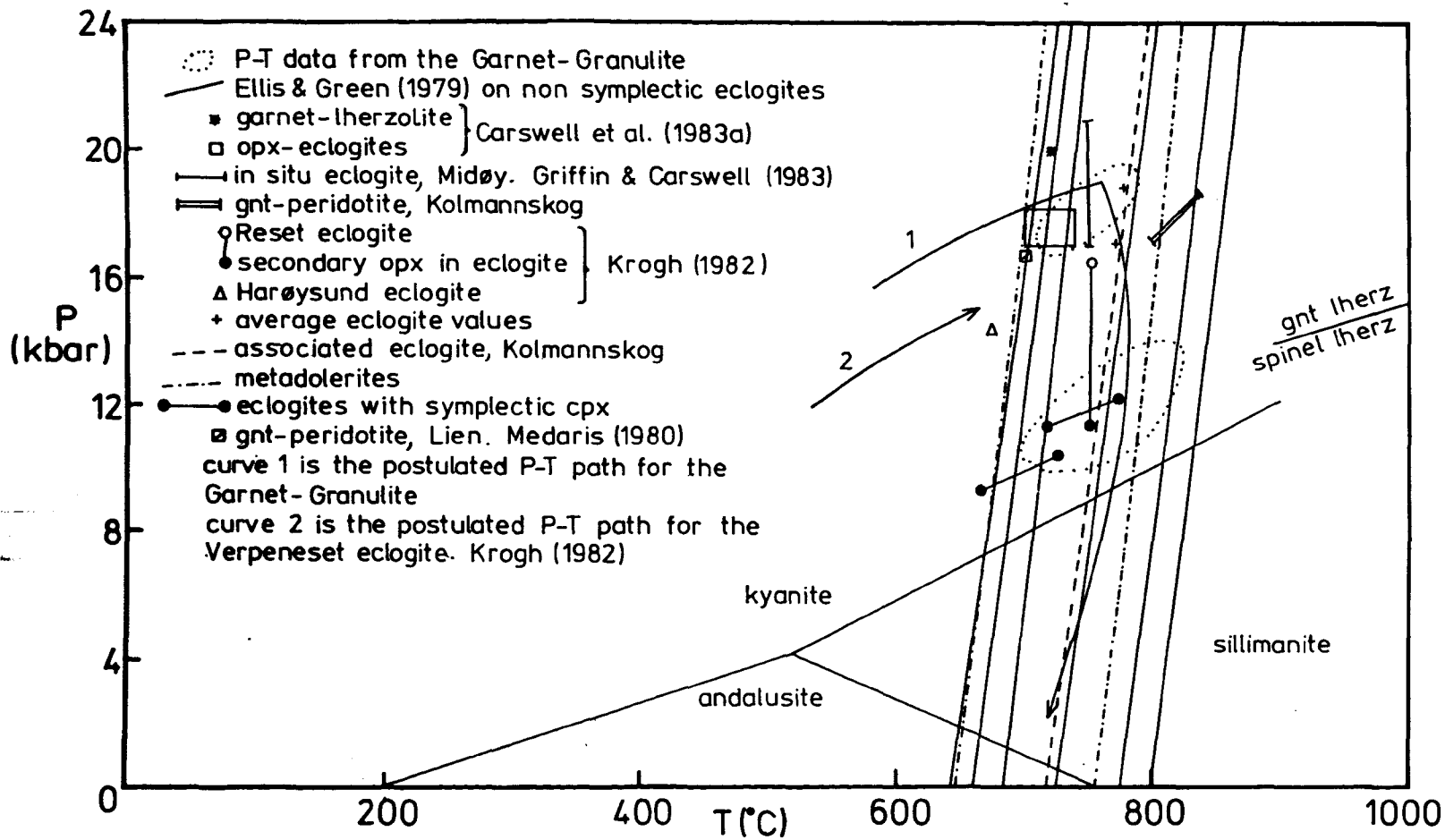
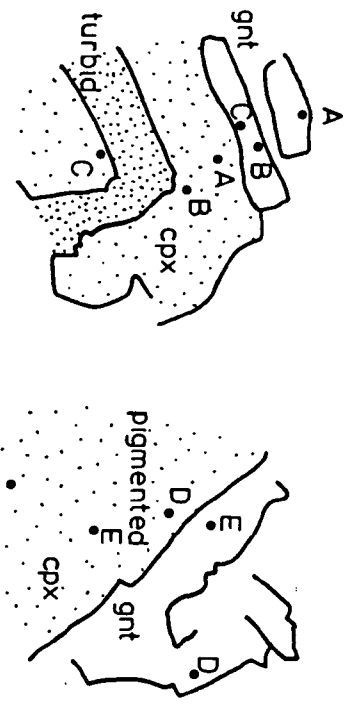


FIG. 7.8(a) Sketches of the textural relationships between the clinopyroxenes and garnets of metadolerite, sample 286, with the positions of the analysis points given in Tables 7.9 and 7.10.

(b) Pressure-temperature grid for the data from the eclogites, metadolerites and garnet-peridotite compared to P-T data from other sources. Garnet-lherzolite/spinel-lherzolite transition from Jenkins & Newton (1979).

(b)



(a)

FIG. 7.8

(sample F4 - see section 5.4), and those in the Augen Gneiss (Carswell & Harvey, 1983) they are less grossular and more almandine-rich, effects likely to be the result of the more acidic bulk compositions of sample F4 and the Augen Gneiss. Compared to the garnets in the Garnet-Granulite (section 3.4), those in the eclogites are slightly more almandine-rich again reflecting the generally more Fe-rich bulk compositions of the eclogites. Within the eclogites themselves, the garnet compositions reflect the bulk compositions of the rocks: e.g. D38 (an equivalent sample to D37 in Table 7.2) is an Fe-rich eclogite and has garnets with high Fe-contents, giving exceptionally high almandine values (see Table 7.5). It is interesting to note that although D38 is an Fe-Ti type eclogite, the contained garnets contain as little Ti as those from other, less titaniferous eclogites perhaps reflecting the expulsion of Ti from this phase postulated by Pinet & Smith (1982) for silicates formed under eclogite facies conditions.

The analyses of the clinopyroxenes are given in Table 7.6 and are of both unaltered discrete grains and symplectic grains. All the analyses come from matrix clinopyroxenes. The varying degrees of symplectite formation are reflected in the depleted Na_2O contents, enrichment in FeO and lower calculated jadeite contents of the grains, on Fig. 7.6(b), only a few analysed grains are true omphacites according to the division of Essene & Fyfe (1967), the remainder being 'augites', in fact dominated by diopside component. The plot of Lovering & White (1969) shows that the majority of the analyses are of eclogite facies pyroxenes (Fig. 7.7(a)). Although the apparently unaltered grains show no evidence of compositional zoning their compositions are fairly variable as a result of the symplectitisation. As in the garnets, the compositions of the clinopyroxenes tends to reflect the bulk composition

of the rocks: D38 exhibits Fe-rich clinopyroxenes in a Fe-rich rock; although these pyroxenes are not particularly Ti-rich. Overall, these clinopyroxenes in Table 7.6 are not particularly omphacitic for eclogites, considering that the generally retrogressed Garnet-Granulite had relict eclogite facies clinopyroxenes with jadeite contents of 30-40%. Analyses of clinopyroxenes from eclogites elsewhere in Norway also tend to have higher jadeite contents: 35-40% in the Ulsteinvik eclogite (Mysen, 1972); 44% in eclogites at Sunnfjord (Krogh, 1980a); 50% in the eclogites of the Seve Nappe (van Roermund, 1983).

In addition to the spot analyses performed on these phases, analytical traverses were made across several grains of clinopyroxene and garnet in the eclogites to investigate the nature of the zoning. For these analyses the EMP was programmed to analyse for Mg and Fe, over a counting time of 10 secs, in steps of 50 μ across the grain. Towards the rims of the grains, the steps were decreased to 10 μ in order to pick up any small scale zoning resulting from partial re-equilibration of the rims.

Fig. 7.7(b) shows typical zoning profiles from garnets and clinopyroxenes in the eclogites; these particular profiles are from sample D8. The profiles are virtually flat, except for a slight prograde rim on the clinopyroxene, where an increase in Fe and a drop in Mg results in a lower Mg/(Mg + Fe) ratio; this pattern is not reflected in an increased Mg/(Mg + Fe) ratio in the garnet. A few garnets show retrograde rims with a drop in the Mg/(Mg + Fe) ratio although these are generally very narrow. These profiles are unlike those from minerals in eclogites elsewhere in the Basal Gneiss Complex which display strong zoning from core to rim in both garnet and clinopyroxene. With increases in Ca and Mg, and decreases in Fe and Mn in the garnet and increases in Na and Al,

and decreases in Ca in the clinopyroxenes, these profiles have been interpreted as reflecting the growth of the minerals in a prograde metamorphic environment (e.g. Bryhni & Griffin, 1971; Krogh, 1982; Cuthbert & Carswell, 1982).

The lack of zoning in the minerals here is in accord with the presence of rutile and omphacite inclusions throughout the garnet grains, whereas the zoned garnets cited above tend to exhibit an ordered distribution of different inclusions, reflecting growth in a prograde metamorphic environment, such as amphibole at the core and omphacite at the rim (Krogh, 1982 and see section 1.3). The lack of chemical, or mineral inclusion zoning suggests that these garnets have been homogenised by volume diffusion (Freer, 1979; Tracy, 1982) at temperatures above the diffusion threshold for garnets of this composition. Although cooling rate affects closure temperatures, such that the faster the cooling rate, the higher the closure temperature, the following relationships apply to the closure temperatures of garnets:

almandine-pyrope is higher than grossular is higher than pyrope (Humphries & Cliff, 1982). Since this terrain, and the enclosed eclogites, has been postulated as having had a rapid uplift subsequent to the Caledonian metamorphism (Chapter 3, and Cuthbert et al., 1983), and the compositions of these garnets are almandine-pyrope, they can be expected to have had fairly high closure temperatures, perhaps $> 700^{\circ}\text{C}$ from the data in Humphries & Cliff. The presence of slight prograde or retrograde rims on some of these phases, including the clinopyroxenes probably reflect the different responses of these minerals to temperature variations and their different diffusion coefficients (Tracy, 1982).

The amphibole analyses in Table 7.7 are of two secondary amphiboles (samples 284 and M7) and one primary amphibole (sample M26). All are

Ca-rich amphiboles in the classification of Leake (1978) with $(Ca + Na)_B \geq 1.34$. The primary amphibole in M26 is more Mg, Na and Al rich, but poorer in Fe and K than the secondary amphiboles. This particular amphibole classifies as a pargasite according to Leake, which confirms the petrographic identification (see section 7.1.1). The two secondary amphiboles are of broadly similar composition although they are from different rocks, and both replace clinopyroxenes. As noted by Lappin & Smith (1978) these secondary amphiboles are richer in Ti than the early (their 'primary') amphiboles which has been attributed to variations in oxidation conditions during the eclogite-facies and subsequent retrograde metamorphic events (Pinet & Smith, 1982). Both are classed as Mg-Hastingsites on Leake's classification.

7.3.2 The metadolerites

The analyses of the garnets and clinopyroxenes from sample 286 are given in Tables 7.9 and 7.10 respectively; the relationship between the analysed points and the mineral texture is shown in Fig. 7.8(a). The analyses are plotted on Figs. 7.6 and 7.7(a) with the data from the eclogites. The garnets show little zoning, as found by Griffin & Råheim (1973) in the eclogitic dolerites at Kristiansund, and have comparable chemistries to those in the eclogites: almandine-pyrope-grossular types and consequently plot in roughly the same position on Fig. 7.6(a). The clinopyroxenes, however, are well zoned, although not in the prograde fashion observed by Griffin & Råheim (1973) with increasing jadeite content from core to rim. The unusual zoning pattern observed here is difficult to explain unless the original igneous pyroxenes were similarly zoned, or the phases have reacted with ophitic igneous plagioclases, no longer present. The consistency of the zoning trends in the two different grains favours the first possibility. As found by Griffin & Råheim

TABLE 7.9 Analyses of garnets from metadolerite

(wt. %)	286 A (1)	286 B (1)	286 C (1)	286 D (1)	286 E (1)
SiO ₂	38.75	38.60	38.42	39.04	38.97
TiO ₂	0.04	0.02	0.05	0.02	0.04
Al ₂ O ₃	21.69	21.86	21.87	21.60	21.75
FeO	24.92	25.05	25.03	26.73	26.48
MnO	0.45	0.48	0.47	0.56	0.51
MgO	7.24	7.19	7.10	8.38	7.42
CaO	7.38	7.49	7.71	4.46	5.90
TOTAL	100.47	100.69	100.65	100.79	101.07
MINERAL FORMULAE (12 OXYGENS)					
Si	2.973	2.957	2.944	2.986	2.980
Ti	0.003	0.001	0.003	0.001	0.003
Al	1.962	1.974	1.975	1.947	1.961
Fe ³⁺	0.088	0.112	0.132	0.079	0.074
Fe ²⁺	1.512	1.491	1.473	1.630	1.620
Mn	0.029	0.031	0.031	0.037	0.033
Mg	0.828	0.821	0.811	0.855	0.846
Ca	0.607	0.615	0.633	0.366	0.484
TOTAL	8.002	8.002	8.002	8.001	8.001
END-MEMBERS (%)					
ANDR	4.33	5.62	6.60	3.96	3.61
PYROPE	27.82	27.75	27.51	3.98	28.35
SPESS	0.98	1.05	1.04	1.22	1.11
GROSS	15.98	15.12	14.79	8.23	12.53
ALM	50.80	50.41	49.97	54.57	54.33
SCHORL	0.08	0.04	0.10	0.04	0.08

Fe³⁺ calculated by charge-balance

Figures in brackets refer to the number of analysis points

TABLE 7.10 Analyses of clinopyroxenes from metadolerite

(wt. %)	286 A (1)	286 B (1)	286 C (1)	286 D (1)	286 E (1)	286 F (1)
SiO ₂	54.61	54.72	54.38	54.39	52.87	53.10
TiO ₂	0.58	0.68	0.66	1.56	1.36	0.62
Al ₂ O ₃	7.85	5.72	6.66	5.07	4.22	6.58
FeO	6.86	6.59	6.67	8.26	7.56	7.95
MgO	9.40	10.79	10.10	10.73	12.03	10.83
CaO	15.88	18.26	17.09	17.01	20.11	18.44
Na ₂ O	4.94	3.90	4.50	3.85	2.30	2.98
TOTAL	100.12	100.66	100.06	100.87	100.45	100.50
MINERAL FORMULAE (6 OXYGENS)						
Si	1.973	1.975	1.969	1.964	1.935	1.937
Ti	0.016	0.018	0.018	0.042	0.037	0.017
Al	0.334	0.243	0.284	0.236	0.182	0.283
Fe ³⁺	0.039	0.055	0.063	0.090	0.046	0.020
Fe ²⁺	0.169	0.144	0.139	0.159	0.186	0.223
Mg	0.506	0.580	0.545	0.577	0.656	0.589
Ca	0.615	0.706	0.663	0.658	0.789	0.721
Na	0.346	0.273	0.316	0.270	0.163	0.211
TOTAL	3.998	3.994	3.997	3.996	3.994	4.001
END-MEMBERS (%)						
Ca-Ti-Ts	1.35	1.29	1.55	1.89	3.25	1.70
Ca-Ts	-	-	-	-	-	2.89
Jd	30.86	21.97	25.44	18.61	11.85	19.12
Ac	3.87	5.55	6.28	9.36	4.61	1.96
Di	45.09	55.58	51.57	50.07	59.02	48.96
Hd	15.03	13.78	13.19	13.81	16.70	18.54
En	2.85	1.48	1.57	4.92	3.56	1.88
Fs	0.95	0.37	0.40	1.36	1.01	4.96

Fe³⁺ calculated on the basis of the structural formula (cf. Mysen & Griffin, 1973)

Figures in brackets refer to the number of analysis points

the clinopyroxenes are Ti-rich and significantly more so than those in the eclogites (see Table 7.6), even when compared to those in the Fe-Ti type eclogites (D8 and D38). These high Ti values appear to be a reflection of the pigmentation of the pyroxenes (see Plates 7.3(a) and (b)), considered by Griffin & Råheim to be due to exsolved rutile lamellae. This expulsion of Ti by silicates under eclogite facies conditions illustrates the conjecture of Pinet & Smith (1982) that such a process occurs during such high grade metamorphism. The appearance of apparent primary, igneous exsolution lamellae in these highly jadeitic pyroxenes suggests that the primary phases have been 'made over' to these new compositions by diffusion processes (cf. Griffin & Råheim, 1973).

Together with the data from the eclogite clinopyroxenes on Fig. 7.7(a), these data from the metadolerite clinopyroxenes illustrate well the path of prograde eclogite facies mineral development from low-P igneous assemblages, and their subsequent retrograde path to high-P granulite, with exsolved feldspars in the clinopyroxenes (cf. that postulated by Griffin & Råheim, 1973).

7.3.3 The garnet-peridotite

The mineral analyses of the phases in the Kolmannskog garnet peridotite and associated eclogite are given in Table 7.11 and all of them reflect well the Fe-Ti nature of the bulk compositions of these rocks (see section 7.2.3), with Fe-rich olivine (Fo 81), orthopyroxene (En 82) and a garnet of (Pyr₅₆Alm₂₉Gross₉). In the Mg-Cr type of garnet peridotite of Carswell et al. (1983b) the constituent phases have typical values of: ol (Fo 82-92), orthopyroxene (En 84-93) and garnet (Pyr₆₀₋₇₅Alm₁₅₋₃₀Gross₅₋₁₀). The garnets and pyroxenes in the Mg-Cr type peridotites also tend to have substantial contents of Cr (0.6-4.35 wt. %) and (0.47-2.6 wt. %) respectively; these two phases in this

TABLE 7.11 Analyses of minerals occurring in the peridotite and associated eclogite at Kolmannskog.

	185 Perid. Gnt (3)	182 Eclo. Gnt (3)	185 Perid. Cpx (3)	182 Eclo. Cpx (6)	185 Perid. Opx (6)	185 Perid. Ol (5)	185 Perid. Spinel (1)	185 Perid. Mica (2)	185 Eclo. Mica (2)	185 Perid. Amph (5)			
SiO ₂	40.80	40.06	54.62	54.07	56.22	39.72	-	38.16	38.10	43.82			
TiO ₂	0.01	0.03	0.10	0.11	0.04	0.01	0.02	0.83	2.12	0.43			
Al ₂ O ₃	22.63	22.17	1.02	2.54	1.44	-	63.62	16.69	14.01	14.66			
Cr ₂ O ₃	-	0.13	0.08	0.08	0.01	0.01	0.13	-	0.07	-			
FeO	15.56	20.47	4.06	5.87	11.23	17.44	18.15	6.17	10.13	7.80			
MnO	0.90	0.68	-	-	-	0.28	-	0.03	0.05	-			
MgO	15.34	12.49	17.18	14.43	30.84	42.77	18.38	21.60	18.39	15.37			
CaO	4.94	4.76	22.62	21.35	0.27	-	-	-	0.07	12.69			
Na ₂ O	-	-	0.31	1.53	0.01	-	-	0.18	0.39	0.93			
K ₂ O	-	-	-	-	-	-	-	9.78	9.19	1.54			
TOTAL	100.18	100.79	99.99	99.98	100.06	100.23	100.30	93.44	92.52	97.24			
MINERAL FORMULAE													
	12 'O'	12 'O'	6 'O'	6 'O'	6 'O'	4 'O'	4 'O'	22 'O'	22 'O'	23 'O'			
Si	2.983	2.975	1.988	1.976	1.979	1.005	-	5.564	5.722	6.270			
Ti	0.001	0.002	0.003	0.003	0.001	0.000	0.000	0.091	0.240	0.046			
Al	1.951	1.940	0.044	0.109	0.060	-	1.912	2.869	2.481	2.472			
Cr	-	0.008	0.002	0.002	0.000	0.000	0.003	-	0.008	-			
Fe ³⁺	0.082	0.098	0.000	0.039	0.000	0.000	0.090	-	-	0.465			
Fe ²⁺	0.869	1.173	0.124	0.140	0.331	0.369	0.297	0.753	1.272	0.468			
Mn	0.056	0.043	-	-	-	0.006	-	0.004	0.006	-			
Mg	1.672	1.383	0.932	0.786	1.618	1.613	0.698	4.694	4.116	3.278			
Ca	0.387	0.379	0.882	0.836	0.010	-	-	-	0.011	1.946			
Na	-	-	0.022	0.108	0.001	-	-	0.051	0.114	0.258			
K	-	-	-	-	-	-	-	1.819	1.762	0.281			
TOTAL	8.001	8.001	3.997	3.999	4.000	2.993	3.000	15.845	15.732	15.484			
END-MEMBERS (%)													
ANDR	4.11	4.91	Ca-Ti-Ts	0.28	0.30	0.11	Fo	81	SPINEL	95.37	Mg/Fe	6.23	3.24
PYROPE	56.02	46.44	Ca-Ts	0.63	1.82	0.93			MAGN.	4.50			
SPESS	1.87	1.44	Ko	0.23	0.23	0.03			CHROM.	0.13			
GROSS	8.84	7.37	Jd	1.97	6.69	0.04							
ALM	29.14	39.40	Ac	-	3.92	-							
SCHORL	0.02	0.06	Di	77.47	69.13	-							
UVAR	-	0.39	Hd	10.27	12.34	-							
			Jo	-	-	-							
			En	8.09	4.73	82.12							
			Fs	1.07	0.84	16.78							
			Rh	-	-	-							

Fe³⁺ calculated by charge-balance (garnets and spinel); on the basis of the structural formula (cf. Mysen & Griffin 1973 for pyroxenes); and the iterative method of Leake (1978) (amphibole).

Fe-Ti type peridotite are notably poor in Cr (cf. Carswell et al., 1983b). Furthermore, the spinel is notably Cr-poor (0.13% chromite), those in the Mg-Cr type peridotites have typical chromite contents of 8-24%.

The clinopyroxene from the associated eclogite is only slightly omphacitic, but is comparable to those in the external eclogites (see Figs. 7.6(b) and 7.7(a)). The garnet is also fairly comparable to those in the external eclogites although slightly more pyropic (Fig. 7.6(a)).

The micas from both the peridotite and associated eclogite are Ti-phlogopites, with Mg/Fe ratios > 3 . Of all the analysed phases in this body only these show any degree of Ti enrichment.

The secondary hornblende, although occurring in a rock with a significantly different composition to the 'external' eclogites has a chemistry very similar to the amphiboles occurring in those eclogites apart from some MgO-enrichment. It is a Tschermakite on the basis of Leake's (1978) classification.

7.3.4 Pressure and temperature calculations

The pressure and temperature data calculated for the eclogites, metadolerite and garnet-peridotite from the data in Tables 7.5-7.11 are given in Fig. 7.8(b) and in Table 7.12. Only adjacent rim compositions have been used in these calculations to ensure, as far as is practicably possible, that the two phases are in equilibrium and will therefore reflect the P and T of final equilibration.

The P-T values for the non-symplectitic eclogites of metadolerites are shown as P-T lines on Fig. 7.8(b), using the calibration of Ellis & Green (1979) as there is no method of obtaining a P estimate for these rocks from their assemblages. For the symplectite bearing eclogites (i.e. retrograde granulite facies assemblages) the methods of Ellis & Green (1979), Krogh (1983) and Newton & Perkins (1982) were solved

TABLE 7.12 Pressure and temperature data calculated for the meta-basic and meta-ultrabasic bodies

	PARAMETERS					METHODS (P in kbars, T in °C)												
	K_D^*	K_D	x_{Ca}^{gnt}	x_{An}^{plag}	% Jd	M & G T	E & G/N & P T	N & P P	K/N & P T	P	W/Wo T	P	M & G/Wo T	P	E & G/Wo T	P	O & W/Wo T	P
NON-SYMPLECTITE ECLOGITES																		
D8	4.74	5.78	.2599	-	-	747												
D30	4.10	4.19	.1742	-	-	804												
D38	4.15	5.70	.1233	-	-	799												
D102	3.81	5.80	.1255	-	-	835												
182	4.09	4.76	.1273	-	-	804												
283	3.53	5.34	.0922	-	-	869												
M26	4.64	4.64	.1310	-	-	847												
SYMPLECTIC ECLOGITES																		
284	5.50	6.55	.2023	.789	.32	694	723	10.3	665	9.6								
M7	5.30	5.77	.1211	.824	3.12	707	771	12.2	717	11.5								
METADOLERITES																		
286/1	3.95	5.44	.2147	-	-	819												
286/2	4.79	6.95	.1623	-	-	743												
GARNET PERIDOTITE																		
185	4.29	3.92	.1297	-	-	785					953	24.7	822	17.9	839	18.8	802	16.9

K_D^* = garnet/cpx Fe-Mg partitioning with all Fe as Fe²⁺

K_D = garnet/cpx Fe-Mg partitioning with calculated Fe³⁺

x_{Ca}^{gnt} = Ca/(Ca + Mg + Fe + Mn)

286/1 = cpx A + gnt C in Tables 7.9 and 7.10

286/2 = cpx D + gnt E in Tables 7.9 and 7.10

M & G = Mori & Green (1978); C & C = Currie & Curtis (1976); E & G = Ellis & Green (1979); K = Krogh (1983); N & P = Newton & Perkins (1982); W = Wells (1977); Wo = Wood (1974); O & W = O'Neill & Wood (1979)

See Appendix B for calculation procedures

iteratively. The values for the garnet peridotite were calculated using the computer program 'NODMINS' written by F.G.F. Gibb. Each pair of methods was solved simultaneously, except for Mori & Green/Wood since the method of Mori & Green does not include a pressure dependence factor.

With regard to the values in Table 7.12, for the garnet peridotite, the T from the method of Wells (1977) is perhaps overestimated due to the Fe-rich nature of the rocks which may be inadequately accounted for in the method (Carswell & Griffin, 1981); this high T value then results in a high P value for the method of Wood (1974). The Fe-rich nature of the rocks may also be the cause of the high temperatures from the methods of Ellis & Green (1979) and Mori & Green (1978). Overall, the range of temperatures for this rock are at slightly higher values than the data calculated for comparable rocks by other workers although the pressure values are fairly similar (see Fig. 7.8(b)). Unfortunately, the Fe-rich nature of the spinel in the garnet-peridotite did not allow the calculation of meaningful pressure values by the method of O'Neill (1981) due to the uncertainties over the effects of Fe^{2+} and Fe^{3+} on the garnet-lherzolite/spinel-lherzolite transition (MacGregor, 1970; O'Neill, 1981). Besides, the method of O'Neill (1981) is for Cr-rich spinels, and those in the garnet-peridotite are very low in Cr and would not be expected to give a very large correction to the garnet-orthopyroxene barometer (see section B.1.2(a)). Using the pressure brackets of 17 and 19 kbar from this rock, temperature values can be obtained for the non-symplectite bearing eclogites. It is felt that these pressure values are applicable to the eclogites for two reasons:

(i) the eclogites and garnet-peridotite are considered to be coeval in formation and are likely to have suffered the same subsequent metamorphic history;

(ii) the pressure values for the orthopyroxene-bearing eclogites (U19, U206, U243) obtained by Carswell et al. (1983a) are comparable (see Fig. 7.8(b)).

At 17 kbar the mean temperature for the eclogites is 769°C and 19 kbar the mean temperature is 775°C. (If the method of Krogh (1983) had been used to calculate these P-T lines, these temperature values would be ~ 50°C lower.) This temperature value is only slightly higher than the value obtained by Krogh (1982) for the eclogite at Reset (on Aukra to the W of the Molde Peninsula); but is significantly higher than the value obtained by Krogh for the eclogite at Harøysund on the NW coast of the Molde Peninsula (see Fig. 7.8(b)). However, this temperature value fits in well with the regional distribution of temperatures derived from eclogites across the Basal Gneiss Complex, from which temperatures > 750°C would be expected for eclogites in this area (Krogh, 1977; Griffin et al., 1983; see Fig. 1.3).

The data for the symplectite-bearing eclogites, on the other hand, indicate slightly lower temperatures than those for the retrograded and symplectised Garnet-Granulite at Tverrfjella, but agrees very well with the P-T values obtained by Krogh (1982) from secondary orthopyroxenes in the Reset eclogite (see Fig. 7.8(b)).

Unfortunately, the lack of zoning in the garnets and clinopyroxenes does not permit the derivation of a prograde path of metamorphism for these rocks as done by Krogh (1980) for the Verpeneset eclogite at Nordfjord shown on Fig. 7.8(b). However, an important point here is that the data for the metadolerites are very comparable to the eclogites at pressures of 17-19 kbar (Fig. 7.8(b)) although the rocks exhibit relict igneous textures. This evidence implies that these rocks have been transformed from low-P igneous protoliths to 'eclogitic' rocks

through prograde metamorphism. Furthermore, from the suggestion that these rocks are genetically related to the eclogites (see section 7.2.2), which are also considered to have low P igneous protoliths from the chemical evidence (section 7.2.1), it seems reasonable to suppose that those eclogites have also suffered a prograde metamorphism, perhaps along a similar trajectory as that proposed by Krogh for the Verpeneset eclogite. The retrograde textures in the symplectite-bearing eclogites reflects the subsequent decompression of the rocks, as seen in the Garnet-Granulite at Tverrfjella and other high-P granulites on the Molde Peninsula (Fig. 5.5). Indeed the postulated metamorphic path for the Garnet-Granulite could equally well be applied to the metamorphic conditions calculated for these eclogites. Furthermore, the garnet-peridotite exhibits textures indicative of a virtually isothermal decompression, as spinel-orthopyroxene symplectites on garnets (section 7.1.3), marking the passage of the rocks from garnet-lherzolite to spinel-lherzolite (see curve on Fig. 7.8(b)).

The constancy of the P-T data from the various analysed rocks on the Molde Peninsula is encouraging and supports the idea that the whole of this area has suffered the same eclogite facies metamorphic event. The data are not compatible with those of Lappin & Smith (1978) (30-45 kbar at 700-900°C) for eclogites at Selje and are not considered to represent equilibration under upper mantle conditions. In addition, the data of Lappin & Smith are not considered to adequately reflect equilibration of the co-existing phases since the points analysed by them are of core compositions of minerals, which cannot reliably be demonstrated to have been in equilibrium and hence to give reliable P-T values. Furthermore, the model presented by Lappin & Smith (1978) for the eclogites as tectonically introduced bodies into the lower crust,

perhaps as part of the 'mega-mélange' postulated by Smith (1980), during continent-continent collision is considered not to be geologically viable and unnecessarily complex. Such large-scale lithological mixing is not considered to be consistent with the regional distribution of the equilibration temperatures derived from the eclogites (cf. Griffin et al., 1983). Also, if the eclogite bodies were intruded tectonically, it would be expected that they would be along large crustal dislocations or at major lithological boundaries. From the evidence on the Molde Peninsula, neither of these situations have been observed. The present disposition of the eclogites as relatively small bodies with tectonic margins to the country rock gneisses does not require such large tectonic movements; localised disruption from larger bodies, as suggested in Chapter 2, will also give such contacts (cf. Mørk, 1982).

From the postulated time of intrusion of the igneous precursors to the meta-basic rocks (section 7.3.4) and the recent radiometric age determinations on these rocks which indicate a Caledonian eclogite metamorphic facies event (Krogh et al., 1973; Griffin & Brueckner, 1980; Gebauer et al., 1982; Mearns & Lappin, 1982a), the formation of these high-grade assemblages is considered to have occurred at that time, during a continent-continent collision between the Baltic and Greenland 'plates', as set out in Cuthbert et al. (1983): considerable crustal thickening occurred during that collision, up to 65 km, resulting from imbrication of the crustal rocks and over-riding nappe sheets giving maximum metamorphic conditions of $\sim 750^{\circ}\text{C}$ and 20 kbar, now observed on the W coast of Southern Norway (Fig. 1.3). Subsequent underthrusting of the Baltic 'plate' under the now eclogite-bearing crustal rocks, plus tectonic stripping and erosion, rapidly uplifted the rocks, giving the decompression textures seen, plus hydration, leading to their eventual exposure at the present land surface.

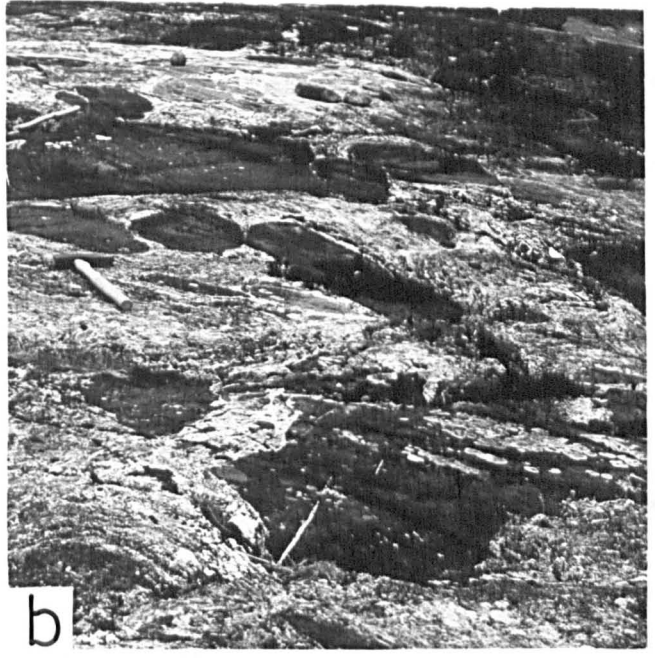
PLATE 7.1

- (a) Typical appearance of a pod of eclogite in outcrop. Note: the lensoidal form; the sharp contact with the host gneisses, partly filled by a quartz vein; and the small-scale mineralogical banding of the rock. Julneset point (970569).
- (b) A 'zone' of fairly small, amphibolitised eclogite pods. Note the variable sizes of the pods. Hammer indicates the general direction of the local strike direction. N coast Vågøy (995684).
- (c) General appearance of a Class I eclogite. Clinopyroxene lies above centre and centre bottom. Note irregular form of the garnet with slight amphibole development on the rim. (Sample D8, plane-polarised light.)
- (d) Sample of eclogite displaying small, rounded, sub-idioblastic garnets, clinopyroxene to the right. (Sample M26, cross-polarised light.)
- (e) General appearance of a Class II eclogite. Note incipient symplectite in the clinopyroxene, top right of centre and amphibole development around the garnet (left and centre bottom). This sample also displays an orientation of the phases in a 'flasar' structure. (Sample D37, plane-polarised light.)
- (f) A 'front' of symplectite development from a grain of clinopyroxene at top centre into another at bottom of picture. Note coarsening of the intergrowth of secondary clinopyroxene and plagioclase away from the leading edge of the symplectite. (Sample T3, cross-polarised light.)

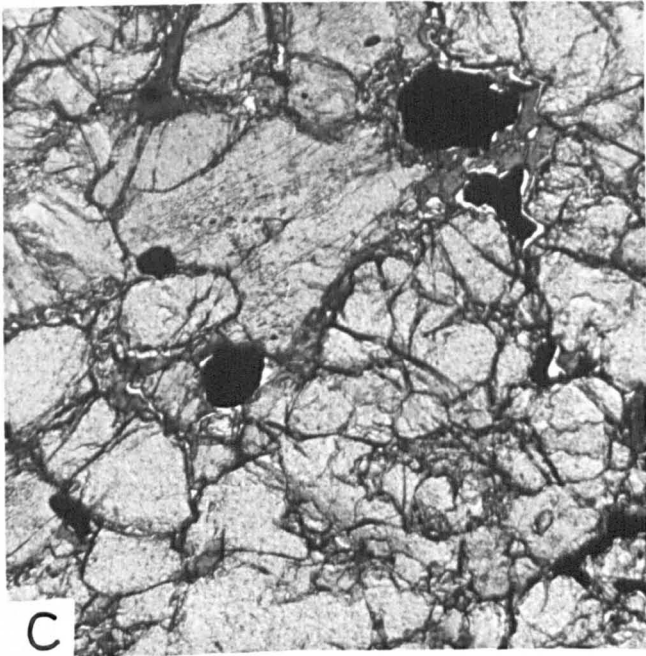
PLATE 7.1



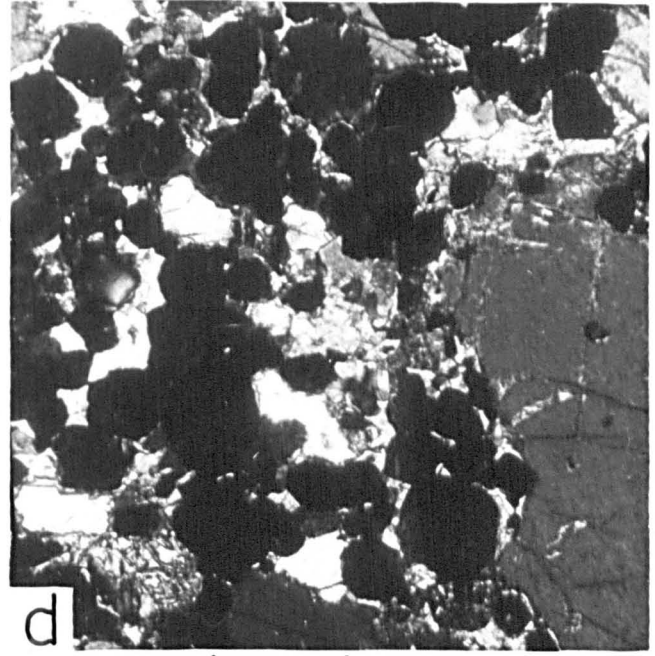
a



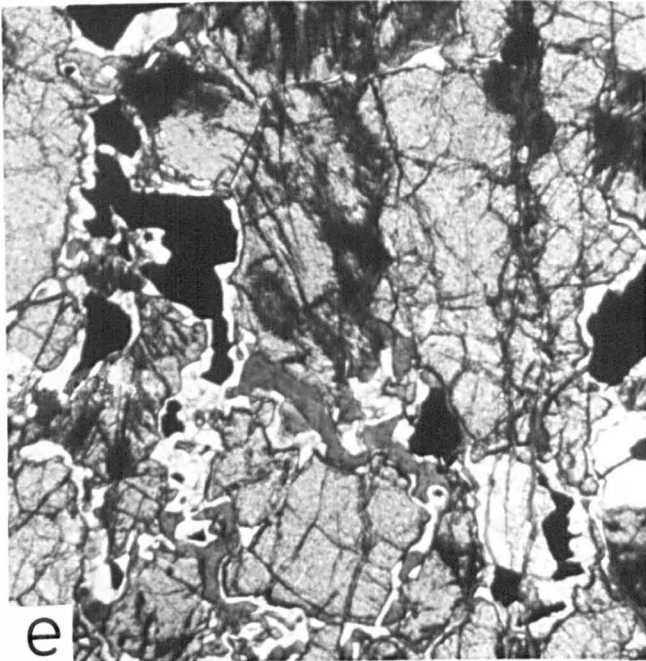
b



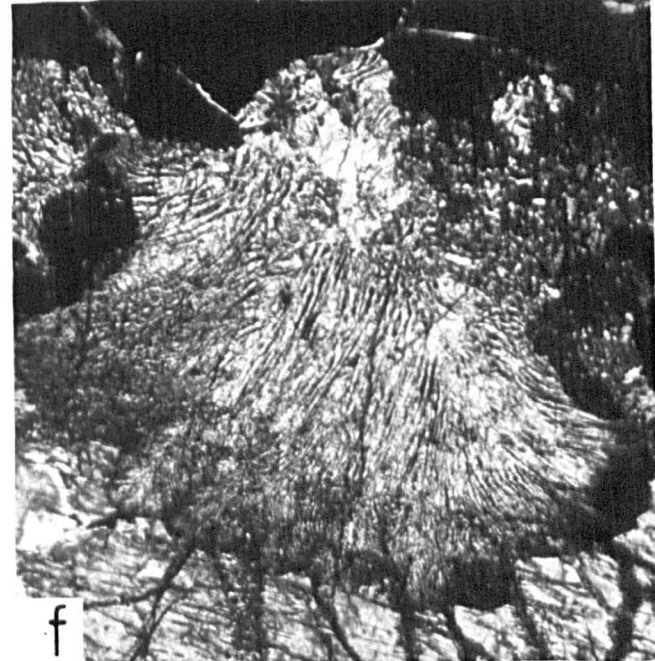
c



d



e



f

PLATE 7.2

- (a) General appearance of a Class III eclogite with some development of symplectite in the clinopyroxene and coarse amphibole/plagioclase kelyphite around the garnets. The clinopyroxene displays slight amphibolitisation. (Sample H1, plane-polarised light.)
- (b) General appearance of a Class IV eclogite. The clinopyroxene displays both coarse and fine symplectite development, much of the clear areas are secondary plagioclase. Note the partial amphibolitisation of the secondary clinopyroxene at top of picture and corroded rim of the garnet at bottom of the picture. (Sample M9, plane-polarised light.)
- (c) General appearance of a Class V eclogite. The clinopyroxene is thoroughly amphibolitised with a coarse symplectite texture. A relict clinopyroxene lies on the left of the picture. The garnets are corroded and do not display an obvious kelyphite rim. (Sample T4, plane-polarised light.)
- (d) The appearance of the primary amphibole in eclogites. Note apparent equilibrium contact with the garnet at the top of the picture. (Sample T3, plane-polarised light.)
- (e) Photograph of a sample of eclogite at Svartnakken (985618) containing a vein of omphacitic clinopyroxene which itself contains porphyroblastic garnets.

PLATE 7.2

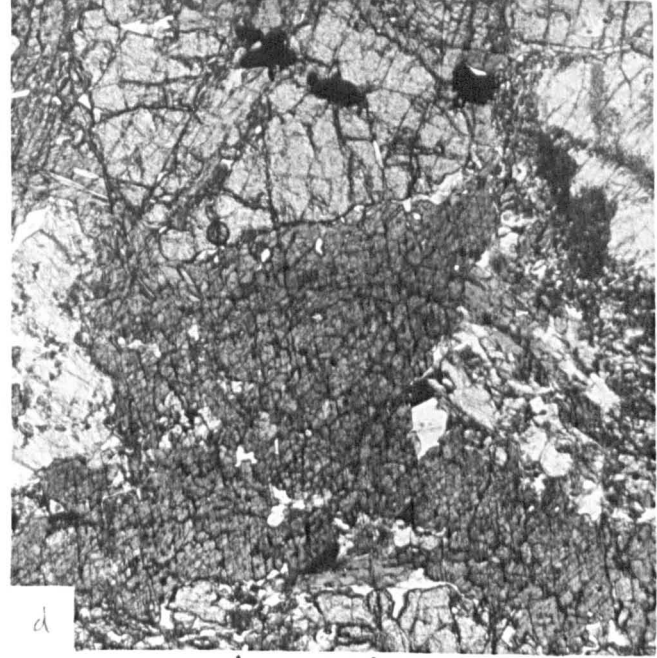
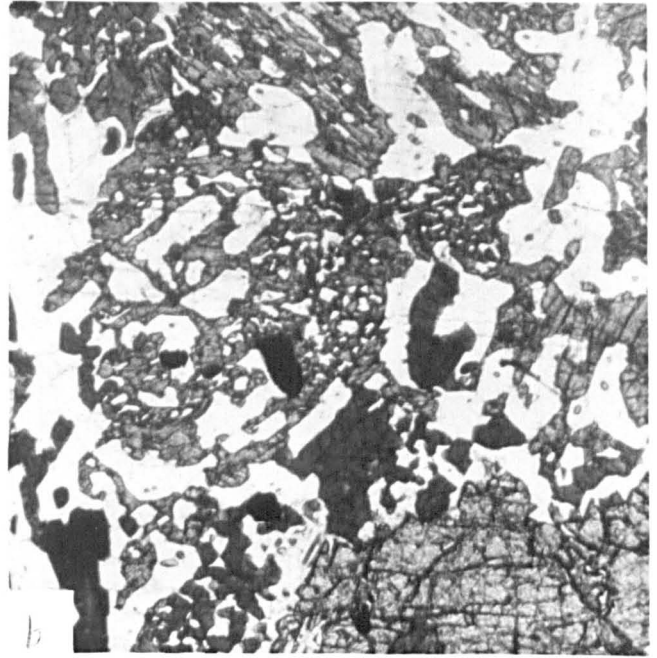
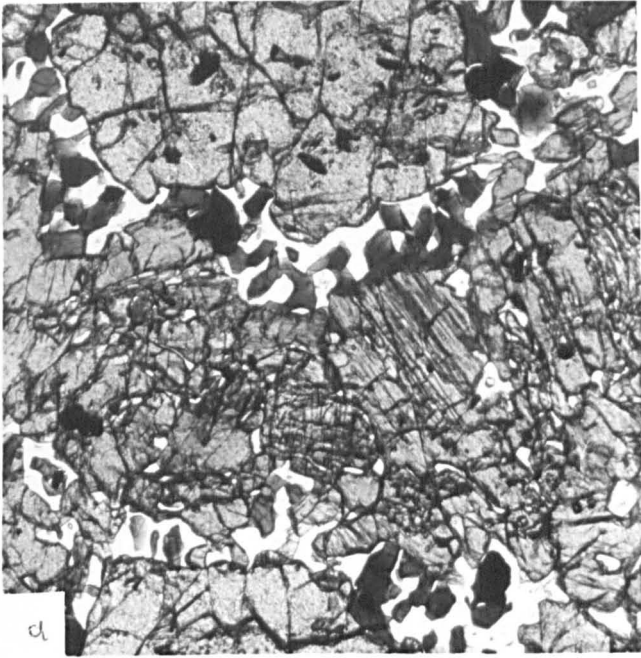
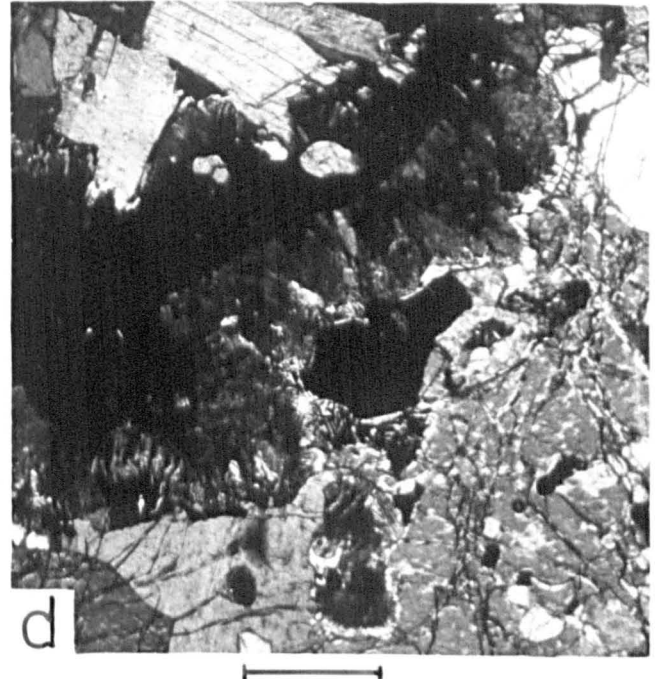
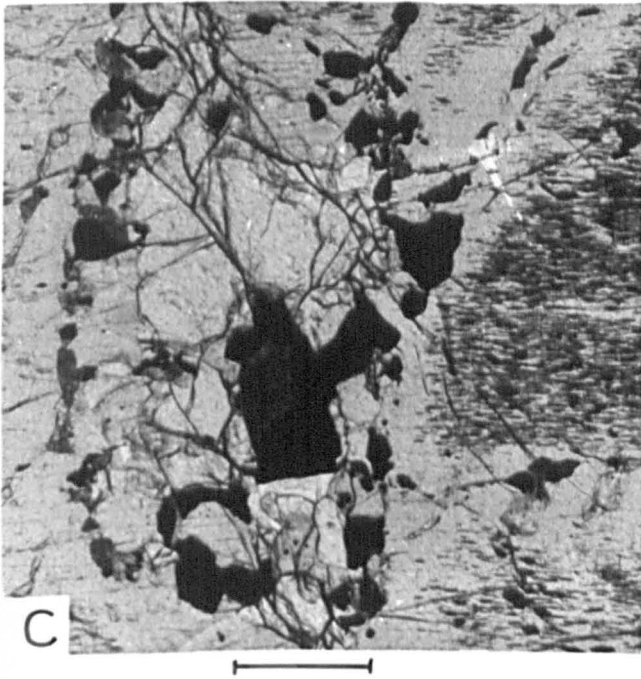
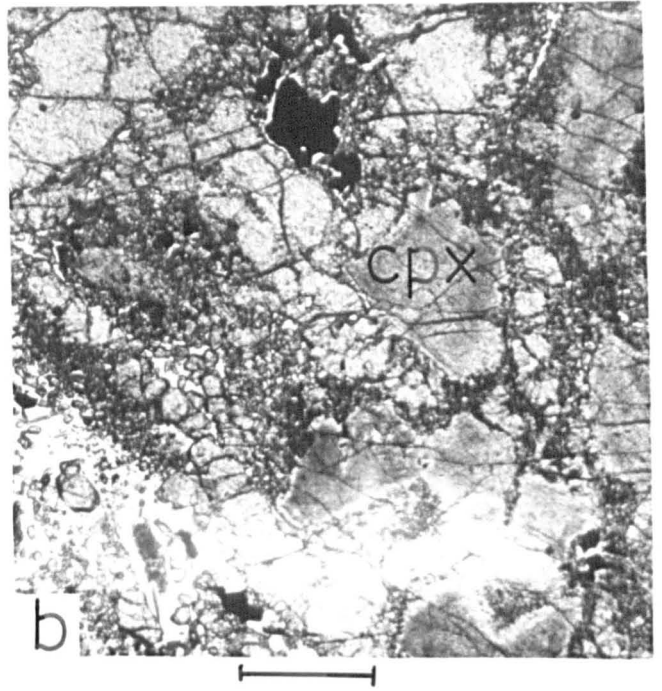
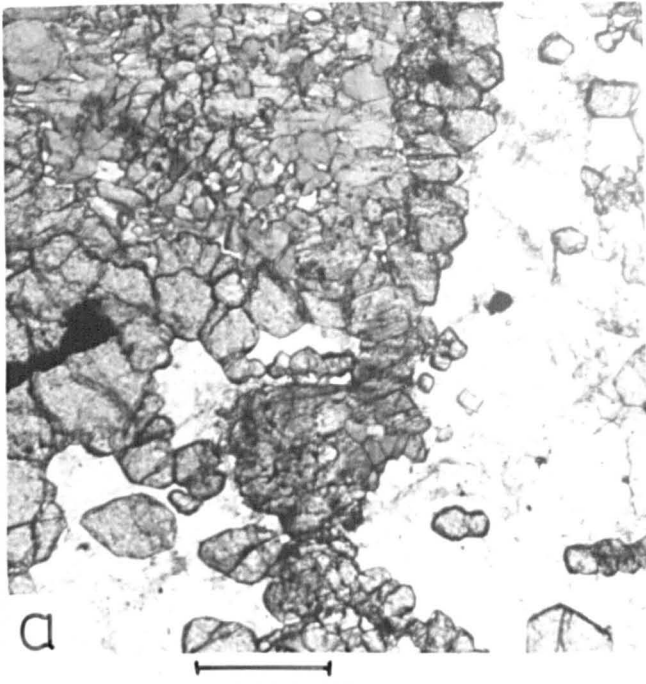


PLATE 7.3

- (a) Corona texture in a metadolerite. Partially amphibolitised initial clinopyroxene lies at top left, surrounded by a thin rim of garnet. The clear area to the right is polygonal plagioclase containing small, sub-idioblastic garnets. (Sample D41, plane-polarised light.)
- (b) Metadolerite displaying a 'fish-net' texture. Pigmented clinopyroxenes are indicated. The garnets have replaced laths of plagioclase. Note the partial retrogression of the rims of the clinopyroxene. The opaque phase at the top of the picture is rutile. (Sample 286, plane-polarised light.)
- (c) Orthopyroxene in the garnet-peridotite displaying profuse needles of magnetite, on the right of the picture. Magnetite is also seen adjacent to the olivine in the centre of the picture. The large magnetite contains a grain of dark green pleonaste spinel. (Sample 185, plane-polarised light.)
- (d) Symplectite development in the garnet-peridotite. Mica at top left, then a thin band of garnet (extinct) developing a fine symplectite of spinel + opaques + amphibole adjacent + an olivine at bottom right. Note the coarser orthopyroxene-opaque symplectite below the large grain of magnetite right of centre. (Sample 184, cross-polarised light.)

PLATE 7.3



CHAPTER 8

SUMMARY OF CONCLUSIONS

In Chapter 1 it was stated that two specific problems were to be tackled in this study:

(i) the discrimination between the basement and 'cover' rocks, if they existed, on the Molde Peninsula;

(ii) an attempt to unravel some of the controversy over the origin of the eclogite rocks in the area.

With regard to the first of these problems, several of the ideas put forward in this work contradict those of earlier workers. Firstly, there appear to be two distinct units of Archaean basement rocks on the Peninsula. The oldest is the Heterogeneous Quartzo-Feldspathic Gneiss Unit, and possibly the rocks of the Moldefjord coast and the Tingvoll Group of rocks on Bolsøy. These are considered to be a calc-alkaline suite, with sediments, deposited in an Andean-type continental margin $\sim 2000 \pm 300$ m.y. ago (Chapters 5 and 6). The other basement unit is the Augen Gneiss Unit, which is considered to have been intruded into the older rocks at 1477 ± 21 m.y. ago. This Unit appears to be related to the extensive anorthosite-rapakivi suite of rocks which was intruded in tensional crustal conditions at that time (Chapter 4).

Both of these basement Units lie in the Frei Group of Hernes (1955) which is considered to be of Svecofennian age (~ 1700 m.y.) (Råheim, 1972). However, it can be seen that this age of metamorphism can only be applied to the older calc-alkaline rocks. The rocks of the Moldefjord coast are not envisaged to be of Palaeozoic age as suggested by Carswell (1973).

The 'cover' rocks have been identified definitely at one locality on the Tverrfjella mountains and possibly also on Bolsøy. The two

localities may be related lithologically although direct comparison of the rock types is hindered by the profound retrogression suffered by the rocks on Bolsøy. The rocks on the Tverrfjella mountains are interpreted as an allochthonous unit, of marginal basin derivation, possibly related to similar units in the Trondheim region, to the NE. The suggestion that these rocks are perhaps only \sim 500-600 m.y. is a major departure from the interpretation of Hernes (1954b) who considered the rocks to be part of the Precambrian-aged Frei Group (Chapter 3).

With respect to the eclogites, two distinct types have been recognised on the Molde Peninsula. The type occurring as relatively small pods is considered to be the result of the metamorphism and disruption of a swarm of tholeiite dykes which were intruded \sim 1200-850 m.y. ago under the tensional crustal conditions which instigated the intrusion of the precursors to the Auger Gneiss Unit. A layered basic intrusion was also emplaced at this time, now represented by the garnet-peridotite at Kolmannskog. The interpretation of these eclogites as meta-igneous rocks is in opposition to the idea of Lappin & Smith (1978) that they are tectonically introduced fragments of rocks equilibrated at upper-mantle conditions (Chapter 7). The other type of eclogite is the large Garnet-Granulite of the Tverrfjella Unit which sporadically preserves relict eclogite facies assemblages. This rock is interpreted as a volcanoclastic deposited in a marginal basin environment with other metasediments, including limestones. The production of an eclogite-facies mineralogy in these postulated sedimentary rocks is again indicated as evidence for eclogite-facies metamorphism in the crust (Chapter 3).

The major conclusions of this study can be placed in chronological order:

1. Formation of a calc-alkaline suite of orthogneisses with meta-sediments in a subduction zone 'plate' margin at $\sim 2000 \pm 300$ m.y. ago.
2. Metamorphism in the Svecofennian orogeny $\sim 1800-1700$ m.y. ago (Pidgeon & Råheim, 1972), with formation of some migmatites.
3. Intrusion of the precursor to the Auger Gneiss Unit as a rapakivi-like, anorogenic pluton at 1477 ± 21 m.y. in the extensional crustal regime dominant in northern Europe and America at that time.
4. Possible metamorphism during the Sveconorwegian orogeny (~ 1100 m.y. ago) although the effects may not have extended this far north.
5. Intrusion of the precursors to the eclogites, metadolerites and garnet-peridotite as dykes, sills and layered gabbroic bodies during the waning stages of the extensional tectonics at $\sim 1200-850$ m.y. ago.
6. Initiation of a compressional crustal regime during the closure of the Iapetus Ocean, subduction on the margins of this ocean resulted in the formation of a marginal basin environment: the precursor to the rocks of the Tverrfjella Unit.
7. Continent-continent collision during the Caledonian with extreme crustal thickening as a result of continental plate underthrusting and compression of a nappe pile. One of the thrust units in this nappe pile ultimately formed the Tverrfjella Unit.
8. Metamorphic culmination at ~ 425 m.y. ago gave P-T conditions of $\sim 750^{\circ}-800^{\circ}\text{C}$ and $\sim 18-20$ kbar, and the formation of eclogite facies assemblages. The formation of the early flat-lying foliation was at this time.
9. Rapid uplift of the gneiss terrain resulted in several retrograde reactions: symplectite clinopyroxenes and kelyphite garnets in the eclogites and Garnet-Granulite of Tverrfjella, and magnetite symplectites in the garnet-peridotite of Kolmannskog. Oxidising conditions prevailed

at this time assisting in the formation of the clinopyroxene symplectites and magnetite symplectites. Partial melting in the pelites also occurred.

10. Large scale folding accompanied this uplift; the steep-limbed syncline in the S of the area assisted in the hydration of the rocks there; these rocks are also locally mylonitised. Continuing oxidising conditions during hydration resulted in the formation of orthite-clinozoisite zoned epidote minerals.

11. High temperatures $\sim 750^{\circ}$ must have been retained during this hydration event to allow for the development of the extensive veining by pegmatites and other granite veins throughout the area.

REFERENCES

- ABDEL-MONEM, A.A. & BRYHNI, I. (1978). A Rb-Sr date from anorthosite-suite rocks of the Gloppen-Eikefjord area, western Norway. Norsk. Geol. Tidsskr., 58, 229-232.
- AITKEN, B.G. (1983). T-X_{CO₂} stability relations and phase equilibria of a calcic carbonate scapolite. Geochim. Cosmochim. Acta, 47, 351-362.
- ALDERMAN, A.R. (1936). Eclogites in the neighbourhood of Glenelg, Inverness-shire. Q. J. Geol. Soc. Lond., 92, 488-530.
- ANDERSON, E.M. (1948). On lineation and petrofabric structure and the shearing movement by which they have been produced. Q. J. Geol. Soc. Lond., 104, 99-132.
- ANDERSON, J.L. & CULLERS, R.L. (1978). Geochemistry and evolution of the Wolf River Batholith, a late Precambrian rapakiva massif in North Wisconsin, U.S.A. Precambrian Res., 7, 287-324.
- ANDREASSON, P.-G. & GORBATSHEV, R. (1980). Metamorphism in extensive nappe terrains: a study of the central Scandinavian Caledonides. Geol. Förel. Stockholm Förel., 102, 335-357.
- ANDREASSON, P.G., JOHANSSON, I. & SOLYOM, Z. (1981). Petrochemistry of metabasites of the basal Seve, Scandinavian Caledonides. Abstr. Uppsala Caled. Symp., Terra Cognita, 1, 32.
- ANDRESEN, A. (1980). The age of the Precambrian basement in western Troms, Norway. Geol. Förel. Stockholm Förel., 101, 291-298.
- ANDRESEN, A. & FAERSETH, R. (1982). An evolutionary model for the south-west Norwegian Caledonides. Am. J. Sci., 282, 756-782.
- ANHAEUSSER, C.R., MASON, R., VILJOEN, M.J., VILJOEN, R.P. (1969). A reappraisal of some aspects of Precambrian shield geology. Geol. Soc. Am. Bull., 80, 2175-2200.
- AUSTRHEIM, H. (1981). Bergen Arcs. In: W.L. Griffin & M.-B.E. Mørk (eds.), Eclogites and Basal Gneisses in west Norway. Excursion Bl., Uppsala Caled. Symp., 74-82.
- AUSTRHEIM, H. & RÅHEIM, A. (1981). Age relationships within the high grade metamorphic rocks of the Bergen Arcs, western Norway. Abstr. Uppsala Caled. Symp., Terra Cognita, 1, 33.
- AUSTRHEIM, H. & GRIFFIN, W.L. (1982). Shear deformation and eclogite formation within granulite-facies anorthosites of the Bergen Arcs, western Norway. Abstr. First Int. Eclogite Conf., Clermont Ferrand. Terra Cognita, 2, 315.
- B.S. Handbook No. 19 (1970). Carbon method 4. Methods for sampling and analysis of iron, steel and other ferrous metals.

- BANHAM, P.H., GIBBS, A.D. & HOPPER, F.W.M. (1979). Geological evidence in favour of Jotunheimen Caledonian suture. Nature, 277, 289-291.
- BANNO, S. (1970). Classification of eclogites in terms of physical conditions of their origin. Phys. Earth and Planet. Inter., 3, 405-421.
- BARKER, F., ARTH, J.G. & HUDSON, T. (1981). Tonalites in crustal evolution. Phil. Trans. R. Soc. London, A301, 293-303.
- BARTH, T.F.W. (1936). The large Precambrian intrusive bodies in the southern part of Norway. 16th Int. Geol. Congr. Wash. Rept., 1, 297-309.
- BARTH, T.F.W. (1938). Progressive metamorphism of sparagmite rocks of southern Norway. Norsk Geol. Tidsskr., 18, 54-65.
- BARTH, T.F.W. (1945). Studies on the igneous rock complex of the Oslo region. II. Systematic petrography of the platonitic rocks. Skr. Norske Vidensk.-Akad. i Oslo, Mat.-naturv. kl.
- BARTH, T.F.W. (1961). The feldspar geologic thermometers. Norsk. Geol. Tidsskr., 42, 330-339.
- BATEMAN, P.C. & DODGE, F.C.W. (1970). Variations of major chemical constituents across the central Sierra Nevada Batholith. Geol. Soc. Am. Bull., 81, 409-420.
- BATEMAN, P.C. & CHAPPELL, B.W. (1979). Crystallisation, fractionation, and solidification of the Tuolumne Intrusive series, Yosemite National Park, California. Geol. Soc. Am. Bull., 90, 465-482.
- BATTEY, M.H. & McRITCHIE, W.D. (1973). A geological traverse across the pyroxene-granulites of Jotunheimen in the Norwegian Caledonides. Norsk. Geol. Tidsskr., 53, 237-265.
- BATTEY, M.H., DAVISON, W. & OAKLEY, P.J. (1979). Almandine pseudomorphous after plagioclase in a metadolerite dyke from the Jotunheim, Norway. Min. Mag., 43, 127-130.
- BEACH, A. & TARNEY, J. (1978). Major and trace element patterns established during retrogressive metamorphism of granulite-facies gneisses, NW Scotland. Precamb. Res., 7, 325-348.
- BINNS, R.A. (1967). Barroisite-bearing eclogite from Naustdal, Sogn og Fjordane, Norway. J. Petrol., 8, 349-371.
- BOHLEN, S.R. & ESSENE, E.J. (1980). Evaluation of coexisting garnet-biotite, garnet-clinopyroxene and other thermometers in Adirondacks granulites. Geol. Soc. Am. Bull., 91, 685-719.
- BOUSEILY, A.M. & SOKKARY, A.A. (1975). The relation between Rb, Ba and Sr in granitic rocks. Chem. Geol., 16, 207-219.
- BOWDEN, P. (1974). Oversaturated alkaline rocks: granites, pantellerites and comendites. In: H. Sørensen (ed.), The Alkaline Rocks, Wiley, 109-123.

- BOWEN, N.L. & TUTTLE, O.F. (1950). The system $\text{NaAlSi}_3\text{O}_8$ - kAlSi_3O_8 - H_2O . J. Geol., 58, 489-511.
- BOWES, D.R. (1976). Archaean crustal history in the Basaltic Shield. In: B.F. Windley (ed.), The Early History of the Earth, Wiley, 481-488.
- BOYD, F.R. & ENGLAND, J.L. (1964). The system enstatite-pyrope. Carnegie Inst. Wash. Yearb., 63, 157-161.
- BOYD, F.R. & SCHAIRER, J.F. (1964). The system MgSiO_3 - $\text{CaMgSi}_2\text{O}_6$. J. Petrol., 5, 275-309.
- BRASTAD, K. (1983). Relations between anorthosites, eclogites and ultramafics in Bjørkedalen, west Norway. In: B.A. Sturt & D.G. Gee (eds.), The Caledonide Orogen - Scandinavia and related areas, Wiley (in press).
- BRIDGEWATER, D. & WINDLEY, B.F. (1973). Anorthosites, post-orogenic granites, acid volcanic rocks, and crustal development in the North Atlantic Shield during the Mid-Proterozoic. In: L.A. Lister (ed.), Symp. on Granites, Gneisses and Related Rocks, Geol. Soc. S. Afr. Sp. Publ., 3, 307-318.
- BRIDGEWATER, D., SUTTON, J. & WATTERSON, J. (1974). Crustal down-folding associated with igneous activity. Tectonophysics, 21, 57-77.
- BROOKS, C., WENDT, I. & HARRE, W. (1968). A two error regression treatment and its application to Rb-Sr and initial $^{87}\text{Sr}/^{86}\text{Sr}$ ratios of younger Variscan granitic rocks from the Schwartzwald massif, south-west Germany. J. Geophys. Res., 73, 6071-6084.
- BROWN, W.L. & PARSONS, I. (1981). Towards a more practical two-feldspar geothermometer. Contrib. Mineral. Petrol., 76, 369-377.
- BRUECKNER, H.K. (1972). Interpretation of Rb-Sr ages from the Precambrian and Palaeozoic rocks of southern Norway. Am. J. Sci., 272, 334-358.
- BRUECKNER, H.K. (1974). 'Mantle' Rb/Sr and $^{87}\text{Sr}/^{86}\text{Sr}$ ratios for clinopyroxenes from Norwegian garnet peridotites and pyroxenites. Earth Planet. Sci. Lett., 26, 26-32.
- BRUECKNER, H.K. (1975). Contact and fracture ultramafic assemblages from Norway: Rb-Sr evidence for crustal contamination. Contrib. Mineral. Petrol., 49, 39-48.
- BRUECKNER, H.K. (1977a). A structural, stratigraphic and petrologic study of anorthosites, eclogites and ultramafic rocks and their country rocks, Tafjord area, Western South Norway. Norges. Geol. Unders., 332, 1-53.
- BRUECKNER, H.K. (1977b). A crustal origin for eclogites and a mantle origin for garnet peridotites: Strontium isotopic evidence from clinopyroxenes. Contrib. Mineral. Petrol., 60, 1-15.

- BRUECKNER, H.K. (1979). Precambrian ages from the Geiranger-Tafjord-Grotli area of the Basal Gneiss Region, west Norway. Norsk. Geol. Tidsskr., 59, 141-153.
- BRUECKNER, H.K., WHEELER, R.L. & ARMSTRONG, R.L. (1968). Rb-Sr isochron for older gneisses of the Tafjord area, Basal Gneiss Region, south-western Norway. Norsk. Geol. Tidsskr., 48, 127-131.
- BRYHNI, I. (1966). Reconnaissance studies of gneisses, ultrabasites, eclogites and anorthosites in outer Nordfjord, western Norway. Norges Geol. Unders., 241, 1-68.
- BRYHNI, I., BOLLINGBERG, J. & GRAFF, P.-R. (1969). Eclogites in quartzofeldspathic gneisses of Nordfjord, west Norway. Norsk. Geol. Tidsskr., 49, 193-225.
- BRYHNI, I., GREEN, D.H., HEIER, K.S. & FYFE, W.S. (1970). On the occurrence of eclogite in Western Norway. Contrib. Mineral. Petrol., 26, 12-19.
- BRYHNI, I., FITCH, F.J. & MILLER, J.A. (1971). $^{40}\text{Ar}/^{39}\text{Ar}$ dates from recycled precambrian rocks in the gneiss region of the Norwegian Caledonides. Norsk Geol. Tidsskr., 51, 391-406.
- BRYHNI, I. & GRIFFIN, W.L. (1971). Zoning in eclogite garnets from Nordfjord, west Norway. Contrib. Mineral. Petrol., 32, 112-125.
- BRYHNI, I. & GRIMSTAD, E. (1970). Supracrustal and infracrustal rocks in the gneiss region of the Caledonides west of Breimsvatn. Norges. Geol. Unders., 266, 105-140.
- BUDDINGTON, A.F. (1939). Adirondack igneous rocks and their metamorphism. Geol. Soc. Am. Mem., 7, pp. 354.
- BUGGE, C. (1905). Kalksten og marmor i Romsdals amt. Norges Geol. Unders., 43.
- BUGGE, C. (1934). Grønne trondhjemsskifre på øyene ved Molde. Norges Geol. Unders., 43, 167-175.
- BUGGE, J.A.W. (1978). Mineral deposits in the Precambrian of southern Norway. In: J.H.V. Bowie, A. Kvalheim & H.W. Haslam (eds.), Mineral deposits of Europe, vol. 1, Northwest Europe, 212.
- BULLARD, E., EVERETT, J.E. & SMITH, A.G. (1965). The fit of the continents around the Atlantic. Phil. Trans. R. Soc. London, A258, 41-51.
- CARMICHAEL, D.M. (1978). Metamorphic bathozones and bathograds: a measure of the depth of post-metamorphic uplift and erosion on the regional scale. Am. J. Sci., 278, 769-797.
- CARSWELL, D.A. (1968a). Picritic magma-residual dunite relationships in garnet peridotite at Kalskaret near Tafjord, southern Norway. Contrib. Mineral. Petrol., 19, 97-124.

- CARSWELL, D.A. (1968b). Possible primary upper mantle peridotite in Norwegian basal gneiss. Lithos, 1, 322-355.
- CARSWELL, D.A. (1973a). The age and status of the basal gneiss complex of north-west southern Norway. Norsk Geol. Tidsskr., 53, 65-78.
- CARSWELL, D.A. (1973b). Garnet pyroxenite lens within Uglevik layered garnet peridotite. Earth Planet. Sci. Lett., 20, 347-352.
- CARSWELL, D.A. (1980). Mantle derived lherzolite nodules associated with kimberlite, carbonatite and basalt magmatism: A review. Lithos, 13, 121-138.
- CARSWELL, D.A. (1981). Clarification of the petrology and occurrence of garnet lherzolites, garnet websterites and eclogite in the vicinity of Rødhaugen, Almklovdalen, west Norway. Norsk Geol. Tidsskr., 61, 249-260.
- CARSWELL, D.A., CURTIS, C.D. & KANARIS-SOTIRIOU, R. (1974). Vein metasomatism in peridotite at Kalskaret, near Tafjord, south Norway. J. Petrol., 15, 383-402.
- CARSWELL, D.A. & GIBB, F.G.F. (1980a). The equilibration conditions and petrogenesis of European crustal garnet lherzolites. Lithos, 13, 19-29.
- CARSWELL, D.A. & GIBB, F.G.F. (1980b). Geothermometry of garnet lherzolite nodules with special reference to those from kimberlites of northern Lesotho. Contrib. Mineral. Petrol., 74, 403-416.
- CARSWELL, D.A. & HARVEY, M.A. (1983). The intrusive history and tectono-metamorphic evolution of the Basal Gneiss Complex in the Moldefjord area, west Norway. In: B.A. Sturt & D.G. Gee (eds.), The Caledonide Orogen - Scandinavia and related areas, Wiley (in press).
- CARSWELL, D.A., KROGH, E.J. & GRIFFIN, W.L. (1983a). Norwegian orthopyroxene eclogites: calculated equilibration conditions and petrogenetic implications. In: B.A. Sturt & D.G. Gee (eds.), The Caledonide Orogen - Scandinavia and related areas, Wiley (in press).
- CARSWELL, D.A., HARVEY, M.A. & AL-SAMMAN, A. (1983b). The petrogenesis of contrasting Fe-Ti and Mg-Cr garnet peridotite types in the high grade gneiss complex of western Norway. Abstr. First Int. Eclogite Conf. Clermont Ferrand, Terra Cognita, 2, 327.
- CAWTHORN, R.G. & COLLERSON, K.D. (1974). The set recalculation of pyroxene end-member parameters and the estimation of ferrous and ferric iron content from electron microprobe analyses. Am. Mineral., 59, 1203-1208.
- CATTERJEE, N.D. & JOHANNES, W. (1974). The thermal stability and standard thermodynamic properties of synthetic $2M_1$ muscovite, $KAl|AlSi_3O_{10}(OH)_2$. Contrib. Mineral. Petrol., 48, 89-114.
- CHENHALL, B.E., PHILLIPS, E.R. & GRADWELL, R. (1980). Spotted structures in gneiss and veins from Broken Hill, New South Wales, Australia. Min. Mag., 43, 779-787.

- CHINNER, G.A. (1960). Pelitic gneisses with varying ferrous/ferric ratios from Glen Cova, Angus, Scotland. J. Petrol., 1, 178-217.
- CLAESSON, S. (1981). Caledonian metamorphism of Proterozoic Seve rocks on Mt. Åreskutan, southern Swedish Caledonides. Geol. För. Stockholm Förh., 103, 291-304.
- CLIFFORD, P.M. (1968). Flood basalts, dike swarms and sub-crystal flow. Can. Jour. Earth Sci., 5, 93-96.
- COLEMAN, R.G., LEE, D.E., BEATTY, L.B. & BRANNOCK, W.W. (1965). Eclogites and eclogites: their differences and similarities. Geol. Soc. Am. Bull., 76, 483-508.
- COX, K.G., BELL, J.D. & PANKHURST, R.J. (1979). The Interpretation of Igneous Rocks, 1st ed., Allen & Unwin, pp. 450.
- CRESSEY, G., SCHMID, R. & WOOD, B.J. (1978). Thermodynamic properties of almandine-grossular garnet solid solutions. Contrib. Mineral. Petrol., 67, 397-404.
- CURRIE, K.L. & CURTIS, L.W. (1976). Application of multicomponent solution theory to jadeitic pyroxenes. J. Geol., 84, 179-194.
- CURTIS, C.D. & BROWN, P.E. (1969). The metasomatic development of zoned ultrabasic bodies in Unst, Shetland. Contrib. Mineral. Petrol., 24, 275-292.
- CUTHBERT, S.J. & CARSWELL, D.A. (1982). Petrology and tectonic setting of eclogites and related rocks from the Dalsfjord area, Sunnfjord, west Norway. Abstr. First Int. Eclogite Conf. Clermont Ferrand, Terra Cognita, 2, 315.
- CUTHBERT, S.J., HARVEY, M.A. & CARSWELL, D.A. (1983). A tectonic model for the metamorphic evolution of the Basal Gneiss Complex, western south Norway. J. metamorphic Geol., 1, 63-90.
- DAVIS, B.T.C. & BOYD, F.R. (1966). The join $Mg_2Si_2O_6$ - $CaMgSi_2O_6$ at 30 kilobars pressure and its application to pyroxenes from kimberlites. J. Geophys. Res., 71, 3567-3576.
- DAWES, P.R. (1966). Genesis of Rapakivi. Nature, 209, 569-571.
- DEER, W.A., HOWIE, R.A. & ZUSSMAN, J. (1963). Rock Forming Minerals, Vol. I, Ortho- and ring silicates. Longmans, London, 333 pp.
- DEER, W.A., HOWIE, R.A. & ZUSSMAN, J. (1963). Rock Forming Minerals, Vol. II, Single-chain silicates. Longmans, London, 333 pp.
- DEER, W.A., HOWIE, R.A. & ZUSSMAN, J. (1963). Rock Forming Minerals, Vol. III, Sheet-silicates. Longmans, London, 270 pp.
- DEER, W.A., HOWIE, R.A. & ZUSSMAN, J. (1963). Rock Forming Minerals, Vol. IV, Framework silicates. Longmans, Lond, 435 pp.

- den TEX, E. (1969). Origin of ultramafic rocks, their tectonic setting and history: a contribution to the discussion of the paper "The origin of ultramafic and ultrabasic rocks" by P.J. Wyllie.
- de WAARD, D. (1965). The occurrence of garnet in the granulite-facies terrane of Adirondack Highlands. J. Petrol., 6, 165-191.
- de WAARD, D. (1969). The anorthosite problem: the problem of the anorthosite-charnockite suite of rocks. In: Y.W. Isachsen (ed.), Origin of Anorthosites and Related Rocks. Memoir 18, New York State Museum and Science Service, 71-91.
- de WAARD, D. (1970). The anorthosite-charnockite suite of rocks of Roaring Brook Valley in the eastern Adirondacks. Am. Mineral., 55, 2063-2075.
- de WAARD, D. & WHEELER, E.P. II (1971). Chemical and petrologic trends in anorthositic and associated rocks of the Nain Massif, Labrador. Lithos, 4, 367-380.
- DEWEY, J.F. (1969). Evolution of the Appalachian/Caledonian orogen. Nature, 222, 124-129.
- DRURY, S.A. (1974). Chemical changes during retrogressive metamorphism of Lewisian granulite facies rocks from Coll and Tiree. Scott. J. Geol., 10, 237-256.
- DYRELIUS, D. (1980). Aeromagnetic interpretation in a geotraverse area across the central Scandinavian Caledonides. Geol. För. Stockholm Förh., 102, 403-420.
- ELLIOT, R.B. & COWAN, D.R. (1966). The petrochemistry of the amphibolites of the Holleindalen Greenstone Group, Jotunheimen, Norway. Norsk Geol. Tidsskr., 46, 309-325.
- ELLIS, D.E. (1978). Stability and phase equilibria of chloride and carbonate bearing scapolites at 750°C and 4000 bar. Geochim. Cosmochim. Acta, 42, 1271-1281.
- ELLIS, D.J. & GREEN, D.H. (1979). An experimental study of the effect of Ca upon Garnet-Clinopyroxene Fe-Mg exchange equilibria. Contrib. Mineral. Petrol., 71, 13-22.
- EMMETT, T.F. (1982). The petrography and geochemistry of corona-bearing dolerites from the Jotun Nappe, central southern Norway. Min. Måg., 46, 43-48.
- EMSLIE, R.F. (1973). Some chemical characteristics of anorthosite suites and their significance. Can. J. Earth Sci., 10, 54-71.
- EMSLIE, R.F. (1978). Anorthosite massifs, rapakivi granites, and late Proterozoic rifting of North America. Precambrian Research, 7, 61-98.
- ENGLAND, P.C. & RICHARDSON, S.W. (1977). The influence of erosion upon the mineral facies of rocks from different metamorphic environments. Q. J. Geol. Soc. Lond., 134, 201-213.

- ESKOLA, P. (1921). On the Eclogites of Norway. *Skr. Norske Vidensk.-Akad. i Oslo, Mat.-naturv. kl.*, 8, pp. 118.
- ESKOLA, P. (1963). The Precambrian of Finland. In: K. Rankama (ed.), The Precambrian, Vol. 1, Wiley, 145-264.
- ESSENE, E.J. (1982). Geologic thermometry and barometry. In: J.M. Ferry (ed.), Characterisation of metamorphism through mineral equilibria. *Reviews in Mineralogy, Vol. 10*. *Min. Soc. Am.*, 153-206.
- ESSENE, E.J. & FYFE, W.S. (1967). Omphacite in Californian metamorphic rocks. Contrib. Mineral. Petrol., 15, 1-23.
- EUGSTER, H.P. & WONES, D.R. (1962). Stability relations of the ferruginous biotite, annite. J. Petrol., 3, 82-125.
- EVANS, B.W. (1965). Application of a reaction rate method to the breakdown equilibria of muscovite and muscovite + quartz. Am. J. Sci., 263, 647-667.
- EVANS, B.W. (1977). Metamorphism of Alpine peridotite and serpentine. Ann. Rev. Earth Planet. Sci., 5, 397-447.
- EVANS, B.W., SHAW, D.M. & HAUGHTON, D.R. (1969). Scapolite stoichiometry. Contrib. Mineral. Petrol., 24, 293-305.
- FAURE, G. & POWELL, J.L. (1972). *Strontium Isotope Geology*, Springer-Verlag, Berlin, pp. 188.
- FERRY, J.M. (1976a). Metamorphism of calcareous sediments in the Waterville-Vassalboro area, south-central Maine: mineral reactions and graphical analysis. Am. J. Sci., 276, 841-882.
- FERRY, J.M. (1976b). P, T, f_{CO_2} and $f_{\text{H}_2\text{O}}$ during metamorphism of calcareous sediments in the Waterville-Vassalboro area, South-Central Maine. Contrib. Mineral. Petrol., 57, 119-143.
- FERRY, J.M. & BURT, D.M. (1982). Characterisation of metamorphic fluid composition through mineral equilibria. In: J.M. Ferry (ed.), Characterisation of metamorphism through mineral equilibria. *Reviews in Mineralogy, vol. 10*, *Min. Soc. Am.*, 207-262.
- FIELD, D. & RÅHEIM, A. (1979). Rb-Sr total rock isotope studies on precambrian charnockitic gneisses from south Norway: evidence for isochron resetting during a low-grade metamorphic-deformational event. Earth Planet. Sci. Lett., 45, 32-44.
- FERRY, J.M. & SPEAR, F.S. (1978). Experimental calibration of the partitioning of Fe and Mg between biotite and garnet. Contrib. Mineral. Petrol., 66, 113-117.
- FLINN, D. (1962). On folding during three-dimensional progressive deformation. Q. J. Geol. Soc. Lond., 118, 385-433.

- FLOYD, P.A. & WINCHESTER, J.A. (1975). Magma type and tectonic setting discrimination using immobile elements. Earth Planet Sci. Lett., 27, 211-218.
- FLOYD, P.A. & WINCHESTER, J.A. (1978). Identification and discrimination of altered and metamorphosed volcanic rocks using immobile elements. Chem. Geol., 21, 291-306.
- FLOYD, P.A. & WINCHESTER, J.A. (1983). Element mobility associated with meta-shear zones within the Ben Hope amphibolite suite, Scotland. Chem. Geol., 39, 1-15.
- FORBES, R.B. (1965). The comparative chemical composition of eclogite and basalt. J. Geophys. Res., 70, 1515-1521.
- FORSTER, R. (1947). Geologisch-Petrographische Untersuchungen inn Gebiete nördlich Locarno. Schweiz. Mineral. Petr. Mitt., 27, 249-471.
- FRANCIS, G.H. (1956). Facies boundaries in pelites at the middle grades of regional metamorphism. Geol. Mag., 93, 353-368.
- FREER, R. (1979). An experimental measurement of cation diffusion in almandine garnet. Nature, 280, 220-222.
- FREY, M. & ORVILLE, P.M. (1974). Plagioclase in margarite-bearing rocks. Am. J. Sci., 274, 31-47.
- FRY, N. & FYFE, W.S. (1969). Eclogites and water pressure. Contrib. Mineral. Petrol., 24, 1-6.
- FURNES, H., SKJERLIE, F.J. & TYSSSELAND, M. (1976). Plate tectonic model based on greenstone geochemistry in the late Precambrian-Lower Palaeozoic sequence in the Solund-Stavfjorden areas, west Norway. Norsk Geol. Tidsskr., 56, 161-186.
- FURNES, H., ROBINS, B., STEPHENS, M.B. & STURT, B.A. (1981). Igneous activity within the Scandinavian Caledonides. Abstr. Uppsala Caled. Symp., Terra Cognita, 1, 43.
- FYFE, W.S. (1972). The generation of batholiths. Tectonophysics, 17, 273-283.
- FYFE, W.S., TURNER, F.J. & VERHOOGEN, J. (1958). Metamorphic reactions and metamorphic facies. Geol. Soc. Am. Mem., 73, pp. 259.
- GALE, G.H. & PEARCE, J.A. (1982). Geochemical patterns in Norwegian greenstones. Can. J. Earth Sci., 19, 385-397.
- GALE, H.G. & ROBERTS, D. (1974). Trace-element geochemistry of Norwegian Lower Palaeozoic basic volcanics and its tectonic implications. Earth Planet. Sci. Lett., 22, 380-390.
- GANGULY, J. (1979). Garnet and clinopyroxene solid solutions, and geothermometry based on Fe-Mg distribution coefficients. Geochim. Cosmochim. Acta, 43, 1021-1029.

- GANGULY, J. & KENNEDY, G.C. (1974). The energetics of natural garnet solid solution. I: Mixing of the aluminosilicate end-members. Contrib. Mineral. Petrol., 48, 137-148.
- GAVELIN, S. (1975). Replacement veins in gneiss from the Precambrian of south-eastern Sweden. Geol. Förel. Stockholm Förel., 97, 56-73.
- GEBAUER, D., LAPPIN, M., GRUENENFELDER, M., KOESTLER, A. & WYTTEBACH, A. (1982). Age and origin of some Norwegian eclogites: a V-Pb zircon and REE study. First Int. Eclo. Conf., Terra Cognita, 2, 323.
- GEE, D.G. (1978). Nappe displacement in the Scandinavian Caledonides. Tectonophysics, 47, 393-419.
- GEE, D.G. (1980). Basement-cover relationships in the central Scandinavian Caledonides. Geol. Förel. Stockholm Förel., 102, 455-474.
- GHEENT, E.D. (1976). Plagioclase-garnet- Al_2SiO_5 -quartz a potential geobarometer-geothermometer. Am. Mineral., 61, 710-714.
- GHEENT, E.D., ROBBINS, D.B. & STOUT, M.Z. (1979). Geothermometry, geobarometry, and fluid compositions of metamorphosed calc-silicate and pelites, Mica Creek, British Columbia. Am. Mineral., 64, 874-885.
- GIBBS, A.D. (1982). Northerly transport and exotic olistostrome in northern Jotunheim: Possible interpretations. Abstr. Scandinavian Caledonides Research Seminar, Bedford College, London. Convenor: P. Banham.
- GJELSVIK, T. (1951). Oversikt over bergartene i Sunnmøre og Tilgrensende deler av Nordfjord. Norges Geol. Unders., 179, pp. 45.
- GJELSVIK, T. (1952). Metamorphosed dolerites in the gneiss area of Sunnmøre on the west coast of southern Norway. Norsk Geol. Tidsskr., 30, 33-134.
- GJELSVIK, T. (1953). Det nordvestlige gneis-område i det sydlige Norge, aldersforhold og tektonisk-stratigrafisk stilling. Norges Geol. Unders., 184, 71-94.
- GLASSLEY, W.E. (1982). Aqueous SiO_2 control on eclogite stability. Abstr. First Int. Eclogite Conf., Clermont Ferrand, Terra Cognita, 2, 332.
- GODOVIKOV, A.A. & KENNEDY, G.C. (1968). Kyanite eclogites. Contrib. Mineral. Petrol., 19, 169-176.
- GOLDMAN, D.S. & ALBEE, A.L. (1977). Correlation of Mg/Fe partitioning between garnet and biotite with $^{18}O/^{16}O$ partitioning between quartz and magnetite. Am. J. Sci., 277, 750-767.
- GOLDSCHMIDT, V.M. (1916). Geologisch-petrographische Studien in Hochgebirge der südlichen Norwegens. IV. Uebersicht der Eruptivgesteine im kaledonischen Gebirge Zwischen Stavanger und Trondheim. Vid.-Selsk. Kristiania Skrifter, I. Mat.-Natur. kl. 1916, 2, pp. 140.

- GOLDSMITH, J.R. (1976). Scapolites, granulites, and volatiles in the lower crust. Geol. Soc. Am. Bull., 87, 161-168.
- GOLDSMITH, J.R. & NEWTON, R.C. (1977). Scapolite-plagioclase stability-relations at high pressures and temperatures in the system $\text{NaAlSi}_3\text{O}_8\text{-CaAl}_2\text{Si}_2\text{O}_8\text{-CaCO}_3\text{-CaSO}_4$. Am. Mineral., 62, 1063-1081.
- GORBATSHEV, R. (1981). Basement and Precambrian nappe elements in the south-central Scandinavian Caledonides. Abstr. Uppsala Caledonide Symp., Terra Cognita, 1, 46.
- GREEN, D.H. & MYSEN, B.P. (1972). Genetic relationship between eclogite and hornblende + plagioclase pegmatite in W Norway. Lithos, 5, 147-161.
- GREEN, D.H. & LAMBERT, I.B. (1965). Experimental crystallisation of anhydrous granite at high pressures and temperatures. J. Geophys. Res., 70, 5259-5268.
- GREEN, D.H. & RINGWOOD, A.E. (1967a). An experimental investigation of the gabbro to eclogite transformation and its petrological applications. Geochim. Cosmochim. Acta, 31, 767-833.
- GREEN, D.H. & RINGWOOD, A.E. (1967b). The stability fields of aluminous pyroxene peridotite and garnet peridotite and their relevance in upper mantle structure. Earth Planet. Sci. Lett., 3, 151-160.
- GREEN, D.H. & RINGWOOD, A.E. (1970). Mineralogy of peridotitic compositions under upper mantle conditions. Phys. Earth Planet. Interiors, 3, 359-371.
- GRIFFIN, W.L. (1971). Genesis of coronas in anorthosites of the upper Jotun Nappe, Indre Sogn, Norway. J. Petrol., 12, 219-243.
- GRIFFIN, W.L. & MURTHY, V.R. (1968). Abundances of K, Rb, Sr and Ba in some ultrabasic rocks and minerals. Earth Planet. Sci. Lett., 4, 497-501.
- GRIFFIN, W.L. & HEIER, K.S. (1973). Petrological implications of some corona structures. Lithos, 6, 315-335.
- GRIFFIN, W.L. & RÅHEIM, A. (1973). Convergent metamorphism of eclogites and dolerites, Kristiansund area, Norway. Lithos, 6, 21-40.
- GRIFFIN, W.L., HEIER, K.S., TAYLOR, P.N. & WEIGAND, P.W. (1974). General geology, age and chemistry of the Raftsund mangerite intrusion, Lofoten-Vesterålen. Norges Geol. Unders., 312, pp. 30.
- GRIFFIN, W.L. & BRUECKNER, H.K. (1980). Caledonian Sm-Nd ages and a crustal origin for Norwegian eclogites. Nature, 285, 319-321.
- GRIFFIN, W.L. & QVALE, H. (1981). Superferric eclogites and the crustal origin of garnet peridotite. Abstr. Uppsala Caled. Symp., Terra Cognita, 1, 48.

- GRIFFIN, W.L. & BRUECKNER, H.C. (1982). Rb-Sr and Sm-Nd studies of Norwegian eclogites. Abstr. First Int. Eclo. Conf., Clermont-Ferrand, Terra Cognita, 2, 324.
- GRIFFIN, W.L. & CARSWELL, D.A. (1983). In situ metamorphism of Norwegian eclogites: an example. In: B.A. Sturt & D.G. Gee (eds.), The Caledonide Orogen - Scandinavia and related areas, Wiley (in press).
- GRIFFIN, W.L., AUSTRHEIM, H., BRASTAD, K., BRYHNI, I., KRILL, A.G., MØRK, M.-B.E., QVALE, H. & TØRUDBAKKEN, B. (1983). High-pressure metamorphism in the Scandinavian Caledonides. In: B.A. Sturt & D.G. Gee (eds.), The Caledonide Orogen - Scandinavia and related areas, Wiley (in press).
- HANSEN, B.T., OBERLI, F. & STEIGER, R.H. (1973). The geochronology of the Scoursby Sund Area. Program report 4. Rb/Sr whole rock and mineral ages. Rapp. Grønland Geol. Unders., 58, 55-58.
- HARIYA, Y. & KENNEDY, G.C. (1968). Equilibrium study of anorthite under high pressure and high temperature. Am. J. Sci., 266, 196-203.
- HARLEY, S.L. & GREEN, D.H. (1982). Garnet-orthopyroxene barometry for granulites and peridotites. Nature, 300, 697-701.
- HART, S.R. & BROOKS, C. (1970). Rb-Sr mantle exsolution models. Carnegie Inst. Wash. Yearb., 69, 426-429.
- HARVEY, M.A. (1983). A geochemical and Rb-Sr study of the Proterozoic augen orthogneisses on the Molde peninsula, west Norway. Lithos, (in press).
- HEARD, H.C. (1963). Effect of large changes in strain rate in the experimental deformation of Yale marble. J. Geol., 71, 162-195.
- HEARD, H.C. & RALEIGH, C.B. (1972). Steady-state flow in marble at 500°C to 800°C. Geol. Soc. Am. Bull., 83, 935-956.
- HEIER, K.S. & COMPSTON, W. (1969). Interpretation of Rb-Sr age patterns in high-grade metamorphic rocks, north Norway. Norsk Geol. Tidsskr., 49, 257-283.
- HEIER, K.S. & THORESEN, K. (1971). Geochemistry of high-grade metamorphic rocks, Lofoten-Vesterålen, North Norway. Geochim. Cosmochim. Acta, 35, 89-99.
- HEINRICH, C.A. (1982). Kyanite-eclogite to amphibolite facies evolution of hydrous mafic and pelitic rocks, Adula Nappe, Central Alps. Contrib. Mineral. Petrol., 81, 30-38.
- HERMANS, G.A.E.M., TOBI, A.C., POORTER, R.P.E. & MAIJER, C. (1975). The high-grade metamorphic precambrian of the Sirdal-Ørsdal area, Rogalands/Vest-Ayder, South-west Norway. Norges Geol. Unders., 318, 51-74.
- HERNE, I. (1954a). Trondhjemsskifrene ved Molde (The Trondheim schists of Molde). Norsk Geol. Tidsskr., 34, 123-137.

- HERNES, I. (1954b). Eclogite-amphibolite on the Molde peninsula, southern Norway. Norsk Geol. Tidsskr., 33, 163-184.
- HERNES, I. (1955). Geologisk oversikt over Molde - Kristiansundsområdet. Det kgl. Norske Vidensk. Selsk. Skifter, 5, 17 pp.
- HERNES, I. (1956a). Surnadalssynklinalen. The Surnadal syncline, Central Norway. Norsk Geol. Tidsskr., 36, 25-39.
- HERNES, I. (1956b). Kaledonsk-tektonikk i midt-Norge. Norsk Geol. Tidsskr., 36, 157-166.
- HERNES, I. (1965). Die Kaledonische Schichtenfolge in Mittel norwegen. Neues Jahrb. Geol. Paläont. Mh., 2, 69-84.
- HERNES, I. (1967). The late Pre-Cambrian stratigraphic sequence in the Scandinavian mountain chain. Geol. Mag., 104, 557-563.
- HIETANEN, A. (1975). Generation of potassium-poor magmas in the northern Sierra Nevada and the Svecofennian of Finland. J. Res. U.S. Geol. Surv., 3, 631-645.
- HIGGINS, N.W. (1971). Cataclastic rocks. Prof. Pap. U.S. Geol. Surv., 687, pp. 97.
- HOBBS, B.E., MEANS, W.D. & WILLIAMS, P.F. (1976). An Outline of Structural Geology, Wiley, pp. 571.
- HOFMANN, A.W. (1975). Diffusion of Ca and Sr in a basalt melt. Carnegie Inst. Wash. Yearb., 74, 183.
- HOLDAWAY, M.J. (1971). Stability of andalusite and the aluminium silicate phase diagram. Am. J. Sci., 271, 97-131.
- HOLDAWAY, M.J. & LEE, S.M. (1977). Fe-Mg cordierite stability in high-grade pelitic rocks based on experimental, theoretical, and natural observations. Contrib. Mineral. Petrol., 63, 175-193.
- HOLLAND, T.H. (1900). The charnockite series, a group of Archaen hyperthentic rocks in peninsular India. Geol. Surv. India Mem., 28, 119-249.
- HOLLAND, T.J.B. (1979). Experimental determination of the reaction pargasite = jadeite + kyanite + H₂O, and internally consistent thermodynamic data for part of the system Na₂O-Al₂O₃-SiO₂-H₂O with applications to eclogites and Uneschists. Contrib. Mineral. Petrol., 68, 293-301.
- HOLLAND, J.G. & LAMBERT, R.St.J. (1973). Comparative major element geochemistry of the Lewisian of the mainland of Scotland. In: R.G. Park & J. Tarney (eds.), The Early Precambrian of Scotland and Related Rocks of Greenland, Keele, 51-63.
- HOLLOWAY, J.R. (1981). Compositions and volumes of supercritical fluids in the Earth's crust. In: L.S. Hollister & M.L. Crawford (eds.), Fluid Inclusions: Applications to Petrology, Mineral. Assoc. Canada, Calgary, 13-38.

- HOLM, P.E. (1982). Non-recognition of continental tholeiites using the Ti-Y-Zr diagram. Contrib. Mineral. Petrol., 79, 308-310.
- HOLTEDAHL, O. (1936). Trekk av det skandinaviske fjellkjedestrøks historie. Nordiska naturforskarmötet i Helsingfors 1936, 129-145.
- HOLTEDAHL, O. (1938). Geological observations in the Opdal-Sunddal-Trollheimen district. Norsk Geol. Tidsskr., 18, 29-53.
- HOLTEDAHL, O. (1944). On the Caledonides of Norway with some scattered local observations. Skr. Norske Vidensk.-Akad. i Oslo, Mat.-naturv. kl., 1944, 4, pp. 31.
- HOLTEDAHL, O. (1953). Norges Geologi. Norges Geol. Unders., 164.
- HOLTEDAHL, O. (1960). Geology of Norway. Norges Geol. Unders., 208, pp. 540.
- HOLTEDAHL, O. & DONS, J.A. (1960). Geologiske kart over Norges, Bergrunnskart 1:1000000. Norges Geol. Unders., 208.
- HOOPER, P.R. (1968). The 'a' lineation and the trend of the Caledonides of northern Norway. Norsk Geol. Tidsskr., 48, 261-268.
- HOSSACK, J.R. (1962). Pebble deformation and thrusting in the Bygdin area (S. Norway). Tectonophysics, 5, 315-339.
- HOSSACK, J.R. (1978). The correction of stratigraphic sections for tectonic finite strain in the Bygdin area, Norway. Q. J. Geol. Soc. Lond., 135, 229-241.
- HOSSACK, J.R. (1982). A geological section from the foreland across the Valdres and Jotunheim areas to the west coast of Norway. Abstr. Scandinavian Caledonides Research Seminar, Bedford College, London. Convenor: P. Banham.
- HOSSACK, J.R., NICKELSEN, R.P. & GARTON, M. (1981). The geological section from the foreland up to the Jotun sheet in the Valdres area, south Norway. Abstr. Uppsala Caled. Symp., Terra Cognita, 1, 52.
- HUBBARD, F.H. & WHITLEY, J.E. (1978). Rapakivi granite, anorthosite and charnockite plutonism. Nature, 271, 439-440.
- HUDLESTON, P.J. (1973). The analysis and interpretation of minor folds developed in the Moine rocks of Monar, Scotland. Tectonophysics, 17, 89-132.
- HUMPHRIES, F.J. & CLIFF, R.A. (1982). Sm-Nd dating and cooling history of Scourian granulites, Sutherland. Nature, 295, 515-517.
- HUNT, J.A. & KERRICK, D.M. (1977). The stability of sphene; experimental redetermination and geological implications. Geochim. Cosmochim. Acta, 41, 279-288.
- HUNZIKER, J.C. (1982). Systematics and problems in isotope work on eclogites. Abstr. First Int. Eclogite Conf., Clermont Ferrand, Terra Cognita, 2, 302.

- HUTCHISON, C.S. (1974). Laboratory handbook of petrographic techniques, Wiley, 527 pp.
- IDEN, I.K. (1981). Geochemistry of precambrian basal gneisses in Lofoten-Vesterålen, northern Norway. Precambrian Res., 14, 135-166.
- IIYAMA, J.T. (1966). Contribution a l'étude des équilibres sub-solidus du système tonaire orthose-albite-anorthite à l'aide des réactions d'échange d'ions Na-K au contact d'une solution hydrothermale. Bull. Soc. Fr. Mineral. Cristallogr., 89, 442-454.
- IGRENS, M. & HIORTDAHL, T. (1864). Om de geologiske forhold paa kyststraekningen af Nordre Bergenhus Amt. Universitets program 2, Halvaar, Christiania 1864, pp. 14.
- IRVINE, T.N. & BARAGAR, W.R.A. (1971). A guide to the chemical classification of the common volcanic rocks. Can. J. Earth Sci., 8, 523-548.
- ISACHSEN, Y.W. (1969). Origin of anorthosite and related rocks - a summarisation. In: Y.W. Isachsen (ed.), Origin of Anorthosite and related rocks, Memoir 18, New York State Mus. Sci. Serv., 435-445.
- JACKSON, E.D. & THAYER, J.P. (1972). Some criteria for distinguishing between stratiform, concentric and alpine peridotite-gabbro complexes. 24th Int. Geol. Congr. Montreal Proc. Sect., 2, 289-296.
- JACOBSEN, S.B. & HEIER, K.S. (1978). Rb-Sr isotope systematics in metamorphic rocks, Kongsberg sector, south Norway. Lithos, 11, 257-276.
- JAEGER, J.C. (1969). Elasticity, fracture and flow with engineering and geological application. Methuen, 268 pp.
- JENKINS, D.M. & NEWTON, R.C. (1979). Experimental determination of the spinel peridotite to garnet peridotite inversion at 900°C and 1000°C in the system CaO-MgO-Al₂O₃-SiO₂ and at 900°C with natural garnet and olivine. Contrib. Mineral. Petrol., 68, 407-420.
- KERRICK, D.M. (1972). Experimental determination of muscovite + quartz stability with $P_{H_2O} < P_{total}$. Am. J. Sci., 272, 946-958.
- KERRICK, D.M. (1974). Review of metamorphic mixed volatile (H₂O-CO₂) equilibrium. Am. Mineral., 59, 729-762.
- KEY, R.M. & WRIGHT, E.P. (1982). The genesis of the Gaborone rapakivi granite complex in southern Africa. Q. J. Geol. Soc. Lond., 139, 109-126.
- KNORRING, O. von & KENNEDY, W.Q. (1958). The mineral paragenesis and metamorphic status of garnet-hb-pyx-scapolite gneiss from Ghana (Gold Coast). Min. Mag., 31, 846.
- KOLBE, P. & TAYLOR, S.R. (1966). Major and trace element relationships in granulites and granites from Australia and South Africa. Contrib. Mineral. Petrol., 12, 202-222.
- KOLDERUP, C.F. (1923). Kvamshestens devonfelt. Bergen Mus. Arb. 1920-21. Naturvidensk, R4, pp. 96.

- KOLDERUP, N.-H. (1928). Fjellbygningen i kyststrøket mellom Nordfjord og Sognfjord. Bergen Mus. Årb. 1928, Naturvidensk., R7, pp. 222.
- KOLDERUP, N.-H. (1952). The age of gneisses and migmatites in the 'North-West Block' of southern Norway. Trans. Edin. Geol. Soc., 15, 234-240.
- KOLDERUP, N.-H. (1960). Origin of Norwegian eclogites in gneisses. Norsk Geol. Tidsskr., 40, 73-76.
- KOLDERUP, C.F. & KOLDERUP, N.-H. (1940). Geology of the Bergen Arc System. Bergen Mus. Skr., 20, pp. 137.
- KRATZ, K.O., GERLING, E.K. & LOBACH-ZHUCHENKO, S.B. (1968). The isotope geology of the Precambrian of the Baltic Shield. Can. J. Earth Sci., 5, 657-660.
- KRAUSKOPF, K.B. (1967). Introduction to geochemistry. McGraw-Hill, New York, pp. 721.
- KRILL, A.G. (1980). Tectonics of the Oppdal area, central Norway. Geol. Förr. Stockholm, Förrh., 102, 523-530.
- KRILL, A.G. (1981). Rb-Sr study of metamorphosed dolerite dikes and psammite: "Precambrian" vs. "Caledonian" orogenesis in the western gneiss region of Norway. Abstr. Uppsala Caledonide Symp., Terra Cognita, 1, 56.
- KRILL, A.G. (1983). Relationships between the western gneiss region and the Trondheim region: Stockwerk-tectonics reconsidered. In: B.A. Sturt & D.G. Gee (eds.), The Caledonide Orogen - Scandinavia and related areas, Wiley (in press).
- KRILL, A.G. & GRIFFIN, W.L. (1981). Interpretation of Rb-Sr dates from the Western Gneiss Region: a cautionary note. Norsk Geol. Tidsskr., 61, 83-86.
- KROGH, E.J. (1977). Evidence of Precambrian continent-continent collision in Western Norway. Nature, 267, 17-19.
- KROGH, E.J. (1980a). Geochemistry and petrology of glaucophane-bearing eclogites and associated rocks from Sunnfjord, western Norway. Lithos, 13, 355-380.
- KROGH, E.J. (1980b). Compatible P-T conditions for eclogites and surrounding gneisses in the Kristiansund area, western Norway. Contrib. Mineral. Petrol., 75, 387-393.
- KROGH, E.J. (1982). Metamorphic evolution of Norwegian country-rock eclogites, as deduced from mineral inclusions and compositional zoning in garnets. Lithos, 15, 305-321.
- KROGH, E.J. (1983). Granat.-clinopyroksen geothermometri-en retolkning av eksisterende eksperimentelle data. N.G.F. Geolognytt, 17, 33.

- KROGH, T.E. & DAVIS, G.L. (1973). The effect of regional metamorphism on U-Pb system in zircon and a comparison with Rb-Sr systems in the same whole rock and its constituent minerals. Carnegie Inst. Wash. Yearb., 73, 601.
- KROGH, T.E., MYSEN, B.O. & DAVIS, G.L. (1973). A Paleozoic age for the primary minerals of a Norwegian eclogite. Carnegie Inst. Wash. Yearb., 73, 575-576.
- KVALE, A. (1953). Linear structures and their relation to movement in the Caledonides of Scandinavia and Scotland. Q. J. Geol. Soc. Lond., 109, 51-73.
- KVOVO, O. & TILTON, G.R. (1966). Mineral ages from the Finnish Precambrian. J. Geol., 74, 421-442.
- LAMBERT, I.B. & HEIER, K.S. (1968). Geochemical investigation of deep seated rocks in the Australian shield. Lithos, 1, 30-53.
- LAMBERT, R.St.J., CHAMBERLAIN, V. & HOLLAND, J.G. (1976). The geochemistry of Archaean rocks. In: B.F. Windley (ed.), The Early History of the Earth, Wiley, 377-387.
- LAPORTE, L.F. (1968). Ancient Environments, Prentice-Hall Inc., pp. 116.
- LAPPIN, M.A. (1960). On the occurrence of kyanite in the eclogites of the Selje and Aheim districts, Nordfjord. Norsk Geol. Tidsskr., 40, 289-296.
- LAPPIN, M.A. (1962). The eclogites, dunites and anorthosites of the Selje and Almklovdalen districts, Nordfjord, S.W. Norway. Unpubl. Ph.D. thesis, University of Durham.
- LAPPIN, M.A. (1966). The field relationships of basic and ultrabasic masses in the Basal Gneiss Complex of Stadlandet and Almklovdalen, Nordfjord, S.W. Norway. Norsk Geol. Tidsskr., 46, 439-495.
- LAPPIN, M.A. (1974). Eclogites from the Sunndal-Grubse ultramafic mass, Almklovdalen, Norway and the T-P history of the Almklovdalen masses. J. Petrol., 15, 567-601.
- LAPPIN, M.A. & SMITH, D.C. (1978). Mantle equilibrated orthopyroxene eclogite pods from the Basal Gneisses in the Selje district, western Norway. J. Petrol., 19, 530-584.
- LAPPIN, M.A., PIDGEON, R.T. & VAN BREEMEN, O. (1979). Geochronology of basal gneisses and mangerite syenites of Stadlandet, west Norway. Norsk Geol. Tidsskr., 59, 161-181.
- LASNIER, B. (1982). Recrystallisation processes in eclogites. Abstr. First Int. Eclogite Conf., Clermont Ferrand, Terra Cognita, 2, 233.
- LEAKE, B.E. (1964). The chemical distinction between ortho- and para-amphibolites. J. Petrol., 5, 238-254.
- LEAKE, B.E. (1969). The discrimination of ortho and para charnockitic rocks, anorthosites and amphibolites. Ind. Mineral., 10, 89-104.

- LEAKE, B.E. (1978). Nomenclature of amphiboles. Min. Mag., 42, 533-563.
- LETTENEY, C.D. (1969). The anorthosite-norite-charnockite series of the Thirteenth Lake Dome, south central Adirondacks. In: Y.W. Isachsen (ed.), Anorthosites and related rocks, Memoir 18, New York State Mus. and Sci. Service, 329-342.
- LIÉGEOIS, J.-P. & DUCHESNE, J.-C. (1981). The Lac Cornu retrograded eclogites (Aiguilles Rouges massif, western Alps, France): evidence of crustal origin and metasomatic alteration. Lithos, 14, 35-48.
- LIPSON, R.D. (1980). The granitic rocks surrounding the Aygeneyssberge - a metamorphosed rapakivi suite. Trans. geol. Soc. S. Afr., 83, 179-192.
- LOVERING, J.F. & WHITE, A.J.R. (1969). Granulitic and eclogitic inclusions from basic pipes at Delegate, Australia. Contrib. Mineral. Petrol., 21, 9-52.
- LUNDQVIST, T. (1980). The Precambrian of Sweden. In: The Geology of the European Countries, Denmark, Finland, Iceland, Sweden, Norway. 24th Int. Geol. Congr., p. 219-271.
- LØSET, F. (1977). Three fold phases in the northern part of Trollheimen in the Norwegian Caledonides. Norsk Geol. Tidsskr., 57, 121-131.
- MCDUGALL, I. & GREEN, D.H. (1964). Excess radiogenic argon in pyroxenes and isotopic ages on minerals from Norwegian eclogites. Norsk Geol. Tidsskr., 44, 183-196.
- MCGREGOR, V.R. (1973). The early Precambrian gneisses of the Godthaab district, west Greenland. Phil. Trans. R. Soc. Lond., A273, 343-358.
- MAALØE, S. & WYLLIE, P.J. (1975). Water content of a granite magma deduced from the sequence of crystallisation determined experimentally with water-undersaturated conditions. Contrib. Mineral. Petrol., 52, 175-191.
- MacGREGOR, I.D. (1970). The effect of CaO, Cr₂O₃, Fe₂O₃ and Al₂O₃ on the stability of spinel and garnet peridotites. Phys. Earth Planet. Int., 3, 372-377.
- MARTIGNOLE, J. (1979). Charnockite genesis and the Proterozoic crust. Precambrian Res., 9, 303-310.
- MASON, B. (1966). Principles of Geochemistry, 3rd ed., Wiley, pp. 329.
- MEARNS, E.W. & LAPPIN, M.A. (1982a). A Sm-Nd study of 'internal' and 'external eclogites', garnet lherzolite and grey gneiss from Almklovdalen, western Norway. First Int. Eclogite Conf., Clermont Ferrand, Terra Cognita, 2, 324.
- MEARNS, E.W. & LAPPIN, M.A. (1982b). The origin and age of 'external eclogites' and gneisses from the Selje district of the western gneiss region, Norway. First Int. Eclogite Conf., Clermont Ferrand, Terra Cognita, 2, 324.

- MEDARIS, L.G. (1980). Petrogenesis of the Lien peridotite and associated eclogites, Almklovdalen, western Norway. Lithos, 13, 339-353.
- MEHNERT, K.R. (1968). Migmatites and the Origin of Granitic Rocks. Elsevier, Amsterdam, pp. 393.
- MICHOT, P. (1969). Geological environments of the anorthosites of south Rogaland, Norway. In: Y.W. Isachsen (ed.), Origin of Anorthosites and Related Rocks, Memoir 18, New York State Mus. and Sci. Services, 411-423.
- MICHOT, J. & PASTEELS, P. (1969). The prospects of the Rb-Sr and the U-Pb methods for an advanced geochronological investigation of the Precambrian of southern Norway. Norges Geol. Unders., 258, 17-24.
- MISCH, P. (1969). Paracrystalline microboudinage of zoned grains and other criteria for synkinematic growth of metamorphic minerals. Am. J. Sci., 267, 43-63.
- MILNE, K.P. & STARMER, I.C. (1982). Extreme differentiation in the Proterozoic Gjerstad-Morkeheia Complex of south Norway. Contrib. Mineral. Petrol., 79, 381-393.
- MITCHELL, A.H.G. (1975). Evolution and global tectonics: Petrogenetic view: Discussion. Bull. Geol. Soc. Am., 86, 1487.
- MOINE, B. & LA ROCHE, H. (1968). Nouvelle approche du problème de l'origine des amphibolites à partir de leur composition chimique. Comptes Rendues Acad. Sci. Paris, serie D, 267, 2084-2087.
- MORGAN, B.A. (1970). Petrology and mineralogy of eclogite and garnet amphibolite from Puerto Cabello, Venezuela. J. Petrol., 11, 101-145.
- MORI, T. & GREEN, D.H. (1978). Laboratory duplication of phase equilibria observed in natural garnet lherzolites. J. Geol., 86, 83-97.
- MORSE, S.A. (1970). Alkali feldspars with water at 5 kbar pressure. J. Petrol., 11, 221-251.
- MOTTANA, A. (1977). Petrochemical characteristics of the western Alps eclogites. N. Jb. Mineral. Abh., 130, 78-88.
- MULLEN, E.D. (1983). MnO/TiO₂/P₂O₅: a minor element discriminant for basaltic rocks of oceanic environments and its implication for petrogenesis. Earth Planet. Sci. Letts., 62, 53-62.
- MURET, C. (1960). Partie S.E. de la culmination du Romsdal, Chaîne Caledonienne Norvège. Int. Geol. Congr. Norden, 1960, 19, 28-32.
- MIYASHIRO, A. (1973). Metamorphism and Metamorphic Belts. Allen & Unwin, pp. 492.
- MYERS, J.S. (1978). Formation of banded gneisses by deformation of igneous rocks. Precambrian Res., 6, 43-64.
- MYSEN, B. (1972). Five clinopyroxenes in the Hareidland eclogite, Western Norway. Contrib. Mineral. Petrol., 34, 315-325.

- MYSEN, B.O. & GRIFFIN, W.L. (1973). Pyroxene stoichiometry and the breakdown of omphacite. Am. Mineral., 58, 60-63.
- MYSEN, B.O. & HEIER, K.S. (1972). Petrogenesis of eclogites in high grade metamorphic gneisses exemplified by the Hareidland eclogite, western Norway. Contrib. Mineral. Petrol., 36, 73-94.
- MØRK, M.B.E. (1982). A gabbro-eclogite transition on Flemsøy, Sunnmøre, western Norway. Abstr. First Int. Eclogite Conf., Clermont Ferrand, Terra Cognita, 2, 316.
- NEUMANN, E.-R. (1976). Two refinements for the calculation of structural formulae for pyroxenes and amphiboles. Norsk Geol. Tidsskr., 56, 1-6.
- NEWTON, R.C. & GOLDSMITH, J.R. (1975). Stability of the scapolite meionite ($3\text{CaAl}_2\text{Si}_2\text{O}_7\text{CaCO}_3$) at high pressures and storage of CO_2 in the deep crust. Contrib. Mineral. Petrol., 49, 49-62.
- NEWTON, R.C. & GOLDSMITH, J.R. (1976). Stability of the end-member scapolites: $3\text{NaAlSi}_3\text{O}_8\cdot\text{NaCl}$, $3\text{CaAl}_2\text{Si}_2\text{O}_8\cdot\text{CaCO}_3$, $3\text{CaAl}_2\text{Si}_2\text{O}_8\cdot\text{CaSO}_4$. Z. kristallogr., 143, 333-353.
- NEWTON, R.C. & HASELTON, H.T. (1981). Thermodynamics of the garnet-plagioclase- Al_2SiO_5 -quartz geobarometer. In: R.C. Newton, A. Navrotsky and B.J. Wood (eds.), Thermodynamics of minerals and melts, Springer-Verlag, 131-147.
- NEWTON, R.C. & PERKINS III, D. (1982). Thermodynamic calibration of geobarometers based on the assemblages garnet-plagioclase-orthopyroxene (clinopyroxene)-quartz. Am. Mineral., 67, 203-222.
- NICKELSEN, R.P., GARTON, M. & HOSSACK, J.R. (1981). Late Precambrian to Ordovician sedimentology and stratigraphic correlation of the Valdres and Synnfjell thrust sheets in the Valdres area, central southern Norway. Abstr. Uppsala Caled. Symp., Terra Cognita, 1, 61.
- NOCKOLDS, S.R. & ALLEN, R. (1952). The geochemistry of some igneous rock series. Geochim. Cosmochim. Acta, 4, 105-142.
- NORRISH, K. & HUTTON, J.T. (1969). An accurate X-ray spectrographic method for the analysis of a wide range of geological samples. Geochim. Cosmochim. Acta, 33, 431-453.
- OFTEDAHL, C. (1964). The nature of the basement contact. Norges Geol. Unders., 227, 5-12.
- OFTEDAHL, C. (1980). Norway. In: The Geology of the European Countries. Denmark, Finland, Iceland, Sweden, Norway. 24th Int. Geol. Congr., 347-356.
- O'HARA, M.J. & MERCY, E.L.P. (1963). Petrology and petrogenesis of some garnetiferous peridotites. Trans. Roy. Soc. Edin., 65, 251-314.
- O'HARA, M.J., RICHARDSON, S.W. & WILSON, G. (1971). Garnet peridotite stability and occurrence in crust and mantle. Contrib. Mineral. Petrol., 32, 48-68.

- O'HARA, M.J. & YARWOOD, G. (1978). High pressure-temperature point on an Archaean geotherm, implied magmagenesis by crustal anatexis, and consequences for garnet-pyroxene thermometry and barometry. Phil. Trans. R. Soc. Lond., A288, 441-456.
- O'NEILL, H.St.C. (1981). The transition between spinel lherzolite and garnet lherzolite and its use as a geobarometer. Contrib. Mineral. Petrol., 77, 185-194.
- O'NEILL, H.St.C. & WOOD, B.J. (1979). An experimental study of Fe-Mg partitioning between garnet and olivine and its calibration as a geothermometer. Contrib. Mineral. Petrol., 70, 59-70.
- O'NEILL, H.St.C. & WOOD, B.J. (1979). An experimental study of Fe-Mg partitioning between garnet and olivine and its calibration as a geothermometer: corrections. Contrib. Mineral. Petrol., 72, 337.
- ORVILLE, P.M. (1963). Alkali ion exchange between vapor and feldspar phases. Am. J. Sci., 261, 201-237.
- ORVILLE, P.M. (1972). Plagioclase cation exchange equilibria with aqueous chloride solution: Results at 700°C and 2000 bars in the presence of quartz. Am. J. Sci., 72, 234-272.
- ORVILLE, P.M. (1975). Stability of scapolite in the system Ab-An-NaCl-CaCO₃ at 4 kb and 750°C. Geochim. Cosmochim. Acta, 39, 1091-1105.
- OSBORN, E.F. (1959). Role of oxygen pressure in the crystallisation and differentiation of basaltic magma. Am. J. Sci., 257, 609-647.
- PAPANASTASSIOU, D.A. & WASSERBURG, G.J. (1969). Initial strontium isotopic abundances and the resolution of small time differences in the formation of planetary objects. Earth Planet. Sci. Lett., 5, 361-376.
- PAPIKE, J.J., CAMERON, K.L. & BALDWIN, K. (1974). Amphiboles and pyroxenes: Characterisation of other than quadrilateral components and estimates of ferric iron from microprobe data (abstr.). Geol. Soc. Am. Abstr. with Prog., 6, 1053.
- PARRAS, K. (1958). On the charnockites in the light of a highly metamorphic rock complex in southwestern Finland. Bull. Comm. géol. Finlande, 181.
- PARSONS, I. (1978). Feldspars and fluids in cooling plutoan. Min. Mag., 42, 1-17.
- PASTEELS, P. & MICHOT, J. (1975). Geochronologic investigation of the metamorphic terrain of southwestern Norway. Norsk Geol. Tidsskr., 55, 111-134.
- PEACOCK, M.A. (1931). Classification of igneous rock series. J. Geol., 39, 54-67.
- PEARCE, J.A. (1975). Basalt geochemistry used to investigate past tectonic environments on Cyprus. Tectonophysics, 25, 41-67.

- PEARCE, J.A. (1976). Statistical analysis of major element patterns in basalts. J. Petrol., 17, 15-43.
- PEARCE, J.A. & CANN, J.R. (1973). Tectonic setting of basic volcanic rocks determined using trace element analyses. Earth Planet. Sci. Lett., 19, 290-300.
- PEARCE, J.A. & NORRY, J.N. (1979). Petrogenetic implications of Ti, Zr, Y & Nb variations in volcanic rocks. Contrib. Mineral. Petrol., 69, 33-47.
- PEDERSEN, S. & FALKUM, T. (1975). Rb-Sr isochrons for the granitic plutons around Farsund, southern Norway. Chem. Geol., 15, 97-101.
- PERCHUK, L.L. & RYABCHIKOV, I.D. (1968). Mineral equilibria in the system nepheline-alkali feldspar-plagioclase and their petrological significance. J. Petrol., 9, 123-167.
- PERCIVAL, J.A. & HELMSTAEDT, H. (1978). Zoned epidote nodules from sedimentary rocks of the Eastport formation, south west New Brunswick. Can. J. Earth Sci., 15, 1194-1200.
- PETERSEN, J.S. (1980a). The zoned kleivan granite - an end member of the anorthosite suite in S.W. Norway. Lithos, 13, 79-95.
- PETERSEN, J.S. (1980b). Rare-earth element fractionation and petrogenetic modelling in charnockitic rocks, southwest Norway. Contrib. Mineral. Petrol., 73, 161-172.
- PHILLIPS, F.C. (1937). A fabric study of some Moine schists and associated rocks. Q. J. Geol. Soc. Lond., 93, 581-620.
- PHILLIPS, F.C. (1971). The use of Stereographic Projection in Structural Geology. Arnold, 3rd ed., pp. 90.
- PHILPOTTS, A.R. (1966). Origin of the anorthosite-mangerite rocks in Southern Quebec. J. Petrol., 7, 1-64.
- PIDGEON, R.T. & RÅHEIM, A. (1972). Geochronological investigation of the gneisses and minor intrusive rocks from Kristiansund, West Norway. Norsk Geol. Tidsskr., 52, 241-256.
- PIPER, J.D.A. (1976). Palaeomagnetic evidence for a Proterozoic supercontinent. Phil. Trans. R. Soc. Lond., A280, 469-490.
- PINET, M. & SMITH, D.C. (1982). A reconnaissance petrochemical study of opaque minerals in some Norwegian eclogites. Abstr. First Int. Eclogite Conf., Terra Cognita, 2, 334.
- PLOQUIN, A. (1975). Etude géochimique et pétrographique du complexe de gneiss, migmatites et granites du Téliemark - Aust Agder. Sa place dans l'ensemble Epizonal à Catazonal profond du Haut Téliemark au Bamble. Thèse Doctorat d'Etat, Nancy, pp. 940.
- PLOQUIN, A. (1977). Présentation sommaire du socle précambrien de Norvège méridionale et continuités trans-Atlantique nord. Revue de Géographie Physique et de Géologie Dynamique, 19, 399-404.

- POINT, R. (1975). Mylonites et orogénèse tangentielle: nature, géochimie, origine et âge des gneiss ocilles dans les nappes Calédoniennes ecternes. Bull. Soc. géol., France, 7, 22, 664-679.
- POWELL, M. & POWELL, R. (1977). Plagioclase-alkali-feldspar geothermometry revisited. Min. Mag., 41, 253-256.
- PRIEM, H.N.A. (1967). Progress report on the isotopic dating project in Norway. Z.W.O. Laboratorium veer isotopen, Amsterdam.
- PRIEM, H.N.A., BOELRIJK, N.A.I.M., HEBEDA, E.H., VERDURMEN, E.A.Th. & VERSCHURE, R.H. (1973). A note on the geochronology of the Hestbrepiggen Granite in west Jotunheimen. Norges Geol. Unders., 289, 31-35.
- QUENARDEL, J.-M. & PLOQUIN, A. (1980). Présentation générale de la réunion extraordinaire dans les Calédonides centro-méridionales (segments Bergen-Jotun et Otta-Grong). Bull. Soc. géol. France, 7, 22, 251-295.
- QVALE, H. & STIGH, J. (1983). Ultramafic rocks in the Scandinavian Caledonides. In: B.A. Sturt & D.G. Gee (eds.), The Caledonide Orogen - Scandinavia and related areas, Wiley (in press).
- RAMSAY, J.G. (1960). The deformation of early linear structures in areas of repeated folding. J. Geol., 68, 75-93.
- RAMSAY, J.G. (1967). Folding and fracturing of rocks. McGraw-Hill, York, pp. 568.
- RAMSAY, J.G. (1979). Shear zone geometry: a review. J. Struct. Geol., 2, 83-99.
- RAMSAY, J.G. & GRAHAM, R.H. (1970). Strain variation in shear belts. Can. J. Earth Sci., 7, 786-813.
- REUSCH, H.H. (1881). Konglomerat-Sandsternfelterne i Nordfjord, Søndfjord og Sogn. Nyt. Mag. Naturvitensk, 26, 93-170.
- REYMER, A.P.S., BOELRIJK, N.A.I.M., HEBEDA, E.H., PRIEM, H.N.A., VERDURMEN, E.A.Th. & VERSCHURE, R.H. (1980). A note on Rb-Sr whole-rock ages in the Seve Nappe of the central Scandinavian Caledonides. Norsk Geol. Tidsskr., 60, 139-147.
- REYNOLDS, R.C., WHITNEY, J.R. & ISACHSEN, Y.W. (1969). K/Rb ratios in anorthositic and associated charnockitic rocks of the Adirondacks and their petrogenetic significance. In: Y.W. Isachsen (ed.), Anorthosites and related rocks, Memoir 18, New York State Mus. and Sci. Service, 267-280.
- RICE, J.M. & FERRY, J.M. (1982). Buffering, infiltration, and the control of intensive variables during metamorphism. In: J.M. Ferry (ed.), Characterisation of metamorphism through mineral equilibria, Reviews in Mineralogy, vol. 10, Min. Soc. Am., 263-326.
- RICKARD, M.J. (1981). The Surnadal synform. Abstr. Uppsala Caled. Symp., Terra Cognita, 1, 68.

- RICKWOOD, P.C. (1968). On recasting analyses of garnet in end-member molecules. Contrib. Mineral. Petrol., 18, 175-198.
- RIVALENTI, G. (1976). Geochemistry of metavolcanic amphibolites from south-west Greenland. In: B.F. Windley (ed.), The Early History of the Earth, Wiley, 213-223.
- ROBERTS, J.L. (1977). Allochthonous origin of the Jotunheim Massif in southern Norway: a reconnaissance study along its northwest margin. Q. J. Geol. Soc. Lond., 134, 351-362.
- ROBERTS, D. & GEE, D.G. (1981). Caledonian tectonics in Scandinavia. Abstr. Uppsala Caled. Symp., Terra Cognita, 1, 69.
- ROBERTS, D., SPRINGER, J. & WOLFF, F.C. (1970). Evolution of the Caledonides in the northern Trondheim region, Central Norway: a review. Geol. Mag., 107, 133-145.
- ROBERTS, D., THON, A., GEE, D.G. & STEPHENS, M.B. (1981). Scandinavian Caledonides-Tectonostratigraphy map, scale 1:1,000,000. Uppsala Caledonide Symp.
- ROBERTSON, J.K. & WYLLIE, P.J. (1971). Rock-water systems, with special reference to the water deficient region. Am. J. Sci., 271, 252-277.
- ROBINSON, D. & LEAKE, B.E. (1975). Sedimentary and igneous trends on AFM diagrams. Geol. Mag., 112, 305-307.
- RODDICK, J.C. & COMPSTON, W. (1977). Strontium isotopic equilibration: a solution to a paradox. Earth Planet. Sci. Lett., 34, 238-246.
- van ROERMUND, H.L.M. (1983). On the eclogites of the Seve Nappe central Scandinavian Caledonides. In: B.A. Sturt & D.G. Gee (eds.), The Caledonide Orogen - Scandinavia and related areas, Wiley (in press).
- ROLLINSON, H.R. (1980). Mineral reactions in a granulite facies calc-silicate rock from Scourie. Scott. J. Geol., 16, 153-164.
- ROLLINSON, H.R. (1982). Evidence from feldspar compositions of high temperatures in granite sheets in the Scourian complex, N.W. Scotland. Min. Mag., 46, 73-76.
- ROMEY, W.D. (1971). Basic igneous complex, mangerite and high grade gneisses of Flakstadøy, Lofoten, northern Norway: I. Field relations and speculations on origin. Norsk Geol. Tidsskr., 51, 33-61.
- ROSENBLUM, S. (1958). Magnetic susceptibilities of minerals in the Frantz isodynamic magnetic separator. Am. Mineral., 43, 170-173.
- ROSENQVIST, I.Th. (1941). Om øyengneisdannelse i fjellkjeder. Norsk Geol. Tidsskr., 21, 165-180.
- RÖSHOFF, K. (1978). Structure of the Tännäs Augen Gneiss Nappe and its relation to under- and overlying units in the central Scandinavian Caledonides. Sveriges Geol. Unders., C739, 1-35.

- RUMBLE, D. III, FERRY, J.M., HOERING, T.C. & BOUCOT, A.J. (1982). Fluid flow during metamorphism at the Beaver Brook fossil locality, New Hampshire. Am. J. Sci., 282, 886-919.
- RYBURN, R.J., RÅHEIM, A. & GREEN, D.H. (1976). Determination of the P,T paths of natural eclogites during metamorphism - record of subduction. Contrib. Mineral. Petrol., 9, 161-164.
- RYDER, G. (1974). A rationale for the origins of massif anorthosites. Lithos, 7, 139-146.
- RÅHEIM, A. (1972). Petrology of the high grade metamorphic rocks of Kristiansund area. Norges Geol. Unders., 279, 1-75.
- RÅHEIM, A. (1975). Mineral zoning as a record of P,T history of Precambrian metamorphic rocks in W. Tasmania. Lithos, 8, 221-236.
- RÅHEIM, A. (1977). A Rb, Sr study of the rocks of the Surnadal syncline. Norsk Geol. Tidsskr., 57, 193-204.
- RÅHEIM, A. (1979). Structural and metamorphic break between the Trondheim basin and the Surnadal synform. Norsk Geol. Tidsskr., 59, 195-198.
- RÅHEIM, A. & GREEN, D.H. (1974). Experimental determination of the T and P dependence of the Fe-Mg partition coefficient for coexisting garnet and clinopyroxene. Contrib. Mineral. Petrol., 48, 179-203.
- RÅHEIM, A. & GREEN, D.H. (1975). P,T paths of natural eclogites during metamorphism - a record of subduction. Lithos, 8, 317-328.
- RÅHEIM, A., GALE, G.H. & ROBERTS, D. (1979). Rb, Sr ages of basement gneisses and supracrustal rocks in the Grong area, Nord-Trøndelag, Norway. Norges Geol. Unders., 354, 131-142.
- SAHAMA, T.G. (1945). On the chemistry of the east Fennoscandian rapakivi granites. Compt. Rendu. Soc. Geol. Fin., 18, 15-64.
- SARKAR, A., BHANUMATHI, L. & BALASUBRAHMANYAN, M.N. (1981). Petrology, geochemistry and geochronology of the Chilka Lake igneous complex, Orissa State India. Lithos, 14, 93-111.
- SAXENA, S.K. (1979). Garnet-clinopyroxene geothermometer. Contrib. Mineral. Petrol., 70, 229-235.
- SCHMID, R. & WOOD, B.J. (1976). Phase relationships in granulitic metapelites from the Ivea-Verbanò Zone (Northern Italy). Contrib. Mineral. Petrol., 54, 255-279.
- SCHMITT, H.H. (1963). Petrology and structure of the Eiksundsdal eclogite complex, Hareidland, Sunnmøre, Norway. Unpublished doctoral thesis, Harvard University.
- SCHMITT, H.H. (1964). Metamorphic eclogites of the Eiksund area, Sunnmøre Norway. Abstr. Am. Geophys. Union, 43, 128.

- SCHUILING, R.D. & VINK, B.W. (1967). Stability relations of some titanium minerals (sphene, perovskite, rutile, anatase). Geochim. Cosmochim. Acta, 31, 2399-2413.
- SECK, H.A. (1971). Koexistierende Alkalifeldspate und Plagioclase im System $\text{NaAlSi}_3\text{O}_8$ - KAlSi_3O_8 - $\text{CaAl}_2\text{Si}_2\text{O}_8$ - H_2O Dei Temperaturen von 650°C bis 900°C. Neues Jahrb. Mineral. Abh., 115, 315-345.
- SEDERHOLM, J.J. (1928). On orbicular granites, spotted and nodular granites, and on the rapakivi texture. Bull. Comm. Geol. Soc. Finland, 83, pp. 105.
- SEN, S.K. (1959). Potassium content of natural plagioclases and the origin of antiperthites. J. Geol., 67, 479-495.
- SHAND, S.J. (1922). The problem of the alkaline rocks. Proc. geol. Soc. S. Afr., 25, 19-33.
- SHAND, S.J. (1947). Eruptive Rocks, 3rd ed., Wiley, pp. 488.
- SHAW, D.M. (1956). Geochemistry of pelitic rocks. Part III: Major elements and general geochemistry. Geol. Soc. Am. Bull., 67, 919-934.
- SHAW, D.M. (1960). The geochemistry of scapolite. Part II: trace elements, petrology and general geochemistry. J. Petrol., 1, 261-285.
- SHERATON, J.W., SKINNER, A.C. & TARNEY, J. (1973). The geochemistry of the Scourian gneisses of the Assynt district. In: R.G. Park & J. Tarney (eds.), The early Precambrian of Scotland and related rocks of Greenland, Keele, 13-30.
- SHERVAIS, J.W. (1982). Ti-V plots and the petrogenesis of modern and ophiolitic lavas. Earth Planet. Sci. Letts., 59, 101-118.
- SIMONEN, A. (1980). The Precambrian of Finland. In: The Geology of the European Countries, Denmark, Finland, Iceland, Sweden, Norway. 24th Int. Geol. Congr., 51-108.
- SKJERLIE, F.J. (1969). The Pre-Devonian rocks in the Askvoll-Gaular area and adjacent districts, Western Norway. Norges Geol. Unders., 258, 325-359.
- SKJERLIE, F.J. (1974). The Lower Palaeozoic sequence of the Stavfjord district, Sunnfjord. Norges Geol. Unders., 302, 1-32.
- SKJERLIE, F.J. & PRINGLE, I.R. (1978). A Rb/Sr whole-rock isochron data from the lowermost gneiss complex of the Gaular area, west Norway and its regional implications. Norsk Geol. Tidsskr., 58, 259-265.
- SMITH, D.C. (1980). A tectonic melange of foreign eclogites and ultramafites in west Norway. Nature, 287, 366-367.
- SMITH, D.C. (1982). Petrochemical notes on the hydrous minerals in the Aarsheimneset eclogite pod, Selje district, Norway. Abstr. First Int. Eclogite Conf., Clermont Ferrand, Terra Cognita, 2, 317.

- SMITH, J.V. (1974). Feldspar minerals. Vol. 2, Chemical and Textural Properties. Springer-Verlag, pp. 690.
- SMITHSON, S.B. & RAMBERG, I.B. (1979). Gravity interpretation of the Egersund anorthosite complex, Norway: its petrological and geo-thermal significance. Geol. Soc. Am. Bull., 90, 199-204.
- SMITHSON, S.B., RAMBERG, I.B. & GRØNLIE, G. (1974). Gravity interpretation of the Jotun Nappe of the Norwegian Caledonides. Tectonophysics, 22, 205-222.
- SOLHEIM, S. (1980). Geochronological investigations in the Oppdal area, central Norway. Norsk Geol. Tidsskr., 60, 175-188.
- SØRENSEN, H. (1974). Introduction. In: H. Sørensen (ed.), The Alkaline Rocks, Wiley, 1-11.
- STARMER, I.C. (1972). The Sveconorwegian regeneration and earlier orogenic events in the Bamble Series, south Norway. Norges Geol. Unders., 277, 37-52.
- STEEL, R. (1981). Devonian basins of Norway. Abstr. Uppsala Caled. Symp., Terra Cognita, 1, 75.
- STEIGER, R.H. & JÄGER, E. (1977). Subcommission on geochronology: convention on the use of decay constants in geo- and cosmochronology. Earth Planet. Sci. Lett., 36, 359-362.
- STORMER, J.C. Jnr. (1975). A practical two-feldspar geothermometer. Am. Min., 60, 667-674.
- STORRE, B. & NITSCH, K.H. (1972). Die Reaktion $2 \text{Zoisit} + 1 \text{CO}_2 = 3 \text{Anorthit} + 1 \text{Calcit} + 1 \text{H}_2\text{O}$. Contrib. Mineral. Petrol., 35, 1-10.
- STRAND, T. (1949). On the gneisses from a part of the north-western gneiss area of southern Norway. Norges Geol. Unders., 173, pp. 45.
- STRAND, T. (1953). The relation between the basal gneiss and the overlying metasediments in the Surnadal district (Caledonides of southern Norway). Norges Geol. Unders., 184, 100-121.
- STRAND, T. (1960). The region with the Basal Gneiss in the N.W. part of S. Norway. In: D. Høltedahl (ed.) Geology of Norway. Norges Geol. Unders., 208, 230-245.
- STRAND, T. (1969). Geology of the Gvotli area. Norsk Geol. Tidsskr., 49, 341-360.
- STRECKEISEN, A. (1976). Classification of the common igneous rocks by means of their chemical composition. A provisional attempt. Neues Jahrb. Mineral. Mh., 1, 1-15.
- STURT, B.A., SKARPENES, O., OHANIAN, A.T. & PRINGLE, I.R. (1975). Reconnaissance Rb/Sr isochron study in the Bergen Arc System and regional implications. Nature, 253, 595-599.

- STURT, B.A. & THON, A. (1976). The age of orogenic deformation in the Swedish Caledonides. Am. J. Sci., 276, 385-390.
- TARNEY, J. (1976). Geochemistry of Archaean high-grade gneisses with implications as to the origin and evolution of the Precambrian crust. In: B.F. Windley (ed.), The Early History of the Earth, Wiley, 405-417.
- TARNEY, J., DALZIEL, I.W.D. & de WIT, M.J. (1976). Marginal basin 'Rocas Verdes' complex from S. Chile: A model for Archaean Greenstone belt formation. In: B.F. Windley (ed.), The Early History of the Earth, Wiley, 131-146.
- TARNEY, J., SKINNER, A.C. & SHERATON, J.W. (1972). A geochemical comparison of major Archaean gneiss units from north-west Scotland and east Greenland. Rept. 24th Int. Geol. Congr., Montreal, 1, 162-174.
- TAYLOR, S.R. (1964). Abundance of chemical elements in the continental crust: a new table. Geochim. Cosmochim. Acta, 28, 1273-1285.
- TAYLOR, S.R. (1965). The application of trace element data to problems in petrology. In: L.A. Ahrens, F. Press, S.K. Runcorn & C. Vrey (eds.), Physics and Chemistry of the Earth, 6, Pergamon Press, 133-214.
- THOMPSON, A.B. (1975). Mineral reactions in a calc-mica schist from Gassetts, Vermont, U.S.A. Contrib. Mineral. Petrol., 53, 105-127.
- THOMPSON, A.B. (1976). Mineral reactions in pelitic rocks. II: Calculations of some P-T-X (Fe-Mg) phase relations. Am. J. Sci., 276, 425-494.
- THOMPSON, A.B. (1982). Dehydration melting of pelitic rocks and the generation of H₂O-undersaturated granitic liquids. Am. J. Sci., 282, 1567-1595.
- THOMPSON, A.B. & TRACY, R.J. (1979). Model systems for anatexis of pelitic rocks. II: Facies series melting and reactions in the system CaO-KAlO₂-NaAlO₂-Al₂O₃-SiO₂-H₂O. Contrib. Mineral. Petrol., 70, 429-438.
- THORNTON, C.P. & TUTTLE, O.F. (1960). Chemistry of igneous rocks. I. Differentiation Index. Am. J. Sci., 258, 664-684.
- TILLEY, C.E. (1937). The paragenesis of kyanite eclogites. Min. Mag., 24, 422-432.
- TORSKE, T. (1977). The south Norway Precambrian region - a Proterozoic cordilleran-type orogenic segment. Norsk Geol. Tidsskr., 57, 97-120.
- TOZER, C.F. (1955). The mode of occurrence of sillimanite in the Glen district, Co. Donegal. Geol. Mag., 92, 310-320.
- TRACY, R.J. (1978). High-grade metamorphic reactions and partial melting in pelitic schist, west-central Massachusetts. Am. J. Sci., 278, 150-178.

- TRACY, R.J. (1982). Compositional zoning and inclusions in metamorphic minerals. In: J.M. Ferry (ed.), Characterisation of metamorphism through mineral equilibria. Reviews in Mineralogy, vol. 10, Min. Soc. America, 355-397.
- TUREKIAN, K.K. & WEDEPOHL, K.H. (1961). Distribution of the elements in some major units of the earth's crust. Geol. Soc. Am. Bull., 72, 175-192.
- TURNER, F.J. (1968). Metamorphic petrology, mineralogical and field aspects. McGraw-Hill, New York, pp. 403.
- TUTTLE, O.F. & BOWEN, N.L. (1958). The origin of granites in the light of experimental studies. In the system: $\text{NaAlSi}_3\text{O}_8\text{-KAlSi}_3\text{O}_8\text{-SiO}_2\text{-H}_2\text{O}$. Geol. Soc. Am. Mem., 74, 1-153.
- TØRUDBAKKEN, B. (1981). Trondheim-Surnadal. In: W.L. Griffin & M.-B.E. Mørk (eds.), Eclogites and Basal Gneisses in west Norway. Excursion Bl, Uppsala Caled., 13-19.
- VALLEY, J.W. & ESSENE, E.J. (1980). Calc-silicate reactions in Adirondack marbles: the role of fluids and solid solution: Summary. Geol. Soc. Am. Bull., 91, 114-117.
- VAN DE KAMP, P.C., LEAKE, B.E. & SENIOR, A. (1976). The petrography and geochemistry of some Californian arkoses with application to identifying gneisses of metasedimentary origin. J. Geol., 84, 195-212.
- VELDE, B. (1965). Phengite micas: synthesis, stability and natural occurrence. Am. J. Sci., 263, 886-913.
- VERNON, R.H. (1979). Formation of late sillimanite by hydrogen metasomatism (base-leaching) in some high-grade gneisses. Lithos, 12, 143-152.
- VERSTEEVE, A.J. (1975). Isotope geochronology in the high-grade metamorphic precambrian of southwestern Norway. Norges Geol. Unders., 318, 1-50.
- VIDAL, J.-L., KUBIN, L., DEBAT, P. & SOULA, J.-C. (1980). Deformation and dynamic recrystallisation of K feldspar augen in orthogneiss from Montagne Noire, Occitania, southern France. Lithos, 13, 247-255.
- VIDALE, R.J. & HEWITT, D.A. (1973). 'Mobile' components in the formation of calc-silicate bands. Am. Mineral., 58, 991-997.
- VOGT, J.H.L. (1896). Norsk Marmor. Norges Geol. Unders., 22.
- VOGT, J.H.L. (1924). The physical chemistry of the magmatic differentiation of igneous rocks. Vid.-Selsk. Kristiania Skrifter. I. Mat.-natur. kl. 1924, 15, pp. 132.
- WAGER, L.R. & BROWN, G.M. (1968). Layered Igneous Rocks, Oliver & Boyd, 588 pp.

- WASHINGTON, H.S. (1916). The charnockite series of igneous rocks. Am. J. Sci., 191, 323-338.
- WELLS, P.R.A. (1977). Pyroxene thermometry in simple and complex systems. Contrib. Mineral. Petrol., 62, 129-139.
- WELLS, P.R.A. (1979). P-T conditions in the Moines of the central Highlands, Scotland. Q. J. Geol. Soc. Lond., 136, 663-671.
- WHEELER II, E.P. (1969). Minor intrusives associated with the Nain anorthosite. In: Y.W. Isachsen (ed.), Origin of Anorthosites and related rocks, Memoir 18, New York State Mus. and Sci. Service, 189-206.
- WHITE, A.J.R. (1964). Clinopyroxenes from eclogites and basic granulites. Am. Mineral., 49, 883-888.
- WHITE, S. (1975). Tectonic deformation and recrystallisation of oligoclase. Contrib. Mineral. Petrol., 50, 287-305.
- WHITNEY, J.A. & STORMER, J.C. (1977). The distribution of NaAlSi₃O₈ between coexisting microcline and plagioclase and its effect on geothermometric calculations. Am. Mineral., 62, 687-691.
- WIEBE, R.A. (1980). Anorthositic magmas and the origin of Proterozoic anorthosite massifs. Nature, 286, 564-567.
- WIKSTRØM, A. (1970a). Note of the alteration of kyanite in the eclogites from the Nordfjord area, Norway. Norsk Geol. Tidsskr., 50, 184-186.
- WIKSTRØM, A. (1970b). Hydrothermal experiments in the system jadeite-diopside. Norsk Geol. Tidsskr., 50, 1-14.
- WIKSTRØM, A. (1970c). Electron microprobe studies of the alteration of omphacite in eclogites from the Nordfjord area, Norway. Norsk Geol. Tidsskr., 50, 137-155.
- WILSON, A.D. (1955). A new method for the determination of ferrous iron in rocks and minerals. Bull. Geol. Surv. Gt. Br., 9, 56-58.
- WILSON, J.R. (1977). Farsundite - a suitable term for charnockite nomenclature? Neues Jahrb. Mineral. Mh., 7, 324-332.
- WILSON, J.R., PEDERSEN, S., BERTHELTSEN, C.R. & JAKOBSEN, B.M. (1977). New light on the precambrian Holum granite, south Norway. Norsk Geol. Tidsskr., 57, 347-360.
- WINCHESTER, J.A., PARK, R.G. & HOLLAND, J.G. (1980). The geochemistry of Lewisian semipelitic schists from the Gairloch District, Wester Ross. Scott. J. Geol., 16, 165-179.
- WINCHESTER, J.A. & FLOYD, P.A. (1976). Geochemical magma type discrimination: application to altered and metamorphosed basic igneous rocks. Earth Planet. Sci. Lett., 28, 459-469.
- WINDLEY, B.F. (1977). The evolving continents, Arrowsmith, pp. 385.
- WINKLER, H.G.F. (1976). Petrogenesis of metamorphic rocks, 4th ed., Springer-Verlag, pp. 334.

- WOOD, B.J. (1974). The solubility of alumina in orthopyroxene co-existing with garnet. Contrib. Mineral. Petrol., 46, 1-15.
- WOOD, B.J. & BANNO, S. (1973). Garnet-orthopyroxene and orthopyroxene-clinopyroxene relationships in simple and complex systems. Contrib. Mineral. Petrol., 42, 109-124.
- WOOD, D.S. (1973). Patterns and magnitude of natural strains in rocks. Phil. Trans. R. Soc. Lond., A274, 373-382.
- WYNNE-EDWARDS, H.R. & HASAW, Z. (1972). Grey gneiss complexes and the evolution of the continental crust. 24th Int. Geol. Congr., Montreal, p. 175.
- YODER, H.S., STEWART, D.B. & SMITH, J.R. (1957). Ternary feldspars. Carnegie Inst. Wash. Yearb., 56, 206-214.
- YODER, H.S. & TILLEY, C.E. (1962). Origin of basalt magmas. J. Petrol., 13, 342-532.
- YORK, D. (1969). Least squares fitting of a straight line with correlated errors. Earth Planet. Sci. Lett., 5, 320-324.
- ZECK, H.P. & MORTHORST, J.R. (1982). Continental tholeiites in the Ti-Zr-Y discrimination diagram. Neues Jahrb. Mineral. Mh., 5, 193-200.
- ZWART, H.J. & DORNSIEPEN, U.F. (1978). The tectonic framework of central and western Europe. Geologie en Mijnbouw, 57, 627-654.

APPENDIX A

ANALYTICAL METHODS

This appendix briefly describes the geochemical methods employed to obtain the whole-rock and mineral analyses used in this study, and the difficulties encountered. Also presented is the method for the Rb-Sr isotopic dating of the augen gneiss, and the method of mineral separation for sample 1428 of the garnet-granulite from Tverrfjella dated by Griffin & Brueckner (1980) using the Sm-Nd isotopic method.

A.1 WET CHEMICAL METHODS

The analyses were performed on powdered rock. The samples were initially crushed into small chips using a jaw-crusher then 'TEMA' ground, for ~ 20 seconds, to a powder. Care had to be taken to prevent any contamination from the steel components of the jaw-crusher, although Co contamination from the tungsten 'TEMA' grinder could not be prevented. Prolonged grinding of the powder is considered to cause partial oxidation of the rock, although no evidence for such was found in this study. Conversely, short periods of grinding does not comminute the rock sufficiently for it to be fully digested in the acids used in the analytical methods. The resulting powders were oven-dried at 110°C for 24 hours prior to any analysis.

A.1.1 Combined water

Determined using 'Penfield's' method. Approximately 0.5 g of sample was placed at the end of a Penfield tube (~ 20 cm long, ~ 0.5 cm diameter) which was then strongly heated with a Meker burner for 10 minutes to drive off any water, which condensed in the cooler part of the tube. The tube was then drawn into two parts and that part contain-

ing the sample discarded. The remainder of the tube was stoppered, to prevent evaporation, allowed to cool and weighed. The tube was then oven-dried at 110°C for at least 1 hour, cooled and weighed. The difference in the weights was the weight of water given off.

$$\% \text{H}_2\text{O} = \frac{\text{weight of water given off (g)} \times 100}{\text{sample weight (g)}}$$

A.1.2 Ferrous iron

As the X-ray fluorescence spectrometry analysis of rocks gives total Fe as Fe_2O_3 , and as Fe can also exist as FeO, the latter oxide had to be determined by chemical methods. Two methods were used: hot-digestion and cold-digestion.

For hot-digestion, approximately 0.5 g of sample was weighed into a 30 ml Pt crucible, and a little distilled H_2O , 5 ml of 50% H_2SO_4 and 10 ml of 40% HF were added. The crucible was covered with a well-fitting Pt lid and heated until the mixture boiled; gentle boiling was continued for 7 minutes. The crucible and lid were then immediately plunged into 250 ml of 5% H_3BO_3 , 10 ml of indicator were added and the solution titrated with a standard $\text{K}_2\text{Cr}_2\text{O}_7$ solution to a stable purple end-point.

$$\% \text{FeO} = \frac{0.2(\text{K}_2\text{Cr}_2\text{O}_7 \text{ titre (ml)}) \times 100}{\text{weight of sample (mg)}}$$

The cold-digestion method is after Wilson (1955) in which the sample was placed in a polythene container with HF and NH_4VO_3 (ammonium metavanadate) and put to one side until the sample is digested. During digestion the V^{5+} is reduced to V^{3+} , which replaces the Fe^{3+} in the sample, and the remaining V^{5+} is titrated for. The original amount of V^{5+} in the NH_4VO_3 solution was initially measured by titration against a standard $\text{Fe}(\text{NH}_4)\text{SO}_4 \cdot 6\text{H}_2\text{O}$ solution.

The original method of Wilson is for rocks with up to 20 wt. % FeO. Some of the rocks in this study have large quantities of FeO, up to 25 wt. %, and to allow for this 5 ml of NH_4VO_3 solution were added to each sample rather than 4 ml as stipulated by Wilson.

A disadvantage experienced with the hot digestion method was the incomplete breakdown of refractory phases, such as garnet and rutile, within the 7 minutes boiling time. In an attempt to assist the digestion boiling was sometimes continued for up to 15 minutes, although beyond this time there was a danger of oxidation of the sample as the acids evaporated. Many difficulties were also experienced with the cold digestion method thereby demanding many repeats of some samples before satisfactory analyses were obtained. As with the hot digestion method, it was found that incomplete breakdown of refractory phases occurred. In the original method of Wilson (1955) 2-4 days is given as the recommended digestion period, although it was found necessary to extend this to 5 or 6 weeks to obtain a maximum FeO value. However, it was found that when samples were left for these long periods, deterioration of the solution and oxidation of the sample often occurred, resulting in low FeO values. This oxidation was visible as a loss of the blue colour, which developed during digestion, from V compounds, the more FeO present, the darker the blue colour. This oxidation appeared to be totally random between samples and no satisfactory explanation could be found such as badly fitting lids, impurition in the vanadium solution or oxidising agents in the samples.

In an attempt to accelerate the process of digestion and retain a closed environment, trials with 'Teflon' pressure digestion vessels were attempted. Here the sample, NH_4VO_3 solution, and HF were placed in a 'Teflon' 'bomb', with a screw lid, and heated in an oven at $\sim 160^\circ\text{C}$ for

5 hours. After this time the 'bomb' was removed, allowed to cool and the contents titrated in the manner described above. Although the digestion appeared to be complete, from the lack of garnet residue, low FeO values were once again recorded.

It is suggested the more rapid, hot-digestion method is suitable for rocks without refractory phases such as garnet, rutile and chromite which cannot be adequately digested in the short boiling time. The cold-digestion method is probably better for rocks containing these refractory phases as they are better dissolved over a longer period of time, although care must be taken with the fitness of the polythene containers used, to prevent oxidation of the sample.

A.1.3 Carbon dioxide

As an initial test, a small amount of sample was mixed with a little HCl to see if any gas would be evolved; if so, that sample would be analysed for CO₂ although the gas produced may have been SO₂ or H₂S. Two methods were used: absorption by soda asbestos and non-aqueous titration.

For the absorption method, approximately 0.5 g of sample was heated in a flask with 25 ml H₃P₂O₄, the gas evolved passed through a condenser and into the absorption train. This consisted of a small flask of sulphuric/chromic acid mixture to absorb water, a U-tube, half-filled with magnesium perchlorate and half with manganese dioxide to remove any SO₂ and SO₃ respectively, and two U-tubes of one-third calcium chloride and two-thirds soda asbestos. The calcium chloride removed any remaining traces of water, whilst the soda asbestos absorbed the CO₂. To ensure complete absorption, a small pump was used to draw the gases through the train. The two tubes of soda asbestos were weighed before

and after the evolution of gas and any weight increase was calculated as CO_2 evolved.

$$\% \text{CO}_2 = \frac{\text{weight increase of tubes (mg)} \times 100}{\text{sample weight (mg)}}$$

The non-aqueous titration is a method modified after: carbon method 4 in B.S. Handbook No. 19 (1970). The gases evolved were passed into a fixed burette containing a mixture of: 150 ml dimethylformamide, 5 ml mono-ethanolamine and 2 ml of 0.1% thymolphthalein (indicator), which absorbed the carbon. The titrant was tetra-n-butyl ammonium hydroxide. Both of these chemicals are toxic and give off fumes which attack rubber, consequently only polythene tubing was used. As before, approximately 0.5 g of sample was heated with 25 ml of $\text{H}_3\text{P}_2\text{O}_4$ and the gases passed through a condenser. An absorption train of silica gel, calcium chloride, magnesium perchlorate, and magnesium dioxide absorbed any H_2O , SO_2 or SO_3 whilst a U-tube of soda asbestos placed before the reaction vessel absorbed any atmospheric CO_2 . After the burette the gases passed through a tower of charcoal where any organic fumes were removed. A small pump was used to assist the flow of gas through the train. Initially, air was drawn through the system to flush out any residual CO_2 ; on titration the dimethylformamide and butyl ammonium hydroxide form a blue colour when there is no CO_2 present. The sample was then reacted with the acid and the CO_2 evolved removed the blue colour, after 10 minutes heating, the butyl ammonium hydroxide was titrated back to the blue end-point. Air was then drawn through the system for a further 5 minutes to ensure that all the CO_2 had been evacuated, and titrated further if necessary.

$$\% \text{CO}_2 = \frac{\text{ml of titrant} \times 4.4}{\text{weight of sample (g)} \times 10}$$

The standard limestone: KH and a synthetic carbonate: K_2CO_3 were analysed as standards and gave acceptable values.

The first method is fairly slow with each analysis taking 30-40 minutes, although this time can be shortened by using two sets of U-tubes. The absorption of H_2O by the $CaCl_2$ causes the grains to aggregate into a cement-like substance which is very difficult to remove from the U-tubes. The only way to circumvent this problem is to replace the $CaCl_2$ at frequent intervals although this slows down the procedure.

The non-aqueous titration is more rapid with each analysis taking about 20 minutes. A disadvantage of this method is the noxious nature of the chemicals involved which requires careful handling of the apparatus.

A.1.4 Sodium (Na_2O)

Approximately 0.1 g of sample was weighed into a very clean Pt crucible followed by 1 ml of 50% H_2SO_4 and 5 ml of 40% HF. The crucible was heated until most of the HF had been removed and the H_2SO_4 started to fume; the heat was then increased until the mixture was dry. Once cool, one drop of 50% H_2SO_4 was added, and the crucible three-quarters filled with distilled water. This was warmed until most of the residue had gone into solution and then washed into a graduated flask (generally 1000 ml). This solution was then analysed on a Perkin-Elmer atomic absorption spectrophotometer using a monochromatic light source and standard solutions of NaOH. The latter were used to calibrate the instrument, which calculated a concentration curve from them, against which the unknown samples were compared. Each sample was analysed three times.

$$\%Na_2O = 100 \times \frac{\text{concentration of } Na_2O \text{ (mg/ml)} \times \text{dilution factor}}{\text{sample weight (mg)}}$$

Care had to be taken with these analyses to prevent contamination of the solutions by Na from the skin, particularly the fingers.

A.2 INSTRUMENTAL METHODS

A.2.1 X-ray fluorescence spectrometry

The elements: Mg, K, Fe, Mn, Ti, Si, Ca, Al, P and S were determined using a fusion technique modified after Norrish & Hutton (1969) with glass specimens; these reduce matrix absorption effects and eliminate mineral grains. A quantity of lanthanum oxide was added to all the specimens, this as a heavy absorber of X-rays and thus dilutes the rocks' absorption and lessens the variation in the mass absorption coefficients in different rocks, thereby enabling calibrations to be made on a wide range of rock types. During analysis, background values were determined on a 'blank' specimen of spec-pure silica prepared in an identical way to the rock samples. Background intensities were measured at the analysis peak positions so that the unknown rock specimens need only be measured for the peak counts, thus saving a large amount of instrument time.

Specimens were prepared by fusing a mixture of: 0.373 g of sample with 0.027 g of NaNO_3 and 2.0 g of flux (a mixture of La_2O_3 , Li_2CO_3 and $\text{Li}_2\text{B}_4\text{O}_7$ ignited at 1000°C) at 1000°C in a Pt-Rh-Au alloy crucible. After heating for 10 minutes the crucible was allowed to cool and reweighed, any weight loss was corrected for the loss due to the decomposition of the NaNO_3 the remaining loss was due to oxidation of Fe and S, and loss of volatiles: H_2O , CO_2 , SO_2 . The mixture was then re-heated for 5 minutes until molten and poured onto a graphite disc kept at 230°C on a hot plate. An aluminium plunger, also kept at 230°C was immediately brought down to quench the molten glass and form a disc approximately 31 mm in diameter and 1.5 mm thick. Before analysis the discs had to be

polished to remove any surface 'bloom' resulting from hydration of the hydrophilic flux.

The analyses were performed on a Phillips 1220 spectrometer using a Cr X-ray tube under standard operating conditions. One of the four sample positions in the spectrometer was always occupied by the standard glass FS48. For each batch of samples the silica blank was included as the first and last specimen analysed. During fusion, element oxidation occurs, principally affecting the Fe and S which were measured as Fe_2O_3 and SO_3 respectively. In natural rocks a certain proportion of the Fe occurs in the ferrous state and S generally in sulphides. Consequently, the determined Fe_2O_3 was adjusted to include the FeO from the wet-chemical analyses, whilst SO_3 was corrected to oxygen equivalent S. As NaNO_3 was used as an oxidising agent it was not possible to determine Na in the analyses. However, trials with other oxidising agents (e.g. NH_4NO_3) were undertaken during the project which permitted the determination of Na_2O by X.R.F.

As fusion discs give lower X-ray intensities than powders, a consequence of dilution of the sample by the flux, their increased absorption and interference from La lines, the glass discs are not suitable for the determination of many heavy elements occurring as traces in the samples. Consequently, the elements: V, Cr, Mn, Ni, Cu, Zn, Rb, Sr, Y, Zr, Ba, Pb, Ce, Ga, Nb and Th were determined using undiluted, self-supporting, pressed powder pellets.

Several samples were analysed for trace elements at Glasgow University on a similar machine, although the method of preparation of the samples was slightly different. The rock powder was mixed with resin (phenol formaldehyde), pressed at 30 tons for 1 minute and baked at 110°C to cure the resin.

A.2.2 Electron microprobe analyses

The constituent minerals of selected samples were analysed in carbon-coated polished thin sections by standard techniques on a Cambridge Instruments Microscan IX electron microprobe using a 15 kV accelerating voltage. The calibrating standards used were natural and synthetic minerals and pure metals. The counts were corrected for X-ray absorption, characteristic fluorescence and atomic number effects (ZAF correction). The silicates were analysed for: Si, Ti, Al, Fe, Mg, Mn, Ca, Na, K, Cr, S and Cl. Total Fe was determined as FeO.

A.2.3 Rb-Sr isotopic analyses

This work was performed at the Mineralogisk-Geologisk Museum, Oslo. The samples were prepared by: weighing approximately 500 g of powder into a 100 ml 'Teflon' beaker and adding a little distilled water. The following quantities and types of acids were successively added and evaporated off: 20 ml HCl; 5 ml HNO₃ plus 5 ml HF; 5 ml 6M HCl. Finally, 3-5 ml of 2.5M HCl were then passed through a series of ion-exchange columns to separate the Sr. The final, very small, amount of sample was loaded onto a tungsten filament and placed in the spectrometer.

The analyses were performed on a V6 micromass 30 mass spectrometer which measured peaks for ⁸⁸Sr, ⁸⁷Sr and ⁸⁶Sr. Variable mass discrimination in ⁸⁷Sr/⁸⁹Sr was corrected by normalising ⁸⁶Sr/⁸⁸Sr = 0.1194 (Faure & Hurley, 1963). Regression lines were calculated, using the technique of York (1969) and the ISOCH VO2-02 computer program made available at the Museum.

A.3 MINERAL SEPARATION

The methods employed followed the descriptions in Hutchison (1958, p. 113). Five samples of eclogite: D8, D37, H1, 182 and 1428 were put

through the process in order to separate the garnets and clinopyroxenes for Sm-Nd dating. The rock samples were ground in a similar way to those for whole-rock analyses, but only as far as small chips and not 'TEMA' ground to a powder. The intention was to obtain a size fraction which would be mainly composed of monomineralic grains. To reduce contamination from the jaw-crusher, only short bouts of crushing were done on small amounts of sample. After sieving through mesh sizes: 100, 120, 150 and 170 the crushing was repeated, until sufficient sample was obtained. The monomineralic grains occurred in the 150 and 170 mesh fractions; the portion finer than 170 mesh, although monomineralic, was too fine to work with. After washing with acetone to remove dust from the crushing the initial separation was made by removing magnetite (and any steel from the crusher) with a hand magnet. Mica was removed by rolling the grains down a piece of filter paper, the platy grains were trapped in the 'flock'.

Much of the separation was done with a Franz isodynamic magnetic separator. The forward slope was set at 25° and the side tilt at 15° whilst the amperage on the magnets was varied in accordance with the table of mineral susceptibilities given in Rosenblum (1958). By starting at low amperages, rutile was removed first, then garnet and pyroxene, leaving hornblende, plagioclase and quartz. However, it was found that the garnet and pyroxene contaminated each other, having similar magnetic susceptibilities, whilst hornblende and plagioclase contaminated the pyroxene, usually through the grains not being monomineralic as a result of secondary alteration. To separate the pyroxene and garnets further, methylene iodide (di-iodo-methane, CH_2I_2) was used in a heavy liquid separation technique. With this liquid of specific gravity 3.325, at 20°C , it was found that both garnet (S.G. $\sim 3.5-4.3$) and pyroxene (S.G. $\sim 3.2-3.7$) had a tendency to sink whereas the pyroxene/feldspar grains

floated, as did hornblende. To separate the garnet and clinopyroxene the CH_2I_2 was cooled in ice-water which increased its S.G. Even so it was found that hand picking was still necessary to remove any grains with inclusions. Of the five samples put through this process only one (1428) had separates of sufficient purity for isotopic dating.

APPENDIX B

TEMPERATURE, PRESSURE AND MINERAL CALCULATIONS

Because of the number of geothermometers and geobarometers used in different parts of this study, it was considered that some outline of these methods should be given as a separate section rather than repeatedly referring to them in the text. Similarly, because of the necessity to calculate mineral formulae, including allowances for Fe^{3+} , at various points in the text, an outline and discussion of these methods is also given here.

B.1 PRESSURE AND TEMPERATURE CALCULATIONS

A number of experimentally calibrated mineral thermometers and barometers are currently available and a review article by Essene (1982) discusses many of the methods.

Many of the geothermometers are based upon the exchange of elements. Essentially, two types of exchange thermometry exist: the interchange of two similar atoms between different sites in one mineral (intracrystalline exchange) or between sites in two different minerals (intercrystalline). The ΔV (volume change) of these exchanges is small and therefore they make good thermometers, although they are prone to resetting by element diffusion (Essene, 1982).

Intercrystalline exchange is usually formulated as:

$$K_D = \frac{(m/n)^C}{(m/n)^D}$$

where m and n are mole fractions of chemical components in phases C and D. The relationship between K_D , T and P is:

$$\Delta\bar{H}^{\circ} - T\Delta S^{\circ} + (P-1)\Delta\bar{V}^{\circ} + RT\ln K_D + RT\ln K_Y = 0$$

The superscript 'o' denotes a hypothetical end-member and K_Y is the ratio of activity coefficients:

$$\frac{(a_m/a_n)^C}{(a_m/a_n)^D}$$

$\Delta\bar{V}^{\circ}$ is small and can be ignored for thermometers. Hence, $\Delta\bar{H}^{\circ}$, ΔS° and K_Y must be known and can be derived from thermodynamic data. However, solution models of varying complexity can be devised for K_Y , depending upon the assumptions made, resulting in the value of K_Y being only an approximation because of the large number of components involved, even in a simple exchange system (Essene, 1982).

It is important that care is exercised when using these calculation methods since certain assumptions are made in their construction which would result in meaningless or misleading temperatures if the method chosen is not applicable to the rocks under investigation.

(i) The system should be well calibrated with reversal of the runs.

(ii) The system should be calibrated at the expected P-T conditions of the rocks under investigation since extreme extrapolation to lower, or higher, P-T could introduce large errors. A common fault, in this respect, is the application of calibrations for garnet-peridotites of sub-crustal origin to rocks in crustal ranges of P and T for which the methods are not calibrated.

(iii) Solid solution models are greatly simplified and some components, not accounted for in the model, could have a large effect on the calculated P-T if they were to be included.

(iv) Minerals with variable structural states prove very difficult to use, e.g. feldspars.

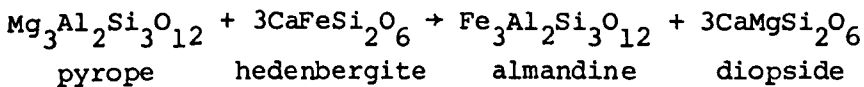
(v) Petrography is very important to ensure that the phases under investigation are truly in equilibrium and that any resetting by subsequent metamorphism is accounted for (Essene, 1982). Furthermore, if sufficient phases are present it may be possible to estimate the equilibration conditions from critical assemblages to provide a cross-check on any calculated P-T values.

B.1.1 Intercrystalline exchange

One of the most widely studied exchange systems is $Mg \rightleftharpoons Fe^{2+}$, and several geothermometers have been calibrated for different mineral pairs.

B.1.1(a) Garnet-clinopyroxene

This method is based on the reaction:



Banno (1970) noted that Fe was partitioned preferentially to garnet from clinopyroxene and he defined K_D for the reaction as:

$$\frac{(Fe^{2+}/Mg)_{gnt}}{(Fe^{2+}/Mg)_{cpx}}$$

He predicted that K_D would be sensitive to T but not greatly to P. The thermometer was first successfully calibrated by Råheim & Green (1974), using glasses of tholeiitic composition, in the range: 600°C-1400°C and 20 Kbar-40 Kbar thereby intending the calibration for eclogites of basaltic composition. During the experiments all Fe was retained as Fe^{2+} . The calibration showed that K_D was rather more P dependant than predicted by Banno (1970). They also showed that the bulk composition,

expressed as: $Mg/(Mg + Fe)$, did not perceptibly affect the K_D in the range: $0.06 < Mg/(Mg + Fe) < 0.85$. The derived expression was:

$$T(^{\circ}K) = \frac{3686 + 28.35 P(\text{kbar})}{\ln K_D + 2.33}$$

Although the garnets produced in the experiments were Ca-poor ($\sim 7\%$) and the pyroxenes were Na-poor ($\sim 4\%$), atypical of eclogite mineralogies (Essene, 1982 and see Table 3.6, Chapter 3). R  heim & Green (1975) and R  heim (1975) used the calibration on eclogites with Ca-rich garnets and Na-rich pyroxenes and at lower P-T conditions than used for the calibration necessitating extrapolation from experimental conditions.

Banno (1970) also considered that the K_D would be dependant upon additional components in the phases such as grossular (Ca) in garnet and jadeite (Na) in pyroxene. Ellis & Green (1979) recalibrated this thermometer with the intention of testing to see if any such dependance existed. Their experiments were conducted in glasses in the system: CaO-MgO-FeO- Al_2O_3 - SiO_2 in the range $750^{\circ}C$ - $1300^{\circ}C$ at 24 kbar-30 kbar. All Fe was kept divalent. Again, no dependance of K_D upon bulk composition was found (cf. R  heim & Green, 1974) nor was there any effect from the Na in the clinopyroxene. However, there was dependance upon the Ca-content of the garnet such that the derived expression was:

$$T(^{\circ}K) = \frac{3104 X_{ca}^{gnt} + 3030 + 10.86 P(\text{kbar})}{\ln K_D + 1.9034}$$

This calibration is suitable for a large range of compositions: Ellis & Green demonstrated that calculated temperatures agreed well with those for garnet-peridotites, a conclusion also reached by Medaris (1980).

Krogh (1982) has recalibrated this thermometer using further experimental data in the temperature interval $600^{\circ}C$ - $1500^{\circ}C$, i.e. lower temperatures than used by Ellis & Green (1979) to give:

$$T(^{\circ}\text{K}) = \frac{3104 x_{\text{Ca}}^{\text{gnt}} + 2443 + 10.86 P(\text{kbar})}{\ln K_{\text{D}} + 1.5049}$$

for a rectilinear relationship, and:

$$T(^{\circ}\text{K}) = \frac{-5708 (x_{\text{Ca}}^{\text{gnt}})^2 + 6555 x_{\text{Ca}}^{\text{gnt}} + 1869 + 10.86 P(\text{kbar})}{\ln K_{\text{D}} + 1.3963}$$

for a curvilinear relationship. Both these expressions are valid for: $0.1 < x_{\text{Ca}}^{\text{gnt}} < 0.5$, and both give temperature values $\sim 50^{\circ}\text{C}$ lower than the method of Ellis & Green.

Mori & Green (1978) have also calibrated this method for ultra-mafic compositions at 950°C - 1500°C and 30 kbar-40 kbar, using artificial pyrolite (minus 40% olivine), synthetic glasses and mineral mixes from natural garnet lherzolites. The K_{D} was calculated using total Fe as Fe^{2+} , although the experimental methods did not control the oxygen fugacity.

$$T(^{\circ}\text{K}) = \frac{2800}{\ln K_{\text{D}} + 1.19}$$

An important point here is that there is no pressure dependence factor included in this formulation.

From a comparison of these methods, Raheim & Green (1974) and Mori & Green (1978) seem to work best on minerals of similar compositions, equilibrated at similar P-T conditions to those in the experiments, and not at lower P-T conditions (Carswell & Gibb, 1980b; Essene, 1982). Ellis & Green's (1979) method appears to work best in granulites (Essene, 1982).

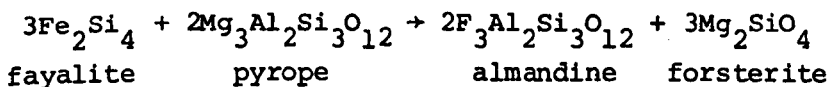
Saxena (1979) calibrated this method in the system: MgO-FeO-MnO- Al_2O_3 - Na_2O - SiO_2 in the temperature interval 800°C - 1400°C , and incorporated mixing parameters. Carswell & Gibb (1980b) considered that this method

gave erratic results, especially at low temperatures, for garnet lherzolites. Indeed, Saxena did not take into account the effect of Na in the clinopyroxene which would be present in some quantity as jadeite in pyroxenes formed at high grade conditions. Consequently, this method gives errors for jadeite-rich pyroxenes at $T < 800^{\circ}\text{C}$. Carswell & Gibb (1980b) found that the method gave very low temperatures whereas the calibration of Ganguly (1979) gave consistently high temperatures.

An important consideration to be made when employing these calibrations is the nature of the experimental procedure used, since this will have a bearing on the amount of Fe^{3+} present and the value of the K_D . Medaris (1980) and Carswell (1981) have discussed this factor in relation to the garnet-clinopyroxene thermometers and point out that Mori & Green (1978) formulated their K_D by taking all the iron in the garnet and clinopyroxene as Fe^{2+} , although it was likely that these phases contained some Fe^{3+} . By contrast, Råheim & Green (1974) and Ellis & Green (1979) controlled the oxidation state of their samples thereby preventing the conversion of Fe^{2+} to Fe^{3+} . Consequently, when calculating the K_D for Mori & Green's method, it is preferable to regard all the iron in the garnet and clinopyroxene as Fe^{2+} and to allow for the presence of Fe^{3+} in these phases (by calculation if using EMP analyses: see section B.2.1) when using the other two methods.

B.1.1(b) Garnet-olivine

This method is based on the reaction:



and has been calibrated by O'Neill & Wood (1979, 1980) with $K_{\text{gnt-oliv}}^{\text{Fe-Mg}}$ as:

$$\frac{(X_{Mg}^{ol})(X_{Fe}^{gnt})}{(X_{Fe}^{ol})(X_{Mg}^{gnt})}$$

In their experiments Fe^{2+} remained divalent. Although it is accepted that this method is not as sensitive as that for garnet and clinopyroxene (as noted by Mori & Green (1978) who also gave a calibration for garnet-olivine from their experiments) olivine is a simple binary solid solution and therefore does not suffer from solution with substantial amounts of Ca, Fe^{3+} or Al. However, the K_D is strongly dependant upon the Fe/Mg ratio and Ca content of the garnet (O'Neill & Wood, 1979).

$$902 + DV + (X_{Mg}^{ol} - X_{Fe}^{ol})(498 + 1.51)(P(\text{kbar}) - 30)T(^{\circ}\text{K}) =$$

$$\frac{-98(X_{Mg}^{gnt} - X_{Fe}^{gnt}) + 1347 X_{Ca}^{gnt}}{\ln K + 0.357}$$

where DV is a volume expression for almandine, pyrope, forsterite and fayalite components (O'Neill & Wood, 1980):

$$-462.5 [1.091 + (T-1073)(2.87 \times 10^{-5})] (P - 2.63 \times 10^{-4} P^2 - 29.76)$$

$$-262.4 [1.0292 + (T-1073)(4.5 \times 10^{-5})] (P - 3.9 \times 10^{-4} P^2 - 29.65)$$

$$+454 [1.020 + (T-1073)(2.84 \times 10^{-5})] (P - 2.36 \times 10^{-4} P^2 - 29.79)$$

$$+278.3 [1.0234 + (T-1073)(2.3 \times 10^{-5})] (P - 4.5 \times 10^{-4} P^2 - 29.6)$$

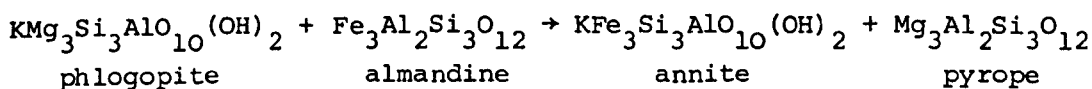
(P in kbar)

The method works best when $K \gg 1$ and is good for peridotites formed at $T \lesssim 1300^{\circ}\text{C}$, but not good for Fe-rich compositions at any T or Mg-rich compositions at $T \gg 1300^{\circ}\text{C}$ (O'Neill & Wood, 1979). Carswell & Gibb (1980b) used this method on kimberlite nodules and found that the derived temperatures agreed well with other element partition calibrations and the two-pyroxene solvus methods (see section B.1.2(a)). O'Neill & Wood (1979) compared the calibration with that of Wells (1977) for the two-

pyroxene solvus and also found good agreement although they considered the garnet-olivine method to be superior at low temperatures and the two-pyroxene method to be superior at higher temperatures when the pyroxene miscibility gap is smaller. At higher pressures, large differences appear between the figures derived from the two methods due to a widening of the pyroxene miscibility gap (Mori & Green, 1978) which affects the solvus thermometer (Carswell, 1980).

B.1.1(c) Garnet-biotite

This mineral pair has long been regarded as a potential thermometer and is based on the reaction:



This has been calibrated by Ferry & Spear (1978) by using synthetic garnet and biotite at 600°C and 700°C at 2.07 kbar. Their derived formulation was:

$$T(^{\circ}\text{K}) = \frac{12454 + 0.057P(\text{kbar}) + 3RT \ln K}{4.662}$$

$$\text{where } K = \frac{(\text{Mg}/\text{Fe}^{2+})^{\text{gnt}}}{(\text{Mg}/\text{Fe}^{2+})^{\text{bi}}}$$

They also showed that Mg and Fe mix ideally in biotite and garnet solid solutions in the compositional range: $0.8 \leq \text{Fe}/(\text{Fe} + \text{Mg}) \leq 1.00$.

However, K is also a function of Ca and Mn in garnet, and Ti and Al^{VI} in biotite. Consequently, Ferry & Spear suggest that the thermometer is best used for garnet compositions where $(\text{Ca} + \text{Mn})/(\text{Ca} + \text{Mn} + \text{Fe} + \text{Mg}) \lesssim 0.2$ and for biotite compositions where $(\text{Al}^{\text{VI}} + \text{Ti})/(\text{Al}^{\text{VI}} + \text{Ti} + \text{Fe} + \text{Mg}) \lesssim 0.15$. This method gives temperatures ~50°C higher than those from

the oxygen isotope thermometer of Goldman & Albee (1977); although a comparison with the empirical thermometer of Thompson (1975), based on field observations in conjunction with critical mineral assemblages, gave very close values.

A major problem is that Fe^{3+} in biotite can be present up to 20 wt. % - 30 wt. % (Essene, 1982), such that using total Fe as Fe^{2+} in the K values results in significantly lower temperatures.

The method appears to be valid for rocks of moderate grades of metamorphism, but at amphibolite-granulite facies the biotites incorporate Ti, F and Cl giving erratic results (Bohlen & Essene, 1980).

B.1.1(d) Scapolite-plagioclase

Scapolite minerals appear in many rocks, including high-grade metamorphics; early workers suspected an increase in S content with grade (Knorring & Kennedy, 1958).

Newton & Goldsmith (1975, 1976) made a study of scapolite in general whilst Orville (1975) found that meionite-scapolite (Ca) was unstable at 750°C and 4 kbar. In further experiments Goldsmith & Newton (1977) found that pure meionite ($\text{Ca}_4\text{Al}_6\text{Si}_6\text{O}_{24}\text{CO}_3$) was unstable at temperatures $>875^{\circ}\text{C}$ at all pressures and that there was a temperature-dependant Na-Ca partitioning between scapolite and plagioclase. However, this dependance was only appropriate for plagioclase compositions $>\text{An } 70\%$ since the more Na-plagioclases have more complex relationships with scapolite due to the non-ideality of the solid solution and the slower reaction kinetics. In the Ca-rich range above $\sim 700^{\circ}\text{C}$, the plagioclase-meionite activities are probably nearly ideal.

Goldsmith & Newton (1977) expressed these relationships on T-X_{An}^{SCAP} diagrams in the temperature range 800°C - 1300°C where:

$$T(^{\circ}\text{C}) = f_1 (X_{\text{An}}^{\text{plag}}) X_{\text{Me}}^{\text{scap}} + f_2 (X_{\text{An}}^{\text{plag}})$$

$$f = A + B X_{\text{An}}^{\text{plag}} + C (X_{\text{An}}^{\text{plag}})^2 \quad \text{where}$$

	A	B	C
f_1	5179	-9023	6518
f_2	-3968	10842	-8313

They also experimented with SO_4^{2-} scapolites which exhibited a temperature dependence, but required greater amounts of Na for stabilisation resulting in non-ideality even at temperatures as low as 1300°C . The temperature relationship is identical to that for the CO_3^{2-} scapolites, but the A, B and C parameters for the 'f'-polynomial are different:

	A	B	C
f_1	1164	-413.4	1296
f_2	-883.2	4826	-4531

The evidence suggests that the partitioning of Na and Ca is roughly proportional between the sulphate and carbonate end-members of scapolite. Consequently, after the temperature is calculated for the SO_4^{2-} and CO_3^{2-} end-members the temperature for the whole sulphate-carbonate-plagioclase assemblage can be calculated by proportioning these two values in the same ratio as the $\text{CaCO}_3 / (\text{CaCO}_3 + \text{CaSO}_4)$ value for the scapolite. This is only applicable for assemblages where plagioclase is between An 70%-98% (Goldsmith & Newton, 1977).

Rollinson (1980) has used these expressions for a scapolite co-existing with plagioclase of An 45 and An 46 and obtained very high temperatures as these plagioclase compositions lie outside the limit imposed by Goldsmith & Newton. Rollinson attempted to calculate the activity of An in scapolite, to allow for these more Na compositions, by assuming the substitution $\text{NaSi} = \text{AlCa}$ and ideal mixing on the anion site.

With the thermodynamic data of Goldsmith and Newton (1977) he obtained temperatures in broad agreement with other thermometers applied to the rocks. His distribution coefficient was:

$$K = \frac{a_{\text{scap}}}{(a_{\text{plag}})^3 (a_{\text{CaCO}_3})}$$

where $a_{\text{scap}} = (X_{\text{Me}}^{\text{Ca}})^4 (X_{\text{Anion}}^{\text{CaCO}_3})$ (cf. Orville, 1975)

and the activity coefficient $\gamma_{\text{An}}^{\text{plag}} = 1.2$ (from Windom & Boettcher, 1976), in the expression:

$$\Delta H - T\Delta S + (P-1)\Delta V = -RT \ln K$$

where $\Delta H = 10332 \pm 574$ cal at 875°C

$$\Delta S = 9 \pm 5 \text{ cal}/^\circ\text{C}$$

$$\Delta V = 1.22 \text{ cm}^3 \text{ (approaches 0 at high T)}$$

He also formulated a similar expression for the sulphate end-members where:

$$K = \frac{a_{\text{scap}}}{(a_{\text{plag}})^3 (a_{\text{CaSO}_4})}$$

where $a_{\text{scap}} = (X_{\text{Me}}^{\text{Ca}})^4 (X_{\text{Anion}}^{\text{CaSO}_4})$

Here there is a pressure dependance, and

$$\Delta H = 11833 \text{ at } 875^\circ\text{C and } 9 \text{ kbar}$$

$$\Delta S = 9 \pm 5 \text{ cal}/^\circ\text{C}$$

$$\Delta V = 1.22 \text{ cm}^3 \text{ (approaches 0 at high T)}$$

B.1.1(e) Orthopyroxene-clinopyroxene

The earliest experimental work on the enstatite ($\text{Mg}_2\text{Si}_2\text{O}_6$)-diopside ($\text{CaMgSi}_2\text{O}_6$) system was by Boyd & Schairer (1964) and Davis & Boyd (1966)

who considered it to be sensitive to changes in T but not to P, and only suitable as a thermometer above $\sim 900^{\circ}\text{C}$. In order to extend the applicability of the thermometer to natural assemblages, which contain considerable amounts of FeO, Wood & Banno (1973) developed a semi-empirical extrapolation of the solvus data using an ideal two-site mixing model in the pyroxenes:

$$T(^{\circ}\text{K}) = \frac{-10202}{\ln K - 7.65 X_{\text{Fe}}^{\text{opx}} + 3.88 (X_{\text{Fe}}^{\text{opx}})^2 - 4.6}$$

where $K = \frac{a_{\text{Ens}}^{\text{cpx}}}{a_{\text{Ens}}^{\text{cpx}}}$ (and in all subsequent formulae for this mineral pair)

In a further development of the solvus, Wells (1977) used simple mixing models to derive a semi-empirical equation over the temperature range 875°C - 1500°C . Besides allowing for solubility of Fe, this formulation is applicable to Mg-rich assemblages, unlike that of Wood & Banno (1973); and is best applied in the compositional range: $X_{\text{Fe}}^{\text{opx}} = 0.0$ - 1.0 and $\text{Al}_2\text{O}_3^{\text{cpx}} = 0$ - 10% . His derived equation was:

$$T(^{\circ}\text{K}) = \frac{7341}{3.355 + 2.44 X_{\text{Fe}}^{\text{opx}} - \ln K}$$

From their application of this method, Carswell & Gibb (1980b) found that it gave slightly underestimated temperatures, possibly due to the failure of the method to allow for the effect of pressure on the form of the solvus as found by Mori & Green (1978).

Mori & Green (1978) have also calibrated this thermometer, based on experiments on natural systems of garnet-lherzolites over a range of: 950 - 1500°C and 30 - 40 kbar such that:

$$T = \frac{-6860}{\ln K - 3.03}$$

This calibration lacks a correction for Fe, shown to be an important component of garnet-peridotites (Wood & Banno, 1973), and is only strictly applicable to orthopyroxenes with $0.04 < \text{Fe}/(\text{Fe} + \text{Mg}) < 0.13$. Furthermore, the method appears to overestimate temperatures (Carswell & Gibb, 1980b).

B.1.1(g) Albite-K-feldspar/ternary feldspars

The alkali-feldspar solvus has been studied by several workers in an attempt to locate the limbs in relation to temperature, pressure and bulk composition (Bowen & Tuttle, 1950; Orville, 1963; Luth & Tuttle, 1966; Morse, 1970; Goldsmith & Newton, 1972 - see review by Parsons, 1978). The location of the limbs is uncertain due to experimental difficulties of unmixing an homogeneous feldspar, and the effect of Al-Si disorder which varies with temperature (Essene, 1982). The two-feldspar exchange has received more attention as a geothermometer.

The partition of albite between plagioclase and K-feldspar, in the ternary feldspar system, as a function of T was first proposed by Barth (1961) based on field calibrations and some experimental work. This early thermometer was based on the distribution coefficient:

$$K_D = \frac{x_{\text{Ab}}^{\text{ksp}}}{x_{\text{An}}^{\text{plag}}}$$

which he considered to be a function of T, but not P, Al-Si order, or the bulk composition of the feldspars. However, Iiyama (1966)

showed that K_D is not constant at any temperature. Perchuk & Ryabchikov (1968) investigated the ternary feldspars as a double-binary system (i.e. Or-Ab and Ab-An) and demonstrated that the composition of the feldspars was a function of temperature. Similarly, Stormer (1975) realised that it was not possible to calculate chemical potentials or activity coefficients for the ternary system, and he assumed that there is no solubility of Or in plagioclase or An in K-feldspar, thereby reducing the ternary system to a double binary. In his formulated thermometer, Stormer (1975) further assumed that the mixing of Ab in plagioclase would be ideal. Such ideality is unlikely in Na-rich compositions and so Whitney & Stormer (1977) attempted to improve the solution model by taking this into account. Their expression is:

$$T = [7973.1 - 16910.6X_{Ab}^{ksp} + 9901.9(X_{Ab}^{ksp})^2 + (0.11 - 0.22X_{Ab}^{ksp} + 0.11(X_{Ab}^{ksp})^2)P] / [-1.9872 \ln(X_{Ab}^{ksp}/a_{Ab}^{plag}) + 6.48 - 21.58X_{Ab}^{ksp} + 23.72(X_{Ab}^{ksp})^2 - 8.62(X_{Ab}^{ksp})^3]$$

$$\text{where } \ln \gamma_{Ab}^{plag} = -1/RT(1-X_{Ab}^{ksp})^2 [w_G^{plag} + 2X_{Ab}^{ksp}(w_G^{or} - w_G^{Ab})]$$

As X_{Ab}^{ksp} approaches 0 then γ_{Ab}^{plag} approaches 1, since X_{Ab}^{ksp} is generally small $\gamma_{Ab}^{plag} \approx 0.99-1.0$.

Powell & Powell (1977) have also attempted to improve Stormer's (1975) thermometer by taking into account An in K-feldspar.

Brown & Parsons (1981) have reviewed the various formulations for feldspar thermometers and have compared them to Seck's (1971) work on the ternary system from which they derived the correct form of a graphical

thermometer. However, before accurate estimations of temperature can be gained from this method improved thermodynamic data must first be used to calibrate it correctly. With regard to the thermometer of Whitney & Stormer (1977), Brown & Parsons consider that the exclusion of Or in plagioclase and An in K-feldspar is not sufficiently realistic, unless these components are present in very small amounts. Furthermore, Whitney & Stormer's method is very sensitive to the values of the Margules parameters (W) and Brown & Parsons consider that these values are insufficiently known even for a binary thermometer let alone a double binary.

The formulation used in Powell & Powell's (1977) method is almost identical to that of Stormer (1975) except that there is a choice as to whether An be added to Ab or to Or. As Brown & Parsons point out Powell & Powell did neither of these and effectively ignored the effect of An in the K-feldspar. In relation to the work of Seck (1971) this formulation has little application (Brown & Parsons, 1981).

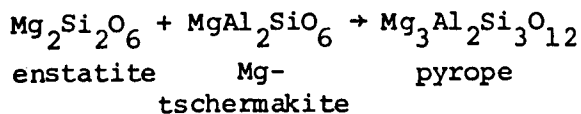
When using the thermometer formulated by Brown & Parsons it is necessary to ensure that the feldspars involved are in equilibrium, and they have suggested several chemographic and petrographic methods to test for this. With regard to metamorphic rocks they considered that the method was restricted to upper-amphibolite/granulite facies rocks since at higher temperatures the exact form of the ternary feldspar solvus is insufficiently known. Furthermore, the calculation of temperatures of unmixing of perthites is unreliable as done by O'Hara & Yarwood (1978) and Rollinson (1982) since the reconstruction of the pre-existing feldspar may not be a true composition due to loss of Na on exsolution (Brown & Parsons, 1981; Essene, 1982).

B.1.2 Geobarometry

Solid-solid reactions are suited to use in geobarometry since their position in P-T space is not dependant upon the presence of a fluid phase. Although solid-solid reactions generally have a dependance upon T as well as P, which requires an estimate of T for the calculation of P, those best suited to geobarometry have a small dependance on T. Major problems with their use are the corrections for solid solution activities, and assumptions therein, and evaluation of the thermodynamic data for the reactions (Essene, 1982).

B.1.2(a) Garnet-orthopyroxene

The earliest experimental work on the enstatite (MgSiO_3)-pyrope ($\text{Mg}_3\text{Al}_2\text{Si}_3\text{O}_{12}$) system was by Boyd & England (1964) via the reaction:



which has a large ΔV . They showed that the Al content of the orthopyroxene decreases with decreasing temperature or increasing pressure and therefore the Al content of enstatite in equilibrium with pyrope could be used as a geobarometer.

Subsequently, Green & Ringwood (1967b) demonstrated that the solubility of Al_2O_3 in pyroxenes was lower in model assemblages (pyrolite) than in the simple system. As a result of adding olivine to the garnet-orthopyroxene assemblage, the above reaction took place at lower pressures.

Wood & Banno (1973) attempted to reconcile the discrepancies between the model and simple systems by formulating a thermodynamic method from simple mixing models of orthopyroxene and garnet solid solution which took into account the effect of CaO and FeO on the system. Wood (1974) conducted further experiments on the solubility of Al in

orthopyroxene at 8-30 kbar and 800-1200°C which gave results in good agreement with the model of Wood & Banno. The formulation of Wood (1974) is:

$$P(\text{bar}) = \frac{RT(^{\circ}\text{K})}{\Delta V_r} \ln \frac{(X_{\text{Al}}^{\text{M1}})(1-X_{\text{Al}}^{\text{M1}})}{(1-y)_{\text{gnt}}^3} + \frac{7012 - 3.89T(^{\circ}\text{K}) - C}{\Delta V_r} (X_{\text{Fe}})_{\text{opx}} (1-2X_{\text{Al}}^{\text{M1}})$$

where $\Delta V_r = \Delta V$ of above reaction, this value depends on $X_{\text{Al}}^{\text{M1}}$, and can be found from Table 1, in Wood (1974).

$$(X_{\text{Fe}})_{\text{opx}} = \text{Fe}^{2+} / (\text{Fe}^{2+} + \text{Mg})$$

$$(1-y)_{\text{gnt}}^3 = [(X_{\text{Fe1}}^{\text{gnt}} + X_{\text{Mg1}}^{\text{gnt}})^3 (X_{\text{Al2}}^{\text{gnt}})^2]$$

$C = 10450$ bars

$X_{\text{Al}}^{\text{M1}}$ is taken as half the number of Al atoms present. If a correction is made for the substitution of Al by Cr, the calculated pressure decreases by a small amount (<1 kbar) which is insignificant considering other uncertainties in the method. One of these uncertainties is that $X_{\text{Al}}^{\text{M1}}$ is dependant upon both P and T such that any errors in the calculated temperature will be compounded in the calculated pressure (Carswell & Gibb, 1980a). Carswell & Gibb (1980b) also consider that this formulation does not adequately take into account the effect of varying Cr/(Cr + Al) ratios on the garnet-orthopyroxene equilibria which will affect the accuracy of the calculated pressures, especially in the 5-phase assemblage: garnet-clinopyroxene-orthopyroxene-olivine-spinel. MacGregor (1970) has shown that the stability field of such an assemblage appears to increase in size with increasing Cr/(Cr + Al) in the bulk composition.

O'Neill (1981) has studied the spinel lherzolite-garnet lherzolite transition in the CMAS and CMASCr systems and found that Cr_2O_3 is heavily partitioned into spinel resulting in a wide transitional 5-phase stability

field. However, the relationship is further complicated by Cr entering garnet with increasing pressure, and non-ideal mixing of MgAl_2O_4 - MgCr_2O_4 spinels. His derived relationship between P and $X_{\text{Cr}}^{\text{Sp}}$ was:

$$P(\text{kbar}) = P^{\circ}(\text{kbar}) + \alpha(X_{\text{Cr}}^{\text{Sp}} + X_{\text{Fe}^{3+}}^{\text{Sp}})$$

where $\alpha = 27.9$, from experimental work

P = experimental pressure

P° = invariant reaction pressure

Fe_2O_3 also has to be taken into account as it behaves in a similar manner to Cr_2O_3 . He also calculated the effect of FeO on the two systems from published data on Fe-Mg partitioning between olivine-'mineral' pairs. This indicated that the spinel lherzolite-garnet lherzolite transition occurs at lower pressures with increasing bulk FeO content.

Harley & Green (1982) have extended the work of Wood (1974) to include FeO in the system (i.e. to give FMAS and CFMAS) over the range of bulk compositions appropriate to crustal granulites at 800-1150°C and 5-20 kbar. They retained the simple solution model for orthopyroxenes (cf. Wood & Banno, 1973) but used ternary regular solution models for the Ca-Mg-Fe garnets (cf. O'Neill & Wood, 1979). Their derived expression was:

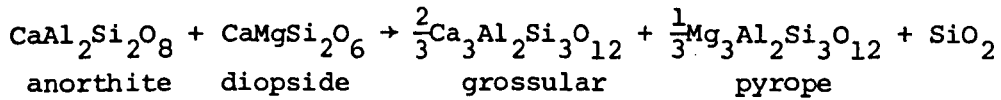
$$P(\text{kbar}) = \frac{1}{\Delta V_r} \left[(R \ln K - 2.93) T(^{\circ}\text{K}) + 5650 + 5157(1 - X_{\text{Al}}^{\text{Ml}})(1 - 2X_{\text{Al}}^{\text{Ml}}) X_{\text{Fe}}^{\text{opx}} \right. \\ \left. - 6300 \left[X_{\text{Ca}}^{\text{gnt}} X_{\text{Fe}}^{\text{gnt}} + (X_{\text{Ca}}^{\text{gnt}})^2 \right] \right]$$

where $K = \left[\frac{X_{\text{Al}}^{\text{Ml}}(1 - X_{\text{Al}}^{\text{Ml}})}{(1 - X_{\text{Ca}}^{\text{gnt}})^3} \right]$

$$\Delta V_r = - \left[183.3 + 178.98(X_{\text{Al}}^{\text{Ml}}(1 - X_{\text{Al}}^{\text{Ml}})) \right] \text{ cal kbar}^{-1}$$

B.1.2(b) Garnet-plagioclase-clinopyroxene-quartz

This assemblage is fairly common in granulite facies rocks and arises in the reaction:



which has a large ΔV and therefore is suitable for a geobarometer.

Newton & Perkins (1982) have constructed an expression for this reaction:

$$P(\text{kbar}) + 675 + 17.179 T(^{\circ}\text{K}) + 3.5962 T(^{\circ}\text{K}) \ln K$$

$$\text{where } K = \frac{(a_{\text{Ca}}^2 \cdot a_{\text{Mg}})_{\text{gnt}}}{(a_{\text{Ca}}^{\text{pl}}) (a_{\text{CaMg}}^{\text{cpx}})}$$

from measured thermodynamic quantities. The major difficulty with this method is the evaluation of the activities of the various components of the phases. Here they are based upon calorimetry (for the garnets) or an ideal two-site model for the pyroxene (cf. Wood & Banno, 1973). Due to non-ideal mixing of Mn with Mg, Fe^{2+} and Ca in the garnets, which cannot be easily formulated, this method is not suitable for assemblages where $\text{Mn} \geq \text{Mg}/3$ in the garnet. The thermodynamic values used give the following expressions for the activity coefficients in garnet:

$$RT \ln K_{\text{Ca}} = (3300 - 1.5T) (X_{\text{Mg}}^2 + X_{\text{Mg}} X_{\text{Fe}})$$

$$\text{and } RT \ln K_{\text{Mg}} = (3300 - 1.5T) (X_{\text{Ca}}^2 + X_{\text{Ca}} X_{\text{Fe}})$$

and for plagioclases:

$$a_{\text{An}} = X_{\text{An}} (1 + X_{\text{An}})^2 \exp \left(\frac{(1 - X_{\text{An}})^2 (2025 + 9442 X_{\text{An}})}{4} \right)$$

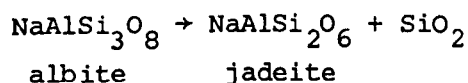
and for clinopyroxene:

$$a_{Di} = X_{Ca}^{M2} \cdot X_{Mg}^{M1}$$

Using the expression on Krogh's (1980b) data, gave a calculated pressure of ~ 13 kbar compared to 18 ± 3 kbar from Krogh. The method appears to underestimate the pressure, perhaps due to re-equilibration during uplift or the inadequacy of the thermodynamic expressions (Newton & Perkins, 1982). A possible refinement of the method could lie in the calculation of the activity of the clinopyroxene, perhaps by using a sub-regular solution model (cf. Currie & Curtis, 1976 - see next section) rather than the ideal model.

B.1.2(c) Albite-jadeite-quartz

A sub-regular solution model has been applied to the clinopyroxene in the reaction:



by Currie & Curtis (1976) assuming that $a_{Ab}^{\text{plag}} = 1$.

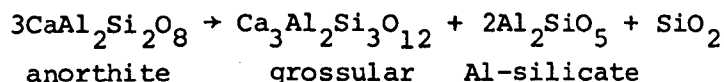
Although a pyroxene can contain five or more components, which would result in at least 10 binary solutions, some of these components mix ideally which simplifies the situation. From the assumptions made in this method, the clinopyroxene can be reduced to three components: jadeite, diopside and hedenbergite. Their derived equation calibrated with experimental data (T in $^{\circ}\text{K}$ and P in bars):

$$\begin{aligned} 0 = & 7.63T - 36 - 0.406P + RT \ln(X_{jd}/X_{alb}) \\ & + [2(X_{Di} + X_{Hd})^2 - 2(X_{Di} + X_{Hd})^3 - 2X_{Di}X_{Hd}(X_{jd} - 0.5 - \Sigma X_m) \\ & - (X_{Di} + X_{Hd})(0.5\Sigma(X_m)^2 - \Sigma(X_m X_n)) + 1.5(X_{Di} + X_{Hd})\Sigma X_m] (10T - 7987 - 0.026P) \\ & + [2(X_{Di} + X_{Hd})^3 - (X_{Di} + X_{Hd})^2 + 2X_{Di}X_{Hd}(X_{jd} - 0.5 - \Sigma X_m) \\ & + 2(X_{Di} + X_{Hd})(0.5\Sigma(X_m)^2 - \Sigma(X_m X_n)) - 0.5(X_{Di} + X_{Hd})\Sigma X_m] 0.1136P - 12850 \end{aligned}$$

From this formulation Currie & Curtis were able to show that omphacitic pyroxenes cannot contain more than 40% jadeite component, and that jadeite-rich pyroxenes cannot contain more than trace amounts of hedenbergite and diopside.

B.1.2(d) Garnet-plagioclase-Al-silicate-quartz

This assemblage, with the Al-silicate being one of: kyanite, sillimanite or andalusite is common in regionally metamorphosed rocks. It was Ghent (1976) who first recognised the potential of the reaction:



as a geobarometer. He formulated an expression from the thermodynamic data on the reaction, including the activities of garnet and plagioclase:

$$0 = \frac{-3272}{T(^{\circ}\text{K})} + 8.3969 - \frac{0.3448 (P(\text{bar}) - 1)}{T(^{\circ}\text{K})} + \log K_D$$

$$\text{where } \log K_D = (3 \log a_{\text{gross}}^{\text{gnt}} - 3 \log a_{\text{An}}^{\text{plag}})$$

In this formulation Ghent took the garnet to be a simple, ideal, grossular-almandine binary (i.e. $\gamma = 1$), and the activity coefficient of anorthite was taken as 1.276 (Orville, 1972). The values of $\log K_D$ vary with the Al-silicate polymorph: -0.5 to -1.4 for kyanite and -2.1 to -3.4 for sillimanite and andalusite.

Ghent et al. (1979) improved on this method by including a parameter for the activity coefficient of garnet:

$$0 = \frac{-3272}{T(^{\circ}\text{K})} + 8.3969 - \frac{0.3448 (P(\text{bar}) - 1)}{T(^{\circ}\text{K})} + \log K_D + \log K_{\gamma}$$

where $K_D = (X_{\text{gross}}^{\text{gnt}})^3 / (X_{\text{an}}^{\text{plag}})^3$

and $K_\gamma = (\gamma_{\text{gross}}^{\text{gnt}})^3 / (\gamma_{\text{an}}^{\text{plag}})^3$

To obtain $\gamma_{\text{gross}}^{\text{gnt}}$, Ghent et al. used a value of $W_{\text{Ca-Fe}} \approx 1\text{Kcal/mole}$ in the standard equation:

$$\ln \gamma_{\text{gross}}^{\text{gnt}} = \frac{(1 - X_{\text{gr}})^2 W_{\text{Ca-Fe}}}{RT}$$

which results in $\gamma > 1$ except for Ca-rich compositions. A problem with this assumption of simple mixing is that in natural parageneses the grossular content in complex garnets is at small concentrations, which results in its activity being significantly larger than its mole fraction (i.e. $\gamma \gg 1$ - Ganguly & Kennedy, 1974). The mole fraction of grossular in garnet is taken as:

$$X_{\text{Ca}}^{\text{gnt}} = \text{Ca} / (\text{Ca} + \text{Mg} + \text{Fe} + \text{Mn})$$

which results in a maximum value for $X_{\text{Ca}}^{\text{gnt}}$ and hence a maximum pressure. However, if Fe^{3+} is calculated and assigned to an andradite component with the necessary amount of Ca, the value of $X_{\text{Ca}}^{\text{gnt}}$ is reduced, as is the calculated pressure.

Newton & Haselton (1981) have attempted to formulate an expression for this reaction using more complex binary mixing models for the garnet (cf. Newton & Perkins, 1982 and the garnet-clinopyroxene-plagioclase-quartz geobarometer section B.1.2(b)). Their expression is:

$$\Delta G_A^\circ + RT(^{\circ}\text{K}) \ln \frac{(a_{\text{gr}})^3}{(a_{\text{an}})} + P(\text{bar}) \Delta \bar{V} \approx 0$$

where: $\Delta G_A^\circ \approx -P^\circ \Delta V_A^\circ$ (P° (kbar) = $-2.1 + 0.0232T(^{\circ}\text{C})$ for kyanite)

(P° (kbar) = $-0.6 + 0.0236T(^{\circ}\text{C})$ for sillimanite)

$$RT \ln \gamma_{gr} = (3300 - 1.5T) (X_{py}^2 + X_{py} X_{al})$$

$$a_{an} = X_{an} (1 + X_{an})^2 \exp \left(\frac{(1 - X_{an})^2 (2050 + 9392 X_{an})}{RT} \right)$$

Some difficulty was experienced in applying this method. Although the procedure for the calculation of the mineral activities was well set out in the paper, the calculated pressure values could not be obtained from the given data. There are three major problems not fully explained in the text.

(i) The volume change for the reaction (ΔV_A^O) is quoted in cm^3 in the text although units of cals bar^{-1} are used in the calculation; to convert, divide value in cm^3 by 41.83.

(ii) Only the volume change for the reaction producing kyanite is given in the text (-66.2 cm^3 , or $1.582 \text{ cal bar}^{-1}$); if the method is applied to a sillimanite-bearing assemblage a value of -54.58 cm^3 , or $1.3045 \text{ cal bar}^{-1}$ must be used (from Schmid & Wood, 1976).

(iii) The derivation of the value of $\Delta \bar{V}$ is not made clear. This is obtained thus: $\Delta V_A^O - V_{gr}^O + \bar{V}_{gr}$ i.e. the volume change for the reaction in cm^3 , depending upon the Al_2SiO_5 polymorph formed, minus the partial molal volume of grossular minus the partial molal volume of the grossular garnet in the assemblage under investigation. The values for V_{gr}^O and \bar{V}_{gr} are obtained from Cressey et al., 1978. The value for $\Delta \bar{V}$ is then converted to cal bar^{-1} .

Due to uncertainty over the interaction of Mn in garnets this method is restricted to garnets with $\text{Mn} \leq \text{Mg}/3$. The method was compared by Newton & Haselton to published data on this four-phase assemblage and gave good agreement with the Al_2SiO_5 -polymorph stability diagram of Holdaway (1971).

B.2 MINERAL CALCULATION

The calculation of structural formulae and theoretical end-members from EMP analyses of minerals, as done in this study, is intimately connected with the estimation of the Fe^{3+} content necessary for the calculation of many of the geothermometers and geobarometers outlined in the previous sections.

Some minerals, such as olivine contain negligible amounts of Fe^{3+} , others such as garnet and orthopyroxene contain a little, yet others can contain appreciable amounts, e.g. biotite and clinopyroxene.

One method of estimating the Fe^{3+} content of a mineral is by assuming that the mineral is stoichiometric, i.e. there is an equal number of cations and anions in the structure, e.g. for clinopyroxene ($\text{R}_2\text{Si}_2\text{O}_6$) this charge is 12. When the structural formula is calculated on the basis of cations, any discrepancy from the expected charge number can be attributed to the unaccounted - for Fe^{3+} which of course contains one more cation charge than Fe^{2+} . This is the charge-balance method, and was used for the calculation of Fe^{3+} in the spinels in this study. For phases such as mica and amphibole, which contain other anions besides O^- in their structures (e.g. F^- or Cl^-), this method is difficult to apply because of the unknown contents of these anions which cannot be analysed by EMP.

Naturally, the initial premise that the mineral is stoichiometric may not hold true. Furthermore, due to the closure of the analysis (i.e. the sum of cations is finite, therefore the number of cations on one element effectively controls the total number of the remaining cations) the cation charge is susceptible to errors of analysis in the generally most common element: Si. Ryburn et al. (1976) showed that an error in the analysed SiO_2 value of 1% would propagate as an error of 100°C in the calculated temperature, using the method of Råheim & Green (1974).

B.2.1 Pyroxenes

The charge-balance method is the basis of a computer program (PYROX) written by Neumann (1976) which has been widely used for the calculation of Fe^{3+} contents in omphacitic pyroxenes from eclogites (e.g. Krogh, 1977; Krogh, 1982; Griffin et al., 1982), here the assumption is that a charge of 12 is present. However, Cawthorn & Collerson (1974) have shown that the total number of cations in Ca-Tschermakititic and jadeitic pyroxenes deviates from the expected member of 4, causing the total charge on these cations to deviate from 12.

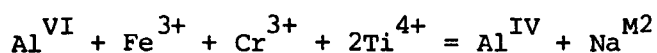
An alternative method is to calculate the structural formula on the basis of 6 oxygens with all the Fe as Fe^{2+} . During the process of calculating the proportions of theoretical end-members, Fe^{3+} is determined by the amount of acmite formed ($\text{NaFe}^{3+}\text{Si}_2\text{O}_6$). However, the structural formula no longer conforms to 6 oxygens. The whole procedure is then iterated until the formula approaches 6 oxygens and there is no further increase in Fe^{3+} (cf. Mysen & Griffin, 1973). This is the basis of a computer program by D.A. Carswell.

Råheim & Green (1975) and Ryburn et al. (1976) have used both of these calculation methods on the same data and found that when applied to the geothermometer of Råheim & Green (1974) the charge-balance method gave generally lower temperatures by about 30°C - 40°C . With clinopyroxenes having low iron contents the charge-balance method gives erratic results (Griffin et al., 1983).

Recently, Rossi (1982, Clermont-Ferrand Conference) has studied the site occupancies of low-temperature omphacites and considers that the tetrahedral site is occupied solely by Si and that all the Al exists as Al^{VI} . As a consequence, in the calculated theoretical end-members Tschermaks molecules are zero (RAlSi_2O_6) and the maximum Al^{VI} value

results in a maximum value for jadeite, any excess Na from jadeite forms acmite. The calculated amount of Fe^{3+} will therefore be lower than in the other methods, consequently Fe^{2+} is higher, as is the $K_D^{\text{gnt-cpx}}$ value and the calculated temperature is lower.

Papike et al. (1974) also provide a charge-balance method for estimating Fe^{3+} :



where the left-hand-side is the sum of the elements in the M1 site, and the right-hand-side is the sum of Al in the tetrahedral site and Na in the M2 site. It was found that this method gave very erratic results, depending upon how siliceous the pyroxene was, since this controlled the Al^{IV} content.

B.2.2 Garnets

The Fe^{3+} contents in this mineral are variable depending upon the dominance of particular end-members within the structure. Andradite ($\text{Ca}_3\text{Fe}_2^{3+}\text{Si}_3\text{O}_{12}$) has substantial Fe^{3+} contents and grossular ($\text{Ca}_3\text{Al}_2\text{Si}_3\text{O}_{12}$) has fairly high contents, which forms a continuous series with andradite. The majority of the garnets analysed in this study are of pyrope-almandine types both of which contain very little Fe^{3+} (Deer et al., 1963, vol. I, p. 97). In general, low Fe^{3+} were expected in the analysed minerals and the charge-balance method used here reflects this. Although the resulting structural formulae are stoichiometric, the sum of the oxides is generally >100% for the garnets. It is suspected that this consistent error arises from the calibration of the EMP with a standard garnet which is not of a sufficiently similar composition to the minerals analysed. As with the pyroxenes the major source of analytical error is probably in the Si.

The end-members were calculated by the method of Rickwood (1968) using a computer program written by D.A. Carswell. The end-members of particular interest were:

Andradite	$\text{Ca}_3\text{Fe}_2^{3+}\text{Si}_3\text{O}_{12}$
Pyrope	$\text{Mg}_3\text{Al}_2\text{Si}_3\text{O}_{12}$
Spessartine	$\text{Mn}_3\text{Al}_2\text{Si}_3\text{O}_{12}$
Grossular	$\text{Ca}_3\text{Al}_2\text{Si}_3\text{O}_{12}$
Almandine	$\text{Fe}_3^{2+}\text{Al}_2\text{Si}_3\text{O}_{12}$
Schorlomite	$\text{Ca}_3\text{Ti}_2\text{Si}_3\text{O}_{12}$
Uvarovite	$\text{Ca}_3\text{Cr}_2\text{Si}_3\text{O}_{12}$

Many other theoretical end-members are included in Rickwood's calculation procedure but they are irrelevant here since they contain elements not analysed for (e.g. goldmanite:V, or kinzigit:Zr). The only major omission is hydrogrossular as H_2O is not analysed by EMP.

B.2.3 Amphiboles

Leake (1978) has presented a formal classification scheme for amphiboles using various chemical parameters: $(\text{Ca} + \text{Na})_B$, Na_A , Ti, $\text{Mg}/(\text{Mg} + \text{Fe}^{2+})$, Si and $\text{Fe}^{3+}/\text{Al}^{3+}$ (the subscripts A and B refer to the sites in the mineral structure). Consequently, the Fe^{3+} content of the amphiboles analysed in this study were estimated solely to assist the classification of the minerals.

In his paper Leake suggests two methods for the estimation of Fe^{3+} : one is by calculating the formula on the basis of 23 anions, assuming that $\text{Na} + \text{Ca} + \text{K}$ are all in the A- and B-sites and that the cations in the C-site (containing Al^{VI} , Fe^{3+} , Fe^{2+} , Mg and Mg) sum to 5. Any excess over 5 in the C-site was allocated to Fe^{3+} . The procedure was then iterated so that ΣC approached 5. The other method was charge-balance, although a major difficulty here is to know the expected charge

(42, 43 or 44) due to variations in A-site occupancy and the possible occurrence of Fe and Mn in the B-site (Neumann, 1976). To remove part of this problem Neumann (1976) suggested that the cations $Si + Al + Ti + Fe + Mg + \frac{1}{2}Mn$ be calculated to sum 13 thereby ignoring the A- and B-sites although there is still the problem of the value of the expected charge.

Papike et al. (1974) also give a charge-balance method, similar to the formulation for the pyroxenes (see previous section) where:

$$(Na + K)_A + Al_C + Fe^{3+}_C + 2Ti_C = Al_T + Na_B$$

this is performed iteratively.

The method used here is the iterative process of Leake (1978) which is incorporated into a computer program written by R. Kanaris-Sotiriou. This method is suitable for Ca-rich amphiboles, as found in the rocks of this study, since the assumption of all Ca, Na and K in the A- and B-sites maximises the amount of $(Ca + Na)_B$ which has to be ≥ 1.34 for Ca-amphiboles in the classification of Leake (1978). However, since $(Ca + Na)_B$ is a maximum, it follows that another diagnostic criterion: Na_A will also be a maximum.

Although this method gave apparently acceptable results, in that there were no instances of negative Fe^{3+} or $Fe^{3+} > Fe^{2+}$ contents, it was felt that the mineral names derived from Leake's classification were perhaps too exact and did not reflect the nature of the analyses (lacking F^- , Cl^- and H_2O) and the estimated Fe^{3+} contents.

B.3 NORMATIVE MINERAL CALCULATION

The normative mineral compositions were calculated using a Fortran IV program (NORM) written by R. Kanaris-Sotiriou. Some care has to be exercised when interpreting the normative mineral compositions calculated from analyses of metamorphic rocks, because of disturbances of the

chemistries resulting from P , T , f_{O_2} and fluid activities. For instance, the degree of silica saturation (reflected by the presence of normative $q \pm \text{hy or ne}$) is dependant upon not only the SiO_2 content, but also the $\text{Fe}_2\text{O}_3/\text{FeO}$ ratio of the rock. If there has been secondary oxidation during metamorphism this ratio will be high, resulting in an increased value of magnetite in the calculated norm. This, in turn, results in less mafic silicates being calculated, which in turn gives more q . Therefore, as the $\text{Fe}_2\text{O}_3/\text{FeO}$ ratio increases the normative calculation moves from ne- to $\text{hy} \pm q$, to q -normative. In addition, the rocks of this study may have underestimated FeO values, resulting from difficulties experienced in the chemical analysis of this oxide, giving higher $\text{Fe}_2\text{O}_3/\text{FeO}$ ratios. A possible remedy for these unknown factors would perhaps be to adopt a standard value for the $\text{Fe}_2\text{O}_3/\text{FeO}$ ratio (cf. Cox, Bell & Pankhurst 1976, p. 413) although this would probably give unrealistic normative mineral values in those rocks which may have suffered oxidation/reduction reactions during their formation.

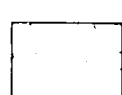

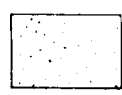













Furthermore, the degree of silica saturation in the norm depends upon the Na_2O and K_2O contents of the rock, with increases in $(\text{Na}_2\text{O} + \text{K}_2\text{O})$ resulting in the calculated mineralogies moving from q to $\text{hy} \pm q$, to ne- normative, i.e. the reverse of the effect of oxidation on the rock. Such increases in Na_2O and K_2O are most likely to result from metasomatic effects in metamorphic rocks, often during hydration of pre-existing anhydrous assemblages.

The normative mineral values given in the Tables of whole rock analyses in this thesis sum to less than 100% due to the omission of H_2O and CO_2 which are not included in the normative calculation.

MAP A

MOLDE PENINSULA: MAIN LITHOLOGICAL UNITS

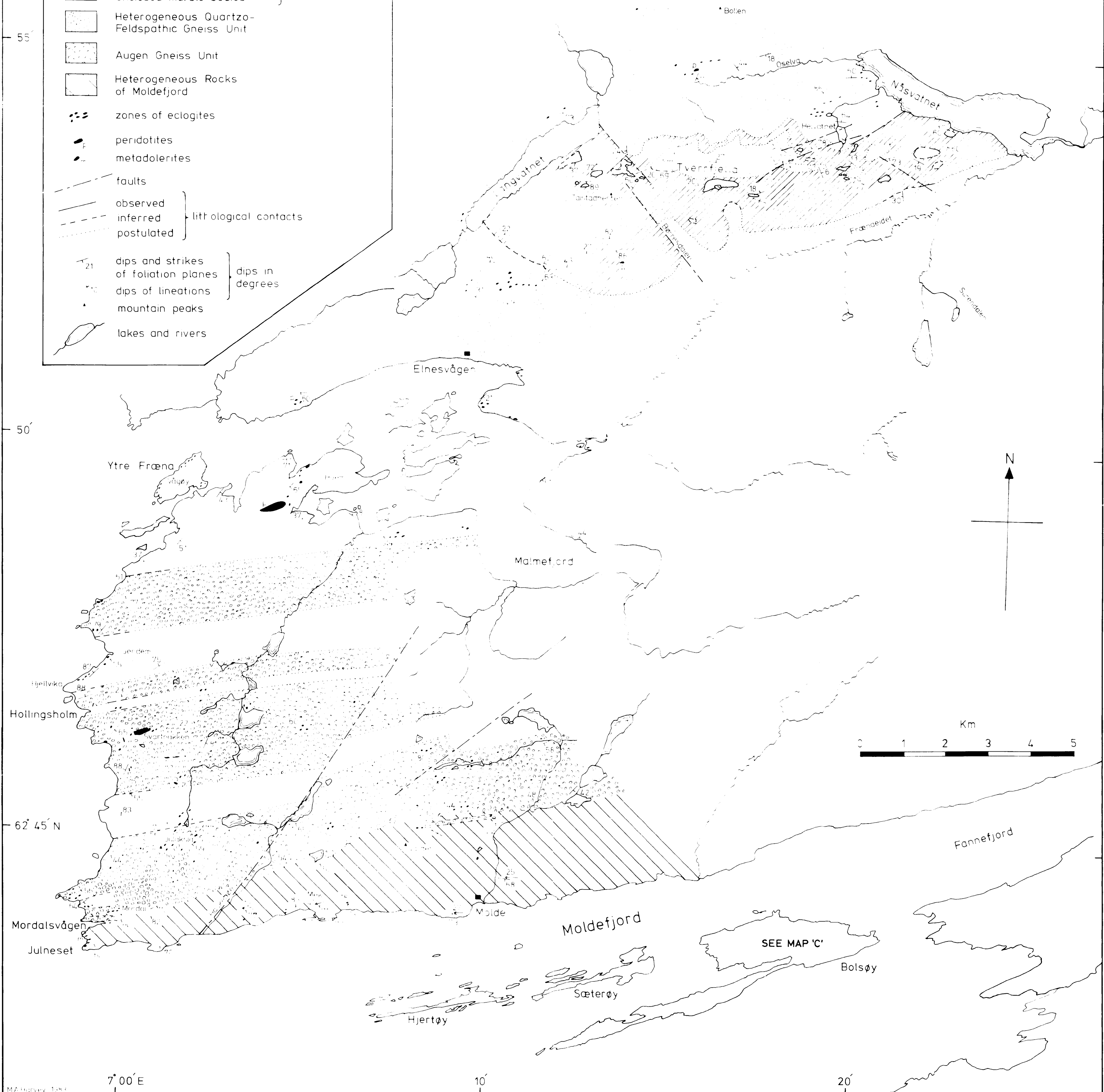
KEY

-  Heterogeneous rocks
-  Garnet-Granulite with enclosed marble bodies
-  Heterogeneous Quartzzo-Feldspathic Gneiss Unit
-  Augen Gneiss Unit
-  Heterogeneous Rocks of Moldefjord
-  zones of eclogites
-  peridotites
-  metadolerites
-  faults
-  observed
-  inferred
-  postulated
-  dips and strikes of foliation planes
-  dips of lineations
-  mountain peaks
-  lakes and rivers

} Tverrfjella Unit

} dips in degrees

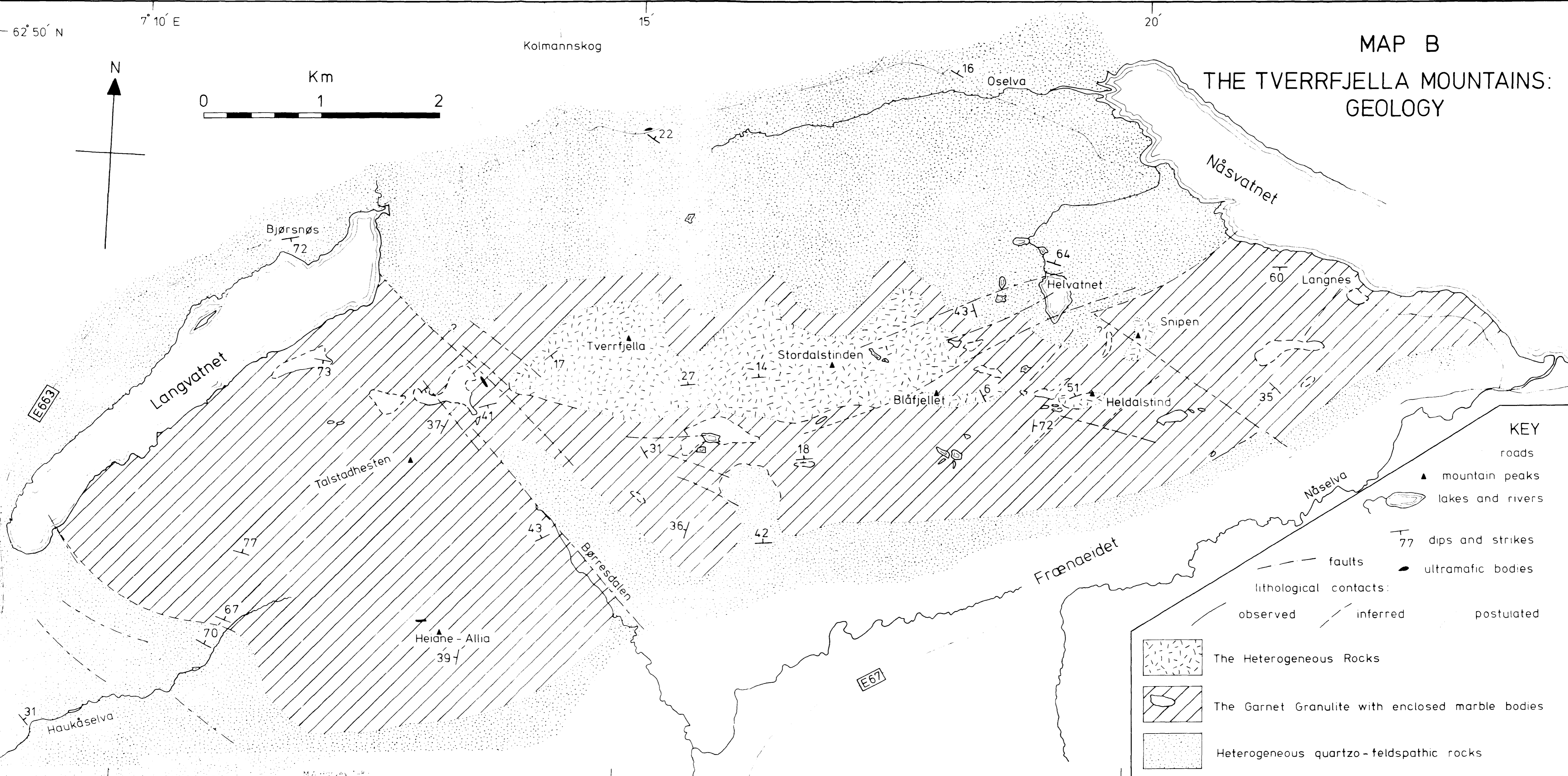
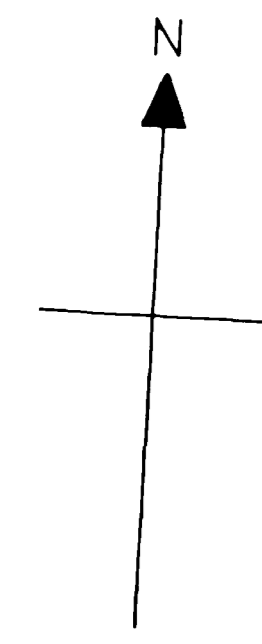
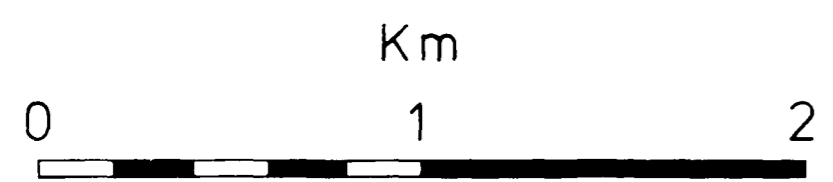
} lithological contacts



62° 50' N 7° 10' E

Kolmannskog

MAP B THE TVERRFJELLA MOUNTAINS: GEOLOGY



KEY

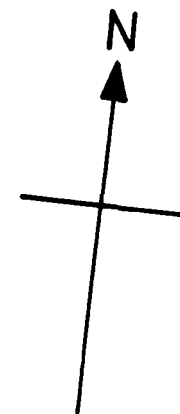
- roads
- ▲ mountain peaks
- lakes and rivers
- 77 dips and strikes
- faults
- ultramafic bodies
- lithological contacts:
 - observed
 - inferred
 - postulated
- The Heterogeneous Rocks
- The Garnet Granulite with enclosed marble bodies
- Heterogeneous quartzo-feldspathic rocks

MAP C

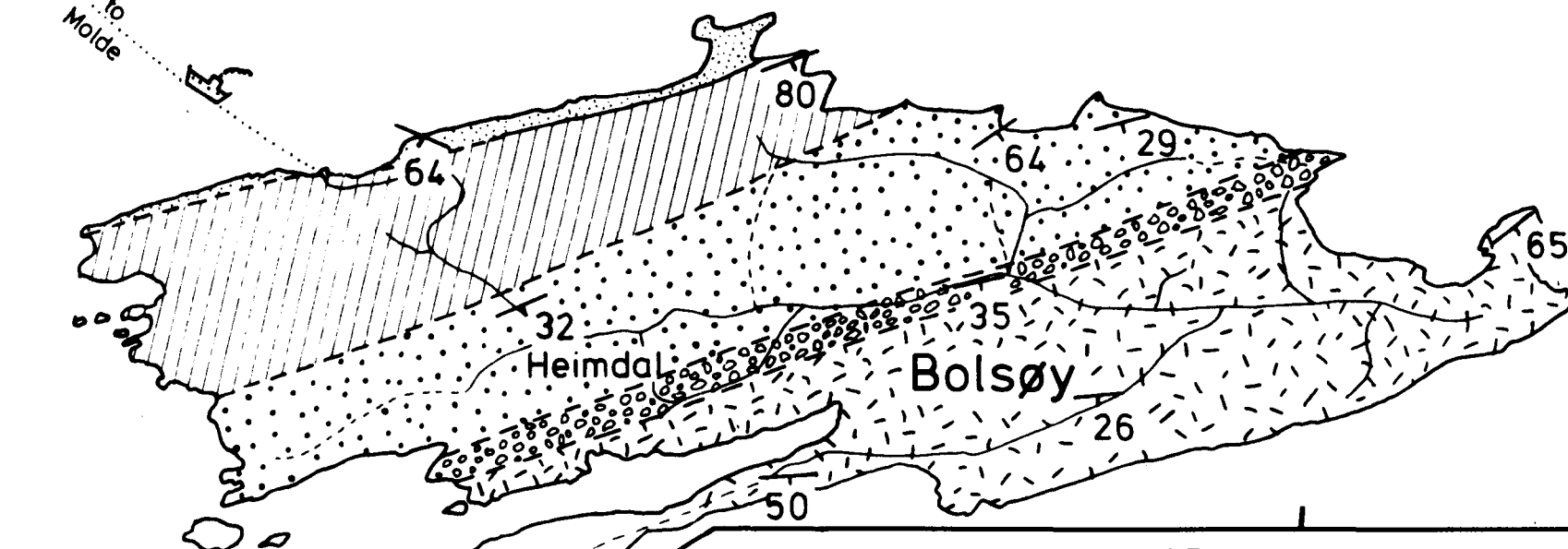
BOLSØY: GEOLOGY

7° 20' E

Km



to
Molde



KEY

roads

67

dips and strikes

lithological contacts:

observed

inferred

Støren Group

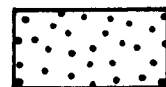


Felsic schists



Amphibole schists + marbles

Røros Group



Mica - schists ± amphibole schists ± marbles

tectonic break?



'Augen' schists

Tingvoll Group



Acid/intermediate gneisses and schists

Moldefjord

Fårøy

MAP D

MOLDE PENINSULA: LINEAR FEATURES DERIVED FROM AERIAL PHOTOGRAPHS

(Some structures were confirmed by field observation others suffer inaccuracies of position due to distortion in the aerial photographs)

① Axes of postulated major structures

① Tverrfjella Syncline

② Halså Anticlinorium

③ Molde - Tingvoll Syncline

▲ mountain peaks

lakes and rivers

representative dips and strikes of foliation planes, from Map A Dips in degrees

